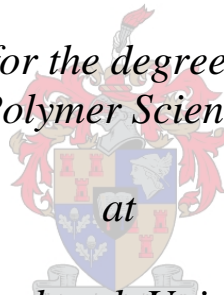


# **The structure - property relationships of polyolefins**

by

**Gareth Harding**

*Dissertation presented for the degree of Doctor of Philosophy  
(Polymer Science)*



*Stellenbosch University*

Promoter: Dr. A.J. van Reenen

*March 2009*

## Declaration

By submitting this dissertation electronically, I declare that the entirety of the work contained therein is my own, original work, that I am the owner of the copyright thereof (unless to the extent explicitly otherwise stated) and that I have not previously in its entirety or in part submitted it for obtaining any qualification.

Signature: .....

Date: .....

## Abstract

Polypropylene is an extremely versatile material and has a broad spectrum of applications due to the variations in properties which are possible with this material. The variations in the properties of the material are governed by the microstructure of the chains constituting the polymer. The microstructure varies according to the production methods, i.e. the polymerisation conditions. Varying the manner in which the polymer is produced therefore changes the properties of the material allowing the polymers' use for different applications. The most important factor affecting the way in which the polymers are produced is the nature of the active sites on the catalyst. Changing the chemical environment of the active sites changes the way in which the polymerisation is controlled and greatly affects the types of chains produced and thus polymer properties.

The study examines the structure-property relationships of polyolefins with specific focus on the polypropylene homopolymer. The temperature rising elution fractionation (TREF) technique is used extensively in order to isolate specific fractions of the polymer. The importance of specific TREF fractions is investigated via a two pronged investigative methodology. On the one hand specific TREF fractions are removed from a sample, allowing the analysis of the properties of the material without that specific fraction, thereby revealing the influence which the fraction in question has on the properties. The other branch of the study investigates the chemical modification of the active sites of a Ziegler-Natta catalyst so as to be able to modify the properties of the polymer in the reactor, in a similar manner to physically removing fractions. The techniques are related and it was discovered that the amount of the fractions of the polymer, found to be important using the one technique, also turned out to be important using the other method.

Initial method development work utilised a polypropylene-1-pentene copolymer since the molecular heterogeneity of this material is such that large differences are observed upon removal of fractions. The technique was then applied to a Ziegler-Natta catalysed polypropylene homopolymer. Each TREF fraction is successively removed and the residual material analysed. Specific TREF fractions were found to play a significant role in determining the polymer properties since there was a drastic reduction in properties upon removal of these fractions.

The polymerisation of propylene was also performed at a variety of conditions in order to investigate different ways in which the catalyst system could be modified. Specific reaction conditions were chosen for in-depth analysis and structure-property correlation. The chemical modification of the active sites was accomplished via the introduction of an external

Lewis base (electron donor) to the polymerisation system, and also by varying the external donor/catalyst ratio used. Two different external donors were used during the study namely Diphenyl-dimethoxysilane (DPDMS) and methyl-phenyl-dimethoxysilane (MPDMS). It is observed that there are definite links between the amounts of specific fractions present in the polymer and the polymer properties, as observed via both the physical removal of fractions and the chemical modification of active sites.



## Opsomming

Polipropileen is 'n baie veelsydige polimeer met 'n wye verskeidenheid van toepassings, as gevolg van die variasie in eienskappe wat moontlik is met die polimeer. Die variasies in die eienskappe van die polimeer word beheer deur die mikrostruktuur van die kettings waaruit die polimeer gebou is. Die mikrostruktuur varieer as gevolg van die manier waarop dit gemaak word, naamlik die omstandighede van die polimerisasie. Veranderinge in die manier waarop die polimeer gemaak word bring dus veranderinge in die fisiese eienskappe van die polimeer, sodat dit gebruik kan word vir ander doeleindes. Die mees belangrike faktor wat die polimerisasie betref is die eienskappe van die aktiewe setels van die katalis. Verandering in die chemiese omgewing van die aktiewe setels verander die manier waarop die polimerisasie beheer word, en bring dus veranderinge mee in die samestelling van die polimeer en die fisiese eienskappe.

Hierdie studie ondersoek die verband tussen die struktuur en die fisiese eienskappe van poli-olefiene wat beklemtoning plaas op die polipropileen homopolimeer. Die TREF tegniek word heelwat gebruik om spesifieke fraksies van die polimeer te isoleer. Die belangrikheid van die TREF fraksies word ondersoek deur middel van twee verskillende denkwyses. Eerstens word spesifieke TREF fraksies verwyder uit die polimeer, sodoende kan die eienskappe van die materiaal ondersoek word sonder die fraksie, en dus kan die belangrikheid van die fraksie uitgelig word. Tweedens word veranderinge aangebring aan die chemiese omgewing van die aktiewe setels van 'n Ziegler-Natta katalis sodat veranderinge aangebring kan word aan die eienskappe van die polimeer in die reaktor op 'n soortgelyke manier as die verwydering van fraksies. Daar is ontdek dat daar 'n verband is tussen die twee denkwyses en dat dieselfde fraksies van belang is by albei denkwyses.

Aanvanklike ontwikkeling van die metodes het gebruik gemaak van 'n polipropileen-1-penteen ko-polimeer as gevolg van die breë verskille in die samestelling van die polimeer, dus behoort daar groot verskille in die eienskappe te wees as 'n fraksie uitgehaal word. Die tegniek is toegepas op 'n polipropileen homopolimeer. Elke TREF fraksie was suksesvol verwyder en die oorblywende materiaal was geanaliseer. Daar is ontdek dat spesifieke TREF fraksies baie belangrik is vir die fisiese eienskappe, as gevolg van die afname in die eienskappe nadat die fraksies uitgehaal is.

Die polimerisasie van propileen was uitgevoer onder verskillende omstandighede, om verskeie maniere te ondersoek waarop die katalis verander kan word. Spesifieke polimerisasies is uitgevoer om polimere te maak wat in meer diepte geanaliseer kan word en wat gebruik kan word om verhoudings te ondersoek tussen die struktuur en die eienskappe.

Die veranderinge in die chemiese omgewing van die aktiewe setels was aangebring deur 'n eksterne Lewis basis (elektron verskaffer) te gebruik teen verkillende hoeveelhede.

Verskillende verhoudings van die Lewis basis tot die katalis is gebruik. Twee verkillende Lewis basisse is gebruik tydens die studie, naamlik di-feniel-dimetoksiesilaan (DPDMS) en metiel-feniel-dimetoksiesilaan (MPDMS). Daar is gevind dat daar 'n definitiewe verband is tussen die hoeveelhede gebruik van spesifieke fraksies, en die fisiese eienskappe soos aangedui deur die verwydering van fraksies, en die verandering aan die chemiese omgewing van die aktiewe setels.

This thesis is dedicated to my family, especially my parents and my fiancée Soraya, for all their unwavering love and support over the years.

## **Acknowledgements**

I would like to thank the following people for their support and assistance during the course of my studies:

Dr. A.J. van Reenen for his guidance and down to earth advice throughout the duration of my studies.

Jean McKenzie and Elsa Malherbe for all their assistance in running the NMR samples and always being willing to help.

The olefins group for all the good times that I have enjoyed throughout the course of my studies and making it a pleasure to be in the office.

Dr. Remy Bucher at Ithemba Labs for assisting with WAXD analysis.

The support and technical staff at the Institute for Polymer Science for all their help in the day to day running of the department and laboratories.

The Department of Labour, Sasol, and the NRF for funding without which this study would not have been possible.

I would also like to thank my entire family and especially my parents and my fiancée Soraya, for their constant, unwavering support throughout my studies.

Finally, to all my friends, for all the good times that I have enjoyed over the past few years, making this time of my life so memorable.

## Table of Contents

Table of Contents .....	I
List of Figures .....	VI
List of Tables.....	XIX
List of Abbreviations.....	XX
Chapter 1. Introduction .....	1
1.1 General introduction.....	1
1.2 Objectives.....	3
1.3 References .....	4
Chapter 2 Historical background.....	5
2.1 Polyolefins: A brief historical overview .....	5
2.1.1 The first steps .....	5
2.1.2 The origins of the Ziegler-Natta catalyst.....	6
2.1.3 The development of stereoregular polymerisation.....	8
2.2 Ziegler-Natta catalysts.....	9
2.2.1 The development of the Ziegler-Natta catalysts .....	9
2.2.2 Polymerisation chemistry .....	12
2.2.2.1 General mechanism of polymerisation.....	12
2.2.2.2 Polymerisation control mechanisms and stereochemistry .....	15
2.2.2.3 Catalyst active sites: The support.....	17
2.2.2.4 Catalyst active sites: Titanium – support complex formation.....	19
2.2.2.5 Catalyst active sites: The internal electron donor .....	20
2.2.2.6 Catalyst active sites: The external electron donor.....	22
2.2.2.7 Catalyst active sites: The effect on the polymer microstructure .....	24
2.2.2.8 Catalyst active sites: Active site models .....	25
2.2.2.9 Polymerisation conditions affecting the reaction .....	27
2.3 Polypropylene.....	27
2.3.1 Structure .....	28
2.3.2 Properties.....	29
2.3.3 Production methods.....	30
2.3.4 Applications .....	31
2.4 Fractionation.....	32
2.4.1 Fractionation by crystallinity .....	32
2.4.1.1 TREF .....	32

2.4.1.2 CRYSTAF .....	35
2.4.1.3 CEF.....	36
2.4.1.4 TFA/SCALLS .....	36
2.4.2 Fractionation by molar mass .....	37
2.4.2.1 SEC.....	37
2.4.2.2 Solvent/non-solvent techniques.....	38
2.4.3 Fractionation by chemical composition distribution.....	38
2.5 Mechanical properties .....	38
2.5.1 General structure-property relationships.....	39
2.5.2 Microhardness .....	40
2.5.2.1 General background and theory .....	40
2.5.2.2 Deformation mechanisms.....	41
2.5.2.3 The effect of microstructure on microhardness.....	42
2.5.3 DMA.....	42
2.5.3.1 General background and theory .....	42
2.5.3.2 The effect of microstructure on the polymer properties.....	44
2.6 Concluding remarks and methodology .....	44
2.7 References .....	45
Chapter 3. General experimental details .....	64
3.1 Polymerisation materials and equipment .....	64
3.2 Fractionation techniques .....	64
3.2.1 TREF .....	64
3.2.1.1 The crystallisation step.....	65
3.2.1.2 The elution step .....	65
3.2.2 CRYSTAF .....	67
3.3 Characterisation techniques.....	67
3.3.1 <sup>13</sup> C NMR.....	67
3.3.2 DSC .....	69
3.3.2.1 Crystallisation and melting data.....	69
3.3.2.2 Lamellar thickness determination .....	69
3.3.3 HT-GPC .....	70
3.4 Mechanical properties .....	70
3.4.1 Extensional DMA.....	70
3.4.2 Compressive DMA.....	71
3.4.3 Microhardness .....	71

3.5 References .....	71
Chapter 4. TREF fraction – property relationships .....	73
4.1 Introduction .....	73
4.2 Experimental .....	74
4.2.1 Polymer materials.....	74
4.2.2 Fractionation and recombination.....	74
4.2.3 Polymer characterisation .....	75
4.2.4 Mechanical properties .....	75
4.3 Results and discussion.....	75
4.3.1 PP-1-pentene .....	75
4.3.1.1 PP-1-pentene characterisation .....	75
4.3.1.2 Fraction removal .....	80
4.3.1.3 Physical properties .....	84
4.3.1.4 Structure – property relationships .....	89
4.3.2 PP homopolymer .....	93
4.3.2.1 PP characterisation .....	93
4.3.2.2 PP fraction removal.....	99
4.3.2.3 Physical properties .....	103
4.3.2.4 Structure – property relationships .....	107
4.4 Conclusions .....	110
4.5 References .....	112
Chapter 5. Polymerisation reactions with a Ziegler-Natta catalyst.....	115
5.1 Introduction .....	115
5.2 Experimental .....	115
5.2.1 Polymerisation details .....	116
5.2.2 Polymer characterisation .....	116
5.3 Results and Discussion.....	117
5.3.1 Catalyst/cocatalyst pre-treatment time .....	117
5.3.2 Polymerisation temperature.....	119
5.3.2.1 Al : Ti = 20 .....	119
5.3.2.2 Al : Ti = 80 .....	123
5.3.3 The catalyst/cocatalyst ratio .....	126
5.3.4 Propylene pressure .....	128
5.3.5 The use of hydrogen as a chain transfer agent .....	130
5.3.6 Varying the external donor type – no hydrogen present .....	132

5.3.6.1 DPDMS .....	132
5.3.6.2 MPDMS .....	137
5.3.7 Polymerisations for in-depth analysis .....	140
5.3.7.1 Polymerisations with DPDMS as external donor.....	141
5.3.7.2 Polymerisations with MPDMS as external donor .....	144
5.4 Conclusions .....	148
5.5 References .....	151
Chapter 6. Active sites, microstructure, and properties .....	156
6.1 Introduction .....	156
6.2 Experimental .....	158
6.2.1 Polymer characterisation .....	158
6.2.2 TREF characterisation.....	158
6.2.3 Mechanical properties .....	158
6.2.4 Molar mass distribution deconvolution.....	159
6.3 Results and Discussion.....	159
6.3.1 Polymer microstructure .....	160
6.3.1.1 Molar mass distributions .....	161
6.3.1.2 <sup>13</sup> C NMR analysis.....	164
6.3.2 Thermal properties .....	167
6.3.3 CRYSTAF analysis .....	174
6.3.4 TREF analysis .....	176
6.3.4.1 Microstructure of TREF fractions .....	179
6.3.4.2 Thermal properties of TREF fractions .....	185
6.3.5 Molar mass distribution deconvolution.....	192
6.3.6 Mechanical properties .....	200
6.3.6.1 Microhardness .....	200
6.3.6.2 DMA.....	209
6.4 Conclusions .....	215
6.5 References .....	218
Chapter 7. Synopsis and conclusions .....	222
7.1 Synopsis and conclusions.....	222
7.2 Recommendations for future work.....	231
7.3 References .....	232
Appendix A. HT-GPC data .....	233
A.1 HT-GPC data from Chapter 4 .....	233



A.2 HT-GPC data from Chapter 5 .....	234
A.3 HT-GPC data from Chapter 6 .....	236
A.4 HT-GPC data from Chapter 7 .....	238
Appendix B. $^{13}\text{C}$ NMR data.....	239
B.1 $^{13}\text{C}$ NMR data from Chapter 4 .....	239
B.2 $^{13}\text{C}$ NMR data from Chapter 5 .....	242
B.3 $^{13}\text{C}$ NMR data from Chapter 6.....	247
B.4 $^{13}\text{C}$ NMR data from Chapter 7 .....	252
Appendix C. DSC data .....	253
C.1 DSC data from Chapter 4 .....	253
C.2 DSC data from Chapter 5 .....	255
C.3 DSC data from Chapter 6 .....	274
C.4 DSC data from Chapter 7 .....	283

## List of Figures

Figure 2.1 The different stereo-conformations of polypropylene. ....	8
Figure 2.2 An illustration of the different types sequence distributions, and the control mechanisms which cause the formation of the sequences in heterogeneous catalysts. ....	16
Figure 2.3 The lateral cuts of the MgCl <sub>2</sub> crystal. ....	18
Figure 2.4 Catalyst active sites on (104) and (110) cuts of the MgCl <sub>2</sub> crystal. ....	19
Figure 3.1 The setup used for the TREF crystallisation step. ....	65
Figure 3.2 Illustration of the column packing. ....	66
Figure 3.3 The TREF elution setup. ....	66
Figure 3.4 The structure of the propylene-1-pentene copolymer. ....	68
Figure 4.1 The TREF fractionation data for sample PP1P. ....	76
Figure 4.2 The weight average molar mass and polydispersity data for the TREF fractions of sample PP1P. ....	77
Figure 4.3 The comonomer content of selected TREF fractions of sample PP1P. ....	78
Figure 4.4 The DSC heating curves for all TREF fractions of sample PP1P. ....	79
Figure 4.5 The degree of crystallinity of each of the TREF fractions of sample PP1P. ....	79
Figure 4.6 The fraction removal data for the PP1P sample. ....	80
Figure 4.7 The weight average molar mass of the PP1P samples with specific fractions removed from the sample (shown in red), and the molar mass of the fraction removed (shown in blue). ....	81
Figure 4.8 The polydispersity of the PP1P samples with specific TREF fractions removed from the sample (shown in red), and the polydispersity of the fractions removed (shown in blue). ....	82
Figure 4.9 The 1-pentene content of the PP1P samples with specific TREF fractions removed from the sample (shown in red), and the 1-pentene content of the material removed (shown in blue). ....	83
Figure 4.10 An illustration of the mass percentage of 1-pentene remaining in the samples after the specific fractions have been removed (shown in red), as well as the mass percentage of the 1-pentene in the fraction removed (shown in blue). ....	84
Figure 4.11 The peak melting temperatures of the PP1P samples with specific TREF fractions removed from the sample (shown in red), and the fractions removed (shown in blue). ....	85

Figure 4.12 The degree of crystallinity of the PP1P sample with specific TREF fractions removed from the sample (shown in red), and the crystallinity of the fraction removed (shown in blue).....	86
Figure 4.13 The weight average lamellar thickness of the PP1P samples with specific fractions removed.....	87
Figure 4.14 The modulus values at 2% strain of the PP1P sample with specific TREF fractions removed from the sample.....	88
Figure 4.15 The relationship between the crystallinity of the samples and the modulus at 2% strain.....	89
Figure 4.16 The relationship between the weight average lamellar thickness of the samples and the percentage crystallinity.....	90
Figure 4.17 The relationship between the weight average lamellar thickness and the 1-pentene content of the PP1P samples.....	91
Figure 4.18 The relationship between the 1-pentene content and the crystallinity of the PP1P samples.....	91
Figure 4.19 The relationship between the comonomer content and the modulus at 2% strain.....	92
Figure 4.20 The TREF fractionation data for the PP homopolymer sample.....	94
Figure 4.21 The molar mass data for the TREF fractions of sample PPH.....	94
Figure 4.22 The polydispersity data for the TREF fractions of sample PPH.....	96
Figure 4.23 The sequence distribution content for the TREF fractions of sample PPH.....	97
Figure 4.24 The melting endotherms of the TREF fractions of sample PPH.....	98
Figure 4.25 The degree of crystallinity of the TREF fractions of sample PPH.....	98
Figure 4.26 The fraction removal data for the PPH sample.....	99
Figure 4.27 The weight average molar mass of the PPH samples with specific fractions removed from the sample (shown in red), and the molar mass of the fraction removed (shown in blue).....	100
Figure 4.28 The polydispersity of the PPH samples with specific fractions removed from the sample (shown in red), and the polydispersity of the fraction removed (shown in blue).....	101
Figure 4.29 The pentad sequence distribution content of the PPH samples with specific TREF fractions removed.....	102
Figure 4.30 The percentage of <i>mmmm</i> pentad sequence content for PPH samples with specific TREF fractions removed (shown in red), and the <i>mmmm</i> pentad sequence content for the fractions removed (shown in blue).....	102

Figure 4.31 The peak melting temperatures of the PPH sample with specific TREF fractions removed from the sample (shown in red), and the peak melting temperatures of the fractions removed (shown in blue).....	104
Figure 4.32 The degree of crystallinity of the PPH samples with specific TREF fractions removed (shown in red), and the crystallinity of the fractions removed (shown in blue).....	105
Figure 4.33 The weight average lamellar thickness of the PPH samples with specific TREF fractions removed.....	106
Figure 4.34 The modulus values at 2% extension of the PPH sample with specific TREF fractions removed from the sample.....	107
Figure 4.35 The relationship between the crystallinity and the modulus at 2% strain for the PPH samples.....	108
Figure 4.36 The relationship between the weight average molar mass and the modulus at 2% strain for the PPH samples. ....	108
Figure 4.37 The relationship between the crystallinity and the lamellar thickness of the PPH samples.....	109
Figure 4.38 The relationship between the lamellar thickness and the average <i>mmmm</i> pentad sequence content of the PPH samples.....	109
Figure 4.39 The relationship between the <i>mmmm</i> pentad sequence content and the crystallinity of the PPH samples. ....	110
Figure 5.1 The structure of the two types of external Lewis base used in the study, namely DPDMS (structure A) and MPDMS (structure B).....	116
Figure 5.2 The effect of the contact time of the catalyst and co-catalyst on the activity of the system.....	117
Figure 5.3 The effect of the contact time of the catalyst and co-catalyst on the molar mass of the polymer.....	118
Figure 5.4 The effect of the contact time of the catalyst and co-catalyst on the crystallinity of the polymer.....	119
Figure 5.5 The effect of temperature on the activity of the catalyst at an Al:Ti = 20.....	120
Figure 5.6 The effect of temperature on the $M_w$ of the polymer produced at an Al:Ti = 20.	121
Figure 5.7 The effect of temperature on the crystallinity of the polymer produced at an Al:Ti = 20.....	122
Figure 5.8 The effect of the polymerisation temperature on the tacticity of the polymer produced at an Al:Ti = 20. ....	123

Figure 5.9 The effect of the polymerisation temperature on the activity of the catalyst at an Al:Ti = 80.....	124
Figure 5.10 The effect of temperature on the crystallinity of the polymer produced at an Al:Ti = 80.....	124
Figure 5.11 Comparison of the activity (closed triangles) and average isotacticity (closed circles) for polymers produced while varying the temperature at Al:Ti = 80.....	125
Figure 5.12 The variation of Al:Ti at a polymerisation temperature of 70 °C.....	126
Figure 5.13 The effect of variation in catalyst/cocatalyst ratio on the weight average molar mass at a polymerisation temperature of 70 °C.....	127
Figure 5.14 The average isotacticity (closed triangles) and percentage crystallinity (closed circles) of the polymers produced while varying the Al:Ti ratio as determined by <sup>13</sup> C NMR. ....	128
Figure 5.15 The influence of the propylene pressure on the activity of the catalyst. ....	129
Figure 5.16 The influence of the propylene pressure on the weight average molar mass of the polymer produced.....	129
Figure 5.17 The effect of the addition of hydrogen to the polymerisation system on the molar mass of the polymer produced. ....	130
Figure 5.18 The effect of hydrogen on the percentage crystallinity of the polymers produced. ....	132
Figure 5.19 The effect of the Si : Ti on the activity of the catalyst.....	133
Figure 5.20 The effect of the Si : Ti on the weight average molar mass of the polymer produced.....	134
Figure 5.21 The effect of the Si : Ti on the <i>mmmm</i> pentad content of the polymer produced. ....	135
Figure 5.22 The effect of the Si : Ti on the crystallinity of the polymer produced. ....	137
Figure 5.23 The effect of the Si : Ti on the activity of the catalyst: Comparisons of the DPDMS and MPDMS as external donors.....	138
Figure 5.24 The effect of the Si : Ti on the weight average molar mass of the polymers: Comparisons of the DPDMS and MPDMS as external donors. ....	139
Figure 5.25 The effect of the Si : Ti on the <i>mmmm</i> pentad content of the polymers: Comparisons of the DPDMS and MPDMS as external donors. ....	139
Figure 5.26 The effect of the Si : Ti on the crystallinity of the polymers: Comparisons of the DPDMS and MPDMS as external donors.....	140

Figure 5.27 The effect of the Si : Ti on the activity of the catalyst using DPDMS as external donor. The activity of the polymerisation performed without external donor is given for comparison.....	141
Figure 5.28 The effect of the Si : Ti on the weight average molar mass of the polymer produced using DPDMS as external donor. The molar mass of the polymer produced without external donor is given for comparison.....	142
Figure 5.29 The effect of the Si : Ti on the polydispersity of the polymer produced using DPDMS as external donor. The polydispersity of the polymer produced without external donor is given for comparison.....	143
Figure 5.30 The effect of the Si : Ti on the peak melting temperatures of the polymer produced using DPDMS as external donor. The melting temperature of the polymer produced without external donor is given for comparison. ....	143
Figure 5.31 The effect of the Si : Ti on the crystallinity of the polymer produced using DPDMS as external donor. The crystallinity of the polymer produced without external donor is given for comparison.....	144
Figure 5.32 The effect of the Si : Ti on the activity of the catalyst using MPDMS as external donor. The activity of the polymerisation performed without external donor is given for comparison.....	145
Figure 5.33 The effect of the Si : Ti on the weight average molar mass of the polymer produced using MPDMS as external donor. The molar mass of the polymer produced without external donor is given for comparison.....	146
Figure 5.34 The effect of the Si : Ti on the polydispersity of the polymer produced using MPDMS as external donor. The polydispersity of the polymer produced without external donor is given for comparison.....	146
Figure 5.35 The effect of the Si : Ti on the peak melting temperatures of the polymer produced using MPDMS as external donor. The melting temperature of the polymer produced without external donor is given for comparison. ....	147
Figure 5.36 The effect of the Si : Ti on the crystallinity of the polymer produced using MPDMS as external donor. The crystallinity of the polymer produced without external donor is given for comparison.....	148
Figure 6.1 An adaptation of the three sites model as proposed by Busico <i>et al.</i> [12, 14].....	157
Figure 6.2 The effect of the Si : Ti on the activity of the catalyst.....	161
Figure 6.3 The molar mass distribution of the polymers synthesised using DPDMS as external donor. The distribution for the sample prepared without external donor is also given for comparison.....	162

Figure 6.4 The molar mass distribution of the polymers synthesised using MPDMS as external donor. The distribution for the sample prepared without external donor is also given for comparison. ....	163
Figure 6.5 The effect of the Si : Ti on the weight average molar mass of the polymers. ....	163
Figure 6.6 The effect of the Si : Ti on the polydispersity of the polymers. ....	164
Figure 6.7 The microstructure distribution for the samples produced using DPDMS as well as the sample polymerised without external electron donor.....	165
Figure 6.8 The microstructure distribution for the samples produced using MPDMS as well as the sample polymerised without external electron donor.....	166
Figure 6.9 The effect of the Si : Ti on the tacticity of the polymers. ....	167
Figure 6.10 A comparison of the crystallisation exotherms of the samples produced using DPDMS as well as the sample without external donor.....	168
Figure 6.11 A comparison of the melting endotherms of the samples produced using DPDMS as well as the sample without external donor.....	168
Figure 6.12 A comparison of the crystallisation exotherms of the samples produced using MPDMS as well as the sample without external donor. ....	170
Figure 6.13 A comparison of the melting endotherms of the samples produced using MPDMS as well as the sample without external donor.....	170
Figure 6.14 A comparison of the peak crystallisation temperatures of the samples.....	171
Figure 6.15 A comparison of the peak melting points of the samples. ....	172
Figure 6.16 A comparison of the degree of crystallinity of the samples. ....	173
Figure 6.17 The differences in the weight average lamellar thickness between the samples produced at different Si:Ti. ....	173
Figure 6.18 A comparison of the CRYSTAF distribution curves of the samples produced using DPDMS as well as the sample without external donor. ....	174
Figure 6.19 A comparison of the CRYSTAF distribution curves of the samples produced using MPDMS as well as the sample without external donor.....	175
Figure 6.20 The distribution of TREF fractions for the samples produced using DPDMS as well as the sample without external donor for comparison.....	176
Figure 6.21 The distribution of TREF fractions for the samples produced using MPDMS as well as the sample without external donor for comparison.....	177
Figure 6.22 The weight average molar mass averages data for the TREF fractions of the samples produced using DPDMS as well as the sample without external donor. ....	180
Figure 6.23 The polydispersity values for the TREF fractions of the samples produced using DPDMS as well as the sample without external donor.....	181

Figure 6.24 The weight average molar mass averages data for the TREF fractions of the samples produced using MPDMS as well as the sample without external donor.	182
Figure 6.25 The polydispersity values for the TREF fractions of the samples produced using MPDMS as well as the sample without external donor. ....	182
Figure 6.26 The percentage of <i>mmmm</i> sequences for selected TREF fractions of the samples produced using DPDMS as well as the sample without external donor. ....	183
Figure 6.27 The percentage of <i>mmmm</i> sequences for selected TREF fractions of the samples produced using MPDMS as well as the sample without external donor.....	184
Figure 6.28 The peak melting temperatures for the TREF fractions of the samples produced using DPDMS as well as the sample without external donor. ....	186
Figure 6.29 The percentage crystallinity for the TREF fractions of the samples produced using DPDMS as well as the sample without external donor.....	187
Figure 6.30 The peak melting temperatures for the TREF fractions of the samples produced using MPDMS as well as the sample without external donor.....	188
Figure 6.31 The weight average lamellar thickness of the fractions of the samples produced using DPDMS as well as those of the sample produced without external donor.	188
Figure 6.32 The weight average lamellar thickness of the fractions of the samples produced using MPDMS as well as those of the sample produced without external donor.	189
Figure 6.33 The percentage crystallinity for the TREF fractions of the samples produced using MPDMS as well as the sample without external donor. ....	190
Figure 6.34 The DSC crystallisation exotherms of the 60 °C TREF fractions of the samples produced using DPDMS and the No ED sample. ....	191
Figure 6.35 The deconvolution of the molar mass distribution of sample DP-1 into Flory distributions.....	192
Figure 6.36 The mass fraction of the various active sites for the deconvolution of the molar mass distribution of the samples produced using DPDMS as well as the No ED sample.....	194
Figure 6.37 The variation in molar mass of the individual Flory distributions at different Si:Ti for the samples produced using DPDMS. ....	195
Figure 6.38 The mass fraction of the various active sites for the deconvolution of the molar mass distribution of the samples produced using MPDMS as well as the No ED sample.....	196
Figure 6.39 The variation in molar mass of the individual Flory distributions at different Si:Ti for the samples produced using MPDMS. ....	197



Figure 6.40 A comparison of the proportion of different active sites and the weight average molar mass of the polymers they produce for the DP-4 and MP-4 samples.....	198
Figure 6.41 A comparison of the proportion of different active sites and the weight average molar mass of the polymers they produce for the DP-1 and MP-1 samples.....	199
Figure 6.42 The microhardness results for the samples produced using DPDMS at different indentation loads and different cooling regimes illustrating the differences in the microhardness upon cooling.....	200
Figure 6.43 A comparison of the microhardness data for the samples produced using DPDMS and MPDMS as well as the No ED sample illustrating the differences between the samples at loads of 49 mN and 98 mN.....	201
Figure 6.44 The effect of the molar mass and polydispersity on the crystallinity of all the samples. ....	202
Figure 6.45 The effect of the molar mass and <i>mmmm</i> pentad content on the crystallinity of the samples. ....	203
Figure 6.46 A closer examination of the effect of small changes in <i>mmmm</i> pentad content as well as changes in the molar mass on the crystallinity of the samples. ....	204
Figure 6.47 The effect of the crystallinity and the molar mass on the microhardness of the samples. ....	204
Figure 6.48 A closer inspection of the effect of crystallinity and molar mass on small changes in microhardness. ....	205
Figure 6.49 The effect of the molar mass and the <i>mmmm</i> pentad content on the microhardness of the samples.....	206
Figure 6.50 The combined effect of the molar mass and the <i>mmmm</i> pentad content on the microhardness of the samples. ....	207
Figure 6.51 The effect of the molar mass on the microhardness of the samples produced using a certain donor type. ....	207
Figure 6.52 The effect of the crystallinity on the microhardness of the polymers produced using a certain donor type. ....	208
Figure 6.53 The effect of the <i>mmmm</i> pentad content on the microhardness of the samples for the different polymers produced using different external donor types. ....	209
Figure 6.54 The $\tan \delta$ curves for the samples produced using DPDMS and the No ED sample. ....	210
Figure 6.55 The $\tan \delta$ curves for the samples produced using MPDMS and the No ED sample. ....	211

Figure 6.56 The magnitude of the area of the $\beta$ -transition as a function of the external donor/catalyst ratio for the samples produced with both DPDMS and MPDMS.	211
Figure 6.57 The storage modulus curves for the samples produced using DPDMS and the No ED sample.	213
Figure 6.58 The storage modulus curves for the samples produced using MPDMS and the No ED sample.	214
Figure 7.1 An illustration of the similarity in TREF profiles of the PPH sample and the No ED sample.	222
Figure 7.2 A more direct comparison between the amount of material eluting in each of the fractions of the PPH and No ED samples.	223
Figure 7.3 The relationship between the <i>mmmm</i> pentad content and the microhardness illustrating the position of the PPH sample relative to the other samples.	224
Figure 7.4 The relationship between the <i>mmmm</i> pentad content and the microhardness illustrating the position of the test sample (produced at an external donor/catalyst ratio of 2) relative to the other samples.	226
Figure 7.5 An illustration of the reciprocal relationship between the microhardness and impact properties as measured by the damping ability of a material in DMA.	227
Figure 7.6 A comparison of the fraction percentage of the different site types responsible for the molar mass distribution of the PPH sample with the 106 – 110 °C fraction removed and the original PPH sample.	228
Figure 7.7 A comparison of the molar mass of the chains produced at each active site type for the sample with the 106 – 110 °C fraction removed and the PPH sample.	229
Figure 7.8 A comparison of the fraction percentage of the different site types responsible for the molar mass distribution of the No ED and DP-3 samples.	230
Figure 7.9 A comparison of the molar mass of the chains produced at each active site type for the No ED and the DP-3 samples.	230
Figure B.1 The $^{13}\text{C}$ NMR spectra of the PPH and PP1P samples.	239
Figure B.2 The $^{13}\text{C}$ NMR spectra for the TREF fractions of the PP1P sample.	240
Figure B.3 The $^{13}\text{C}$ NMR spectra for the PP1P samples with specific TREF fractions removed.	240
Figure B.4 The $^{13}\text{C}$ NMR spectra for the TREF fractions of the PPH sample.	241
Figure B.5 The $^{13}\text{C}$ NMR spectra for the PPH samples with specific TREF fractions removed.	241
Figure B.6 The $^{13}\text{C}$ NMR spectra for the polymerisations conducted at various temperatures at an Al:Ti = 20.	242

Figure B.7 The $^{13}\text{C}$ NMR spectra for the polymerisations conducted at various temperatures at an Al:Ti = 80. ....	243
Figure B.8 The $^{13}\text{C}$ NMR spectra for the polymerisations conducted at various cocatalyst/catalyst ratios.....	243
Figure B.9 The $^{13}\text{C}$ NMR spectra for the polymerisations conducted using DPDMS at varying external donor/catalyst ratios at an Al:Ti = 20.....	244
Figure B.10 The $^{13}\text{C}$ NMR spectra for the polymerisations conducted using DPDMS at varying external donor/catalyst ratios at an Al:Ti = 40.....	244
Figure B.11 The $^{13}\text{C}$ NMR spectra for the polymerisations conducted using DPDMS at varying external donor/catalyst ratios at an Al:Ti = 60.....	245
Figure B.12 The $^{13}\text{C}$ NMR spectra for the polymerisations conducted using DPDMS at varying external donor/catalyst ratios at an Al:Ti = 80.....	245
Figure B.13 The $^{13}\text{C}$ NMR spectra for the polymerisations conducted using MPDMS at varying external donor/catalyst ratios at an Al:Ti = 80.....	246
Figure B.14 The $^{13}\text{C}$ NMR spectra for the polymerisations used for in-depth analysis. ....	247
Figure B.15 The $^{13}\text{C}$ NMR spectra for selected TREF fractions of sample DP-1. ....	248
Figure B.16 The $^{13}\text{C}$ NMR spectra for selected TREF fractions of sample DP-2. ....	248
Figure B.17 The $^{13}\text{C}$ NMR spectra for selected TREF fractions of sample DP-3. ....	249
Figure B.18 The $^{13}\text{C}$ NMR spectra for selected TREF fractions of sample DP-4. ....	249
Figure B.19 The $^{13}\text{C}$ NMR spectra for selected TREF fractions of sample MP-1.....	250
Figure B.20 The $^{13}\text{C}$ NMR spectra for selected TREF fractions of sample MP-2.....	250
Figure B.21 The $^{13}\text{C}$ NMR spectra for selected TREF fractions of sample MP-3.....	251
Figure B.22 The $^{13}\text{C}$ NMR spectra for selected TREF fractions of sample MP-4.....	251
Figure B.23 The $^{13}\text{C}$ NMR spectra for selected TREF fractions of sample No ED.....	252
Figure B.24 The $^{13}\text{C}$ NMR spectrum of the test sample. ....	252
Figure C.1 The DSC crystallisation exotherms for the PP1P samples with selected fractions removed.....	253
Figure C.2 The DSC melting endotherms for the PP1P samples with selected fractions removed.....	253
Figure C.3 The DSC crystallisation exotherms for the PPH samples with selected fractions removed.....	254
Figure C.4 The DSC melting endotherms for the PPH samples with selected fractions removed.....	254

Figure C.5 The DSC crystallisation exotherms for the samples produced while varying the pre-treatment time between the catalyst and cocatalyst. The pre-treatment time is indicated in minutes. ....	255
Figure C.6 The DSC melting endotherms for the samples produced while varying the pre-treatment time between the catalyst and cocatalyst. The pre-treatment time is indicated in minutes. ....	255
Figure C.7 The DSC crystallisation exotherms of the polymers produced at different temperatures at an Al:Ti = 20.....	256
Figure C.8 The DSC melting endotherms of the polymers produced at different temperatures at an Al:Ti = 20. ....	256
Figure C.9 The DSC crystallisation exotherms of the polymers produced at different temperatures at an Al:Ti = 80.....	257
Figure C.10 The DSC melting endotherms of the polymers produced at different temperatures at an Al:Ti = 80. ....	257
Figure C.11 The DSC crystallisation exotherms for the samples produced at different catalyst/cocatalyst ratios.....	258
Figure C.12 The DSC melting endotherms for the samples produced at different catalyst/cocatalyst ratios.....	258
Figure C.13 The DSC crystallisation exotherms for the samples produced at varying hydrogen pressures.....	259
Figure C.14 The DSC melting endotherms for the samples produced at varying hydrogen pressures.....	259
Figure C.15 The DSC crystallisation exotherms for the polymers produced using DPDMS at an Al:Ti=20 while varying the Si:Ti. ....	260
Figure C.16 The DSC melting endotherms for the polymers produced using DPDMS at an Al:Ti=20 while varying the Si:Ti. ....	260
Figure C.17 The DSC crystallisation exotherms for the polymers produced using DPDMS at an Al:Ti=40 while varying the Si:Ti. ....	261
Figure C.18 The DSC melting endotherms for the polymers produced using DPDMS at an Al:Ti=40 while varying the Si:Ti. ....	261
Figure C.19 The DSC crystallisation exotherms for the polymers produced using DPDMS at an Al:Ti=60 while varying the Si:Ti. ....	262
Figure C.20 The DSC melting endotherms for the polymers produced using DPDMS at an Al:Ti=60 while varying the Si:Ti. ....	262

Figure C.21 The DSC crystallisation exotherms for the polymers produced using DPDMS at an Al:Ti=80 while varying the Si:Ti. ....	263
Figure C.22 The DSC melting endotherms for the polymers produced using DPDMS at an Al:Ti=80 while varying the Si:Ti. ....	263
Figure C.23 The DSC crystallisation exotherms for the polymers produced using MPDMS at an Al:Ti=80 while varying the Si:Ti. ....	264
Figure C.24 The DSC melting endotherms for the polymers produced using MPDMS at an Al:Ti=80 while varying the Si:Ti. ....	264
Figure C.25 The DSC crystallisation exotherms for the polymers prepared to investigate repeatability using the DPDMS donor at an external donor/catalyst ratio of 4. ..	265
Figure C.26 The DSC melting endotherms for the polymers prepared to investigate repeatability using the DPDMS donor at an external donor/catalyst ratio of 4. ..	265
Figure C.27 The DSC crystallisation exotherms for the polymers prepared to investigate repeatability using the DPDMS donor at an external donor/catalyst ratio of 8. ..	266
Figure C.28 The DSC melting endotherms for the polymers prepared to investigate repeatability using the DPDMS donor at an external donor/catalyst ratio of 8. ..	266
Figure C.29 The DSC crystallisation exotherms for the polymers prepared to investigate repeatability using the DPDMS donor at an external donor/catalyst ratio of 16. ..	267
Figure C.30 The DSC melting endotherms for the polymers prepared to investigate repeatability using the DPDMS donor at an external donor/catalyst ratio of 16. ..	267
Figure C.31 The DSC crystallisation exotherms for the polymers prepared to investigate repeatability using the DPDMS donor at an external donor/catalyst ratio of 40. ..	268
Figure C.32 The DSC melting endotherms for the polymers prepared to investigate repeatability using the DPDMS donor at an external donor/catalyst ratio of 40. ..	268
Figure C.33 The DSC crystallisation exotherms for the polymers prepared to investigate repeatability using no external donor. ....	269
Figure C.34 The DSC melting endotherms for the polymers prepared to investigate repeatability using no external donor. ....	269
Figure C.35 The DSC crystallisation exotherms for the polymers prepared to investigate repeatability using the MPDMS donor at an external donor/catalyst ratio of 4... ..	270
Figure C.36 The DSC melting endotherms for the polymers prepared to investigate repeatability using the MPDMS donor at an external donor/catalyst ratio of 4... ..	270
Figure C.37 The DSC crystallisation exotherms for the polymers prepared to investigate repeatability using the MPDMS donor at an external donor/catalyst ratio of 8... ..	271

Figure C.38 The DSC melting endotherms for the polymers prepared to investigate repeatability using the MPDMS donor at an external donor/catalyst ratio of 8...	271
Figure C.39 The DSC crystallisation exotherms for the polymers prepared to investigate repeatability using the MPDMS donor at an external donor/catalyst ratio of 16.	272
Figure C.40 The DSC melting endotherms for the polymers prepared to investigate repeatability using the MPDMS donor at an external donor/catalyst ratio of 16.	272
Figure C.41 The DSC crystallisation exotherms for the polymers prepared to investigate repeatability using the MPDMS donor at an external donor/catalyst ratio of 40.	273
Figure C.42 The DSC melting endotherms for the polymers prepared to investigate repeatability using the MPDMS donor at an external donor/catalyst ratio of 40.	273
Figure C.43 The DSC crystallisation exotherms of the TREF fractions of sample DP-1.....	274
Figure C.44 The DSC melting endotherms of the TREF fractions of sample DP-1.....	274
Figure C.45 The DSC crystallisation exotherms of the TREF fractions of sample DP-2.....	275
Figure C.46 The DSC melting endotherms of the TREF fractions of sample DP-2.....	275
Figure C.47 The DSC crystallisation exotherms of the TREF fractions of sample DP-3.....	276
Figure C.48 The DSC melting endotherms of the TREF fractions of sample DP-3.....	276
Figure C.49 The DSC crystallisation exotherms of the TREF fractions of sample DP-4.....	277
Figure C.50 The DSC melting endotherms of the TREF fractions of sample DP-4.....	277
Figure C.51 The DSC crystallisation exotherms of the TREF fractions of sample No ED...	278
Figure C.52 The DSC melting endotherms of the TREF fractions of sample No ED.....	278
Figure C.53 The DSC crystallisation exotherms of the TREF fractions of sample MP-1.....	279
Figure C.54 The DSC melting endotherms of the TREF fractions of sample MP-1.....	279
Figure C.55 The DSC crystallisation exotherms of the TREF fractions of sample MP-2.....	280
Figure C.56 The DSC melting endotherms of the TREF fractions of sample MP-2.....	280
Figure C.57 The DSC crystallisation exotherms of the TREF fractions of sample MP-3.....	281
Figure C.58 The DSC melting endotherms of the TREF fractions of sample MP-3.....	281
Figure C.59 The DSC crystallisation exotherms of the TREF fractions of sample MP-4.....	282
Figure C.60 The DSC melting endotherms of the TREF fractions of sample MP-4.....	282
Figure C.61 The DSC crystallisation exotherm of the test sample.....	283
Figure C.62 The DSC melting endotherm of the test sample.....	283

## List of Tables

Table 3.1 The designation of the carbon atoms in the structure of the propylene-1-pentene copolymer.....	68
Table 3.2 The assignment of the pentad sequences in the methyl region of the PP homopolymer samples.....	68
Table 4.1 The data summary for the polypropylene homopolymer (PPH) and copolymer (PP1P).....	74
Table 6.1 A data summary of all samples with varying donor types and loadings.....	160
Table 6.2 A data summary of all the <sup>13</sup> C NMR data for the polymers.....	165
Table 6.3 The DSC results for all samples.....	167
Table 6.4 The results for the deconvolution of all samples .....	193
Table A.1 The HT-GPC data for the fractions of the TREF characterisation of the PP1P sample.....	233
Table A.2 The HT-GPC data for the PP1P samples with selected fractions removed .....	233
Table A.3 The HT-GPC data for the fractions of the TREF characterisation of the PPH sample .....	233
Table A.4 The HT-GPC data for the PPH samples with selected fractions removed.....	234
Table A.5 The HT-GPC data for the various polymerisations performed.....	234
Table A.6 The HT-GPC data of the TREF fractions of sample DP-1 .....	236
Table A.7 The HT-GPC data of the TREF fractions of sample DP-2 .....	236
Table A.8 The HT-GPC data of the TREF fractions of sample DP-3 .....	236
Table A.9 The HT-GPC data of the TREF fractions of sample DP-4 .....	237
Table A.10 The HT-GPC data of the TREF fractions of sample No ED.....	237
Table A.11 The HT-GPC data of the TREF fractions of sample MP-1.....	237
Table A.12 The HT-GPC data of the TREF fractions of sample MP-2.....	237
Table A.13 The HT-GPC data of the TREF fractions of sample MP-3.....	238
Table A.14 The HT-GPC data of the TREF fractions of sample MP-4.....	238
Table A.15 The HT-GPC data for the test sample .....	238

## List of Abbreviations

$\Delta H_f$	Enthalpy of fusion
$\Delta H_{fc}$	Enthalpy of fusion of ideal 100% crystalline polypropylene
$\Delta T$	Difference in temperature
$^{13}\text{C}$	Carbon thirteen
$\sigma_e$	Free surface energy
A-TREF	Analytical temperature rising elution fractionation
BHT	2,6-di- <i>tert</i> -butyl-4-methylphenol
BOPP	Biaxially oriented polypropylene
CEF	Crystallisation elution fractionation
CM%	Comonomer percentage
CRYSTAF	Crystallisation analysis fractionation
DGMBE	Diethylene-glycol-monobutylether
DIBP	Di- <i>iso</i> -butyl phthalate
DMA	Dynamic mechanical analysis
DMP	Dimethyl phthalate
DNBP	Di- <i>n</i> -butyl phthalate
DPDMS	Diphenyl dimethoxysilane
DSC	Differential scanning calorimetry
$E^*$	Complex modulus
$E'$	Storage modulus
$E''$	Loss modulus
EB	Ethylbenzoate
ED	External electron donor
EGMBE	Ethylene glycol monobutylether
ESR	Electron spin resonance
GC	Gas chromatography
GFC	Gel filtration chromatography
GPC	Gel permeation chromatography
HDPE	High density polyethylene
HT-GPC	High temperature gel permeation chromatography
ID	Internal electron donor
IR	Infra-red



$l_w$	Weight average lamellar thickness
LDPE	Low density polyethylene
$M_n$	Number average molar mass
MFR	Melt flow rate
MH	Microhardness
MPDMS	Methyl phenyl dimethoxysilane
$M_w$	Weight average molar mass
MMD	Molar mass distribution
NMR	Nuclear magnetic resonance spectroscopy
PD	Polydispersity
PP	Polypropylene
RI	Refractive index
SCALLS	Solution crystallisation analysis by laser light scattering
SEC	Size exclusion chromatography
Tan	Tangent
$T_c$	Crystallisation temperature
TCB	Trichlorobenzene
TCE	Tetrachloroethylene
$T_e$	Elution temperature
TEA	Triethylaluminium
TFA	Turbidity fractionation analysis
$T_g$	Glass transition temperature
$T_m$	Melting temperature
TREF	Temperature rising elution fractionation
USA	United States of America
WAXD	Wide-angle x-ray diffraction
$W_i$	Weight fraction
$W_i\%$	Weight fraction percentage

# Chapter 1. Introduction

## 1.1 General introduction

Polypropylene as a commodity is currently very well known throughout the world as an extremely versatile material with a diverse spectrum of applications. The material has been successful in capturing a large portion of a number of markets due to the excellent properties of the material such as a high melting point (above 160 °C), good stiffness, hardness, and excellent chemical resistance, allowing its use in applications such as car batteries [1]. One weakness of the polypropylene homopolymer has been its low temperature impact strength which is due to the fact that it has a glass transition temperature ( $T_g$ ) range in the region of 0 °C, although this varies according to the characteristics of the polymer.

The spectrum of properties of the material has been significantly broadened by the introduction of comonomers, such as ethylene and butene, to the polymer. A variety of catalyst compositions are available which distribute these comonomers in different ways throughout the polymer chains, producing materials with different properties. The most important property change as a result of the introduction of a comonomer is a reduction in crystallinity of the material. The formation of reactor alloys has also been accomplished with the production of the so-called impact copolymers where the homopolymer is essentially produced along with an ethylene-propylene random copolymer in a multi reactor system, producing a material with greatly improved impact properties.

As far as the homopolymer is concerned, the importance of the hardness and impact strength cannot be underestimated as these are vital properties for a given application. Generally an increase in the hardness of a material comes at the expense of the impact strength and as such a balance must be struck between the two properties. This justifies extensive research in this area since knowledge of the exact reasons behind the physical properties, facilitates the tailoring of the physical properties and improved property development for specific applications.

It is possible to tailor the polymer properties after the polymerisation as evidenced by the production of controlled rheology grades of polypropylene, produced by the chemical vis-breaking of the material by peroxides, resulting in lower molar mass polymer with a narrower polydispersity [2]. However, the most important factor determining the microstructure of the polymers, and thus the polymer properties, is the way in which the chains are originally

polymerised. The production of reactor grades capable of being used for a certain application negates the use of post-production methods to alter the properties of the material.

The most important property of the catalyst is the nature of the active sites on the catalyst, since it is the nature and proportion of the types of sites present which determines the exact types of chains produced. Ziegler-Natta catalysts are extremely regiospecific by nature and thus the main types of defects incorporated into the chains during the polymerisation are stereo-errors, making this the most important factor affecting polymer properties [3]. The molar mass of the chains is also an extremely important factor. The molar mass of the chains produced at the more stereospecific sites is generally higher than the molar mass of material produced at the less stereospecific sites [4, 5].

It is, therefore, the stereospecificity of the active sites which is the dominant factor determining the overall properties of the polymers produced. The stereospecificity of the active sites is mainly controlled by the use of Lewis bases which act as electron donors, coordinating to the catalyst in the vicinity of the active sites thereby altering the chemical environment of the active sites. The chemical environment in turn dictates the manner in which the monomer coordinates and is inserted into the chains at the active sites, thus controlling the stereospecificity of the sites. The degree to which the active sites are controlled thus has an important bearing on the nature of the chains produced during the polymerisation. Heterogeneous catalysts are known to be comprised of a number of different active sites present on the same catalyst; therefore the proportion of the different types of active sites is also extremely important in determining the overall characteristics of the polymer produced.

In terms of the methodology used for this study, it was decided that a two pronged method should be used in order to determine the relationships between the various active site types, the polymer microstructure, and the physical properties of the polymers. On the one hand the composition of a polymer could be changed, and thus its properties altered, via the physical removal of certain fractions of the material using the temperature rising elution fractionation technique (TREF). On the other hand the composition of a polymer could be changed via chemical modification of the active sites responsible for the polymerisation. The physical removal of fractions, with subsequent recombination of the residual material, would give an important indication which fractions were the most important in terms of being responsible for the overall properties of the polymer. The chemical modification of the active sites on the catalyst provides a means to bring about similar changes in the composition of the material in the reactor, thereby altering the properties of the polymer.

## 1.2 Objectives

The overall objective of this study is, therefore, an investigation into the structure-property relationships of the polypropylene homopolymer, with specific attention given to the effect of the molecular characteristics on the hardness-impact balance and an evaluation of the more important fractions of the polymer for polymer properties. This also entails evaluation of the active sites of the catalyst responsible for the production of the chains. There are, however, a number of other important objectives which are also investigated during the course of the study which assist in the investigation of the main objective and as such are mentioned here.

Initially the methodology of selective fraction removal is investigated via the use of a propylene-1-pentene random copolymer, since the molecular heterogeneity of these materials should result in large differences in polymer properties upon removal of fractions. The methodology used is then to be applied to a Ziegler-Natta catalysed polypropylene homopolymer in order to evaluate the relative importance of its TREF fractions on polymer properties.

The chemical modification of the active sites is also to be studied. Initially the effect of various polymerisation conditions on the catalyst system will be investigated, varying conditions such as the cocatalyst/catalyst pre-treatment time, polymerisation temperature, cocatalyst/catalyst ratio, monomer pressure, hydrogen pressure, and external electron donor/catalyst ratio.

A few specific reactions will be undertaken in order to perform in-depth analysis on the polymers produced. To this end the chemical environment of the active sites is to be altered via the use of external electron donors at various external donor/catalyst ratios. The type of external donor shall also be varied in order to provide another means to alter the properties of the polymer produced. Polymer will also be produced with the same catalyst system in the absence of external electron donor so that larger differences in properties can be investigated. Thus the effect of smaller and larger differences in the chemical environment of the active sites will be investigated in order to tailor the properties of the polymers produced. These polymers will be used to evaluate the effect of polymer microstructure on the properties of polypropylene such as the microhardness, modulus, and damping ability of the polymer. The importance of specific fractions of the polymer will also be investigated.

The molar mass distributions of the polymers will also be deconvoluted as a means to evaluate the number of different active sites on the catalyst, and also as an additional means to

investigate the differences in the proportions of the active sites and the molar mass of the polymers produced at the sites, upon variation of the reaction conditions.

The effects of the physical removal of fractions shall also be correlated with the chemical alteration of the active sites in order to demonstrate the feasibility of the technique used.

### 1.3 References

1. Del Duca, D., & Moore, E.P, Jr., *End-use properties*, in *Polypropylene Handbook*, E.P. Moore, Jr., Editor. 2002, Hanser: Munich. p. 237-254.
2. Lieberman, R., *Propylene polymers*, in *Encyclopedia of polymer science and technology*, Mark, H., Editor. 2003, John Wiley & Sons: Hoboken.
3. Albizzati, E., Giannini, U., Collina, G., Noristi, L., & Resconi, L., *Catalysts and polymerizations*, in *Polypropylene handbook*, E.P. Moore, Jr., Editor. 2002, Hanser: Munich. p. 11-111.
4. Chadwick, J.C., Morini, G., Balbontin, G., Camurati, I., Heere, J.J.R., Mingozi, I., Testoni, F., *Effects of internal and external donors on the regio and stereoselectivity of active species in MgCl<sub>2</sub>-supported catalysts for propene polymerization*. *Macromolecular Chemistry and Physics*, 2001. **202**: p. 1995-2002.
5. Chadwick, J.C., van Kessel, G.M.M., & Sudmeijer, O., *Regio- and stereospecificity in propene polymerization with MgCl<sub>2</sub>-supported Ziegler-Natta catalysts: Effects of hydrogen and the external donor*. *Macromolecular Chemistry and Physics*, 1995. **196**: p. 1431-1437.

## Chapter 2 Historical background

### 2.1 Polyolefins: A brief historical overview

#### 2.1.1 The first steps

There were few people in the first half of the 20<sup>th</sup> century who would have thought that the phenomenon which has come to be known as plastic would play such a large role in the everyday life of just about every human being on the planet by the turn of the century. The idea of a polymer is actually far older than one might think, with J. Berzelius having used the term polymeric as early as 1832 [1]. Propylene was actually reported to have been polymerised as early as 1869 by M. Berthelot through a reaction with concentrated sulphuric acid [1]. The product, a viscous oil, was of little use however. Much early work was done by the likes of Goryainov and Butlerov who managed to polymerise pentene, propylene, and isobutylene by the addition of trace amounts of boron trifluoride [1]. Their attempts to polymerise ethylene however failed. It was Butlerov who actually first used the term “polypropylen” in 1876.

Polymerisations of ethylene were also attempted in the 19<sup>th</sup> century with H. von Peckman [2] managing to polymerise small amounts of ethylene to low molar mass by the decomposition of diazomethane, reported in 1898, as illustrated in equation 1.



Soon after this discovery Bamberger and Tschirner [2] managed to produce larger quantities of this material which was given the name “polymethylene”. The decomposition of diazomethane was found to be catalysed by boron compounds, which enabled the complete decomposition of diazomethane into polymethylene and nitrogen [3].

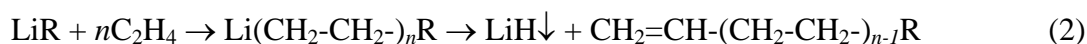
During the first half of the 20<sup>th</sup> century ethylene was polymerised in the presence of diethylmercury [4] and also by the condensation of decamethylene bromine [5]. The Fischer-Tropsch reduction of carbon monoxide with hydrogen was also used by, among others, Koch and Ibing [6], and generally produced low molar mass material although this could be altered by the reaction conditions in order to produce crystalline paraffins [2].

The first commercial polyolefin was low density polyethylene (LDPE) which was first reported in 1933 when Fawcett and Gibson at Imperial Chemical Industries (ICI), used high pressures to try and condense ethylene and benzaldehyde at 200 °C [7]. Due to technical difficulties, such as the high pressures needed and the control required for the highly exothermic reaction, the first plant for commercial production of LDPE was only ready in 1939 [2]. This material was mainly used during the war as insulation for cables used in radar applications [2].

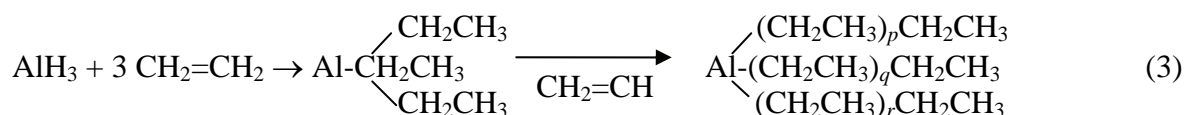
The development of LDPE sparked renewed interest in the more linear form of the polymer, namely high density polyethylene (HDPE). Very high pressures were used by Larson and Krase [8] in order to produce linear polyethylene. In 1943 Bailey and Reid of Phillips Petroleum Company passed ethylene over a nickel oxide catalyst on an aluminium/silica support and managed to produce oligomers. Their colleagues, Hogan and Banks, altered this recipe slightly and passed the ethylene over a chromium salt on an aluminium/silica support and obtained HDPE [9]. This became the dominant method for the production of HDPE worldwide. By the middle of the 20<sup>th</sup> century crystalline polyethylene was known to the world to some extent, however, crystalline polypropylene had not yet been discovered. Advances in this field were soon to come through the groundbreaking research taking place in the laboratories of K. Ziegler and G. Natta.

### **2.1.2 The origins of the Ziegler-Natta catalyst**

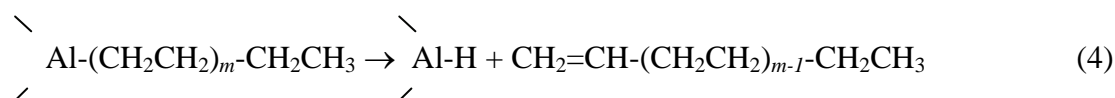
One of the first steps on the road to the discovery of what are commonly known today as the Ziegler-Natta catalysts was made in 1930 when C. Marvel and M. Frederick accidentally polymerised ethylene in the presence of butyllithium and tetraethylarsenium bromide. Ziegler and co-workers followed this up with investigations of alkali metal alkyls and their polymerisation of conjugated dienes [10-12]. In 1937 Hall and Nash used aluminium chloride as a catalyst in ethylene polymerisation and noticed that alkyl aluminium was produced during the reaction [13]. This development eventually led to the production of polyethylene in the presence of aluminium chloride and titanium tetrachloride which was patented by Fischer in 1953 [14]. The lithium alkyls were further investigated by Ziegler who noticed that they could not polymerise to high molar mass due to premature termination of the chain and precipitation of lithium hydride (see equation 2).



Due to the limited solubility of the lithium hydride Ziegler decided to replace it with the more soluble lithium-aluminium hydride which was found to react with ethylene to form  $\text{LiAlEt}_4$  [15]. This led to the discovery that the triethylaluminium (TEA) was more efficient for ethylene polymerisation and enabled the further investigation of the metal alkyl and metal alkyl hydride equilibrium. The process by which Ziegler called the polymerisation of higher molar mass homologues of ethylene in the presence of triethylaluminium was the “Aufbau” reaction as illustrated in equation 3 and involved the insertion of ethylene units into an Al-C bond without the formation of a branch.



Molar masses ( $M_w$ ) in the order of 3000 to 30 000 g/mol were claimed [16]. A displacement reaction prevented the formation of high molar mass material (equation 4).



The discovery of 1-butene during a reaction of ethylene and triethylaluminium was initially a cause for concern as it appeared that the reaction had not worked. What actually happened was crucial to further development work. The displacement reaction had been catalysed by colloidal nickel originating from a previous hydrogenation experiment in the reactor. A systematic investigation followed in order to determine if any other metals affected the polymerisation in a similar way since if one metal could slow down a reaction perhaps there were others which would speed it up. The breakthrough came when HDPE was polymerised in the presence of zirconium acetylacetonate at low pressures [17]. It was discovered that the most active catalyst was made from titanium tetrachloride and triethylaluminium. This was developed for the manufacture of HDPE on a large scale (although most HDPE was eventually made by the Phillips catalyst process) and designated by Ziegler as the “Mulheim Atmospheric Polyethylene Process”.



### 2.1.3 The development of stereoregular polymerisation

At this stage in the development of the polyolefin industry very little was known about the stereoregularity of polymer chains. Indeed it was only during the 1940's that a stereoregular polymer was first observed which had originated from an asymmetric monomer (cis-1,4 isoprene), namely natural rubber [18]. Crystalline polyethylene (PE) was at least partially understood while crystalline polypropylene (PP) had never been observed and all propylene polymerisations at this time had resulted in low molar mass amorphous oils. There were two important discoveries in the late 1940's which showed that stereoregular polymerisation was possible for vinyl and diene monomers. The first discovery by Morton [19] was that a mixture of allyl sodium, sodium isopropoxide, and sodium chloride polymerised butadiene to a *trans*-1,4-polymer. The second development by Schildknecht was the stereoregular polymerisation of a vinyl monomer using vinyl isobutyl ether and  $\text{BF}_3$  etherates in a propane solvent at  $-78\text{ }^\circ\text{C}$  [20, 21]. These steps demonstrated that stereoregular polymerisation was indeed possible.

After developing the Mulheim Atmospheric Polyethylene Process, Ziegler revealed his findings to Montecatini Company (Italy) and Goodrich-Gulf Chemical Company (USA). Giulio Natta, then a consultant for Montecatini, undertook to investigate this new catalyst system [16] and placed three of his assistants in Ziegler's laboratory [1]. In 1954 Natta, working with the Mulheim catalyst, managed to produce a mixture of amorphous and crystalline material. After attempting the reaction with other titanium chlorides such as  $\alpha\text{TiCl}_3$  he managed to produce far more crystalline material which was established to have long sequences of monomeric units having the same configuration.

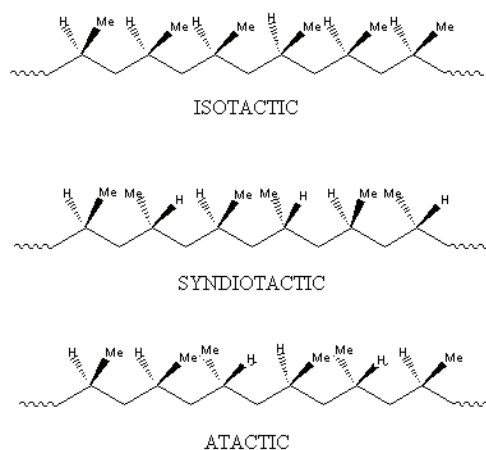


Figure 2.1 The different stereo-conformations of polypropylene.

The polypropylene which was produced had different stereo conformations, the nomenclature of which was actually suggested by Natta's wife. The different stereo configurations of polypropylene were designated as isotactic, syndiotactic, and atactic, and are illustrated in Figure 1.1. Natta applied for a U.S. patent which was assigned to Montecatini. From this point on there were many developments as the new catalyst system was put through its paces, Natta and co-workers alone contributing over 170 reports over the following few years [1]. The polymerisation of stereoregular polymers has enabled the development of a broad range of polymers with different properties, helping the commodity to reach a very strong position in global markets.

## 2.2 Ziegler-Natta catalysts

A Ziegler-Natta catalyst can be defined as a transition metal compound which has a metal-carbon bond that is capable of the repeated insertion of olefin units. The catalyst system used for Ziegler-Natta polymerisations usually consists of the catalyst itself, which is a transition metal salt, and an activator or cocatalyst, which is a main group metal alkyl that generates the active metal-carbon bond. The catalyst as we know it today was not created overnight and it is only after countless hours of investigation by many researchers that the current level of development has been reached.

### 2.2.1 The development of the Ziegler-Natta catalysts

Since the early work of Ziegler and Natta the catalyst has continuously evolved, various improvements having been made over the years.

During the development of the first generation of Ziegler-Natta catalysts the various crystal modifications of  $\text{TiCl}_3$  were investigated, some of which also contained co-crystallised  $\text{AlCl}_3$  or  $\text{AlRCl}_2$ . The various crystal modifications were designated as  $\alpha$ ,  $\gamma$ , and  $\delta$  (violet in colour), and the  $\beta$ -form (brown). The  $\alpha$ -form exhibits hexagonal Cl packing, while the  $\gamma$ -form has cubic packing [22]. The  $\delta$ -form consists of random hexagonal and cubic close packing, while the  $\beta$ -form on the other hand is of a more fibre-like structure [23]. The  $\text{Ti}^{3+}$  coordination is octahedral in all modifications.

These catalysts were prepared by reduction of  $\text{TiCl}_4$  with either aluminium metal or aluminium alkyls. Those reduced by aluminium metal were usually ball-milled in order to

convert the  $\alpha$ - or  $\gamma$ -forms into the more active  $\delta$ -form, and also to reduce the crystallite size thereby increasing the surface area of the catalyst [24]. Reduction by aluminium alkyls has the advantage that if the reaction conditions are carefully controlled then catalysts particles can be formed with a certain shape and a narrow particle size distribution [22].

The most important factors affecting the polymerisations with this type of catalyst were the crystal modification type and the cocatalyst, although the extent of milling and the presence of co-crystallised  $\text{AlCl}_3$  also played a role. Generally the  $\alpha$ ,  $\gamma$ , and  $\delta$ -forms produced material of similar isotacticity while the  $\beta$ -form produced material of significantly lower isotacticity [25, 26]. Co-crystallisation of  $\text{AlCl}_3$  was found to generally decrease the molar mass and slightly broaden the molar mass distribution (MMD). The stereospecificity was not significantly altered although an increase in activity was observed [27]. TEA and diethylaluminium chloride (DEAC) as co-catalysts were found to lead to the most active catalysts. These catalysts are often referred to as AA- $\text{TiCl}_3$  catalysts (aluminium reduced and activated). Removal of catalyst residues (de-ashing) was required however as the activity was not high enough at this stage.

Further developments led to the next generation of catalysts which from a structural viewpoint were characterised by a smaller crystallite size and a much increased surface area. They also contained far less co-crystallised  $\text{AlCl}_3$  and  $\text{AlRCl}_2$ . These advances were mainly reached due to different reduction methods. As much of the development work was done by Solvay [28], these catalysts are often referred to as “Solvay”  $\text{TiCl}_3$  although the term “low-Al” catalysts has also been used [22]. The catalyst shape was claimed to be nearly spherical and to consist of many smaller sub-particles of very small crystallites (50 – 100 Å). Compared to the earlier AA- $\text{TiCl}_3$  catalysts the productivity (12-15 kg PP/g catalyst) and isotacticity ( $\cong 98\%$ ) of these Solvay type catalysts were considerably improved and much better polymer morphology was obtained. Lewis bases were also incorporated into the catalyst recipe at this time and a number of different compounds such as esters, ethers, amides, amines and ketones were experimented with. An increase in stereospecificity was obtained using the Lewis bases and activities were high, however, catalyst residues were still too high, leading to poor quality of products. Solvay used di-isoamyl ether successfully as an electron donor and reported it in 1973 [28].

The next step in the evolution of the Ziegler-Natta type catalysts was the use of a support on which to site the catalyst. Initial work on conventional supports bearing surface functional groups yielded mixed results with some being highly active for ethylene

polymerisation, however, the lower activity of propylene meant that these supports did not work for propylene polymerisations. It was eventually discovered [29] that  $\text{MgCl}_2$  could be used as a very effective support for the catalyst for both ethylene and propylene polymerisation. This group of catalysts became known as the third generation of Ziegler-Natta catalysts and the use of a support became an integral part of further development in the field. The main problem with the original supported catalysts was the low isotacticity (<50%) of the polymer produced as a result of the limited applicability of the early types of Lewis base to the supported catalysts. This led to the investigation of other types of Lewis base more suited to use with a supported catalyst.

The Lewis bases are also often referred to as electron donors and can be separated into two categories, namely the internal donors (ID) which are added during catalyst preparation, and the external electron donors (ED) which are added together with the cocatalyst during the polymerisation. Initially the most common compounds used as electron donors were the aromatic monoesters such as ethylbenzoate (EB), methyl-*p*-toluate, and *p*-ethoxy-ethylbenzoate. If a monoester was employed as internal donor then the best external donor to be used in conjunction with it were also monoesters. The most common monoester used by far being ethylbenzoate. Atactic material removal was, however, still necessary as this still constituted as much as 10% of the material produced.

The three main routes to the incorporation of the electron donors were mechanical, mechanical and chemical, and chemical [22]. Mechanical processes involved the ball milling of the  $\text{MgCl}_2$  support,  $\text{TiCl}_4$ , and an internal donor to form the catalyst. A combination of mechanical and chemical processed involved the milling of the support with the Lewis base followed by treatment with  $\text{TiCl}_4$  in a suitable solvent. Purely chemical routes involve processes such as reaction of the support with a Lewis base to form a complex which is then treated with the internal donor and excess  $\text{TiCl}_4$  and subsequently washed several times. The chemical routes have proved to be the most preferred ones in the later stages of supported catalyst development.

The introduction of the new types of Lewis base, more suited to polymerisations using a supported catalyst, heralded a new era for the production of polyolefins and improvements were soon to be made in the type of compounds used as electron donors. The fourth generation of catalysts utilised diesters, such as diisobutyl phthalate, as internal donors along with alkoxysilanes as external donors. These catalysts are the most common in today's industrial processes due to their improved activity/isotacticity balance. A relatively new development in terms of the Ziegler-Natta catalyst has been the discovery that hindered 1,3-

diethers can be used as internal donors during catalyst preparation and that these catalysts do not require an external donor to be added with the cocatalyst during the polymerisation in order to obtain highly active and stereospecific catalysts [30].

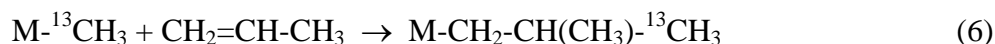
## 2.2.2 Polymerisation chemistry

### 2.2.2.1 General mechanism of polymerisation

A Ziegler-Natta catalyst can be defined as a transition metal compound incorporating a metal-carbon bond which is able to perform the repeated insertion of olefin units [22]. The active centres of Ziegler-Natta catalysts are basically formed due to interaction between a transition metal compound and an organometallic cocatalyst [31, 32]. The most common cocatalysts which have been used in recent times are TEA, DEAC, and tri-isobutylaluminium (TIBA) although the aluminium-alkyl-chlorides usually offer poorer performance and are usually used in conjunction with the aluminium-tri-alkyls [22]. The exchange of a halogen atom from the transition metal compound and an alkyl group from the organometallic cocatalyst is a critical step in the formation of the active centre [16, 31], as illustrated in equation 5 for a  $\text{TiCl}_3/\text{AlEt}_3$  system:



The most important factor regarding the bond between the transition metal atom and the carbon atom is that it has the ability to react with the double bonds of  $\alpha$ -olefins [31]. The insertion mechanism has been proven by the presence of isobutyl chain-end groups formed in the first step of the polymerisation reaction using  $^{13}\text{C}$ -enriched  $\text{Al}(\text{CH}_3)_3$  [33]:



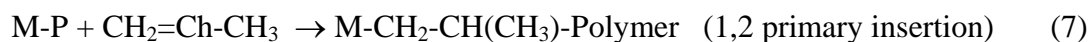
A great number of different models have been proposed with regards to the polymerisation mechanism. Bimetallic models proposed by Patat and Sinn [34], and Natta and Mazzanti [35], were furthered by Rodriguez and van Looy [36] and consist of a ligand, such as a chlorine or alkyl group, and the last carbon atom of the growing chain linking the

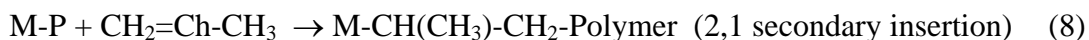
aluminium and titanium through a double bridge. Steric interactions between the metal alkyl and complexed olefin were given as the source of stereoregularity.

There are also a number of monometallic mechanisms such as the trigger mechanism was proposed by Ystenes [37] involving a pseudo-seven coordinated complex in the transition state and two monomer molecules which interact with each other. One monomer molecule is always coordinated to the metal of the active site and is only inserted when another monomer molecule arrives to trigger the insertion. By far the most widely accepted model to date has been that of Cossee [38] and Arlman [39]. Their model consists of two main steps, the first being coordination of the incoming monomer unit at a vacant octahedral coordination site with the double bond of the monomer parallel to the metal-carbon bond. The second step is chain migratory insertion of the monomer unit between the metal atom of the catalyst and the last carbon atom of the growing chain. This takes place via a four-member transition state consisting of the metal atom, the two carbons of the monomer unit and the last carbon of the growing chain. According to the model of Brookhart and Green [40] and theoretical studies by Cavallo *et al.* [41] and Boero *et al.* [42] the insertion is strongly assisted by  $\alpha$ -agostic interactions between the metal atom and the C-H bond of the growing chain. After the insertion the growing chain migrates back to its original position thus preserving the stereoselectivity of the active site.

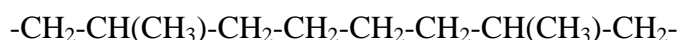
Non-bonded interactions, between the incoming propylene monomer and the  $\beta$ -carbon of the growing chain, have proved to be extremely important in determining the preferential enantioface coordination of the monomer. The methyl group of the coordinating propylene monomer unit lies on the other side of the plane defined by the metal carbon bond and the monomer units' own double bond. This has been shown due to fact that insertion into a Ti-CH<sub>3</sub> bond is not stereospecific, while insertion into a Ti-CH<sub>2</sub>-CH<sub>3</sub> bond is partially stereospecific [43, 44]. If the size of the alkyl group is increased (for example to an isobutyl group) then the insertion is stereospecific. It is therefore clear that the growing chain plays an extremely important role in determining the stereoregularity of the polymer chains produced from a prochiral monomer such as propylene.

The insertion of the  $\alpha$ -olefin into the metal-carbon bond can occur in two different ways [22]:





where P represents the polymer chain. This defines the regiochemistry of the polymer formed. Heterogeneous catalysts have extremely high regiospecificity, resulting in mainly 1,2 insertions [22]. The polymer chain is then grown through the repeated insertions of the monomer units. Secondary insertions can either be followed by a primary insertion, leading to vicinal methyl groups, or by isomerisation of the secondary inserted unit, resulting in 1,3 insertion of the monomer [45]. The 1,3 insertions result in the following structure [46]:

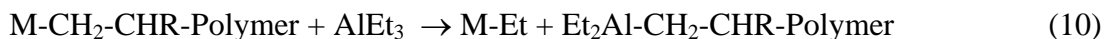


The isomerisation is favoured by a higher polymerisation temperature [45].

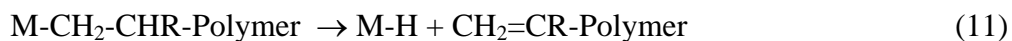
Eventually each growing polymer chain is disengaged from the transition metal atom. There are a number of ways in which this chain termination occurs. The first method of chain termination is chain transfer to monomer [31]. This is the most important chain termination process for the polymerisation of propylene with heterogeneous catalysts (in the absence of hydrogen) [22, 32, 41]. It involves the replacement of a long alkyl chain at the transition metal atom with a short alkyl group derived from the monomer as illustrated in equation 9:



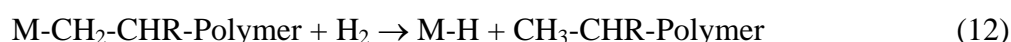
A second reaction which can occur is the alkyl group transfer between the active centre and the organometallic cocatalyst as illustrated in equation 10:



The Al-C bond decomposes on exposure to air and moisture, leaving a polymer molecule [31]. The third way in which termination occurs is by means of a  $\beta$ -hydride elimination (Equation 11), although this process is not considered important in propylene polymerisation with heterogeneous catalyst systems at normal polymerisation temperatures [22]:



Equation 11 does however become a significant chain termination reaction in metallocene-based catalyst systems [22]. There is also the  $\beta$ -methyl elimination method of chain termination, although this process has never been observed during the polymerisation of propylene with heterogeneous catalyst systems [22]. It is, however, important during homogeneous polymerisations. The chain termination reactions occur very infrequently compared to the chain growth reactions [31]. In order to limit the molar mass of the polymer formed, hydrogen is usually introduced to terminate a growing chain according to the so-called chain transfer to hydrogen reaction [47], as illustrated in equation 12:



The chain transfer to hydrogen reaction is the most commercially important method of controlling the molar mass [31].

During the course of a polymerisation the catalyst also undergoes an ageing process and there is a point during the polymerisation where the catalyst is at its most active. After this point has been reached the catalyst begins to decay and productivity decreases. This is due to the over-reduction of the Ti species. The active species for propylene polymerisation is Ti(III). Reduction of Ti(IV) is required to produce Ti(III), however, should the Ti species become over-reduced by the cocatalysts to Ti(II) then that particular site would not be active for propylene polymerisation [48].

### 2.2.2.2 Polymerisation control mechanisms and stereochemistry

One of the most important factors governing the applications of polypropylene is the isotacticity of the material. In order to produce highly crystalline polypropylene the isotacticity of the polymer chains must be very high. Therefore, when one is looking at the perfection of the order of the polymer chains one must consider the stereoregularity of the chains as well as the regioregularity of the insertions. The critical time for the determination of the stereospecificity is during the coordination of the incoming monomer unit to the metal atom during the formation of the four-member transition state. Regioselectivity of the Ziegler-Natta catalysts is generally much better than that of the metallocene catalysts [22, 31]. The majority of the monomer units will therefore be inserted in the primary (1,2) insertion mode during polymerisation with heterogeneous catalysts. The coordination of the enantioface is, however, still an issue for these types of catalysts and a lack of configurational regularity



would result in an atactic polymer with few uses. Multiple insertions of the same enantioface are therefore required for the formation of isotactic polymer.

Two possibilities exist for governing the selection of the enantioface [22]. The first involves control by the chiral induction of the last inserted unit and is referred to as chain-end control. The second possibility is the asymmetry of the initiating site and this is known as enantiomorphic site control. The differences in the polymerisations with the different control mechanisms are illustrated in Figure 2.2.

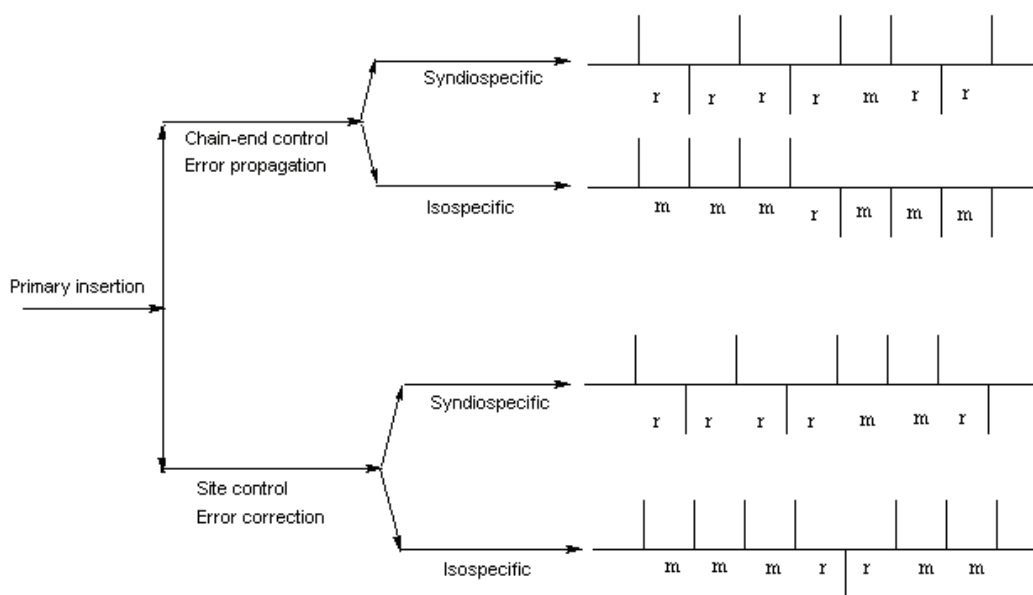


**Figure 2.2** An illustration of the different types sequence distributions, and the control mechanisms which cause the formation of the sequences in heterogeneous catalysts.

The different types of propagation errors that can occur during the polymerisations can be identified using  $^{13}\text{C}$  nuclear magnetic resonance (NMR) spectroscopy (this will be discussed further in Chapter 3). It has been proven via  $^{13}\text{C}$  NMR that the general mechanism for the isospecific polymerisation of propylene with Ziegler-Natta catalysts is enantiomorphic site control. This was achieved by end-group analysis of isotactic polybutene obtained with  $\text{TiCl}_3$  and  $\text{AlEt}_3$  enriched with  $^{13}\text{C}$  at the methylene carbons. The end groups resulting from the first and second monomer insertions during this polymerisation are stereoregular despite the absence of asymmetry in the original ethyl group and alkyl group after first monomer insertion [43, 49]. It is therefore possible to get an idea of the stereoselectivity and regioselectivity of the catalyst through examination of the material produced.

A secondary insertion often leads to a dormant active site as opposed to incorporation of the defect into the chain. Incorporation of the defect into the chain can occur, however, in

the presence of hydrogen, chain transfer to hydrogen almost always takes place [50]. This can have the effect of actually increasing the average isotacticity of the polymer chains as less defects are incorporated into the chains so that the average isotacticity actually increases with increasing hydrogen content [50, 51].

The nature of the active sites on the catalyst is therefore critical in determining the type of polymer chains that are produced by a given catalyst system. This in turn determines the end-use properties of the polymer. A more in depth discussion on the nature of the active sites of Ziegler-Natta catalysts is therefore required in order to understand as comprehensively as possible what effect small changes in catalyst composition will have on the active sites.

### **2.2.2.3 Catalyst active sites: The support**

Although other supports have been used with varying degrees of success, it is  $\text{MgCl}_2$  which has dominated the scene with regards to supported Ziegler-Natta catalysts. This has been due to the unprecedented level of activity and stereospecificity obtained while using this material as a support. There are actually two crystalline modifications of the  $\text{MgCl}_2$  crystal, namely the  $\alpha$ - and  $\beta$ -forms, although the  $\beta$ -form is less stable and so it is the  $\alpha$ -form which is used commercially [22]. The  $\alpha$ -form consists of a cubic-close packing structure of double chlorine layers with interstitial  $\text{Mg}^{2+}$  ions in a sixfold coordination. The actual form of the crystal which are used during the Ziegler-Natta polymerisation is a disordered structure resulting from the translation and rotation of the  $\text{MgCl}_2$  layers with respect to one another in the stacking direction [52] and this is often referred to as activated or  $\delta$ - $\text{MgCl}_2$ . The actual activated support used during the polymerisations can be seen as an agglomeration of smaller crystallites which have exposed lateral surfaces with  $\text{Mg}^{2+}$  ions with different levels of unsaturation and steric hindrance [22].

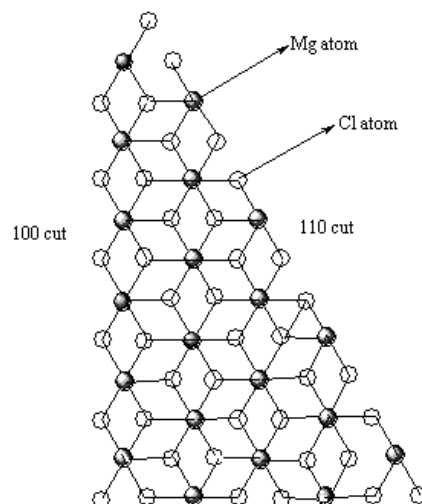


**Figure 2.3 The lateral cuts of the MgCl<sub>2</sub> crystal.**

It had originally been determined experimentally by Giannini [52] that the preferential lateral cuts of the MgCl<sub>2</sub> crystal correspond to the (100) and (110) cuts. These lateral cuts contain coordinatively unsaturated Mg<sup>2+</sup> ions with coordination number 4 on the (110) cut and 5 on the (100) cut as illustrated in Figure 2.3. However, there has been some confusion regarding the assignment of the Miller indexes to the lateral cut with coordination number 5, which was originally assigned the (100) index. Recent studies by Mori [53] and Boero [54] classified this lateral cut as (104) according to the International Tables for Crystallography [55]. This was confirmed by Busico [56] who traced the disagreement to the size of the crystals used to determine the lateral cuts, (100) being accurate for single structural layers while (104) is more accurate for whole MgCl<sub>2</sub> crystals. Since most references have referred to the (100) surface as such, the following discussions will still use this assignment if it is used in a given reference although (104) is actually the correct index and this will be used for general discussion.

Recent work by Andoni *et al.* [57-60], utilising the Ostwald ripening process to increase the size of the MgCl<sub>2</sub> crystals so that they can be observed via AFM and SEM, has shown that MgCl<sub>2</sub> crystals consist of two main lateral cuts with 90° and 120° edge angles. They also showed that polymerisation occurs on these lateral cuts and not on the basal (001) plane of the crystals and concluded that the 90° and 120° lateral cuts referred to the (104) and (110) respectively [60].

### 2.2.2.4 Catalyst active sites: Titanium – support complex formation

During the preparation of the catalyst there must be some degree of coordination of the Ti species to the support. There have been a number of investigations into the manner in which this takes place. Carr-Parrinello investigations of the interaction between mononuclear and dinuclear Ti-species were performed by Boero *et al.* [54]. They observed that the (100) or (104) surface is not able to carry out the polymerisation process efficiently and that the Ti-species can coordinate only in dinuclear configuration. The dinuclear configuration of Ti species was also possible on the (110) surface, however, this was shown to destabilise as well during the polymerisation process. The mononuclear configuration was however a stable active site on the (110) surface, although it was unstable on the (100) surface. Different coordination modes on the different surfaces are illustrated in Figure 2.4.

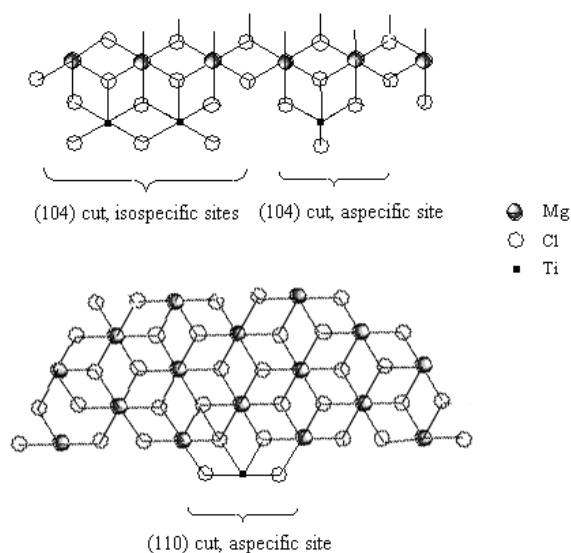


**Figure 2.4 Catalyst active sites on (104) and (110) cuts of the  $\text{MgCl}_2$  crystal.**

Research by Monaco *et al.* [61] supports these results in that their DFT calculations also show that monomeric  $\text{TiCl}_4$  and  $\text{TiCl}_3$  coordination is favoured on the (110) surface. Dinuclear coordination of  $\text{TiCl}_3$  fragments were found to be able to coordinate to the (100) surface. Brambilla *et al.* [62] also showed via Raman spectroscopy that a  $\text{MgCl}_2\text{-TiCl}_4$  complex is formed with Ti atoms in an octahedral coordination. As can be seen from Figure 2.4 the coordination mode of the Ti species is critical in determining the stereoregulating ability of the active site. An isolated Ti atom on the (110) cut would produce atactic material in the absence of a donor while if two donors were bridge-coordinated on either side of the Ti

atom then isotactic material would be produced [63]. The dimeric Ti species on the (104) surface produces isospecific active sites [64], while the monomeric species on (104) produces aspecific active sites. The chiral dimeric species on (104) being the only stereoregulating active site in the absence of electron donors [64]. This is the reason why electron donors have developed into such a vital part of the catalyst system since it is through direct competition with the Ti species that the internal electron donors coordinate to the support and in doing so impose certain configurations of the Ti species on the surfaces.

#### **2.2.2.5 Catalyst active sites: The internal electron donor**

Due to the fact that electron donors play such a large role in the usefulness of a catalyst a great amount of research has been dedicated to this field over the last couple of decades. The internal donors are added during catalyst preparation and thus compete with  $\text{TiCl}_4$  for coordination sites on the support [65]. There have been a number of different types of compounds [16] which have been used as electron donors such as triethylamine used in early work by Burfield and Tait [66] as well as a host of others which were initially investigated [16]. The most prominent internal electron donors which have been reported in the literature are ethyl benzoate, and the bifunctional phthalates and diethers, and it is also these donors which have played the largest role in recent and current industrial processes. Generally the 1,3-diether systems are more active than the diester based systems due to an increase in the number of active centres rather than an increase in propagation rate constant ( $k_p$ ) of the active sites [67].

It has been shown via a number of studies that coordination of the internal donor to the support is dependent on the functionality of the donors. For example, theoretical studies by Correa *et al.* [63] have shown that Lewis bases such as phthalates, succinates, alkoxysilanes, and diethers were found to coordinate strongly to the (100) and (110) lateral cuts of the  $\text{MgCl}_2$  crystal. A single coordination mode was favourable on the (100) lateral cut but several coordination modes were possible on the (110) cut. With regard to the Lewis base a short spacer between the coordinating O atoms of the donor (alkoxysilanes and 1,3 diethers) resulted in a chelating coordination while longer spacers (such as the four atom spacers of phthalates and succinates) allow more configurations such as bridged coordination as well as coordination with vicinal monolayers. Liu *et al.* [68] determined that there was competitive coordination between the =O and -O- oxygen atoms of the monoester-type electron donors with the  $\text{MgCl}_2$  support. The effect of various electron donors on  $\text{TiCl}_4$  in solution were

investigated by Cavallo *et al.* [69] by means of calorimetric investigations and it was discovered that in all cases the stable structure in solution is represented by an octahedral Ti atom with two oxygen atoms coordinated. They also showed that the ether oxygen atom is a much better  $\sigma$ -donor than the ester oxygen atom.

There is a large amount of IR data on the coordination of EB to the catalyst [70-72] and the summation of these results is that there is a shift in the C=O stretching frequency from  $1725\text{ cm}^{-1}$  in the free ester to  $1680\text{ cm}^{-1}$  -  $1700\text{ cm}^{-1}$  in the catalyst mixture as well as in EB/MgCl<sub>2</sub> mixtures. This has been explained as evidence that the ester group coordinates to the Mg and not to the Ti. Data for the phthalates [73-75] have also shown a shift in the C=O stretching frequency from  $1730\text{ cm}^{-1}$  to  $1685\text{ cm}^{-1}$  -  $1700\text{ cm}^{-1}$  in the catalyst/EB and EB/MgCl<sub>2</sub> mixtures. This evidence points to the EB donor coordinating to the support directly and not to the Ti species. There has also been some evidence, however, from both IR [76] and electron spin resonance (ESR) [77] that small amounts of EB or phthalates might be coordinated to both Mg and Ti.

The coadsorption and support mediated interaction between the Ti species and EB donor were investigated by Taniike and Terano [78, 79]. They found that the relative position of both the Ti species and the EB donor were random on both the (100) and (110) lateral cuts. They also discovered that if the Ti species and EB were close together on the support then the MgCl<sub>2</sub> facilitated electronic transfer selectively on the (110) crystal face.

Cui *et al.* [65] examined the effect of a diether on the polymerisation and concluded that as the donor/Mg ratio increased the Ti content decreased and that this was due to the donor coordinating directly with the MgCl<sub>2</sub> support and thus competing directly with the Ti species. Toto *et al.* [80] found that diethers coordinated preferentially on the (110) surface when used as internal donors.

A theoretical study [81] of alcohols, esters, and ketones used as electron donors has shown that the alcohols coordinated more strongly on the 5-coordinated Mg atoms on (101) than the 4-coordinated Mg atoms on (110). Esters were more stable coordinated on the (101) surface and ketones were most stable on the (110) surface. Carr-Parrinello investigations have also shown that the internal donor di-*n*-butyl phthalate (DNBP) binds very efficiently to the (100) surface in bidentate configuration with a less strong binding on the (110) where a singly bonded structure was the most stable [54].

A number of studies have also shown that the internal donor can easily be extracted from the surface of the support by the alkyl aluminium cocatalyst [82-86]. Monoesters such as ethylbenzoate are extracted the easiest and soonest [83], while the diesters such as the

phthalates are also extracted to some extent at slightly longer induction times [85] although not to the same degree as the monoesters. The diethers on the other hand do not seem to be extracted at all from the surface of the support as evidenced by the fact that no external donor is required when using the diethers as internal donors [87].

The interaction between the internal donor and the alkyl aluminium cocatalyst has been investigated [88, 89] and it is believed that the interaction involves the formation of an acid-base complex through the carbonyl oxygen of the donor. The complex is thought to occur mainly in a 1:1 ratio for the monoesters. Further reactions are possible with these complexes such as alkylation of the carbonyl group complexed to the alkylaluminium, and also reduction of the carbonyl group.

Specific differences between the effect of the internal donors on the structure of the  $\text{MgCl}_2$  crystallites has also been demonstrated recently [60]. Using a diether as an electron donor lead to the formation of  $120^\circ$  edge angles only, while using a monoester or diester resulted in both  $120^\circ$  and  $90^\circ$  edge angles being formed in the crystallites. Due to the fact that the diethers generally preferentially coordinate to the (110) surface [80] the  $120^\circ$  edge angles have been assigned as the (110) surface while the  $90^\circ$  edge angles correspond to the (104) surface.

It would therefore seem that the roles of the internal donor are as follows:

- Competitive coordination with the Ti species on the support so that the Ti species cannot coordinate to the (110) surface and form aspecific sites.
- Coordination with the support in the region of the Ti-species thereby converting aspecific sites into isospecific sites.
- Deactivation of aspecific sites, although this is mainly achieved via the process of competitive coordination as mentioned in the first point.
- Influencing the formation of  $\text{MgCl}_2$  crystallites with specific surfaces.

#### **2.2.2.6 Catalyst active sites: The external electron donor**

As far as the external donor is concerned there have been a number of different types which have been used over the years, namely different monoesters such as EB and methyl-*p*-toluate representing the third generation of Ziegler-Natta catalysts, and a variety of alkoxy silanes used in conjunction with diethers as internal donors representing the fourth

generation of catalysts. The necessity of having to use an external donor during polymerisations has arisen from the problem of internal donor extraction by the cocatalyst as discussed earlier. However, until the discovery of the diethers as internal donors requiring no external donor, the combination of internal and external donor worked best with the external donor performing more than the simple role of replacing the internal donor in the system. The 1,3 diethers appear to function in much the same way as the silanes when used as external donors.

A complex is also formed between external electron donors such as the alkoxysilanes and the cocatalyst. The complex seems to only involve the oxygen atom from one of the OR groups of the silane irrespective of the number of OR groups present [22]. The complexes formed with the silanes are generally more stable than those of the esters and do not tend to react further. A number of researchers [28, 90] have also shown that in general the silanes favour the removal of the internal donor to a greater extent than the monoester donors. This is due to the fact that the silanes can form a stronger complex with the support than with the cocatalyst while the opposite holds true for the benzoic acid esters.

It has also been shown that the addition of external electron donors increases the amount of isospecific centres but does not increase the total amount of centres, implying the conversion of atactic sites to isotactic sites [91].

The roles of the external donor can be summarised as follows:

- Replaces the internal donor extracted by the cocatalyst.
- Reduces the ability of the alkyl aluminium cocatalyst to extract the internal donor by forming a complex with the cocatalyst.
- Converts aspecific sites into isospecific sites by coordinating to the support in the vicinity of the active sites.

It has also become clear that each type of electron donor has a certain influence on the active sites in its direct vicinity. This has been demonstrated by a number of researchers such as Sacchi *et al.* [87] who showed that the same isospecific centres were obtained when using a diether as an internal donor without any external donor, as were obtained when the same diether was used as an external donor and replaced the DIBP internal donor on the catalyst. This has meant that it is possible to tailor the structural characteristics of the polymers simply by changing the type and amount of the donor modifiers. Specific differences in the polymer microstructure as facilitated by the different donor types will be discussed in the next section.



As far as the structure of the external donors is concerned the molecular shape of the donor greatly affects the performance of the compound [92]. The bulkier silanes are the most effective modifiers of the fourth generation as they are more effective at forming stereoregulating active sites and are not extracted as much due to weaker complexation with the cocatalysts [93]. In general the highest isospecificity is obtained with a silane with at least two small alkoxy groups and a bulky alkyl or aryl group [94]. The methoxy groups in turn perform better than the ethoxy groups. The better the complexation ability of the donor the better the activating effect it will have. The complexation ability improves with the number of alkoxy groups as well as with a decrease in size of the alkoxy groups [95]. Concerning the alkyl or aryl groups on the silane the smaller the substituents, the better they are absorbed on the catalyst, however, the larger the substituents, the better the stereoregulating ability of the donor [95].

Different internal donors were used to investigate catalyst ageing on activity and stereospecificity. Dioctylphthalate was found to form a stronger complex with the catalyst than EB and was extracted to a much lesser extent by the TEA cocatalyst [86].

#### **2.2.2.7 Catalyst active sites: The effect on the polymer microstructure**

The influence of the various donor combinations and types is varied for each specific catalyst system, however, there are some general effects which have been observed and seem to hold true no matter what the system used. Generally the addition of an electron donor to the catalyst increases the isotacticity of the material produced [84, 96, 97]. The manner in which this takes place is a matter of debate, however, the general consensus is that the addition of electron donors increases the amount of isospecific centres via the conversion of atactic sites to isotactic sites [91, 98, 99] as well as converting moderately isotactic sites into highly isotactic sites. The molar mass of the polymers produced upon addition of the donors also increases [84, 97], while the polydispersity and activity generally decrease.

It has also been found that there are differences in the  $k_p$  of the various types of active sites. The  $k_p$  of the active sites have been shown to vary as follows: aspecific < moderately isospecific < highly isospecific [67, 91, 99]. Addition of electron donors generally causes a decrease in the  $k_p$  of non-stereospecific active sites and increases the fraction of stereospecific centres [100]. A copolymerisation study by Busico *et al.* [101] showed that the diether system distributes regiodefects more uniformly than the phthalate/silane systems.

The pre-treatment time of the donor with the catalyst generally results in a decrease in activity as does pre-treatment of the cocatalyst with the external donor, however, the activity decrease due to the latter is generally much less severe [98].

The electron donors are not singularly responsible for the isotactic sites as evidenced in a study by Matsuoka *et al.* [82]. They showed that the rate of internal donor extraction was faster than the rate of loss of isotacticity and so they proposed that the amount of internal donor is not always related to the isotacticity of a polymer. Matsuoka *et al.* [102] have also shown that active sites of highest stereoregularity can be formed without the presence of electron donors.

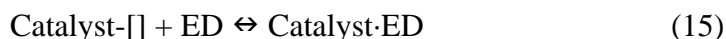
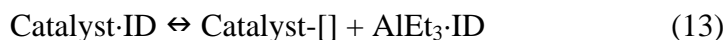
DIBP/silane donor systems generally have a higher stereoregularity [103] and lower hydrogen response than EB based systems. The EB systems have a broader MMD. Diether systems produce polymers with the narrowest distribution [103] of molecular species, however, 2,1 insertions are important in these systems [104].

An increase in polymerisation temperature has been shown to correspond to an increase in the amount and tacticity of the isotactic material, and the isospecific sites produce more material at higher temperatures than moderately isospecific sites [105].

#### **2.2.2.8 Catalyst active sites: Active site models**

A number of attempts have been made over the years to bring together all the information regarding the nature of the active sites in these catalyst systems into models so that better predictions can be made regarding changes in a catalyst's composition. An early model for the isotactic polymerisation of 1-alkenes was proposed by Busico *et al.* [64]. They discussed much of their early work on propene polymerisation in terms of this model [106-108]. According to this early model only the dinuclear Ti species formed on the (100) surface could lead to the formation of a stereospecific active site. Another early model was proposed by Kakugo *et al.* [109] which took into account both the  $\delta$ -TiCl<sub>3</sub> and  $\beta$ -TiCl<sub>3</sub> as well as the case of supported catalysts. The models essentially demonstrated the coordination of the electron donors to a coordination vacancy on catalyst with two vacancies, thereby converting an aspecific site to an isospecific one. It also showed how a donor molecule could coordinate to an active site with a single vacancy and deactivate it.

Sacchi *et al.* [87, 95, 110] have discussed active sites in terms of the equilibria which are present in a catalyst system. These equilibrium reactions are as follows:



Equilibrium (13) is present irrespective of the presence of an external donor. The formation of a complex between the external donor and cocatalyst in equilibrium (14) is also known to occur. Due to the fact that there is generally more cocatalyst present in the system compared to the external donor equilibrium reaction (15) is not so important and to a certain extent can be discounted. Concerning the coordination to the catalyst of the donor/cocatalyst complex it has been shown that the first step insertion stereoregularity is the same when using a diether as internal donor or when replacing a phthalate as internal donor thus showing that the nature of the active site is the same in each case. Equilibrium reaction (17) is therefore considered to be more important than equilibrium reaction (16). Varying the amounts of these compounds in the system will therefore have a significant effect on the equilibrium reactions and therefore the nature of the active sites.

Busico *et al.* [111] proposed a 3-site model in which they proposed active sites for highly isotactic, isotactoid (or weakly isotactic), and syndiotactic material on the basis of microstructural evidence gathered from  $^{13}\text{C}$  NMR data.

The stopped-flow polymerisation technique [98] was used by Nitta *et al.* [85] to validate a model and explain the presence of highly isotactic sites in the absence of electron donors via the formation of a bimetallic complex which can form even in the presence of donors. This model was expanded upon by Liu *et al.* [112] incorporating specific roles of the alkyl aluminium cocatalysts on the formation of isospecific sites in the absence of electron donors [112]. Electron donors were then incorporated into the model [83] and discussed in terms of isotacticity of the sites, referred to as AS, IS<sub>1</sub>, IS<sub>2</sub>, and IS<sub>3</sub> sites depending on the level of stereospecificity of the site.

Liu *et al.* [113] also used the stopped-flow technique to draw up a modified 3-sites model which they use to try and explain the differences in the stereospecific roles of the catalytic Ti species, the cocatalyst, support, and electron donor not specified by the original 3-site model of Busico. Aspecific and weakly-isospecific sites were shown to be transformed into isospecific sites by Ti-Al bimetallic complexation.

Busico *et al.* furthered their work on the general 3-sites model [111] by utilising propene/ethane-[1-<sup>13</sup>C] copolymerisation [101, 114] to investigate catalyst regioselectivity in catalyst systems with and without electron donors. The three-site model appears to hold for a variety of different active site configurations and is generally the model most researchers refer to, or base their own models on. Each of the three sites proposed by Busico can be subdivided into a variety of different sites depending on the ligands coordinated in the vicinity of the active sites.

### 2.2.2.9 Polymerisation conditions affecting the reaction

With regards to the reaction conditions and their effect on the polymerisation the following relationships generally hold true:

- The polymerisation rate is directly proportional to the catalyst concentration [89, 115].
- Increasing the cocatalyst concentration generally increases the reaction rate of supported catalysts [89, 116], however, beyond a certain limit the decay rate increases possibly due to over reduction of the Ti species.
- Supported catalysts usually show a direct relationship between the monomer concentration and the polymerisation rate [24, 52]
- Increasing the reaction temperature generally has a positive influence on the reaction rate up to a certain temperature which is different for different catalyst systems [117, 118]. Beyond this temperature the reaction rate decreases.
- The effect of hydrogen on the system is also varied depending on the monomer and catalyst system [22]. Hydrogen has actually been shown to activate certain fourth and fifth generation catalyst systems presumably by reactivating dormant active sites after 2,1 insertions [119].

## 2.3 Polypropylene

Since its discovery in 1954, isotactic polypropylene as a commodity has grown in leaps and bounds in terms of the production capabilities as well as the applications for the material. The major commercial sources of propylene monomer are via processes for the cracking of hydrocarbons. The major impurity in propylene monomer is propane; however,

minor impurities such as acetylenes, dienes, carbon monoxide, carbon dioxide, water, and alcohols can have more severe effects on the activity and stereospecificity of propylene polymerisation [120].

### 2.3.1 Structure

Polypropylene is essentially a semi-crystalline polymer. This means that there are a number of different regions within the polymer which makes this material so interesting.

On the lowest structural level the polypropylene chains are characterised by varying levels of stereoregularity and regioregularity as discussed previously. The active sites on the catalyst are directly responsible for the variations that are obtained in this regard. Comprehensive analysis of the methyl, methine, and methylene regions and the different microstructures obtained has been performed by Busico *et al.* [121-123]. The microstructure is generally described by the terms *meso* (m) and *racemic* (r) which are used to describe the relative orientation of neighbouring substituents. An isotactic polymer has a high percentage of (m) positions of the methyl groups whereas syndiotactic polypropylene has a high percentage of (r) positions. The chains produced during the polymerisation are also characterised by their molar mass and molar mass distribution.

The chains arrange themselves to form a helical structure and align in layers of right handed and left handed helices [124] in the crystalline regions. Depending on the manner in which these layers come together to form lamellae, different crystal structures are formed. Polypropylene has four crystal forms, namely the  $\alpha$ -form (monoclinic),  $\beta$ -form (trigonal),  $\gamma$ -form (orthorhombic) and a metastable mesomorphic form, often referred to as the smectic form [125, 126]. The smectic form is formed by fast cooling of the polymer melt at low temperatures [127] and represents a state of order intermediate between the amorphous and crystalline states [128]. All forms of the crystal contain chains in the characteristic  $3_1$  helix conformation of polypropylene [126]. There are in fact two types of monoclinic unit cells: the  $\alpha_1$ -form originally indexed by Natta and Corradini in the C2/c space group, and the  $\alpha_2$ -form in the P2<sub>1</sub>/c space group [128]. The type of crystal phase evident in a given polymer is very much dependent on the microstructure of the sample as well as the thermal history of the sample.

The crystal structure of the polymer in turn affects the lamellar structure of the polymer. The cross-hatched structure of the lamellae of  $\alpha$ -phase polypropylene is well known

and one can distinguish between the thicker radial or mother lamellae and the thinner tangential or daughter lamella, which are grown epitaxially from the mother lamellae [128] by a process referred to as homoepitaxy [124]. Lamellae in turn form spherulites which are essentially aggregations of primary crystallites growing from a central nucleus. It has been shown that the spherulites structure depends on the tacticity of the chains. Increasing the tacticity increases the proportion of radial lamellae in the spherulites [129].

### 2.3.2 Properties

The properties of the polymer depend to a great extent on the isotacticity of the chains which in turn affect the crystal type formed. For example the  $\gamma$ -phase crystal has a lower melting point than the  $\alpha$ -phase, and also produces polymer with improved optical properties [130-133]. The molar mass also affects the properties such as the melting point [128], although consensus has not been reached on the exact melting point of a theoretical 100% crystalline polypropylene sample, however, an estimate for an extremely isotactic sample was made by Yamada *et al.* [134, 135] using both differential scanning calorimetry (DSC) and optical microscopy. One cannot discuss the melting properties of polypropylene without mentioning the multiple melting phenomenon which is often observed for these samples. Essentially despite a single, narrow crystallisation exotherm the chains of polypropylene often melt in two distinct regions of varying temperature. There is much debate surrounding the cause of the multiple melting endotherms [128, 136-140]. Multiple melting endotherms could be the result of different polymorphic forms, melting-recrystallisation effects, segregation by tacticity or molar mass, the melting of different regions in the crystalline structure such as radial and transverse lamellae, or even orientation effects [128, 136, 137, 140, 141]. Each case is different and the polymerisation process (i.e. chain microstructure) and thermal histories must be taken into account when discussing the multiple melting endotherms of any given sample. Generally speaking polypropylene samples have a reasonably high melting point of around 150 °C to 170 °C depending on the tacticity of the sample with more perfect chains being able to form thicker lamellae which in turn melt at higher temperatures.

The degree of crystallinity of a given polypropylene sample is usually determined either by density measurements or by a comparison of the melting enthalpy of the sample with that of a theoretical 100% crystalline sample. A value of 209 J/g [142] is often taken as the enthalpy of fusion for the ideal 100% crystalline polypropylene. The crystallinity of a sample

varies significantly depending on the tacticity of the chains, molar mass and molar mass distribution. The degree of crystallinity plays a critical role in many of the applications of polypropylene since properties such as hardness, modulus and yield stress all depend on the level of crystallinity in the sample.

Since polypropylene is a semi-crystalline material it also exhibits a  $T_g$  which occurs over a certain temperature range depending on the crystallinity of the sample although it is usually in the region of  $-10\text{ }^{\circ}\text{C}$  to  $0\text{ }^{\circ}\text{C}$ . The  $T_g$  is often too weak to be detected by DSC especially in highly crystalline samples although other analytical techniques such as dynamic mechanical analysis (DMA) are able to detect the transition. The polymer is also generally only soluble in high boiling aliphatic and aromatic hydrocarbons at high temperature. One of the more useful properties of polypropylene is its excellent chemical resistance

### **2.3.3 Production methods**

Production of polypropylene has grown in leaps and bounds over the last few decades and the growth rate in annual production has remained at around 7% for the last three decades [143]. Much of the growth has been maintained due to developing countries increasing their capacity dramatically over the last few years.

Early commercial processes were batch polymerisations using  $\text{TiCl}_3$  catalysts which took place in a hydrocarbon medium. The demand soon became such that continuous processes became the norm such as the Hercules process used during the 60's and 70's. This involved a continuous feed of catalyst suspended in kerosene diluent to a series of stirred overflow reactors, monomer being added to the first reactor. The slurry is then contacted with isopropanol to terminate the reaction. Catalyst residue removal was however still necessary. Montedison utilised a similar process [144], however, the high costs of having to recycle diluent and alcohols used in the processes encouraged further development. Rexall Drug and Chemical and Phillips Petroleum pioneered the use of liquid monomer, which was polymerised in a slurry before being transferred to a cyclone to separate out the gaseous monomer in the Rexall process [145], while Phillips used a continuous loop reactor [146]. BASF were the first company to use a gas-phase process which they called the Novolen process utilising stirred bed reactors [147].

The introduction of high activity, high stereospecificity catalysts by Montedison and Mitsui enabled the development of processes in which removal of catalyst residues was not

necessary, thus saving enormous amounts on operating costs. The most widely used processes at present are the Spheripol, Unipol, and Novolen processes [120].

### 2.3.4 Applications

There is an extremely large variety of applications for polypropylene products due to the versatility of this polymer and the development of the production processes to manufacture the polymer in a cost effective manner. The processes developed have the ability to tailor the polymer for the desired application by altering the reaction conditions or including comonomers in order to manufacture random copolymers with increased flexibility or even impact copolymers which, as the name implies, have very good impact properties.

One of the main uses of isotactic polypropylene is in injection moulding. The molten polymer is generally injected into a cold mould. The orientation of the polymer in the mould is an important factor in this process as is the melt temperature, mould temperature, melt flow rate (MFR), and polydispersity of the sample. Shrinkage of the sample in the mould is also a critical factor for these applications with thicker samples shrinking more than thinner ones. Homopolymers, random copolymers, impact copolymers and filled polymers are all used in the injection moulding process.

Melt spinning of PP fibres is another process where PP has been used extensively. The molten polymer is forced through a spinnerette and is taken up on a reel. The degree of orientation imposed on the crystallites and fibrils in the fibre are important in determining the properties of the fibre.

Melt-blowing of iPP makes use of high MFR (low molar mass) polymer material and involves the extrusion of material through a small die. The material is then disrupted by a flow of hot air followed by cooling by cold air which deposits the fibres onto a collecting plate where a mat of unorientated, very thin fibres is formed. This results in melt-blown fabrics with low tensile strength, however, the fabrics are very soft due to the small fibre diameter.

PP is also used commercially in the production of films either as cast film or as biaxially oriented polypropylene (BOPP) films. Oriented films are much stiffer and stronger than the cast films which lack orientation. The BOPP films can therefore be made much thinner than the cast films and still maintain good physical properties.

Blow moulding is also performed with low melt flow polymers. HDPE is usually preferred for this application but a number of PP grades have also been found to be suitable.



As a result of the fact that PP is the subject of attack by oxygen and excessive heat stabilisers are almost always added to the polymer grades too minimise these effects. Usually phenolic antioxidants are added, with some being added as processing stabilisers while others are added to protect the polymer in its final application. Typical examples are Irganox 1010, Irgafos 168 and BHT.

## **2.4 Fractionation**

It has long been realised that in order to comprehensively characterise a semi-crystalline polymer one cannot simply look at the polymer as a whole. Since the advent of the polyolefin industry there have been constant efforts to find better ways of characterising a material and the most common means of doing this has been by means of fractionation techniques. Fractionating a material has turned out to be an excellent way in which to examine the heterogeneity of molecular species within a given polymer sample, revealing much information regarding the way in which the polymers were made. The two main techniques used for fractionating a polymer, of relevance to this work, are fractionation according to crystallisability and molar mass, while a third technique, separation according to chemical composition distribution, is also discussed due to its importance for future developments.

### **2.4.1 Fractionation by crystallinity**

A number of techniques have been developed over recent years to analyse semi-crystalline polymers on the basis of crystallisability. The most established techniques being temperature rising elution fractionation (TREF) and crystallisation analysis fractionation (CRYSTAF), however, recent developments in the field include new techniques such as crystallisation elution fractionation (CEF) and solution crystallisation analysis by laser light scattering (SCALLS).

#### **2.4.1.1 TREF**

Much of the early work in this field was focused on ways to establish molar mass distributions. Desreux and Spiegels [148] were the first to realise that a semi-crystalline

polymer could be fractionated according to solubility at a given temperature, and that this fractionation was based on the ability of the polymer to crystallise and not simply on its molar mass. Their pioneering work involved the elution of fractions of polyethylene at successively higher temperatures. Further development and refinement occurred in the field, but it was not until Shirayama *et al.* [149] described the method of fractionating low density polyethylene according to the degree of short chain branching that the term “temperature rising elution fractionation” was born. At this time See and Smith [150] were investigating the effect of different solvent/non-solvent mixtures of varying compositions on the elution of linear polyethylene and isotactic polypropylene. Their experimental setup was essentially the same as that used for TREF, with the exception that they maintained a constant elution temperature and varied the strength of the eluting solvent. This was similar to the work of Guillet *et al.* [151] on polyethylene. With the development of size exclusion chromatography as an excellent method for determining molar mass distributions, fractionation according to crystallisability became the new area of interest.

Fractionation of a semi-crystalline polymer sample by TREF is based on separation according to crystallisability [152-156]. In other words the actual molecular structure and composition directly affects the ability of the chains to crystallise [154]. The longest crystallisable isotactic sequence in the polymer will therefore determine at what temperature the particular chain will crystallise. The development of the TREF experimental setup occurred for very practical reasons. It is far easier to dissolve polymer off a support than it is to collect fractions which crystallise at successively lower temperatures. The general TREF technique can be divided into two main steps, namely a crystallisation step and an elution step.

During the crystallisation step, the semi-crystalline polymer that is being analysed is first dissolved at high temperature, and then allowed to cool slowly under the control of a programmed temperature profile. According to Wild [152] the maximum cooling rate that should be used for achieving a good separation is 2 °C/hour. Various media have been utilised for the crystallisation step of TREF with the most common being a temperature controlled oil bath [157, 158]. Alternatives do exist such as the oven from a gel permeation chromatography (GPC) setup [159], although in this case heat transfer is not as good. One advantage of an oven is the decreased cycle rotation time due to the fact that the oven can be cooled far quicker than an oil bath, in preparation for the next fractionation [152]. Problems associated with temperature gradients in the column as well as poor heat transfer have been noted by Wild [152]. A single medium can be used for both the crystallisation and elution steps as in

the setup of Bergstrom and Avela [160] and Nakano and Goto [161]. It is often the case that two separate media are used [157, 158], enabling the simultaneous crystallisation of a number of samples, since this is the time-limiting step of TREF [152]. The experimental setups utilising a separate crystallisation and elution step usually consist of an oil bath for the crystallisation step followed by either another oil bath or an oven for the elution step.

The importance of the crystallisation step was not fully recognised at first, although it gradually gained importance as it was eventually recognised as the critical step necessary to obtain good reproducible separations [156]. The cooling step can either be done in the presence of a support [157, 159, 162, 163], or simply in solution [158, 164, 165], which is then later slurried with a support before the elution step. The addition of 0.1% of an antioxidant is advised in order to prevent polymer degradation [166].

During the elution step the polymer is dissolved off the support at successively higher temperatures. Columns thus became an integral part of the experimental setup as they provided a simple medium in which to perform the fractionation. Initially constructed from glass [167, 168] and later from stainless steel [169, 170], the columns developed were of many different sizes. There are a few good reviews in the literature that cover all aspects of TREF [152, 153, 155, 156, 166, 171].

As the experimental techniques were improved and refined a distinction could be drawn between the technique involving an on-line detector for continuous signal detection (analytical TREF), and the technique involving the collection of much larger fractions for subsequent offline analysis (preparative TREF).

Analytical TREF is a relatively recent development in the experimental setup of TREF, with workers such as Usami, Gotoh, and Takayama [159] being among the first to describe their systems in detail. Analytical TREF involves the same slow, controlled crystallisation step as in the preparative version of the fractionation, but instead of collecting the fractions for offline analysis the eluent is sent to an RI/IR detector which constantly monitors the polymer being eluted. Recently the trend has been to use an IR detector set at 3.41  $\mu\text{m}$  (C-H stretch), as this presents less of a problem when compared to an RI detector, with respect to with baseline noise [154, 156], due to the relative insensitivity of IR to temperature fluctuations [152, 153].

Preparative TREF on the other hand involves a step-wise elution, isolating fractions from the eluent which are then sent for further offline analysis by  $^{13}\text{C}$  NMR, DSC, wide-angle x-ray diffraction (WAXD), GPC, and CRYSTAF to name but a few. This allows a complete molecular picture to be drawn up regarding the polymer under investigation.

### 2.4.1.2 CRYSTAF

CRYSTAF, an analogous technique to TREF was developed by Monrabal [172], enabling similar results to be obtained in a far shorter time [166, 173, 174]. The CRYSTAF technique also fractionates a semi-crystalline material on the basis of crystallisability [166], and provides a detailed picture of the chemical composition distribution of the polymer being analysed. The main difference between the TREF and CRYSTAF techniques is that while CRYSTAF separates material based on the ability of the chains to crystallise out of solution, the variation of TREF which utilise a support, involves crystallisation out of solution onto a support and must therefore be treated differently. This is especially important when examining polymers which crystallise in different ways such as the homogeneous crystallisation of polyethylene compared to the heterogeneous crystallisation of polypropylene.

The analytical CRYSTAF technique uses a discontinuous sampling process and is automated for ease of use [166], allowing the simultaneous analysis of five samples [153]. The analysis is carried out in stirred stainless-steel reaction vessels without support [153]. The polymer is dissolved in an appropriate solvent (suitable for use with an IR detector) such as 1,2,4,-trichlorobenzene (TCB) and is allowed to cool under the control of a temperature program [172, 173]. The choice of solvent will not affect the separation mechanism but will influence the crystallisation temperature depending on the solvent power [166]. The addition of 0.1% of an antioxidant is recommended in order to prevent polymer degradation [166]. The concentration of the polymer in solution is monitored by an IR detector [166]. The first data points above the crystallisation temperature of the polymer represent the initial (100%) concentration [166]. As the solution cools the chains are able to crystallise out of solution thereby lowering the concentration of the solution. The precipitate is ignored while the concentration of the solution is measured by taking aliquots of the solution through a filter and analysing them with the IR detector [166, 174-176]. Those chains that can crystallise the easiest (those with least branching, highest tacticity, lowest comonomer content etc.) will precipitate out of solution first [173]. As the temperature drops more and more of the polymer can crystallise out of solution.

Due to the freezing point of the solvent used, there is usually a lower limit for the temperature to which the instrument can be used [177]. This means that there is usually a certain amount of material which remains in solution [166]. This is represented on the CRYSTAF graph by a rectangle of constant base and varying height, the area of which

represents the amount of material remaining in solution [166]. The first derivative of the CRYSTAF graph gives a graph equivalent to that obtained with A-TREF [153]. A calibration curve converting the CRYSTAF data into the number of branches per 1000 carbon atoms is necessary before CRYSTAF samples run with different solvents can be compared [177]. This technique has become a standard means of analysis in many laboratories all over the world, with its ease of use and fast analysis time relative to A-TREF being a key factor in its success.

A preparative CRYSTAF unit has been reported, which is capable of fractionating up to 2 g of polymer into eight fractions [153]. The instrument has two stainless-steel crystallisation vessels connected to eight glass vessels [178]. The preparative CRYSTAF unit can also be operated as a solvent/non-solvent unit, allowing the fractionation of polymers by molar mass [153, 179].

#### **2.4.1.3 CEF**

A recent development in terms of the fractionation of semi-crystalline polymers has been made by Monrabal *et al.* [180]. They have designed and made an instrument which separates polymer according to their chemical composition distribution which work by pumping solvent over the polymer during the crystallisation process. The flow rates are extremely low during the crystallisation process and the must be adapted to the cooling rates, crystallisation rate of the sample and the column volume in order to ensure maximum separation within the column length. This technique looks to become a standard measurement technique in the years to come.

#### **2.4.1.4 TFA/SCALLS**

Another relatively new fractionation technique for semi-crystalline polymer is the fractionation technique, which involves analysis of the turbidity of a polymer solution, developed by Shan *et al.* [181]. The technique involves the observation of the scattering of laser light after it passes through a polymer solution. The temperature of the polymer solution is controlled via a heating block which is subjected to a temperature ramp. The polymer crystallises out of solution upon controlled cooling from high temperature and as this takes place the turbidity of the solution increases. Van Reenen *et al.* [182] have developed a similar instrument which they used to investigate a series of polyolefin copolymers. A molar mass dependence on the separation of the polymer chains was also observed for metallocene

polypropylene samples. Their developmental work resulted in the re-branding of their instrumental technique from turbidity fractionation analysis (TFA) to solution crystallisation analysis by laser light scattering (SCALLS) [182]. The fast analysis times this technique provides are a major positive factor when compared to other techniques such as TREF and CRYSTAF.

## **2.4.2 Fractionation by molar mass**

### **2.4.2.1 SEC**

The best known analytical technique, size exclusion chromatography (SEC), is the most used method for fractionating a polymer based on molar mass. Strictly speaking however, the SEC process fractionates polymers according to their hydrodynamic volume [125, 183, 184]. SEC is the general name for this type of separation of molecules and can be subdivided into gel permeation chromatography (GPC) and gel filtration chromatography (GFC). GPC is the separation of synthetic macromolecules using porous gels or rigid inorganic packing particles, while GFC is a similar process for the separation of biological macromolecules [183].

The sample solution is introduced into the column of the instrument and is carried through the column by means of a suitable solvent [183]. The separation in the column occurs due to the fact that the smaller chains are able to penetrate deeper into the porous packing material than the larger chains [46], resulting in the larger chains having the shortest retention time, with the retention time increasing as the chain size decreases [184]. It is often necessary to run these experiments at high temperature, depending on the solubility of the sample in question in the solvent [183].

The gel-permeation chromatogram is converted to a molar mass distribution via a calibration curve. Polymer standards of known molar mass and narrow molar mass distribution are generally used, with polystyrene standards being the most widely used [183]. The polystyrene calibration is applied to other polymers by means of the universal calibration procedure, calibrating the calibration of many random coil polymers with the product of intrinsic viscosity and molar mass [184].

#### **2.4.2.2 Solvent/non-solvent techniques**

Solvent/non-solvent techniques are usually used for the preparative fractionation by molar mass. The fractionation in this case is molar mass dependent rather than tacticity dependent [185]. Preparative CRYSTAF apparatus can also be used for solvent/non-solvent fractionation [153, 179]. Vilaplana *et al.* [179] used xylene as the solvent and diethylene-glycol-monobutylether (DGMBE) as the non-solvent for an LDPE sample fractionation using the CRYSTAF apparatus. Baijal *et al.* [186] used TCB as the solvent and dimethyl phthalate (DMP) as the non-solvent for their fractionation of polypropylene.

#### **2.4.3 Fractionation by chemical composition distribution**

The complexity of a variety of modern polymer compositions has necessitated new developments in terms of fractionation of the constituent parts. Polymer blends, copolymers, and even terpolymers, are commonplace, however, they are rather complex polymer systems. New techniques such as the recently developed high temperature gradient HPLC have enabled the separation of these chains with such varied chemical composition distributions for the first time. Heinz and Pasch [187] have reported the separation of blends of polypropylene and polyethylene using a mobile phase of ethylene glycol monobutylether (EGMBE) and 1,2,4-trichlorobenzene with silica gel as the stationary phase.

### **2.5 Mechanical properties**

There are a vast number of grades of polypropylene available commercially, each one designed and modified to suit a certain type of application. A detailed discussion of all the different types of grades is beyond the scope of this thesis, however, important relationships between the structure of the polymers and the final properties will be discussed. The main types of polypropylenes which are commercially available are the homopolymer, random copolymers, impact or heterophasic copolymers, and filled grades. There are also speciality nucleated grades available with improved optical and mechanical properties. The discussions that follow will focus mostly on the homopolymers where possible.

## 2.5.1 General structure-property relationships

Some of the more important properties of polypropylene products are the modulus, impact strength, hardness, tensile strength, and maximum use temperature. In order to determine the usefulness of a certain polymer grade these properties must be known. Designing reactor grades that can be used for certain products therefore requires knowledge of the effect of different polymerisation conditions on the physical properties of the polymer. This in turn requires knowledge of the effect of the reaction conditions on the microstructure of the polymer formed since it is the microstructure which determines the physical properties. Generally the modulus values of random and impact copolymers are lower than that of the homopolymer while the opposite holds true for the impact strength [130].

The homopolymer is used for applications requiring high stiffness and high thermal resistance. The properties of the homopolymer are dependent on the tacticity of the polymer as well as the molar mass and molar mass distribution. These structural characteristics mostly affect the properties by affecting the ability of the material to crystallise. Paukkeri and Lehtinen [188] found that the tacticity of the polymer chains had the greatest influence on the ability of the chains to crystallise while the molar mass had only a small influence once the molar mass exceeded approximately 22 000 g/mol. Increasing the tacticity of the polymer generally results in an increase in the stiffness and hardness while the impact strength usually decreases. This is linked to the crystallinity of the sample. Properties which improve with an increase in crystallinity are the stiffness, hardness, and end use temperature while the impact properties generally decrease with increasing crystallinity of the material. Lower molar masses and broader molar mass distributions also improve the ability of the chains to crystallise and thus improve the stiffness and hardness. Higher molar masses also result in a greater degree of orientation in the chains during processing and this factor must also be taken into account when examining data. Polymers with broader molar mass distributions can also show this effect.

The molar mass distribution can be artificially narrowed by degrading the polymer with peroxides, thereby controlling the properties with the amount and type of peroxide added [189]. Crystallinity can also be affected by the addition of nucleating agents which can promote the formation of highly crystalline material characterised by smaller, higher melting spherulites [190, 191]. Specific nucleating agents can also promote the formation of different crystalline phases of polypropylene which also affects the properties [192, 193]. The



introduction of a comonomer used in the random copolymers is another way in which the properties can be varied via the incorporation of a comonomer unit which acts as a discontinuity in the polymer chains preventing them from attaining the levels of crystallinity obtained with the homopolymers.

## 2.5.2 Microhardness

### 2.5.2.1 General background and theory

The microhardness technique has been around for a number of years and has proved to be an extremely useful and sensitive technique to probe small differences in materials not detectable by other large-scale tests. The microhardness technique involves the static penetration of a material with an indenter using a known force. The microhardness of a material is determined by dividing the load used by the residual deformation area on the surface of the material. It is essentially a measure of the irreversible deformation processes characterising the material. There are two main zones of deformation in the material below the indenter. These are the plastic deformation zone and the larger elastic penetration zone [194]. Both zones serve to support the stress imposed on the material by the force of the indenter. The plastic deformation zone involves such processes as phase transformations at low strains, chain tilt and slip within crystals, and also crack formation and chain unfolding at larger strains while the elastic deformation zone mainly involves the elastic yielding of the amorphous component of the material.

There are two main types of indenter used for microhardness measurements, namely the Vickers indenter and the Knoop indenter. The Vickers indenter consists of a square based pyramid of approximately 100  $\mu\text{m}$  in height. The included angles between the opposite faces of the pyramid are  $\alpha = 136^\circ$ , corresponding to the tangential angle of an 'ideal' ball impression. The hardness value is determined according to equation (18):

$$MH_{\text{Vickers}} = \frac{2P \sin\left(\frac{\alpha}{2}\right)}{9.807d^2} = 0.1891 \left(\frac{P}{d^2}\right) \quad (18)$$

P is the applied force in Newton. The Knoop indenter on the other hand utilises a rhombic based pyramidal diamond with angle edges of  $172^\circ$  and  $130^\circ$ . The microhardness is also given

according to the applied force divided by the residual area of impression according to equation (19):

$$MH_{Knoop} = \frac{P}{9.807d^2C} \approx \frac{1.451P}{d^2} \quad (19)$$

Due to the two-fold symmetry of the indentation the Knoop indenter is more sensitive to material anisotropy than the Vickers indenter, however, the Vickers indenter can still detect anisotropy in a material [195, 196].

Sample preparation is a critical part of the microhardness technique. One must ensure that the sample has a smooth, flat surface which is aligned perpendicularly to the indenter. There are also a number of factors regarding sample preparation which affect the microhardness value obtained such as the sample melt pressing method and also sample cooling method post-pressing.

Balta-Calleja [194] has investigated the effect of analysis temperature on the microhardness and discovered that the microhardness generally decreases with an increase in temperature due to the increase in the thermal expansion in the crystalline regions decreasing the resistance to plastic deformation via a decrease in cohesion energy of the crystals. Annealing of the sample generally results in an increase in the microhardness as the lamellae thicken and improve in perfection [197, 198]. Cooling rates during sample preparation also play an important role with an increase in cooling rate correlating to lower hardness values [199]. The mechanical properties such as the yield stress and elastic modulus have also been investigated [200] showing that an increase in the microhardness correlates well to an increase in yield stress and elastic modulus.

### 2.5.2.2 Deformation mechanisms

There are a number of deformation mechanism by which a material such as polypropylene can dissipate energy. These mechanisms absorb the energy placed on the sample via the stresses exerted upon it by the indenter. The smallest mechanisms for deformation involve phase transformation within the lamellae and elastic bending of crystals although these mechanisms occur at very small strains. Slightly larger strains can bring about interlamellar slip involving shearing and deformation of the amorphous layers and partial destruction of some crystalline blocks. At large strains lamellar fracture can occur. Generally

the networks of tie molecules and entanglements contribute significantly to the strength of the material [194]. It is also possible that during an indentation there is also melting of crystals taking place with subsequent rearrangement and recrystallisation which also assists in absorbing energy.

### **2.5.2.3 The effect of microstructure on microhardness**

Microhardness has been used to investigate a number of different aspects of polypropylene such as the differences in the microhardness of the crystal phases [195, 198], which showed that the  $\alpha$ -phase crystals are slightly harder than the  $\beta$ -phase crystals. These results are supported by the nanoindentation results of Labour *et al.* [201].

Koch *et al.* [197] have investigated the effect of the molar mass on the microhardness in both quenched and annealed samples of isotactic polypropylene and have shown that there is a decrease in microhardness with increasing molar mass – especially for higher molar masses. Flores *et al.* [202] have also shown a slight molar mass effect on the microhardness mainly due to the effect of the molar mass on the crystallinity of the samples. In general, microstructures which promote the formation of thicker crystals and a higher overall degree of crystallinity in the samples result in an increase in the microhardness values.

## **2.5.3 DMA**

### **2.5.3.1 General background and theory**

Dynamic mechanical analysis is a well established technique for the analysis of the mechanical properties of a material. The technique can be defined as the application of an oscillating force to a sample and analysis of the materials response to the force [203]. There is a variety of information which one can obtain from DMA measurements and the experiments can be tailored to provide a wealth of data. One can determine the tendency of a material to flow (its viscosity) from the phase lag of the material response to the applied force which is often referred to as the damping ability of the material or rather the ability of the material to lose energy as heat. The stiffness of the material can also be determined via the sample recovery and is a good measure of the ability of the materials ability to recover from deformation.

During the analysis a stress ( $\sigma$ ) is applied to the sample which then undergoes a strain ( $\gamma$ ) as a result of the applied stress. The slope of the stress-strain curve gives us the modulus of the sample. One advantage of DMA over a standard tensile test to determine the modulus is that a modulus value can be obtained for every oscillation applied to the sample. It is therefore possible to obtain modulus values every second. A temperature ramp can also be applied to the sample which allows the determination of the mechanical properties as a function of temperature. There are, however, differences between the Young's modulus obtain from a classical stress-strain experiment and that obtained from DMA. The modulus obtained from DMA consists out of a complex modulus ( $E^*$ ), elastic (storage) modulus ( $E'$ ) and imaginary (loss) modulus ( $E''$ ). These enable us to determine the ability of the material to dissipate energy and also the ability to store energy. The ratio of these two effects is called the damping ability of the material ( $\tan \delta$ ).

Determining these properties for each point on a temperature ramp means that the transitions which take place upon heating the sample can also be determined due to the fact that generally at these transitions there will be a change in the properties of the material. DMA has therefore proven to be an extremely sensitive tool for the determination of the  $T_g$  of a material, as well as even smaller transitions such as side chain or pendant group motions, bending and stretching motions and even local crankshaft rotations of polymer chains. At the higher temperatures chain slip and recrystallisation can both be determined. The area under the  $\tan \delta$  curve is a measure of the ability of the material to damp vibrations via localised chain motions and thus a large area under the curve means the sample has good impact properties compared to a sample with a much smaller area under the curve.

There are a number of different experiments which one can perform using DMA such as creep-recovery testing, stress relaxation experiments, curing of materials, extensional measurements, torsional measurements, 3-point bending tests, and frequency scans to name but a few, however, the majority of these are beyond the scope of this thesis. The functions of the DMA utilised in this study involve the standard temperature scan with a superimposed oscillation as well as the use of the instruments control ability to analyse the extensional stress-strain data for various samples.

### 2.5.3.2 The effect of microstructure on the polymer properties

Studies [201] have shown that the differences in crystal phase of polypropylene also show up in DMA analysis with the crystals of the  $\beta$ -phase showing improved mobility over those of the  $\alpha$ -phase. The molar mass of the sample has been shown to influence the  $T_g$  of the sample with higher molar masses increasing the temperature of the  $T_g$  transition [204]. The inclusion of comonomers reduces the degree of crystallinity and lamellar thickness of a sample resulting in improved impact strength compared to the homopolymer [205] as a result of improved mobility of chains in the amorphous component. The elastic modulus has also been shown to be dependant on the amount of the crystalline phase and the crystal thickness. Stern *et al.* [206] showed that increasing the molar mass decreased the crystallinity of the samples and increased the lamellar thickness. They also showed that the chain mobility depended on the molar mass and the lamellar thickness and that essentially the  $\beta$ -transition increased with molar mass.

Recent studies on metallocene isotactic polypropylene samples [207-209] have highlighted the effect of tacticity on the mechanical properties of polypropylene. Stereoirregularities in the polypropylene chains are shown to influence the crystal phase of the polymer. A linear relationship was found between the amount of the  $\gamma$ -form of the crystals and the average isotactic sequence length. This in turn influenced the stress-strain profiles of the samples.

## 2.6 Concluding remarks and methodology

The complex nature of the polymers produced by the Ziegler-Natta catalysts necessitates thorough fractionation and analysis in order to evaluate the effects of different polymerisation conditions on the polymer microstructure. In order to analyse the effect of certain types of polymer chains on the properties of the whole polymer it is necessary to investigate the differences in the properties brought about by the presence or absence of the specific parts of the polymer in question. Should specific parts of the polymer be required for certain properties, then by default the active sites producing the types of chains which make up that part of the polymer are required for those properties.

Physically removing certain parts of the polymer (via fraction removal and recombination using preparative TREF) would therefore give an indication of the role that the

fraction in question plays in the overall polymer properties. Properties could then be altered by varying the polymerisation conditions with a view to changing the material produced by specific active sites, thus altering the polymer properties in the reactor.

A propylene copolymer would provide a good means to investigate the differences in properties of polymers with selected fractions removed since the presence of the comonomer in the fractions would bring about larger changes in the materials properties once the fractions are removed. Experiments could then be carried out using the homopolymer with greater confidence in the knowledge that differences in the samples are real. Finally reaction conditions could be varied for a series of polymerisations in order to produce polymers with different properties directly from the reactor.

Mechanical analysis of the fractionated and recombined materials as well as the polymers synthesised will be carried out via microhardness and DMA techniques. This will enable the investigation of the hardness and impact properties on a small scale which is necessary due to the small amounts of material available for testing.

## 2.7 References

1. Seymour, R.B., *History of polyolefins*, in *Handbook of polyolefins*, C. Vasile, & Seymour, R.B., Editor. 1993, Marcel Dekker: New York. p. 1.
2. Raff, R., & Lyle, E.L., *Historical developments*, in *Crystalline olefin polymers*, R.A.V. Raff, & Doak, K.W., Editor. 1965, John Wiley & Sons: New York. p. 1.
3. Meerwein, H., *Catalytic decomposition of diazomethane to polymethylene*. *Angewandte Chemie*, 1948. **60**: p. 78.
4. Taylor, H.S., & Jones, W.H., *The thermal decomposition of metal alkyls in hydrogen-ethylene mixtures*. *Journal of the American Chemical Society*, 1930. **52**(3): p. 1111.
5. Carothers, W.H., Hill, J.W., Kirby, J.E., & Jacobsen, R.A., *Polymerization and ring formation. VII. Normal paraffin hydrocarbons of high molecular weight prepared by the action of sodium on decamethylene bromide*. *Journal of the American Chemical Society*, 1930. **52**: p. 5279.
6. Koch, H., & Ibing, G., *The composition of hard paraffins produced in the naphtha synthesis of Franz Fischer and H. Tropsch*. *Brennstoff-Chemie*, 1935. **16**: p. 141.
7. Fawcett, E.W., & Gobson, R.O., *Influence of pressure on a number of organic reactions in the liquid phase*. *Journal of the American Chemical Society*, 1934: p. 386.

8. Larson, A.T., & Krase, N.W., 1946, Polymerizing ethylene, U.S. Patent 2,405,962
9. Hogan, J.P., & Banks, R.L., 1958, Polymerization of olefins, U.S. Patent 2,825,721
10. Ziegler, K.D., F., & Wollthan, H., *Alkali organic compounds. XI. Mechanism of polymerization of unsaturated hydrocarbons by alkali metal and alkali alkyls.* Justus Liebigs Annalen der Chemie, 1934. **511**: p. 13.
11. Ziegler, K., & Jakob, L., *Alkali organic compounds. XII. "Catalysis" of the polymerization of unsaturated hydrocarbons by alkali organic compounds.* Justus Liebigs Annalen der Chemie, 1934. **511**: p. 45.
12. Ziegler, K., Jakob, L., Wollthan, H., & Wenz, A., *Alkali organic compounds. XIII. The first reaction products of alkali metals upon butadiene.* Justus Liebigs Annalen der Chemie, 1934. **511**: p. 64.
13. Hall, F.C., & Nash, A.W., *Formation of organometallic alkyl derivatives of aluminum during the polymerization of ethylene.* Journal of the Institute of Petroleum, 1937. **23**: p. 679.
14. Fischer, M., 1953, Solid polymers from ethylene or gas mixtures rich in ethylene, German Patent 874,215
15. Ziegler, K., *Alumino-organic syntheses in the field of olefinic hydrocarbons.* Angewandte Chemie, 1952. **64**: p. 323.
16. Boor, J., *Ziegler-Natta Catalysts and Polymerizations.* 1979, New York: Academic Press, Chapter 2.
17. Ziegler, K., Holzkamp, E., Breil, H., & Martin, H., *The M.Overddot.uhlheim low-pressure polyethylene process.* Angewandte Chemie, 1955. **67**: p. 541.
18. Moore, E.P., Jr., *Polypropylene Handbook.* 2002, Munich: Hanser. Chapter 1.
19. Morton, A.A., Magat, E.E., & Letsinger, R.L., *Polymerization. VI. The alfin catalysts.* Journal of the American Chemical Society, 1947. **69**: p. 950.
20. Schildknecht, C.E., Zoss, A.O., & McKinley, C., *Vinyl alkyl ethers.* Journal of Industrial and Engineering Chemistry, 1947. **39**: p. 180.
21. Schildknecht, C.E., Gross, C.E.S.T., Davidson, H.R., Lambert, J.M., & Zoss, A.O., *Polyvinyl isobutyl ethers-properties and structures.* Journal of Industrial and Engineering Chemistry, 1947. **40**: p. 2104.
22. Albizzati, E., Giannini, U., Collina, G., Noristi, L., & Resconi, L., *Catalysts and polymerizations,* in *Polypropylene handbook*, E.P. Moore, Jr., Editor. 2002, Hanser: Munich. p. 11.

23. Natta, G., Corradini, P., & Allegra, G., *The different crystalline modifications of  $TiCl_3$ , a catalyst component for the polymerization of  $\alpha$ -olefins. I.* Journal of Polymer Science, 1961. **51**: p. 399.
24. Kissin, Y.V., *Isospecific Polymerization of Olefins with Heterogeneous Ziegler-Natta Catalysts.* 1985, New York: Springer-Verlag.
25. Natta, G., Zambelli, A., Pasquon, I., & Giongo, G.M., *Stereospecific polymerization mechanism of  $\alpha$ -olefins to isotactic polymers in the presence of a bimetallic catalyst system. II. Stereospecificity of some heterogeneous catalyst systems.* Chimica e l'Industria, 1966. **48**: p. 1307.
26. Natta, G., Zambelli, A., Pasquon, I., & Giongo, G.M., *Stereospecific polymerization mechanism of  $\alpha$ -olefins to isotactic polymers in the presence of a bimetallic catalyst system. I. Velocity of chain propagation with various catalytic systems.* Chimica e l'Industria, 1966. **48**: p. 1298.
27. Wilchinsky, Z.W., Looney, R.W., & Tornqvist, E.G.M., *Dependence of polymerization activity on particle and crystallite dimensions in ball milled titanium trichloride and titanium trichloride.0.33 aluminum chloride catalysts components.* Journal of Catalysis, 1973. **28**: p. 351.
28. Hermans, J.P., & Henriouille, P., 1973, Ziegler-Natta type catalyst, U.S. Patent 3,769,233
29. Montedison, 1968, British Patent 1,286,867
30. Soga, K., & Shiono, T., *Ziegler-Natta catalysts for olefin polymerisations.* Progress in Polymer Science, 1997. **22**: p. 1503.
31. Krentsel, B.A., Kissin, Y.V., Kleiner, V.J., & Stotskaya, L.L., *Polymers and copolymers of higher  $\alpha$ -olefins.* 1999, Munich: Hanser. Chapter 1.
32. Zakharov, V.A., Bukatov, G.D., & Yermakov, Y.I., *On the mechanism of olefin polymerization by Ziegler-Natta catalysts.* Advances in Polymer Science, 1983. **51**: p. 61.
33. Zambelli, A., Locatelli, P., Sacchi, M.C., & Tritto, I., *Isotactic polymerization of propene: Stereoregularity of the insertion of the first monomer unit as a fingerprint of the catalytic active site.* Macromolecules, 1982. **15**: p. 831.
34. Patat, P., & Sinn, H., *The course of low-pressure polymerization of  $\alpha$ -olefins. I. Complex polymerization.* Angewandte Chemie, 1958. **70**: p. 496.



35. Natta, G., & Mazzanti, G., *Organometallic complexes as catalysts in ionic polymerizations*. Tetrahedron, 1960. **8**: p. 86.
36. Rodriguez, L.A.M., & van Looy, H.M., *Studies on Ziegler-Natta catalysts. V. Stereospecificity of the active center*. Journal of Polymer Science, Part A-1: Polymer Chemistry, 1966. **4**: p. 1971.
37. Ystenes, M., *The trigger mechanism for polymerization of  $\alpha$ -olefins with Ziegler-Natta catalysts: A new model based on interaction of two monomers at the transition state and monomer activation of the catalytic centers*. Journal of Catalysis, 1991. **129**: p. 383.
38. Cossee, P., *Reaction mechanism of ethylene polymerization with heterogeneous Ziegler-Natta catalysts*. Tetrahedron Letters, 1960. **17**: p. 12.
39. Arlmann, E.J. *The active center in Ziegler-Natta polymerization. The interaction of a crystalline transition metal trichloride with a metal alkyl in hydrocarbon solution*. in *Proc. Intern. Catalysis, 3rd*. 1965. Amsterdam.
40. Brookhart, M., & Green, M.L.H., *Carbon-hydrogen-transition metal bonds*. Journal of Organometallic Chemistry, 1983. **250**: p. 395.
41. Cavallo, L., Guerra, G., & Corradini, P., *Mechanisms of propagation and termination reactions in classical heterogeneous Ziegler-Natta catalytic systems: A nonlocal density functional study*. Journal of the American Chemical Society, 1998. **120**: p. 2428.
42. Boero, M., Parrinello, M., & Terakura, K., *First principles molecular dynamics study of Ziegler-Natta heterogeneous catalysis*. Journal of the American Chemical Society, 1998. **120**: p. 2746.
43. Locatelli, P., Tritto, I., & Sacchi, M.C., *Steric control in the insertion of the first monomeric unit in the stereospecific polymerization of linear 1-alkenes*. Makromolekulare Chemie Rapid Communications, 1984. **5**: p. 495.
44. Erker, G., Nolte, R., Tsay, Y.H., & Kruger, C., *Double stereodifferentiation by the formation of isotactic polypropylene on chiral dichlorobis [methyl(phenyl)methylcyclopentadienyl]zirconium-methylaluminumoxane catalysts*. Angewandte Chemie, 1989. **101**: p. 642.
45. Grassi, A., Zambelli, A., Resconi, L., Albizzati, E., & Mazzocchi, R., *Microstructure of isotactic polypropylene prepared with homogeneous catalysis: Stereoregularity, regioregularity, and 1,3-insertion*. Macromolecules, 1988. **21**: p. 617.

46. Monasse, B., & Haudin, J.M., *Molecular structure of polypropylene homo- and copolymers*, in *Polypropylene: Structure, blends and composites*, J. Karger-Kocsis, Editor. 1995, Chapman & Hall: London. p. 3.
47. Kroschwitz, J.I., Mark, H.F., Bikales, N.M., Overberger, C.G., & Menges, G., ed. *Encyclopedia of Polymer Science and Engineering*. Second ed. Vol. 13. 1985, John Wiley & Sons: New York. p. 488.
48. Fregonese, D., Mortara, S., & Bresadola, S., *Ziegler–Natta  $MgCl_2$ -supported catalysts: Relationship between titanium oxidation states distribution and activity in olefin polymerization*. *Journal of Molecular Catalysis A: Chemical*, 2001. **172**: p. 89.
49. Zambelli, A., Locatelli, P., Sacchi, M.C., & Tritto, I., *Isotactic polymerization of propene: Stereoregularity of the insertion of the first monomer unit as a fingerprint of the catalytic active site*. *Macromolecules*, 1982. **15**: p. 831.
50. Chadwick, J.C., Morini, G., Albizzati, E., Balbontin, G., Mingozzi, I., & Cristofori, A., *Aspects of hydrogen activation in propene polymerization using  $MgCl_2/TiCl_4$ /diether catalysts*. *Macromolecular Chemistry and Physics*, 1996. **197**: p. 2501.
51. Chadwick, J.C., Morini, G., Balbontin, G., Mingozzi, I., & Albizzati, E., *Propene polymerization with  $MgCl_2$ -supported catalysts: Effects of using a diether as external donor*. *Macromolecular Chemistry and Physics*, 1997. **198**: p. 1181.
52. Giannini, U., *Polymerization of olefins with high activity catalysts*. *Macromolecular Chemistry and Physics, Supplement*, 1981. **5**: p. 216.
53. Mori, H., Sawada, M., Higuchi, T., Hasebe, K., Otsuka, N., & Terano, M., *Direct observation of  $MgCl_2$ -supported Ziegler catalysts by high resolution transmission electron microscopy*. *Macromolecular Rapid Communications*, 1999. **20**: p. 245.
54. Boero, M., Parrinello, M., Weiss, H., & Huffer, S., *A first principles exploration of a variety of active surfaces and catalytic sites in Ziegler-Natta heterogeneous catalysis*. *Journal of Physical Chemistry A*, 2001. **105**: p. 5096.
55. Henry, N.F.M., & Lonsdale, K., ed. *International tables for crystallography*. 1952, Kynoch Press: Birmingham, U.K.
56. Busico, V., Causa, M., Cipullo, R., Credendino, R., Cutillo, F., Friederichs, N., Lamanna, R., Segre, A., & Castelli, V.V.A., *Periodic DFT and high-resolution magic-angle-spinning (HR-MAS)  $^1H$  NMR investigation of the active surfaces of  $MgCl_2$ -supported Ziegler-Natta catalysts. The  $MgCl_2$  matrix*. *Journal of Physical Chemistry C*, 2008. **112**: p. 1081.

57. Andoni, A., Chadwick, J.C., Niemantsverdriet, H.J.W., & Thune, P.C., *A preparation method for well-defined crystallites of MgCl<sub>2</sub>-supported Ziegler-Natta catalysts and their observation by AFM and SEM*. *Macromolecular Rapid Communications*, 2007. **28**: p. 1466.
58. Andoni, A., Chadwick, J.C., Milani, S., Niemantsverdriet, H.J.W., & Thune, P.C., *Introducing a new surface science model for Ziegler-Natta catalysts: Preparation, basic characterization and testing*. *Journal of Catalysis*, 2007. **247**: p. 129.
59. Andoni, A., Chadwick, J.C., Niemantsverdriet, H.J.W., & Thune, P.C., *A flat model approach to Ziegler-Natta catalysts for propylene polymerization and a preparation method of well-defined crystallites of MgCl<sub>2</sub>-supported catalysts*. *Macromolecular Symposium*, 2007. **260**: p. 140.
60. Andoni, A., Chadwick, J.C., Niemantsverdriet, H.J.W., & Thune, P.C., *The role of electron donors on lateral surfaces of MgCl<sub>2</sub>-supported Ziegler-Natta catalysts: Observation by AFM and SEM*. *Journal of Catalysis*, 2008. **257**: p. 81.
61. Monaco, G., Toto, M., Guerra, G., Corradini, P., & Cavallo, L., *Geometry and stability of titanium chloride species adsorbed on the (100) and (110) cuts of the MgCl<sub>2</sub> support of the heterogeneous Ziegler-Natta catalysts*. *Macromolecules*, 2000. **33**: p. 8953.
62. Brambilla, L., Zerbi, G., Nascetti, S., Piemontesi, F., & Morini, G., *Experimental and calculated vibrational spectra and structure of Ziegler-Natta catalyst precursor: 50/1 comilled MgCl<sub>2</sub>-TiCl<sub>4</sub>*. *Macromolecular Symposium*, 2004. **213**: p. 287.
63. Correa, A., Piemontesi, F., Morini, G., & Cavallo, L., *Key elements in the structure and function relationship of the MgCl<sub>2</sub>/TiCl<sub>4</sub>/Lewis base Ziegler-Natta catalytic system*. *Macromolecules*, 2007. **40**: p. 9181.
64. Busico, V., Corradini, P., De Martino, L., Proto, A., Savino, V., & Albizzati, E., *Polymerization of propene in the presence of MgCl<sub>2</sub>-supported Ziegler-Natta catalysts, 1: The role of ethyl benzoate as "internal" and "external" base*. *Makromolekulare Chemie*, 1985. **186**: p. 1279.
65. Cui, N., Ke, H., Li, H., Zhang, Z., Guo, C., Lv, Z., & Hu, Y., *Effect of diether as internal donor on MgCl<sub>2</sub>-supported Ziegler-Natta catalyst for propylene polymerization*. *Journal of Applied Polymer Science*, 2006. **99**: p. 1399.
66. Burfield, D.R., & Tait, P.J.T., *Ziegler-Natta catalysis: 6. Effect of electron donors on the course of polymerization*. *Polymer*, 1974. **15**: p. 87.

67. Yaluma, A.K., Chadwick, J.C., & Tait, P.J.T., *Kinetic and active centre studies on the polymerization of propylene using MgCl<sub>2</sub> supported Ziegler-Natta catalysts and 1,3 diether donors*. Macromolecular Symposium, 2007. **260**: p. 15.
68. Liu, B., Cheng, R., Liu, Z., Qiu, P., Zhang, S., Taniike, T., Terano, M., Tashino, K., & Fujita, T., *Experimental and computational approaches on the isospecific role of monoester-type internal electron donor for TiCl<sub>4</sub>/MgCl<sub>2</sub> Ziegler-Natta catalysts*. Macromolecular Symposium, 2007. **260**: p. 42.
69. Cavallo, L., Del Piero, S., Ducere, J-M., Fedele, R., Melchior, A., Morini, G., Piemontesi, A., & Tolazzi, M., *Key interactions in heterogeneous Ziegler-Natta catalytic systems: Structure and energetics of TiCl<sub>4</sub>-Lewis base complexes*. Journal of Physical Chemistry C, 2007. **111**: p. 4412.
70. Yano, T., Inoue, T., Ikai, S., Shimizu, M., Kai, Y., & Tamura, M., *Highly active supported catalysts for olefin polymerization: Preparation and characterization of the catalyst*. Journal of Polymer Science: Part A: Polymer Chemistry, 1988. **26**: p. 477.
71. Terano, M., Kataoka, T., & Keii, T., *A study on the states of ethyl benzoate and titanium tetrachloride in magnesium chloride-supported high-yield catalysts*. Makromolekulare Chemie, 1987. **188**: p. 1477.
72. Terano, M., Kataoka, T., & Keii, T., *Analytical and kinetic approaches for the basic type of magnesium chloride-supported high-yield catalysts*. Journal of Polymer Science: Part A: Polymer Chemistry, 1990. **28**: p. 2035.
73. Mackie, P., Berger, M.N., Grieveson, B.M., & Lawson, D., *Replication in Ziegler polymerization*. Journal of Polymer Science, Polymer Letters Edition, 1967. **5**: p. 493.
74. Terano, M., Kataoka, T., Hosaka, M., & Keii, T., *Transition metals and organometallics as catalysts for olefin polymerization*, W. Kaminsky, & Sinn, H., Editor. 1988, Springer Verlag: Berlin. p. 55.
75. Jeong, Y., Lee, D., Shiono, T., & Soga, K., *Propene polymerization with a diethoxymagnesium-supported titanium tetrachloride catalyst. 3. The role of benzoyl chloride*. Makromolekulare Chemie, 1991. **192**: p. 1727.
76. Jones, P.J.V., & Oldman, R.J., *Transition metals and organometallics as catalysts for olefin polymerization*, W. Kaminsky, & Sinn, H., Editor. 1988, Springer Verlag: Berlin. p. 223.
77. Chien, J.C.W., & Hu, Y., *Superactive and stereospecific catalysts. III. Definitive identification of active sites by electron paramagnetic resonance*. Journal of Polymer Science: Part A: Polymer Chemistry, 1989. **27**: p. 897.

78. Taniike, T., & Terano, M., *Coadsorption and support-mediated interaction of Ti species with ethyl benzoate in MgCl<sub>2</sub>-supported heterogeneous Ziegler-Natta catalysts studied by density functional calculations*. *Macromolecular Rapid Communications*, 2007. **28**: p. 1918.
79. Taniike, T., & Terano, M., *Density functional calculations for electronic and steric effects of ethyl benzoate on various Ti species in MgCl<sub>2</sub>-supported Ziegler-Natta catalysts*. *Macromolecular Symposium*, 2007. **260**: p. 98.
80. Toto, M., Morini, G., Guerra, G., Corradini, P., & Cavallo, L., *Influence of 1,3-diethers on the stereospecificity of propene polymerization by supported Ziegler-Natta catalysts. A theoretical investigation on their adsorption on (110) and (100) lateral cuts of MgCl<sub>2</sub> platelets*. *Macromolecules*, 2000. **33**: p. 1134.
81. Puhakka, E., Pakkanen, T.T., & Pakkanen, T.A., *Theoretical investigations on heterogeneous Ziegler-Natta catalyst supports: Stability of the electron donors at different coordination sites of MgCl<sub>2</sub>*. *Journal of Physical Chemistry A*, 1997. **101**: p. 6063.
82. Matsuoka, H., Liu, B., Nakatani, H., Nishiyama, I., & Terano, M., *Active sites deterioration of MgCl<sub>2</sub>-supported catalyst induced by the electron donor extraction by alkylaluminium*. *Polymer International*, 2002. **51**: p. 781.
83. Liu, B., Nitta, T., Nakatani, H., & Terano, M., *Stereospecific nature of active sites on TiCl<sub>4</sub>/MgCl<sub>2</sub> Ziegler-Natta catalyst in the presence of an internal electron donor*. *Macromolecular Chemistry and Physics*, 2003. **204**: p. 395.
84. Garoff, T., Virkkunen, V., Jaaskelainen, P., Vestberg, T., *A qualitative model for polymerisation of propylene with a MgCl<sub>2</sub>-supported TiCl<sub>4</sub> Ziegler-Natta catalyst*. *European Polymer Journal*, 2003. **39**: p. 1679.
85. Nitta, T., Liu, B., Nakatani, H., & Terano, M., *Formation, deactivation and transformation of stereospecific active sites on TiCl<sub>4</sub>/dibutylphthalate/Mg(OEt)<sub>2</sub> catalyst induced by short time reaction with Al-alkyl cocatalyst*. *Journal of Molecular Catalysis A: Chemical*, 2002. **180**: p. 25.
86. Yang, C.-B., & Hsu, C.C., *Effect of catalyst aging on catalyst activity and stereospecificity for MgCl<sub>2</sub>/ethyl benzoate or dioctyl phthalate/TiCl<sub>4</sub>-triethylaluminium for propene polymerization*. *Macromolecular Rapid Communications*, 1995. **16**: p. 311.
87. Sacchi, M.C., Forlini, F., Tritto, I., Locatelli, P., Morini, G., Noristi, L., & Albizzati, E., *Polymerization stereochemistry with Ziegler-Natta catalysts containing*

- dialkylpropane diethers: A tool for understanding internal/external donor relationships*. *Macromolecules*, 1996. **29**: p. 3341.
88. Lim, S.-Y., & Choung, S.-J., *Effects of external electron donor on catalyst active sites in propylene polymerization*. *Journal of Applied Polymer Science*, 1998. **67**: p. 1779–1787.
89. Barbe, P.C., Cecchin, G., & Noristi, L., *The catalytic system Ti-complex/MgCl<sub>2</sub>*. *Advances in Polymer Science*, 1986. **81**: p. 1.
90. Sacchi, M.C., Tritto, I., Shan, C., Mendichi, R., & Noristi, L., *Role of the pair of internal and external donors in MgCl<sub>2</sub>-supported Ziegler-Natta catalysts*. *Macromolecules*, 1991. **24**: p. 6823.
91. Bukatov, G.D., & Zakharov, V.A., *Propylene Ziegler-Natta polymerization: Numbers and propagation rate constants for stereospecific and non-stereospecific centers*. *Macromolecular Chemistry and Physics*, 2001. **202**: p. 2003.
92. Proto, A., Oliva, L., Pellicchia, C., Sivak, A.J., & Cullo, L.A., *Isotactic-specific polymerization of propene with supported catalysts in the presence of different modifiers*. *Macromolecules*, 1990. **23**: p. 2904.
93. Kissin, Y.V., Chadwick, J.C., Mingozi, I., & Morini, G., *Isoselectivity distribution of isospecific centers in supported titanium-based Ziegler-Natta catalysts*. *Macromolecular Chemistry and Physics*, 2006. **207**: p. 1344.
94. Kang, K.K., Shiono, T., Jeong, Y.-T., & Lee, D.-H., *Polymerization of propylene by using Mg(OEt)<sub>2</sub>-DNBP-TiCl<sub>4</sub> catalyst with alkoxy disilanes as external donor*. *Journal of Applied Polymer Science*, 1999. **71**: p. 293.
95. Sacchi, M.C., Forlini, F., Tritto, I., Mendichi, R., Zannoni, G., & Noristi, L., *Activation effect of alkoxy silanes as external donors in MgCl<sub>2</sub>-supported Ziegler-Natta catalysts*. *Macromolecules*, 1992. **25**: p. 5914.
96. Shimizu, F., Pater, J.T.M., Van Swaaij, W.P.M., & Weickert, G., *Kinetic study of a highly active MgCl<sub>2</sub>-supported Ziegler-Natta catalyst in liquid pool propylene polymerization. II. The influence of alkyl aluminum and alkoxy silane on catalyst activation and deactivation*. *Journal of Applied Polymer Science*, 2002. **83**: p. 2669.
97. Xu, J., Feng, L., Yang, S., Yang, Y., & Kong, X., *Influence of electron donors on the tacticity and the composition distribution of propylene-butene copolymers produced by supported Ziegler-Natta catalysts*. *Macromolecules*, 1997. **30**: p. 7655.
98. Liu, B., Matsuoka, H., & Terano, M., *Stopped-flow techniques in Ziegler catalysis*. *Macromolecular Rapid Communications*, 2001. **22**: p. 1.



99. Zakharov, V.A., Bukatov, G.D., & Barabanov, A.A., *Recent data on the number of active centers and propagation rate constants in olefin polymerization with supported ZN catalysts*. Macromolecular Symposium, 2004. **213**: p. 19.
100. Bukatov, G.D., Zakharov, V.A., & Barabanov, A.A., *Mechanism of olefin polymerization on supported Ziegler–Natta catalysts based on data on the number of active centers and propagation rate constants*. Kinetics and Catalysis, 2005. **46**: p. 166.
101. Busico, V., Chadwick, J.C., Cipullo, R., Ronca, S., & Talarico, G., *Propene/ethene-[1-<sup>13</sup>C] copolymerization as a tool for investigating catalyst regioselectivity. MgCl<sub>2</sub>/internal donor/TiCl<sub>4</sub>-external donor/AlR<sub>3</sub> systems*. Macromolecules, 2004. **37**: p. 7437.
102. Matsuoka, H., Liu, B., Nakatani, H., & Terano, M., *Variation in the isospecific active sites of internal donor-free MgCl<sub>2</sub>-supported Ziegler catalysts: Effect of external electron donors*. Macromolecular Rapid Communications, 2001. **22**: p. 326.
103. Chadwick, J.C., *Advances in propene polymerization using MgCl<sub>2</sub>-supported catalysts. Fundamental aspects and the role of electron donor*. Macromolecular Symposium, 2001. **173**: p. 21.
104. Chadwick, J.C., Morini, G., Balbontin, G., Camurati, I., Heere, J.J.R., Mingozi, I., Testoni, F., *Effects of internal and external donors on the regioand stereoselectivity of active species in MgCl<sub>2</sub>-supported catalysts for propene polymerization*. Macromolecular Chemistry and Physics, 2001. **202**: p. 1995.
105. Chadwick, J.C., Morini, G., Balbontin, G., & Sudmeijer, O., *Effect of polymerization temperature on the microtacticity of isotactic poly(propylene) prepared using heterogeneous (MgCl<sub>2</sub>-supported) Ziegler-Natta catalysts*. Macromolecular Chemistry and Physics, 1998. **199**: p. 1873.
106. Busico, V., Corradini, P., De Martino, L., Proto, A., & Albizzati, E., *Polymerization of propene in the presence of MgCl<sub>2</sub>-supported Ziegler-Natta catalysts, 2 a) Effects of the co-catalyst composition*. Makromolekulare Chemie, 1986. **187**: p. 1115.
107. Busico, V., Corradini, P., Ferraro, A., & Proto, A., *Polymerization of propene in the presence of MgCl<sub>2</sub>-supported Ziegler-Natta catalysts, 3 a) Catalyst deactivation*. Makromolekulare Chemie, 1986. **187**: p. 1125.
108. Busico, V., Cipullo, R., Corradini, P., & De Biasio, R., *Propene polymerization in the presence of MgCl<sub>2</sub>-supported Ziegler-Natta catalysts, 5 a) Microstructural*

- characterization of the "isotactic" (heptane-insoluble) polypropene fractions.* Macromolecular Chemistry and Physics, 1995. **196**: p. 491.
109. Kakugo, M., Miyatake, T., Naito, Y., & Mizunuma, K., *Microtacticity distribution of polypropylenes prepared with heterogeneous Ziegler-Natta catalysts.* Macromolecules, 1988. **21**: p. 314.
110. Sacchi, M.C., Tritto, I., & Locatelli, P., *Stereochemical investigation of the effect of lewis bases in heterogeneous Ziegler-Natta initiator systems.* Progress in Polymer Science, 1991. **16**: p. 331.
111. Busico, V., Cipullo, R., Monaco, G., Talarico, G., Vacatello, M., Chadwick, J.C., Segre, A.L., & Sudmeijer, O., *High-resolution <sup>13</sup>C NMR configurational analysis of polypropylene made with MgCl<sub>2</sub>-supported Ziegler-Natta catalysts. 1. The "model" system MgCl<sub>2</sub>/TiCl<sub>4</sub>-2,6-dimethylpyridine/Al(C<sub>2</sub>H<sub>5</sub>)<sub>3</sub>.* Macromolecules, 1999. **32**: p. 4173.
112. Liu, B., Nitta, T., Nakatani, H., & Terano, M., *Specific roles of Al-alkyl cocatalyst in the origin of isospecificity of active sites on donor-free TiCl<sub>4</sub>/MgCl<sub>2</sub> Ziegler-Natta catalyst.* Macromolecular Chemistry and Physics, 2002. **203**: p. 2412.
113. Liu, B., Nitta, T., Nakatani, H., & Terano, M., *Precise arguments on the distribution of stereospecific active sites on MgCl<sub>2</sub>-supported Ziegler-Natta catalysts.* Macromolecular Symposium, 2004. **213**: p. 7.
114. Busico, V., Cipullo, R., Polzone, C., Talarico, G., & Chadwick, J.C., *Propene/ethene-[1-<sup>13</sup>C] copolymerization as a tool for investigating catalyst regioselectivity. 2. The MgCl<sub>2</sub>/TiCl<sub>4</sub>-AlR<sub>3</sub> system.* Macromolecules, 2003. **36**: p. 2616.
115. Burfield, D.R., *Ziegler-Natta polymerization: the nature of the propagation step.* Polymer, 1984. **25**: p. 1645.
116. Pino, P., & Rotzinger, B., *Recent developments in the polymerization of olefins with organometallic catalysts.* Macromolecular Chemistry and Physics, Supplement, 1984. **7**: p. 41.
117. Spitz, R., Lacombe, J.L., & Guyot, A., *Ziegler-Natta catalysts supported on magnesium chloride for stereocontrolled propene polymerization. II. Simple catalytic system: solid binary magnesium chloride-titanium tetrachloride system and cocatalytic solution of triethylaluminum and ethyl benzoate.* Journal of Polymer Science, Polymer Chemistry Edition, 1984. **22**: p. 2625.



118. Keii, T., Suzuki, E., Tamura, M., Murata, M., & Doi, Y., *Propene polymerization with a magnesium chloride-supported Ziegler catalyst. 1. Principal kinetics.* Makromolekulare Chemie, 1982. **183**: p. 2285.
119. Chadwick, J.C., Miedema, A., & Sudmeijer, O., *Hydrogen activation in propene polymerization with MgCl<sub>2</sub>-supported Ziegler-Natta catalysts: The effect of the external donor.* Macromolecular Chemistry and Physics, 1994. **195**: p. 167.
120. Lieberman, R., *Propylene polymers*, in *Encyclopedia of polymer science and technology*  
H.F. Mark, Editor. 2003, John Wiley & Sons: Hoboken. p. 287.
121. Busico, V., Cipullo, R., Monaco, G., Vacatello, M., & Segre, A.L., *Full assignment of the <sup>13</sup>C NMR spectra of regioregular polypropylenes: Methyl and methylene region.* Macromolecules, 1997. **30**: p. 6251.
122. Busico, V., Cipullo, R., Monaco, G., Vacatello, M., Bella, J., & Segre, A.L., *Full assignment of the <sup>13</sup>C NMR spectra of regioregular polypropylenes: Methine region.* Macromolecules, 1998. **31**: p. 8713.
123. Busico, V., and Cipullo, R., *Microstructure of polypropylene.* Progress in Polymer Science, 2001. **26**: p. 443.
124. Lotz, B., Wittmann, J.C., & Lovinger, A.J., *Structure and morphology of poly(propylenes): a molecular analysis.* Polymer, 1996. **37**: p. 4979.
125. Karger-Kocsis, J., *Polypropylene: an A-Z reference.* 1999, Dordrecht, the Netherlands: Kluwer Academic Publishers.
126. Mathieu, C., Thierry, A., Wittmann, J.C., & Lotz, B., *"Multiple" nucleation of the (010) contact face of isotactic polypropylene, alpha phase.* Polymer, 2000. **41**: p. 7241.
127. Kroschwitz, J.I., Mark, H.F., Bikales, N.M., Overberger, C.G., & Menges, G., ed. *Encyclopedia of Polymer Science and Engineering.* Second ed. Vol. 13. 1985, John Wiley & Sons: New York. p. 464.
128. Phillips, R.A., & Wolkowicz, M.D., *Structure and morphology*, in *Polypropylene Handbook*, E.P. Moore, Jr., Editor. 2002, Hanser: Munich. p. 113.
129. Yamada, K., Matsumoto, S., Tagashira, K., & Hikosaka, M., *Isotacticity dependence of spherulitic morphology of isotactic polypropylene.* Polymer, 1998. **39**: p. 5327.
130. Del Duca, D., & Moore, E.P, Jr., *End-use properties*, in *Polypropylene Handbook*, E.P. Moore, Jr., Editor. 2002, Hanser: Munich. p. 237.

131. Alamo, R.G., Kim, M-H., Galante, M.J., Isasi, J.R., & Mandelkern, L., *Structural and kinetic factors governing the formation of the  $\gamma$  polymorph of isotactic polypropylene*. *Macromolecules*, 1999. **32**: p. 4050.
132. Auriemma, F., & De Rosa, C., *Crystallization of metallocene-made isotactic polypropylene: Disordered modifications intermediate between the  $\alpha$  and  $\gamma$  forms*. *Macromolecules*, 2002. **35**: p. 9057.
133. Busico, V., Corradini, P., De Rosa, C., & Di Benedetto, E, *Physico-chemical and structural characterization of ethylene-propene copolymers with low ethylene content from isotactic-specific Ziegler-Natta catalysts*. *European Polymer Journal*, 1985. **21**(3): p. 239.
134. Yamada, K., Hikosaka, M., Toda, A., Yamazaki, S., & Tagashira, K., *Equilibrium melting temperature of isotactic polypropylene with high tacticity: 1. Determination by differential scanning calorimetry*. *Macromolecules*, 2003. **36**: p. 4790.
135. Yamada, K., Hikosaka, M., Toda, A., Yamazaki, S., & Tagashira, K., *Equilibrium melting temperature of isotactic polypropylene with high tacticity. 2. Determination by optical microscopy*. *Macromolecules*, 2003. **36**: p. 4802.
136. Huang, T.W., Alamo, R.G., & Mandelkern, L., *Fusion of isotactic poly(propylene)*. *Macromolecules*, 1999. **32**: p. 6374.
137. Alamo, R.G., Brown, G.M., Mandelkern, L., Lehtinen, A., & Paukkeri, R., *A morphological study of a highly structurally regular isotactic poly(propylene) fraction*. *Polymer*, 1999. **40**: p. 3933.
138. Paukkeri, R., & Lehtinen, A., *Thermal behaviour of polypropylene fractions: 2. The multiple melting peaks*. *Polymer*, 1993. **34**(19): p. 4083.
139. Bartczak, Z., Chiono, V., & Pracella, M., *Blends of propylene-ethylene and propylene-1-butene random copolymers: I. Morphology and structure*. *Polymer*, 2004. **45**: p. 7549.
140. Zhang, M., Gong, Y., & He, T., *Multiple melting behaviour of isotactic polypropylene and poly(propylene-co-ethylene) after stepwise isothermal crystallisation*. *European Polymer Journal*, 2003. **39**: p. 2315.
141. Wend, J., Olley, R.H., Bassett, D.C., & Jaaskelainen, P., *Crystallization of propylene-ethylene random copolymers*. *Journal of Polymer Science Part B: Polymer Physics*, 2004. **42**(18): p. 3318.
142. Quirk, R.P., & Alsamarraie, M.A.A., *Physical properties of poly(propylene)*. *Polymer Handbook*, ed. E.H. Immergut. 1989, New York: John Wiley & Sons.

143. Moore, E.P., Jr., & Larson, G.A., *Introduction to PP in business*, in *Polypropylene handbook*, E.P. Moore, Jr., Editor. 2002, Hanser: Munich. p. 257.
144. Di Drusco, G., & Rinaldi, R., *High yield polypropylene*. Hydrocarbon Processing, International Edition, 1981. **60**: p. 153.
145. Rexall Drug and Chemical Co., 1981, British patent 1,044,811
146. Smith, D.E., Keeler, R.M., & Guenther, E., 1969, Polymerization process control and apparatus therefor, U.S. Patent 3,476,729
147. Ross, J.F., & Bowles, W.A., *An improved gas-phase polypropylene process*. Industrial & Engineering Chemistry Product Research and Development, 1985. **24**: p. 149.
148. Desreux, V., & Spiegels, M.C., *Fractionation of polyethylene by extraction*. Bulletin des Societes Chimiques Belges, 1950. **59**: p. 476.
149. Shirayama, K., Okada, T. & Kita, S, *Distribution of short-chain branching in low-density polyethylene*. Journal of Polymer Science Part A, 1965. **3**: p. 907.
150. See, B., & Smith, T.G., *Estimating the fractionation conditions for linear polyethylene and isotactic polypropylene*. Journal of Applied Polymer Science, 1966. **10**: p. 1625.
151. Guillet, J.E., Combs, R.L., Slonaker, D.F., & Coover, H.W., *Chromatographic fractionation of polyethylene*. Journal of Polymer Science, 1960: p. 307.
152. Wild, L., *Temperature rising elution fractionation*. Advances in Polymer Science, 1990. **98**(1): p. 1.
153. Soares, J.B.P., & Hamielac, A.E., *Temperature rising elution fractionation*, in *Modern Techniques for Polymer Characterisation*, R.A. Pethrick, and Dawkins, J.V., Editor. 1999, John Wiley & Sons: Chichester. p. 15.
154. Fonseca, C.A., & Harrison, I.R., *Temperature rising elution fractionation*, in *Modern Techniques for Polymer Characterisation*, R.A. Pethrick, and Dawkins, J.V., Editor. 1999, John Wiley & Sons: Chichester. p. 1.
155. Xu, J., & Feng, L., *Application of temperature rising elution fractionation in polyolefins*. European Polymer Journal, 2000. **36**: p. 867.
156. Glockner, G., *Temperature rising elution fractionation: A review*. Journal of Applied Polymer Science: Applied Polymer Symposium, 1990. **45**: p. 1.
157. Wild, L., Ryle, T.R., Knobloch, D.C., & Peat, I.R., *Determination of branching distributions in polyethylene and ethylene copolymers*. Journal of Polymer Science: Polymer Physics Edition, 1982. **20**: p. 441.

158. Mirabella, F.M.J., *Temperature rising elution fractionation (TREF) characterisation of polypropylene copolymers*. Journal of Liquid Chromatography, 1994. **17**(14 & 15): p. 3201.
159. Usami, T., Gotoh, Y., & Takayama, S., *Generation mechanism of short-chain branching distribution in linear low-density polyethylenes*. Macromolecules, 1986. **19**(11): p. 2722.
160. Bergstrom, C., & Avela, E., *Investigation of the composite molecular structure of LDPE by using temperature rising elution fractionation*. Journal of Applied Polymer Science, 1979. **23**: p. 163.
161. Nakano, S., & Goto, Y., *Development of automatic cross fractionation: Combination of crystallisability fractionation and molecular weight fractionation*. Journal of Applied Polymer Science, 1981. **26**: p. 4217.
162. Mirabella, F.M.J., & Ford, E.A., *Characterisation of linear low-density polyethylene: Cross-fractionation according to copolymer composition and molecular weight*. Journal of Polymer Science: Part B: Polymer Physics, 1987. **25**: p. 777.
163. Zhang, Y.-D., Wu, C.-J., & Zhu, S.-N., *Fractionation and characterisation for a propylene-ethylene random copolymer*. Polymer Journal, 2002. **34**(9): p. 700.
164. Wild, L., & Knobloch, D.C., 1991, Process for fractionating polymers, United States of America 5,030,713
165. Wild, L., & Blatz, C., *Development of high performance TREF for polyolefin analysis*. Polymeric Materials: Science and Engineering, 1992. **67**: p. 153.
166. Monrabel, B., *Temperature rising elution fractionation and crystallisation analysis fractionation*. Encyclopaedia of Analytical Chemistry. Vol. 9. 2000, Chichester: John Wiley & Sons Ltd. 8074
167. Zhang, Y.-D., Gou, Q.-Q., Wang, J., & Wu, C.-J., *<sup>13</sup>C NMR, GPC, and DSC study on a propylene-ethylene-1-butene terpolymer fractionated by temperature rising elution fractionation*. Polymer Journal, 2003. **35**(7): p. 551.
168. Feng, Y., & Hay, J.N., *The measurement of compositional heterogeneity in a propylene-ethylene block copolymer*. Polymer, 1998. **39**(26): p. 6723.
169. Xu, J., Fu, Z., Fan, Z., & Feng, L., *Temperature rising elution fractionation of PP/PE alloy and thermal behaviour of the fractions*. European Polymer Journal, 2002. **38**: p. 1739.
170. Mirabella, F.M.J., *Correlation of the elution behaviour in temperature rising elution fractionation and melting in the solid state and in the presence of a diluent of*

- polyethylene copolymers*. Journal of Polymer Science: Part B: Polymer Physics, 2001. **39**: p. 2819.
171. Soares, J.B.P., & Hamielac, A.E., *Temperature rising elution fractionation of linear polyolefins*. Polymer, 1995. **36**(8): p. 1639.
172. Monrabel, B., 1991, Crystallisation analysis fractionation, United States of America 5,222,390
173. Monrabel, B., *Crystallisation analysis fractionation: A new technique for the analysis of branching distribution in polyolefins*. Journal of Applied Polymer Science, 1994. **52**: p. 491.
174. Monrabel, B., *CRYSTAF: Crystallisation analysis fractionation. A new approach to the composition analysis of semi-crystalline polymers*. Macromolecular Symposium, 1996. **110**: p. 81.
175. Britto, L.J.D., Soares, J.B.P., Penlidis, A., & Monrabal, B., *Polyolefin analysis by single-step crystallisation fractionation*. Journal of Polymer Science: Part B: Polymer Physics, 1999. **37**: p. 539.
176. Sarzotti, D.M., Soares, J.B.P., & Penlidis, A., *Ethylene/1-hexene copolymers synthesized with a single-site catalyst: Crystallisation analysis fractionation, modeling, and reactivity ratio estimation*. Journal of Polymer Science: Part B: Polymer Physics, 2002. **40**: p. 2595.
177. Monrabel, B., Blanco, J., Nieto, J., & Soares, J.B.P., *Characterisation of homogeneous ethylene/1-octene copolymers made with a single-site catalyst. CRYSTAF analysis and calibration*. Journal of Polymer Science: Part A: Polymer Chemistry, 1999. **37**: p. 89.
178. Bruaseth, I., Soares, J.B.P., & Rytter, E., *Crystallisation analysis fractionation of ethylene/1-hexene copolymers made with the MAO-activated dual-site (1,2,4-Me<sub>3</sub>Cp)<sub>2</sub>ZrCl<sub>2</sub> and (Me<sub>5</sub>Cp)<sub>2</sub>ZrCl<sub>2</sub> system*. Polymer, 2004. **45**: p. 7853.
179. Vilaplana, F., Morera-Esrich, V., Hierro-Navarro, P., Monrabel, B., & Ribes-Greus, A., *Performance of crystallisation analysis fractionation and preparative fractionation on the characterisation of  $\gamma$ -irradiated low-density polyethylene*. Journal of Applied Polymer Science, 2004. **94**: p. 1803.
180. Monrabal, B., Sancho-Tello, J., Mayo, N., & Romero, L., *Crystallization elution fractionation. A new separation process for polyolefin resins*. Macromolecular Symposium, 2008. **257**: p. 71.

181. Shan, C.L.P., deGroot, W.A., Hazlitt, L.G., Gillespie, D., *A new turbidimetric approach to measuring polyethylene short chain branching distributions*. *Polymer*, 2005. **46**: p. 11755–11767.
182. van Reenen, A.J., Rohwer, E.G., Walters, P., Lutz, M., & Brand, M., *Development and use of a turbidity analyzer for studying the solution crystallization of polyolefins*. *Journal of Applied Polymer Science*, 2008. **109**: p. 3238.
183. Kostanski, L.K., Keller, D.M., & Hamielac, A.E., *Size-exclusion chromatography - a review of calibration methodologies*. *Journal of Biochemical and Biophysical Methods*, 2004. **58**: p. 159.
184. Kroschwitz, J.I., Mark, H.F., Bikales, N.M., Overberger, C.G., & Menges, G., ed. *Encyclopedia of Polymer Science and Engineering*. Second ed. Vol. 7. 1985, John Wiley & Sons: New York. p. 298.
185. Moore, W.R., & Boden, G.F., *Heptane-soluble material from atactic polypropylene. I. Fractionation and characterization of fractions*. *Journal of Applied Polymer Science*, 1965. **9**: p. 2019.
186. Baijal, M.D., Dilter, R.M., & Pool, F.R., *The molecular weight fractionation of polypropylene*. *Macromolecules*, 1969. **2**(6): p. 679.
187. Heinz, L.-C., & Pasch, H., *High-temperature gradient HPLC for the separation of polyethylene–polypropylene blends*. *Polymer*, 2005. **46**: p. 12040–12045.
188. Paukkeri, R., & Lehtinen, A., *Thermal behaviour of polypropylene fractions: I. Influence of tacticity and molecular weight on crystallization and melting behaviour*. *Polymer*, 1993. **34**(19): p. 4075.
189. Becker, R.F., Burton, L.P.J., & Amos, S.E., *Additives*, in *Polypropylene handbook*, E.P. Moore, Jr., Editor. 2002, Hanser: Munich. p. 177.
190. Tang, J., Wang, Y., Liu, H., & Belfiore, L.A., *Effects of organic nucleating agents and zinc oxide nanoparticles on isotactic polypropylene crystallization*. *Polymer*, 2004. **45**: p. 2081.
191. Xu, T., Lei, H., & Xie, C.S., *The effect of nucleating agent on the crystalline morphology of polypropylene (PP)*. *Materials and Design*, 2003. **24**: p. 227–230.
192. Foresta, T., Piccarolo, S., & Goldbeck-Wood, G., *Competition between alpha and gamma phases in isotactic polypropylene: effects of ethylene content and nucleating agents at different cooling rates*. *Polymer*, 2001. **42**: p. 1167.



193. Zhang, P., Liu, X., Li, Y., *Influence of  $\beta$ -nucleating agent on the mechanics and crystallization characteristics of polypropylene*. *Materials Science and Engineering A*, 2006. **434**: p. 310.
194. Balta'-Calleja, F.J., *Microhardness relating to crystalline polymers*. *Advances in Polymer Science*, 1985. **66**: p. 117.
195. Balta'-Calleja, F.J., Martinez-Salazar, J., & Asano, T., *Phase changes in isotactic polypropylene measured by microhardness*. *Journal of Materials Science Letters*, 1988. **7**: p. 165.
196. Henning, S., Michler, G.H., Ania, F., & Balta' -Calleja, F.J., *Microhardness of  $\alpha$ - and  $\beta$ -modified isotactic polypropylene at the initial stages of plastic deformation: analysis of micromechanical processes*. *Colloid Polymer Science*, 2005. **283**: p. 486.
197. Koch, T., Seidler, S., Halwax, E., & Bernstorff, S., *Microhardness of quenched and annealed isotactic polypropylene*. *Journal of Materials Science*, 2007. **42**: p. 5318.
198. Seidler, S., & Koch, T., *Determination of local mechanical properties of  $\alpha$ - and  $\beta$ -PP by means of microhardness measurements*. *Journal of Macromolecular Science: Part B, Physics*, 2002. **B41**: p. 851.
199. Seidler, S., & Koch, T., *Morphology - property correlations of PP materials by means of microhardness*. *Macromolecular Symposium*, 2004. **217**: p. 329.
200. Lorenzo, V., Perena, J.M., & Fatou, J.G., *Vickers microhardness related to mechanical properties of polypropylene*. *Journal of Materials Science Letters*, 1989. **8**: p. 1455.
201. Labour, T., Gauthier, C., Seguela, R., Vigier, G., Bomal, Y., & Orange, G., *Influence of the  $\beta$  crystalline phase on the mechanical properties of unfilled and  $\text{CaCO}_3$ -filled polypropylene. I. Structural and mechanical characterisation*. *Polymer*, 2001. **42**: p. 7127.
202. Flores, A., Aurrekoetxea, J., Gensler, R., Kausch, H.H., & Balta' Calleja, F.J., *Microhardness-structure correlation of iPP/EPR blends: influence of molecular weight and EPR particle content*. *Colloid Polymer Science*, 1998. **276**: p. 786.
203. Menard, K.P., *Dynamic mechanical analysis: A practical introduction*. 1999, Boca Raton: CRC Press.
204. Samios, D., Tokumoto, S., & Denardin, E.L.G., *Investigation of the large plastic deformation of iPP induced by plane strain compression: Stress-strain behavior and*

- thermo-mechanical properties*. International Journal of Plasticity, 2006. **22**: p. 1924–1942.
205. Bartczak, Z., & Pracella, M., *Blends of propylene-ran-ethylene and propylene-ran-(1-butene) copolymers: Crystal superstructure and mechanical properties*. European Polymer Journal, 2006. **42**: p. 1819–1829.
206. Stern, C., Frick, A., & Weickert, G., *Relationship between the structure and mechanical properties of polypropylene: Effects of the molecular weight and shear-induced structure*. Journal of Applied Polymer Science, 2007. **103**: p. 519.
207. De Rosa, C., Auriemma, F., Di Capua, A., Resconi, L., Guidotti, S., Camurati, I., Nifant'ev, I.E., & Laishevtsev, I.P., *Structure-property correlations in polypropylene from metallocene catalysts: Stereodeficient, regioregular isotactic polypropylene*. Journal of the American Chemical Society, 2004. **126**: p. 17040.
208. De Rosa, C., & Auriemma, F., *Structural-mechanical phase diagram of isotactic polypropylene*. Journal of the American Chemical Society, 2006. **128**: p. 11024.
209. De Rosa, C., Auriemma, F., & De Ballesteros, O.R., *The role of crystals in the elasticity of semicrystalline thermoplastic elastomers*. Chemical of Materials, 2006. **18**: p. 3523.



## **Chapter 3. General experimental details**

During the course of the project various materials and analytical methods were used. The following chapter gives the detail on where the materials were sourced from as well as the methods and settings used during the preparation and analysis of materials.

### **3.1 Polymerisation materials and equipment**

The catalyst used for all the polymerisations conducted during the course of the project was obtained from Star Chemicals Co. (China) and is designated as catalyst NT-1. The catalyst contains di-isobutyl phthalate as an internal donor, has a titanium content of 2.78% and magnesium content of 16.9% and was used as received. Triethylaluminium was obtained from Sigma-Aldrich as a 1.0 M solution in hexane and was used as received. Toluene was obtained from Merck and was distilled over sodium/benzophenone according to standard procedures before use. Diphenyl dimethoxy silane and methyl phenyl dimethoxy silane were obtained from Sigma-Aldrich and were used as received. Propylene monomer was obtained from Sigma-Aldrich at a purity > 99% and was used as received. High purity Argon obtained from Afrox was used for all air-sensitive materials in both the glove box and schlenk lines. All catalyst preparation work and subsequent manipulations were performed using standard glove box and schlenk line techniques.

Polymerisations were carried out in a 300 mL stainless steel reactor equipped with inlets for catalyst and monomer gas introduction and a pressure gauge. Reactor temperature was controlled by placing the reactor in an oil bath set at a designated temperature. Details regarding the polymerisation are discussed further in the relevant chapters.

### **3.2 Fractionation techniques**

#### **3.2.1 TREF**

Preparative temperature rising elution fractionation was performed on various samples during the course of the project. The TREF method is based on two separate steps namely the crystallisation step and the elution step. The instrumentation used was built in-house [1].

### 3.2.1.1 The crystallisation step

The crystallisation step of the TREF analysis is illustrated in Figure 3.1.

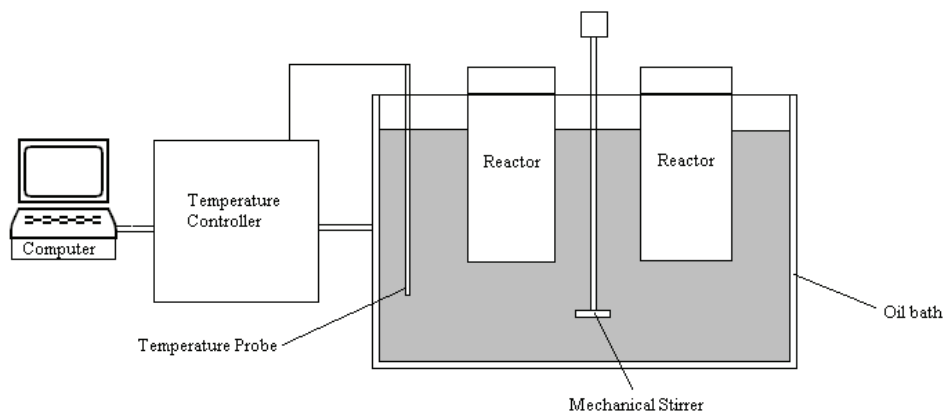


**Figure 3.1** The setup used for the TREF crystallisation step.

The propylene homo- or copolymer (3 g) and Irganox 1010 stabiliser (2% w/v) were dissolved in xylene (300 mL) at 130 °C in a stirred glass reactor which was placed in an oil bath and equipped with a reflux condenser. The reactor containing the dissolved polymer and stabiliser was then transferred to a larger oil bath which had been preheated to 130 °C. This larger oil bath, which was used for the crystallisation step, was large enough to accommodate four reactors so that they could all cool down simultaneously in order to save time. The inert support (washed sand white quartz -50 + 70 mesh) was also preheated to 130 °C before introduction into the reactor in order to prevent premature crystallisation onto cold sand and general lowering of the temperature in the reaction vessel. The hot sea sand was then added to the reactor in sufficient amounts as to cover the solution in the reactor so as to avoid any solution crystallisation in the absence of support material. The reactors in the oil bath were then cooled at 1 °C/h from 130 °C to 20 °C.

### 3.2.1.2 The elution step

The elution step involves the transfer of the polymer and support to a stainless steel column 15 cm in length and an internal diameter of 7.5 cm. The column is equipped with a hole in the bottom for a temperature probe so that the temperature at the middle of the column can be monitored ensuring an accurate fractionation temperature. The column packing is illustrated in Figure 3.2.

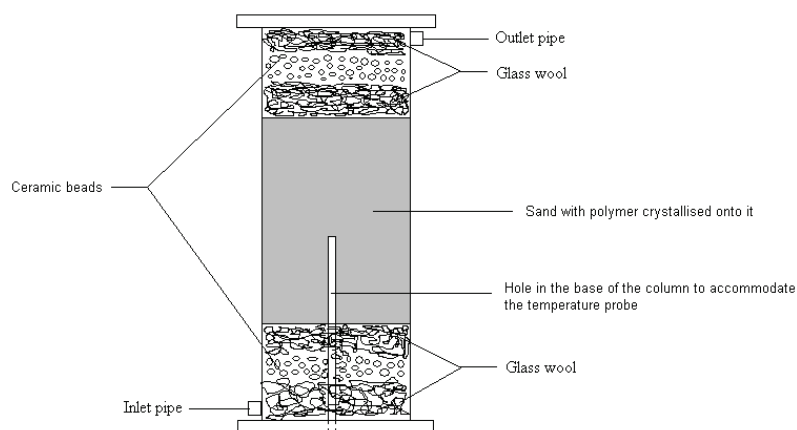


**Figure 3.2 Illustration of the column packing.**

The purpose of the glass wool and beads was to break up the solvent flow so as to prevent preferential solvent channelling. The column was then placed in a GC oven which served as the temperature controlled environment for the elution step. A pump controlled the flow of solvent through the column at a constant rate.

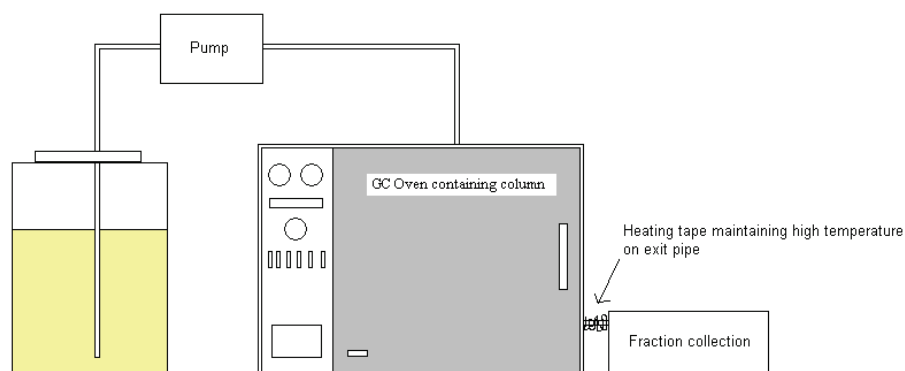


**Figure 3.3 The TREF elution setup.**

Heating tape, maintained at a constant temperature of 130 °C, was wound around the exit pipe as it emerged from the oven so as to prevent deposition of the fractions onto the cold pipe during collection of the fractions. The polymer fractions were then eluted from the column at successively higher temperatures. The column was heated to each predetermined temperature and was maintained at that temperature while the fraction was taken. Fractions were taken at various temperatures depending on the number of fractions that were required. The xylene which was used to elute the polymer was then removed on a rotary evaporator. Fractions isolated on the rotary evaporator were then dried in a vacuum oven until the weight of the fractions remained constant.

### 3.2.2 CRYSTAF

Crystallization analysis fractionation was carried out using a CRYSTAF commercial apparatus model 200 manufactured by Polymer Char S.A. (Valencia, Spain). The crystallization was carried out in 60 mL stirred, stainless steel reactors. Dissolution and filtration took place automatically in the reactors. Exactly 10 mg of each sample was dissolved in 30 mL 1,2,4-trichlorobenzene. The temperature was decreased at a rate of 0.10 °C/min from 100 °C to 30 °C. Fractions were taken automatically and the polymer concentration from solution was determined by an infrared detector, using 3.5 μm as the chosen wavelength.

## 3.3 Characterisation techniques

### 3.3.1 <sup>13</sup>C NMR

<sup>13</sup>C NMR spectra were recorded at 120 °C on a Varian VXR 600 MHz spectrometer in 1,1,2,2-tetrachloroethane-d<sub>2</sub>, using δ 74.3 as internal secondary reference. The pulse angle was 90 degrees, the relaxation delay was 15 seconds, and the acquisition time was 1.8 seconds.

The 1-pentene comonomer content (CM%) in the propylene copolymers used in a section of this study was calculated according to the following equation:

$$CM\% = \frac{C_{Br} + \frac{1}{2}(C_{\alpha})}{C_{\alpha} + C_{Br} + C_{Br-PP} + C_{\alpha-PP}} \times 100 \quad (1)$$

Essentially the carbons of the backbone belonging to the comonomer were integrated and the sum divided by the sum of all backbone carbons as illustrated in Figure 3.4:

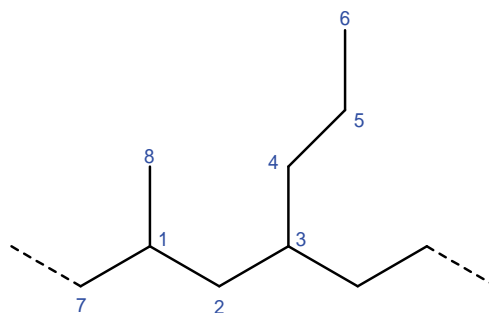


Figure 3.4 The structure of the propylene-1-pentene copolymer.

Table 3.1 The designation of the carbon atoms in the structure of the propylene-1-pentene copolymer

Carbon number in Figure 3.4	Designation	Observed chemical shift (ppm)
1	C <sub>Br-PP</sub>	28.7
2	C <sub>α</sub>	43.8
3	C <sub>Br</sub>	33.5
4	C <sub>α</sub> (1-pentene)	38.5
5	C <sub>β</sub> (1-pentene)	20.0
6	CH <sub>3</sub> (1-pentene)	14.7
7	C <sub>α-PP</sub>	46.4
8	CH <sub>3</sub> (propylene)	21.8

Precisely the same method was used for the determination of the comonomer content of all samples. The determination of the tacticity sequence distribution for the propylene-1-pentene copolymers was not possible due to the overlapping of the resonance of the C<sub>β</sub> (5 at  $\delta = 20.0$  ppm) of the 1-pentene comonomer with the *rrrm* and the *mrrm* steric pentad resonances in the methyl region of the propylene copolymer.

The pentad sequence distribution of the polypropylene homopolymer is assigned for the methyl region according to the nomenclature adopted by Busico *et al.* [2] and is given in Table 3.2.

Table 3.2 The assignment of the pentad sequences in the methyl region of the PP homopolymer samples

Chemical shift (ppm)	22.2-21.7	21.7-21.5	21.5-21.3	21.3-21.0	21.0-20.7	20.7-20.5	20.5-20.0	20.0-19.7
Pentad sequence	<i>mmmm</i> (%)	<i>mmmr</i> (%)	<i>rmmr</i> (%)	<i>mmrr</i> (%)	<i>mmrm</i> + <i>rrmr</i> (%)	<i>mrrm</i> (%)	<i>rrrm</i> + <i>rrrr</i> (%)	<i>mrrm</i> (%)

### 3.3.2 DSC

#### 3.3.2.1 Crystallisation and melting data

Crystallisation and melting points were determined by DSC. Samples were run on a TA Instruments Q100 DSC system calibrated with indium metal according to standard procedures. Heating and cooling rates were maintained at a standard 10 °C/minute. The samples of the standard fractions and original polymers were first subjected to a heating ramp up to 220 °C, after which the temperature was kept isothermally at 220 °C for 5 minutes to remove thermal history. The cooling cycle followed the isothermal stage, with the subsequent second heating scan being recorded for analysis. The crystallinities of the samples were determined by comparing the enthalpy of fusion of the samples ( $\Delta H_f$ ) to that of an ideal 100% crystalline polypropylene sample ( $\Delta H_{fc}$ ) according to equation 2.

$$w_c = \frac{\Delta H_f}{\Delta H_{fc}} \times 100 \quad (2)$$

A value of 209 J/g [3] was used as the enthalpy of fusion for the ideal 100% crystalline polypropylene.

#### 3.3.2.2 Lamellar thickness determination

The lamellar thickness distribution and average lamellar thickness were determined from the DSC melting endotherms using the Thomson-Gibbs equation [4, 5] which is given as equation 3:

$$T_m = T_m^0 \left( 1 - \frac{2\sigma_e}{l\Delta H_f} \right) \quad (3)$$

Where  $T_m$  is the melting temperature of the polymer,  $T_m^0$  is the equilibrium melting temperature (taken as 464 K),  $l$  is the lamellar thickness (longitudinal dimension of the crystal),  $\Delta H_f$  is the melting enthalpy of a perfect crystal (taken as 196 J/cm<sup>3</sup>), and  $\sigma_e$  is the free surface energy of the end faces of the chain fold (taken as 102.9 J/cm<sup>2</sup>). The lamellar thickness distribution can be expressed as equation 4:

$$\frac{1}{M} \frac{dM}{dl} = \frac{dE/dT(T_m^0 - T_m)^2 \rho_c}{2\sigma_e T_m^0 M} \quad (4)$$

The work of Crist and Mirabella [6] is noted for discussions on the distribution of lamellar thickness however for the purpose of this study the Thomson-Gibbs equation and breadth of the melting endotherm was used in order to compare samples.

### 3.3.3 HT-GPC

The molar mass of all samples were determined using high-temperature gel permeation chromatography (HT-GPC) relative to polystyrene standards. All samples were analysed on a PL-GPC 220 high temperature chromatograph (Polymer Laboratories) at a temperature of 160 °C and a flow rate of 1 mL/min. The column set used was four polystyrene/divinylbenzene copolymer packed columns (PL gel MIXED-B [9003-53-6]) from Polymer Laboratories. A 50 mm guard column was also used. The total column length was 1200 mm and the diameter was 7.5 mm. The columns have a particle size of 10 µm. The sample concentration used for all samples was 0.75 mg/mL and the solvent used was 1,2,4-trichlorobenzene, stabilized with 0.0125% 2,6-di-tert-butyl-4-methylphenol (BHT). BHT was used as a flow rate marker. Calibration of the instrument was done with monodisperse polystyrene standards (EasiCal from Polymer Laboratories). The detector used was a differential refractive index detector.

## 3.4 Mechanical properties

### 3.4.1 Extensional DMA

Samples for extensional DMA were analysed on a Perkin Elmer DMA 7e operating in extension mode. The samples analysed were melt pressed at 200 °C into films 50 µm thick. Small tensile bars were then cut out of the films using a special cutter built for this purpose.

### 3.4.2 Compressive DMA

Samples for compressive DMA analysis were examined on a Perkin Elmer DMA 7e calibrated according to standard procedures. The samples for compressive DMA were first melted at 200 °C for 8 minutes and then melt pressed at that temperature at 5 MPa pressure. The samples were analysed using a 5 °C/minute heating ramp with an applied force oscillating at a frequency of 1 Hz. The static force was kept constant at 110% of the dynamic force. The temperature range analysed was between -40 °C and 230 °C.

### 3.4.3 Microhardness

Microhardness measurements were conducted on a UHL microhardness tester equipped with a Vickers indenter. Measurements were obtained using 25 µm/s as the indentation speed and a dwell time of 15 s. Samples were analysed at indentation loads of 5 gf and 10 gf. The samples were first melted at 200 °C for 6 minutes before applying 3 MPa pressure for 3 minutes. The mould was then transferred to an ice bath for quench cooling. 20 measurements were taken for each sample analysed.

## 3.5 References

1. Harding, G.W., & van Reenen, A.J., *Fractionation and characterisation of propylene-ethylene random copolymers: Effect of the comonomer on crystallisation of poly(propylene) in the  $\gamma$ -phase*. *Macromolecular Chemistry and Physics*, 2006. **207**(18): p. 1680-1690.
2. Busico, V., Cipullo, R., Monaco, G., Vacatello, M., & Segre, A.L., *Full assignment of the  $^{13}\text{C}$  NMR spectra of regioregular polypropylenes: Methyl and methylene region*. *Macromolecules*, 1997. **30**: p. 6251-6263.
3. Quirk, R.P., & Alsamarraie, M.A.A., *Physical properties of poly(propylene)*. *Polymer Handbook*, ed. E.H. Immergut. 1989, New York: John Wiley & Sons.
4. Romankiewicz, A., & Sterzynski, T., *The lamellar distribution in isotactic polypropylene modified by nucleation and processing*. *Macromolecular Symposium*, 2002. **180**: p. 241-256.
5. Bershtein, V.A., & Egorov, V.M., *Differential scanning calorimetry of polymers: Physics, chemistry, analysis*. 1994, London: Ellis Horwood.



6. Crist, B., & Mirabella, F.M., *Crystal thickness distributions from melting homopolymers or random copolymers*. Journal of Polymer Science Part B: Polymer Physics, 1999. **37**: p. 3131-3140.

## Chapter 4. TREF fraction – property relationships

### 4.1 Introduction

Polypropylene has developed into one of the most widely used materials on the planet, aided by the diversity of applications available to the product. Research into the material has played an extremely important role in this development, with the correlation between the polymer microstructure and the properties of the polymer being of paramount importance.

The properties of the polypropylene homopolymer are governed on a microstructural level by the molar mass, the molar mass distribution, and the degree of regio- and stereoregularity of the polymer chains. Polypropylene copolymers have the additional, often dominating, influence of the comonomer on the polymer properties. These factors in turn affect the packing of the chains which affects the crystal phase of the crystalline regions. The formation and order of the crystal lamellae thus depend on these factors. The crystallites can in turn affect the formation of the next structural level of the polypropylene, namely the spherulitic morphology, although other structures are also possible (such as the skin-core morphology, cylindrites, axialites, quadrites etc. [1]) depending on a number of factors such as polymer processing.

The TREF technique has been, and is currently, extensively used to analyse semi-crystalline polymers. The ability of the technique to separate polymer chains on the basis of their crystallisability is very useful for the analysis of these materials, where the usefulness of the material is often determined by the manner in which the chains crystallise. The preparative TREF technique in particular is extremely powerful as it allows the subsequent offline analysis of any number of fractions, as designated by the operator. It is therefore possible to perform an in-depth analysis of a material and discover exactly what type of polymer chains are present in the material which crystallises out of solution at varying temperatures.

Since different properties are obtained from materials which crystallise differently due to the presence of different types of polymer chains, it follows that certain sections of a material therefore help to give that material its specific properties. It was therefore decided to investigate this by means of selectively removing TREF fractions from a material and observing the changes in properties. In order to investigate the methodology of selective fraction removal from the polymer we selected a propylene-1-pentene random copolymer as a target material, as we felt that the chemical heterogeneity of this group of polymers [2] would lead to easily observable changes in overall structure and properties upon removal of fractions. The methodology used was therefore to investigate the effect of the various TREF

fractions of a polypropylene-1-pentene copolymer on the polymer properties and then do the same for a polypropylene homopolymer. The data for the propylene-1-pentene copolymers serving as supporting evidence for the trends observed for the polypropylene homopolymer. The technique used, namely selective fraction removal, can therefore be seen as a “physical” method to alter the components of a given material. The “chemical” route to alter the makeup of a given polymer being the alteration of the polymerisation conditions, thereby altering the amount and type of the active sites present and thus forming polymers with different properties as discussed in Chapters 5 and 6.

## 4.2 Experimental

The general experimental procedures and methods used for the analytical techniques were discussed in Chapter 3. There are also various graphs contained in this work that use a dotted line to connect data points. These lines are in no way implying a continuous distribution of data for isolated data points and are simply meant to be a guide to the eye.

### 4.2.1 Polymer materials

Development work on the fractionation of the materials with subsequent removal of fractions was carried out using both a Ziegler-Natta catalysed polypropylene homopolymer (Moplen - Himont, Italy) and a Ziegler-Natta catalysed polypropylene-1-pentene copolymer (Sasol, South Africa).

**Table 4.1 The data summary for the polypropylene homopolymer (PPH) and copolymer (PP1P)**

Sample code	$M_n$ (g/mol)	$M_w$ (g/mol)	PD	$T_m$ (°C)	$T_c$ (°C)	Crystallinity (%)	1-pentene content (%)	<i>mmmm</i> (%)
PPH	1.3E+05	6.9E+05	5.20	158.58	112.28	84.11	N/A	90.49
PP1P	1.5E+05	6.2E+05	4.18	139.74	97.85	63.88	2.35	nd <sup>a</sup>

a = not determined (see Section 3.3.1)

The processing history of the samples is not known and so it is not clear if the samples were vis-broken or not although for the purposes of this study this information is not required.

### 4.2.2 Fractionation and recombination

The general TREF procedure is described in Chapter 3 (Section 3.2.1). The normal TREF characterisation of the two polymers used in the study was conducted according to standard TREF procedures. The samples requiring the removal of a specific TREF fraction

were also subjected to the standard TREF procedures, the main difference being that once the designated fraction had been removed the remaining material was first combined in solution before removal of the solvent on a rotary evaporator. The specific fractions were removed from the bulk material for each experiment, with the removal of each specific fraction requiring a separate TREF fractionation of the bulk material.

### **4.2.3 Polymer characterisation**

The  $^{13}\text{C}$  NMR, DSC, and HT-GPC data of the samples were obtained according to procedures described in Chapter 3 (Sections 3.3.1-3.3.3).

### **4.2.4 Mechanical properties**

The extensional and standard compression DMA data of the samples were obtained according to procedures described in Chapter 3 (Sections 3.4.1 and 3.4.2).

## **4.3 Results and discussion**

### **4.3.1 PP-1-pentene**

As can be seen from Table 4.1 the polypropylene-1-pentene sample is of a reasonably high molar mass with a relatively low polydispersity. The comonomer incorporation is relatively low at only 2.35% although the impact on the melting and crystallisation temperatures and degree of crystallinity compared to the homopolymer is readily apparent, with the peak melting temperature decreasing by almost 20 °C. The preparative TREF fractionation data is presented in the next section.

#### **4.3.1.1 PP-1-pentene characterisation**

The TREF data given in Figure 4.1 illustrate the contribution of each fraction to the composition of the polymer.

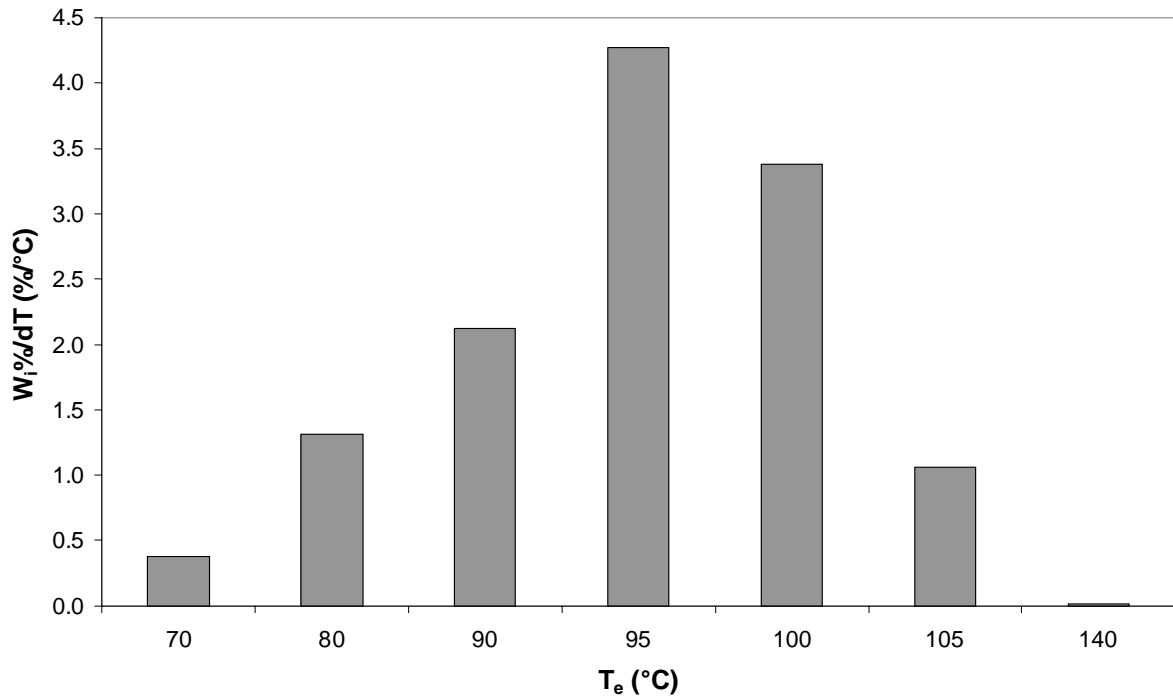


**Figure 4.1** The TREF fractionation data for sample PPI1.

The fractions are shown as the weight percentage of polymer material eluted at a certain temperature divided by the temperature range of that particular elution step thus enabling the direct comparison of the relative importance of each fraction. The fraction eluting at 95 °C clearly comprises the major fraction of material although the fractions at 100 °C and 90 °C also contribute significantly. This is in agreement with the major elution temperatures of earlier work on propylene-ethylene copolymers [3] where small amounts of a comonomer inhibits the ability of the chains to crystallise, thus lowering the temperature at which they crystallise out of solution as compared to the polypropylene homopolymer.

Figure 4.2 gives the weight average molar mass averages and polydispersity values for each TREF fraction. The molar mass tends to increase until the 100 °C fraction followed by a slight decrease in molar mass for the last two fractions. It is believed some lower molar mass material is trapped between the support and those chains that crystallise out of solution first at high temperature. This has also been shown to be the case for polypropylene impact copolymers where part of the high ethylene content copolymer or rubbery material has been found in the highest TREF fractions [4]. This material would not normally crystallise out at these temperatures and so some form of entrapment must be responsible. Degradation of material in the column at high temperature is also a possible reason for the presence of the lower molar mass material in the final two fractions.

The polydispersity of the fractions on the other hand tends to decrease as the elution temperature increases, a notable exception being the 105 °C fraction which seems to buck this trend. The values are all relatively low as one would expect from TREF fractions where small sections of a polymer are isolated.

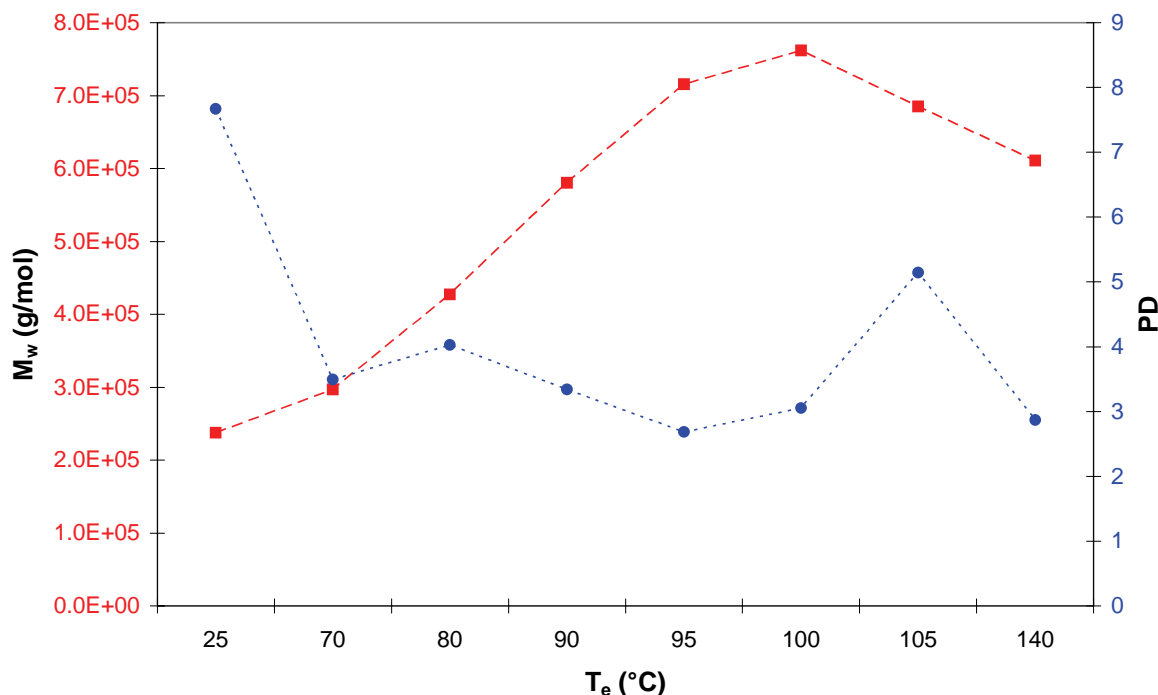


**Figure 4.2** The weight average molar mass and polydispersity data for the TREF fractions of sample PP1P.

The 1-pentene content of each fraction is given in Figure 4.3. There is a definite decrease in 1-pentene content as the fractionation temperature increases as would be expected. This is consistent with Flory's approximation on the effect of a comonomer on the melting point of a copolymer [5, 6]. The comonomer essentially disrupts the crystallisation of the chains, preventing them from crystallising as perfectly as they would have otherwise done. Unfortunately there was insufficient material eluted in the final fraction for <sup>13</sup>C NMR analysis. It should be noted that despite the low amounts of the 1-pentene present in the higher temperature fractions there are quantifiable amounts present indicating that the random inclusion of the comonomer occurs even in chains which can crystallise out of solution at high temperature. This does not mean per se that the 1-pentene is situated in the crystalline regions as it is more than likely mostly excluded from the crystals and is situated in the inter-crystalline regions.

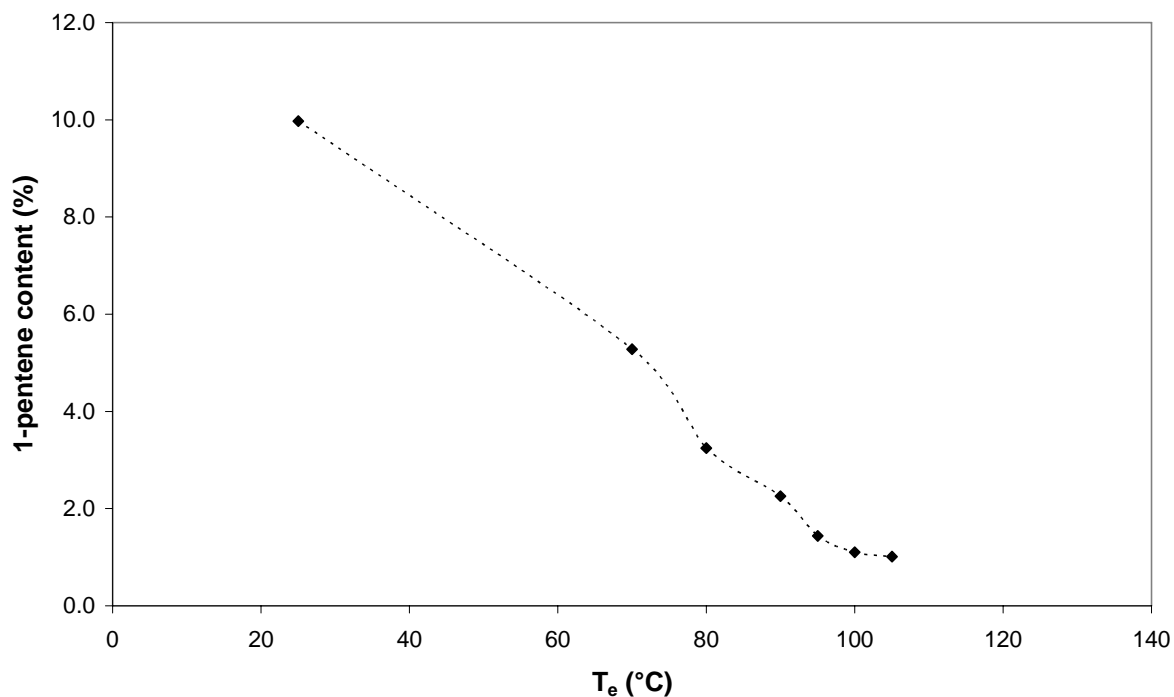


**Figure 4.3** The comonomer content of selected TREF fractions of sample PP1P.

The DSC data for the TREF fractions shown in Figure 4.4 show an increase in the melting temperature of the fractions as the fractionation temperature is increased as would be expected. The peak melting temperatures of the last two fractions are slightly lower than that of the preceding fraction despite the fact that this material crystallises first out of solution. This demonstrates that there is material present in these fractions (of a slightly lower molar mass as mentioned earlier) which is disrupting the crystallisation of the chains of that particular fraction, hence the slightly lowered melting points. This supports the hypothesis that there are lower molar mass chains being trapped during the initial crystallisation process. It is also noted, however, that there is evidence that the higher the molar mass of the chains in the solid state, the lower the rate of crystallisation, and the higher the tacticity (or the lower the comonomer content), the faster the rate of crystallisation [7]. These effects could also play a role in solution and therefore the slightly lower molar mass and low comonomer content could also result in fast crystallisation rates for the chains in the highest temperature fractions. This could in turn influence the melting of the chains since the faster crystallisation rates could lead to the formation of thinner lamellae.

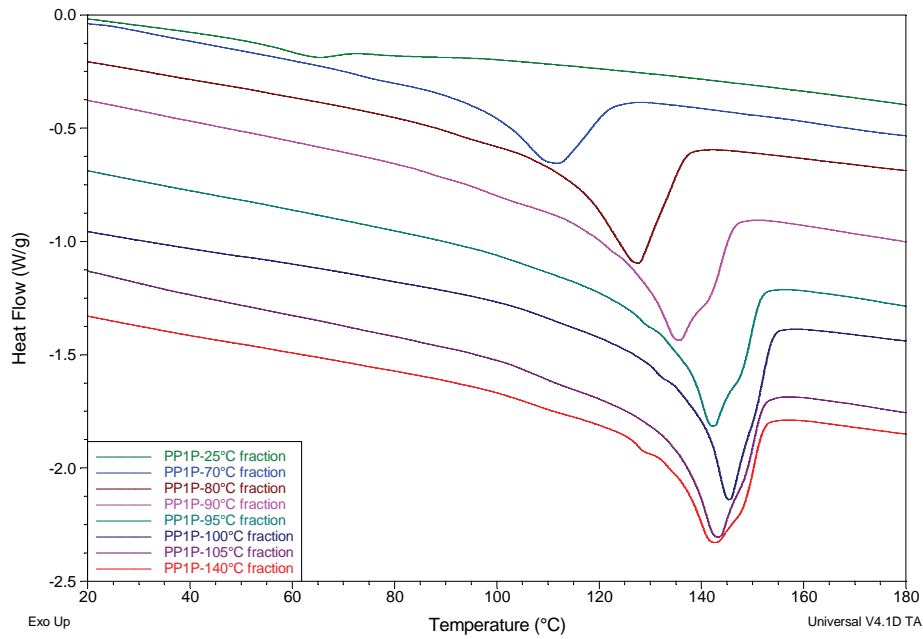


**Figure 4.4** The DSC heating curves for all TREF fractions of sample PP1P.

The crystallinities of the TREF fractions (Figure 4.5) also show the same trends as the melting temperatures and molar mass, namely an increase in crystallinity with TREF fractionation temperature.

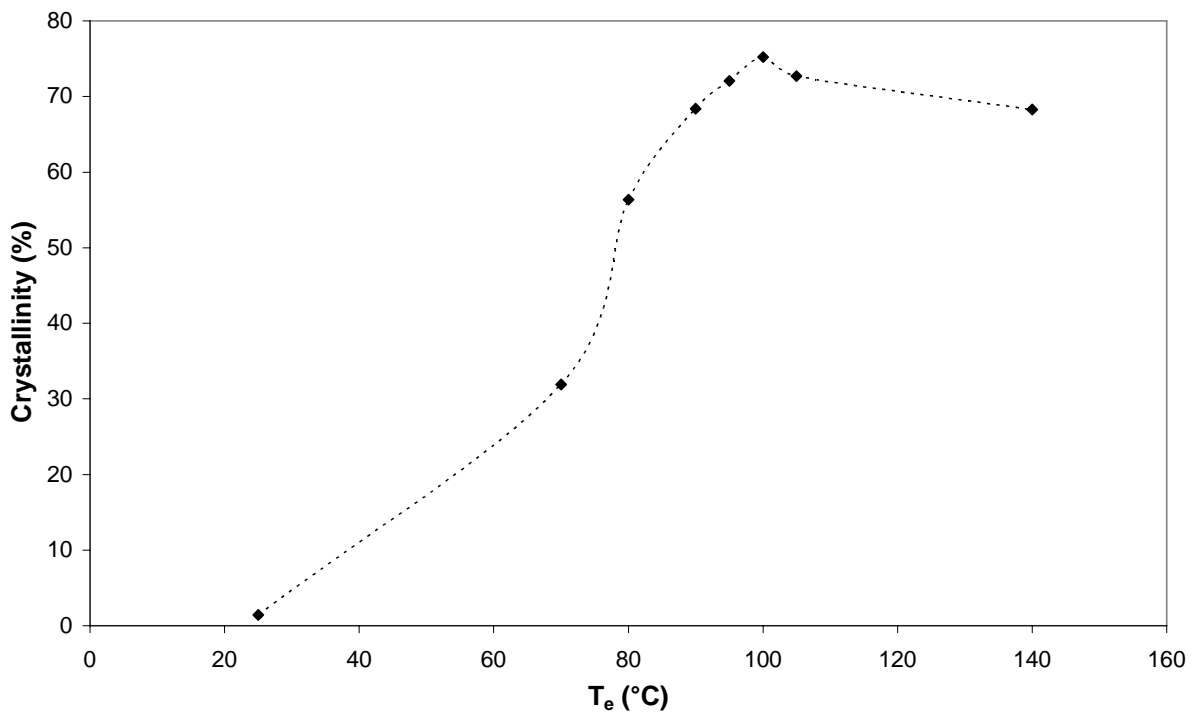


**Figure 4.5** The degree of crystallinity of each of the TREF fractions of sample PP1P.



This is what one would expect to find since the higher the TREF fractionation temperature the more easily the chains can crystallise from solution as a result of a higher level of order in the chains leading to more perfect crystallites. With regards to the final two fractions which exhibit a slightly lower crystallinity than the 100 °C fraction, one can clearly see the effect of the slightly lower molar mass material on the ability of the chains to crystallise. As to whether the average type of chain in this fraction simply cannot crystallise to the same extent and to the same degree of order as the chains in the 100 °C fraction or whether there are simply a few chains present in the final two fractions which are limiting the crystallisability of the other chains one could not say for certain. The amount of material recovered in these two fractions is quite low, allowing for little analysis of any sort, and their relative influence on the properties of the whole can also be safely assumed to be small.

#### 4.3.1.2 Fraction removal

Figure 4.6 gives the information regarding the removal of specific TREF fractions from the PP1P sample and compares the amount of material removed to the amount remaining for the different samples. The individual samples in this section will be referred to by the fraction that has been removed from the material.

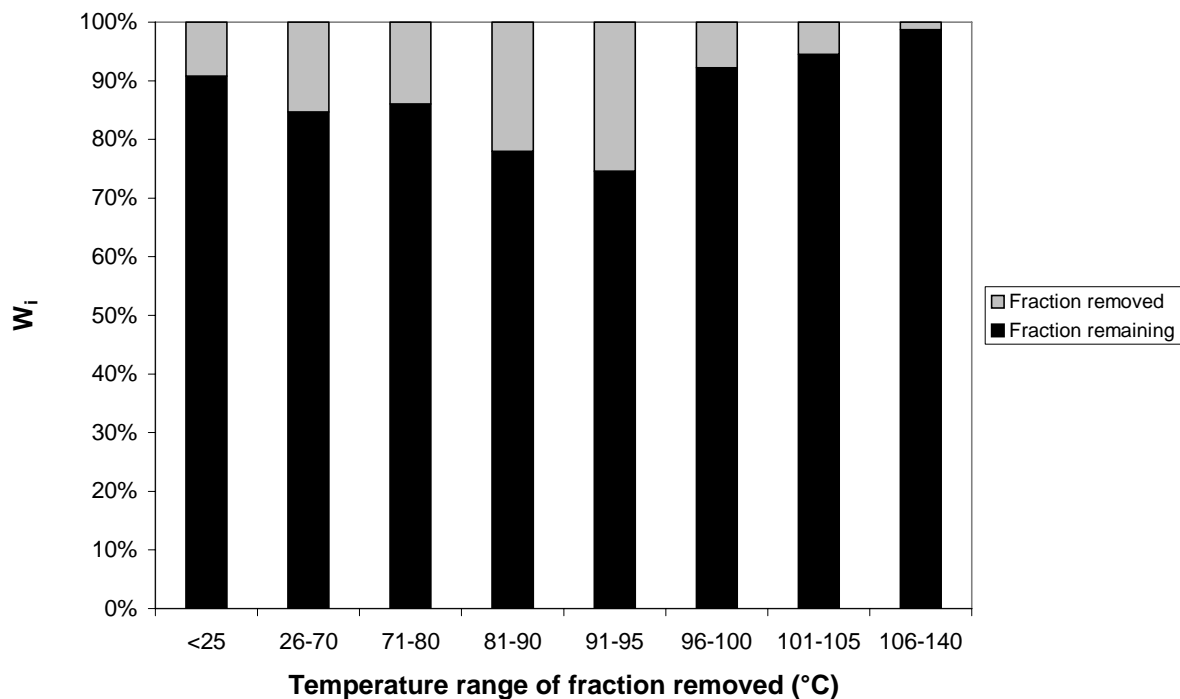


Figure 4.6 The fraction removal data for the PP1P sample.

One can see that the amount of material removed mirrors the TREF characterisation run with the amount being removed increasing for each fraction until the 91 – 95 °C fraction, thereafter decreasing to the 140 °C fraction. The molar mass data are given in Figure 4.7 and it is evident that removing specific fractions has a large effect on the composition of the polymers. Generally the trend for the molar mass data mirrors that of the individual fractions. As the TREF fractionation temperature of the fraction removed increases, there is a drop in the weight average molar mass of the sample. This is consistent with the removal of material from the sample of increasingly higher molar mass as illustrated by the blue data points in Figure 4.8. Removing the fractions eluting at the highest temperatures on the other hand results in a polymer which has a slightly higher molar mass. There is a molar mass decrease for the fractions eluting at the highest temperatures and so this trend is not entirely unexpected. An obvious exception to the general trend is that the sample with the 71 - 80 °C fraction removed has a much higher molar mass than would be expected. This is possibly due to the fact that the amount of material being removed from this sample is less than the amount of material being removed by the removing the preceding and following fractions. This means that despite the material being removed having a higher molar mass than that of the preceding sample, the amount of material removed is less thus leaving a sample of higher molar mass.

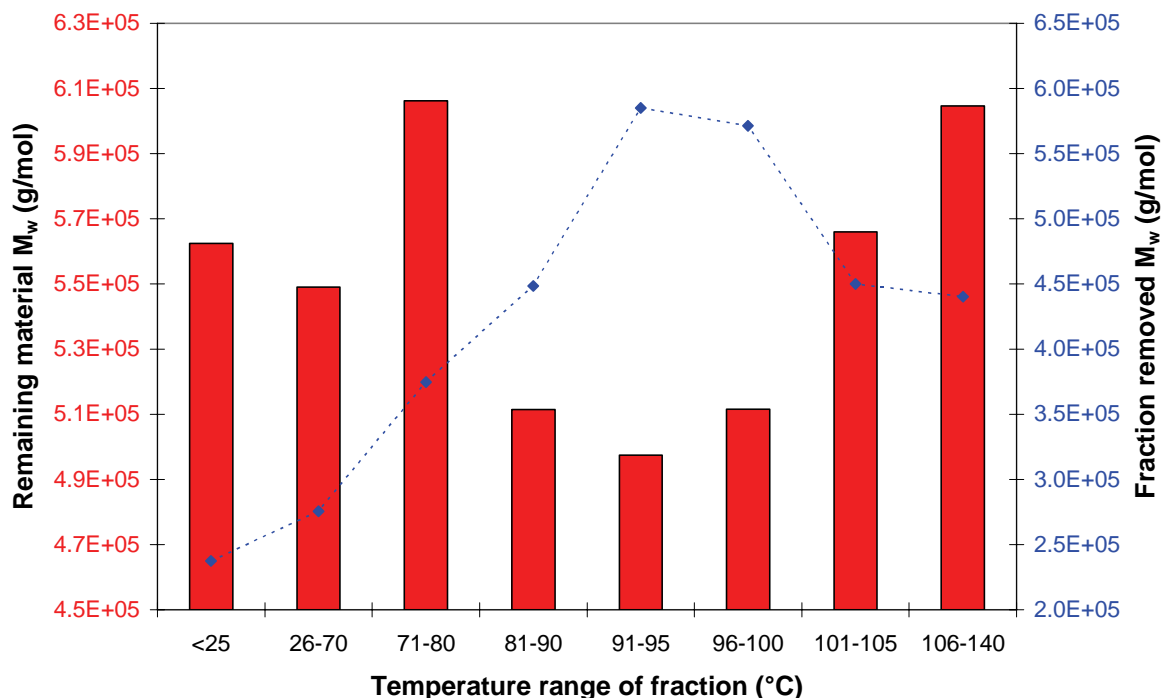
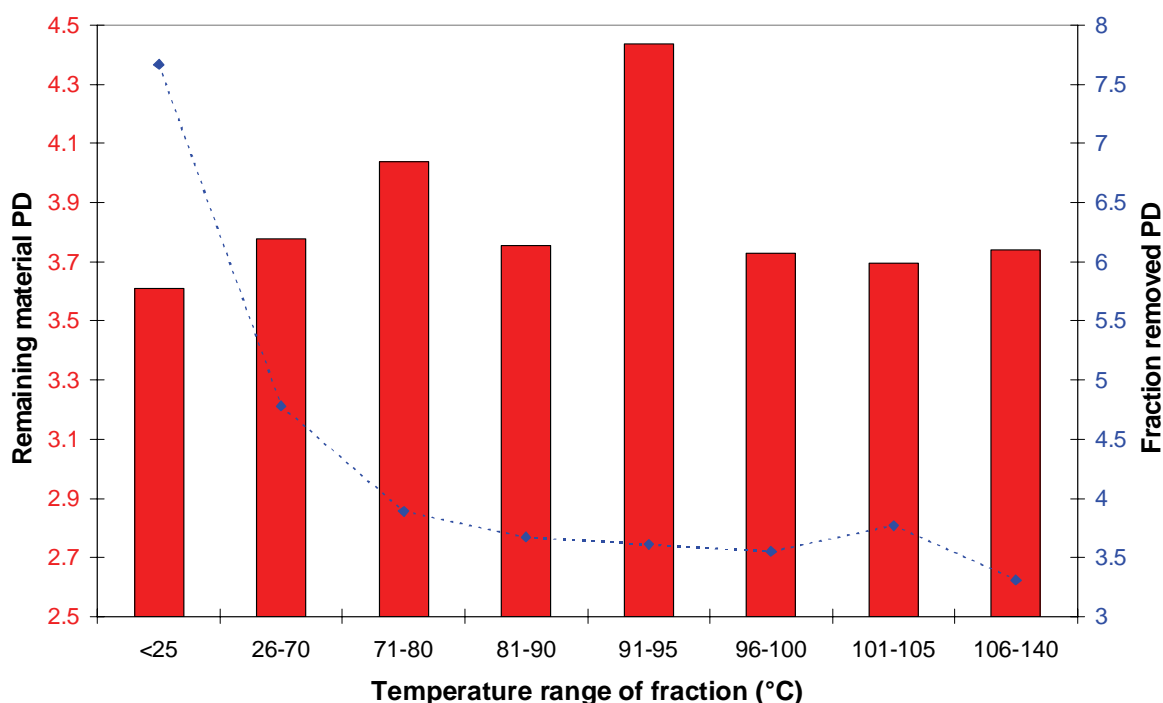


Figure 4.7 The weight average molar mass of the PP1P samples with specific fractions removed from the sample (shown in red), and the molar mass of the fraction removed (shown in blue).

The polydispersity data in Figure 4.8 show that in general there is an increase in the polydispersity of the material remaining for each fraction removed until the 91 - 95 °C fraction. The polydispersity then decreases to a nearly constant value for the remaining three samples. The polydispersity data of the fraction removed given for comparison shows a general decrease for all fractions barring the 101 - 105 °C fraction where a slight increase is observed. It can be said that the narrower the distribution of molar mass of the sample removed the broader the distribution of the sample remaining for the first few TREF fractions removed. Removing the fractions eluting at the highest temperatures does not seem to influence the polydispersity of the remaining material. It is also noted that removing the 81 - 90 °C fraction results in a narrower distribution of molar mass than would be expected.



**Figure 4.8** The polydispersity of the PP1P samples with specific TREF fractions removed from the sample (shown in red), and the polydispersity of the fractions removed (shown in blue).

The data concerning the comonomer content of the samples shown in Figure 4.9 is on first glance a little more complex. There is a decrease in the 1-pentene content with increasing elution temperature for the TREF fractions as mentioned earlier, however, the opposite is not always the case once the selected fraction has been removed. Generally it would seem to hold that the higher the elution temperature of the TREF fraction removed the higher the residual 1-pentene content since there is less and less of the 1-pentene actually being removed. This is true for the majority of the fractions, however, the two main exceptions are the cases where

the room temperature fraction is removed and the case where the 91 - 95 °C fraction is removed. In both cases the 1-pentene content of the residual material is higher than would be expected.

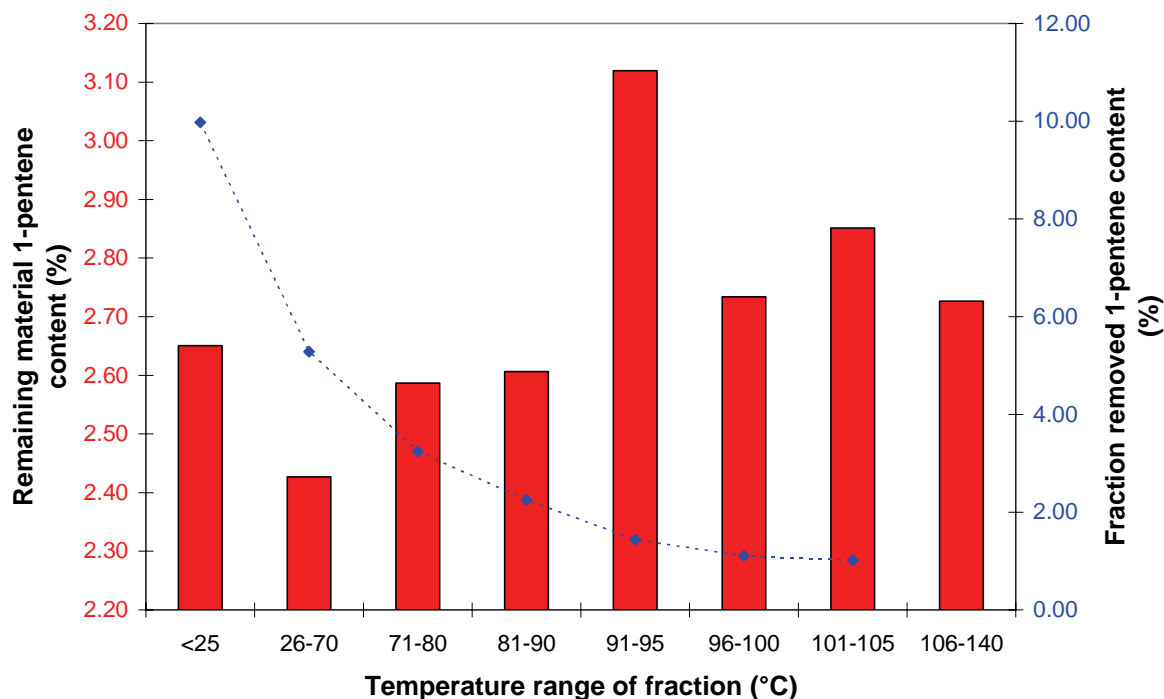


**Figure 4.9** The 1-pentene content of the PP1P samples with specific TREF fractions removed from the sample (shown in red), and the 1-pentene content of the material removed (shown in blue).

The reason for the higher than expected comonomer content for the sample with the 91 - 95 °C fraction removed is related to the amount of material removed from the polymer since this particular fraction contributes the most to the polymer as a whole (25.3%). Thus despite the fact that the 1-pentene content of this fraction is slightly higher than that of the fractions which are eluted at higher temperatures, there are significant amounts of this material being removed, hence the higher residual 1-pentene content. The same could be said for the case where the room temperature fraction is removed since the room temperature fractions' contribution to the whole is approximately 9.2% but this is less than the fractions eluting at the higher temperatures. Therefore despite the presence of a higher percentage of 1-pentene in the 25 °C fraction compared to the 26 - 70 °C fraction, the smaller amount of that fraction being removed is the dominating effect. This effect is illustrated in Figure 4.10 which shows the actual mass percentage of 1-pentene remaining in each sample as well as the actual mass percentage of material which has been removed. The amount of 1-pentene remaining in the sample is clearly linked to the amount of material removed and the higher the fractionation

temperature of the fraction removed the more 1-pentene remains in the residual polymer since less and less is being removed. It is interesting to note that although the percentage incorporation of the 1-pentene decreases constantly with increasing elution temperature (Figure 4.9), the actual mass of 1-pentene contained in each fraction is slightly different at least for the lower temperature fractions.

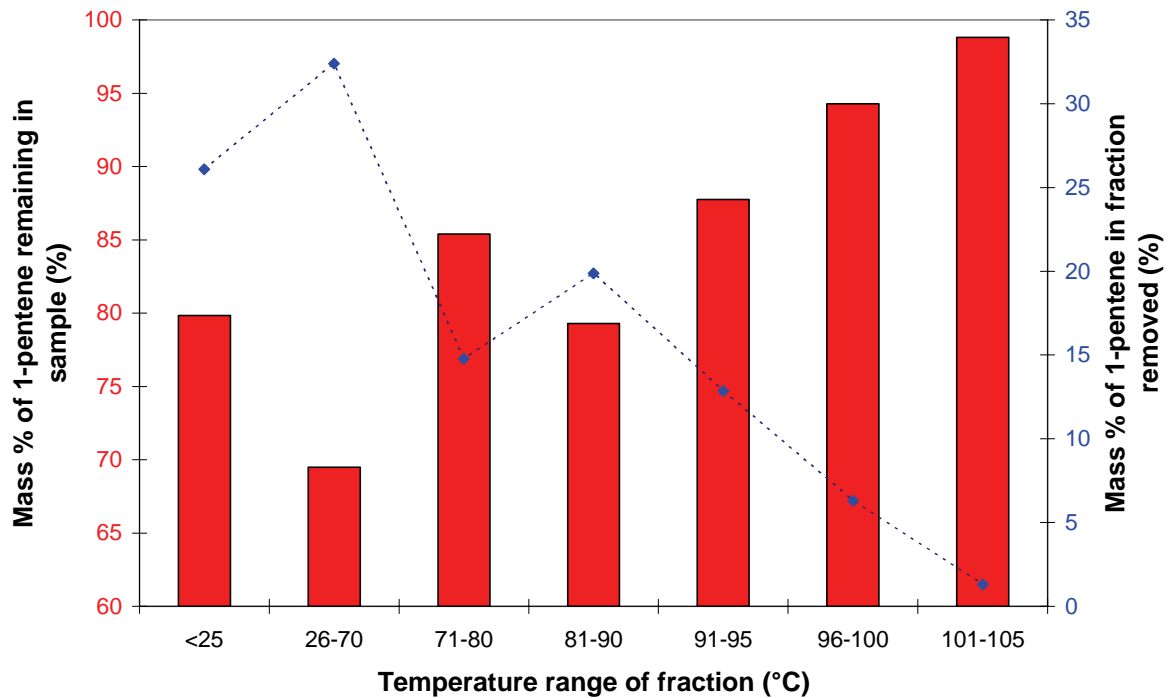


**Figure 4.10** An illustration of the mass percentage of 1-pentene remaining in the samples after the specific fractions have been removed (shown in red), as well as the mass percentage of the 1-pentene in the fraction removed (shown in blue).

This demonstrates that the amount of material being removed for a certain fraction must be taken into account when examining the data.

#### 4.3.1.3 Physical properties

An examination of the thermal properties of the samples is illustrated in Figure 4.11. The peak melting temperatures of the samples with fractions removed decreases as the TREF fractionation temperature of the fraction removed increases. This is consistent with the removal of higher melting material leading to residual material which melts at a lower temperature due to the fact that the chains which can crystallise to form thicker lamellae have been removed.

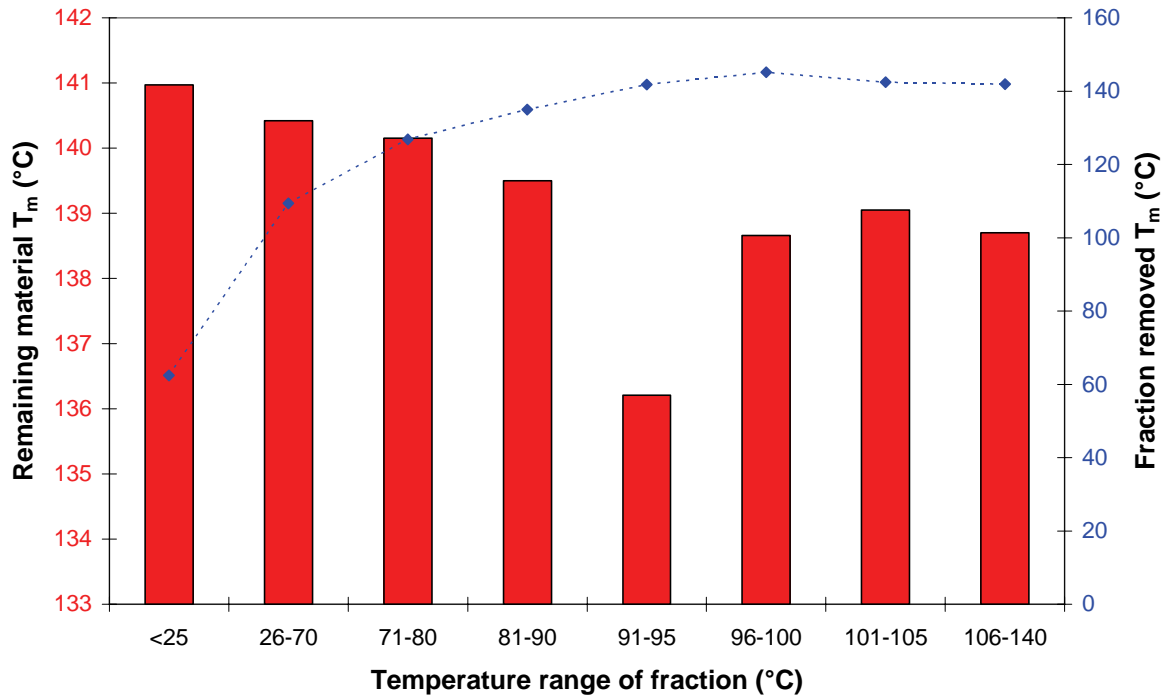


**Figure 4.11** The peak melting temperatures of the PP1P samples with specific TREF fractions removed from the sample (shown in red), and the fractions removed (shown in blue).

Once again the sample which does not seem to follow the trend is the one with the 91 - 95 °C fraction removed. It has a much lower peak melting temperature than would be expected and this is in keeping with the apparent high comonomer content of the residual material (Figure 4.9). The presence of the comonomer has disrupted the chains' ability to crystallise resulting in a noticeably lower melting temperature for the sample. Hosada *et al.* [8] have shown that small amounts of the comonomer can indeed be included in the crystal lattice by investigation of the expansion of the lattice spacing. This means that even small amounts of a defect such as a comonomer can cause a significant change in the crystallisation mechanisms of a material, indeed the effect of a comonomer on the crystallisation of a copolymer has been extensively studied [9-15].

The degree of crystallinity of the samples (Figure 4.12) shows that there are significant differences between the samples depending on which fraction one removes. The percentage crystallinity of the samples decrease up to the sample where the 81 - 90 °C fraction is removed, after which the crystallinity increases again for the samples with higher eluting TREF fractions removed.

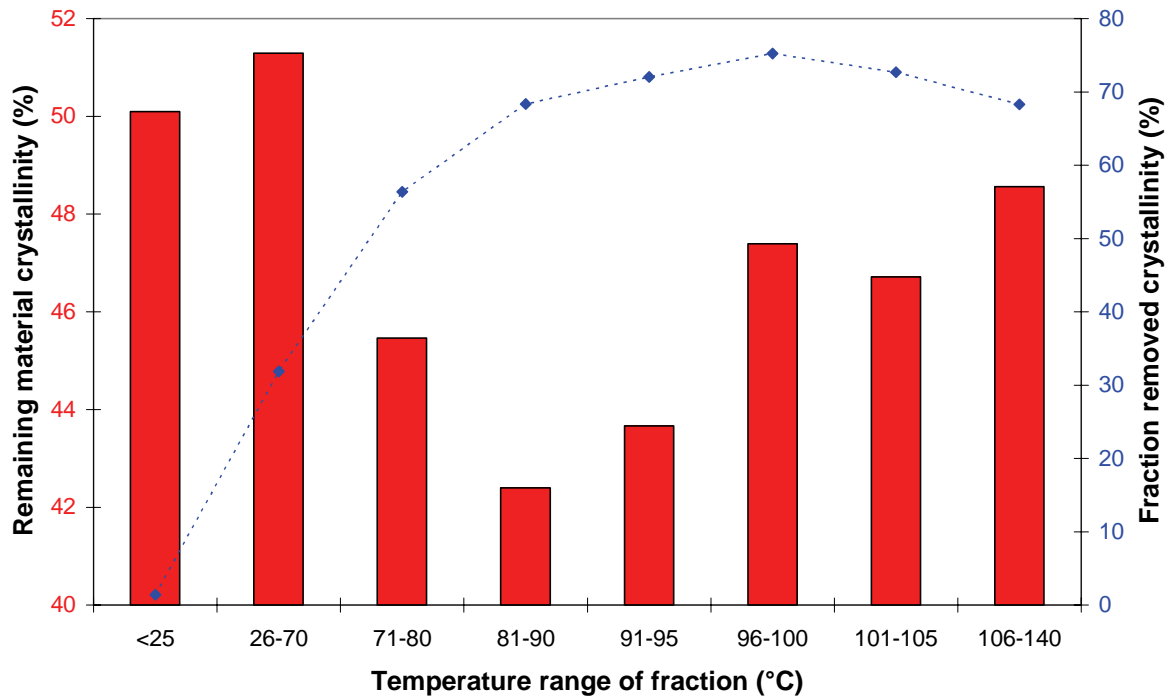


**Figure 4.12** The degree of crystallinity of the PP1P sample with specific TREF fractions removed from the sample (shown in red), and the crystallinity of the fraction removed (shown in blue).

The general trend would seem to be the expected one where removing the more crystalline fractions leaves behind a material with a lower crystallinity. However, there are definitely other factors which play a role such as the amount of material removed. It would seem that this is an important factor in determining the properties of a material and that therefore the amount of material present in each fraction is critical to the properties of the material and not just the quality of the fraction. This implies that modification of a catalyst to alter the amounts of material in the fractions would therefore alter the properties of the material. An interesting comparison can be made between the crystallinity of the sample with the 81 – 90  $^{\circ}\text{C}$  fraction removed and that of the sample with the 91 – 95  $^{\circ}\text{C}$  fraction removed. The 91 – 95  $^{\circ}\text{C}$  fraction is more crystalline than the 81 – 90  $^{\circ}\text{C}$  fraction, however, the samples remaining after removing these fractions show the opposite trend than what would be expected in that the sample with the 81 – 90  $^{\circ}\text{C}$  fraction removed has a lower residual crystallinity despite removing a less crystalline material. This is also not due to the amount of material removed since there is more material being removed upon removing the 91 – 95  $^{\circ}\text{C}$  fraction. Therefore, it seems as if the 81 – 90  $^{\circ}\text{C}$  fraction is very important for enabling the sample as a whole to attain a high degree of crystallinity despite the fact that it is not the most crystalline nor the largest constituent fraction in the sample.

A very similar trend to that of the crystallinity of the samples is observed for the weighted average lamellar thickness ( $l_w$ ) of the samples in Figure 4.13. A general decrease in  $l_w$  is observed until the sample with the 91 - 95 °C fraction removed, after which there is an increase in  $l_w$  for the final three samples. A notable exception to the decreasing trend in the first few samples is the sample with the 26 – 70 °C fraction removed. This sample appears to have a higher than expected crystallinity and  $l_w$ .

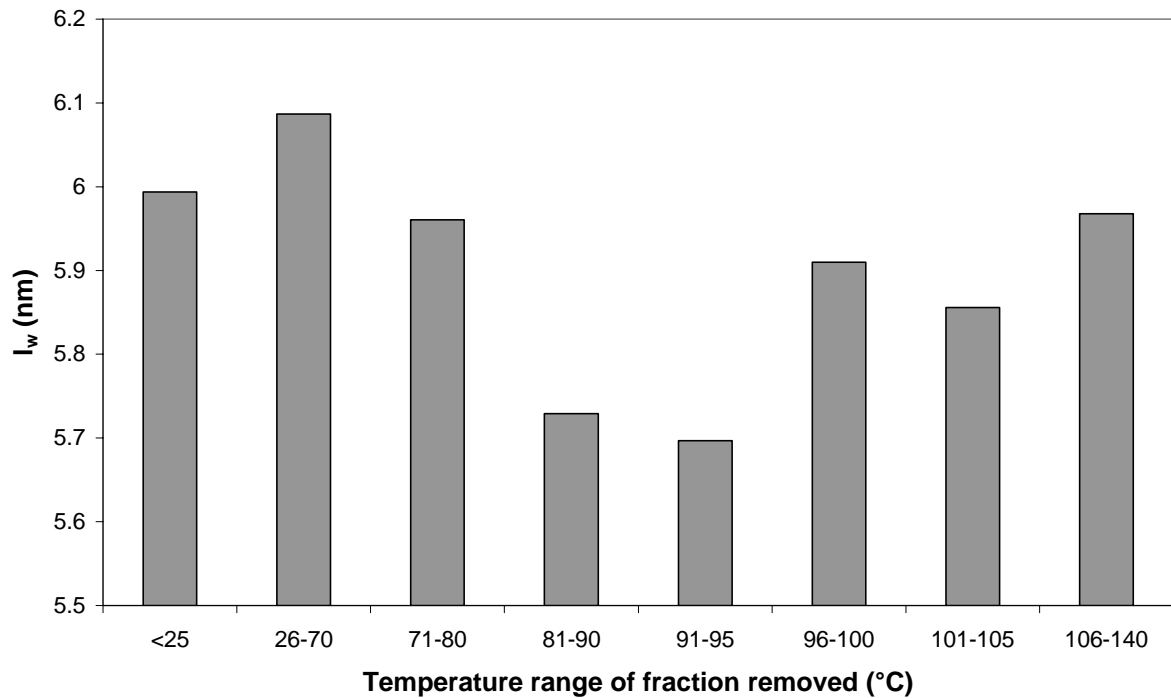


**Figure 4.13** The weight average lamellar thickness of the PP1P samples with specific fractions removed.

This is, however, due to the low amount of comonomer present in this sample as shown in Figure 4.9. The sample contains the least comonomer of all the samples with specific fractions removed and so there is less inhibition of the crystallisation of the chains. The lamellar thickness has been shown in a number of studies [8, 16] to decrease with increasing comonomer content of the sample.

Figure 4.14 shows the observed trends for the modulus values at 2% strain for all the PP1P samples. As more crystalline material is removed from the sample at higher TREF fractionation temperatures the modulus of the sample decreases up to the 81 – 90 °C fraction. It is noted, however, that removing the fractions eluted at the higher temperatures does not seem to affect the modulus values to any great extent with the exception of the sample without the final fraction. Despite very little material being removed from the samples when extracting this fraction, there seems to be a noticeably lower modulus for the sample without



that fraction. It is believed that the low modulus values obtained are due to the lower crystallinity values as well as the absence of the fractions which contain the important tie-molecules and “ordered” amorphous phase. These types of chains play an important role in the absorbing energy during deformation. It is noted that the most important fraction in the sample for maintaining a high tensile strength is the 81 – 90 °C fraction since this fractions removal results in the largest decrease in modulus.

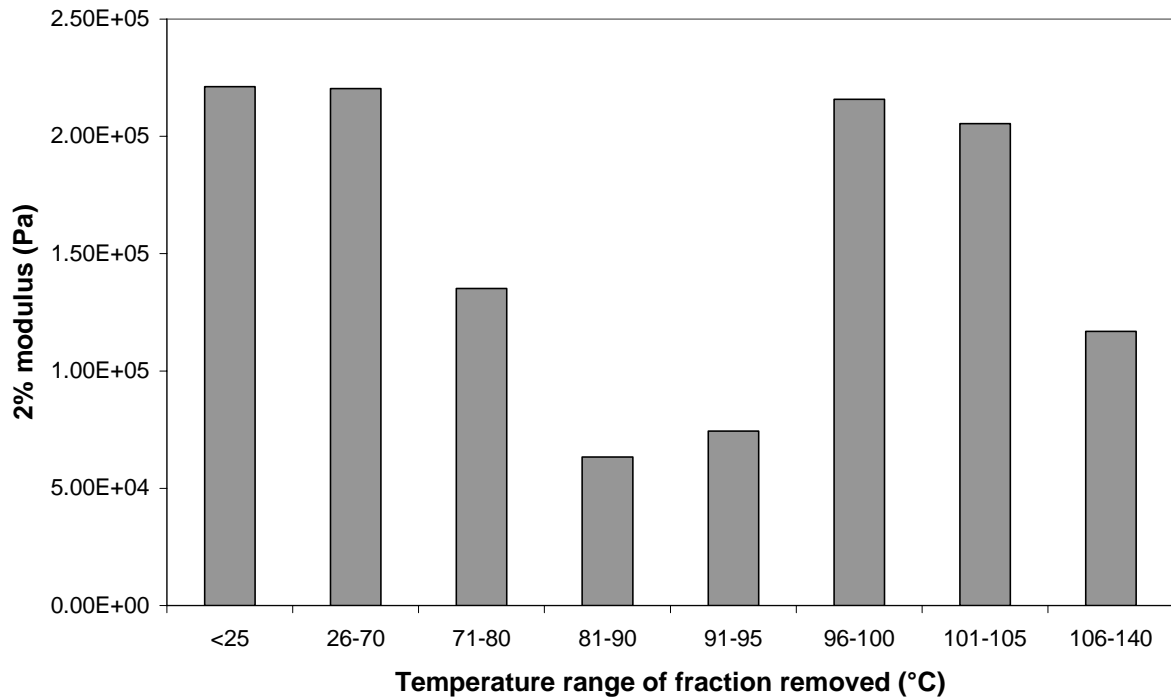


**Figure 4.14 The modulus values at 2% strain of the PP1P sample with specific TREF fractions removed from the sample.**

There are some extremely interesting facts which are revealed via the removal of selected fractions, namely that the fractions of reasonably high crystallinity and molar mass are responsible for giving the material its physical properties. These fractions are not those eluting at the highest temperatures, nor are they the most crystalline fractions in the sample, however, their presence is definitely required for good physical properties. Altering the amount of material in these fractions would therefore have the greatest influence on changing the physical properties of the polymer.

The importance of the various TREF fractions to the properties of the material as a whole is evident from the data presented. The specific relationships observed are discussed in the next section.

#### 4.3.1.4 Structure – property relationships

There is a clear relationship between the modulus at 2% strain and the crystallinity of the sample. This is illustrated in Figure 4.15. The increase in the degree of crystallinity means that there is much more stiffness in the material and that there is less amorphous material present which would have aided in the flow of material. More force is therefore, necessary to induce the crystal-crystal slip involved in the break-up of the crystalline regions, resulting in the extension of the sample under the applied load. It has been observed [17] that fibrils tend to align in the direction of the applied load during such a tensile test and that less crystalline samples exhibit more stretching of the microfibrils than the more crystalline samples. This stretching of the fibrils can account for the lower observed modulus values since the lower crystallinity samples can deform easier than those of higher crystallinity, i.e. have a greater microplasticity.

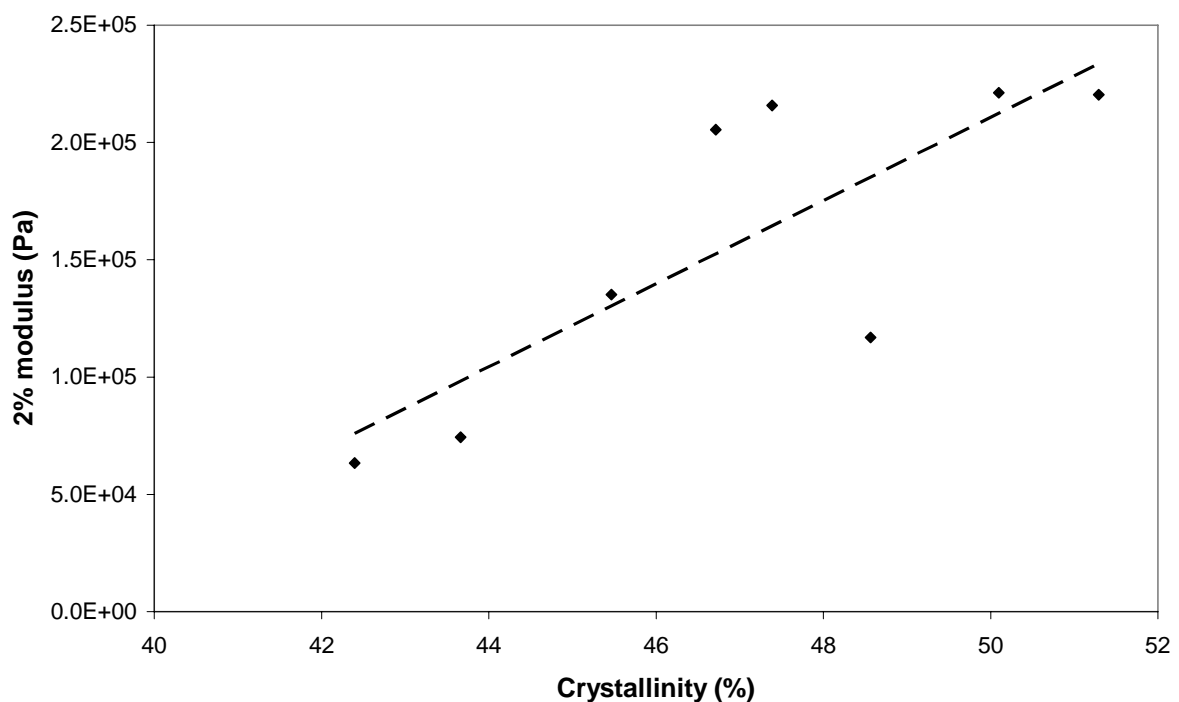
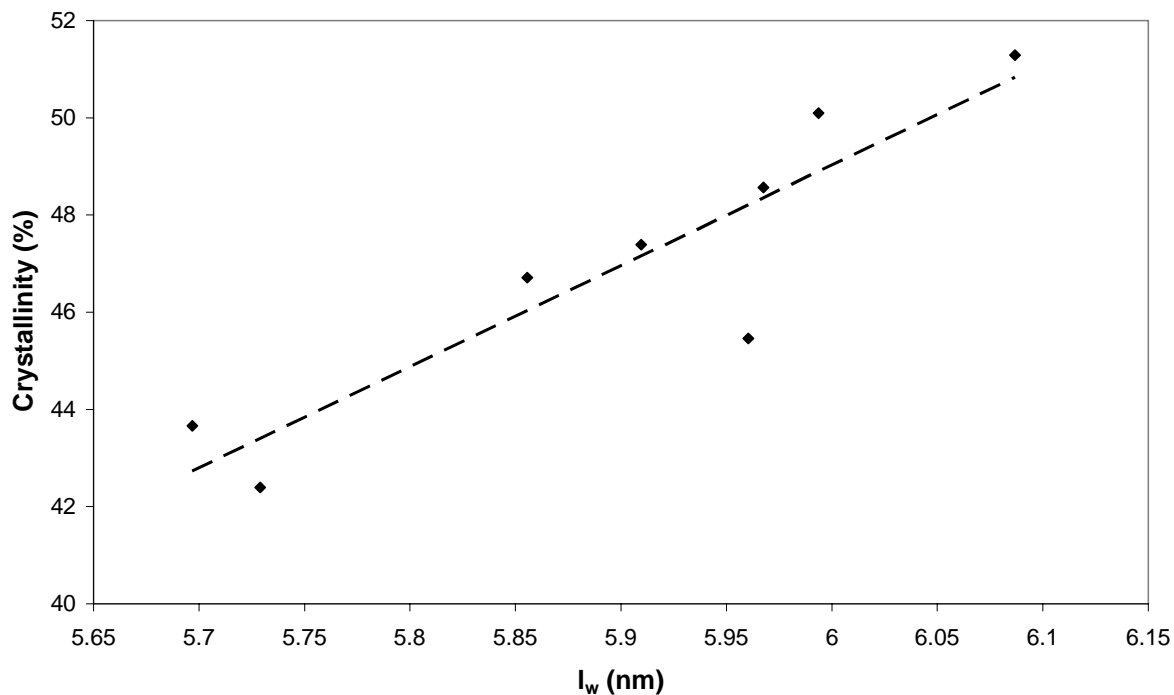
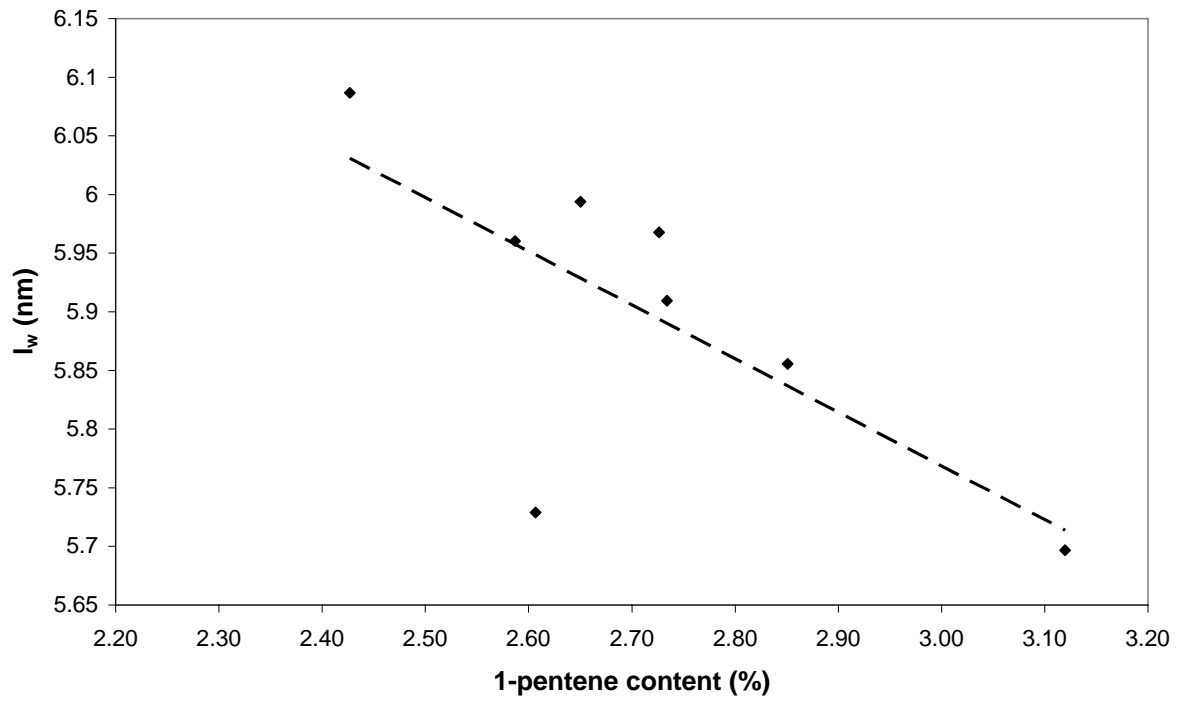


Figure 4.15 The relationship between the crystallinity of the samples and the modulus at 2% strain.



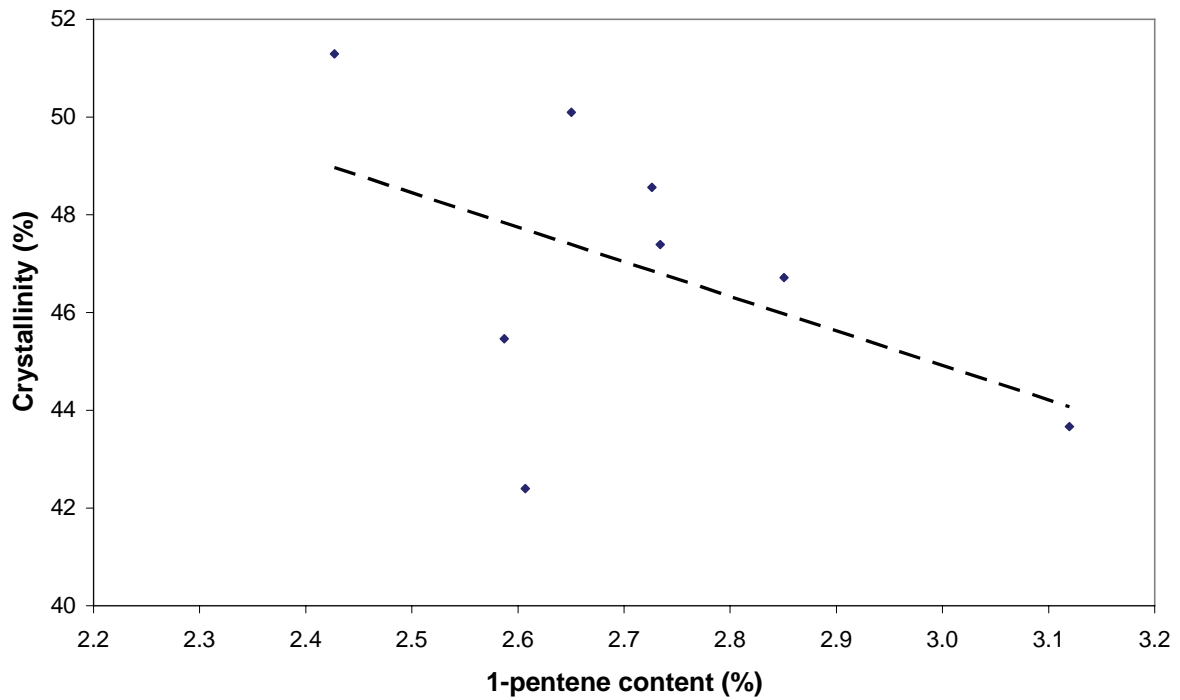
**Figure 4.16** The relationship between the weight average lamellar thickness of the samples and the percentage crystallinity.

The crystallinity of a given sample is in turn dependent on the thickness of the lamellae of that sample. Lamellar thickening has been shown to account for increases in melting temperatures of polypropylene [18] and it is also clear from Figure 4.16 that the thicker lamellae are present in the more crystalline samples. The effect of the comonomer on the lamellar thickness is illustrated in Figure 4.17. The disrupting effect of the 1-pentene units in the formation of the crystals is evident.



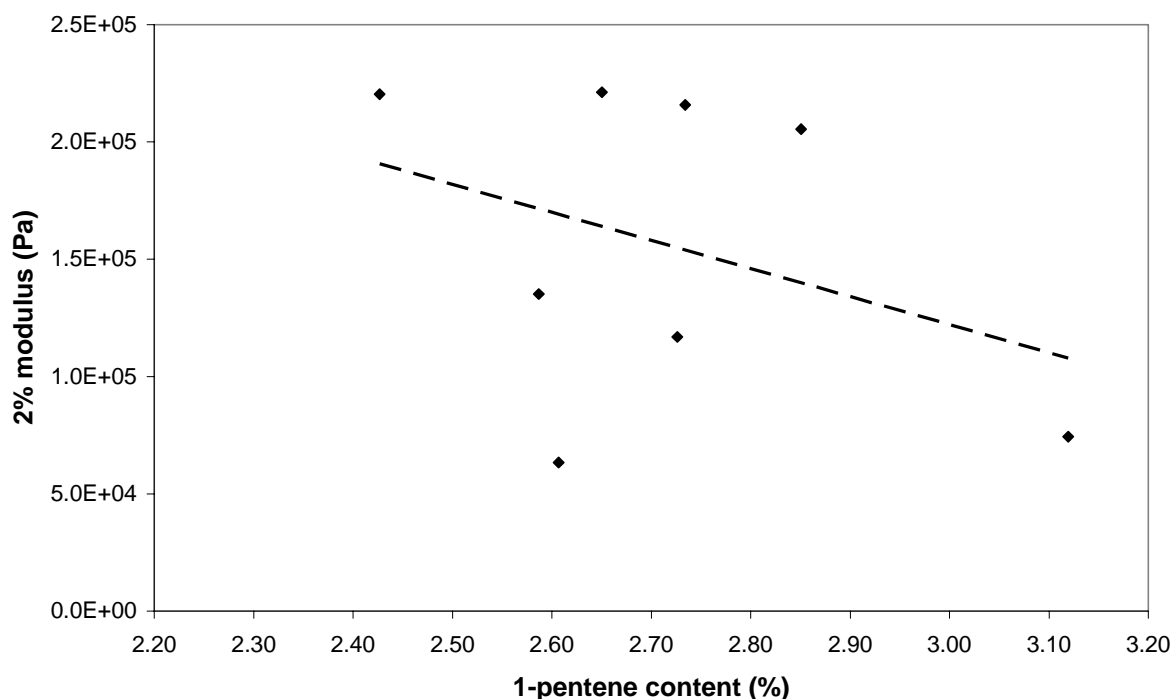
**Figure 4.17** The relationship between the weight average lamellar thickness and the 1-pentene content of the PP1P samples.

Figure 4.18 illustrates the relationship between the crystallinity and the 1-pentene content.



**Figure 4.18** The relationship between the 1-pentene content and the crystallinity of the PP1P samples.

It definitely seems as if the higher the comonomer content, the lower the degree of crystallinity, however, the correlation is not as strong as would be expected. It is important to note that despite the above relationships there is no strong correlation between the 1-pentene content of the samples and the modulus at 2% strain as illustrated in Figure 4.19.



**Figure 4.19** The relationship between the comonomer content and the modulus at 2% strain.

Therefore, it is believed that although the comonomer clearly affects the lamellar thickness which in turn affects the crystallinity there is only a weak correlation between the comonomer content and the modulus. It would therefore, appear as if there are other factors such as the molar mass and molar mass distribution which play an important role in determining the crystallinity of a sample. These factors also affect the modulus of the samples hence the lack of a direct correlation between the comonomer content and the modulus. No singular factor is believed to be responsible since no direct correlation was obtained between the molar mass or molar mass distribution and the modulus.

In general it would seem that for the propylene copolymer the overriding factor determining the properties of the material is the comonomer content. One could say that the molar mass and molar mass distribution also play a role, for the samples with higher molar mass and narrower molar mass distribution tend to form thicker lamellae and have a higher crystallinity. However, this is more due to the fact that the active sites producing the high molar mass material do not incorporate the comonomer to the same extent as the sites

producing lower molar mass chains and so the effect of the comonomer cannot be excluded from these trends. The molar mass, and molar mass distribution, play a significant role in determining the properties as evidenced by the lack of a direct correlation between the modulus and comonomer content.

### **4.3.2 PP homopolymer**

The techniques developed for the analysis of the propylene-1-pentene copolymer were then systematically applied to a polypropylene homopolymer. The molar mass and molar mass distribution of the two materials are similar (Section 4.2.1), however, the homopolymer has significantly higher melting points and degree of crystallinity. Since there is no comonomer present in this sample the main factors affecting the polymer properties are the stereospecificity, molar mass, and molar mass distribution. The regiospecificity of the chains can also be a factor, however, polymers made with Ziegler-Natta catalysts have extremely low amounts of regio-errors unlike those polymers made with metallocene catalysts where these types of errors are more prominent [19, 20].

#### **4.3.2.1 PP characterisation**

The TREF characterisation of the PPH sample is given in Figure 4.20. The distribution of molecular species is reasonably broad with two fractions comprising the majority of the material. The elution temperatures of the major fractions are at 110 °C and 115 °C, considerably higher than those of the copolymer used in the first section as one would expect for an isotactic polypropylene homopolymer sample.

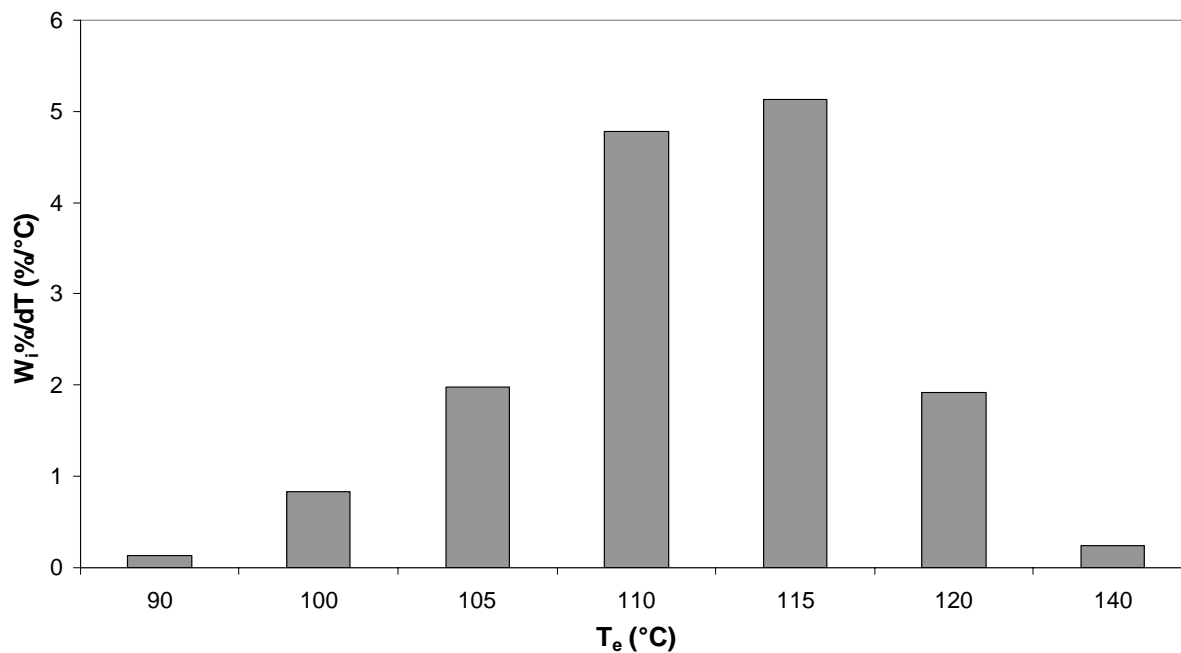


Figure 4.20 The TREF fractionation data for the PP homopolymer sample.

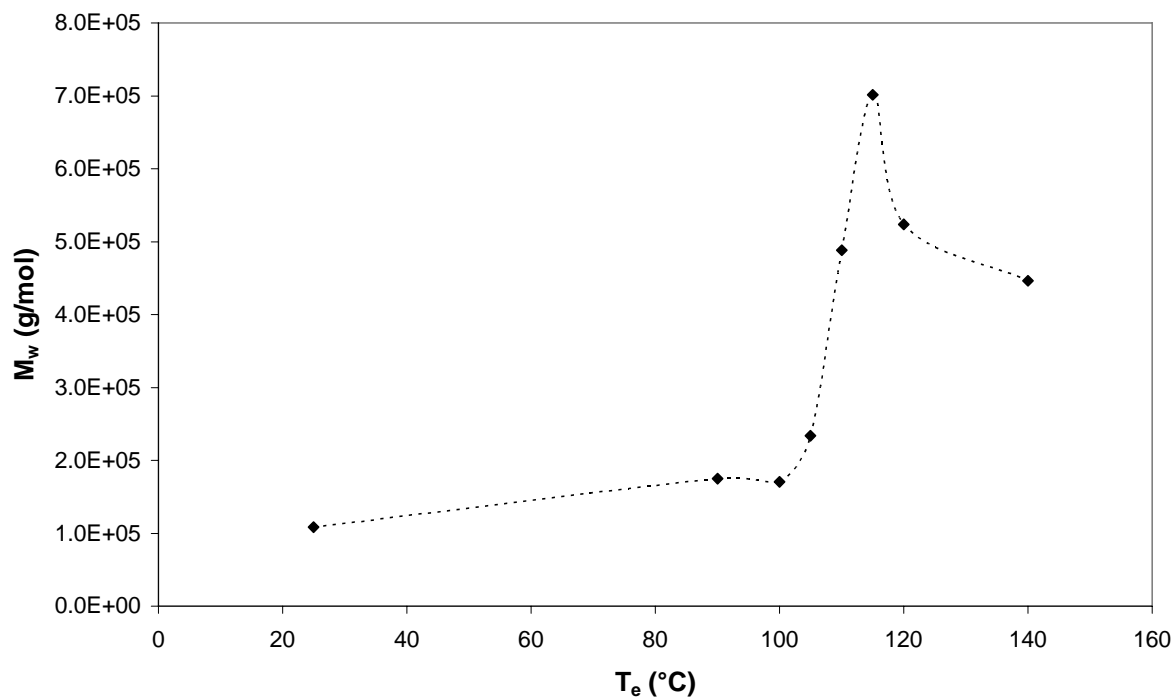


Figure 4.21 The molar mass data for the TREF fractions of sample PPH.

The trend for the weight average molar mass of the TREF fractions (Figure 4.21) is similar to that of the copolymer and is the same trend we have observed for a number of

different fractionation experiments of different materials. There is a rather sharp increase in molar mass for the samples eluting above 105 °C indicating that those chains that crystallise out of solution at high temperatures are of a much higher molar mass than those which crystallise out at low temperatures. Since there is no comonomer present in this sample the ability of the chains to crystallise is mainly dependent on the tacticity of the chains [21, 22]. Since the active sites which produce material with a high degree of stereoregularity also have a high  $k_p$  [23-26], it therefore follows that the majority of chains with high molar mass also have high stereospecificity and are able to crystallise out of solution at higher temperatures. What is noted, however, is that while the increase in molar mass of the PPH sample's fractions increases drastically from the 105 °C fraction to the 115 °C fraction, the PP1P sample's fractions' molar masses increase over a broader range of temperatures, from the 80 °C fraction to the 100 °C fraction. This implies that the comonomer is playing a larger role in the separation of chains for the PP1P sample than the tacticity is for the PPH sample, and that the molar mass of the homopolymer's fractions possibly plays a more significant role in the separation mechanism.

The polydispersity of the fractions (Figure 4.22) decreases as the fractionation temperature increases with the exception of the fraction eluting at 90 °C, however, the temperature range over which this material is collected is extremely broad hence the broader distribution of molecular species obtained for this fraction. It would appear that the active sites producing the material with the ability to crystallise out of solution at higher temperatures are more uniform and therefore produce a more uniform distribution of molecular species. In general the majority of the fractions show a narrow distribution with PD values between 3 and 3.5.



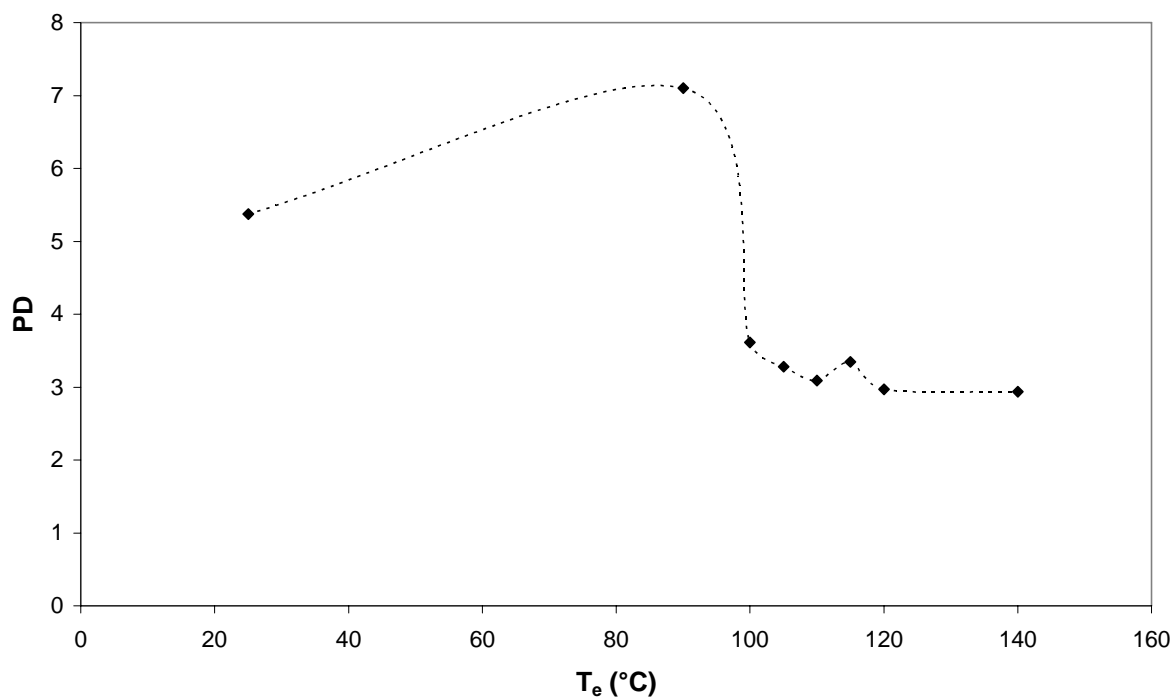


**Figure 4.22** The polydispersity data for the TREF fractions of sample PPH.

The  $^{13}\text{C}$  NMR data for the fractions is shown in Figure 4.23. The distribution of the various sequences is given for each fraction. The now familiar trend in properties is observed with the average *mmmm* pentad sequence distribution increasing up to the 110 °C fraction as one would expect since the higher the stereoregularity of the chains, the more easily they can crystallise. There is a slight decrease in the stereoregularity of the chains of the final few fractions indicating that despite the fact that these chains crystallise out of solution before the chains contained in the preceding fractions they are less isotactic and are of a lower molar mass. There is the possibility that the chains can crystallise out of solution before the more perfect chains located in the 110 °C fraction for example due to the slightly lower molar mass since too high a molar mass can inhibit the crystallisation of the chains. This is the only possible reason on a molecular level for the presence of these chains in the higher fractions since it is unlikely that the reduced tacticity of these chains would lead to an increased likelihood of crystallisation. There would have to exist a balance in terms of molar mass and tacticity which would then determine the temperature at which the chains would crystallise out of solution. The possibility of the entrapment of chains cannot be discounted.

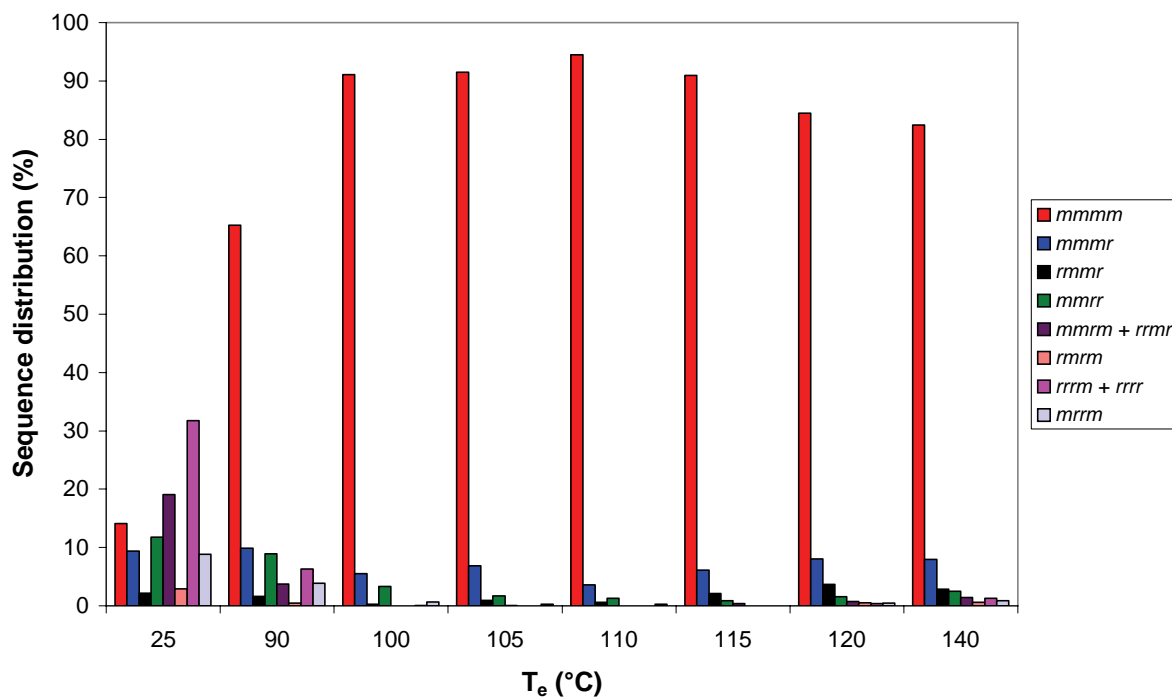


**Figure 4.23** The sequence distribution content for the TREF fractions of sample PPH.

It is also important to note the high amount of syndiotactic material that is present in the room temperature soluble fraction implying a degree of chain end control for certain active sites in the catalyst. Material of this type is also evident in the 140 °C fraction which is another indication that entrapment of material occurred during the fractionation process.

Analysis of the melting endotherms of the TREF fractions (Figure 4.24) also shows the characteristic increase in melting temperature with increasing fractionation temperature until the final couple of fractions where the decrease in stereospecificity of the material is evident in the slightly lower melting temperatures of the chains. The characteristic double melting peaks of polypropylene are evident in some of the lower temperature fractions and it is believed in that in this case the double melting peaks are the result of melting of different crystalline areas in the samples, namely the thicker radial and thinner tangential lamellae.

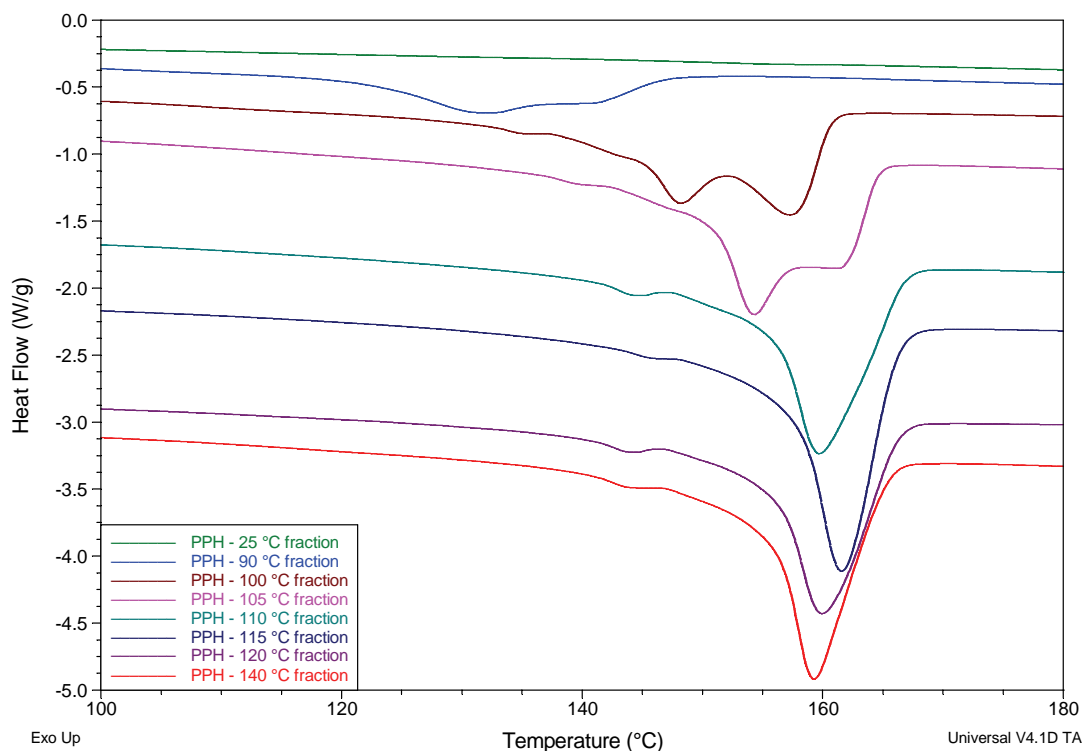


**Figure 4.24** The melting endotherms of the TREF fractions of sample PPH.

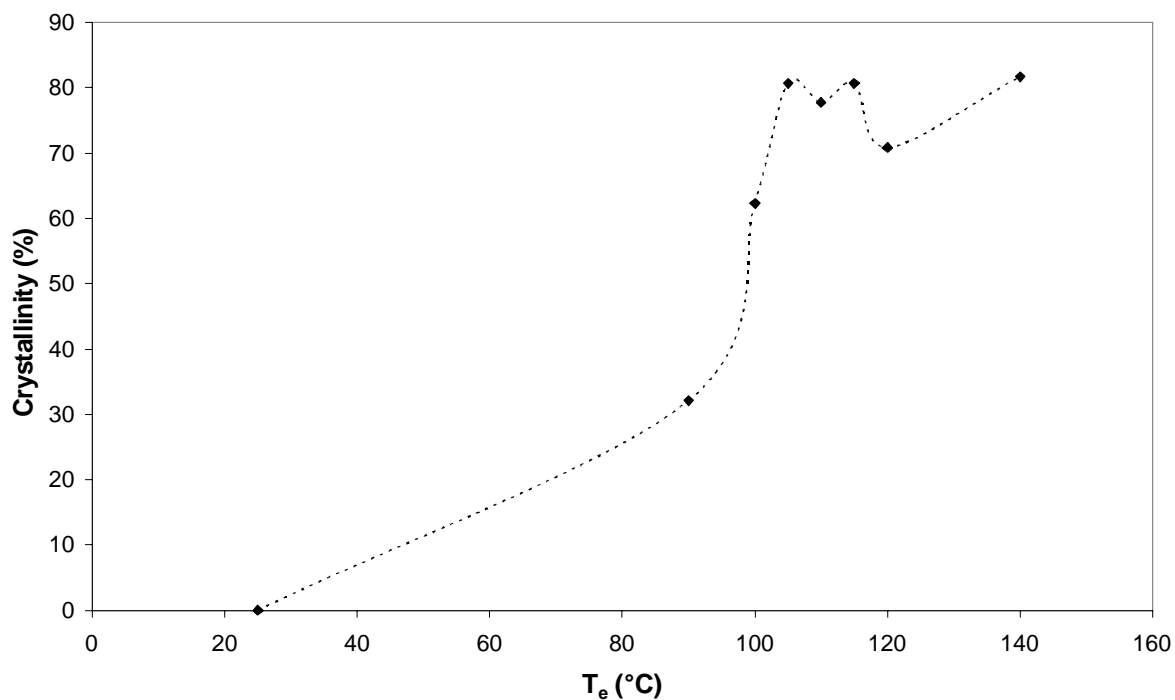


**Figure 4.25** The degree of crystallinity of the TREF fractions of sample PPH.

The degree of crystallinity of the fractions (Figure 4.25) also increases with fractionation temperature over the temperature range of the first few fractions. From the 105 °C fraction there is little further increase in crystallinity and the values are relatively constant

with the exception of the 120 °C fraction which shows a slight decrease. The reason for this could only be the difference in the molar mass of the samples since the tacticity values for this fraction are higher than that of the final fraction and the polydispersity of the fractions are similar. The slightly higher molar mass compared to the final fraction preventing the crystallisation of the chains to the same extent. The previous fraction at 115 °C has a higher molar mass (Figure 4.21) and crystallinity, however, it is believed that the higher crystallinity is due to the higher tacticity of the sample enabling the improvement in crystallisation of the chains despite the higher molar mass of the chains. It is clear that a balance must be struck in order to obtain the maximum degree of crystallisation.

#### 4.3.2.2 PP fraction removal

The PPH samples with specific fractions removed are again referred to by the temperature range of the fraction removed from the sample.

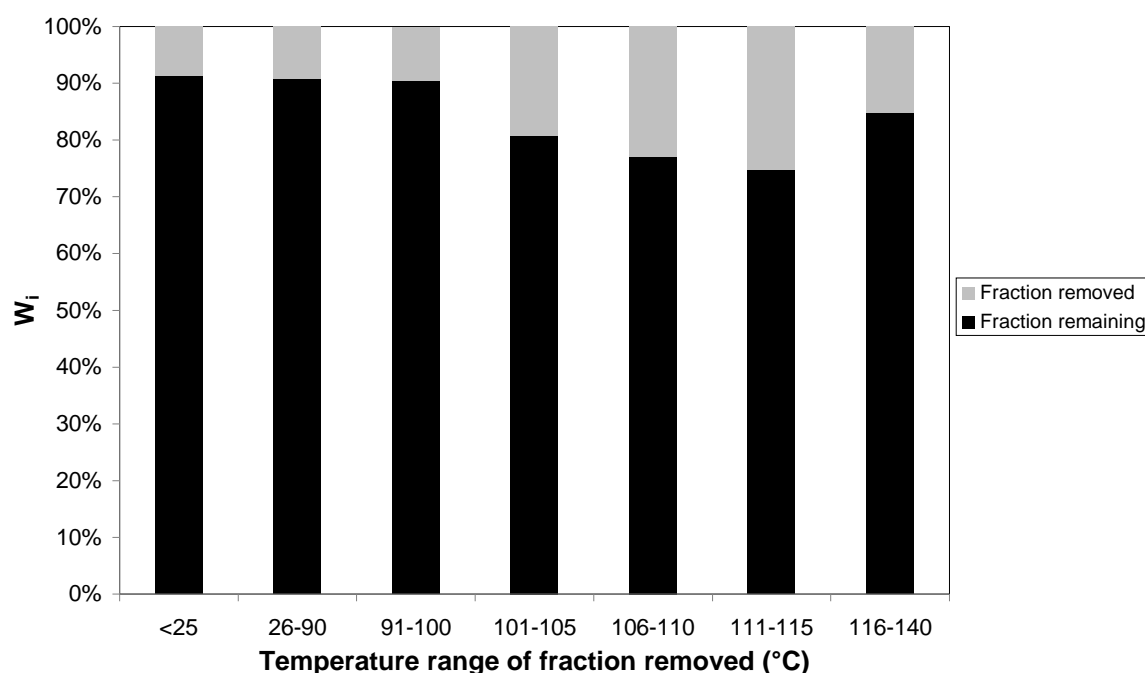
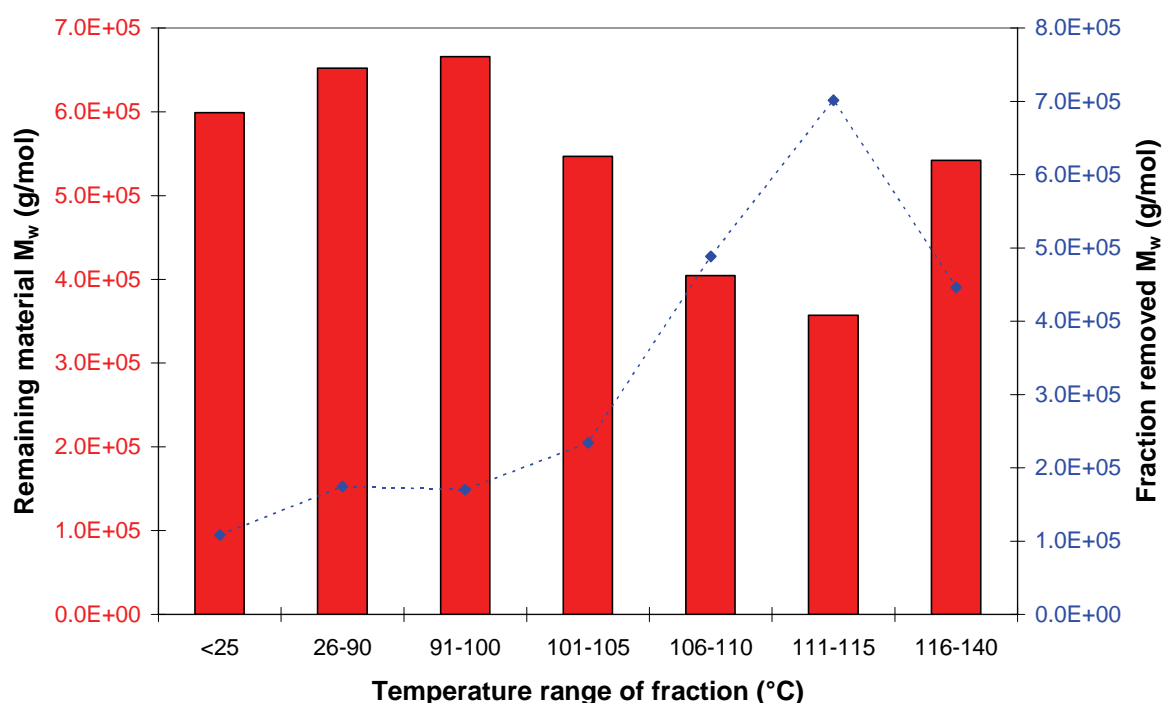


Figure 4.26 The fraction removal data for the PPH sample.

Figure 4.26 shows the amount of each fraction removed from the sample as a whole for each temperature range analysed. The major fractions are those at 110 °C and 115 °C and there are significant amounts of material being removed upon removal of these fractions which, as observed for the 1-pentene copolymer, plays a significant role in the properties of the materials and the trends formed upon removing the different fractions.

The weight average molar mass of each sample is given in Figure 4.27 and it is observed that initially there is a slight increase in the molar mass of the samples if the 26 – 90 °C and 91 – 100 °C fractions are removed. It is important to note, however, that there is little material being removed from these samples and that the molar mass of the fractions removed are also similar, therefore, it is proposed that the amount of material removed is the overriding factor regarding the molar mass of the residual material. Removing the fractions eluting at higher temperatures, results in a clear and significant decrease in the molar mass of the residual material. Generally it is observed that removing materials of lower molar mass, leaves behind a material with a higher molar mass than removing material of a high molar mass eluting in higher temperature fractions.



**Figure 4.27** The weight average molar mass of the PPH samples with specific fractions removed from the sample (shown in red), and the molar mass of the fraction removed (shown in blue).

As far as the broadness of the molar mass distribution is concerned an examination of the polydispersity data reveals that there is no obvious relationship between the polydispersity of the fraction removed and that of the material remaining. It can be said that the polydispersity of all the samples is higher once a fraction has been removed and that in general removing a fraction with a relatively narrow distribution leaves behind material with a broader distribution of molar mass. Once again it is believed that trends observed in Figure 4.28 are mainly the results of the amount of material removed, as opposed to the quality of the material

removed, since the polydispersity of the TREF fractions removed are rather similar with the exception of the first two fractions.

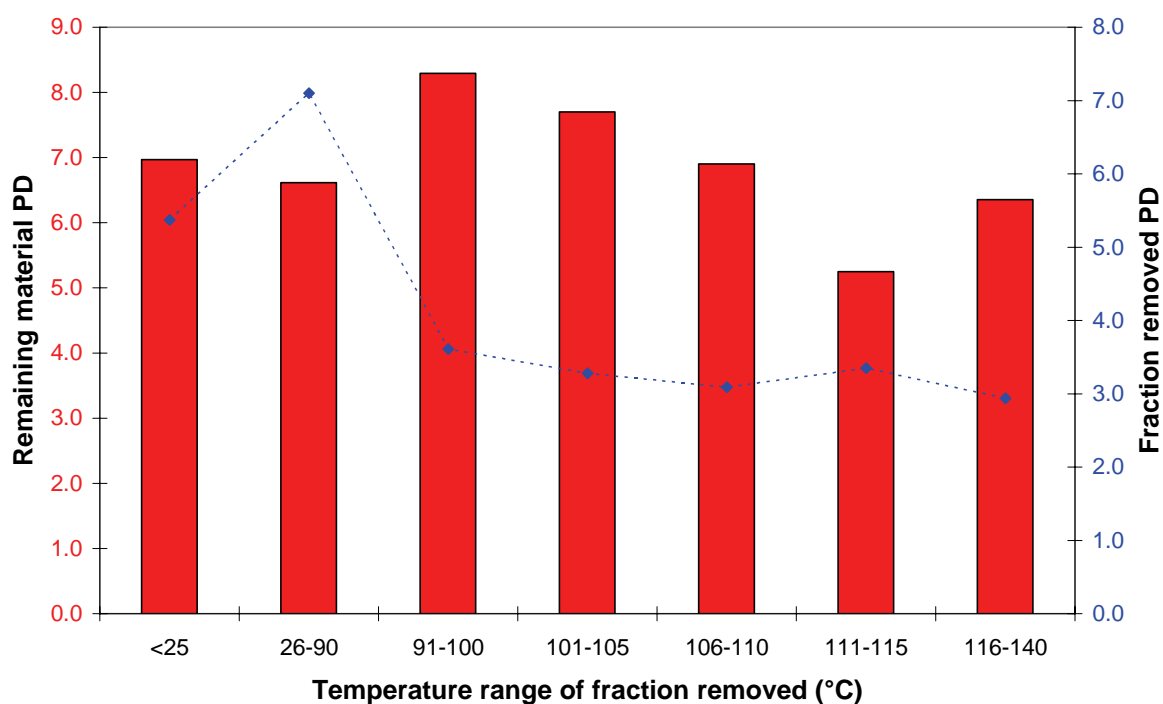


**Figure 4.28** The polydispersity of the PPH samples with specific fractions removed from the sample (shown in red), and the polydispersity of the fraction removed (shown in blue).

An examination of the various sequence distributions as determined by  $^{13}\text{C}$  NMR is given in Figure 4.29. In general one can observe that all the samples contain material with a degree of stereo-errors and that the syndiotactic material produced by means of the chain end control mechanism is evident in all samples with the exception of the sample with the room temperature fraction removed as one would expect since it is the room temperature soluble fraction which contains the majority of these chains (see Figure 4.23). A more in-depth look at the average *mmmm* sequence distribution is given in Figure 4.30. A decrease in the average *mmmm* sequence content is observed as the temperature range of the fraction removed is increased up to the 101 – 105 °C sample. The highest temperature fractions have slightly lower average *mmmm* sequence contents and thus removing these fractions leaves behind material with a slightly higher *mmmm* sequence content than for example removing the 101 – 105 °C fraction.

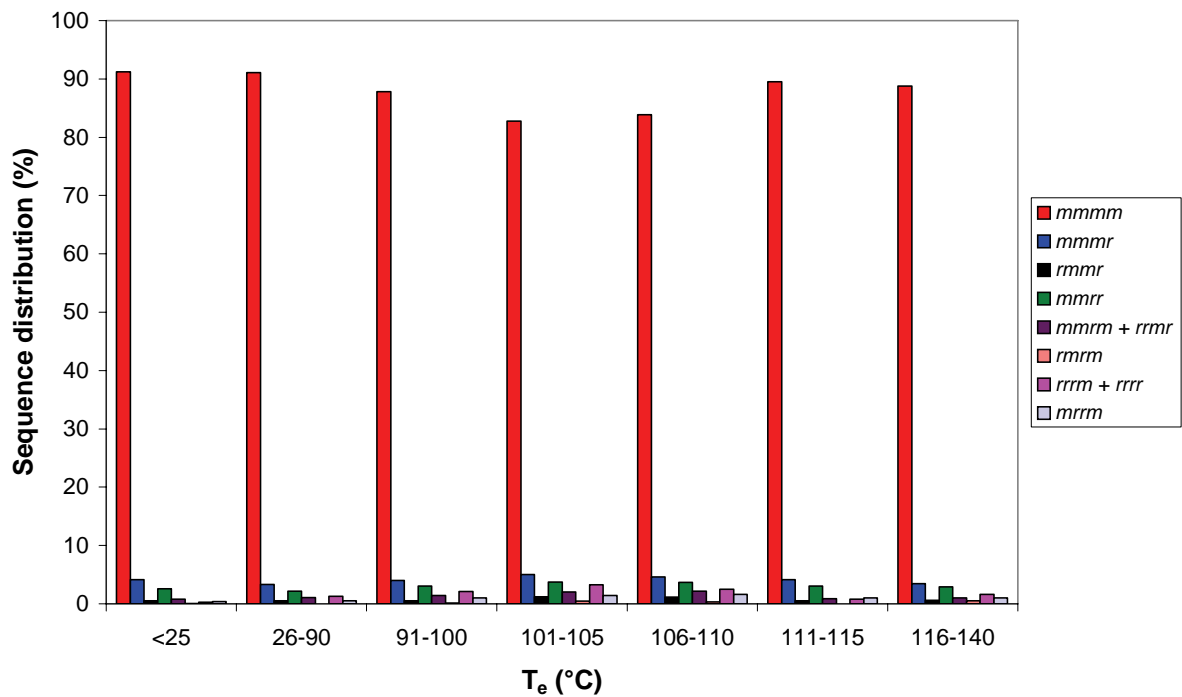


Figure 4.29 The pentad sequence distribution content of the PPH samples with specific TREF fractions removed.

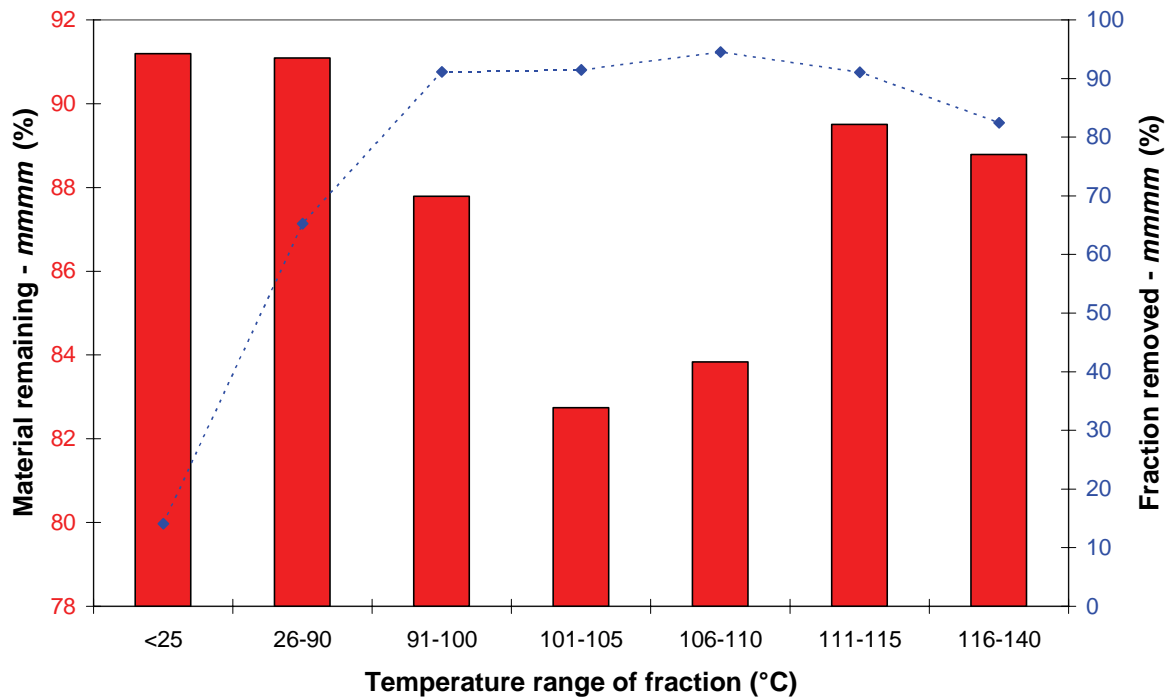


Figure 4.30 The percentage of *mmmm* pentad sequence content for PPH samples with specific TREF fractions removed (shown in red), and the *mmmm* pentad sequence content for the fractions removed (shown in blue).

The amount of material removed also seems to play a significant role. This is evident if one compares the 91 – 100 °C fraction removal and the 101 – 105 °C fraction removal. The *mmmm* sequence content of the fractions being removed are practically the same at 91.1% and 91.4% respectively. However, there is a 5% difference in the *mmmm* sequence content once the fractions are removed. This is due to the greater amount of material being removed when one extracts the 101 – 105 °C fraction. Similarly to the case of the propylene-1-pentene copolymer discussed earlier, it is apparent that the amount of material produced by a certain type of active site is very important with regards to the properties of the material as a whole and not just the nature of the material produced by a certain site.

#### **4.3.2.3 Physical properties**

An examination of the thermal properties of the PPH samples leads one to conclude that the higher the melting temperature of the fraction removed the lower the melting temperature of the material remaining. This is a generalisation and a closer look at Figure 4.31 shows that it is indeed the case for the majority of the fractions concerned. There are obvious exceptions to this generalisation, notably the removal of the final fraction and also the removal of the 25 °C fraction.



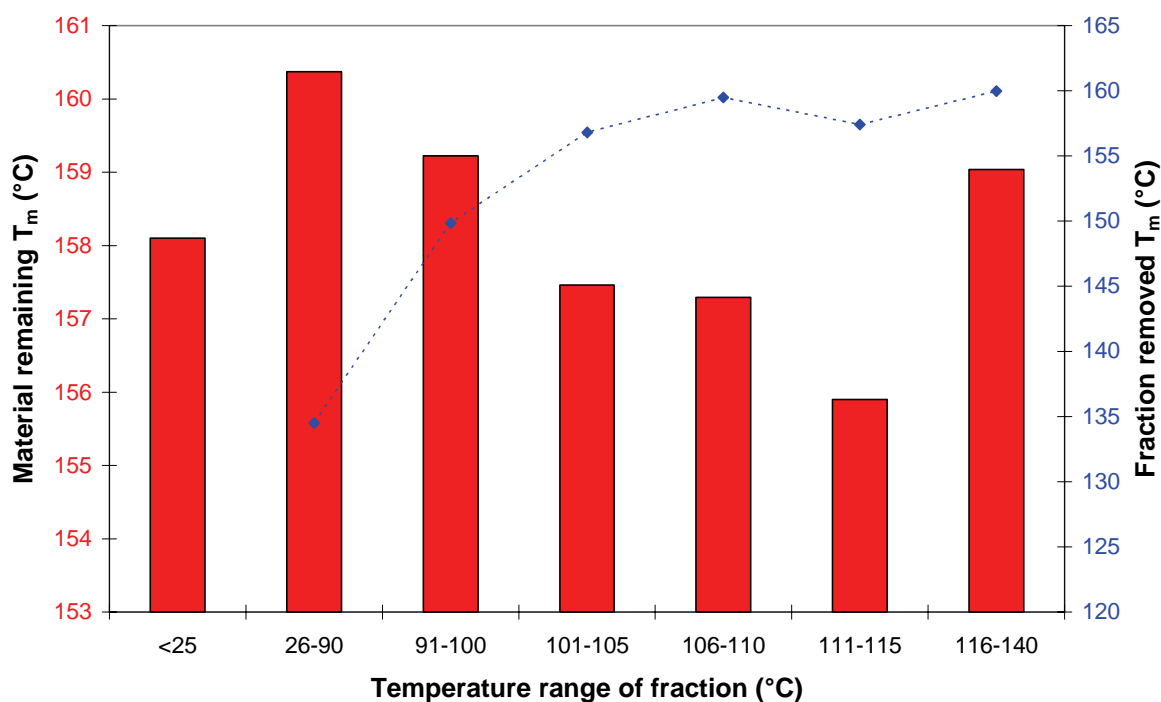


**Figure 4.31** The peak melting temperatures of the PPH sample with specific TREF fractions removed from the sample (shown in red), and the peak melting temperatures of the fractions removed (shown in blue).

With regards to the removal of the final fraction, the molar mass of this fraction is lower than that of the preceding fraction, the tacticity is approximately the same, and the polydispersity of the fraction is slightly higher. It would appear that the broader polydispersity and lower molar mass enable the formation of thicker lamellae which melt at high temperatures for this particular sample. Removal of the 25 °C fraction is interesting in that the fraction itself does not crystallise under the temperature conditions of analysis, however, removal of this material, compared to removal of the following fraction which is semi-crystalline, results in a sample which does not contain lamellae which are as thick and melt at a lower temperature than the following sample. It would appear that the presence of the amorphous material in the 25 °C fraction aids in enhancing the mobility of the chains which can crystallise, thus enabling them to come together to form more perfect and thicker lamellae which melt at slightly higher temperatures.

Analysis of the degree of crystallinity of the samples (Figure 4.32) on the other hand indicates that despite the thinner lamellae the amount of crystalline material is still higher for the sample with the 25 °C fraction removed as one would expect if a significant portion of amorphous material is removed from a sample. There is a definite trend in the crystallinity

data that the more crystalline the material removed, the less crystalline the remaining material as one would expect.

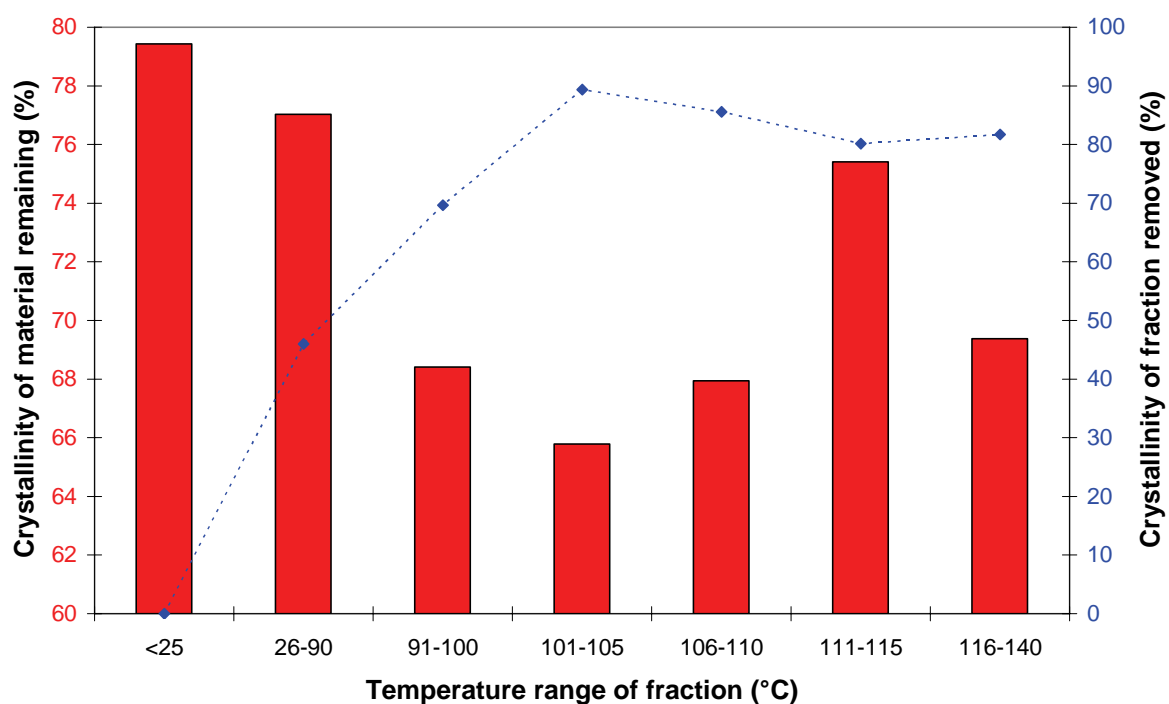


**Figure 4.32** The degree of crystallinity of the PPH samples with specific TREF fractions removed (shown in red), and the crystallinity of the fractions removed (shown in blue).

Similarly to the case of the PP1P sample there are some interesting points to be noted regarding the crystallinity of the samples. If one compares the crystallinity of the sample with the 91 – 100 °C fraction removed with that of the sample with the 106 – 110 °C fraction removed it is observed that although both samples have approximately the same degree of crystallinity, the crystallinity of the fraction being removed is significantly higher for the 106 – 110 °C fraction. There is also significantly less of the 91 – 100 °C fraction being removed than is being removed by taking out the 106 – 110 °C fraction. This implies that once again the fractions which are reasonably crystalline but not the most crystalline are very important in facilitating the crystallisation of the polymer as a whole.

A similar trend is observed for the weight average lamellar thickness as is observed for the crystallinity of the samples. There is a decrease in the thickness of the lamellae as the temperature range of the fraction removed increases (Figure 4.33). The sample with the 25 °C fraction removed has a slightly lower average lamellar thickness which correlates well with the lower melting point. The sample with the 111 – 115 °C fraction removed shows a slightly higher level of crystallinity than would be predicted, however, this sample does have the

lowest molar mass of the samples (Figure 4.25) and also a relatively high *mmmm* sequence content and so it would seem that these factors combined lead to the higher average lamellar thickness of the sample.

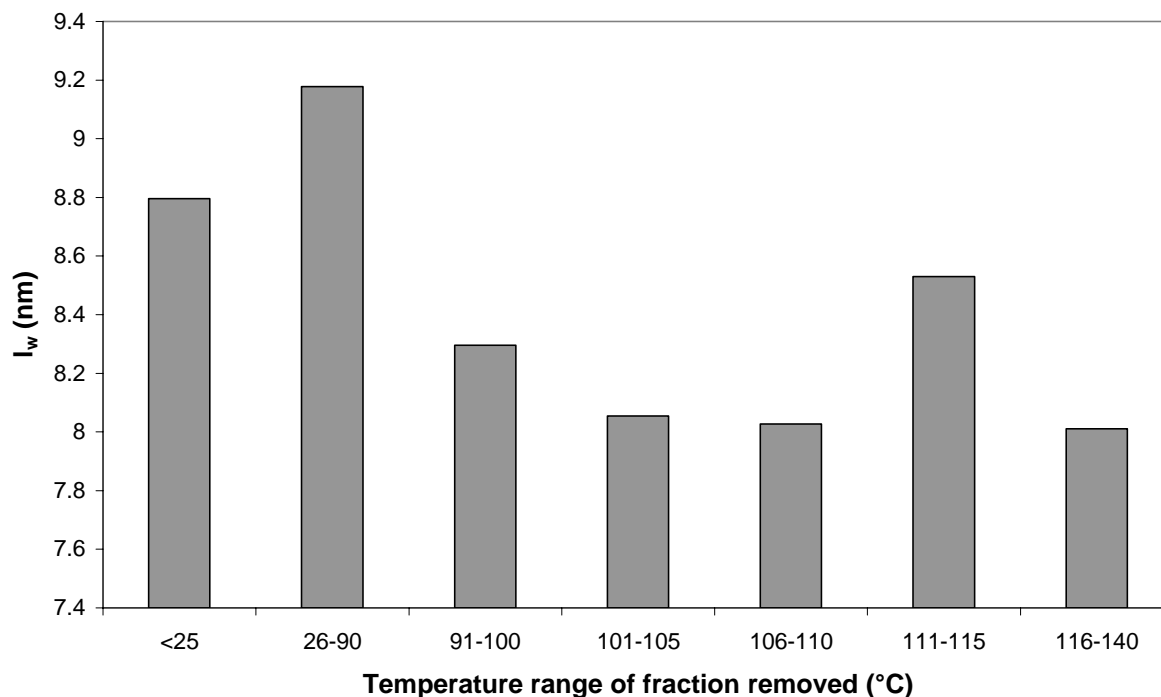


**Figure 4.33** The weight average lamellar thickness of the PPH samples with specific TREF fractions removed.

Figure 4.34 shows the effect of removing different fractions on the modulus value at 2% strain. In general there would appear to be a decrease in the modulus as the temperature range of the fraction removed increases. It would appear that the 26 – 90 °C fraction is very important for the stiffness of the material despite the relatively high crystallinity of the PPH sample with this fraction removed and the high lamellar thickness of the sample. The chains of intermediate crystallinity which melt at lower temperatures possibly act as tie molecules and help in holding together the crystallites in different regions. Removing this material might result in a crystallinity increase, however, on application of a tensile load the energy absorption mechanisms are not as strong as when this fraction is present. Despite this the samples with a lower average lamellar thickness and lower crystallinity generally have a lower modulus value as would be expected with a more crystalline sample being stiffer than a less crystalline one.

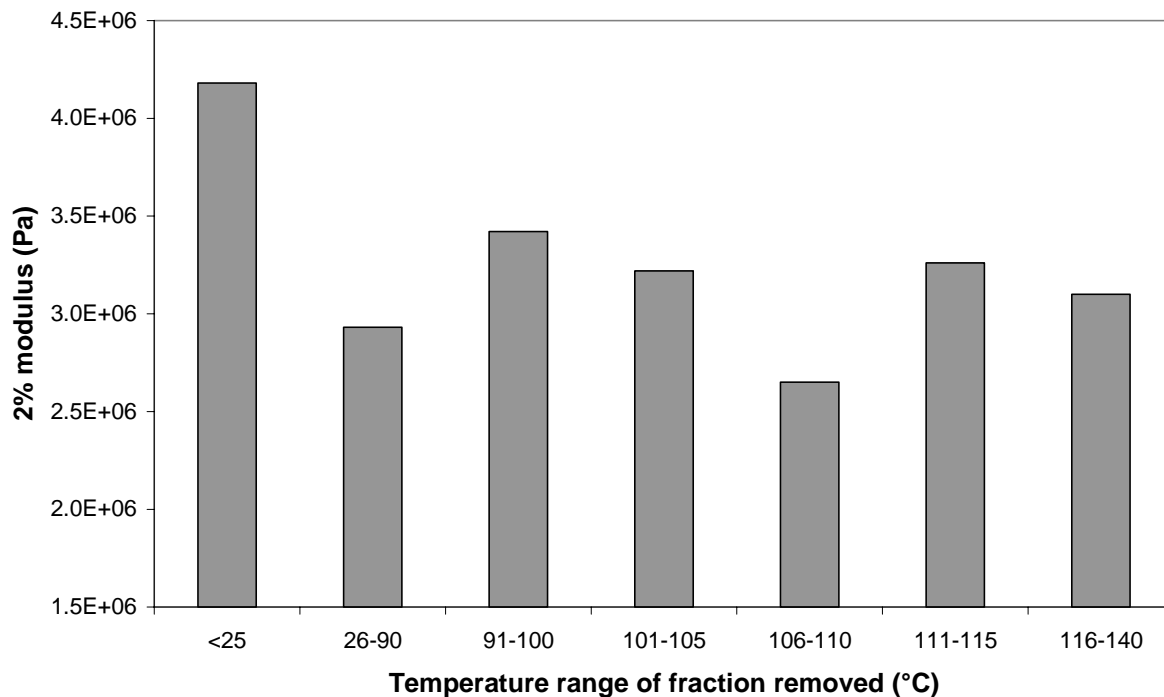


**Figure 4.34** The modulus values at 2% extension of the PPH sample with specific TREF fractions removed from the sample.

#### 4.3.2.4 Structure – property relationships

A closer examination of the properties of the PPH samples reveals a few relationships between the polymer microstructure and the physical properties of the materials. Figure 4.35 illustrates the correlation between the degree of crystallinity of the samples and the modulus of the samples. An increase in the crystallinity would definitely appear to result in an increase in the modulus of the samples although this is not the only factor affecting the properties. Similarly there is an effect of molar mass on the modulus (Figure 4.36) and it would appear that the higher molar mass samples have a higher stiffness than the lower molar mass samples possibly related to the degree of molecular entanglements which is higher for higher molar mass samples. There was, however, no direct correlation of molar mass with crystallinity implying that a combination of affects are at work regarding the properties of the materials upon loading.

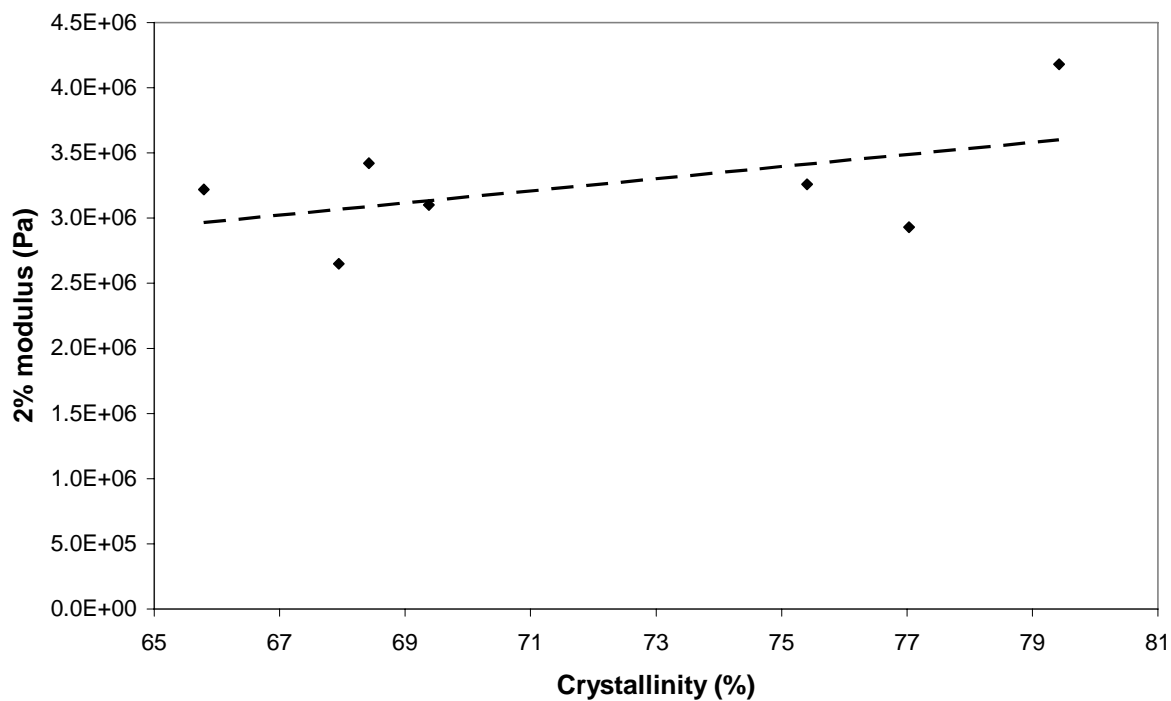


Figure 4.35 The relationship between the crystallinity and the modulus at 2% strain for the PPH samples.

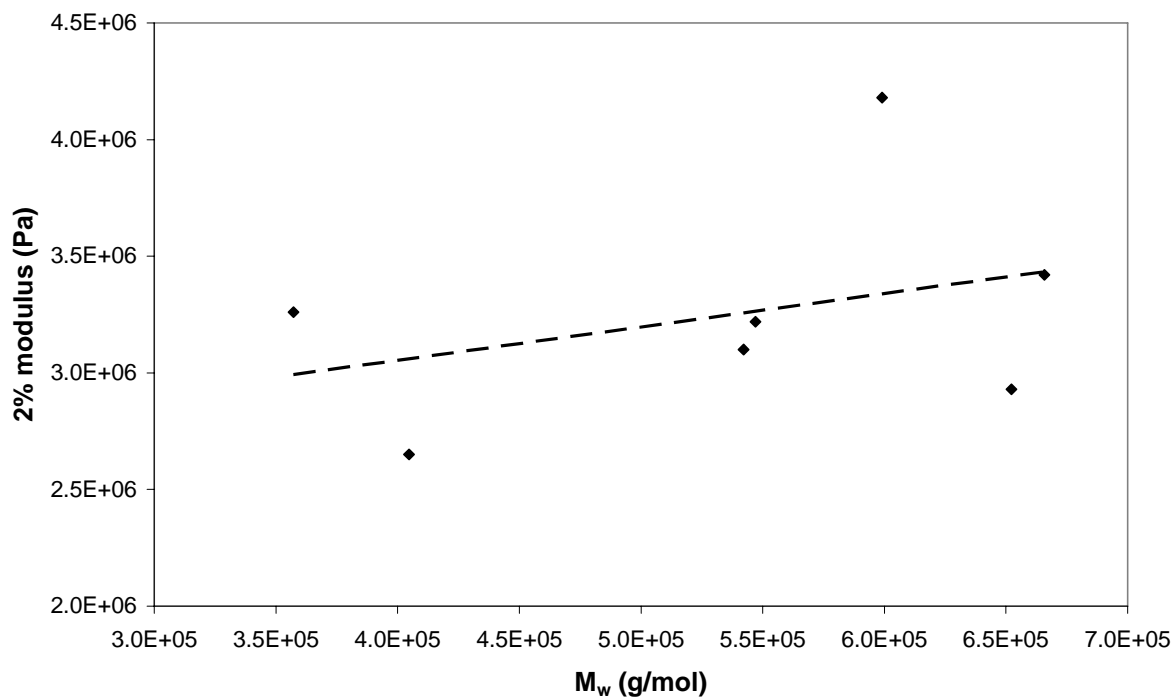


Figure 4.36 The relationship between the weight average molar mass and the modulus at 2% strain for the PPH samples.

The crystallinity on the other hand appears to be related to the lamellar thickness of the samples as a good relationship between the two properties is illustrated in Figure 4.37.

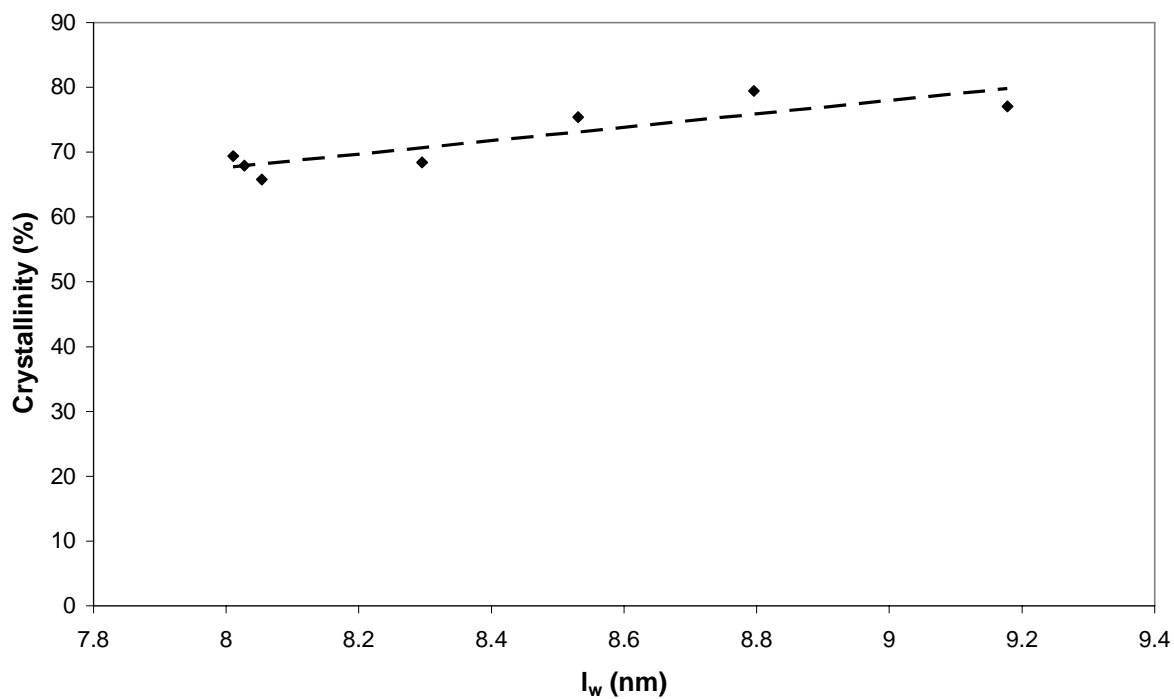


Figure 4.37 The relationship between the crystallinity and the lamellar thickness of the PPH samples.

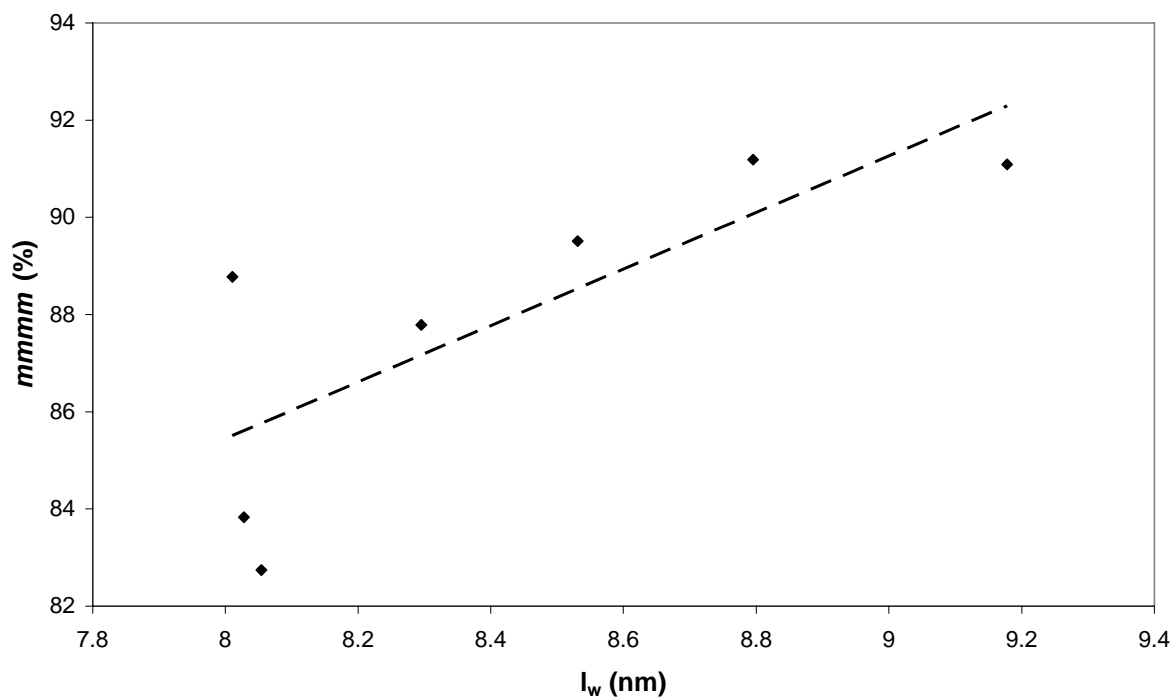
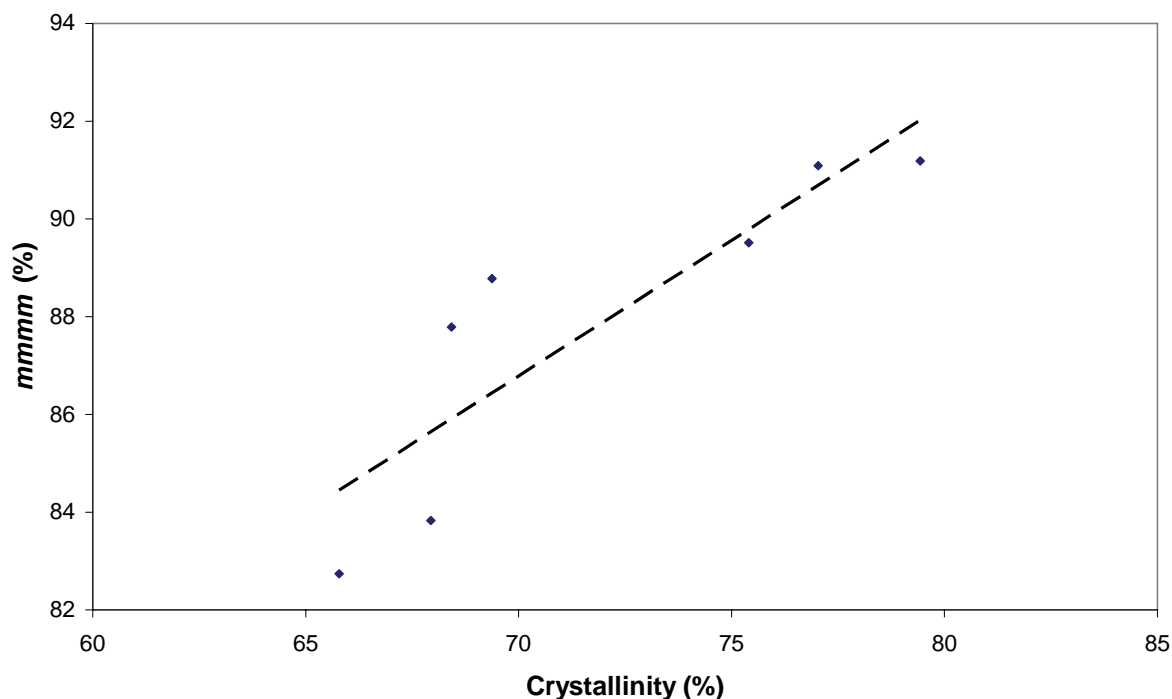


Figure 4.38 The relationship between the lamellar thickness and the average *mmmm* pentad sequence content of the PPH samples.

There is also a tacticity effect on the lamellar thickness (Figure 4.38) as the higher the tacticity of a given sample, the thicker the lamellae. This is a clear indication that the

stereoregularity of the chains is a dominant factor in determining the lamellar thickness of the crystals in the homopolymer. The tacticity therefore also plays an important role in determining the crystallinity of the samples as expected (Figure 4.39).



**Figure 4.39** The relationship between the *mmmm* pentad sequence content and the crystallinity of the PPH samples.

The importance of the molecular structure on the properties of the polymer is clearly evident from the differences observed between the samples.

## 4.4 Conclusions

The thorough analysis of the two propylene polymers undertaken in this section of the study, have yielded some interesting results. Generally it can be said that for both the copolymer and homopolymer the microstructure plays an extremely important role in determining the properties of the polymers. Both polymers were successfully characterised and the distinct differences between the homopolymer and copolymer were evident. The effect of the comonomer on the fractionation of the copolymer, and on the properties of the copolymer as compared to the homopolymer were observed. The comonomer clearly disrupts the crystallisation of the propylene segments. The nature of this section of the work is such that one could not say with any certainty that the comonomer is present in the crystalline

regions itself, however, the comonomer is incorporated to such an extent that there are highly isotactic chains present which include isolated 1-pentene units in the chains and these comonomer units do indeed have an effect on the crystallisation of the polymer. A more in depth analysis on the location of the comonomer is beyond the scope of this work.

As far as the correlation between the polymer microstructure and the physical properties are concerned a number of relationships were established. The modulus of both the copolymer and the homopolymer was dependant on the crystallinity of the samples, with a higher crystallinity resulting in a higher modulus value for a given polymer. It is also evident that the modulus values for the homopolymer are much higher than those of the copolymer indicating that the disruption of the crystallisation of the polymer by the comonomer plays a significant role in determining the properties of the material. In turn the crystallinity of the copolymer samples was shown to be strongly dependant on the lamellar thickness of the samples which in turn were dependant on the 1-pentene content of the sample. There was no direct correlation between the comonomer content and the modulus indicating that the molar mass and molar mass distribution also play a significant role.

Similarly the crystallinity of the homopolymer was dependent on the lamellar thickness of the samples and this in turn was dependant on the *mmmm* pentad sequence content. Irrespective of which polymer system is analysed it appears that any structural defect inhibiting the crystallisation of the chains plays a large role in determining the physical properties. There was also no direct correlation between the *mmmm* pentad content and the modulus despite the formers influence on the crystallinity. There was also a slight molar mass effect on the modulus values for the homopolymer indicating the possibility that molecular entanglements and tie molecules contribute to the stiffness of the polymer.

It was also discovered that the amount of a certain type of material present in a polymer system plays an important role in determining the properties. Changing the amount of materials physically constituting a polymer was possible using preparative TREF and this showed that the alteration of a polymer properties is possible by altering the amounts of certain types of chains in the polymer. The alteration of the properties demonstrated that certain specific TREF fractions are extremely important for the properties of the polymer as a whole, as the properties decreased significantly in the absence of these fractions. It is also noted that the most important fractions are not necessarily the most crystalline fractions or even those eluting at the highest temperatures but that the fractions eluting in the intermediate to high temperatures are the most important. These fractions possibly serve as tie molecules and form part of the crystalline and ordered amorphous phases, aiding in the linkup of different crystalline regions and thus improving polymer properties.



Alteration of the amount of certain fractions in the polymer was done on a physical basis for the work in this chapter, however, the same methodology can be applied to the scenario whereby the composition of a polymer is altered by changing the nature of the active sites actually producing the polymer. This chemical alteration of the active sites is made possible by alteration of the polymerisation conditions. There are a number of different ways in which this can be done and these are discussed further in the following chapters.

## 4.5 References

1. Varga, J., & Ehrenstein, G.W., *Crystallization, melting and supermolecular structure of isotactic polypropylene*, in *Polypropylene: Structure, blends and composites*, J. Karger-Kocsis, Editor. 1995, Chapman & Hall: London.
2. Lutz, M., Structure/property relationships of commercial propylene/1-pentene random copolymers. 2006. PhD Thesis. University of Stellenbosch: Stellenbosch
3. Harding, G.W., & van Reenen, A.J., *Fractionation and characterisation of propylene-ethylene random copolymers: Effect of the comonomer on crystallisation of poly(propylene) in the  $\gamma$ -phase*. *Macromolecular Chemistry and Physics*, 2006. **207**(18): p. 1680-1690.
4. De Goede, E. 2008. Unpublished work, University of Stellenbosch.
5. Beuche, F., *Physical properties of polymers*. 1962, New York: Interscience Publishers.
6. Wild, L., *Temperature rising elution fractionation*. *Advances in Polymer Science*, 1990. **98**(1): p. 1-47.
7. De Rosa, C., Auriemma, F., Paolillo, M., Resconi, L., & Camurati, I., *Crystallization behavior and mechanical properties of regiodefective, highly stereoregular isotactic polypropylene: Effect of regiodefects versus stereodefects and influence of the molecular mass*. *Macromolecules*, 2005. **38**: p. 9143-9154.
8. Hosoda, S., Hori, H., Yada, K., Nakahara, S., & Tsuji, M., *Degree of comonomer inclusion into lamella crystal for propylene/olefin copolymers*. *Polymer*, 2002. **43**: p. 7451-7460.
9. Ran, S., Hsiao, B.S., Agarwal, P.K., Varma-Nair, M., *Structure and morphology development during deformation of propylene based ethylene-propylene copolymer and its blends with isotactic polypropylene*. *Polymer*, 2003. **44**: p. 2385-2392.
10. Feng, Y., & Hay, J.N., *The characterisation of random propylene-ethylene copolymer*. *Polymer*, 1998. **39**(25): p. 6589-6596.

11. Feng, Y., and Hay, J.N., *Crystalline structure of propylene-ethylene copolymer fractions*. Journal of Applied Polymer Science, 1998. **68**: p. 381-386.
12. Feng, Y., & Hay, J.N., *The measurement of compositional heterogeneity in a propylene-ethylene block copolymer*. Polymer, 1998. **39**(26): p. 6723-6731.
13. Bartczak, Z., Chiono, V., & Pracella, M., *Blends of propylene-ethylene and propylene-1-butene random copolymers: I. Morphology and structure*. Polymer, 2004. **45**: p. 7549-7561.
14. Laihonon, S., Gedde, U.W., Werner, P.-E., & Martinez-Salazar, J., *Crystallization kinetics and morphology of poly(propylene-stat-ethylene) fractions*. Polymer, 1997. **38**: p. 361-369.
15. Flory, P.J., *Theory of crystallization in copolymers*. Transactions of the Faraday Society, 1955. **51**: p. 848-857.
16. Hosier, I.L., Alamo, R.G., & Lin, J.S., *Lamellar morphology of random metallocene propylene copolymers studied by atomic force microscopy*. Polymer, 2004. **45**: p. 3441-3455.
17. Dasari, A., Rohrmann, J., & Misra, R.D.K., *Surface microstructural modification and fracture behavior of tensile deformed polypropylene with different percentage crystallinity*. Materials Science and Engineering, 2003. **A360**: p. 237-248.
18. Mezghani, K., Campbell, R.A., & Phillips, P.J., *Lamellar thickening and the equilibrium melting point of polypropylene*. Macromolecules, 1994. **27**: p. 997-1002.
19. Albizzati, E., Giannini, U., Collina, G., Noristi, L., & Resconi, L., *Catalysts and polymerizations*, in *Polypropylene handbook*, E.P. Moore, Jr., Editor. 2002, Hanser: Munich. p. 11-111.
20. Krentsel, B.A., Kissin, Y.V., Kleiner, V.J., & Stotskaya, L.L., *Polymers and copolymers of higher  $\alpha$ -olefins*. 1999, Munich: Hanser. Chapter 1.
21. Kakugo, M., Miyatake, T., Naito, Y., & Mizunuma, K., *Microtacticity distribution of polypropylenes prepared with heterogeneous Ziegler-Natta catalysts*. Macromolecules, 1988. **21**: p. 314-319.
22. Virkkunen, V., Laari, P., Pitkanen, P., & Sundholm, F., *Tacticity distribution of isotactic polypropylene prepared with heterogeneous Ziegler-Natta catalyst. I. Fractionation of polypropylene*. Polymer, 2004. **45**: p. 3091-3098.
23. Zakharov, V.A., Bukatov, G.D., & Barabanov, A.A., *Recent data on the number of active centers and propagation rate constants in olefin polymerization with supported ZN catalysts*. Macromolecular Symposium, 2004. **213**: p. 19-28.

24. Yaluma, A.K., Chadwick, J.C., & Tait, P.J.T., *Kinetic and active centre studies on the polymerization of propylene using MgCl<sub>2</sub> supported Ziegler-Natta catalysts and 1,3 diether donors*. Macromolecular Symposium, 2007. **260**: p. 15-20.
25. Bukatov, G.D., Zakharov, V.A., & Barabanov, A.A., *Mechanism of olefin polymerization on supported Ziegler–Natta catalysts based on data on the number of active centers and propagation rate constants*. Kinetics and Catalysis, 2005. **46**: p. 166-176.
26. Bukatov, G.D., & Zakharov, V.A., *Propylene Ziegler-Natta polymerization: Numbers and propagation rate constants for stereospecific and non-stereospecific centers*. Macromolecular Chemistry and Physics, 2001. **202**: p. 2003-2009.

# Chapter 5. Polymerisation reactions with a Ziegler-Natta catalyst

## 5.1 Introduction

The research into Ziegler-Natta catalysts and the polymers they produce is a reasonably mature field, driven on by the huge consumer demand for the products which are produced from these polymers. Since the discovery of these catalysts in the 1950's the number of applications for the materials have grown extensively as a direct result of research, the result of which has been the ability to manipulate the properties of the polymers produced via a number of means such as varying reaction conditions, new catalysts and copolymerisation. Manipulation of the properties of the material via modification of the polymerisation conditions is therefore, a key step in the development of different polymer grades and is the modification mechanism focussed on in this chapter. The polymerisation conditions in turn affect the active sites of the catalyst and the manner in which they polymerise the monomer. Variations in the active sites and their effect on polymer properties were discussed in detail in Chapter 2.

The following chapter discusses the results for the development work done on the conditions used for the polymerisations. It was decided to perform a number of different reactions with the catalyst in order to examine the effects of different polymerisation temperatures, catalyst/cocatalyst ratio's, monomer pressures, the presence or absence of electron donor, the type of electron donor, and the external donor/catalyst ratio. Due to the fact that the polymerisations were conducted in relatively small 300 mL reactors, many of the initial developmental reactions were focussed on the activity of the system so as to ensure that sufficient material was produced for further analysis, especially for the reactions used for more in-depth studies. Once a good understanding was obtained on the manner in which the catalyst functions a number of more specific reactions were performed for the in-depth analysis.

## 5.2 Experimental

The majority of the experimental details are given in Chapter 3, however, a few specific to the polymerisations are given here.

## 5.2.1 Polymerisation details

All polymerisations were conducted in a 300 mL stainless steel reactor equipped with a pressure gauge, gas inlet, and sample introduction port. A specified amount of catalyst was first weighed off into a schlenk tube in a glove box under an argon atmosphere. The schlenk tube was then sealed and transferred to a schlenk line adjacent to the reactor. To the catalyst was added 5 mL toluene as solvent, as well as the cocatalyst and external electron donor (depending on whether this was required during the reaction or not) into the schlenk tube. Subsequent to initial investigations on the matter, the contact time in the schlenk tube was maintained at a constant 1 minute. The reactor was repeatedly evacuated and flushed with argon prior to the polymerisation reaction. 20 mL of toluene was then added to the reactor. The catalyst solution was then introduced to the reactor. The reactor was then charged with hydrogen (if required for the reaction in question), followed by propylene monomer. All reactions were left to take place over one hour after which they were terminated via the addition of a 10% solution of hydrochloric acid in methanol.

The two types of external electron donor used in this study are illustrated in Figure 5.1. The only difference between the two donors being the exchange of a phenyl group for a methyl group so that the substituents on the silane are less bulky for external donor B in order to investigate this effect on the polymerisations.

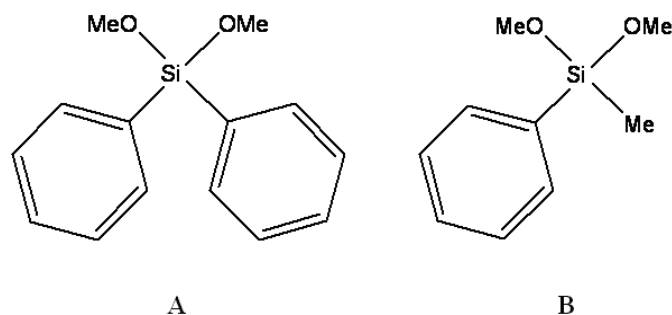


**Figure 5.1** The structure of the two types of external Lewis base used in the study, namely DPDMS (structure A) and MPDMS (structure B).

## 5.2.2 Polymer characterisation

The  $^{13}\text{C}$  NMR, DSC, and HT-GPC data of the samples were obtained according to procedures described in Chapter 3 (Sections 3.3.1-3.3.3).

## 5.3 Results and Discussion

Each of the different reaction conditions investigated during the course of the study are discussed in turn.

### 5.3.1 Catalyst/cocatalyst pre-treatment time

Initial reactions focussed on the contact time between the catalyst and cocatalyst. This is an important factor since it is known that although the cocatalyst activates the catalyst to form the metal-carbon bond, it can also over-reduce the titanium species resulting in sites on the catalyst which are inactive for polymerisation [1, 2]. Stopped-flow reactions have also shown this deactivation of the catalyst and have shown that there is a reduction in the active centre concentration ( $C^*$ ) when the catalyst is pre-treated with the cocatalyst [3].

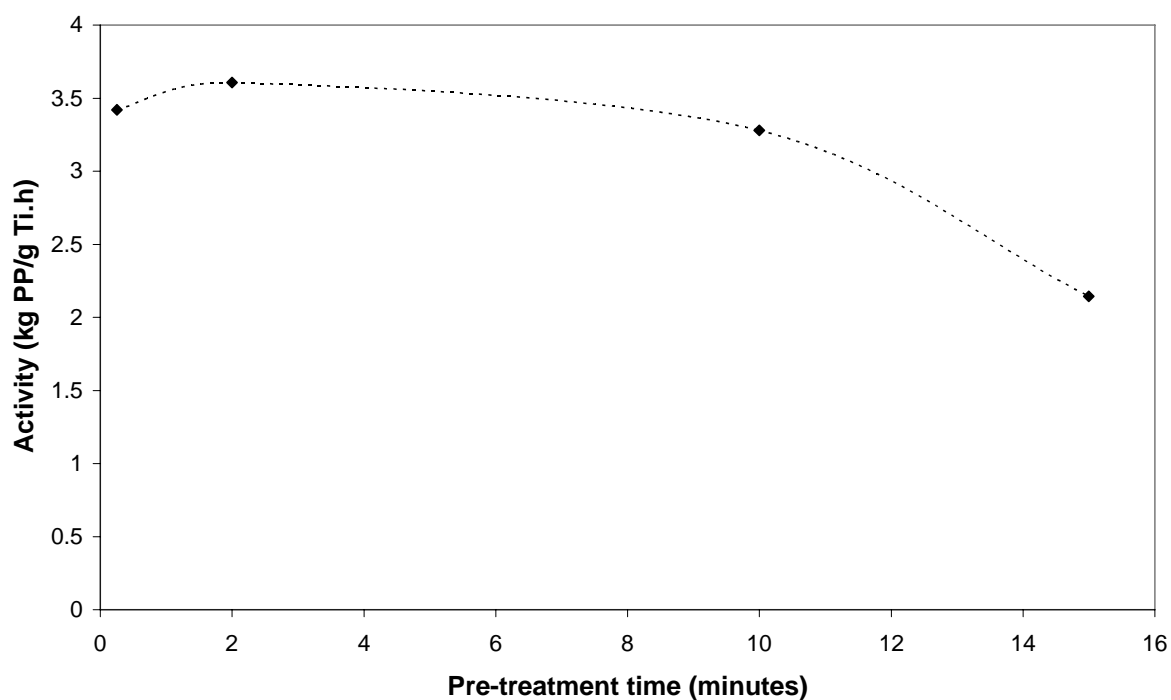


**Figure 5.2** The effect of the contact time of the catalyst and co-catalyst on the activity of the system.

Figure 5.2 illustrates the catalyst-cocatalyst contact times investigated. It is clear that after an initial increase over the first couple of minutes the activity decreases sharply as the contact time is increase further. This is consistent with the over-reduction of the titanium species reducing the number of sites actually active for the polymerisation, thereby lowering the activity of the catalyst as a whole. Evidence that the polymer chains that are produced are also inherently different is given in Figure 5.3. The decrease in molar mass as the contact time

is extended past the optimum time is shown, implying that the active sites on the catalyst are not able to produce material of the highest chain lengths. A reduction in molar mass with reduction of the active species has been shown by other researchers [2].

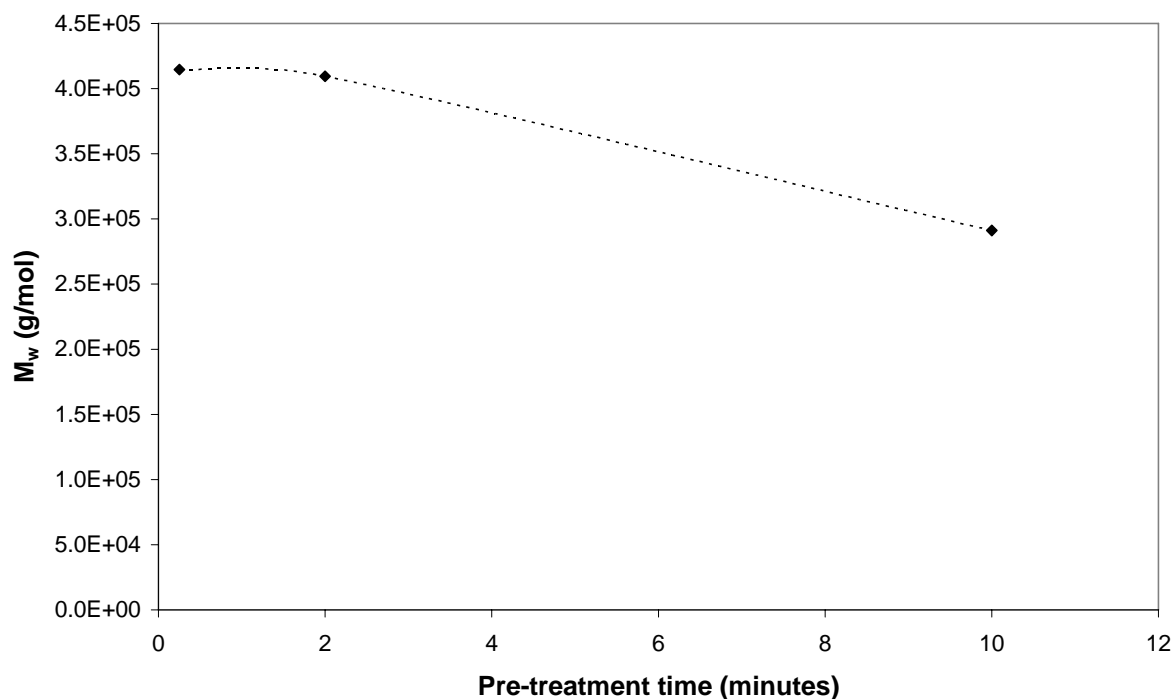


**Figure 5.3** The effect of the contact time of the catalyst and co-catalyst on the molar mass of the polymer.

The thermal properties of the samples were also investigated and the effect of the over reduction of titanium species has also been observed to have an affect on the crystallinity of the samples as illustrated in Figure 5.4. There is an initial increase in the degree of crystallinity, however, this soon decreases again for the longer catalyst-cocatalyst contact times. This is most likely due to the extraction of the internal donor from the catalyst by the cocatalyst, thereby reducing the stereospecificity of the active sites. It is also possible that over-reduction of the titanium species also aids in the formation of less stereospecific active sites. The lower stereospecificity of the active sites would result in the production of chains of a lower stereoregularity and lower molar mass due to a reduction in  $k_p$  for the sites of lower stereoregularity. This would result in the chains not being able to crystallise as perfectly as prior to the over-reduction and indeed a decrease in isospecificity of overly reduced titanium species has been observed [2]. Mori *et al.* [4] have shown a decrease in the isotacticity of the polymer and an increase in the polydispersity of the polymer produced as the reducing ability of the cocatalyst is increased. This also indicates that the over-reduction of the titanium species plays an important role in altering the composition of the active sites of the catalyst.

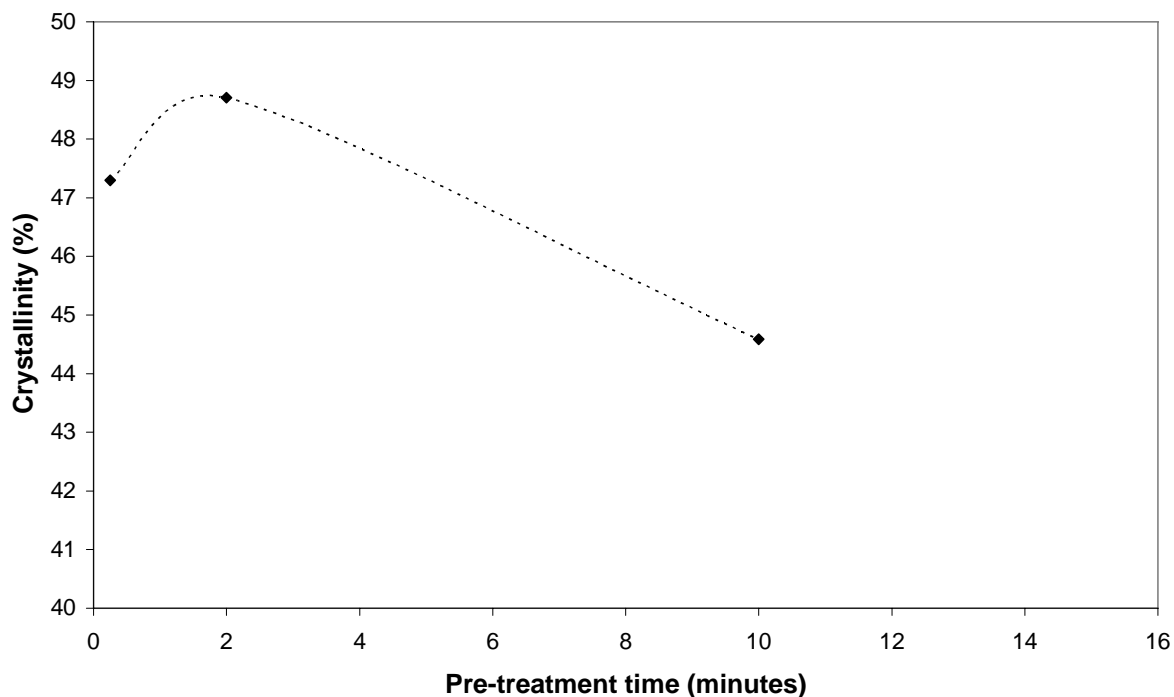


Figure 5.4 The effect of the contact time of the catalyst and co-catalyst on the crystallinity of the polymer.

### 5.3.2 Polymerisation temperature

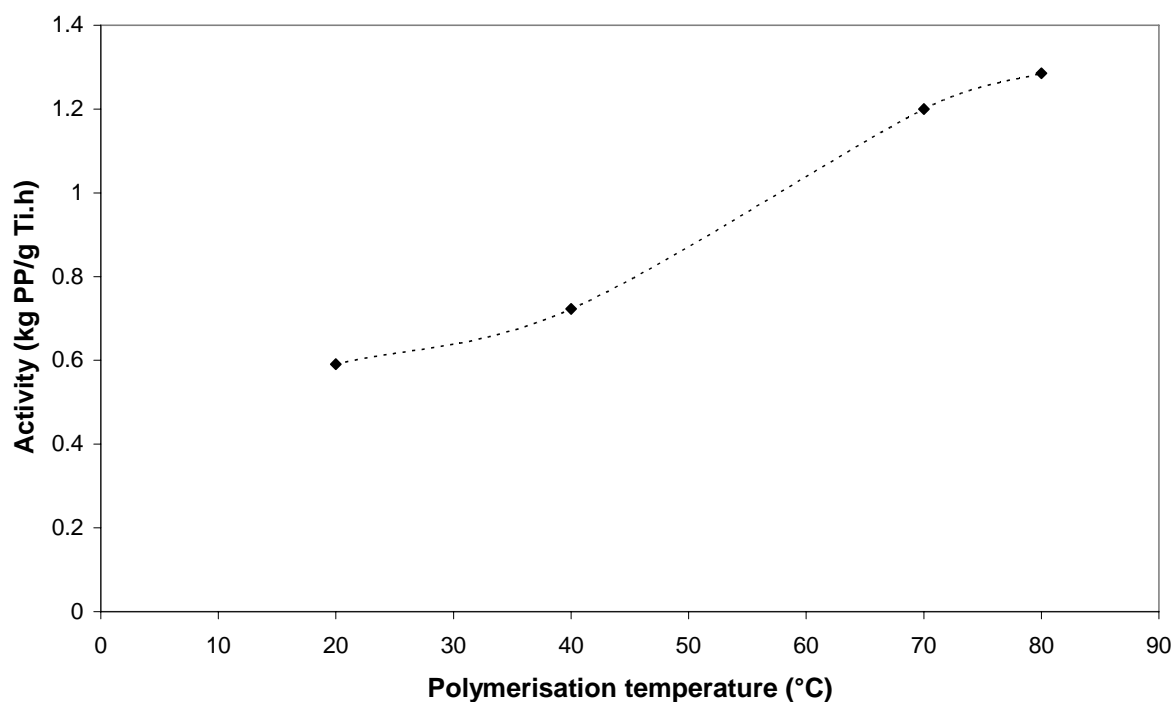
The polymerisation temperature is known to play an important role in determining the activity [5] of the active sites as well as other parameters such as the isospecificity [6, 7] and molar mass [8, 9] and morphology of the catalyst particle [10]. Various temperatures were investigated at two different cocatalyst-catalyst ratios in order to investigate the differences in this parameter for the varying conditions. The two different ratios investigated were Al:Ti = 20 and Al:Ti = 80. The polymerisations conducted to investigate the effect of temperature were conducted in the absence of both hydrogen and external electron donors.

#### 5.3.2.1 Al : Ti = 20

Figure 5.5 illustrates the change in activity as the polymerisation temperature is increased from 20 °C to 80 °C. There is a clear increase in activity with polymerisation temperature over the temperature range investigated. Zhong *et al.* [7] have shown, however, that too high a polymerisation temperature, especially using the highly active triethylaluminium cocatalyst used in this study, results in a decrease in activity. This

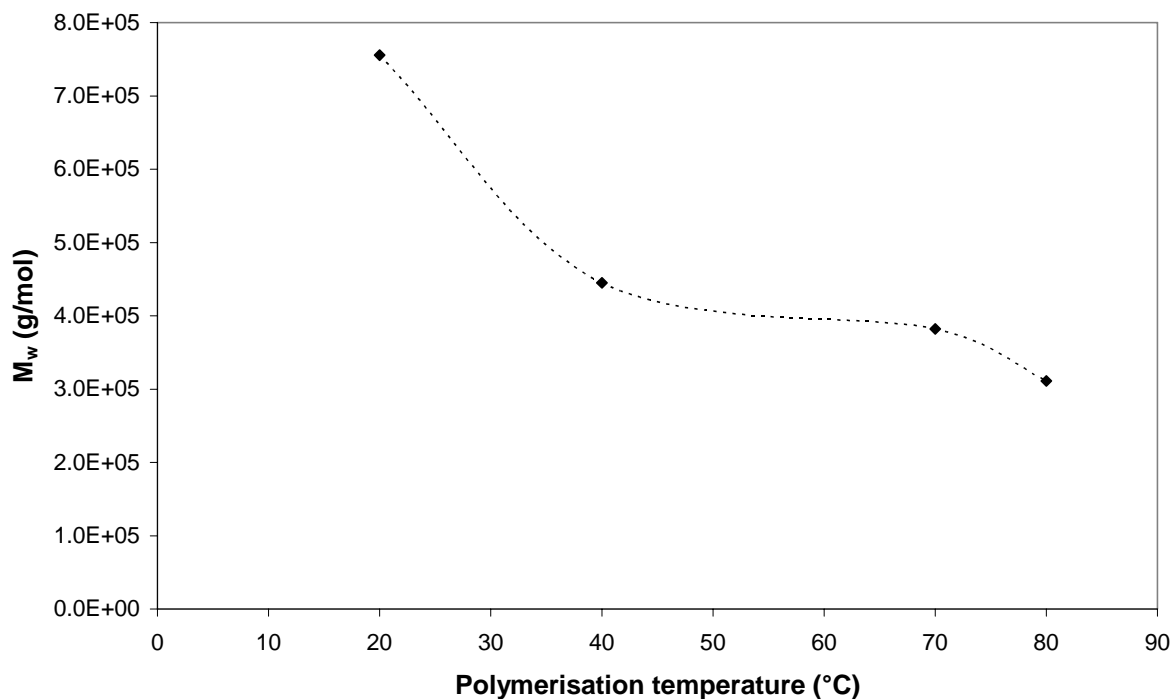


temperature at which the activity begins to decrease is over 80 °C for the relatively low cocatalyst-catalyst ratio of 20.



**Figure 5.5** The effect of temperature on the activity of the catalyst at an Al:Ti = 20.

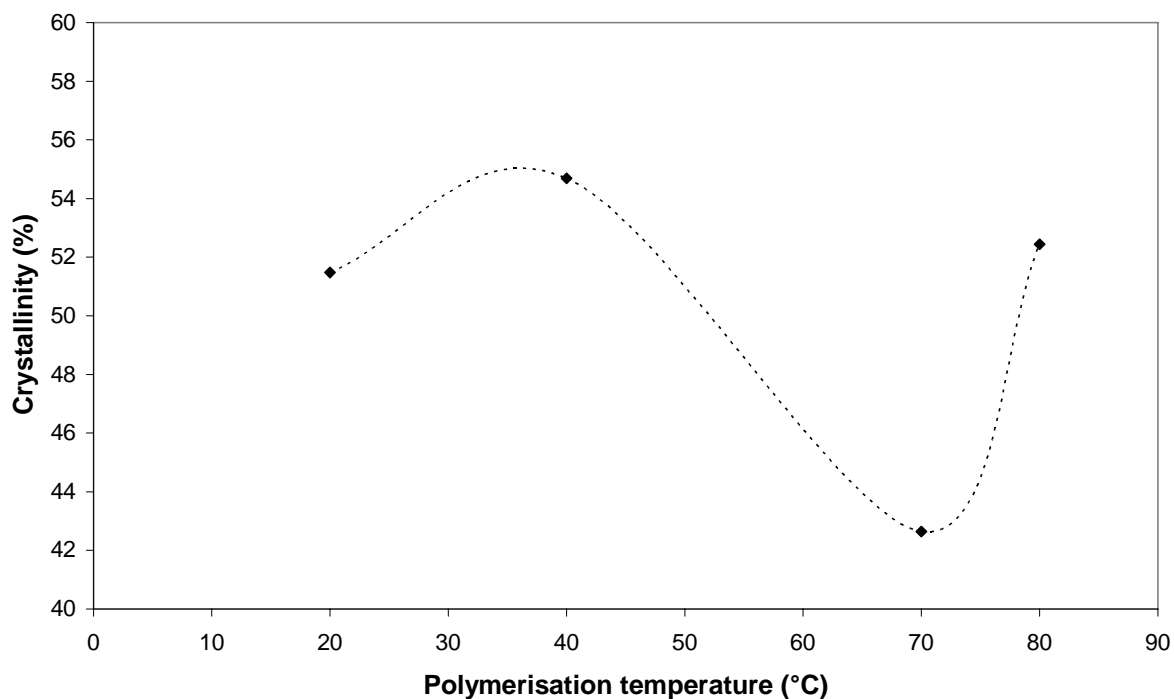
The activity increase with increasing temperature is most likely due to an increase in the propagation rate constant of the sites as well as the possibility of an increase in the ability of the cocatalyst to activate the catalyst, thereby producing more active centers for polymerisation as was revealed by Zakharov *et al.* [5].



**Figure 5.6** The effect of temperature on the  $M_w$  of the polymer produced at an Al:Ti = 20.

The molar mass of the samples generally decrease with increasing polymerisation temperature as can be seen in Figure 5.6. The reduction in molar mass with increasing polymerisation temperature has also been shown to occur in studies by Zhong *et al.* [7], Wang *et al.* [9], and Zohuri *et al.* [11]. Chadwick *et al.* [6] also observed a decrease in molar mass with increasing polymerisation temperature for a donor free catalyst and an increase in molar mass when an external donor was present in the system. They also used a catalyst system with DIBP as internal donor and observed a decrease in viscosity (which is an indication of a decrease in molar mass) with increasing polymerisation temperature in the absence of external donor.

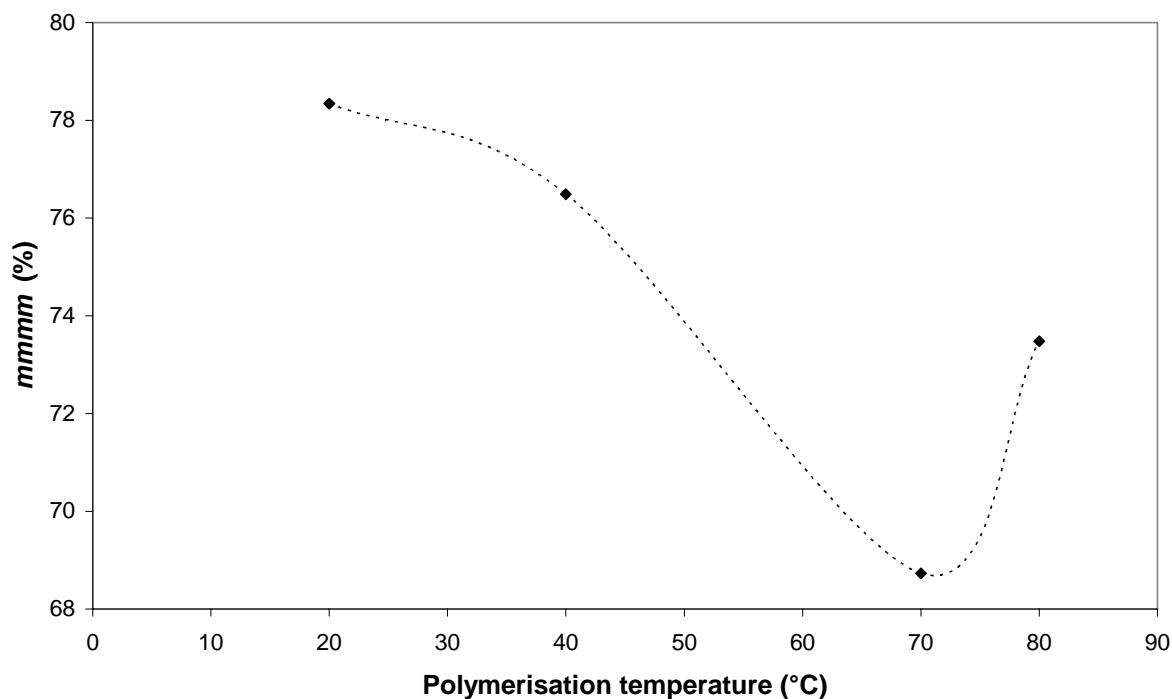
The degree of crystallinity of the samples was also investigated and the results are given in Figure 5.7. No definite trend was observed for the crystallinity of the samples although there is possibly a slight overall decrease with increasing polymerisation temperature. There would appear to be a correlation between the crystallinity of the samples and the *mmmm* pentad sequence content (Figure 5.8) as would be expected. The increase in crystallinity at the highest polymerisation temperature of 80 °C, occurs as a result of an increase in *mmmm* pentad content at the same temperature.



**Figure 5.7** The effect of temperature on the crystallinity of the polymer produced at an Al:Ti = 20.

Generally a decrease in tacticity of the samples was observed with increasing polymerisation temperature (Figure 5.8). Kissin *et al.* [8] have also discovered a general decrease in the average tacticity of samples with increasing polymerisation temperature. Chadwick *et al.* [6] on the other hand have observed an increase in the stereoselectivity of a catalyst containing a diether as donor with increasing polymerisation temperature, both in the presence and absence of hydrogen. The use of the diether in their system mean that their results would be different since the diether is not extracted to any great extent by the cocatalyst, thus preventing the over-reduction of the titanium species at higher temperatures. Their reactions, using DIBP as internal donor, did not show any increase in tacticity with polymerisation temperature.

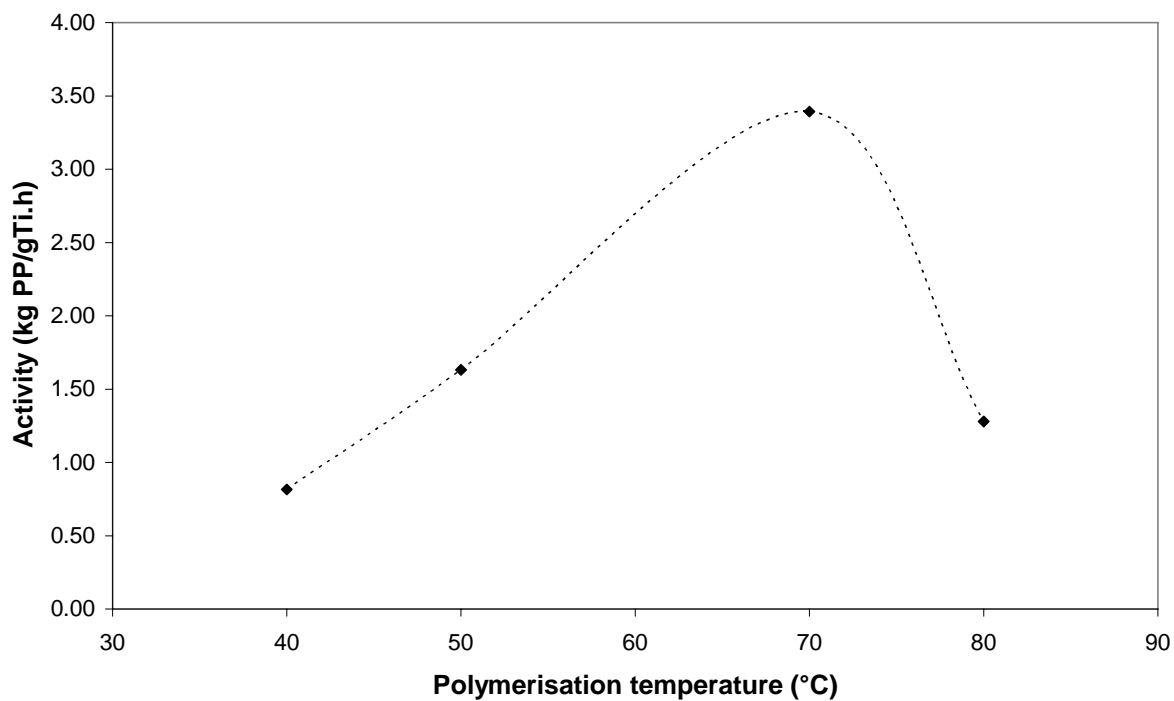
An increase in tacticity is observed if the polymerisation temperature is raised from 70 °C to 80 °C as seen in Figure 5.8. This is possibly due to faster propagation at the higher temperatures for the more stereospecific sites thereby increasing their productivity [6], although this effect would also be counterbalanced by the over-reduction of titanium species and extraction of internal donor.



**Figure 5.8** The effect of the polymerisation temperature on the tacticity of the polymer produced at an Al:Ti = 20.

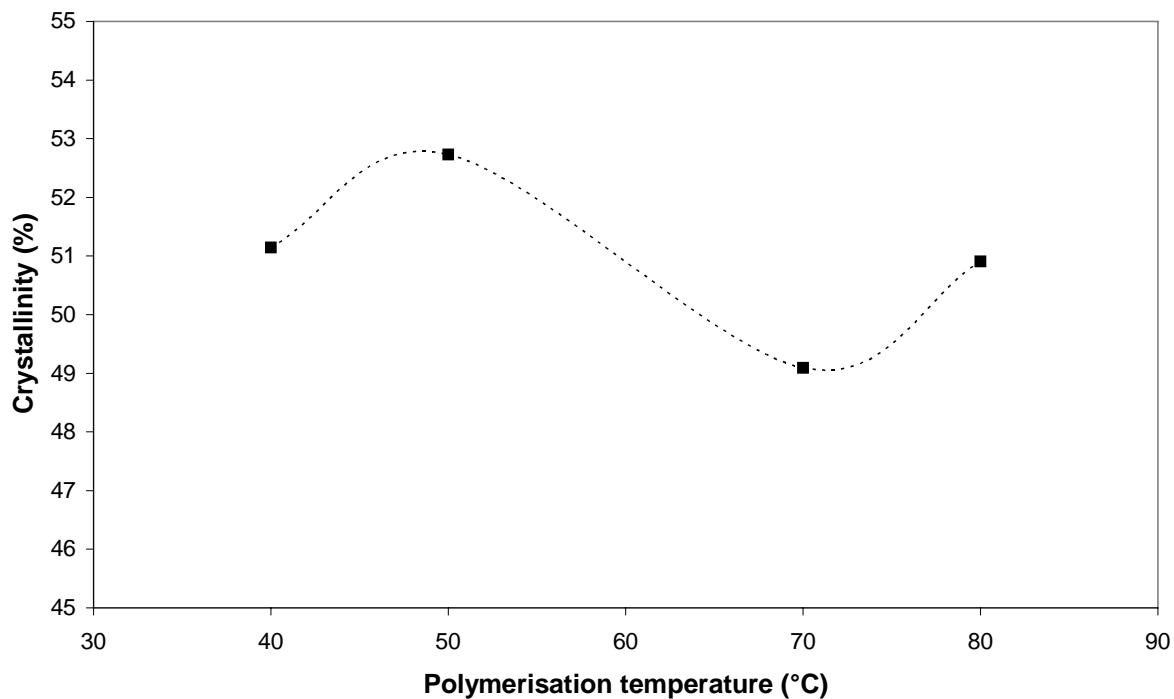
### 5.3.2.2 Al : Ti = 80

Figure 5.9 shows the effect of polymerisation temperature at the higher cocatalyst-catalyst ratio of 80. The same increase in activity with polymerisation temperature is observed for the higher cocatalyst loading, however, the decrease in activity at high temperature is evident at 80 °C as opposed to the earlier case at a lower cocatalyst-catalyst ratio where the decrease is not yet evident at 80 °C. This is more than likely due to the fact that at the higher cocatalyst-catalyst ratio there is more cocatalyst present in the system, and therefore the likelihood of reduction of the catalyst is greater.



**Figure 5.9** The effect of the polymerisation temperature on the activity of the catalyst at an Al:Ti = 80.

There was once again no distinct relationship between the polymerisation temperature and the degree of crystallinity of the samples (Figure 5.10).



**Figure 5.10** The effect of temperature on the crystallinity of the polymer produced at an Al:Ti = 80.

However, it is noted that the same trends are observed at both cocatalyst/catalyst ratios, in that an increase in temperature first brings about an increase in crystallinity, followed by a decrease at higher temperatures and finally another increase at the highest temperature investigated.

Comparison of the *mmmm* pentad sequence content of the sample polymerised at varying temperatures and at a cocatalyst-catalyst ratio of 80 show that there is an opposing effect with regards to the stereospecificity and the activity of the catalyst. Increasing the polymerisation temperature increases the activity up to 70 °C, however, this comes at the cost of a reduction in tacticity of the polymer produced. This is due to the increased activation of the catalyst by the cocatalyst at the higher temperatures due to the increased level of energy in the system. The active centre activation is more indiscriminate and so the active sites activated are not necessarily those that are highly stereospecific. Since there is more energy in the system a factor such as a 2,1 insertion which would normally result in a species having a low activity in chain propagation, does not slow down the polymerisation mechanism to the same extent as it would at lower polymerisation temperatures. There is therefore also the increased likelihood of stereo-errors along with the higher activity.

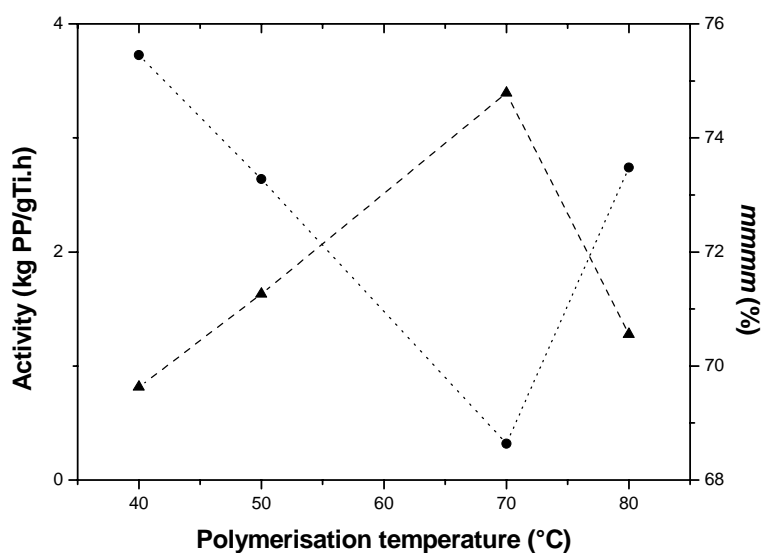


**Figure 5.11 Comparison of the activity (closed triangles) and average isotacticity (closed circles) for polymers produced while varying the temperature at Al:Ti = 80.**

The higher cocatalyst content also means that there is greater extraction of the internal electron donor, compared to the lower cocatalyst-catalyst ratio, which occurs relatively easily for the  $\text{MgCl}_2/\text{TiCl}_4/\text{DIBP-AlEt}_3$  system, although not as easily as for the  $\text{MgCl}_2/\text{TiCl}_4/\text{EB-}$

AlEt<sub>3</sub> system [12, 13]. This appears to be the case at least for the lower temperatures, while at higher temperatures the *mmmm* pentad content appears to be very similar for the two cocatalyst-catalyst ratios as the polymerisation temperature becomes the dominant factor affecting the active sites.

### 5.3.3 The catalyst/cocatalyst ratio

The next polymerisation variable under investigation is the cocatalyst-catalyst ratio. The polymerisation temperature was kept constant at 70 °C for these investigations. The reactions were also conducted in the absence of both hydrogen and external electron donors.

Figure 5.12 shows the effect of the cocatalyst-catalyst ratio on the activity of the system. A clear increase in activity is observed with increasing level of cocatalyst in the system as is expected since there is more of the cocatalyst present to activate more sites on the catalyst, which produces more polymer. This effect would be expected to change at higher cocatalyst-catalyst ratios due to the over-reduction of the titanium species [2]. It is also possible that the higher cocatalyst levels in the system also aid in removing contaminants from the reactor system, thereby allowing the reaction to proceed better than if the contaminants were still present.

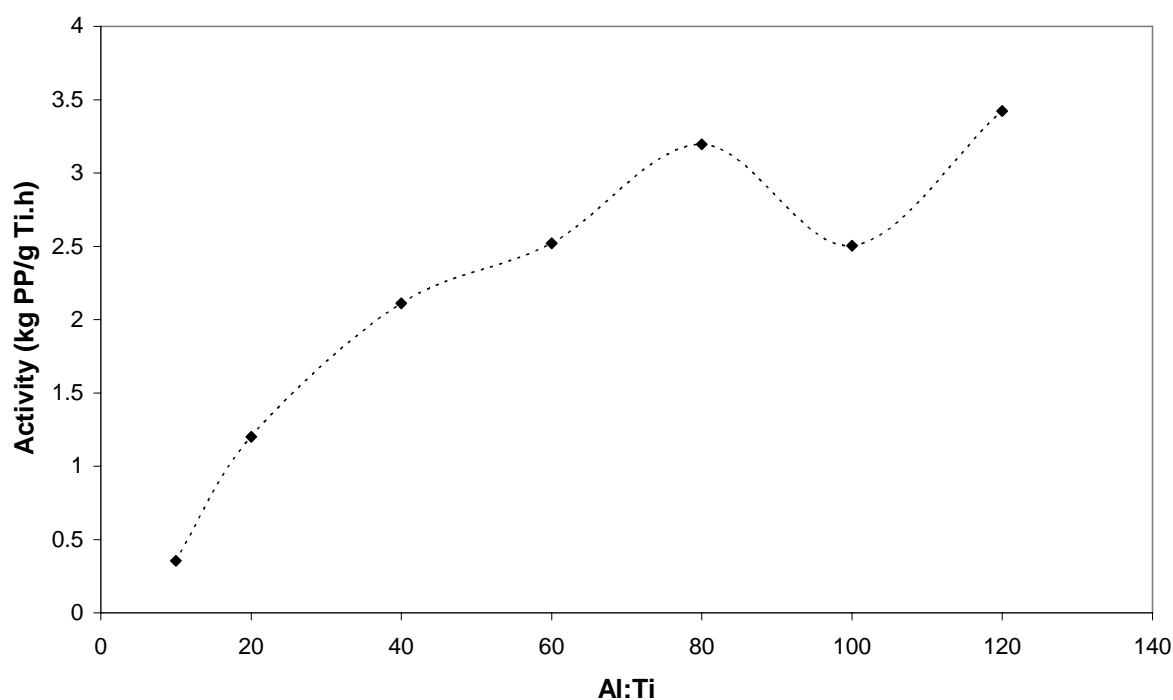
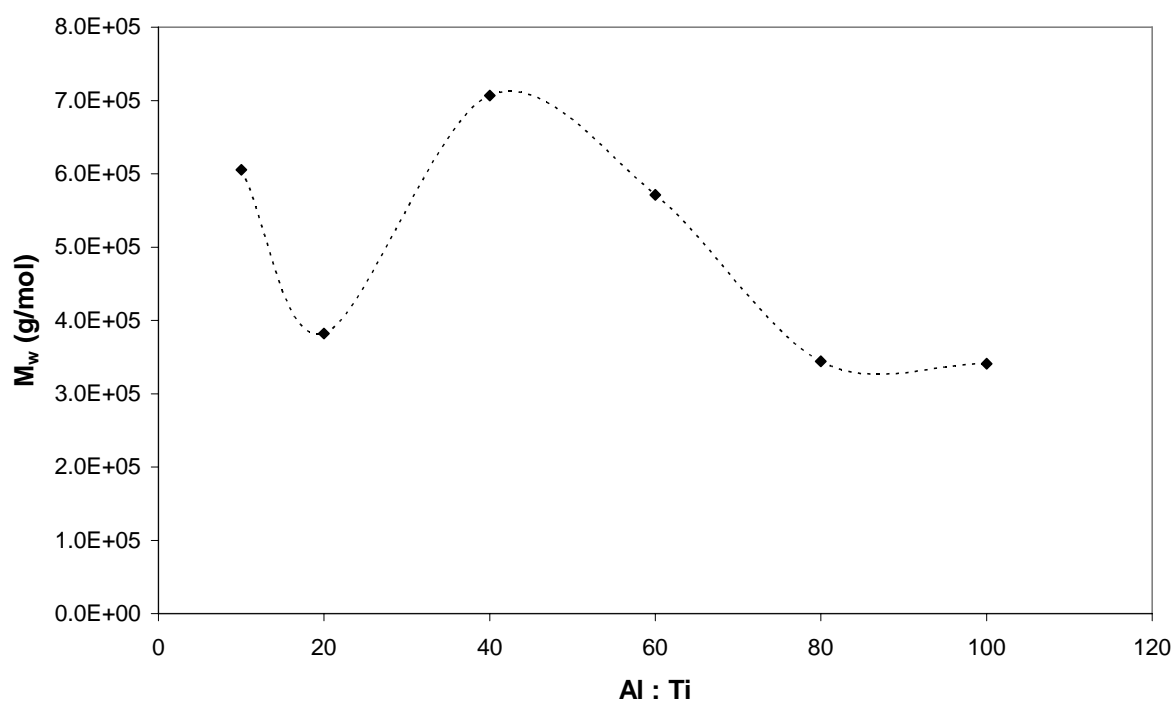


Figure 5.12 The variation of Al:Ti at a polymerisation temperature of 70 °C.

In turn the increased activation of the catalyst yielding more polymer results in a general decrease in the molar mass of the polymer especially at higher cocatalyst/catalyst ratios (Figure 5.13). Increased chain transfer to the cocatalyst is thought to be a possible cause of the molar mass decrease. However, it is believed that the main reason for the decrease in molar mass is the extraction of the internal electron donor (DIBP) from the system since this is known to occur. This results in the formation of active sites with lower propagation rate constants and lower stereospecificity, thus the polymer produced is of a lower molar mass and, as observed in Figure 5.14, a lower *mmmm* pentad content as well. The sites will therefore also be more “open”, allowing chain transfer reactions to take place easier. The sites without electron donor present are also likely to be less stable than when the donor was present at the active site.



**Figure 5.13** The effect of variation in catalyst/cocatalyst ratio on the weight average molar mass at a polymerisation temperature of 70 °C.

The variation in the *mmmm* pentad content of the polymers produced at varying cocatalyst-catalyst ratios is illustrated in Figure 5.14. The correlation with the crystallinity of the samples is also given for comparison and a clear relationship is observed between the *mmmm* pentad content and the crystallinity. The decrease in both the *mmmm* pentad content and crystallinity with increasing cocatalyst-catalyst ratio is also noted, as a result of the



increasing extraction of the internal electron donor from the surface of the catalyst. Similar results were obtained by Zohuri *et al.* [11] for both monosupported and bisupported catalysts.

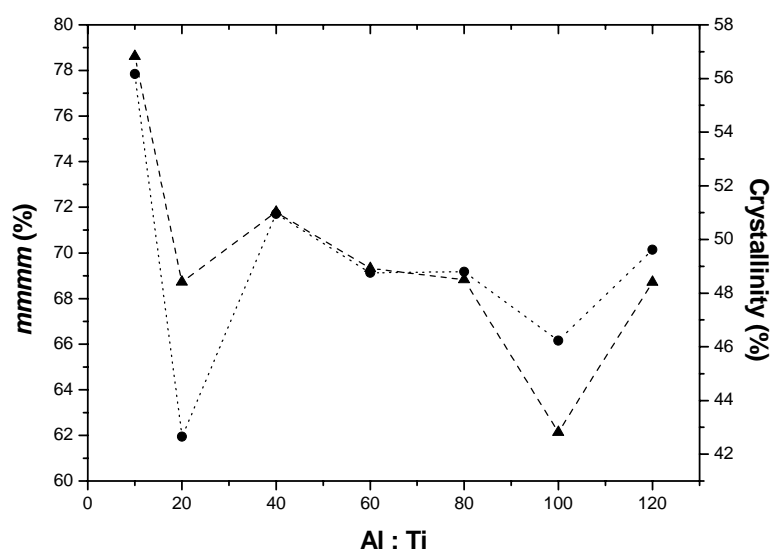


**Figure 5.14** The average isotacticity (closed triangles) and percentage crystallinity (closed circles) of the polymers produced while varying the Al:Ti ratio as determined by  $^{13}\text{C}$  NMR.

### 5.3.4 Propylene pressure

Investigations into the effect of the propylene pressure on the activity of the catalyst were performed at 40 °C using DPDMS as an external donor, however, no hydrogen was present in the reactions.

Figure 5.15 indicates the influence of the monomer pressure on the activity of the catalyst. There is an increase in activity with increasing monomer pressure as one would expect since a number of researchers have established a first order dependence with regards to the monomer pressure on the polymerisation rate [14-16].

The effect of the higher monomer pressure on the molar mass of the polymer produced is illustrated in Figure 5.16. A decrease in molar mass with increasing monomer pressure is observed. Increased chain transfer to monomer is a possible cause of the molar mass decrease since this is the most important form of chain transfer in the absence of hydrogen [17-19], and indeed these reactions were conducted in the absence of hydrogen. However, if propagation and chain transfer rates are first order with regards to the monomer concentration, then the decrease in molar mass is more likely due to insufficient temperature control. It has also been shown that in general the isotacticity of the polymer produced is higher for reactions with a

lower propylene pressure [20], due to the fact that the back-skip of the growing chain is preferred to less regio- or stereo-insertion.

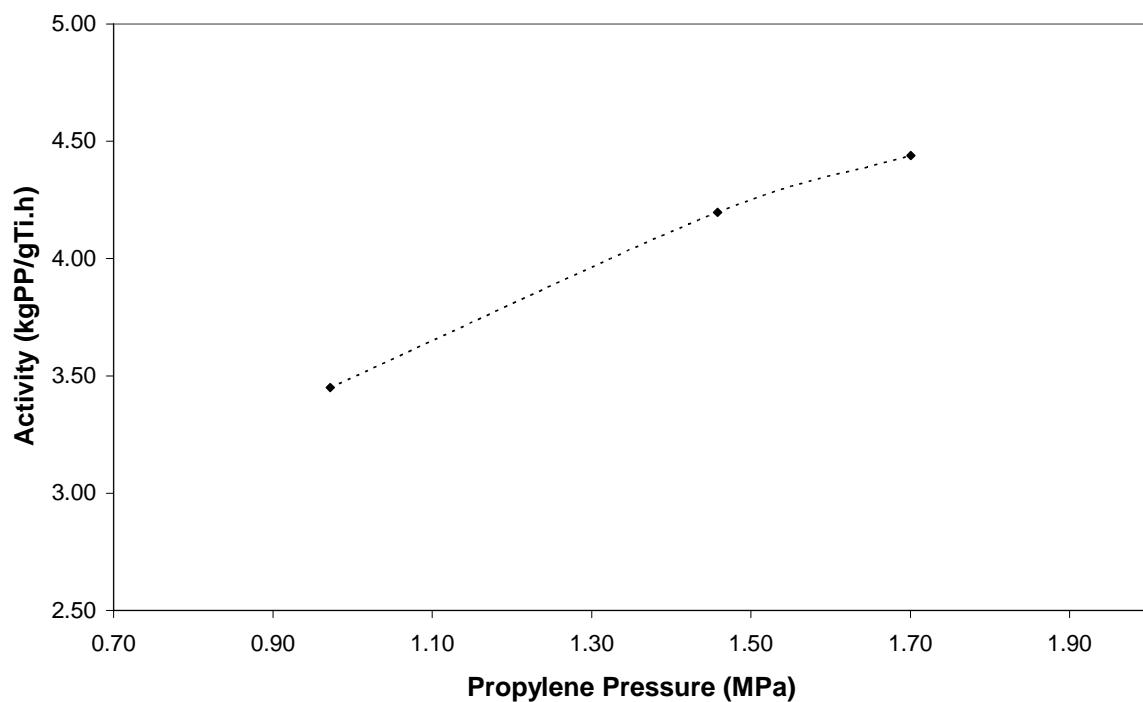


Figure 5.15 The influence of the propylene pressure on the activity of the catalyst.

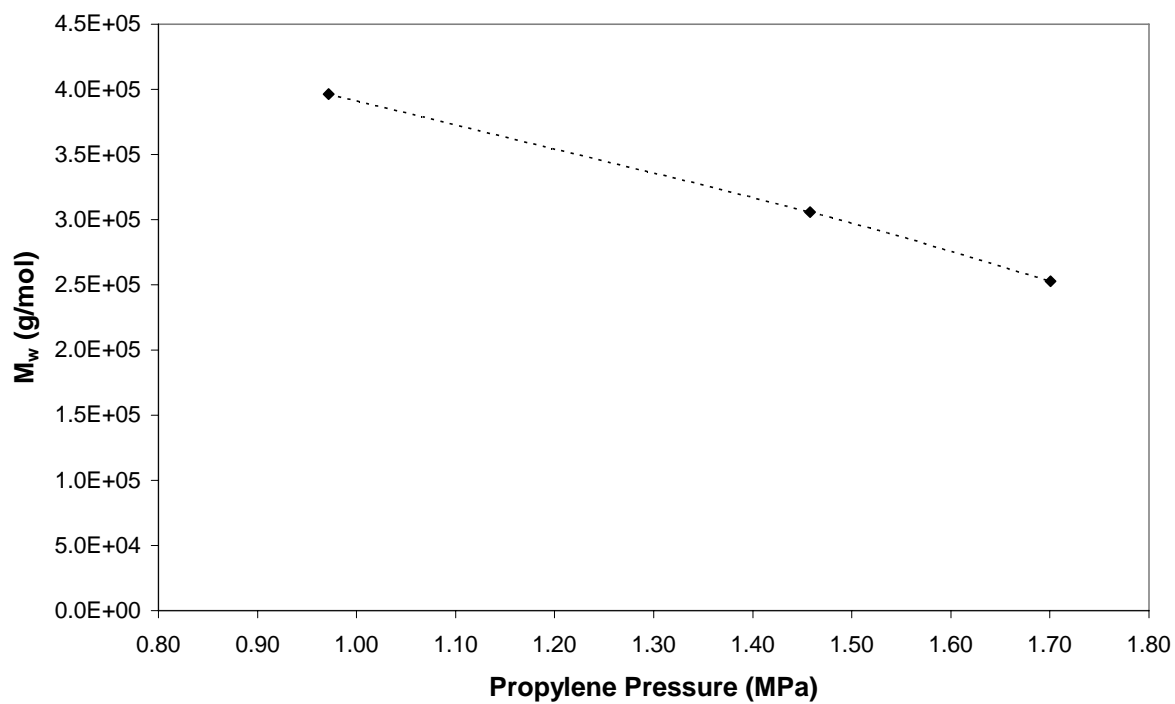
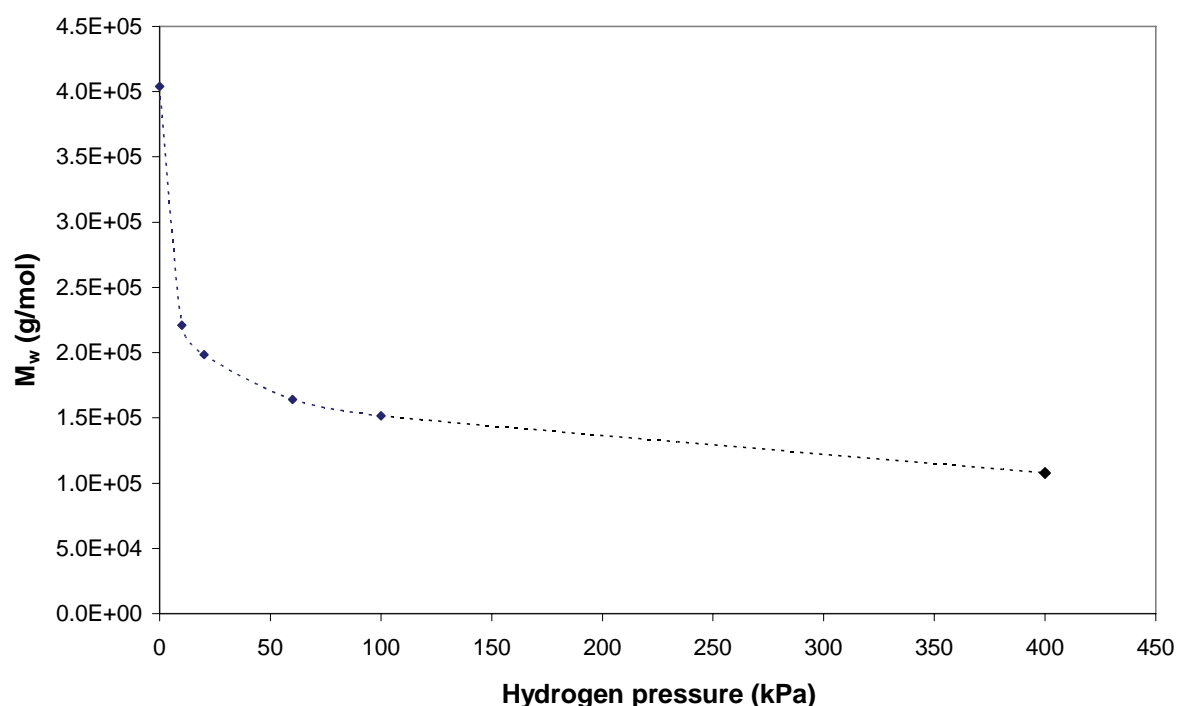


Figure 5.16 The influence of the propylene pressure on the weight average molar mass of the polymer produced.

### 5.3.5 The use of hydrogen as a chain transfer agent

The polymerisations conducted to investigate the effect of hydrogen were performed using DPDMS as an external donor during the course of the polymerisations which were conducted at 40 °C. Hydrogen is a well known, and the most industrially used, chain transfer agent for Ziegler-Natta polymerisations. It is by far the most efficient chain transfer process and a half-order dependence with respect to the hydrogen concentration has generally been found [17].



**Figure 5.17** The effect of the addition of hydrogen to the polymerisation system on the molar mass of the polymer produced.

The decrease in molar mass with increasing hydrogen concentration illustrated in Figure 5.17 is very clear. It is noted that a large decrease in molar mass is obtained with the addition of a small amount of hydrogen to the system but that significantly more hydrogen must be added in order to decrease the molar mass further, becoming increasingly more difficult as the hydrogen pressure increases. The limited ability of the effect of hydrogen to control the molar mass of the polypropylene at high hydrogen concentrations has been discussed in detail by Kissin *et al.* [21].

It has also been noted that various researchers have observed an activating effect when hydrogen is used during the reaction. The activation effect was not observed for the reactions

undertaken in this section of the study and in the remaining sections the hydrogen concentration was kept constant when used in a reaction, however, a brief discussion of the topic is deemed relative to the overall picture of the polymerisation reaction.

Kouzai *et al.* [22] discovered that there was no effect of the hydrogen on the aspecific sites, while the molar mass of the polymer produced at the isospecific sites decreased upon hydrogen addition. Liu *et al.* [23] investigated the hydrogen dissociation sites on the catalysts and they concluded that deactivation of certain active titanium species could be associated with the formation of hydrogen dissociation sites, subsequently confirmed by H<sub>2</sub>-D<sub>2</sub> exchange reactions. Busico *et al.* [24] investigated diester and diether based systems and discovered that the better hydrogen response of the diether based system was due to the more uniform distribution of the regiodefects in the polymer chains. The relatively hindered active sites present in a system after a 2,1 insertion are preferential points for the hydrogen to terminate the growing chain [25], thus enabling the reactivation of the site and the subsequent continuation of the polymerisation. This is the reason for the activating effect of hydrogen observed by a number of researchers since the formation of a site of relatively lower activity is prevented and chain propagation can continue at a faster rate. There is also the possibility that the regio- and stereo-regularity of the chains could increase as a result of this mechanism of chain transfer. Essentially what would have been a defect incorporated into the chain is converted into a chain end and so it is possible that the average tacticity of the samples can increase with increasing hydrogen concentration. An alternative mechanism for the molar mass control of polymers by hydrogen was proposed by Kissin and Rishina [26]. They propose that the hydrogenolysis of the Ti-*iso*-C<sub>3</sub>H<sub>7</sub> group formed either after secondary propylene coordination after β-hydride transfer or transfer to hydrogen, or by chain transfer to monomer if the propylene is coordinated in the secondary orientation. Essentially they propose that the Ti-*iso*-C<sub>3</sub>H<sub>7</sub> group is relatively stable and so the hydrogenolysis of this group plays a significant role in reactivating dormant centers in the catalyst. It is therefore clear that the presence of the hydrogen in the polymerisation system is extremely important as it performs a very important role with a number of related consequences.

The crystallinity of the samples with varying hydrogen content varies considerably as the hydrogen content is increased. Figure 5.18 illustrates the general increase in crystallinity of the samples between the hydrogen pressures of 10 kPa and 100 kPa. The lower molar mass of the samples would appear to be the main driving force behind the improvement in crystallinity, although a possible slight increase in average tacticity of the samples cannot be discounted which would also aid in improving the degree of crystallinity. It is also noted that

increasing the hydrogen pressure from 100 to 400 kPa does not result in any change in the crystallinity.

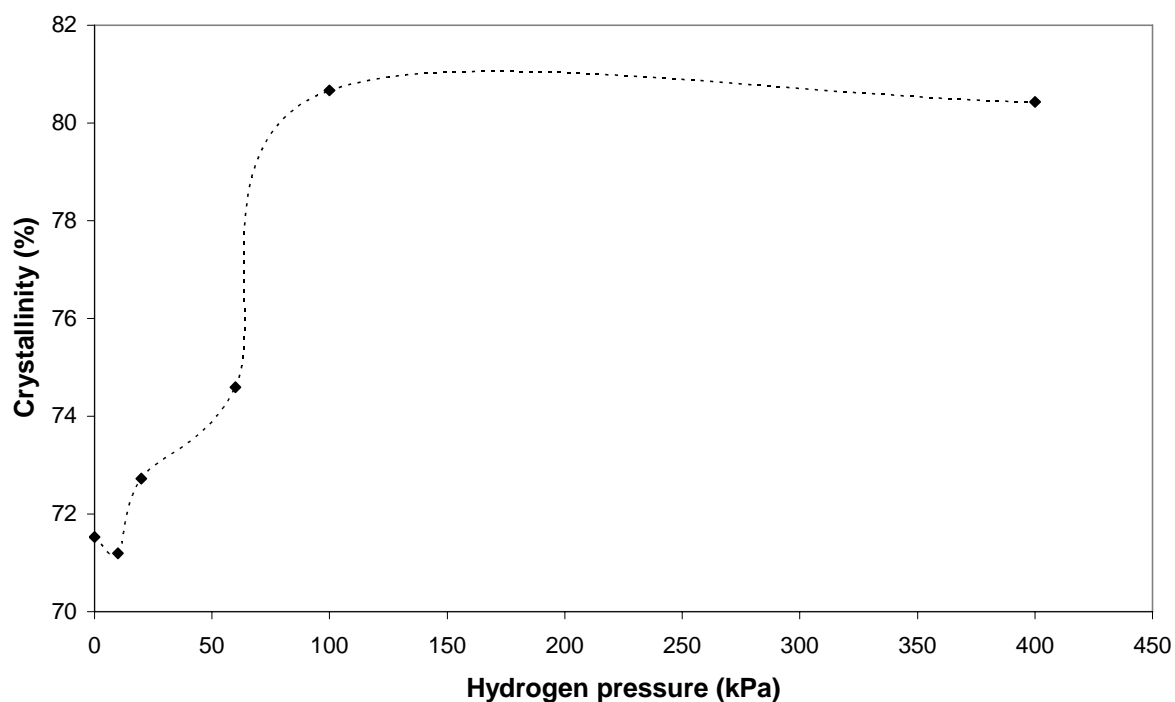


Figure 5.18 The effect of hydrogen on the percentage crystallinity of the polymers produced.

### 5.3.6 Varying the external donor type – no hydrogen present

The following section of the work examined the effect of the amount and type of external Lewis base which was introduced to the reactor system. The two Lewis bases used were DPDMS and MPDMS. The effect of the amount of the external donor used was also investigated by varying the external donor/catalyst ratio. The reactions in this section were conducted in the absence of hydrogen at 40 °C. The reactions with DPDMS as external donor will be discussed first followed by those using MPDMS.

#### 5.3.6.1 DPDMS

The reactions conducted with DPDMS as external donor were also used to investigate the effect of varying the cocatalyst/catalyst ratio on the reactions while also varying the external donor/catalyst ratio. The trends observed for the activities of the reactions are illustrated in Figure 5.19. In general if one first examines the effect of varying the amount of external donor for a given cocatalyst/catalyst ratio it would seem as if the activity of the

system generally decreases with increasing amount of external donor present in the reaction as one would expect since the external donor is proposed to eradicate aspecific active sites, thereby reducing the overall number of active centers [27], and thus lowering the activity of the catalyst. It is also well known that the external donor forms a complex with the cocatalyst [17, 28] and therefore it is also possible that at high donor levels in the reaction there is less free cocatalyst to activate the sites. The complex between the external donor and the cocatalyst is also capable of activating the catalyst but the activating power is not as strong as that of the free cocatalyst.

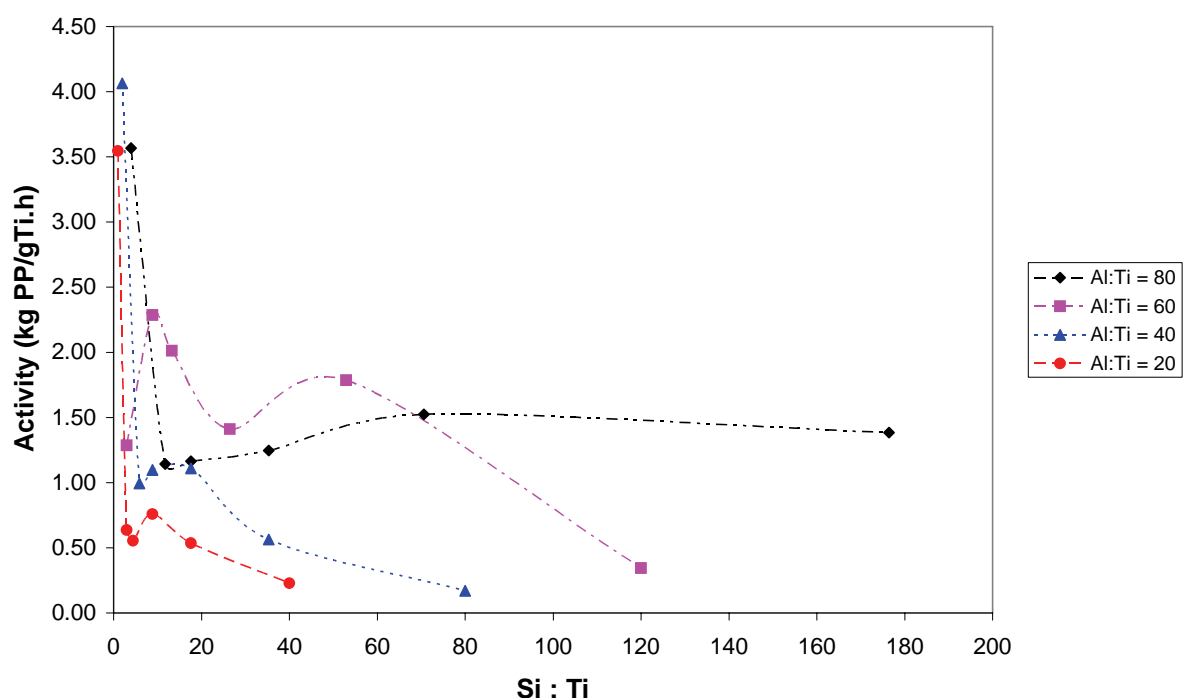


**Figure 5.19** The effect of the Si : Ti on the activity of the catalyst.

It is also noted that as a generalisation there is an increase in the activity at a certain external donor loading for each of the different cocatalyst/catalyst ratios used. It would also appear that the higher the cocatalyst loading in the reaction, the broader the region of activity increase (in terms of the external donor/catalyst ratio), and that the higher the cocatalyst loading the more external donor is required to attain the activity increase. There is therefore a clear relationship between the external base and cocatalyst in the system which results in a slight activity increase at a certain external donor/catalyst ratio. It is also noted that in general the activity of the catalyst is higher at higher cocatalyst/catalyst ratios as expected and discussed in Section 5.3.3. The slightly lower than expected activity at the cocatalyst/catalyst ratio of 80 is possibly due to over-reduction of some of the titanium species.

Similar trends are observed upon examination of the molar mass data in Figure 5.20. There is an initial decrease in molar mass as the external donor level is increased slightly, however, upon further increase in the external donor level there is a sharp increase in molar mass of the polymers formed. This trend is observed at all cocatalyst/catalyst ratios with the sharp increase in molar mass seemingly related once again to the amount of cocatalyst and external donor in the system since generally the molar mass increase occurs at higher external donor loadings for higher cocatalyst/catalyst ratios.

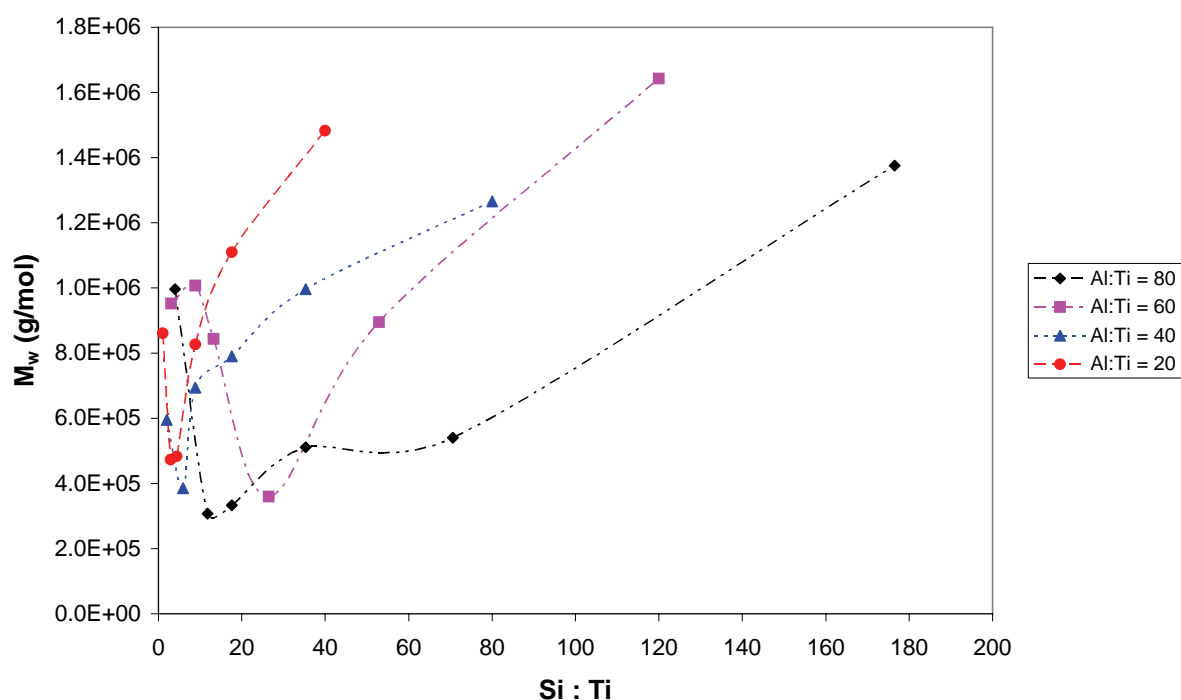


**Figure 5.20** The effect of the Si : Ti on the weight average molar mass of the polymer produced.

Analysis of the  $^{13}\text{C}$  NMR data reveal that there is also an initial sharp increase in the average *mmmm* pentad sequence content of the polymers as the external donor level is increased (Figure 5.21), but that upon further increase in the donor levels there is actually a slight decrease in *mmmm* pentad content which then seems to remain relatively constant. Once again the higher the cocatalyst level in the system, the higher the silane loading is before the slight decrease in *mmmm* pentad content is observed.

There is a decrease in activity of the catalyst, and the polymer produced increases in relative average *mmmm* pentad content and decreases in molar mass upon increasing the external donor/catalyst ratio slightly. This is consistent with the external donor forming a complex with the cocatalyst and coordinating in the vicinity of the active sites thereby improving their stereospecificity. The decrease in activity would be the results of the

deactivation of some aspecific sites as a result of the coordination of the external donor and this appears to be the overriding effect upon increasing the external donor levels even to extremely high loadings. It is also probable that increasing the level of the external donor prevents the extraction of the internal donor to the same extent, thereby aiding in the prevention of the formation of more aspecific sites, and also reducing the activity of the catalyst by preventing the reactivation of dormant sites.

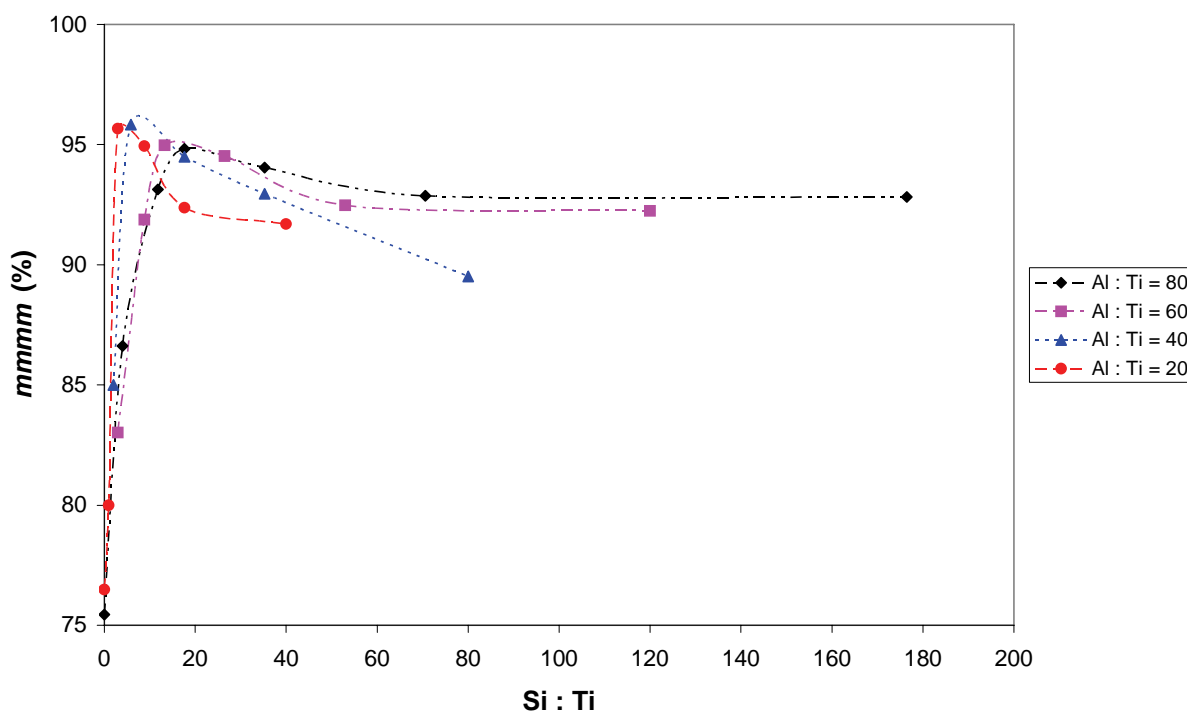


**Figure 5.21** The effect of the Si : Ti on the *mmmm* pentad content of the polymer produced.

The molar mass decrease over the same region of initial increase in external donor loading would have to be the result of increased termination of the chains via transfer reactions. This is due to the fact that increasing the stereospecificity of the active sites, as is the case for a small increase in silane loading, increases the  $k_p$  of the sites since the  $k_p$  of isospecific sites is generally higher than that of aspecific sites [29-31]. Therefore the reduction in molar mass would seem to be more than likely due to increased transfer reactions. The most important chain transfer reaction in the absence of hydrogen being the chain transfer to monomer, which contrary to chain transfer to hydrogen, takes place preferentially after a primary insertion [12]. The transfer to monomer is also strongly related to the stereospecificity of the active sites with an increase in stereospecificity of the active site leading to lower occurrences of chain transfer to monomer. The fact that the *mmmm* pentad content increases should mean that the  $k_p$  of the active sites also increases and that the



likelihood of chain transfer to monomer decreases, however, the molar mass decreases significantly when the external donor level is initially increased and so chain transfer must be the reason and is possibly energetically preferred to the inclusion of a defect in the chain.

Higher external donor levels result in higher molar mass polymer being produced at a slightly lower level of stereospecificity. The main reason for the increase in molar mass is thought to be due to the reduction in the number of propagating centers due to the deactivation of a number of sites by the external donor, thereby increasing the molar mass of those centres still active for polymerisation. It seems as if the stability of the active sites increases at higher external donor loadings. There is the possibility that the higher molar mass is due to a drastic reduction in the amount of transfer reactions taking place. This could be due to the fact that practically all the cocatalyst is complexed to the external donor and so the chain transfer to cocatalyst is possibly eliminated as a chain termination mechanism. However, the rate of chain transfer to cocatalyst has been shown to be at least an order of magnitude less than the chain transfer to monomer [32]. Therefore the reduction in chain transfer reactions would seemingly have to include a reduction in chain transfer to monomer in order to account for the increase in molar mass observed. A reduction in chain transfer reactions would also allow for the inclusion into the chains of more stereo-errors thus reducing the average tacticity of the chains at the same time.

The slight increase in activity at a certain external donor/catalyst ratio would appear to be due to a balance between the decrease in the number of active sites via coordination of external donor to the catalyst and the increase in molar mass of the polymer produced at the sites which are still active producing more material. This in turn is related to the chain termination reactions and so it would seem that the reduction in transfer reactions coinciding with increasing molar mass and decreasing number of active sites as a result of increasing donor levels are the reasons for the observed trends in activity.

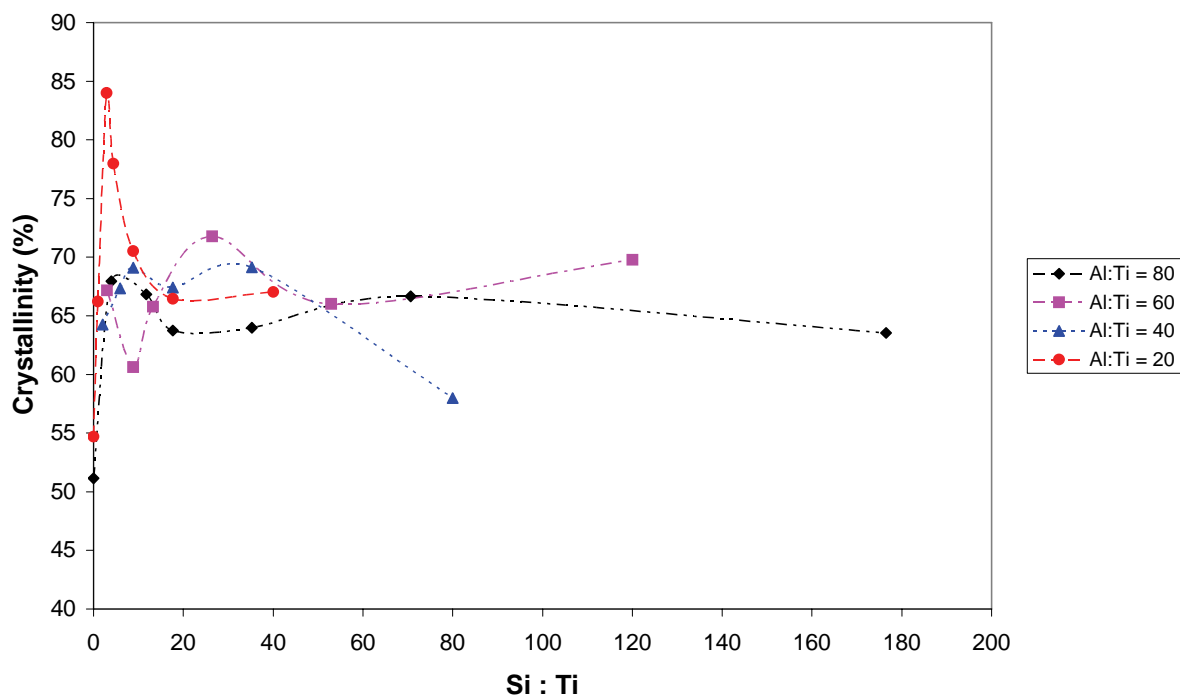


**Figure 5.22** The effect of the Si : Ti on the crystallinity of the polymer produced.

The crystallinities of the samples are given in Figure 5.22. There would appear to be an initial increase in crystallinity with increasing external donor loading for the samples at all the different cocatalyst/catalyst ratios investigated. However, there are no other distinct trends observed for higher external donor loadings.

### 5.3.6.2 MPDMS

A few reactions were also conducted using MPDMS as external donor in the absence of hydrogen. All reactions in this section were conducted at a cocatalyst/catalyst ratio of 80. Data on the reactions using DPDMS as external donor, also at a cocatalyst/catalyst ratio of 80, are given for comparison. A number of studies [33-36] have pointed out that the best alkoxy silane donors are those with bulky substituents in order to give selective poisoning of the active sites. Therefore it is predicted that using DPDMS as external donor would produce active sites which were on average more hindered than those produced using MPDMS.

It would appear that using MPDMS as external donor results in a catalyst with a generally higher activity at similar external donor loadings at least for the lower external donor/catalyst ratios (Figure 5.23).

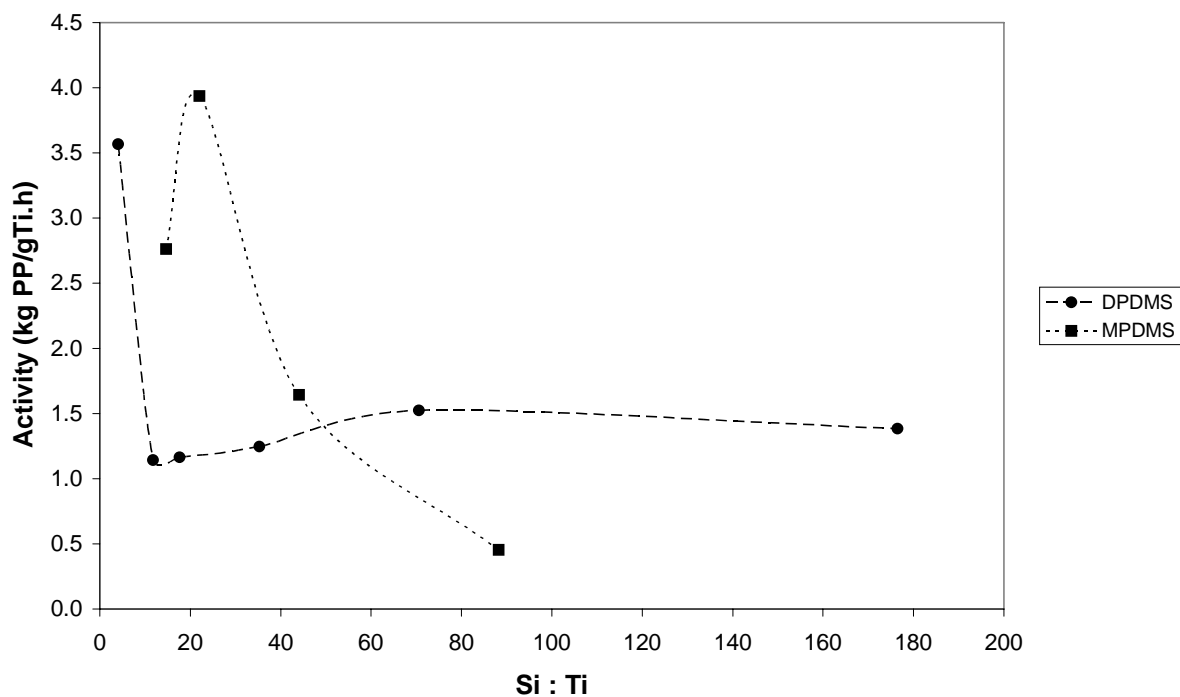


**Figure 5.23 The effect of the Si : Ti on the activity of the catalyst: Comparisons of the DPDMS and MPDMS as external donors.**

This could be due to the active sites with MPDMS in close proximity being more open than those where DPDMS is present. The molar mass data given in Figure 5.24 would appear to support this due to the fact that the molar mass of the polymers produced using MPDMS is significantly higher than that produced with DPDMS in the absence of hydrogen. The same trend of increasing molar mass with increasing external donor/catalyst ratio is observed for the polymers produced with MPDMS.

There is also an increase in the average *mmmm* pentad sequence content, of the polymer produced with MPDMS, with increasing external donor/catalyst ratio. It appears as if the tacticity of the polymers produced using MPDMS can attain the same levels of stereospecificity as those produced with DPDMS but that higher external donor loadings are necessary to attain this same high level of tacticity.

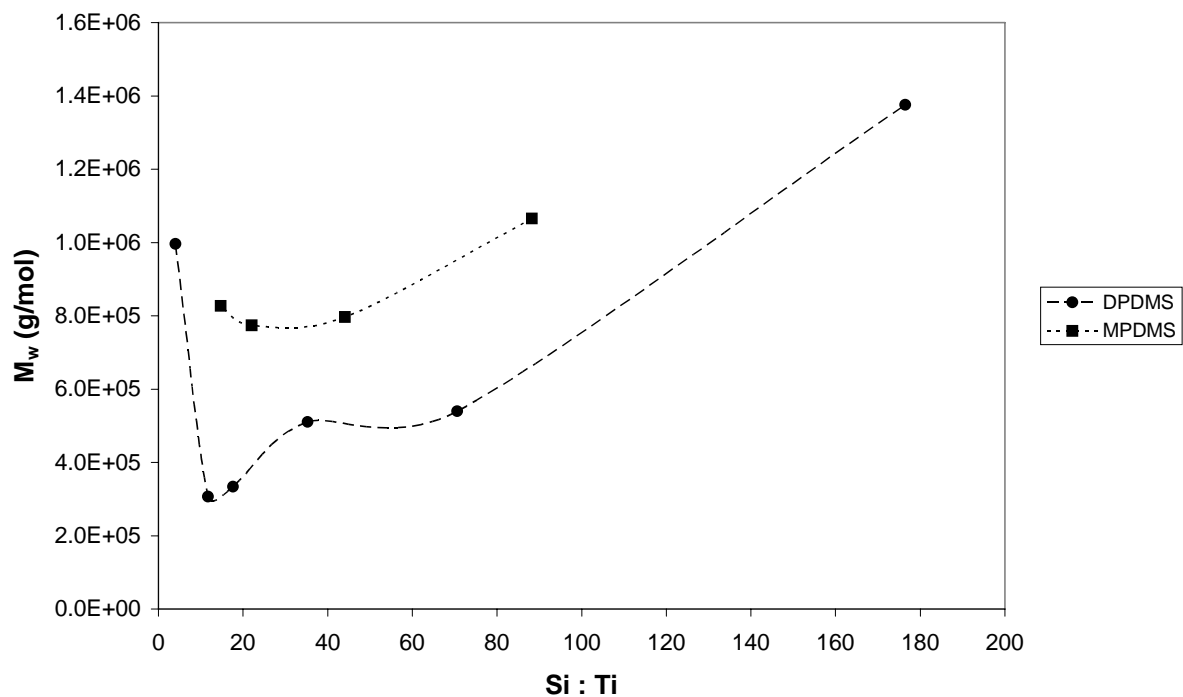


Figure 5.24 The effect of the Si : Ti on the weight average molar mass of the polymers: Comparisons of the DPDMS and MPDMS as external donors.

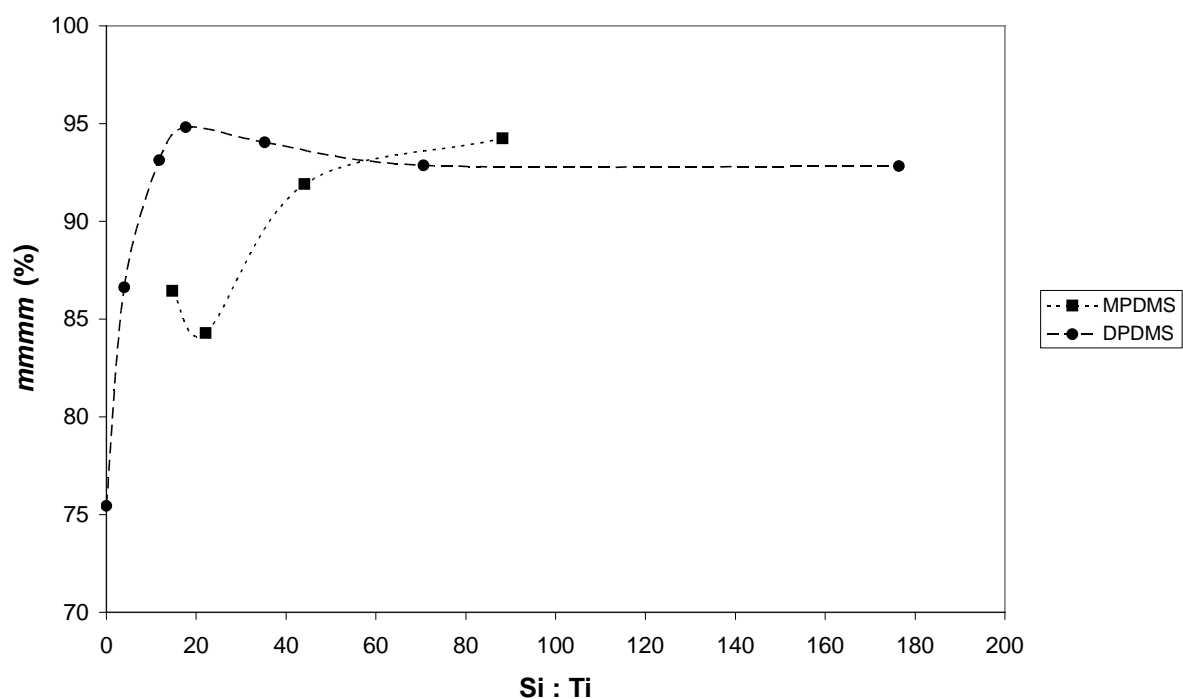
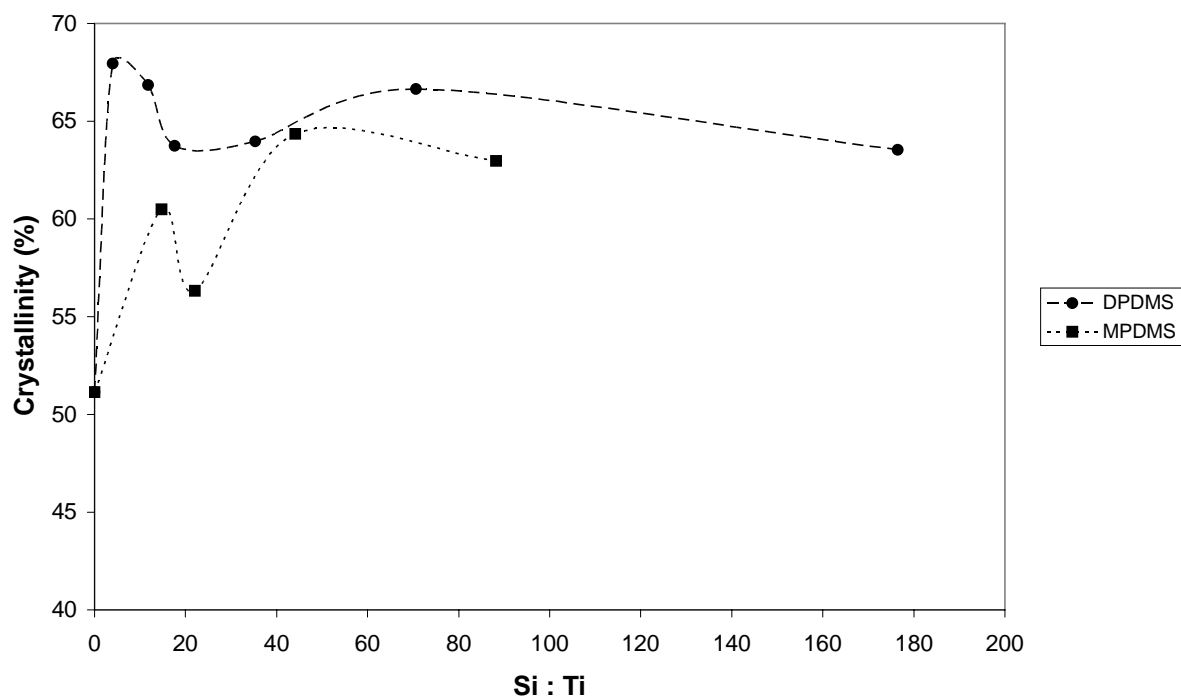


Figure 5.25 The effect of the Si : Ti on the  $mmmm$  pentad content of the polymers: Comparisons of the DPDMS and MPDMS as external donors.

As far as the crystallinity of the polymer is concerned it would appear that the generally higher tacticity and lower molar mass of the samples produced with DPDMS enable the chains to crystallise to a greater extent.



**Figure 5.26 The effect of the Si : Ti on the crystallinity of the polymers: Comparisons of the DPDMS and MPDMS as external donors.**

### 5.3.7 Polymerisations for in-depth analysis

It was decided that in order to investigate the effect of different polymerisation conditions on the properties of polypropylene homopolymers it would be necessary to conduct a few specific polymerisations with the aim of obtaining polymers with different properties which could be related back to the microstructure, which in turn could be related to the polymerisation conditions. To this effect it was decided to conduct polymerisations using both types of electron donors (DPDMS and MPDMS) and at different external donor/catalyst ratios for each type of donor. The polymerisation in the absence of the external donors was also performed so that this larger difference in polymerisation conditions could also be used for comparison with the other samples. The external donor ratios used for each type of donor were 0, 4, 8, 16, and 40. All the reactions were conducted at 40 °C, with a hydrogen pressure of 20 kPa, and at a cocatalyst/catalyst ratio of 80. A number of reactions were performed at

each of the specified reaction conditions in order to make sure that the polymer produced was representative of the reactions conditions and that the reactions were repeatable.

### 5.3.7.1 Polymerisations with DPDMS as external donor

The activities of the polymerisations using DPDMS are given in Figure 5.27. A general decrease in activity is observed with increasing donor/catalyst ratio due to the external donor selectively poisoning the aspecific active sites thus lowering the number of propagation centers in the catalyst [27].

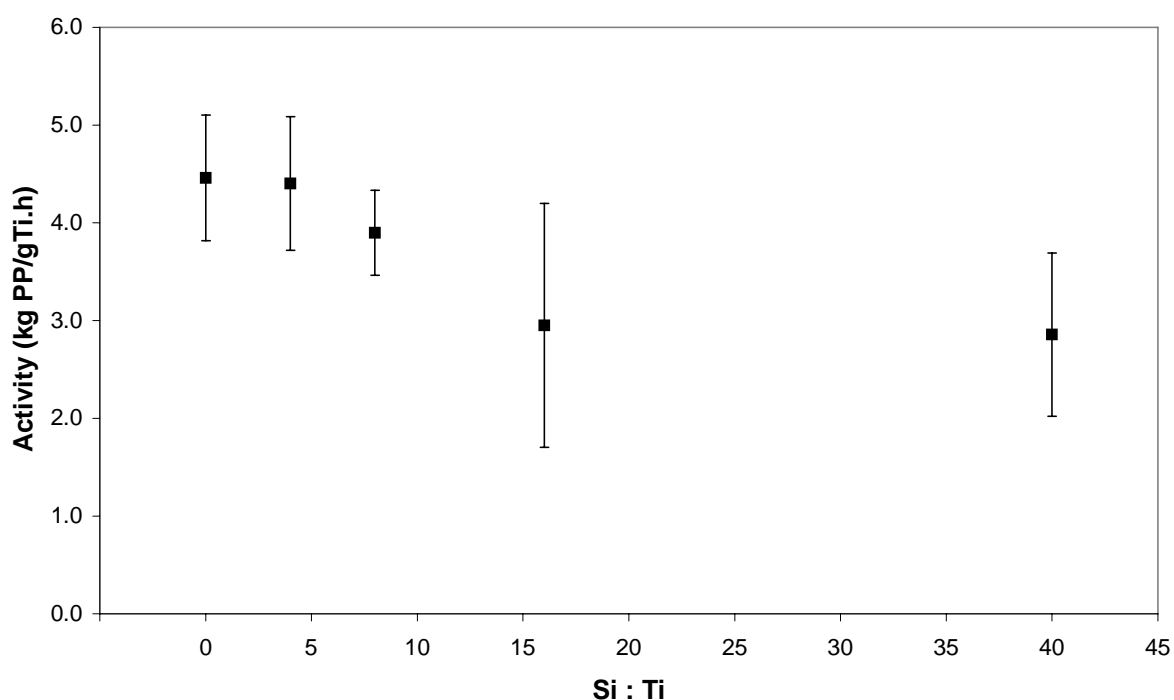


**Figure 5.27** The effect of the Si : Ti on the activity of the catalyst using DPDMS as external donor. The activity of the polymerisation performed without external donor is given for comparison.

The molar mass data are given in Figure 5.28 and the increase in molar mass with increasing donor/catalyst ratio is observed. The repeatability of the results is generally quite good and polymers are produced with significant differences in molar mass at different donor/catalyst ratios. The increase in molar mass at higher external donor loadings is most probably due to an increase in  $k_p$  due to an increase in the stereoselectivity of the active sites with the external donor in the vicinity of the sites, as well as the possibility of a reduction in chain transfer reactions. Contrary to the case discussed earlier in Section 5.3.6.1 hydrogen was used as a chain transfer agent in these reactions and would be by far the most dominant

chain transfer reaction. It is therefore proposed that the increase in molar mass is related to the increase in  $k_p$  as opposed to any significant decrease in chain transfer to hydrogen.

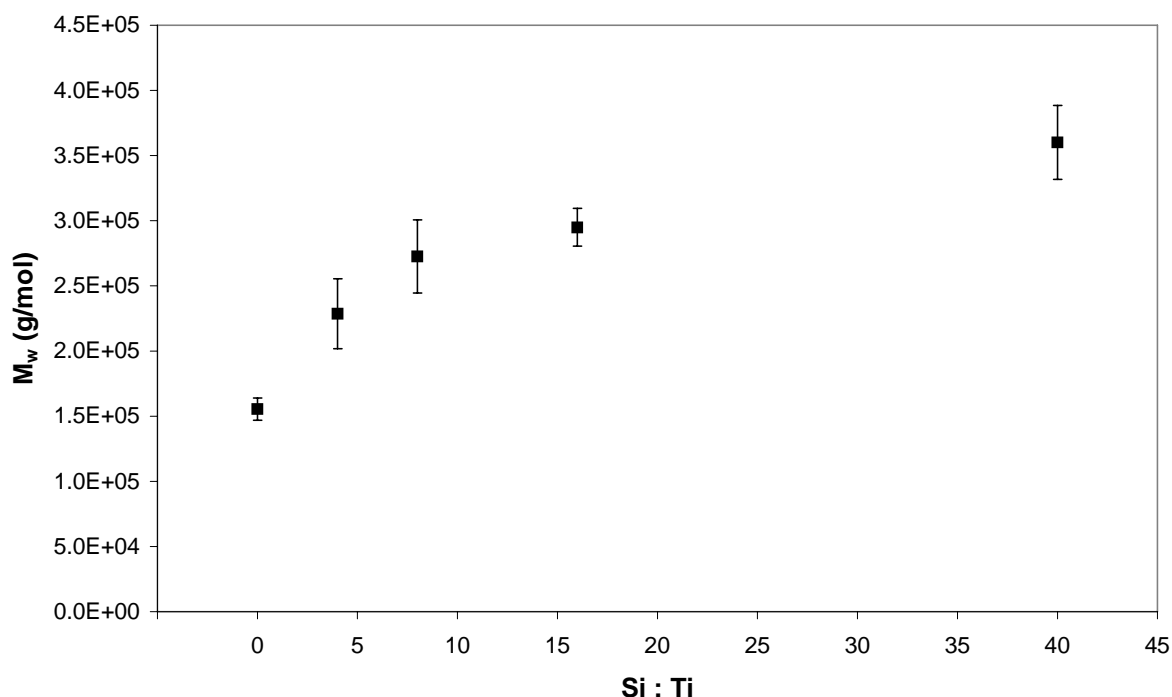


**Figure 5.28** The effect of the Si : Ti on the weight average molar mass of the polymer produced using DPDMS as external donor. The molar mass of the polymer produced without external donor is given for comparison.

The molar mass distribution (Figure 5.29) narrows significantly upon introduction of an external donor to the polymerisation, however, further increase of the external donor content does not produce any further reduction in polydispersity. It is believed that the initial decrease in polydispersity is due to the eradication of the aspecific sites producing a variety of material and that once these sites have been eliminated there is no further effect on the molar mass distribution.

With regards to the thermal properties of the polymers the addition of an external donor to the polymerisation can immediately be seen on the peak melting temperatures of the samples (Figure 5.30). There is an immediate jump of 5 °C as soon as even a small amount of external donor is added to the system. Further increase of the external donor/catalyst ratio above 4 only results in a slight increase in peak melting temperature. The repeatability of the samples is quite good at all external donor loadings indicating that the same type of material is being produced in each reaction.

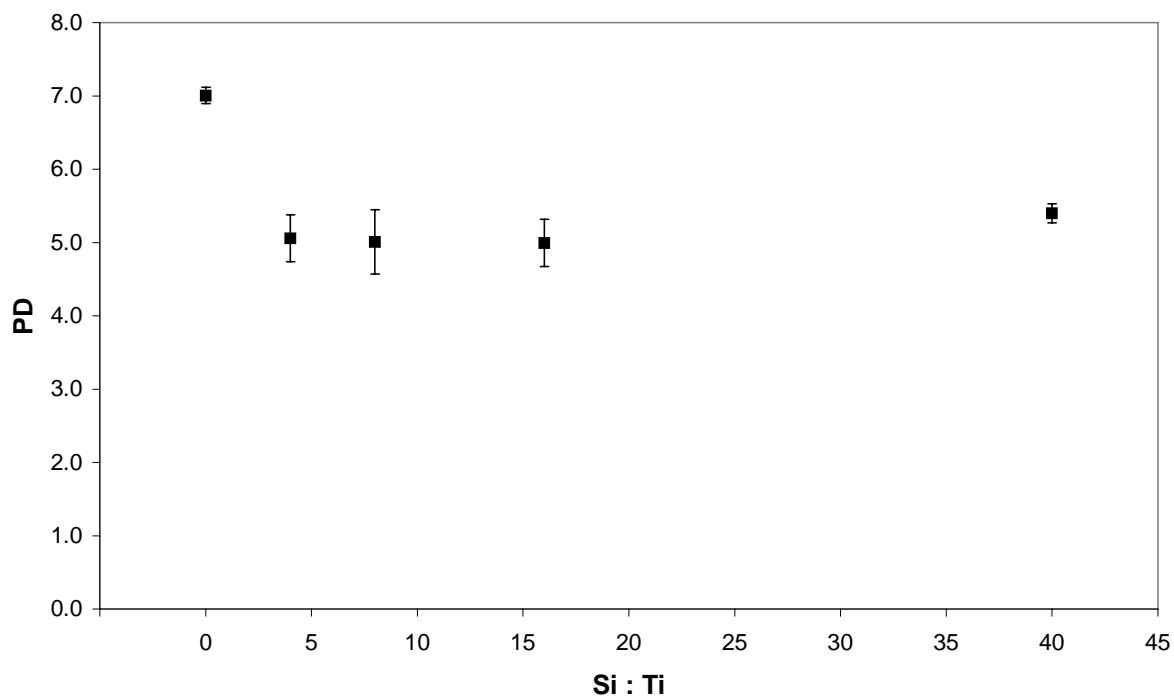


**Figure 5.29** The effect of the Si : Ti on the polydispersity of the polymer produced using DPDMS as external donor. The polydispersity of the polymer produced without external donor is given for comparison.

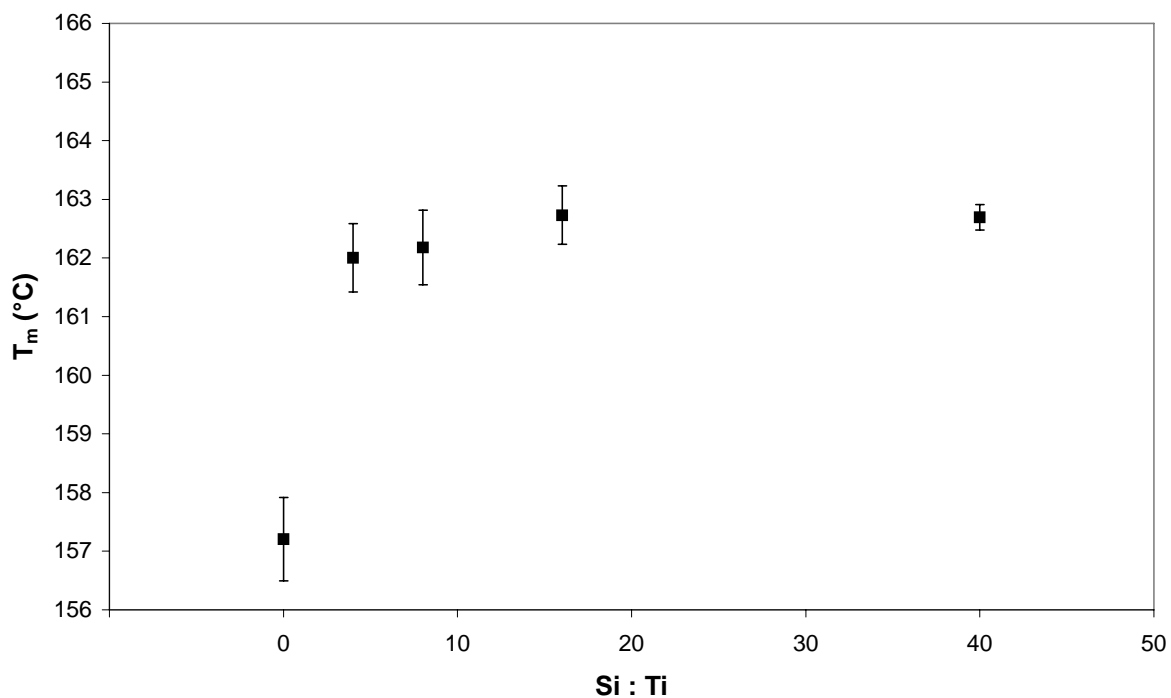


**Figure 5.30** The effect of the Si : Ti on the peak melting temperatures of the polymer produced using DPDMS as external donor. The melting temperature of the polymer produced without external donor is given for comparison.



The data for the crystallinities of the samples (Figure 5.31) shows similar results to the peak melting temperatures as one would expect. The impact of the addition of the external donor is readily apparent with an increase of approximately 15% in the degree of crystallinity compared to the samples polymerised without external donor. This implies that the stereospecificity of the active sites increases initially upon addition of the external donor but that there is little improvement in stereospecificity at higher external donor loadings.

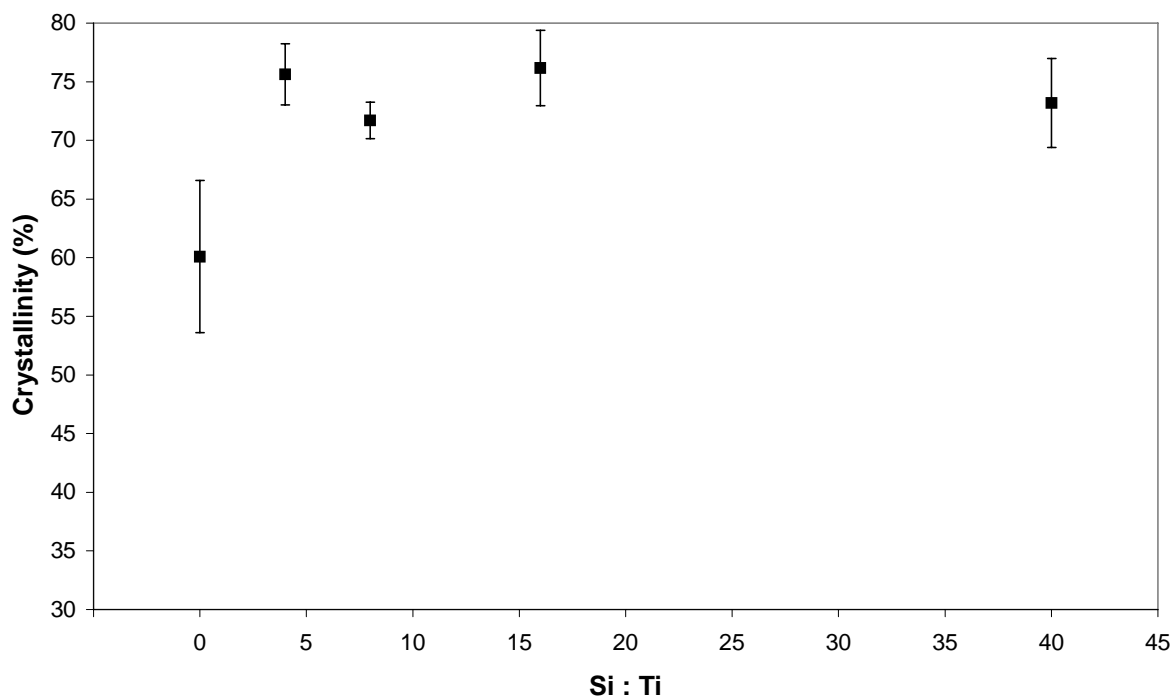


**Figure 5.31** The effect of the Si : Ti on the crystallinity of the polymer produced using DPDMMS as external donor. The crystallinity of the polymer produced without external donor is given for comparison.

Further increase in the external donor content does not bring any noticeable increase in the crystallinity of the samples.

### 5.3.7.2 Polymerisations with MPDMS as external donor

Figure 5.32 shows the effect of MDMS as external donor on the activity of the system. It is readily apparent that there is little effect shown by increasing the external donor loading on the activity of the catalyst as the values remain relatively constant.

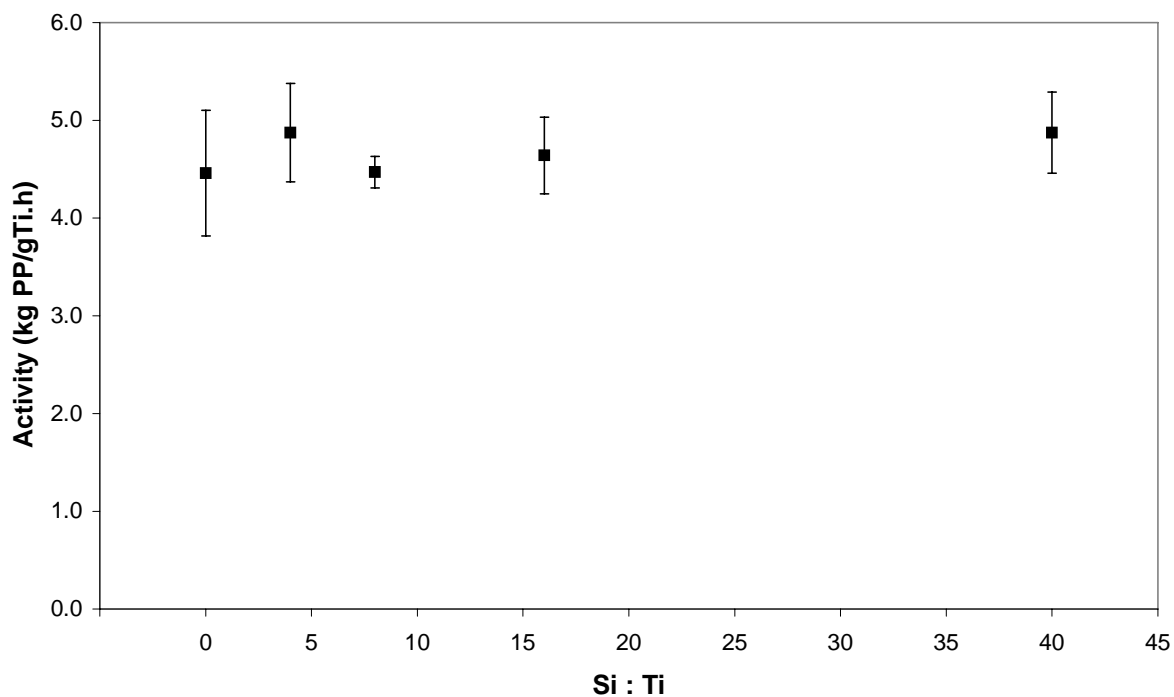


**Figure 5.32** The effect of the Si : Ti on the activity of the catalyst using MPDMS as external donor. The activity of the polymerisation performed without external donor is given for comparison.

The weight average molar mass data for the MPDMS samples show the same trends as the DPDMS samples in that there is a gradual increase in molar mass with external donor/catalyst ratio. This is consistent with the increase in stereospecificity of the active sites leading to an increase in  $k_p$  for the active sites, resulting in higher molar mass polymer being produced. The variation between reactions is extremely small and reveals good repeatability between reactions with the exception of the highest external donor/catalyst ratio where some difference is observed.

The polydispersity of the polymers does not change significantly with increasing external donor/catalyst ratio and remains relatively constant between 7 and 8 (Figure 5.33). It is noted that the polydispersity of the MPDMS samples is higher than that of the DPDMS samples implying that DPDMS as external donor imparts a greater degree of regularity to the active sites than MPDMS.

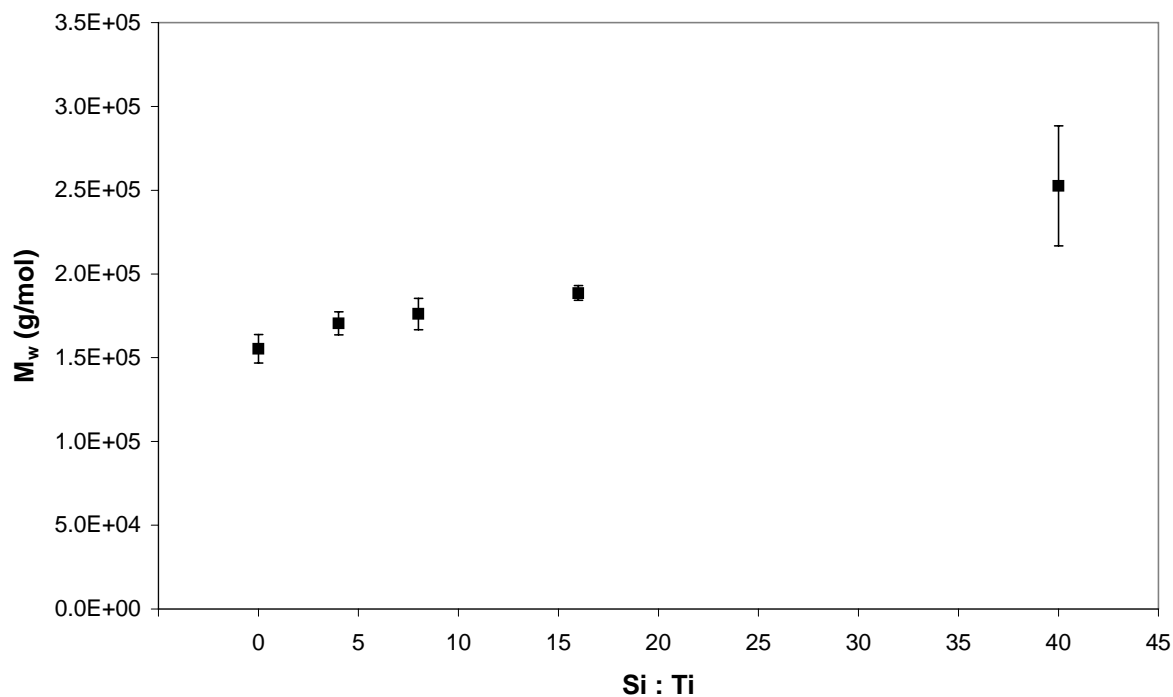


**Figure 5.33** The effect of the Si : Ti on the weight average molar mass of the polymer produced using MPDMS as external donor. The molar mass of the polymer produced without external donor is given for comparison.

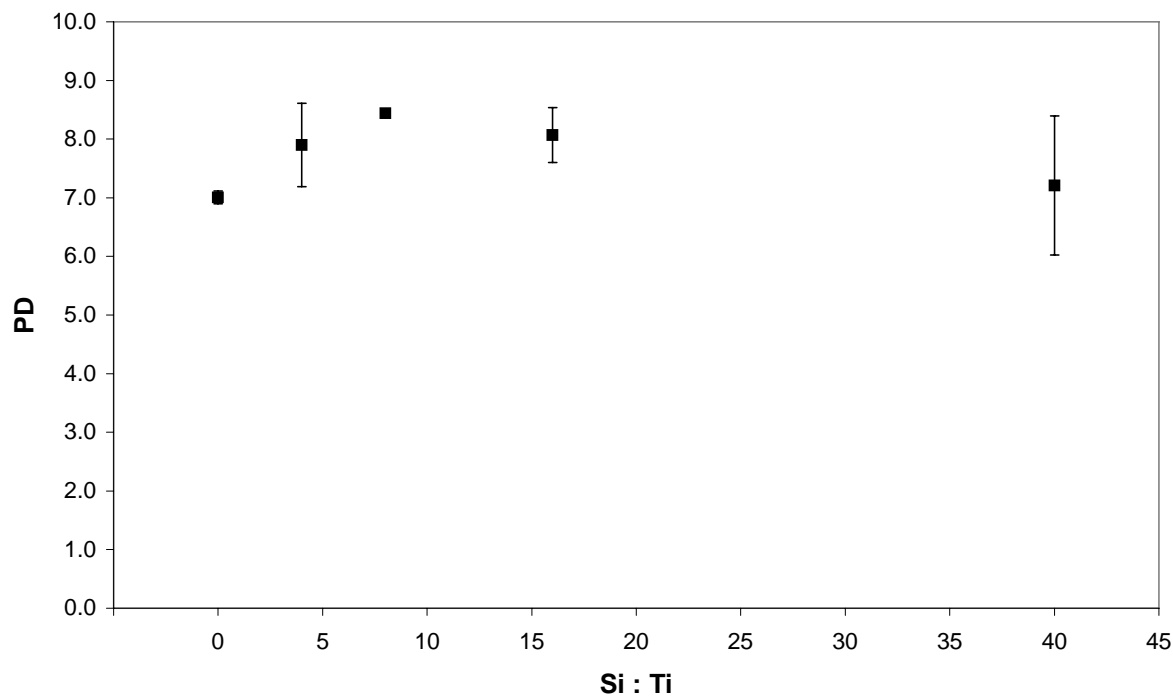


**Figure 5.34** The effect of the Si : Ti on the polydispersity of the polymer produced using MPDMS as external donor. The polydispersity of the polymer produced without external donor is given for comparison.

The thermal properties of the MPDMS samples are given in Figures 5.35 and 5.36. There is once again a distinct increase in peak melting temperature upon addition of external donor and that the addition of greater amounts of external donor can produce material which melts at a slightly higher temperature although the increase is relatively small and is only at very high silane loadings.

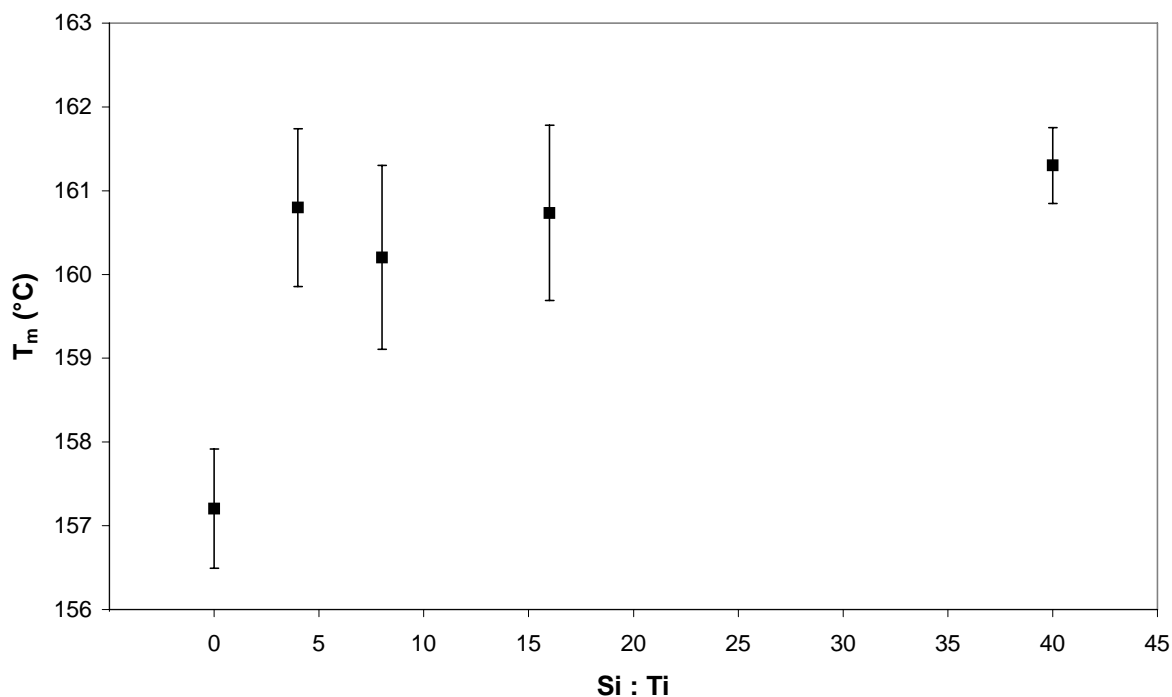


**Figure 5.35** The effect of the Si : Ti on the peak melting temperatures of the polymer produced using MPDMS as external donor. The melting temperature of the polymer produced without external donor is given for comparison.

As far as the crystallinity of the samples is concerned the addition of external donor also yields a material which is considerably more crystalline than that produced without external donor. It is also noted that the degree of crystallinity is reduced slightly at high external donor/catalyst ratios. It would appear that the tacticity of the samples decreases slightly for the higher external donor/catalyst ratios compared to the lower ratios and that the higher molar mass of the polymers produced at high external donor/catalyst ratios inhibits the crystallisation slightly.

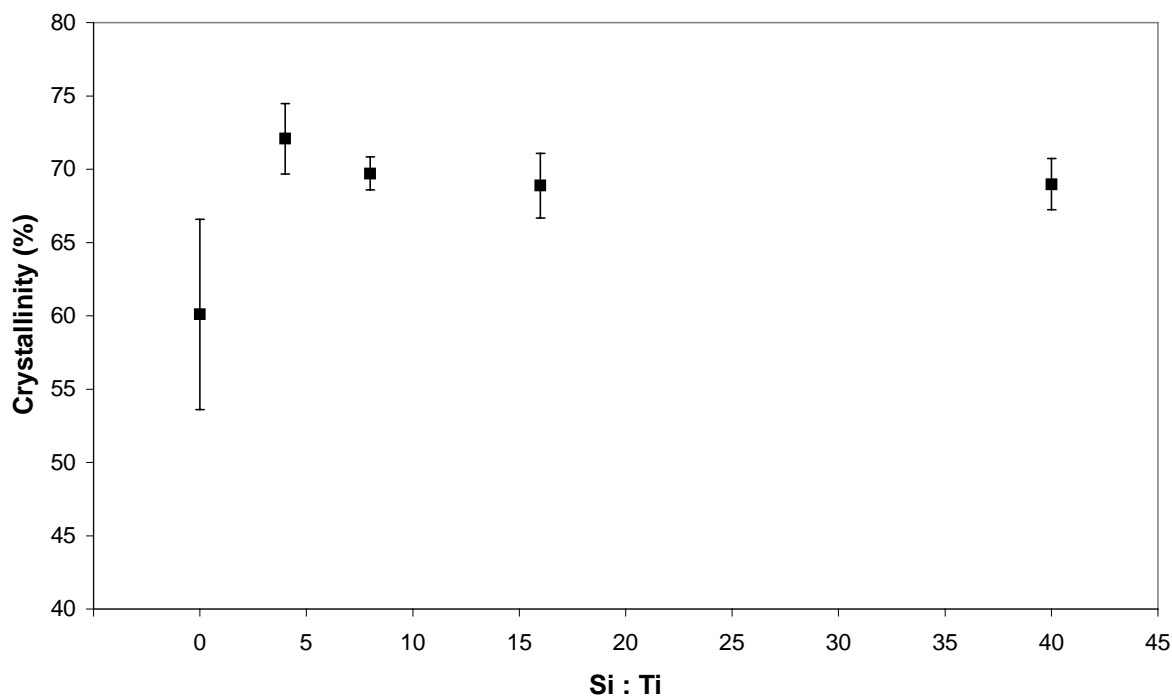


**Figure 5.36** The effect of the Si : Ti on the crystallinity of the polymer produced using MPDMS as external donor. The crystallinity of the polymer produced without external donor is given for comparison.

## 5.4 Conclusions

A number of conclusions can be drawn from the results presented in this chapter. Firstly it is evident that the polymerisation conditions play a significant role in the production of materials with distinct differences in their composition. It is shown that there are a number of different ways to manipulate the composition of the polymers produced by these catalysts, and that therefore the microstructure of the properties can be tailored via the polymerisation conditions to obtain polymers with certain characteristics. The conditions can essentially be tailored to suit a certain application for which the material is required.

Conclusions can also be drawn regarding the specific reaction conditions used. Pre-treatment of the catalyst and cocatalyst prior to the introduction of monomer can be beneficial to the activity and properties of the polymer produced. The highest activity was obtained after a pre-treatment time of two minutes (for the pre-treatment with TEA only), further increase of the pre-treatment time leading to a drop in activity as well as the molar mass of the polymer produced. The crystallinity of the polymer was also affected and a significant decrease was observed at longer catalyst/cocatalyst contact times.

The polymerisation temperature was also investigated and it was found that in general the activity increases with polymerisation temperature. This was the case for reactions at both

a cocatalyst/catalyst ratio of 20 and at 80. The higher level of cocatalyst in the system (Al:Ti = 80) brought about a drop in activity at 80 °C, most likely brought about by an over-reduction of the titanium species occurring at a lower temperature for a higher cocatalyst loading in the system. The increase in polymerisation temperature also brought about a decrease in the molar mass of the chains produced most likely due to an increase in the number of propagating centres producing more, lower molar mass, polymer. The *mmmm* pentad content of the chains decreased in general up to the polymerisation temperature of 70 °C and then increased slightly at 80 °C. The decrease is thought to be due to the extraction of the internal donor by the cocatalyst and the slight increase possibly due to a balance between this effect and the greater productivity of isospecific sites at higher temperatures. The effect of polymerisation temperature on the crystallinity of the samples was varied, however, the same trends were observed at both cocatalyst/catalyst ratios investigated indicating a link between the polymerisation temperature and the crystallisation ability of the material produced.

The effect of the cocatalyst/catalyst ratio was also investigated and an increase in the amount of cocatalyst in the system increases the activity of the system as would be expected. The greater degree of activation due to the increase in cocatalyst content also brings about a decrease in the average molar mass of the chains, and since it is thought that there is an increase in the number of propagation centers, the average chain length at each centre decreases. This effect is enhanced by the fact that the more cocatalyst there is present in the system, the more internal donor is extracted, thereby lowering the stereospecificity of a number of active sites, thus decreasing their  $k_p$  of the sites and lowering the average molar mass of the chains produced. Indeed the *mmmm* pentad sequence content of the samples decreases as the cocatalyst/catalyst ratio is increased as a result of the aforementioned extraction of internal donor. The crystallinity is also decreased with increasing cocatalyst/catalyst ratio and there is a good correlation between the tacticity of the polymers and the degree of crystallinity.

With regards to the monomer pressure a clear increase in activity was observed with increasing monomer pressure as was expected. There is also an accompanying decrease in the molar mass of the polymer most likely due to insufficient temperature control leading to higher temperatures at high monomer pressures.

The effect of various amounts of hydrogen was also investigated principally in order to determine the effect on the molar mass of the polymer produced. The decrease in molar mass with increasing hydrogen pressure was observed and it is noted that the addition of a small amount of hydrogen can cause a significant drop in the molar mass of the chains but that further decreases in molar mass come at an every increasing price in terms of hydrogen

pressure. A sharp increase in the degree of crystallinity of the chains was also observed upon increasing the hydrogen pressure, most likely due to the lower molar mass facilitating improved molecular motion of the chains allowing the reorganisation of the chains in order to crystallise more perfectly. It is also possible that the tacticity of the chains could have improved slightly as the hydrogen pressure was increased due to increased chain transfer to hydrogen after 2,1 insertions, thus forming chain ends rather than incorporating defects into the chains. This would have the overall effect of increasing the chains stereoregularity.

The type and amount of external donor introduced to the system was also investigated. DPDMS as external donor was investigated at different external donor/catalyst ratios and also at different cocatalyst/catalyst ratios. General conclusions are that the activity is higher when the cocatalyst concentration is higher. A decrease in activity with increasing external donor ratio is observed, thought to be due to the deactivation of certain sites on the catalyst by the external donor. Increasing the external donor/catalyst ratio brings about an initial decrease in molar mass which soon changes to become a drastic increase in molar mass at higher external donor loadings. The effect on the *mmmm* pentad content of increasing the external donor/catalyst ratio is an initial sharp increase in *mmmm* pentad content up to a maximum level, after which further increases in external donor levels bring about a slight decrease in tacticity. It would seem as if the number of active sites at the extremely high external donor/catalyst ratios is so low that defects are incorporated into the chains, allowing the production of high molar mass polymer and also accounting for the slight decrease in tacticity. The slight increase in activity observed at a certain external donor/catalyst ratio would appear to be due to a balance between the decrease in the number of active sites via coordination of external donor to the catalyst and the increase in molar mass of the polymer produced at the sites which are still active producing more material.

A few reactions were also conducted with MPDMS as the external donor at different external donor/catalyst ratios. The catalyst containing MPDMS is a bit more active than the case where DPDMS was used, possibly due to the decreased steric bulk of the methyl group compared to the phenyl group. This has the effect that the active sites protected by the external donor are less hindered than those with DPDMS in the vicinity. Further evidence of this is the higher molar mass of the polymer produced by the catalysts containing MPDMS in the absence of hydrogen. The stereospecificity of the sites is, however, lower for the polymers made using MPDMS at least at lower external donor loadings. On the premise that the  $k_p$  of the sites is higher for the more stereospecific sites, it would appear that the higher molar mass is due to less chain transfer reactions and the easier incorporation of defects such as 2,1 insertions into the chains, allowing the chains to grow longer. The crystallinity of the

polymers produced using MPDMS is also slightly lower than those produced using DPDMS. It is noted that differences in the type and amount of the external donor clearly result in differences in the microstructure of the polymer produced.

In order to relate the properties of the polypropylene homopolymer to the microstructure it was necessary to produce material for further analysis with distinct differences based on the reaction conditions. It was therefore decided to produce polymers at four different external donor/catalyst ratios using each of the external donors obtained as well as in the absence of external donor. Repeatability of the specified reactions was generally good and sufficient material was obtained for a more in-depth analysis and investigation of the structure – property relationships and correlation with polymerisation conditions.

For reactions in the presence of hydrogen, an increase in molar mass was observed upon increasing the external donor/catalyst ratio for both types of donors used. The polydispersity of the DPDMS samples decreased upon increasing the external donor/catalyst ratio while little effect was observed for the samples produced using MPDMS. The crystallinities of the samples increased sharply on addition of a small amount of external donor but further increases in external donor content did not bring any significant increase in crystallinity. The activity of the catalyst using MPDMS remained relatively constant while a general decrease in activity with increasing external donor loading was observed for the DPDMS samples.

In-depth analysis of the material produced using these final reaction conditions is the subject of Chapter 6.

## 5.5 References

1. Fregonese, D., Mortara, S., & Bresadola, S., *Ziegler–Natta MgCl<sub>2</sub>-supported catalysts: Relationship between titanium oxidation states distribution and activity in olefin polymerization*. Journal of Molecular Catalysis A: Chemical, 2001. **172**: p. 89-95.
2. Al-arifi, A.S.N., *Propylene polymerization using MgCl<sub>2</sub>/ethylbenzoate/TiCl<sub>4</sub> catalyst: Determination of titanium oxidation states*. Journal of Applied Polymer Science, 2004. **93**: p. 56-62.
3. Murayama, N., Liu, B., Nakatani, H., & Terano, M., *Plausible guard effect on the active sites of heterogeneous Ziegler–Natta catalyst by coordinating monomers and growing polymer chains in the initial stage of propene polymerization*. Polymer International, 2004. **53**: p. 723-727.



4. Mori, H., Hasebe, K., & Terano, M., *Variation in oxidation state of titanium species on MgCl<sub>2</sub>-supported Ziegler catalyst and its correlation with kinetic behavior for propylene polymerization*. *Polymer*, 1999. **40**: p. 1389–1394.
5. Zakharov, V.A., Chumaevskii, N.B., Bukatov, G.D., & Yermakov, Y.I., *Study of the mechanism of propagation and transfer reactions in the polymerization of olefins by Ziegler-Natta catalysts, 2\*) The influence of polymerization temperature on the kinetic characteristics of propagation*. *Die Makromolekulare Chemie*, 1976. **177**: p. 763-775.
6. Chadwick, J.C., Morini, G., Balbontin, G., & Sudmeijer, O., *Effect of polymerization temperature on the microtacticity of isotactic poly(propylene) prepared using heterogeneous (MgCl<sub>2</sub>-supported) Ziegler-Natta catalysts*. *Macromolecular Chemistry and Physics*, 1998. **199**: p. 1873-1878.
7. Zhong, C., Gao, M., & Mao, B., *Effect of high polymerization temperature on the microstructure of isotactic polypropylene prepared using heterogeneous TiCl<sub>4</sub>/MgCl<sub>2</sub> catalysts*. *Journal of Applied Polymer Science*, 2003. **90**: p. 3980-3986.
8. Kissin, Y.V., Ohnishi, R., & Konakazawa, T., *Propylene polymerization with titanium-based Ziegler-Natta catalysts: Effects of temperature and modifiers on molecular weight, molecular weight distribution and stereospecificity*. *Macromolecular Chemistry and Physics*, 2004. **205**: p. 284-301.
9. Wang, Q., Lin, Y., Zhang, Z., Liu, B., & Terano, M., *High temperature polymerization of propylene catalyzed by MgCl<sub>2</sub>-supported Ziegler–Natta catalyst with various cocatalysts*. *Journal of Applied Polymer Science*, 2006. **100**: p. 1978-1982.
10. Pater, J.T.M., Weickert, G., Swaaij, W.P.M., *Polymerization of liquid propylene with a fourth-generation Ziegler–Natta catalyst: Influence of temperature, hydrogen, monomer concentration, and prepolymerization method on powder morphology*. *Journal of Applied Polymer Science*, 2003. **87**: p. 1421-1435.
11. Zohuri, G.H., Jamjah, R. & Ahmadjo, S., *Comparative study of propylene polymerization using monosupported and bisupported titanium-based Ziegler–Natta catalysts*. *Journal of Applied Polymer Science*, 2006. **100**: p. 2220-2226.
12. Chadwick, J.C., *Advances in propene polymerization using MgCl<sub>2</sub>-supported catalysts. Fundamental aspects and the role of electron donor*. *Macromolecular Symposium*, 2001. **173**: p. 21-35.

13. Liu, B., Nitta, T., Nakatani, H., & Terano, M., *Stereospecific nature of active sites on  $TiCl_4/MgCl_2$  Ziegler–Natta catalyst in the presence of an internal electron donor*. *Macromolecular Chemistry and Physics*, 2003. **204**: p. 395-402.
14. Giannini, U., *Polymerization of olefins with high activity catalysts*. *Macromolecular Chemistry and Physics, Supplement*, 1981. **5**: p. 216-229.
15. Keii, T., Suzuki, E., Tamura, M., Murata, M., & Doi, Y., *Propene polymerization with a magnesium chloride-supported Ziegler catalyst. I. Principal kinetics*. *Makromolekulare Chemie*, 1982. **183**: p. 2285-2304.
16. Kissin, Y.V., *Isospecific Polymerization of Olefins with Heterogeneous Ziegler-Natta Catalysts*. 1985, New York: Springer-Verlag.
17. Albizzati, E., Giannini, U., Collina, G., Noristi, L., & Resconi, L., *Catalysts and polymerizations*, in *Polypropylene handbook*, E.P. Moore, Jr., Editor. 2002, Hanser: Munich. p. 11-111.
18. Zakharov, V.A., Bukatov, G.D., & Yermakov, Y.I., *On the mechanism of olefin polymerization by Ziegler-Natta catalysts*. *Advances in Polymer Science*, 1983. **51**: p. 61-100.
19. Cavallo, L., Guerra, G., & Corradini, P., *Mechanisms of propagation and termination reactions in classical heterogeneous Ziegler-Natta catalytic systems: A nonlocal density functional study*. *Journal of the American Chemical Society*, 1998. **120**: p. 2428-2436.
20. Busico, V., Cipullo, R., Talarico, G., Segre, A.L., & Chadwick, J.C., *New evidence on the nature of the active sites in heterogeneous Ziegler-Natta catalysts for propene polymerization*. *Macromolecules*, 1997. **30**: p. 4786-4790.
21. Kissin, Y.V., Rishina, L.A., & Vizen, E.I., *Hydrogen effects in propylene polymerization reactions with titanium-based Ziegler–Natta catalysts. II. Mechanism of the chain-transfer reaction*. *Journal of Polymer Science: Part A: Polymer Chemistry*, 2002. **40**: p. 1899-1911.
22. Kouzai, I., Wada, T., Taniike, T., & Terano, M., *Hydrogen effects for propylene polymerization with ultra low  $TiCl_3$  loading  $MgCl_2$ -supported catalyst*. *Macromolecular Symposium*, 2007. **260**: p. 179-183.
23. Liu, B., Murayama, N., & Terano, M., *Transformation of polymerization sites into hydrogen dissociation sites on propylene polymerization catalyst Induced by the reaction with Al-alkyl cocatalyst*. *Industrial Engineering Chemistry Research*, 2005. **44**: p. 2382-2388.

24. Busico, V., Chadwick, J.C., Cipullo, R., Ronca, S., & Talarico, G., *Propene/ethene- $[1-^{13}C]$  copolymerization as a tool for investigating catalyst regioselectivity.  $MgCl_2$ /internal donor/ $TiCl_4$ -external donor/ $AlR_3$  systems.* *Macromolecules*, 2004. **37**: p. 7437-7443.
25. Chadwick, J.C., van Kessel, G.M.M., & Sudmeijer, O., *Regio- and stereospecificity in propene polymerization with  $MgCl_2$ -supported Ziegler-Natta catalysts: Effects of hydrogen and the external donor.* *Macromolecular Chemistry and Physics*, 1995. **196**: p. 1431-1437.
26. Kissin, Y.V., & Rishina, L.A., *Hydrogen effects in propylene polymerization reactions with titanium-based Ziegler-Natta catalysts. I. Chemical mechanism of catalyst activation.* *Journal of Polymer Science: Part A: Polymer Chemistry*, 2002. **40**: p. 1353-1365.
27. Matsuoka, H., Liu, B., Nakatani, H., & Terano, M., *Variation in the isospecific active sites of internal donor-free  $MgCl_2$ -supported Ziegler catalysts: Effect of external electron donors.* *Macromolecular Rapid Communications*, 2001. **22**: p. 326-328.
28. Sacchi, M.C., Tritto, I., & Locatelli, P., *Stereochemical investigation of the effect of lewis bases in heterogeneous Ziegler-Natta initiator systems.* *Progress in Polymer Science*, 1991. **16**: p. 331-360.
29. Yaluma, A.K., Chadwick, J.C., & Tait, P.J.T., *Kinetic and active centre studies on the polymerization of propylene using  $MgCl_2$  supported Ziegler-Natta catalysts and 1,3 diether donors.* *Macromolecular Symposium*, 2007. **260**: p. 15-20.
30. Bukatov, G.D., & Zakharov, V.A., *Propylene Ziegler-Natta polymerization: Numbers and propagation rate constants for stereospecific and non-stereospecific centers.* *Macromolecular Chemistry and Physics*, 2001. **202**: p. 2003-2009.
31. Zakharov, V.A., Bukatov, G.D., & Barabanov, A.A., *Recent data on the number of active centers and propagation rate constants in olefin polymerization with supported ZN catalysts.* *Macromolecular Symposium*, 2004. **213**: p. 19-28.
32. Yaluma, A.K., Tait, P.J.T., & Chadwick, J.C., *Active center determinations on  $MgCl_2$ -supported fourth- and fifth-generation Ziegler-Natta catalysts for propylene polymerization.* *Journal of Polymer Science: Part A: Polymer Chemistry*, 2006. **44**: p. 1635-1647.
33. Sacchi, M.C., Forlini, F., Tritto, I., Mendichi, R., Zannoni, G., & Noristi, L., *Activation effect of alkoxysilanes as external donors in  $MgCl_2$ -supported Ziegler-Natta catalysts.* *Macromolecules*, 1992. **25**: p. 5914-5918.

34. Kissin, Y.V., Chadwick, J.C., Mingozi, I., & Morini, G., *Isoselectivity distribution of isospecific centers in supported titanium-based Ziegler-Natta catalysts*. *Macromolecular Chemistry and Physics*, 2006. **207**: p. 1344-1350.
35. Kang, K.K., Shiono, T., Jeong, Y-T., & Lee, D-H., *Polymerization of propylene by using  $Mg(OEt)_2$ -DNBP- $TiCl_4$  catalyst with alkoxy disilanes as external donor*. *Journal of Applied Polymer Science*, 1999. **71**: p. 293-301.
36. Proto, A., Oliva ,L., Pellecchia, C., Sivak, A.J., & Cullo, L.A., *Isotactic-specific polymerization of propene with supported catalysts in the presence of different modifiers*. *Macromolecules*, 1990. **23**: p. 2904-2907.

## Chapter 6. Active sites, microstructure, and properties

### 6.1 Introduction

Chapter 4 dealt with the physical removal of fractions, ascertaining the differences in properties that exist if different fractions are removed from the material, while Chapter 5 examined the differences that exist in the microstructure of the polymer produced at different reaction conditions. The main focus of the current chapter will be to attempt to bring all the data together by relating the polymerisation conditions of a few specific reactions to the microstructure of the chains produced, and this in turn with the physical properties of the polymers.

The physical properties of polypropylene are influenced by a number of factors. Probably the most influential property of polypropylene on the physical properties is the degree of crystallinity of the sample in question. An increase in crystallinity is often related to an increase in properties such as the stiffness or modulus of a sample while other factors such as the impact strength generally decrease with increasing crystallinity. Molar mass also plays an important role both in determining the degree of crystallinity, crystallisation rate, and also the physical properties themselves [1]. The molar mass has also been shown to influence the  $T_g$  of polymers with higher molar mass samples having a higher  $T_g$  [2]. This in turn influences the mobility of chains at room temperature, and since polypropylene has a glass transition temperature range in the region of 0 °C, variations in the temperature range of the  $T_g$  can have an effect on the ability of the material to displace energy at low temperatures. The tacticity of polypropylene samples is also important for the physical properties. Generally polymers of higher tacticity show an improvement in crystallinity and form stiffer materials [3]. The regio- and stereo-regularity can also influence the crystal phase of the polymer and, since the different phases have slightly different properties, changes in the relative content of each phase can change the overall properties of the polymer.

The polymerisation conditions determine the molar mass, molar mass distribution, and overall tacticity of the polymer chains produced. The conditions are thus vitally important and knowledge of which conditions yield which properties is critical in being able to pre-determine the types of chains which would be produced in a given reaction. The molar mass is generally controlled by the amount of hydrogen present in the system and this has proven to be an excellent way in which to tailor the molar mass of polymers. The electron donors introduced to a system on the other hand are mainly responsible for the improvement of the stereospecificity of the active sites thus improving the tacticity of the samples and limiting the

amount of atactic polymer produced. It should be noted, however, that upon increasing the stereospecificity of the active sites there is a concurrent increase in the  $k_p$  of the sites [4] and generally a reduction in chain transfer to monomer (in the absence of hydrogen), and so the electron donors can also influence the molar mass and molar mass distribution of the polymer as well [5-7]. The electron donors present at a given active site also influence the regioselectivity of the sites which can have a significant influence on the molar mass and molar mass distribution via the high probability of chain transfer to hydrogen after a 2,1 insertion [8]. The stereo- and regio-selectivity can also influence the hydrogen activating effect which is also essentially due to the increased chain transfer and the elimination of semi-dormant sites after a secondary coordination of a monomer unit [9].

The nature of the active sites therefore plays an important role in determining the microstructure of the chains produced by a catalyst. The electron donors are the main factors governing the type of active sites present in a given catalyst system. It should be noted, however, that highly stereospecific active sites are present even in the absence of electron donors [10] and active site models involving the formation of a bimetallic complex have been proposed to account for this effect since the cocatalyst is observed to have an influence on the stereospecificity [11].

A three site model was proposed by Busico *et al.* [12] to account for the presence in the same chains of highly isotactic material as well as poorly isotactic material [13], essentially forming stereo-blocks in the same chain.

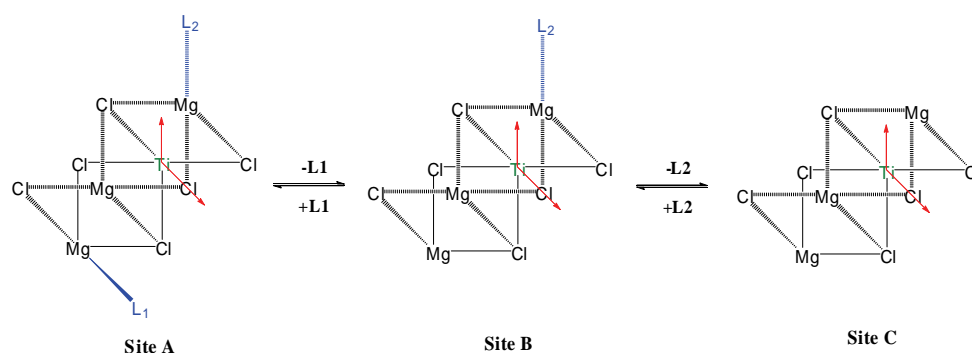


**Figure 6.1** An adaptation of the three sites model as proposed by Busico *et al.* [12, 14].

The three sites in the model have the ability to produce highly isotactic chains (site **A**), poorly isotactic chains (site **B**), and syndiotactic or atactic chains (site **C**). The ligands in the L1 or L2 positions can be electron donors, aluminium-alkyls, or chlorine atoms. Active site **C** can produce syndiotactic material if chain end control predominates during the polymerisation since there is a lack of steric hindrance at the active site. Active site **A** on the other hand produces highly isotactic material when ligands are coordinated to both positions, while active

site **B** is mainly responsible for the production of poorly isotactic material. The type of material produced at this site could be strongly dependant on the nature of the ligand in the L2 position.

The degree to which the ligands are labile plays an important role in the stereoregulating ability of the sites. The fast switching (within the lifetime of a growing chain) between the sites is thought to account for the presence of highly isotactic and syndiotactic segments in the same chain. This emphasises the importance of the equilibria which are present during a polymerisation as discussed in Section 2.2.2.8. It is clear, based on the three sites model, that extraction of the internal donor for example would change the nature of the site completely. There are of course a number of different permutations of the sites depending on which ligands are coordinated in the vicinity of the sites and therefore the actual number of sites in any given Ziegler-Natta catalyst is usually more than three. Modified three-sites models have been proposed to account for the variations [15, 16], however, the three sites model serves as an excellent generalisation.

The polymerisations conducted in order to obtain polymers for further analysis involved variation of the amount of external donor as well as the type of external donor. This would in turn affect the amounts of each of the three sites present in the catalyst. The largest difference in properties is expected for the sample produced without external donor as the extraction of the internal donor would proceed unhindered.

## **6.2 Experimental**

### **6.2.1 Polymer characterisation**

The CRYSTAF,  $^{13}\text{C}$  NMR, DSC, and HT-GPC data of the samples were obtained according to procedures described in Chapter 3 (Section 3.2.2 and Sections 3.3.1-3.3.3).

### **6.2.2 TREF characterisation**

The general TREF procedure is described in Chapter 3 (Section 3.2.1).

### **6.2.3 Mechanical properties**

The standard compression DMA data and microhardness data of the samples were obtained according to procedures described in Chapter 3 (Sections 3.4.2 and 3.4.3).

## 6.2.4 Molar mass distribution deconvolution

The deconvolution of molar mass data has become a standard tool for researchers in order that quantification of the different active sites in a polymerisation can be performed. Essentially the procedure involves the deconvolution of the molar mass distribution into a number of constituent Flory distributions [17] (equation 1), each of which have an  $M_w/M_n$  value of 2. This can be done since a single Flory distribution can describe the molar mass distribution of the polymer produced using single-site metallocene catalysts. The method involves the use of the instantaneous chain length distributions:

$$w(r) = r\tau^2 \exp(-r\tau) \quad (1)$$

where  $w(r)$  is the weight chain length distribution for all polymer chains of length  $r$ , and  $\tau$  is the ratio of all chain transfer rates to the propagation rate. The instantaneous chain length distribution of the polymer as a whole is obtained by averaging the distributions of each individual site type [18] as shown in equation 2:

$$\hat{W}(r) = \sum_{j=1}^n m(j)w(r, j) \quad (2)$$

where  $\hat{W}(r)$  is the instantaneous weight chain length distribution of the whole polymer produced by  $n$  site types. Then  $m(j)$  is the mass fraction of polymer made by site type  $j$ . The procedure is discussed in detail in the literature and the reader is directed here for a more in-depth discussion on the subject [18-22]. The method developed by Soares and Hamielec [18] was used during this study.

## 6.3 Results and Discussion

The general characterisation of the materials will be discussed first, followed by fractionation analysis by CRYSTAF and TREF, and finally the deconvolution of the HT-GPC data and physical properties of the samples. The polymerisation conditions were noted in Chapter 5 (Section 5.3.7).



### 6.3.1 Polymer microstructure

Table 6.1 comprises of a data summary for all the samples used in this section of the work.

Table 6.1 A data summary of all samples with varying donor types and loadings

Sample Code	Si:Ti	Activity (kg PP/gTi.h)	T <sub>m</sub> (°C)	Crystallinity (%) <sup>d</sup>	M <sub>w</sub> (g/mol)	PD	mmmm (%) <sup>e</sup>
DP-1 <sup>a</sup>	40	2.86	162.66	64.83	321000	4.9	96.11
DP-2 <sup>a</sup>	16	2.95	162.80	63.73	288000	5.0	94.78
DP-3 <sup>a</sup>	8	3.90	160.99	73.30	246000	5.2	95.13
DP-4 <sup>a</sup>	4	4.40	161.27	74.64	226000	5.9	94.56
No ED <sup>c</sup>	0	4.46	157.08	54.21	158000	7.5	83.84
MP-1 <sup>b</sup>	40	4.87	161.44	66.12	262000	6.5	96.00
MP-2 <sup>b</sup>	16	4.64	159.30	66.75	192000	8.8	95.44
MP-3 <sup>b</sup>	8	4.47	159.35	74.80	182000	8.7	93.72
MP-4 <sup>b</sup>	4	4.87	159.49	69.04	183000	8.5	94.57

*a* = polymerisations conducted using DPDMS as external donor

*b* = polymerisations conducted using MPDMS as external donor

*c* = polymerisation conducted with no external donor present

*d* = crystallinity (%) as determined by DSC from the melting enthalpy

*e* = pentad sequence content as determined by <sup>13</sup>C NMR

Each aspect of the samples is discussed individually in the following sections. It is noted, however, that as far as the activity of the individually systems are concerned (Figure 6.2), increasing the external donor/catalyst ratio for the polymers made using MPDMS as external donor does not appear to yield any significant change in the activity. Using DPDMS on the other hand results in a decrease in activity as the external donor/catalyst ratio is increased. This implies that either the DPDMS is more effective at deactivating certain active sites or that there is the possibility that the  $k_p$  of the active sites that remain is not as high as when the MPDMS is present in the system. It is thought that the overriding factor is more likely the more effective blocking of certain sites than a lower  $k_p$  since the average *mmmm* pentad sequence contents are generally very similar using both types of donors and also the molar mass of the polymers produced using DPDMS is generally higher than that of the polymers produced using MPDMS. Garoff *et al.* [5] also found a decrease in activity at high external donor/catalyst ratios using dicyclopentyl dimethoxysilane (DCPDMS) as external donor

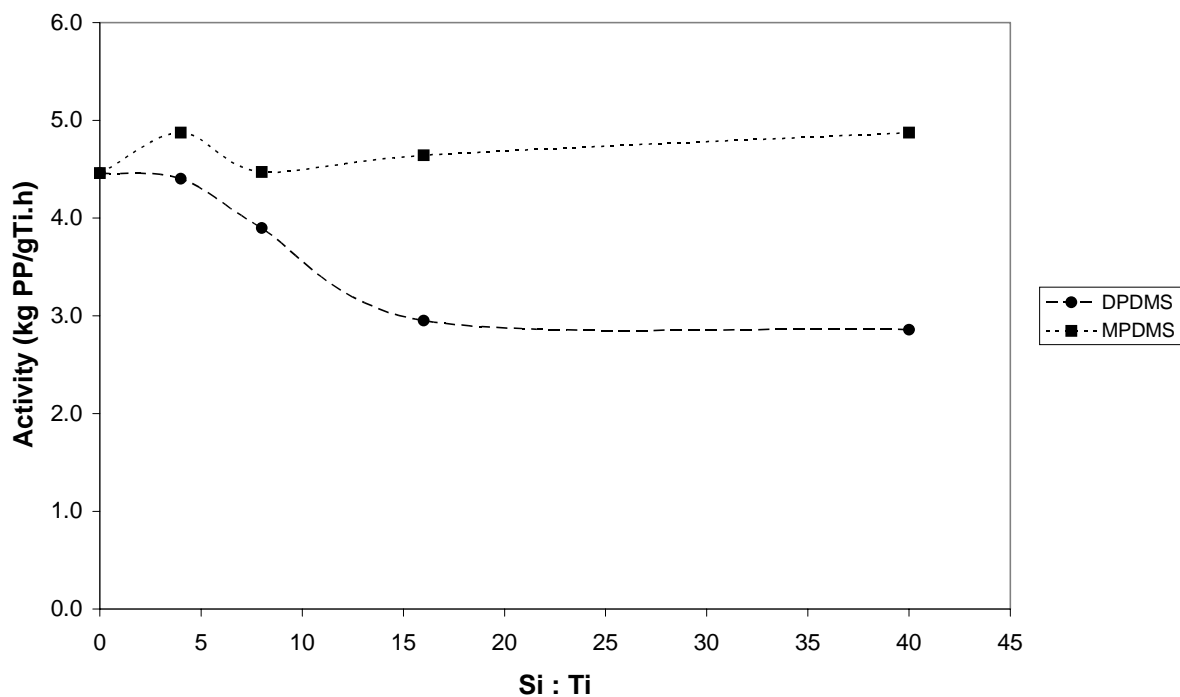
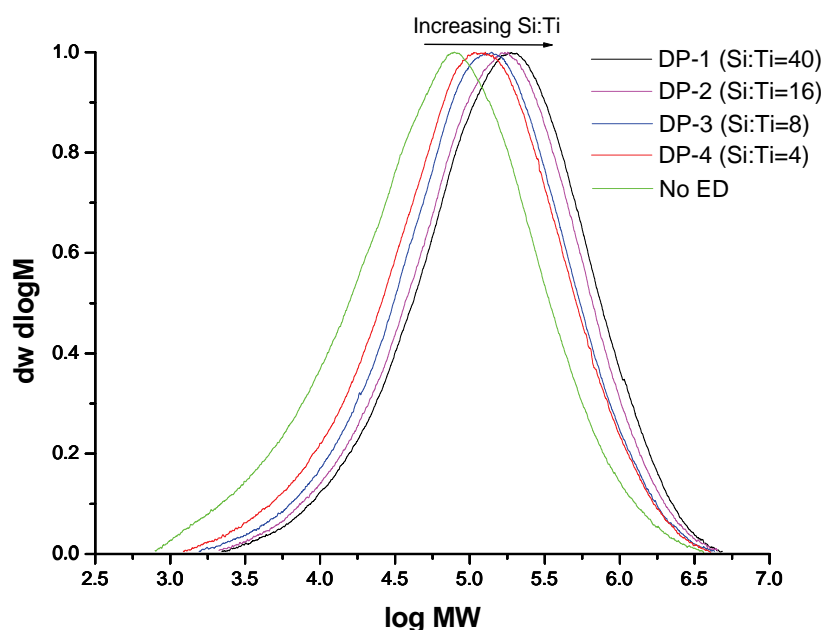


Figure 6.2 The effect of the Si : Ti on the activity of the catalyst.

### 6.3.1.1 Molar mass distributions

The molar mass distributions for the samples produced using DPDMS as external donor, as well as the sample without external donor, are given in Figure 6.3. There is a clear shift in the distribution to higher molar masses as the external donor/catalyst ratio is increased. The broadness of the distribution remains relatively similar, narrowing slightly for the highest external donor/catalyst ratio. Since it is believed that the number of propagating centers decreases upon increasing the external donor levels in the system, due to deactivation of certain active sites in the system such as the aspecific sites, it is also thought that the increase in molar mass is primarily due to an increase in the  $k_p$  of the active sites as the isospecificity of the sites increases. Chadwick *et al.* [7, 23] have demonstrated that different external donors affect the molar mass of the polymer produced and that active sites with higher stereoregulating ability produced higher molar mass polymers. Active sites formed using certain external donors, yielded sites characterised by a lower hydrogen response, and thus higher molar mass polymers were formed at these sites. It would therefore seem that the higher molar masses obtained at higher external donor/catalyst ratios are indeed the result of increased stereospecificity of the active sites. Kouzai *et al.* [24] have demonstrated that at low titanium loadings on the catalyst the hydrogen is not effective as a chain transfer agent for aspecific sites due to the absence of hydrogen dissociation sites near isolated titanium species.

Hydrogen was still an effective transfer agent for the isospecific sites irrespective of titanium content of the catalyst. The possibility therefore exists that the high external donor/catalyst ratios also result in blocking some of the hydrogen dissociation sites in the vicinity of the propagating centres thereby allowing the production of chains of increased molar mass although an independent study would be required to ascertain if this was indeed the case.



**Figure 6.3** The molar mass distribution of the polymers synthesised using DPDMS as external donor. The distribution for the sample prepared without external donor is also given for comparison.

The molar mass distributions of the samples prepared using MPDMS as external donor, as well as the sample prepared without external donor, are presented in Figure 6.4. A slight shift is observed to higher molar masses upon addition of a small amount of external donor, however, the molar mass of the polymers then remains relatively similar (although a small increase is observed) until the external donor/catalyst ratio reaches 40 where a significant increase is again observed. It is noted that there are actually more, lower molar mass chains produced when the external donor is present than when the external donor is absent but that at the same time there are significantly more higher molar mass chains produced when the external donor is present. The distribution is definitely broader for the samples containing external donor with the exception of the sample produced at an external donor/catalyst ratio of 40 which shows a distinctly narrower distribution. Comparisons between the samples with respect to the molar mass and polydispersity are given in Figures 6.5 and 6.6.

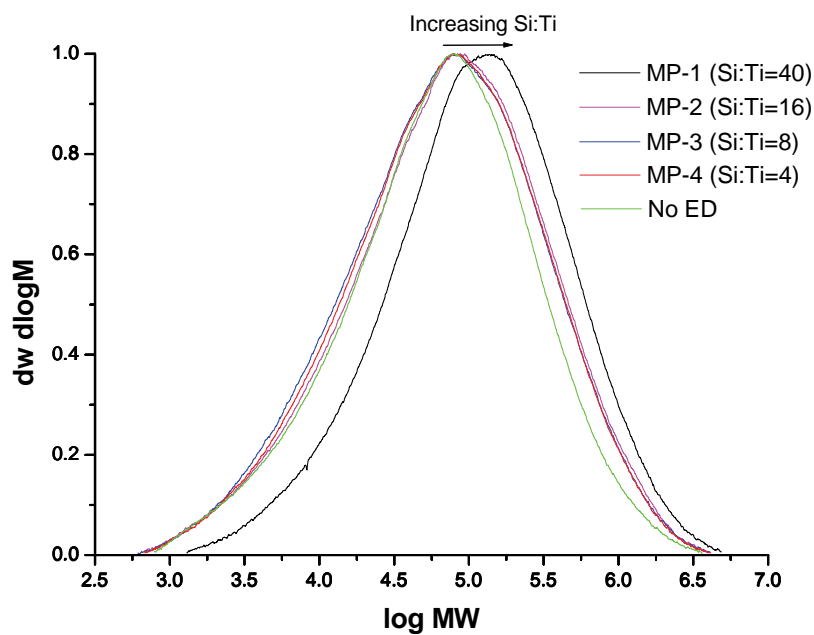


Figure 6.4 The molar mass distribution of the polymers synthesised using MPDMS as external donor. The distribution for the sample prepared without external donor is also given for comparison.

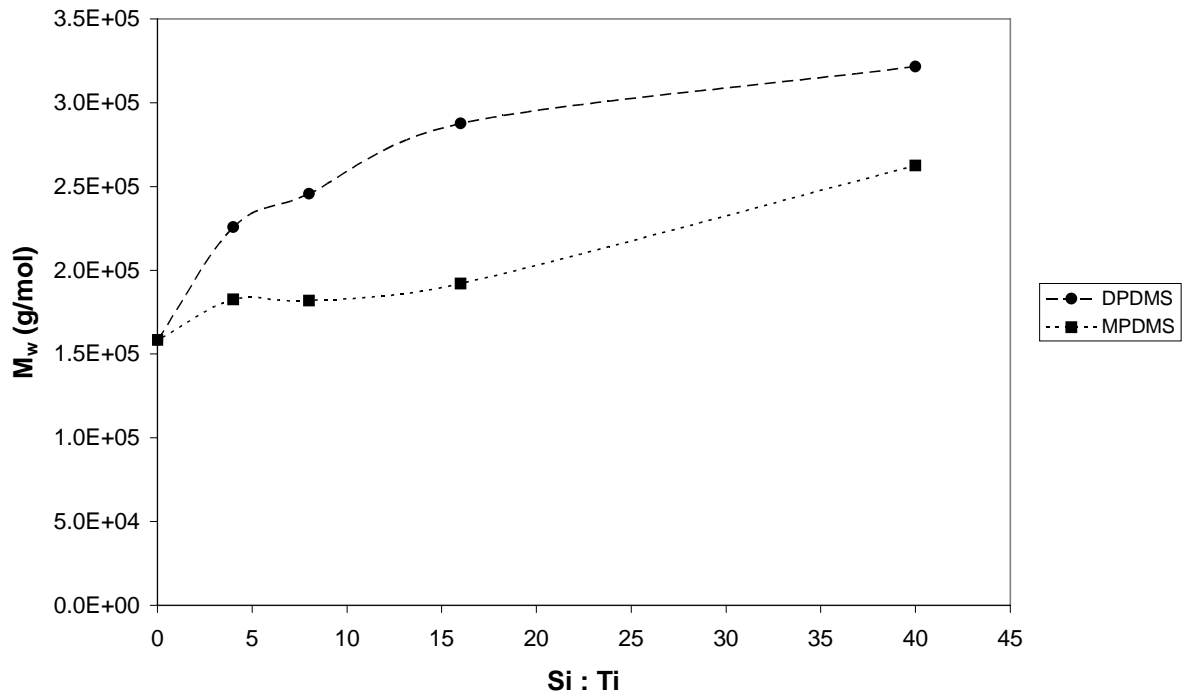
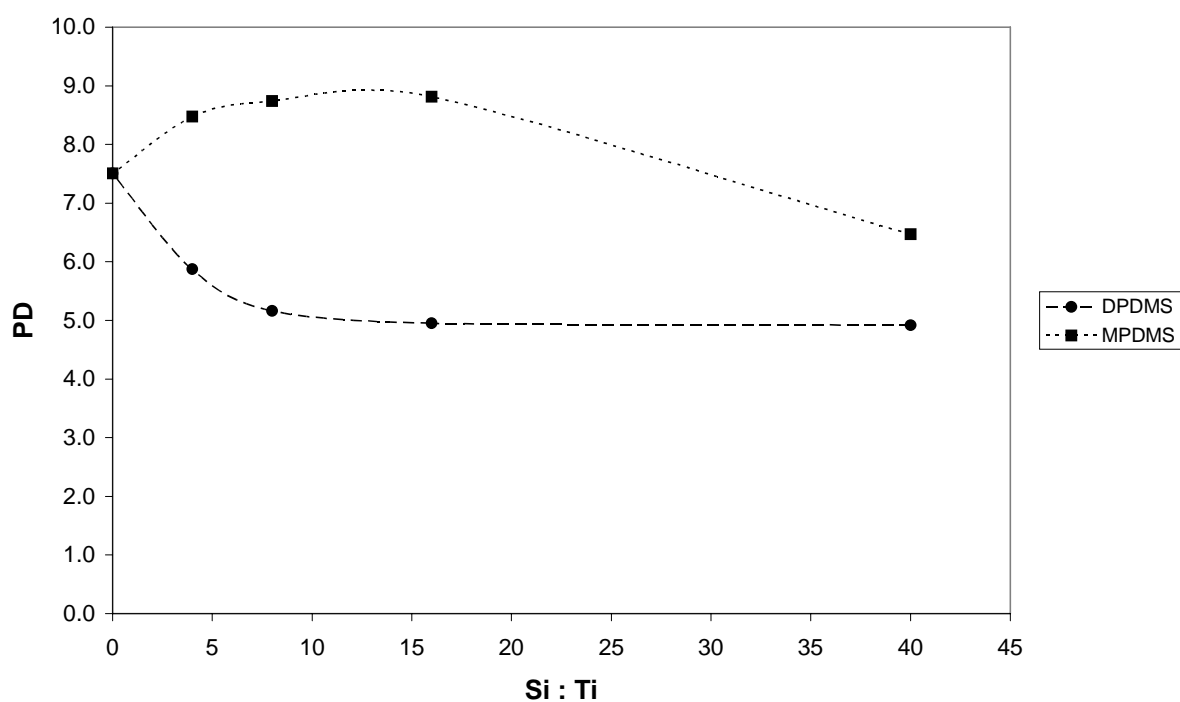


Figure 6.5 The effect of the Si : Ti on the weight average molar mass of the polymers.

If one were to discuss the different donors in terms of how labile the donor is, it would appear as if the MPDMS donor is definitely the more labile of the two as indicated by the higher polydispersity and lower molar mass of the polymers produced using this donor compared to the samples prepared using DPDMS. In terms of Busico's three site model discussed earlier it would therefore appear as if using DPDMS as external donor results in more stable active sites and less reversible coordination of the donor to the site, meaning that the site exists in a more stereospecific form for more of the time. MPDMS seems to be more labile and therefore there is more of the reversible coordination of the donor to the site and so the molar mass is lower and the polydispersity higher due to more variation in the nature of the sites. The bulkiness of the two phenyl groups on the silane definitely seems to be better as compared to the methyl and phenyl groups on the silane in terms of active site stability.



**Figure 6.6** The effect of the Si : Ti on the polydispersity of the polymers.

### 6.3.1.2 $^{13}\text{C}$ NMR analysis

A summary of the pentad sequence distribution is given in Table 6.2. It is apparent that the external donor has a significant effect on the microstructure of the chains formed. It should be noted at this stage that these are essentially average values over the entire sample.

Table 6.2 A data summary of all the  $^{13}\text{C}$  NMR data for the polymers

Sample Code	Si : Ti	<i>mmmm</i> (%)	<i>mmmr</i> (%)	<i>rmmr</i> (%)	<i>mmrr</i> (%)	<i>mmrm + rrrm</i> (%)	<i>rrrm</i> (%)	<i>rrrm + rrrr</i> (%)	<i>mrrm</i> (%)
DP-1	40	96.11	1.40	0.18	1.07	0.52	0.00	0.62	0.29
DP-2	16	94.78	1.30	0.16	1.30	1.00	0.07	0.71	0.66
DP-3	8	95.13	1.78	0.00	1.47	0.67	0.00	0.75	0.47
DP-4	4	94.56	1.72	0.12	1.47	0.72	0.00	0.93	0.49
No ED	0	83.84	4.15	0.49	4.03	1.89	0.31	3.37	1.93
MP-1	40	96.00	1.59	0.00	1.28	0.45	0.00	0.38	0.51
MP-2	16	95.44	1.65	0.43	1.31	0.52	0.00	0.56	0.28
MP-3	8	93.72	2.18	0.53	1.38	0.41	0.14	1.08	0.55
MP-4	4	94.57	1.92	0.38	1.19	0.33	0.00	1.17	0.56

Figure 6.7 illustrates the distribution in pentad sequences for the samples prepared using DPDMS as well as the sample prepared without external donor for comparison. The sharp increase in *mmmm* pentad content is clear once even a small amount of external donor is added to the system. Further increase in the amount of external donor added does not bring about any significant increase in the *mmmm* pentad content.

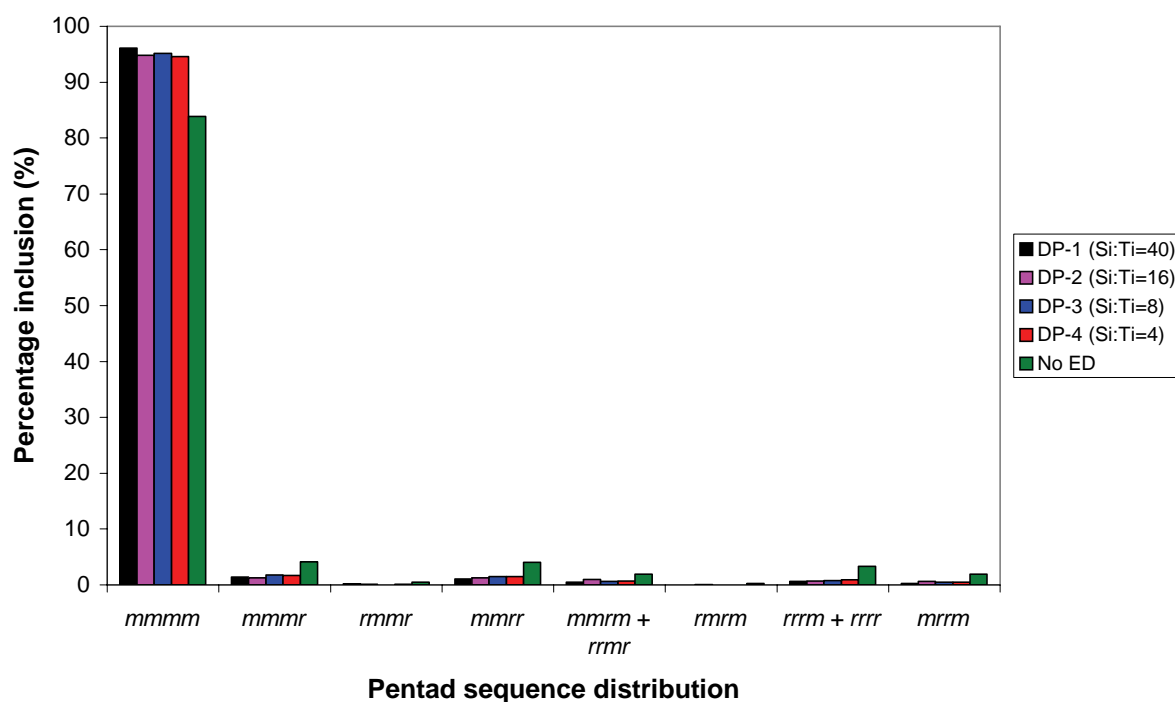
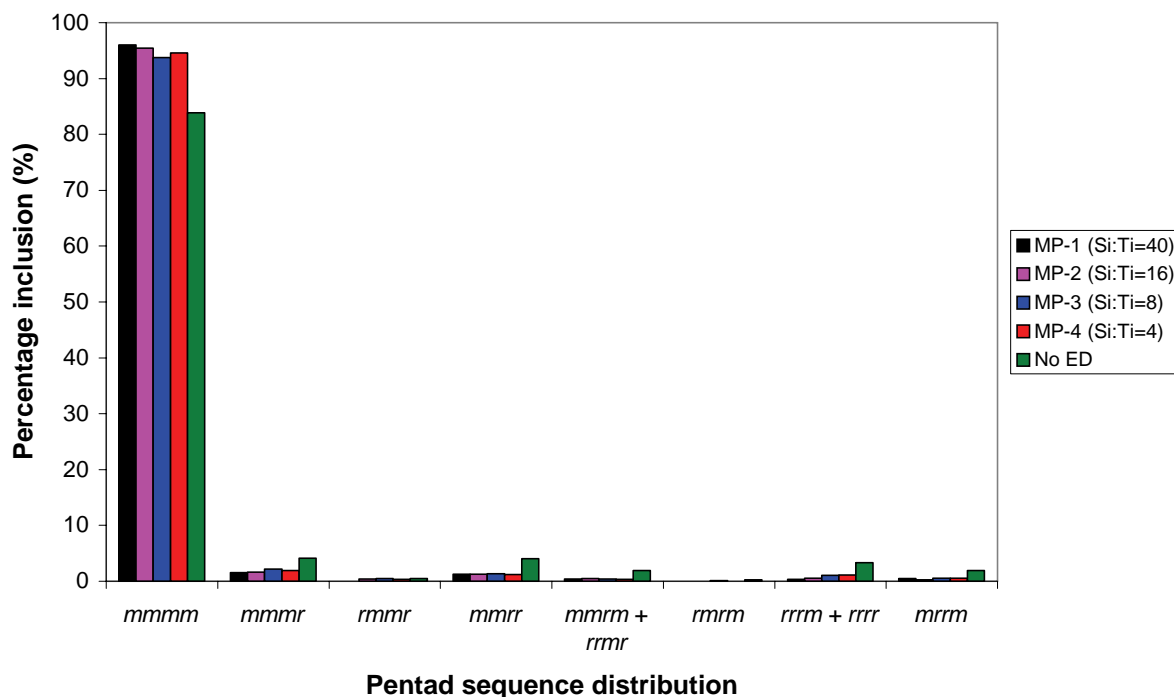


Figure 6.7 The microstructure distribution for the samples produced using DPDMS as well as the sample polymerised without external electron donor.

It is noted, however, that the *rrrm* and *rrrr* sequence content decreases constantly with increasing external donor/catalyst ratio, indicating that increasing the amount of external donor present does inhibit the production of syndiotactic material produced via chain end control to a certain extent, even if there is no significant increase in *mmmm* pentad content.

Figure 6.8 illustrates the pentad sequence distribution for the samples produced using MPDMS. Once again the increase in *mmmm* pentad content is evident upon addition of a small amount of external donor and that further increase in the external donor/catalyst ratio does not improve the *mmmm* pentad content significantly.



**Figure 6.8** The microstructure distribution for the samples produced using MPDMS as well as the sample polymerised without external electron donor.

The same constant decrease in the *rrrm* and *rrrr* pentad contents is observed for the samples produced using MPDMS indicating less syndiotactic material production at higher external donor loadings. It appears that increasing the external donor/catalyst ratio essentially systematically removes active site **C** in terms of Busico's model. A comparison of the *mmmm* pentad content of all samples is given in Figure 6.9. The values obtained are similar for both external donor types with the values being practically identical at external donor/catalyst ratios of 4 and 40, while at a ratio of 8 there is a drop in the stereospecificity of the sample produced using DPDMS to a level below that of the sample produced using MPDMS with the opposite occurring at a ratio of 16.

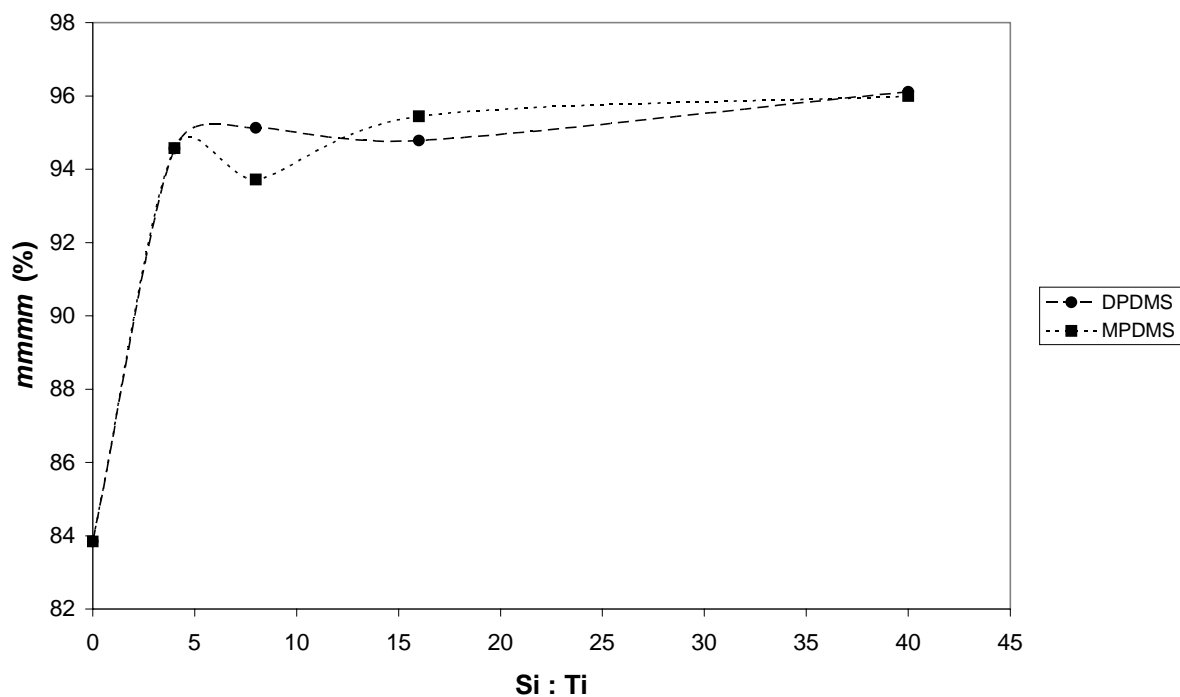


Figure 6.9 The effect of the Si : Ti on the tacticity of the polymers.

It is important to note that despite the indication from the GPC data that MPDMS is more labile than the DPDMS the average *mmmm* pentad sequence contents are very similar, indicating the presence of active sites of similar stereoregulating ability on the catalyst for each donor type.

### 6.3.2 Thermal properties

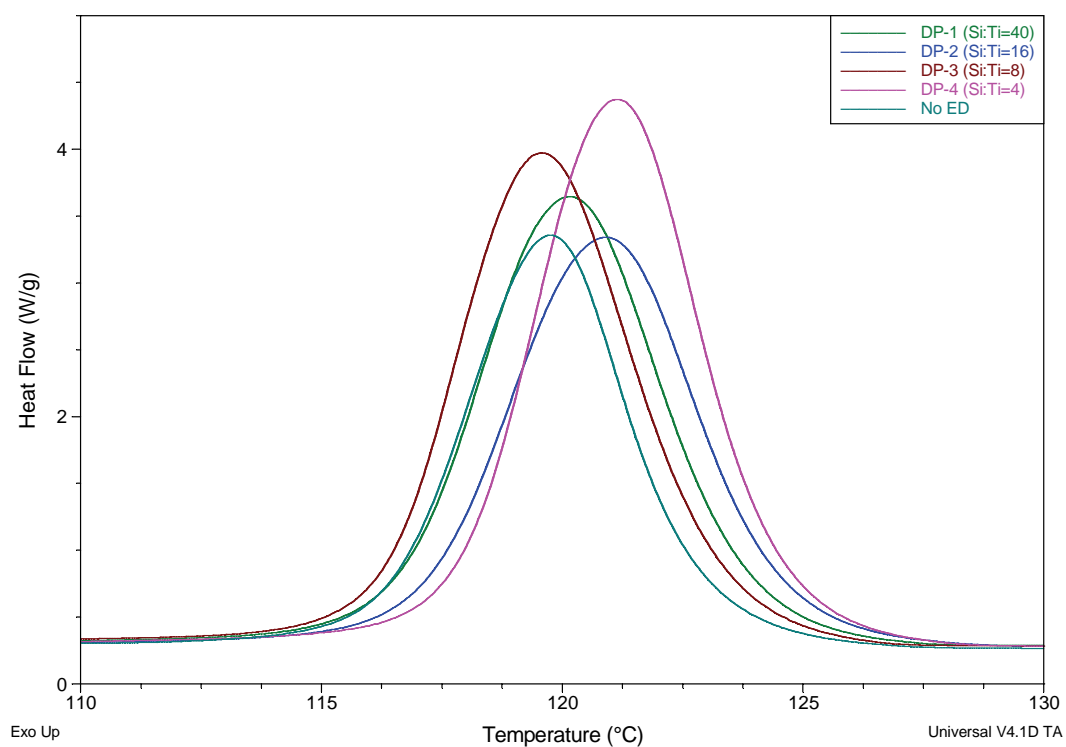
The thermal properties of all the samples are given in Table 6.3.

Table 6.3 The DSC results for all samples

Sample Code	Si:Ti	$T_m$ (°C)	$T_m$ onset (°C)	$T_c$ (°C)	$T_c$ onset (°C)	Crystallinity (%)
DP-1	40	162.7	158.6	120.1	123.9	64.8
DP-2	16	162.8	158.4	120.9	124.6	63.7
DP-3	8	161.0	157.2	119.6	123.3	73.3
DP-4	4	161.3	157.4	121.1	124.5	74.6
No ED	0	157.1	151.5	119.7	122.8	54.2
MP-1	40	161.4	157.9	120.6	124.1	66.1
MP-2	16	159.3	155.8	120.7	123.9	66.7
MP-3	8	159.4	154.6	120.7	124.1	74.8
MP-4	4	159.5	155.8	121.9	124.9	69.0



Figures 6.10 and 6.11 show the crystallisation and melting curves respectively for the samples produced using DPDMS as well as the sample produced without external donor.



**Figure 6.10** A comparison of the crystallisation exotherms of the samples produced using DPDMS as well as the sample without external donor.

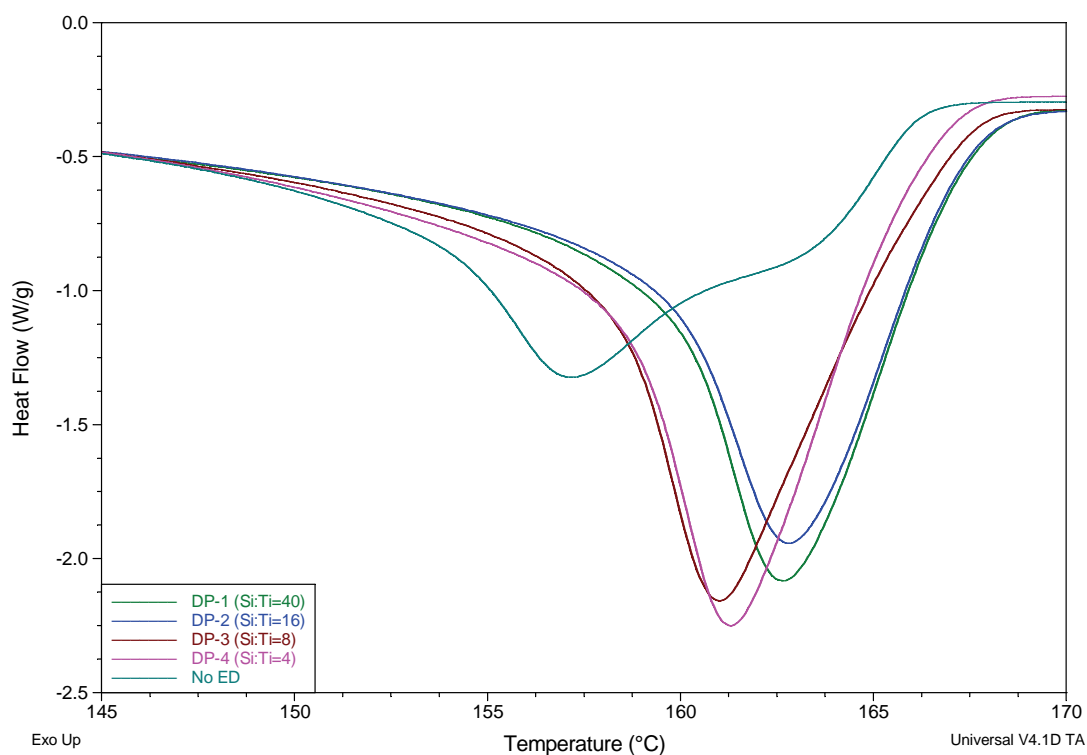


**Figure 6.11** A comparison of the melting endotherms of the samples produced using DPDMS as well as the sample without external donor.

The onset of crystallisation is lowest for the sample prepared without external donor as would be expected due to the lower *mmmm* pentad content of the chains. The melting endotherm for this sample also occurs at significantly lower temperatures than the samples prepared with an external donor and the sample exhibits a clear bimodality in terms of the melting profile indicating that although there are still some crystals present which melt at the same temperatures as the samples prepared with external donors, the majority of the lamellae melt at lower temperatures and are as such less perfect and generally thinner.

It is interesting to note that the sample with the highest onset of crystallisation temperature is the sample with an external donor/catalyst ratio of 4, and that this sample also has the highest crystallisation temperature of the samples prepared using DPDMS. The onset of crystallisation occurs at lower temperatures for the various external donor/catalyst ratios in the following order: 4, 16, 40, 8. The ratio of 8 appears to crystallise noticeably lower than where it is expected in terms of the series of samples at increasing external donor loadings. It is also interesting to note that the general order of the onset of crystallisation is that the samples with lower external donor/catalyst ratios crystallise out first and that the higher the ratio the lower the onset of crystallisation. This would seem to be related to the molar mass of the polymers since the *mmmm* pentad sequence content of the samples are similar, however, the molar mass of the samples decreases for the external donor/catalyst ratios in the order 40, 16, 8, 4. Therefore it is the lower molar mass of the sample at similar *mmmm* pentad contents which enables the crystallisation of the chains at higher temperatures. The molar mass effect on crystallisation of iPP was studied by De Rosa *et al.* [25] who demonstrated faster crystallisation for samples of lower molar mass. Similar results were obtained by Ibadon [26]. What is also interesting is that the higher crystallisation temperature of a sample does not necessarily result in higher melting temperatures. Figure 6.11 illustrates that the samples produced at an external donor/catalyst ratio of 4 and 8 melt at similar temperatures but that the samples produced at the higher ratios of 16 and 40 melt at distinctly higher temperatures.

The crystallisation and melting curves of the samples produced with MPDMS as external donor as well as the sample produced without external donor are given in Figures 6.12 and 6.13. The crystallisation and melting of the samples prepared with external donor are higher than the sample prepared without external donor as expected. It is interesting to note that the crystallisation of the samples with external donor/catalyst ratios of 8, 16, and 40 are very similar, and that as was the case with the samples produced with DPDMS the sample with an external donor/catalyst ratio of 4 crystallises out at the highest temperature. The melting curves also show important differences between the samples and it is once again the

sample produced at a high external donor/catalyst ratio (40) which melts at the highest temperature (Figure 6.13).

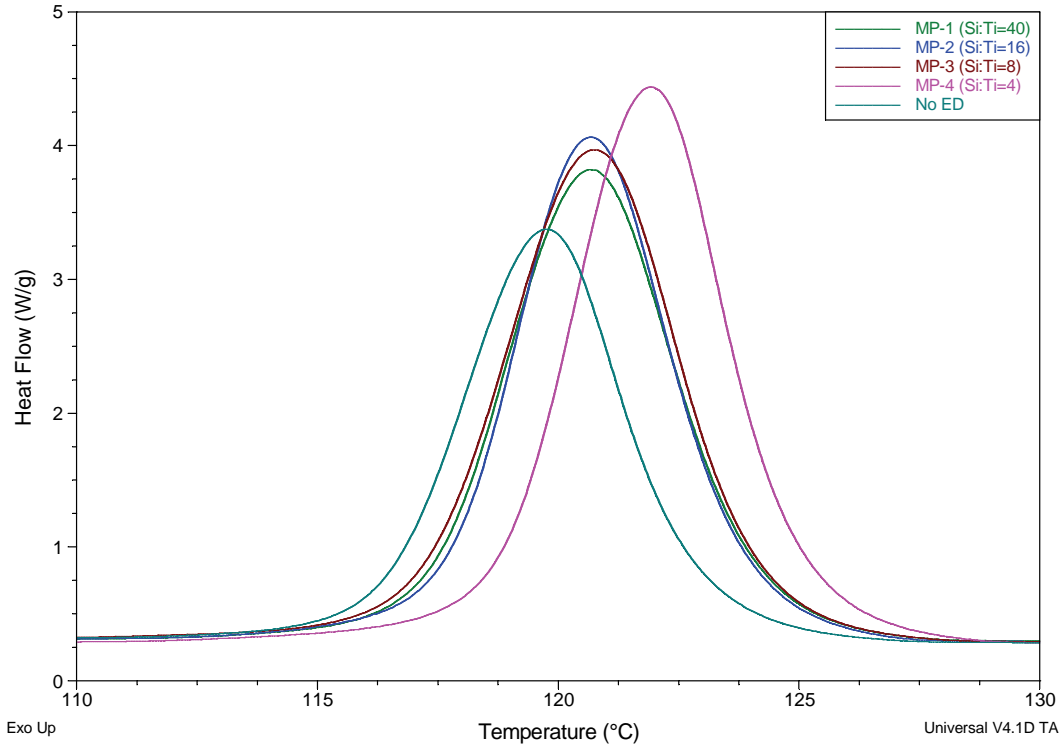


**Figure 6.12** A comparison of the crystallisation exotherms of the samples produced using MPDMS as well as the sample without external donor.

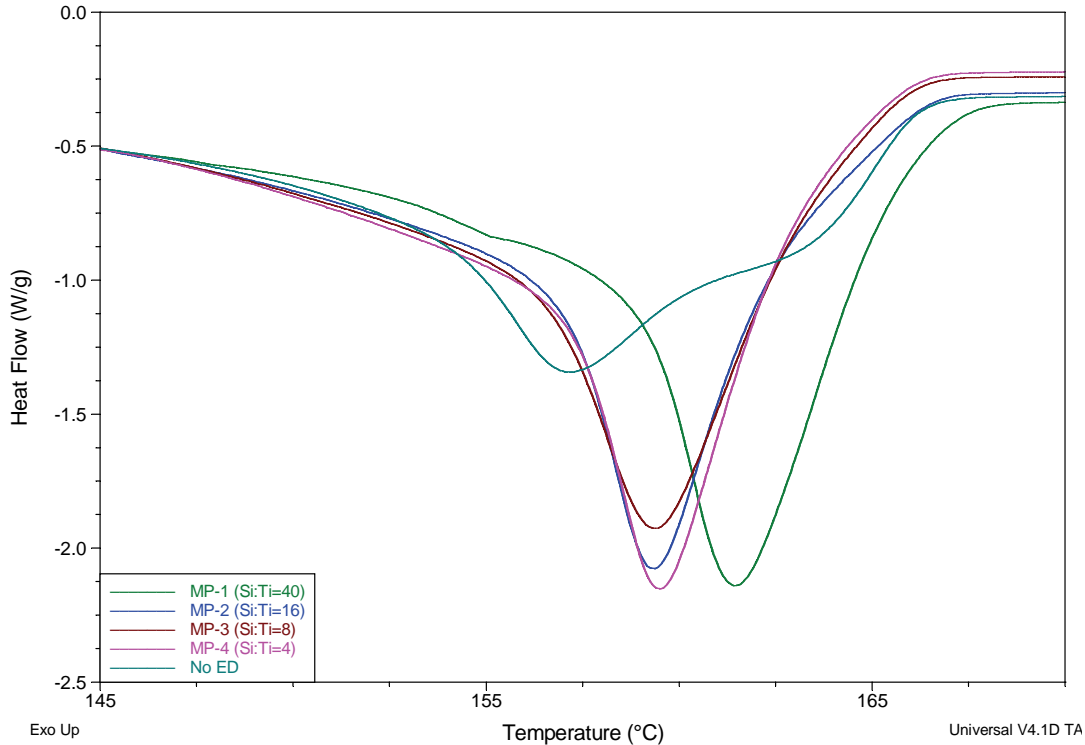


**Figure 6.13** A comparison of the melting endotherms of the samples produced using MPDMS as well as the sample without external donor.

The rest of the samples show very similar melting characteristics. The materials clearly contain small differences which play an important role in determining the properties of the polymers. Since the *mmmm* pentad contents of the samples are similar it is once again thought that the molar mass of the samples is critical in determining the crystallisation and melting of the samples. The higher molar mass of sample MP-1 appearing to results in the formation of crystals which melt at high temperatures. Samples DP-1 and DP-2 also show significant increases in molar mass compared to the other samples in that series and so it would definitely seem as if the molar mass plays a very important role on the melting properties of the polymers.

Figure 6.14 illustrates the comparison of the crystallisation temperature for the samples. Generally speaking the samples produced using MPDMS crystallise at higher temperatures than the samples produced using DPDMS with the exception of the case where the external donor/catalyst ratio is 16.

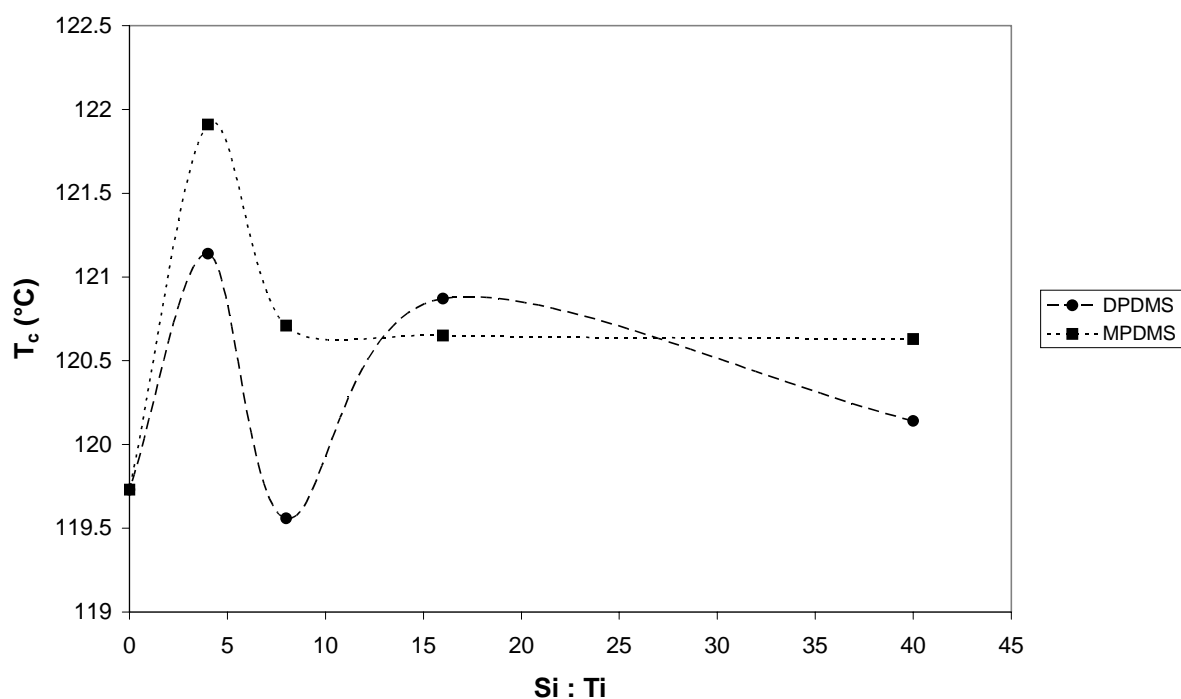


**Figure 6.14** A comparison of the peak crystallisation temperatures of the samples.

The differences are more than likely due to the lower molar mass and broader molar mass distribution of the samples produced using MPDMS. The slightly higher crystallisation temperature of sample DP-2 as compared to MP-2 is possibly related to the slightly higher *mmmm* pentad content of the DP-2 sample compared to the MP-2 sample. The noticeably low crystallisation temperature for sample DP-3 is also more than likely linked to the lower

*mmmm* pentad content of this sample as well superimposed on the effect of the higher molar mass.

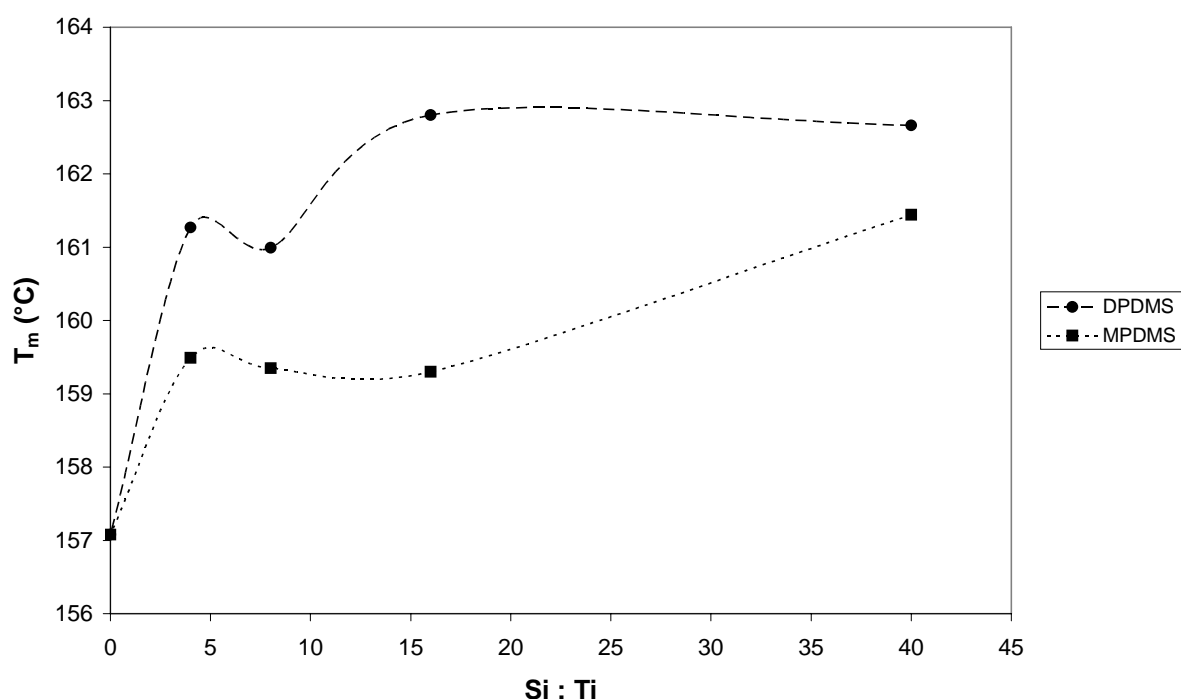


**Figure 6.15** A comparison of the peak melting points of the samples.

An examination of the melting points for the two types of donor used (Figure 6.15) reveal that the samples produced using DPDMS as external donor clearly have a higher peak melting temperature. The main reason is due to the ability of the chains present in each sample to crystallise as lamellae of increased thickness. The samples produced with DPDMS have in general a higher molar mass and narrower molar mass distribution and it thus appears as if these factors result in thicker lamellae being formed. The crystallinities of the samples are compared in Figure 6.16 and it is evident that the trends observed for both external donors are the same. It is interesting to note that, with the exception of the external donor/catalyst ratio of 4, the samples produced with MPDMS as external donor are slightly more crystalline than the samples produced using DPDMS. This is thought to be mainly due to the lower molar mass of the samples. The decrease in crystallinity for the higher external donor/catalyst ratios is also thought to be linked to the higher molar mass of the samples. The case where the external donor/catalyst ratio is 4 is interesting in that the two samples have identical tacticity and the molar mass of the DP-4 sample is higher than that of the MP-4 sample.

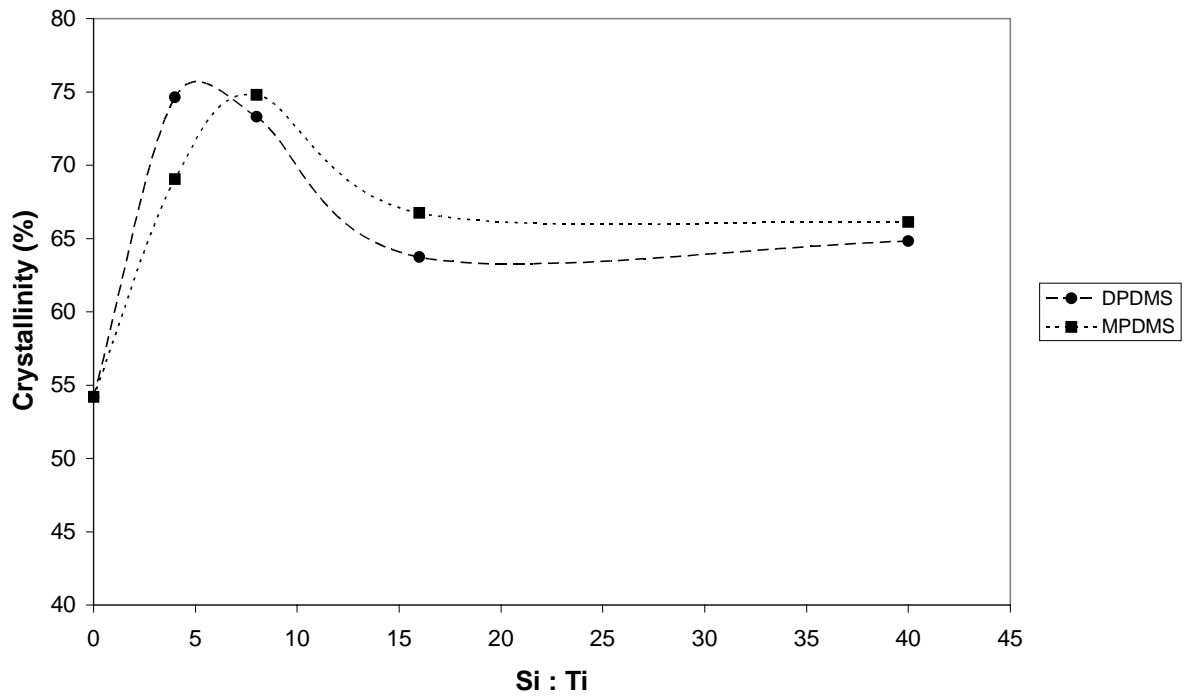


Figure 6.16 A comparison of the degree of crystallinity of the samples.

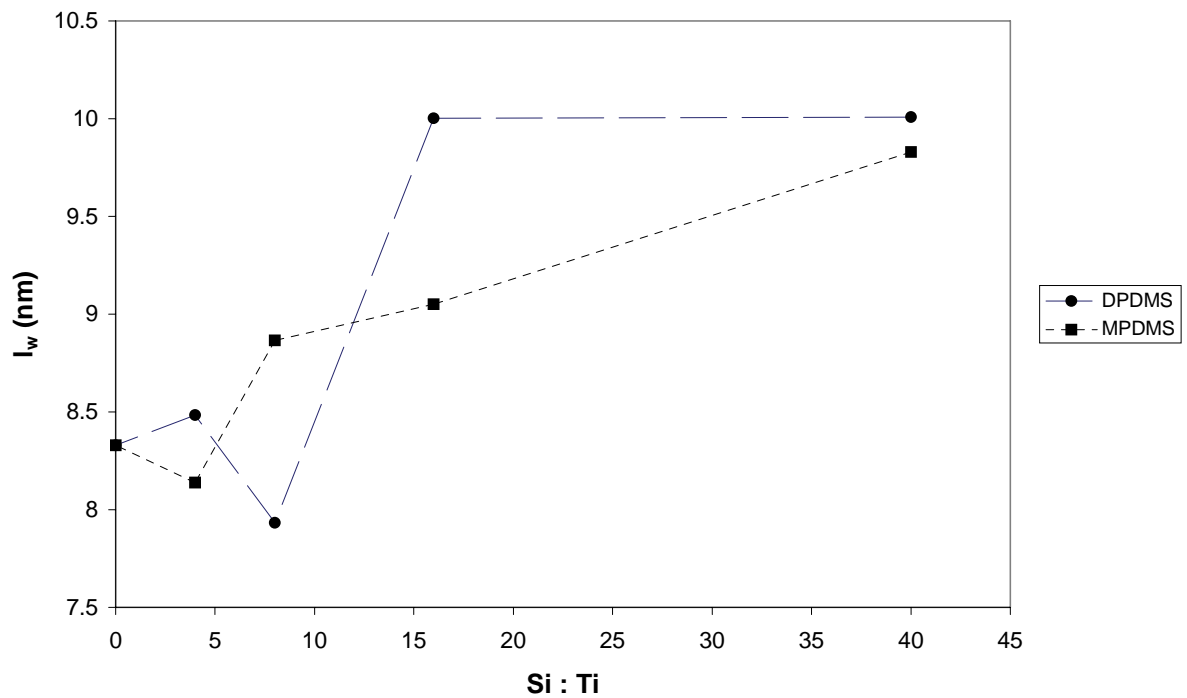


Figure 6.17 The differences in the weight average lamellar thickness between the samples produced at different Si:Ti.

Analysis of the average lamellar thickness of the samples (Figure 6.17) indicates a link to the crystallisation temperatures and the *mmm* pentad content at least in the case of the

samples produced using DPDMS. The case for the samples produced using MPDMS is less clear although in general for all samples there is an increase in lamellar thickness with increasing external donor/catalyst ratio. This could possibly be related to increased molar mass as well as increased *mmmm* pentad content. The higher molar masses seem to result in slower crystallisation, and thus the formation of thicker lamellae. Flores *et al.* [27] have demonstrated an increase in lamellar thickness with increasing molar mass of the polymers which is the same trend observed in this study.

### 6.3.3 CRYSTAF analysis

Figure 6.18 presents the CRYSTAF curves for the samples produced using DPDMS as well as the sample produced without external donor. The bimodality of the No ED sample is again evident as it was in the melting endotherms discussed earlier. The effect of adding even a small amount of external donor is immediately apparent since the bimodality disappears immediately.

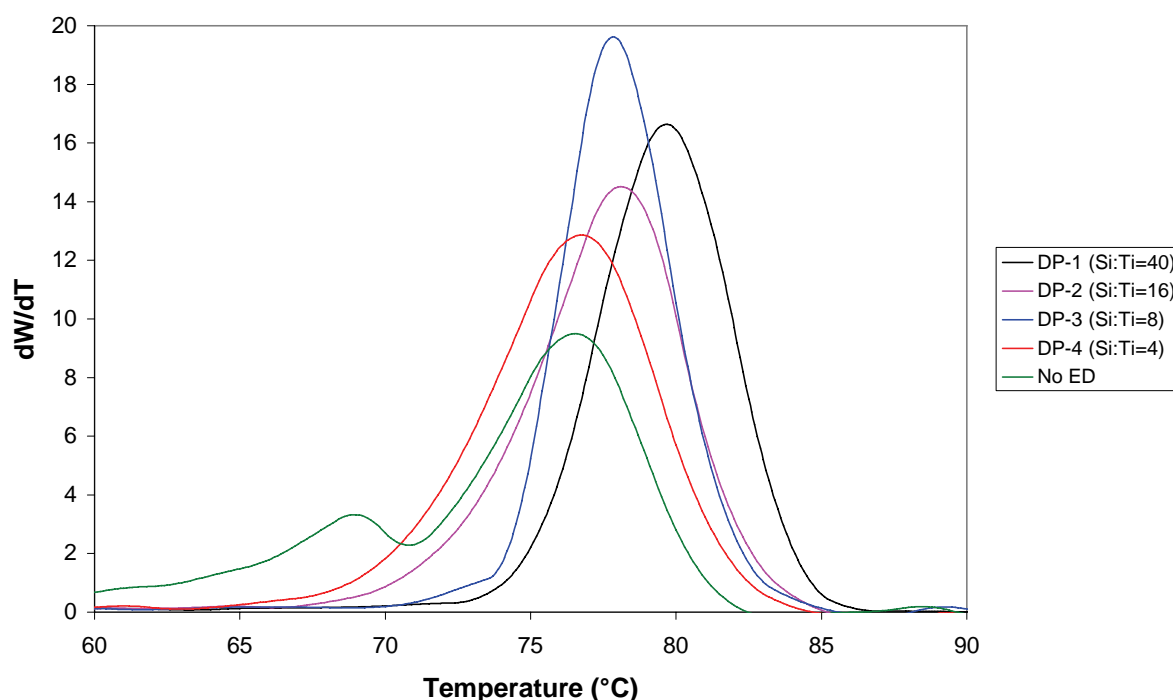


**Figure 6.18** A comparison of the CRYSTAF distribution curves of the samples produced using DPDMS as well as the sample without external donor.

The differences observed between the crystallisation of the samples are interesting if one compares the CRYSTAF data to the DSC data. Whereas in the case of the crystallisation

in the solid state, the first sample to begin crystallising was DP-4 followed by DP-2, DP-1, DP-3 and finally as expected the No ED sample, the case in solution appears to be somewhat different as far as the order is concerned. The sample which crystallises out first at high temperature is the DP-1 sample, followed by DP-2, DP-3, and DP-4. This is interesting in that there is almost a direct reversal of the trends observed for crystallisation in the solid state. It is evident that the samples crystallise out of solution in the order of decreasing external donor/catalyst ratio with the higher donor/catalyst ratios crystallising out of solution at higher temperatures. It is noted that sample DP-3 (with an external donor/catalyst ratio of 8) has a particularly narrow distribution of molecular species relative to the other samples in the series. The largest difference between the samples is the molar mass and so it would appear that the molar mass plays an important role in crystallisation from solution, with the longer chains crystallising out of solution first.

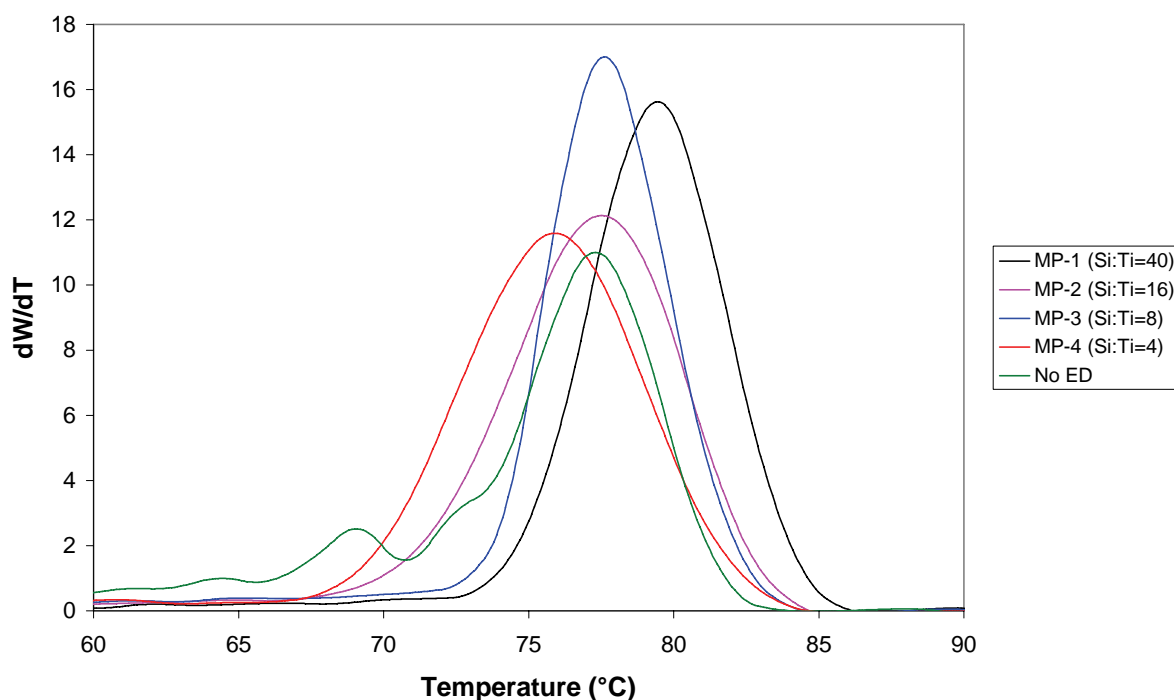


**Figure 6.19** A comparison of the CRYSTAF distribution curves of the samples produced using MPDMS as well as the sample without external donor.

An examination of the CRYSTAF data for the samples produced with MPDMS as external donor reveals the same trend (Figure 6.19). The higher the external donor/catalyst ratio, the higher the temperature of the onset of crystallisation from solution. It is also noted that the crystallisation temperatures from solution are slightly lower for the samples produced using MPDMS as compared to the samples produced using DPDMS, with the MP-4 sample



for example crystallising out of solution at a lower temperature than the No ED sample. The slightly higher crystallisation temperatures for the DPDMS samples are possibly due to the presence of longer isotactic sequences. Sample MP-3 (with an external donor/catalyst ratio of 8) also shows a relatively narrow distribution of molecular species compared to the other samples in the MPDMS series, indicating that the distribution of molecular species at this external donor/catalyst ratio is narrower irrespective of external donor type.

### 6.3.4 TREF analysis

All samples were fractionated by preparative TREF technique and the fractions analysed. The majority of the material constituting the No ED sample clearly elutes at lower temperatures than the samples prepared using DPDMS as external donor. The major fractions of this sample being those at 110 °C and 115 °C while the major fractions for the DPDMS samples are at 115 °C and 120 °C.

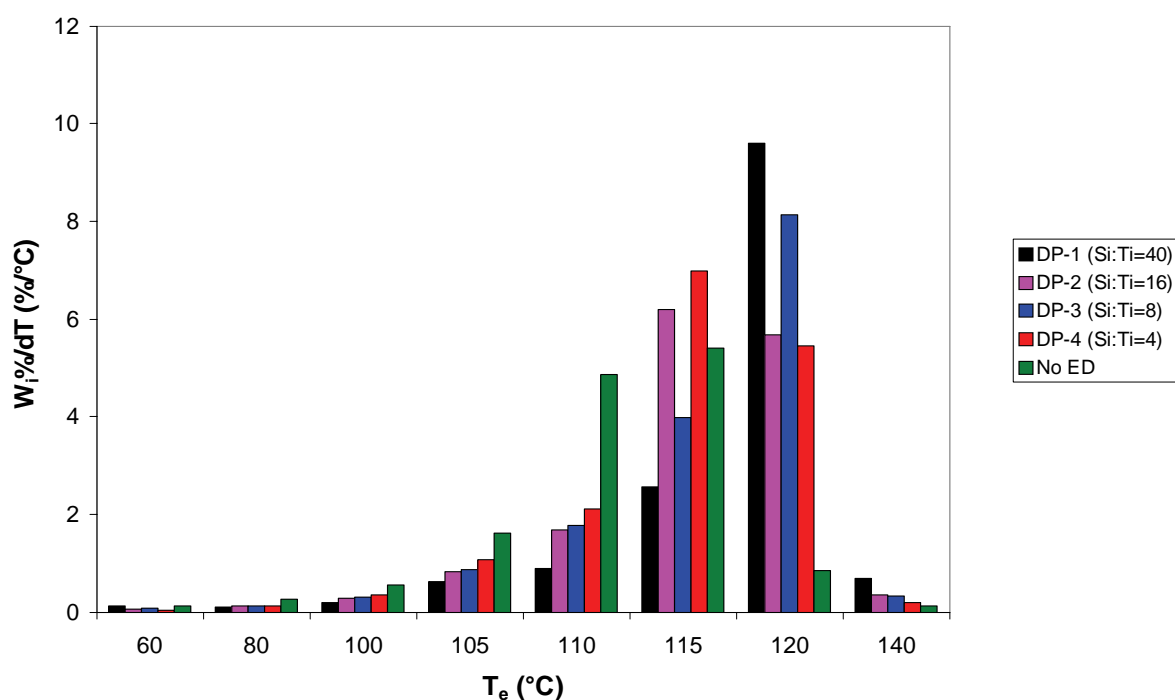


**Figure 6.20** The distribution of TREF fractions for the samples produced using DPDMS as well as the sample without external donor for comparison.

What is also interesting is that the lower temperature fractions, containing chains produced by less stereospecific active sites (site **B** according to Busico's model) since the chains can only crystallise out of solution at lower temperatures, vary in their content relative to the amount of

external donor in the system. The higher the external donor/catalyst ratio the lower the amount of material produced which elutes in these fractions. This trend is evident for the 80, 100, 105, and 110 °C fractions. As demonstrated in Chapter 4 these fractions are of paramount importance in determining the physical properties of the polymers since the removal of these fractions drastically affects the properties. However, the difference in this case is that although there is less material being produced in these fractions there is more material produced which elutes in the higher temperature fractions due to the conversion of the type of active site from site type **B** to site type **A**. The opposite trend is observed for the 140 °C fraction as one would expect with the higher external donor/catalyst ratios producing more material eluting in this fraction. Similar trends are observed for the 115 °C and 120 °C fractions with regards to the samples containing external donor. For the 115 °C fraction there is more material present in the fraction, the lower the external donor/catalyst ratio, with the exception of the DP-2 sample which appears to have more material in this fraction than would be expected. This demonstrates that increasing the external donor/catalyst ratio has an effect on the higher temperature fractions as well. The same but reversed trend is evident in the 120 °C fraction. The higher the external donor/catalyst ratio the larger the portion of material eluting in this fraction with once again the exception of the DP-2 sample where less material is eluted than expected since more of the material has eluted in the preceding 115 °C fraction.

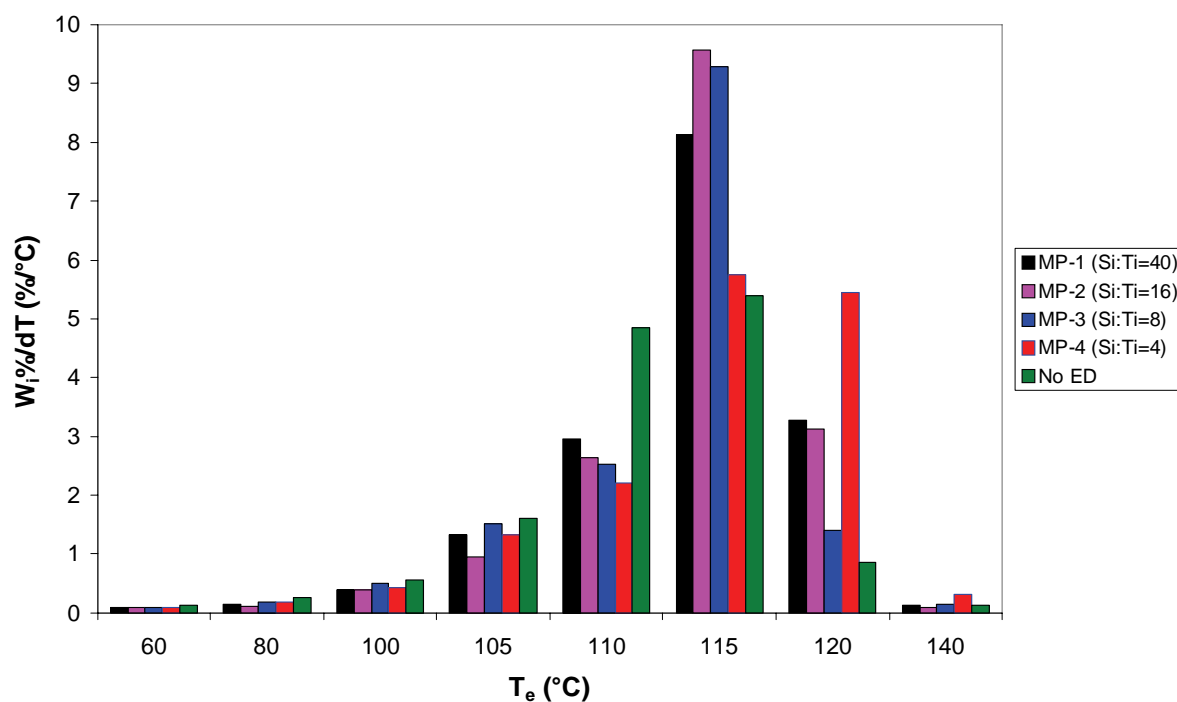


**Figure 6.21** The distribution of TREF fractions for the samples produced using MPDMS as well as the sample without external donor for comparison.

It appears as if the majority of the material produced by the converted active sites elutes in the 120 °C and 140 °C fractions.

The fraction content for the samples produced using MPDMS are slightly different with regards to the amount of material eluting in each fraction (Figure 6.21). Firstly the major fractions appear to be the 110, 115, and 120 °C fraction with the 115 °C fraction being the more dominant one for most of the samples. It appears in general that the material is more broadly distributed over the fractions for these samples. The trend observed in the CRYSTAF analysis was that the onset of crystallisation temperature was higher for the higher molar mass polymers when crystallising out of solution. This is a possible reason for the slight shift in the major elution temperatures to lower temperatures for the MPDMS samples since they have lower molar mass than the samples produced using DPDMS. Secondly the trends observed for the DPDMS samples are not as clear for the samples produced using MPDMS. There would appear to be trends in the major fractions since for the 110, 115, and 120 °C fractions the higher the external donor/catalyst ratio, the higher the amount of material being eluted in each of these fractions. This means that the converted active sites produce material which elutes in these fractions since increasing the external donor/catalyst ratio increases the proportion of these sites. This also indicates that despite the presence of the external donor in the vicinity of the active sites the material produced by the sites does not elute at as high a temperature as the material produced using DPDMS as external donor. A notable exception is the 115 °C fractions where less material than expected is eluted for sample MP-1, and also the 120 °C fraction where more of sample MP-4 is eluted than would be expected relative to the other samples in the series. In general the lower temperature fractions contribute less to the overall sample the higher the external donor/catalyst ratio although the effect is not as clear cut as in the case of the DPDMS samples. Sample MP-4 elutes at a higher temperature than would be expected, however, one should take note of the fact that this sample did start crystallising at the highest temperature during DSC analysis indicating a more solid-state-like crystallisation mechanism than from solution although there is the possibility that the high elution temperatures is due to a very high tacticity in the fractions crystallising out of solution first.

Comparing the DPDMS and MPDMS samples overall it would appear that the DPDMS as external donor exerts more control over a wider range of active sites since it demonstrates better control over the material eluting over a wider range of elution temperatures, with especially good control over the active sites producing poorly isotactic material eluting in the middle range of elution temperatures. It would also seem as if MPDMS as external donor exerts a positive influence over a broader range of active sites with regards to the sites producing significant quantities of material eluting at high temperatures. This

would be due to the fact that it MPDMS as external donor enhances the production of material which elutes at 110, 115, and 120 °C, as opposed to the enhancement of only the 120 °C fraction for the DPDMS samples (as well as for the 140 °C fraction, however, there is little material eluting in these fractions). It would appear as if the active sites affected by the MPDMS produce material with a broader distribution of molecular species than the sites affected by the DPDMS donor. The DPDMS would definitely seem to have the stronger influence on the sites. There are definitely interesting differences between the samples and so further analysis was performed on the fractions of each sample.

#### **6.3.4.1 Microstructure of TREF fractions**

The molar mass data for all of the fractions for samples DP-1, DP-2, DP-3, DP-4 and No ED are given in Figure 6.22. The overall picture is that there is initially a very small increase in the molar mass of the fractions at low temperature and that after the 100 °C fraction the molar mass increases dramatically for the remaining fractions. As observed and discussed in Chapter 4 there is a slight decrease in molar mass for the highest temperature fractions. The trends observed follow the observations of a number of researchers [4, 7, 23] that the highly stereospecific active sites also produced high molar mass material due to an increase in  $k_p$  and decrease in transfer reactions. The overall trend in molar mass for the bulk samples increases in the following order No ED, DP-4, DP-3, DP-2, and finally DP-1. In general the fractions seem to follow the same trends, however, it is interesting to note that sample DP-1's fractions for example, have the highest molar mass for the high temperature fractions, however, the lower temperature fractions molar masses are not the highest. The No ED sample's fractions have relatively high molar masses for the low temperature fractions compared to the other samples in the series. In fact the No ED sample has by far the highest molar mass for the fractions at 80 °C, 105 °C, and 110 °C. Since these fractions are deemed extremely important for the properties of the material and the molar mass was observed to have an affect on the modulus of the samples as investigated in Chapter 4 it is believed that the molar mass of these fractions is also possibly an important factor affecting the properties. One can therefore already observe the effect of the external donor on the type of material produced by the various sites. The external donor affects the sites producing chains which elute at low temperatures as well as the sites which produce chains eluting at higher temperatures.

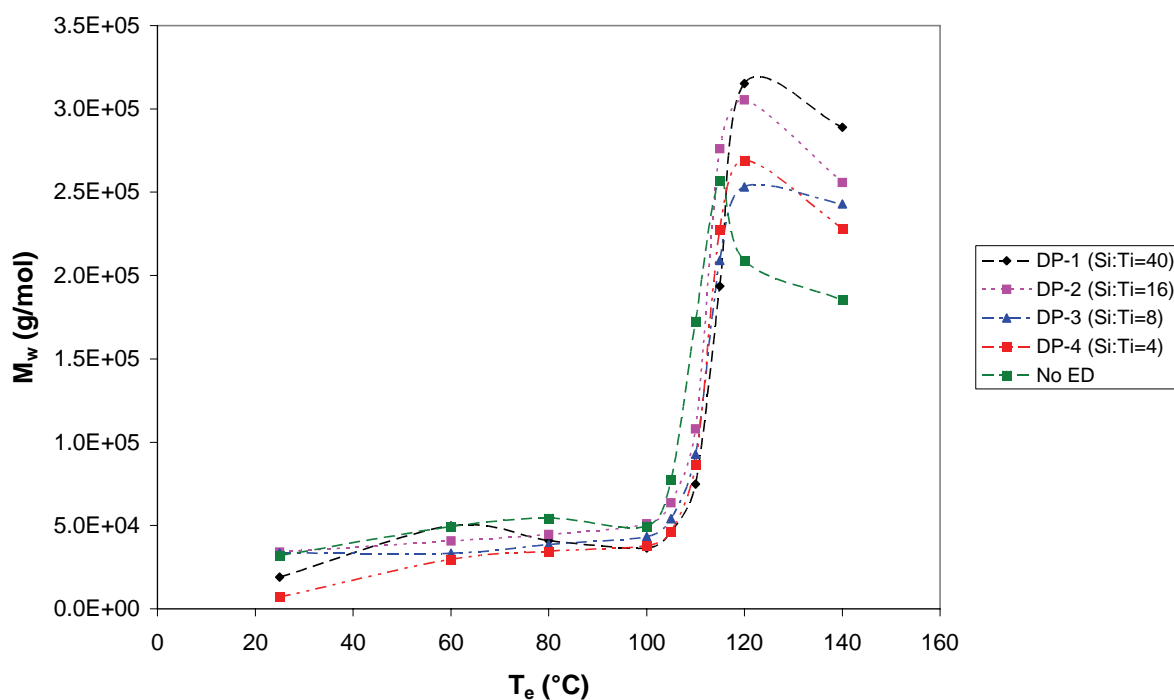


**Figure 6.22** The weight average molar mass averages data for the TREF fractions of the samples produced using DPDMS as well as the sample without external donor.

In terms of the polydispersity of the fractions, the fractions eluting at lower temperatures have a rather broad distribution while those fractions eluting at higher temperatures show a narrower distribution of molar mass. The minimum of the polydispersity is observed for the 105 °C fraction for all samples in the series. It is also observed that over the region of the greatest increase in molar mass, namely the 105 -115 °C fractions there is a slight broadening of the molar mass distribution, after which the polydispersity remains relatively constant. A sharp decrease in molar mass is also observed between the 80 °C fraction and the 100 °C fraction for all external donor/catalyst ratios. The same significant drop in polydispersity occurs between the 60 and 80 °C fractions for the No ED sample. The molar mass of the 80 °C and 100 °C fractions does not differ significantly therefore it would appear as if the 100 °C fraction is the first fraction where a certain type of active sites chains are no longer eluted and that either the number of sites contributing to the fractions decreases or that the nature of the sites changes in terms of molar mass distribution of the polymer produced.

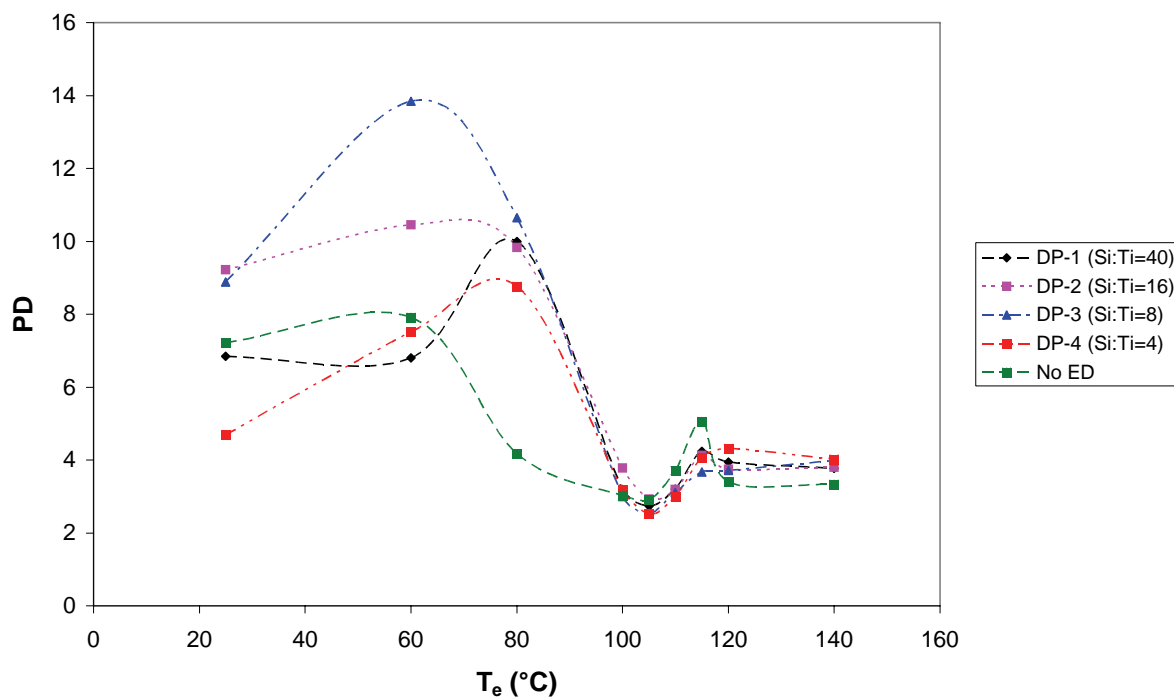


**Figure 6.23** The polydispersity values for the TREF fractions of the samples produced using DPDMS as well as the sample without external donor.

The molar mass data for the samples produced with MPDMS (Figure 6.24) show a very similar trend to those discussed previously for the sample produced with DPDMS. The molar mass remains relatively constant for the lower temperature fractions while after the 100 °C fraction there is a sharp increase in molar mass of the fractions. Once again the molar masses of the lower temperature fractions of the samples produced using an external donor are relatively low compared to the molar mass of the fractions of the No ED sample, with the No ED sample's fractions at 60, 80, 100, 105, and 110 °C having the highest molar mass relative to the MPDMS samples' fractions. Once again the external donor clearly affects the fractions eluting at lower temperatures as well as those eluting at higher temperatures. The highest molar mass in the higher temperature fractions belongs to the MP-1 sample with the highest external donor/catalyst ratio. This is consistent with the overall molar mass of the samples in that overall the MP-1 sample has significantly higher molar mass than the other samples in the series. The familiar drop in weight average molar mass for the final two fractions is observed.

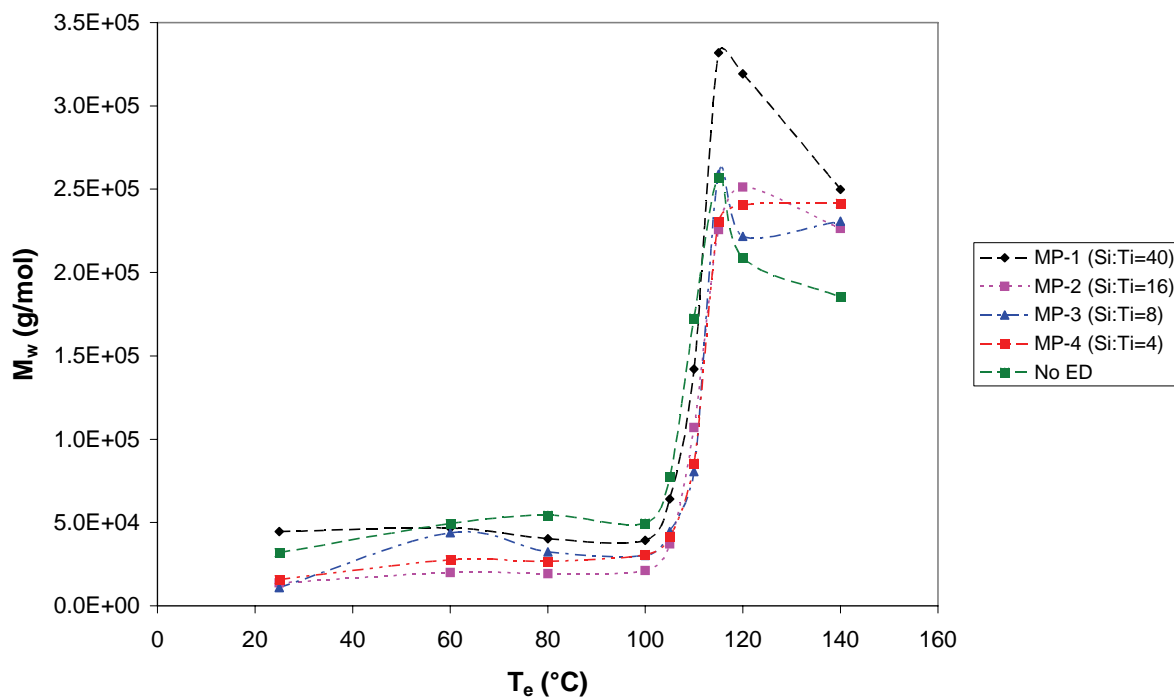


Figure 6.24 The weight average molar mass averages data for the TREF fractions of the samples produced using MPDMS as well as the sample without external donor.

Figure 6.25 illustrates the polydispersity of the TREF fractions for the samples produced using MPDMS.

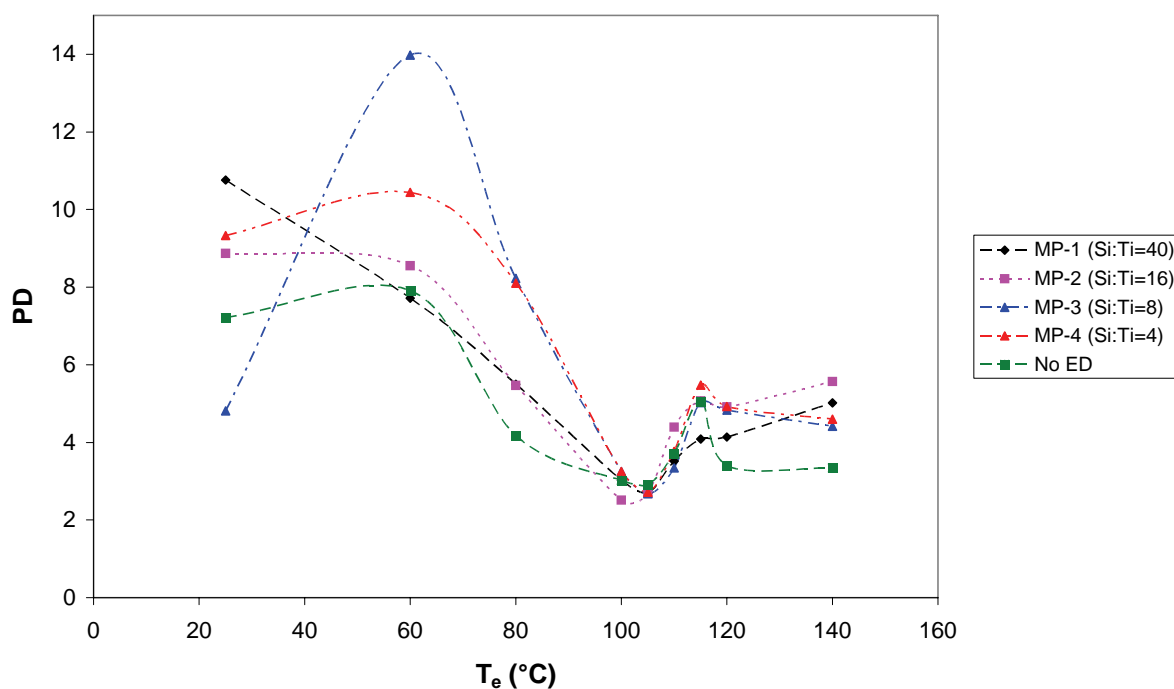
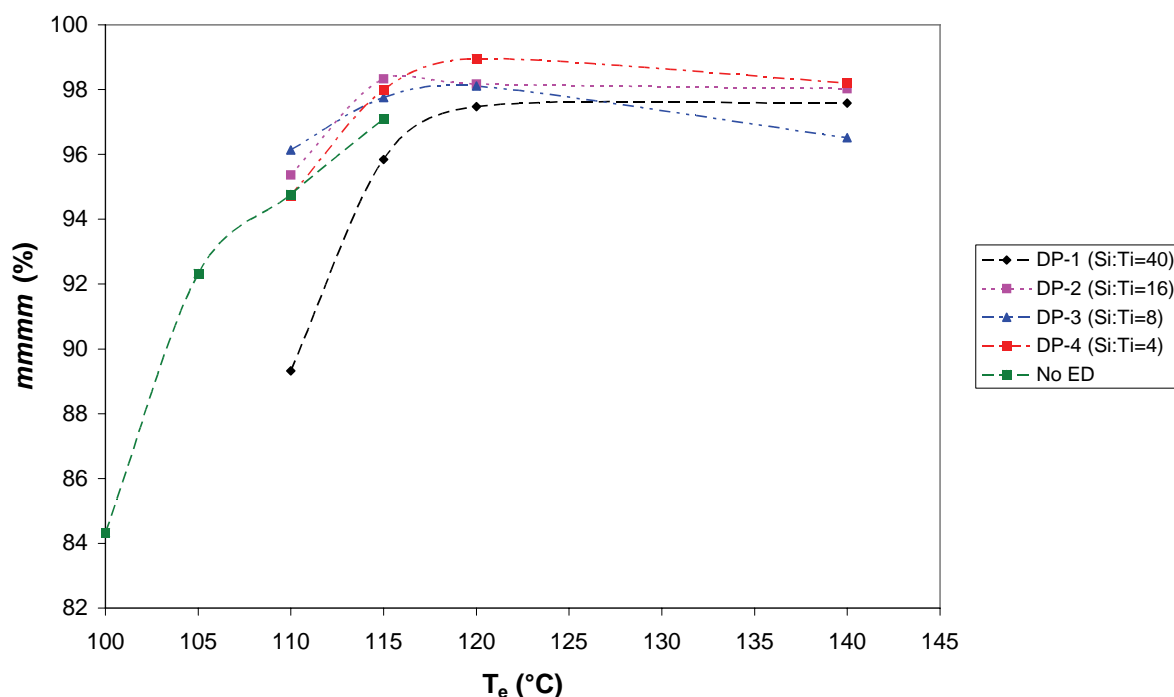


Figure 6.25 The polydispersity values for the TREF fractions of the samples produced using MPDMS as well as the sample without external donor.

Similarly to the case with the DPDMS samples there is a minimum in the polydispersity of the fractions which also occurs at the 105 °C fraction. A similar slight broadening of the distribution is also observed for the fractions showing the sharp increase in molar mass, namely the 105, 110, and 115 °C fractions. There is also a similar decrease in the polydispersity of the fractions as one increases the elution temperature from 60 °C and 80 °C to 100 °C. This is further evidence that specific types of sites are no longer contributing to the composition of the fractions eluting at 100 °C and higher.

The *mmmm* pentad sequence content of selected fractions of the samples produced with DPDMS as well as the No ED sample are given in Figure 6.26. The major fractions of the No ED sample elute at slightly lower temperatures hence slightly lower temperature fractions were analysed by <sup>13</sup>C NMR. It is interesting to note that highly isotactic material is produced even in the absence of an external electron donor, with the 115 °C fraction of the No ED sample containing material with a *mmmm* pentad content of 97%.



**Figure 6.26** The percentage of *mmmm* sequences for selected TREF fractions of the samples produced using DPDMS as well as the sample without external donor.

It is also interesting to note that the fractions of the sample with the highest external donor/catalyst ratio contain chains which on average are slightly less stereoregular than the same fractions of samples produced at lower external donor/catalyst ratios. It is also observed



that the addition of a small amount of external donor (sample DP-4) appears to result in the highest stereoregularity of the highest temperature fractions. This is possibly the reason why the sample has the highest onset of crystallisation temperature as observed for the DSC data. In general one can say that the higher the TREF fractionation temperature the higher the *mmmm* pentad sequence content up to a limiting value for each sample.

The *mmmm* pentad sequence content for selected fractions of the samples produced using MPDMS are given in Figure 6.27. In general the same trends are observed in that the higher TREF fractions contain chains with a higher *mmmm* pentad content as expected since TREF fractionates polymers on their ability to crystallise [28] and a higher *mmmm* pentad content enables easier crystallisation although the molar mass plays a significant role as shall be discussed shortly.

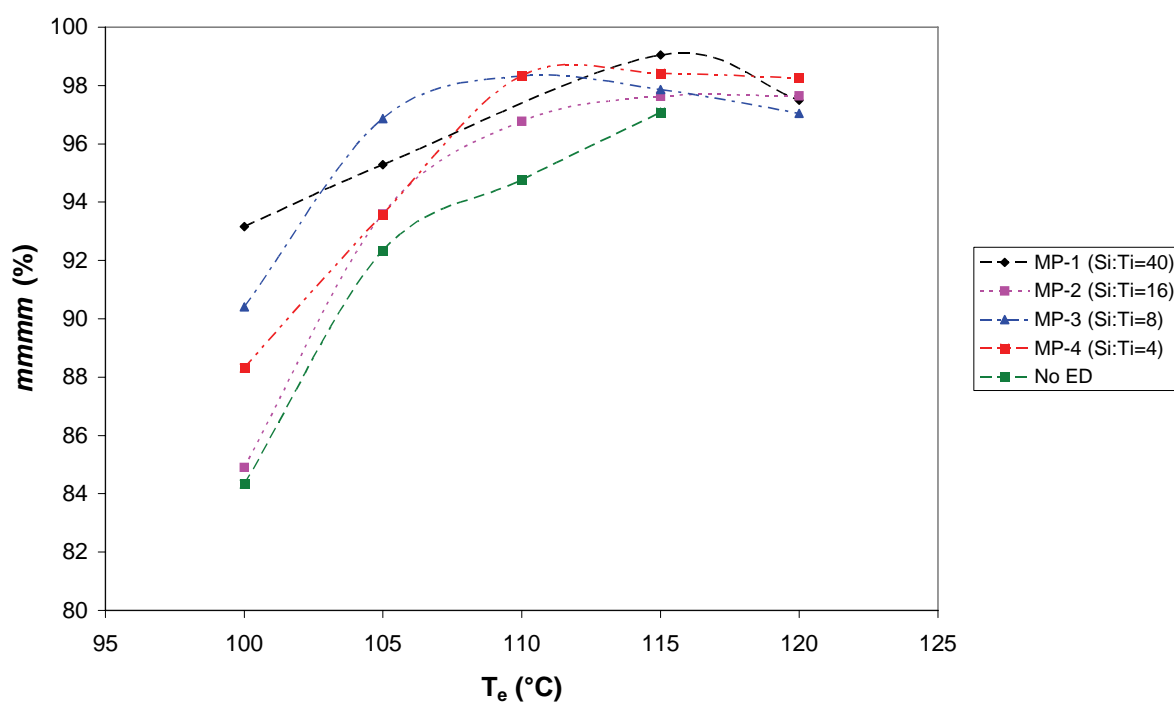


**Figure 6.27** The percentage of *mmmm* sequences for selected TREF fractions of the samples produced using MPDMS as well as the sample without external donor.

Compared to the DPDMS samples the elution temperatures of the major fractions are slightly lower for the samples produced using MPDMS. It is observed that the fractions produced using MPDMS contain chains with an *mmmm* pentad content equal to the fractions of the samples produced using DPDMS at least for the highest temperature fractions analysed. The range of fractions analysed for the MPDMS samples is slightly broader hence the lower values observed for the lower elution temperatures analysed. Once again the addition of a

small amount of external donor (MP-4) produces chains which elute in the highest temperature fractions and contain very high *mmmm* pentad contents, indicating that this is possibly the reason why the sample crystallises at the highest temperatures during DSC analysis. The lower *mmmm* pentad content values for the highest external donor/catalyst ratio (MP-1) are not observed for the MPDMS sample and the values for this sample are generally very high, as opposed to the case for sample DP-1. It is also observed that the lower temperature fractions are affected more by the increase in the external donor/catalyst ratio (at least for the MPDMS samples) than the higher temperature fractions, indicating that the external donor plays a more significant role in increasing the stereospecificity of these sites. This would appear to be evidence of the role of the external donor in converting poorly isospecific sites into more highly isospecific sites, so that the active sites are in a stable state with a donor coordinated in the vicinity of the sites for a longer time. With regards to the separation mechanism of TREF there is a clear contribution of molar mass to the mechanism. As an example an examination of the *mmmm* pentad content of the 110 and 115 °C fractions of sample MP-4 reveal no significant difference in the stereoregularity of the chains. However, the molar mass of the fractions increases from, approximately, 85 kg/mol to 230 kg/mol. The higher molar mass chains elute in the higher temperature fraction thus proving that the molar mass plays a significant role in the fractionation mechanism of TREF.

#### **6.3.4.2 Thermal properties of TREF fractions**

An investigation of the thermal properties of the TREF fractions for the samples produced using DPDMS reveal that the fractions of all the samples containing external donor, irrespective of external donor/catalyst ratio, melt at significantly higher temperatures than the fractions of the No ED sample.

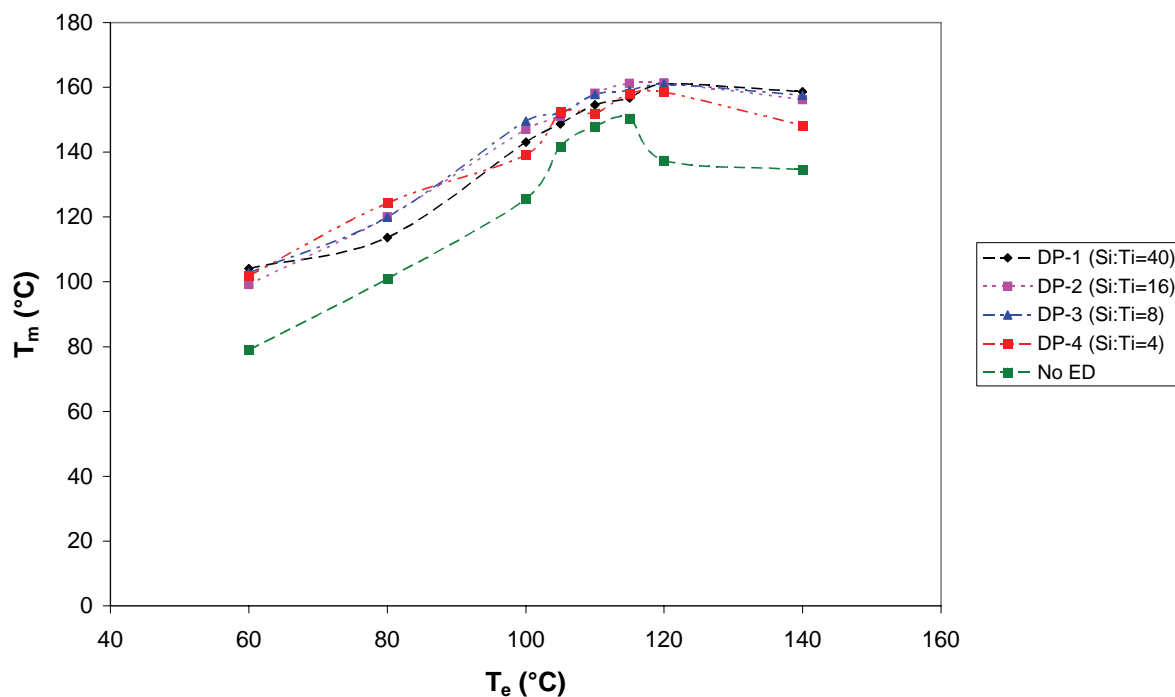


**Figure 6.28** The peak melting temperatures for the TREF fractions of the samples produced using DPDMS as well as the sample without external donor.

There is a general increase in melting temperature as the fractionation temperature increases for all samples as expected and also a slight decrease in melting points for the highest temperature fractions. This is in agreement with known trends for TREF fractions and thus the influence of the increased tacticity, higher molar mass and narrower molar mass distribution on the formation of thicker lamellae is evident.

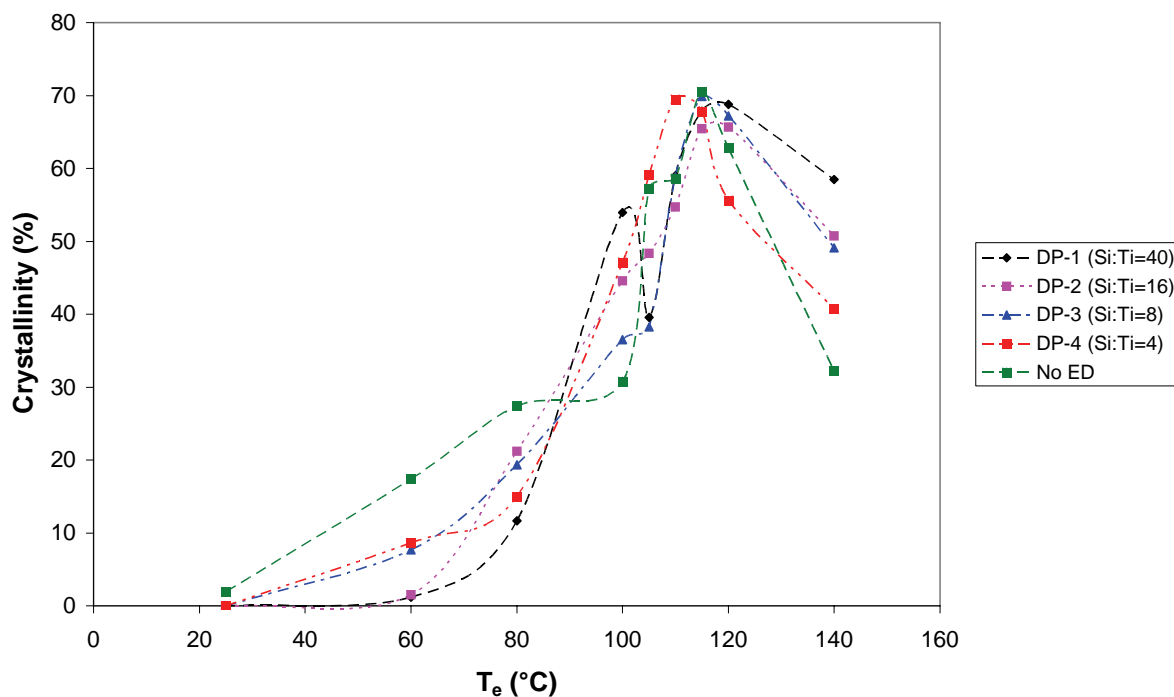


**Figure 6.29** The percentage crystallinity for the TREF fractions of the samples produced using DPDMS as well as the sample without external donor.

With regards to the crystallinity of the fractions (Figure 6.29), the fractions eluting at lower temperatures possess a lower degree of crystallinity than those fractions eluting at higher temperatures as expected due to the influence of the low stereoregularity and molar mass on the crystallisability of the chains present in those fractions. It is also interesting that the lower temperature fractions of the No ED sample are significantly more crystalline than the same fractions of the samples produced with an external electron donor present in the system. The fractions of the No ED sample eluting at high temperatures such as 105, 110, and 115 °C also possess high crystallinity, as high if not higher than the same fractions of the DPDMS samples. The No ED fractions in question also have relatively high molar mass and narrow molar mass distribution compared to the samples produced with DPDMS and it seems to be a combination of these factors which results in the high degree of crystallinity of the samples. Another possibility, however, is the presence of significantly more, shorter, isotactic sequences in these fractions of the No ED sample.

The peak melting temperatures of the fractions of the samples produced using MPDMS are given in Figure 6.30. Unlike the case for the DPDMS samples, all fractions of all samples produced using MPDMS as external donor, have similar peak melting temperatures to those of the No ED sample. The samples would appear to be more uniform.

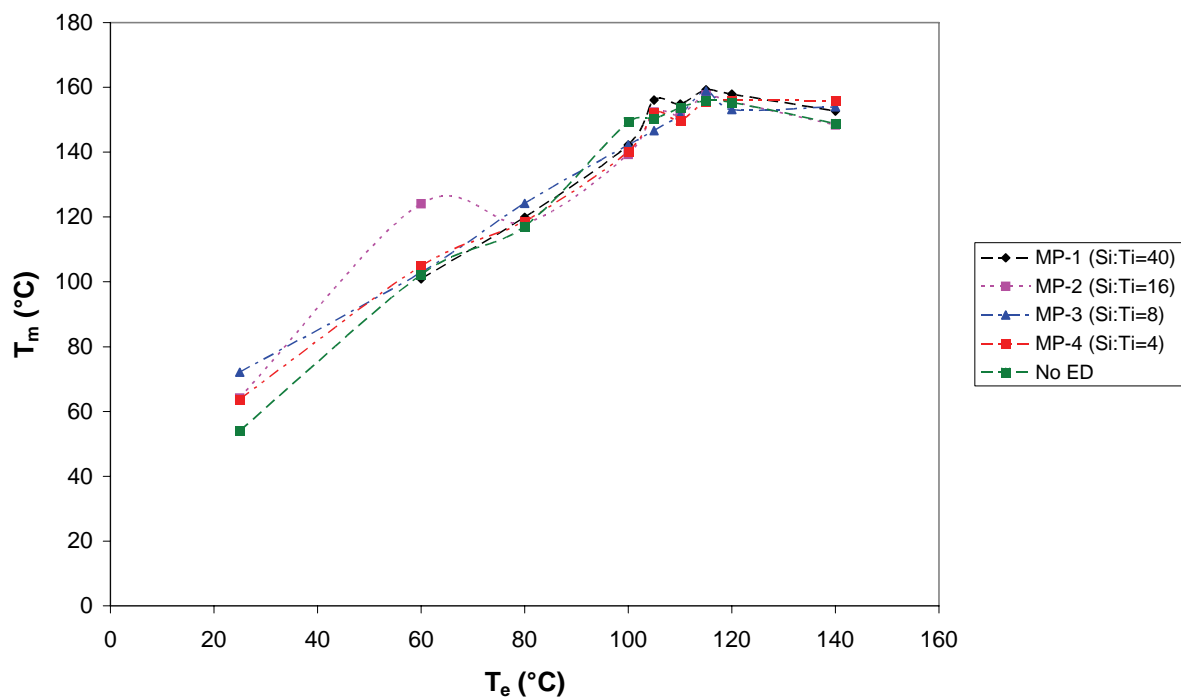


Figure 6.30 The peak melting temperatures for the TREF fractions of the samples produced using MPDMS as well as the sample without external donor.

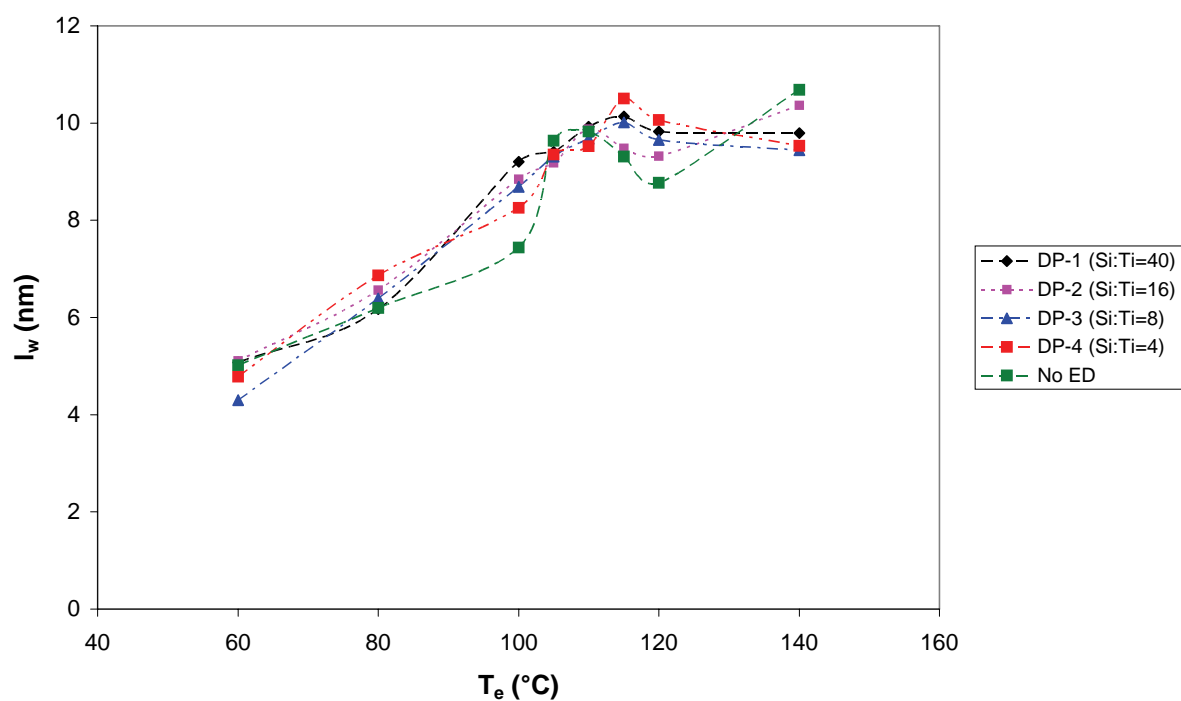
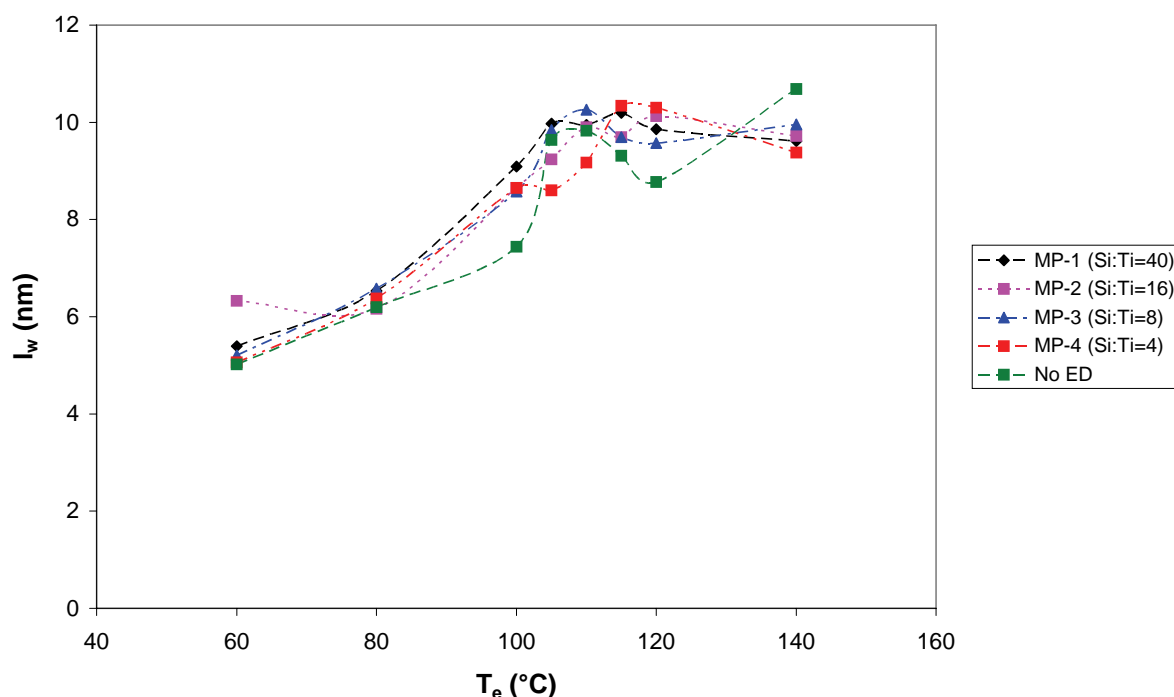


Figure 6.31 The weight average lamellar thickness of the fractions of the samples produced using DPDMS as well as those of the sample produced without external donor.

This would seem to indicate that MPDMS as external donor does not influence the ability of the chains to crystallise into lamellae of increasing thickness as much as DPDMS as external donor. Lamellar thickness calculations, however, do not reveal any major differences in the thickness of the lamellae in the different fractions irrespective of the donor type. The weight average lamellar thickness of the fractions for the DPDMS samples and MPDMS samples are given in Figures 6.31 and 6.32 respectively.



**Figure 6.32** The weight average lamellar thickness of the fractions of the samples produced using MPDMS as well as those of the sample produced without external donor.

A look at the degree of crystallinity of all of the fractions of the samples produced using MPDMS (Figure 6.33) reveal that, as was the case for the samples produced using DPDMS, the high temperature fractions of the No ED samples are as crystalline as the fractions of the samples produced using an external donor. The lower temperature fractions of the No ED sample, such as those at 60 °C and 80 °C, are not much more crystalline than some of the fractions of the samples produced with an external donor. This is in contrast to the degree of crystallinity of the same fractions produced using DPDMS as external donor, where the No ED samples' fractions are considerably more crystalline for these two fractionation temperatures. Examination of the 60 °C fraction of the samples produced using DPDMS reveals that external donor/catalyst ratios of 4 and 8 reduces the crystallinity of the fraction to

a certain extent but that increasing the external donor content further to ratios of 16 and 40 decreases the crystallinity still further.

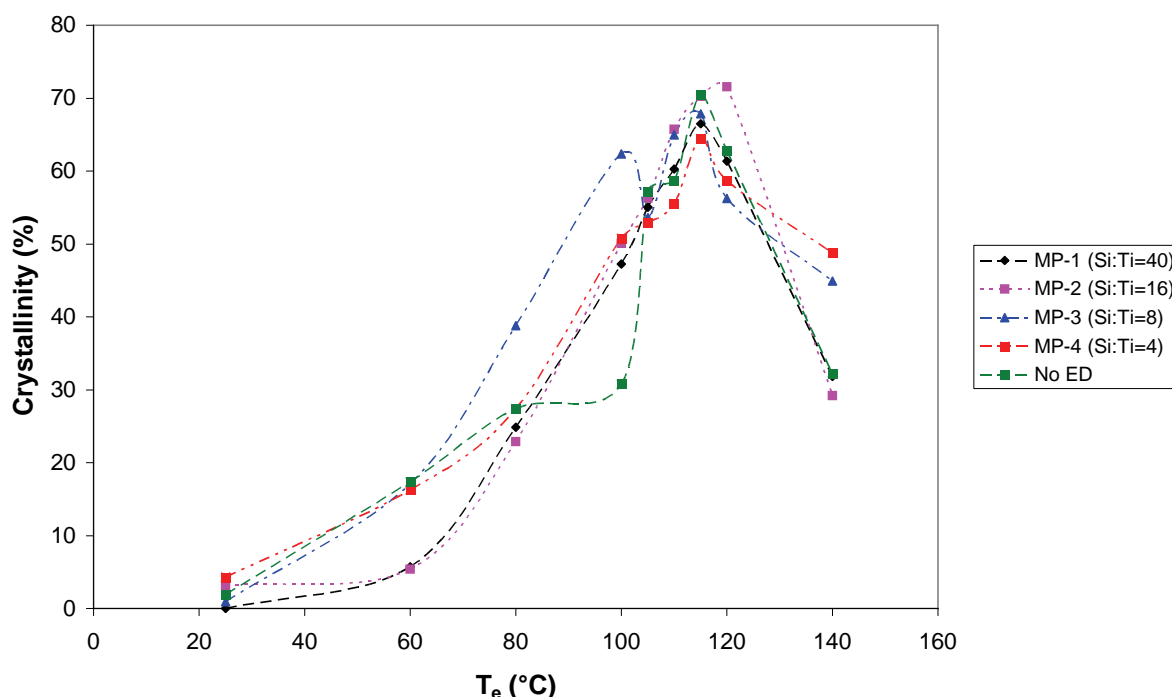


**Figure 6.33** The percentage crystallinity for the TREF fractions of the samples produced using MPDMS as well as the sample without external donor.

Analysis of the same scenario for the samples produced using MPDMS reveal that at an external donor/catalyst ratio of 4 or 8 there is practically no change in the degree of crystallinity of the fractions, but that at a ratio of 16 and 40 there is also a considerable reduction in crystallinity of the fractions. It would appear that to bring about the same effect on these fractions with the MPDMS donor one requires more of the donor in the system as compared to a bulkier donor such as DPDMS. The effect of the donor on these fractions is important since it is the conversion of aspecific or poorly isospecific sites to highly isospecific sites and/or the deactivation of the sites which is in question, and this is an extremely important requirement for an external donor since the conversion of the active sites has a significant effect on the physical properties.

The effect of the donor on the poorly isospecific active sites is illustrated in Figure 6.34 by examining the crystallisation of the 60 °C fractions of the No ED sample and the samples produced using DPDMS. It is evident that addition of a small amount of external donor (DP-4) increases the crystallisation temperature of the chains dramatically although the magnitude of the crystallisation peak decreases. This indicates that although less material is

crystallising out at this point, the chains which are crystallising are slightly more perfect than they were in the absence of external donor. There is definitely a molar mass effect involved since the molar mass of this particular fraction of the No ED sample is the highest and the crystallisation temperature is the lowest. Sample DP-4 has the lowest molar mass for this particular fraction and the highest crystallisation temperature. The molar mass of the fractions then increases in the order DP-3, DP-2 and finally DP-1 which has a molar mass approximately the same as the No ED sample. The crystallisation temperature of the 60 °C fraction clearly decreases with increasing molar mass as would be expected for the faster crystallisation of lower molar mass chains in the solid state. It is evident that alteration of the molar mass of a certain fraction plays an important role in determining the crystallisation of that fraction. The differences in crystallisation temperature for the same temperature TREF fractions is observed since the temperature range of the fraction is large 26 – 60 °C and therefore the chains crystallise out over the range of temperatures.

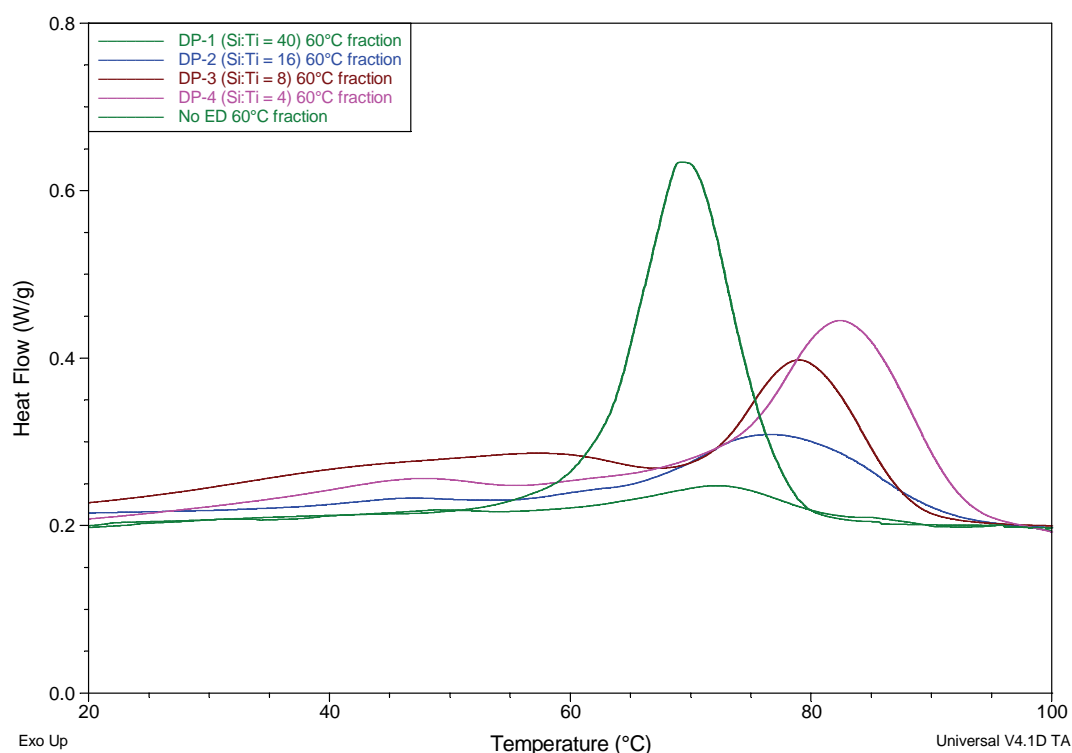


**Figure 6.34 The DSC crystallisation exotherms of the 60 °C TREF fractions of the samples produced using DPDMS and the No ED sample.**

Increasing the amount of external donor therefore simply reduces the degree of crystallisation as well as the peak crystallisation temperature indicating that there is less material crystallising out and at lower temperatures due to the high external donor loadings deactivating the sites producing this material.



### 6.3.5 Molar mass distribution deconvolution

The deconvolution of the molar mass data of all the samples was performed and an example of the results obtained is given in Figure 6.35 for the DP-1 sample. Overall, a good fit of the experimental data was obtained when using 6 sites to describe the molar mass distribution. Deconvolution into 6 sites proved to be the optimum solution for all samples analysed. Irrespective of sample type, slightly correlated residuals (the difference in the sum of the squares) were observed at low molar mass although this was also observed by Soares and Hamielec [18] and ascribed to higher chromatogram noise levels and increased variance of observation or peak broadening in the GPC analysis.

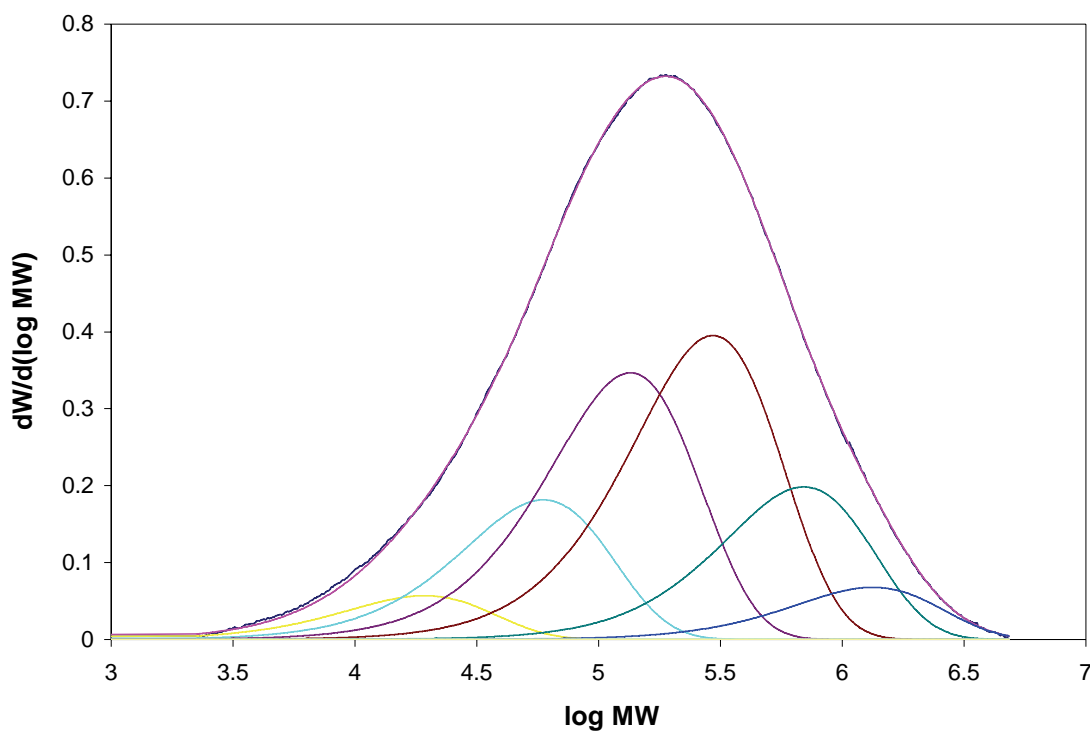


**Figure 6.35** The deconvolution of the molar mass distribution of sample DP-1 into Flory distributions.

Each deconvoluted active site type has a characteristic molar mass ( $M_n$  and  $M_w$ ) and produces chains which constitute a certain mass fraction ( $m$ ) of the polymer as a whole.

**Table 6.4 The results for the deconvolution of all samples**

Sample Code	Si:Ti		Flory distribution number					
			1	2	3	4	5	6
DP-1	40	m	0.05	0.15	0.28	0.32	0.16	0.05
		M <sub>n</sub> (g/mol)	9.6E+03	3.0E+04	6.8E+04	1.5E+05	3.5E+05	6.7E+05
		M <sub>w</sub> (g/mol)	1.9E+04	5.9E+04	1.4E+05	2.9E+05	7.0E+05	1.3E+06
DP-2	16	m	0.05	0.15	0.31	0.29	0.14	0.06
		M <sub>n</sub> (g/mol)	8.7E+03	2.7E+04	6.5E+04	1.4E+05	3.0E+05	6.2E+05
		M <sub>w</sub> (g/mol)	1.7E+04	5.5E+04	1.3E+05	2.9E+05	6.1E+05	1.2E+06
DP-3	8	m	0.05	0.16	0.31	0.29	0.14	0.05
		M <sub>n</sub> (g/mol)	7.2E+03	2.4E+04	5.5E+04	1.2E+05	2.7E+05	5.8E+05
		M <sub>w</sub> (g/mol)	1.4E+04	4.8E+04	1.1E+05	2.4E+05	5.5E+05	1.2E+06
DP-4	4	m	0.03	0.08	0.24	0.33	0.22	0.09
		M <sub>n</sub> (g/mol)	4.4E+03	1.1E+04	3.1E+04	7.3E+04	1.7E+05	4.7E+05
		M <sub>w</sub> (g/mol)	8.8E+03	2.3E+04	6.1E+04	1.5E+05	3.5E+05	9.3E+05
No ED	0	m	0.05	0.12	0.28	0.31	0.18	0.06
		M <sub>n</sub> (g/mol)	2.6E+03	8.4E+03	2.5E+04	6.1E+04	1.5E+05	4.4E+05
		M <sub>w</sub> (g/mol)	5.2E+03	1.7E+04	5.1E+04	1.2E+05	3.1E+05	8.8E+05
MP-1	40	m	0.06	0.14	0.29	0.28	0.17	0.06
		M <sub>n</sub> (g/mol)	6.0E+03	2.0E+04	4.8E+04	1.1E+05	2.7E+05	6.6E+05
		M <sub>w</sub> (g/mol)	1.2E+04	3.9E+04	9.6E+04	2.3E+05	5.4E+05	1.3E+06
MP-2	16	m	0.05	0.12	0.25	0.29	0.20	0.09
		M <sub>n</sub> (g/mol)	2.7E+03	8.4E+03	2.5E+04	6.3E+04	1.6E+05	4.5E+05
		M <sub>w</sub> (g/mol)	5.4E+03	1.7E+04	5.0E+04	1.3E+05	3.2E+05	8.9E+05
MP-3	8	m	0.06	0.13	0.26	0.29	0.19	0.07
		M <sub>n</sub> (g/mol)	3.0E+03	8.8E+03	2.5E+04	6.5E+04	1.7E+05	4.7E+05
		M <sub>w</sub> (g/mol)	6.0E+03	1.8E+04	5.0E+04	1.3E+05	3.4E+05	9.4E+05
MP-4	4	m	0.06	0.13	0.25	0.28	0.20	0.08
		M <sub>n</sub> (g/mol)	2.9E+03	8.9E+03	2.5E+04	6.2E+04	1.6E+05	4.4E+05
		M <sub>w</sub> (g/mol)	5.9E+03	1.8E+04	5.0E+04	1.2E+05	3.2E+05	8.8E+05

The data for the deconvolution of all the samples is given in Table 6.4. An examination of the mass fractions of each active site for the samples produced using DPDMS is given in Figure 6.36. There are definitely some interesting differences in the amount of material being produced at each active site. The addition of a small amount of external donor (DP-4) noticeably changes the amount of material produced at the active sites compared to the sample prepared without external donor. There is a lot less material being produced at sites 1, 2, and 3 while at the same time there is more material being produced at sites 4, 5, and 6 for the DP-4 sample.

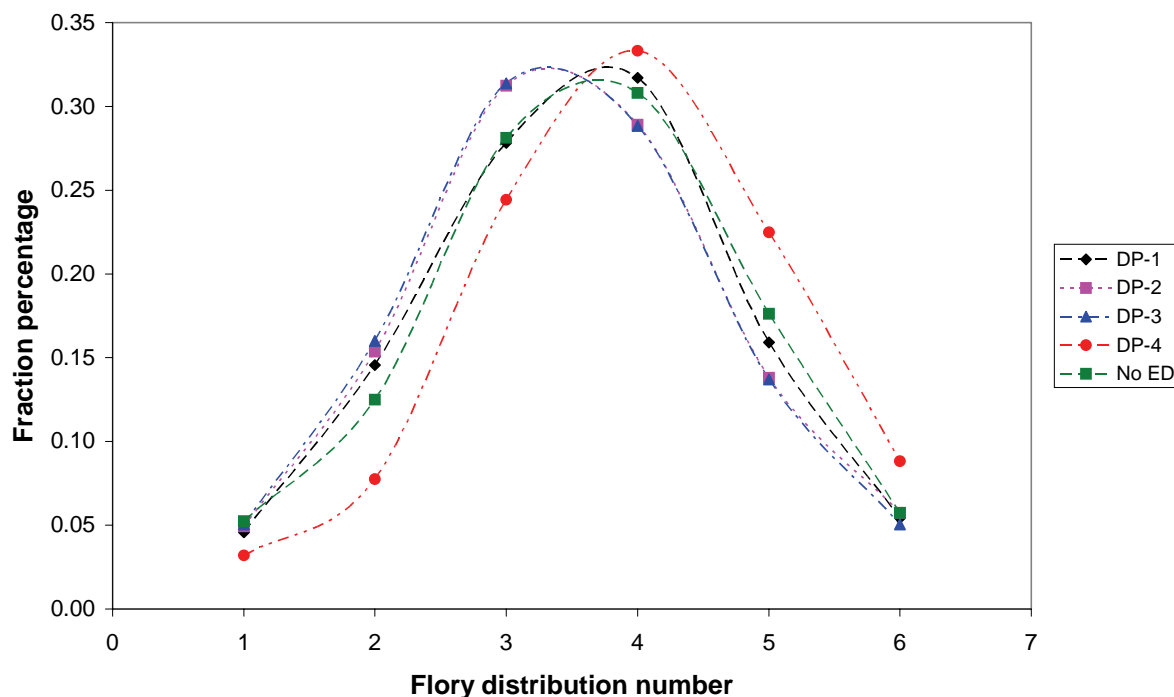


**Figure 6.36** The mass fraction of the various active sites for the deconvolution of the molar mass distribution of the samples produced using DPDMS as well as the No ED sample.

The molar mass produced at each active site is given in Figure 6.37 for the samples produced using DPDMS. It is immediately apparent that the molar mass of the material produced at each of the active sites increases as the external donor/catalyst ratio increases with the largest increases in molar mass to be found in the sites producing higher molar mass chains. This would be expected if the external donors coordinate in the vicinity of the active sites and convert aspecific sites to isospecific sites, thereby exerting more influence on the more stereospecific sites whose  $k_p$  increases in conjunction with the increase in stereospecificity.

Examination of Figures 6.36 and 6.37 reveal that addition of a small amount of DPDMS to the system does not significantly alter the molar mass of the material produced at each site but rather the proportion of sites producing higher molar mass material increases. Further increase in the external donor/catalyst ratio to 8 or 16 produces very similar results, in that the proportion of active sites producing high molar mass material decreases and the proportion of sites producing lower molar mass increases, while at the same time the molar mass of the chains produced at all the sites increases significantly. Increasing the external donor/catalyst ratio still further to 40, brings about a combined increase in the proportion of active sites producing high molar mass material (although not to the same extent as a ratio of

4), as well as an increase in the molar mass of the chains produced at those sites producing high molar mass chains.

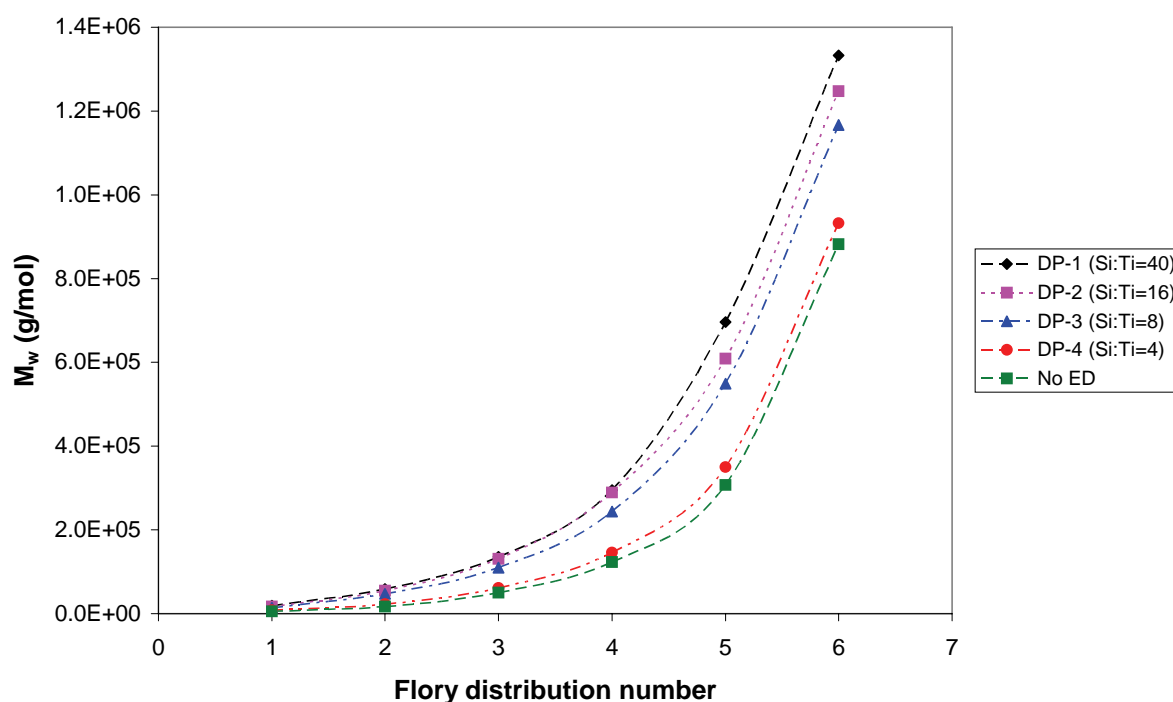


**Figure 6.37** The variation in molar mass of the individual Flory distributions at different Si:Ti for the samples produced using DPDMS.

It would seem as if the addition of a small amount of external donor is mainly responsible for converting a number of aspecific sites into isospecific sites with a higher  $k_p$  as evidenced by the fact that the proportion of active sites producing higher molar mass chains increases significantly. Increasing the external donor/catalyst level to 8 or 16 increases the molar mass significantly for all active sites implying an increase in  $k_p$  at all the sites and a decrease in transfer reactions. This indicates that the higher external donor/catalyst ratios result in the deactivation of more sites but that the remaining sites produce higher molar mass chains. The highest external donor loading studied (DP-1) exerts an influence not only on the molar mass of the chains produced at each site but also the proportion of sites producing higher molar mass relative to the ratios of 8 and 16.

The results for the samples produced using MPDMS are a little different as illustrated in Figure 6.38. Increasing the external donor/catalyst ratio to 4, 8, and 16 increases the proportion of active sites producing high molar mass material slightly while the ratio of 40 reduces that same proportion of sites.

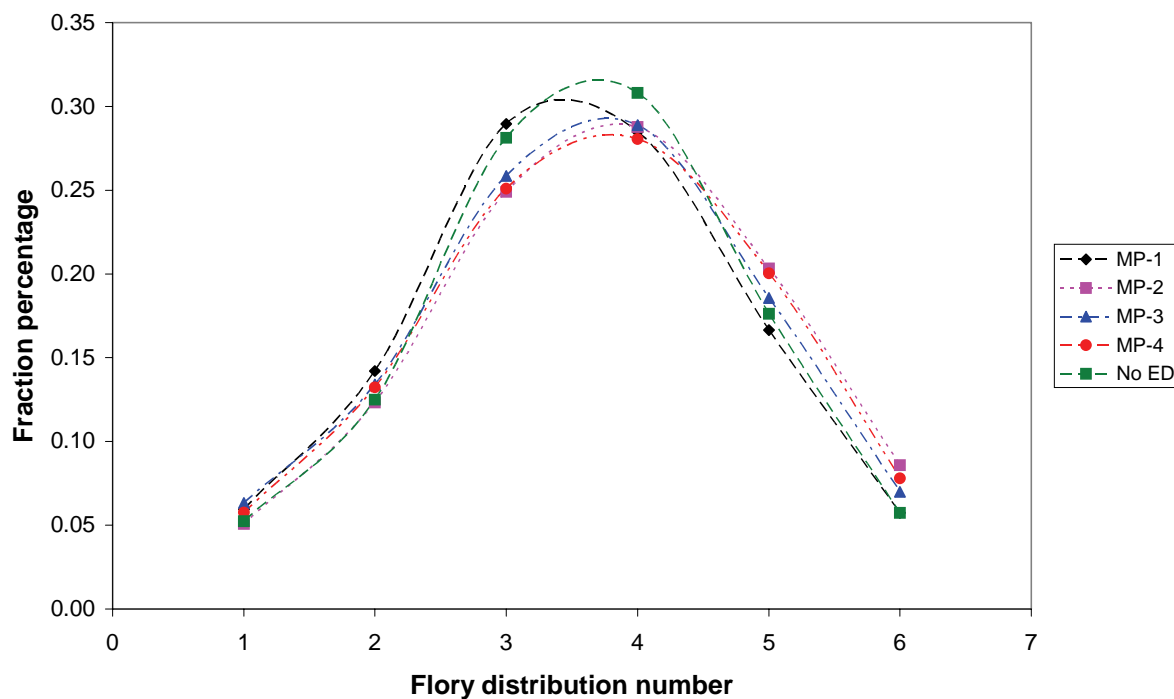


**Figure 6.38** The mass fraction of the various active sites for the deconvolution of the molar mass distribution of the samples produced using MPDMS as well as the No ED sample.

A look at the molar mass of the chains produced at each of the site type (Figure 6.39) also tells a different story to that of the samples produced using DPDMS. The molar mass of the chains produced at all site types remains relatively constant for all the external donor/catalyst ratios with the exception of the ratio of 40 where a sharp increase is observed. Relating this data to the overall molar mass of the samples, it seems as if the slight increases in molar mass for the lower external donor/catalyst ratios are due to a slight increase in the proportion of sites producing higher molar mass material while the highest external donor/catalyst ratios sharp increase in molar mass is due to the increase in the molar mass of the chains produced at all site types.

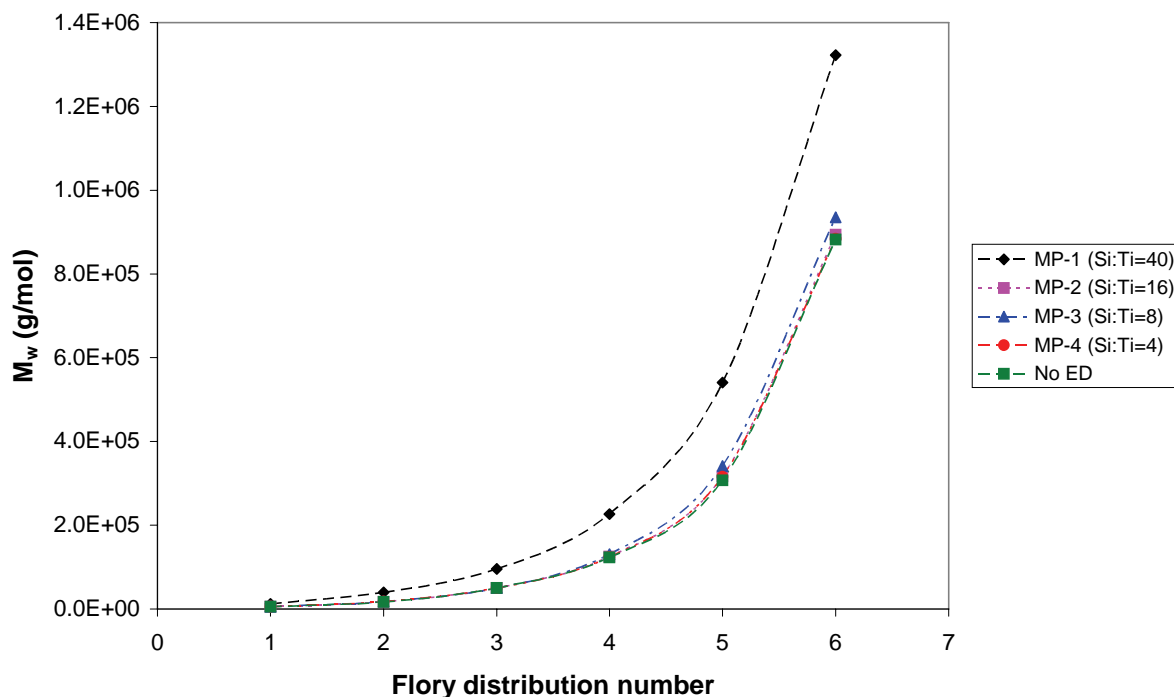


**Figure 6.39** The variation in molar mass of the individual Flory distributions at different Si:Ti for the samples produced using MPDMS.

On the basis of these results it would appear as if the lower external donor/catalyst ratios are mainly responsible for the conversion of aspecific sites to isospecific sites but that the stereoselectivity of the sites are not increased much. The highest ratio of 40 brings about a noticeable increase in the molar mass of the chains and it would seem that at this ratio the external donor exerts more influence on the active sites in general and also the stereoregular sites in particular.

The data for both donor types seem to indicate that in general the conversion of sites from aspecific (site type **C**), or poorly isospecific (site type **B**) to isospecific (site type **A**) is accomplished at low donor loadings and that the deactivation of sites occurs at higher external donor loadings. More of the MPDMS donor seems to be required in order to deactivate certain sites compared to the case of the DPDMS donor where deactivation of sites seems to occur at lower external donor/catalyst ratios. It is also evident that the conversion of active sites to the more stereospecific site (type **A**) is accomplished at an external donor/catalyst ratio of 4 for the DPDMS samples but that at the same ratio for the MPDMS samples there are still sites remaining requiring conversion to the more stereospecific type as evidence by the conversion of sites at the higher ratios of 8 and 16. Figure 6.40 compares the effect of the type of external donor on the proportion of the different active sites and the molar mass of the chains they produce, at the lowest external donor/catalyst ratio investigated (4). It is evident

that using the DPDMS donor causes an increase in the proportion of active sites producing high molar mass polymers and that the molar mass of the polymers produced at those sites is slightly higher than that of the sites in the MPDMS system but not much higher. This confirms that at the same external donor loading the DPDMS is much better at converting sites to those producing high molar mass polymers especially at low external donor/catalyst ratios.

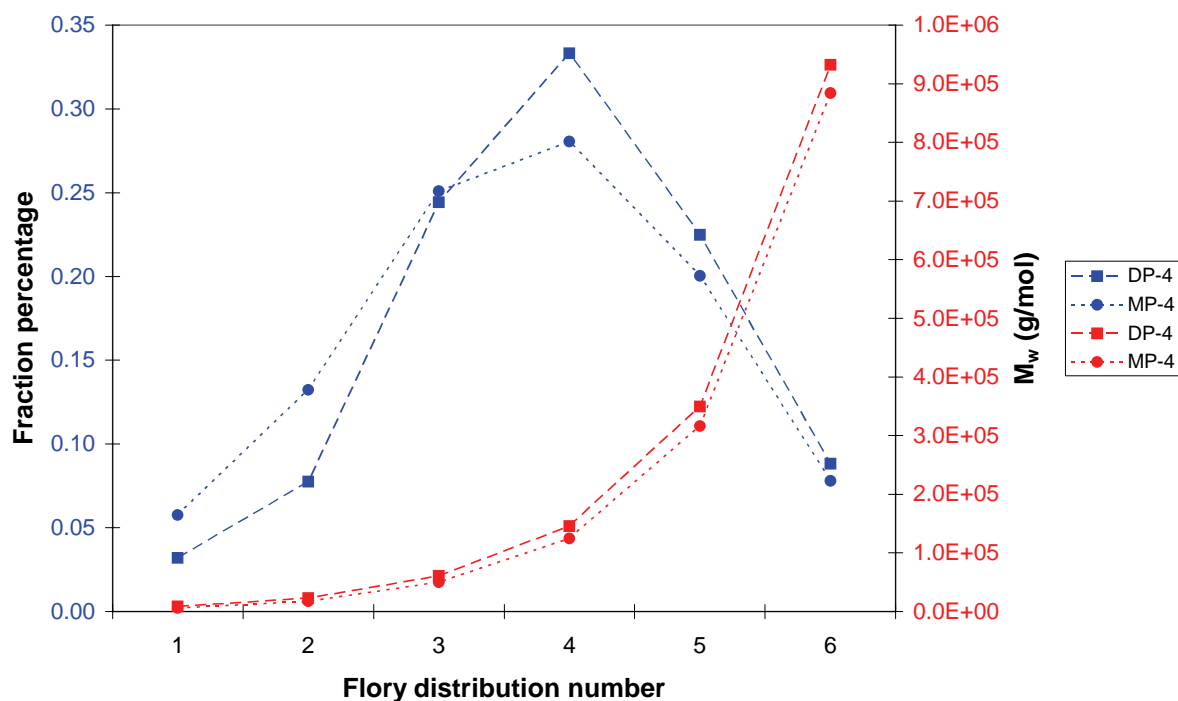


**Figure 6.40** A comparison of the proportion of different active sites and the weight average molar mass of the polymers they produce for the DP-4 and MP-4 samples.

A similar comparison at the highest external donor/catalyst ratio investigated (40) is illustrated in Figure 6.41. It is clear that at the higher external donor/catalyst ratio the proportion of the different types of active sites is very similar for the two different donor types used, unlike the case at the lower external donor/catalyst ratio. The main difference in the overall molar mass of the polymers (DP-1 having a higher molar mass than MP-1), lies in the differences in the molar mass of the polymers produced by active site numbers 3, 4, and 5. It is interesting to note that since the proportion of site types are similar that the higher molar mass of the chains produced using DPDMS lies in the greater ability of the sites (with the DPDMS donor coordinated in the vicinity of the site) to produce higher molar mass polymers. It is believed that the DPDMS therefore exerts a stronger influence on the sites than MPDMS

due to the bulkiness of the two phenyl groups and that the  $k_p$  of the sites is higher with DPDMS coordinated in the vicinity of the sites.

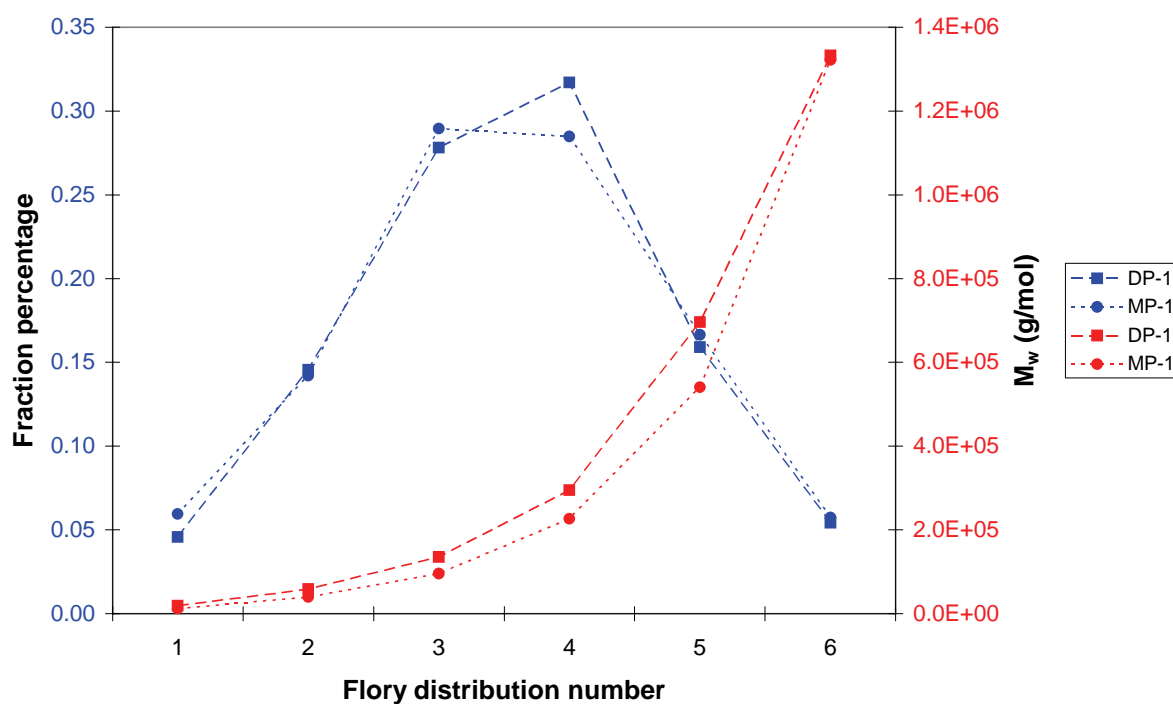


**Figure 6.41** A comparison of the proportion of different active sites and the weight average molar mass of the polymers they produce for the DP-1 and MP-1 samples.

It should also be noted that the same deconvolution procedure was applied to one of the higher temperature TREF fractions (with a narrow polydispersity of 3.5) and it was observed that the optimum solution involved contributions from 4 different active sites all of which would have to be of type **A** according to Busico's model. This means that there are isospecific sites present on the catalyst which produce material covering a wide range of molar masses and that thus there are a few different types of sites which have the ability to produce highly isotactic chains although with varying lengths. These differences could be due to the coordination of different ligands for active site **A** as discussed for the model proposed by Busico. The result would be isospecific sites which are slightly different and thus produce different distributions of chains. It is therefore noted that there are a significant number of different active sites and that the nature of the active sites are constantly changing via the equilibrium reactions present in the system and that so the values presented are average numbers of site types rather than a specific number of absolute active sites. For example, isospecific sites present in the catalyst can be located on different parts of the support and although the sites might have a very similar chemical configuration there are factors such as



the amount of steric hindrance (due to the location of site on the surface not due to the donor) at a site which might influence the material produced at a given site.

### 6.3.6 Mechanical properties

In order to correlate the structure of the polymers with the physical properties all samples were analysed by microhardness and DMA.

#### 6.3.6.1 Microhardness

At first a brief examination was undertaken to investigate the effect of cooling of the sample from the mould in order to determine the effects of sample preparation on the properties of the material. Figure 6.42 illustrates the difference in microhardness for the samples prepared using DPDMS at two different indentation loads and also for two different cooling regimes, namely slow cooling over 5 minutes at ambient conditions and quench cooling.

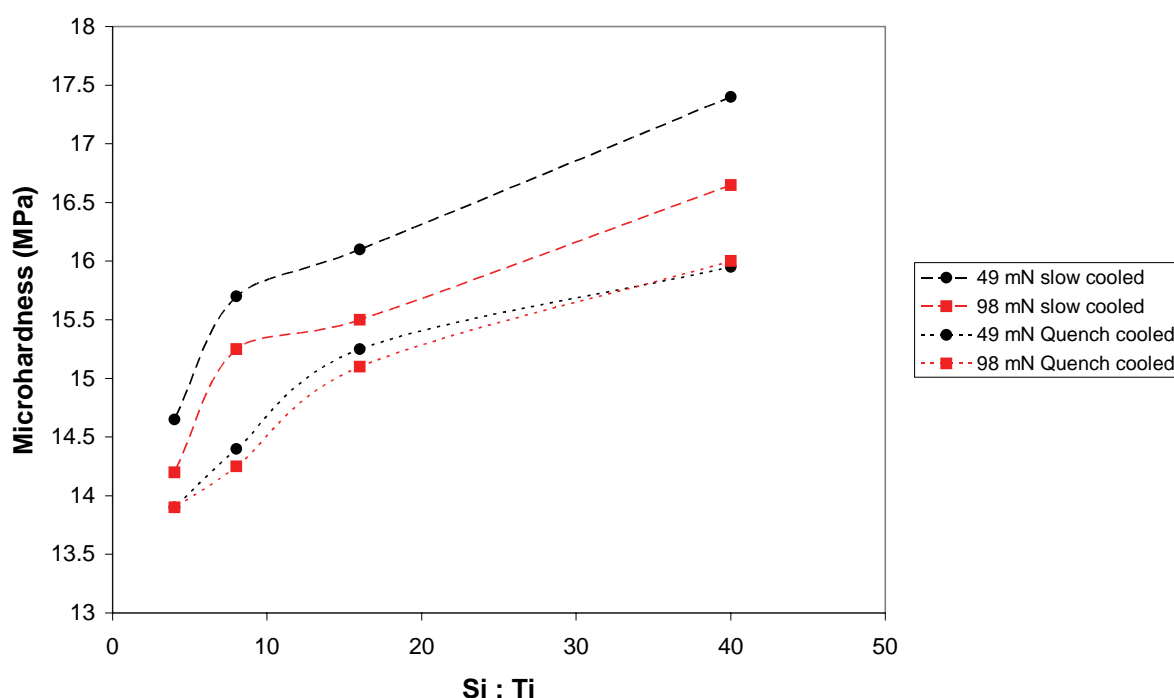
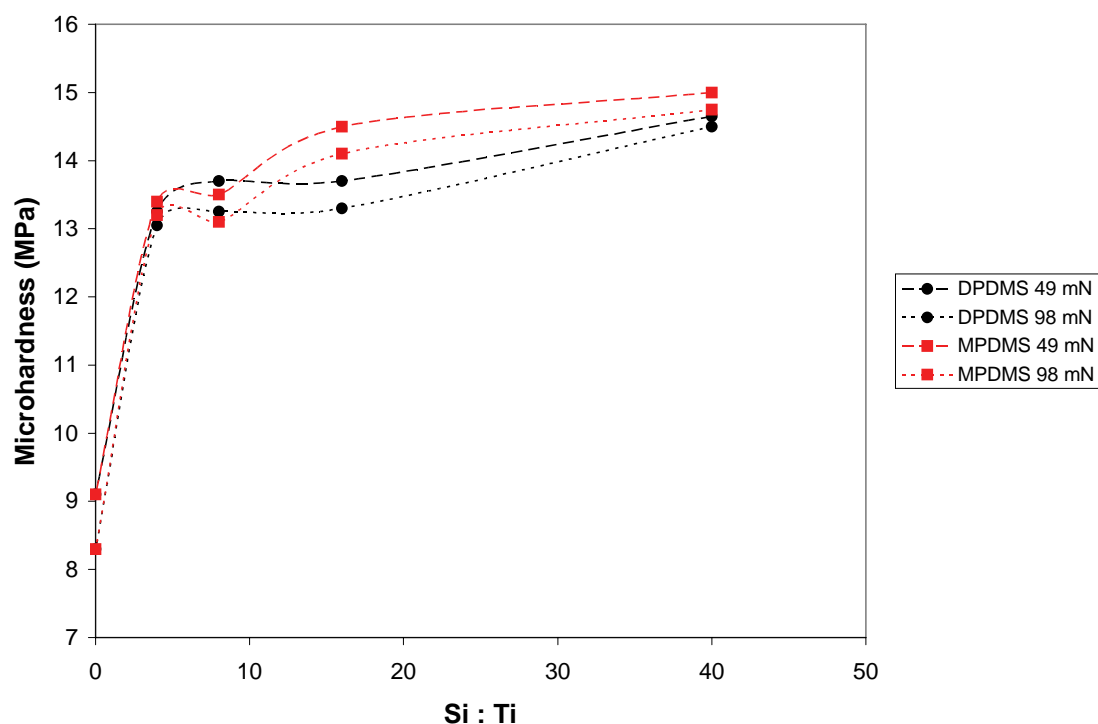


Figure 6.42 The microhardness results for the samples produced using DPDMS at different indentation loads and different cooling regimes illustrating the differences in the microhardness upon cooling.

It is immediately apparent that the slow cooled samples are slightly harder than those which were quench-cooled. This is to be expected since upon slow cooling the chains have more time to order themselves and crystallise out while for the quench cooled samples there is little time and so the crystals are not as perfect as those subjected to the slow cooling. Similar results were obtained by Koch *et al.* [29] who found an increase in microhardness upon annealing after quenching, similarly giving the chains more time to order themselves and form a harder material. It is also noted that there is a general increase in the microhardness of the samples with increasing external donor/catalyst ratio. Flores *et al.* [27] also discovered an increase in microhardness on annealing.

These results were subsequently confirmed in a second batch of experiments (Figure 6.43) in which all samples were subjected to the quench cooling process at two different indentation loads.



**Figure 6.43 A comparison of the microhardness data for the samples produced using DPDMS and MPDMS as well as the No ED sample illustrating the differences between the samples at loads of 49 mN and 98 mN.**

There is a sharp increase in the microhardness of the samples upon addition of the external electron donors to the polymerisation system. Further increase in the external donor/catalyst ratio does bring about a slight increase in the microhardness although the increase is not as dramatic as for the addition of a small amount of donor compared to the No ED sample.

In order to evaluate the effect of the polymer microstructure on the microhardness of the material there are a few key relationships which need investigating. The effect of the molar mass and molar mass distribution on the crystallinity of the samples is investigated and illustrated in Figure 6.44. The three dimensional plots show the projections of data points in three dimensional space on the surface of each plane. The actual data points have been omitted for clarity.

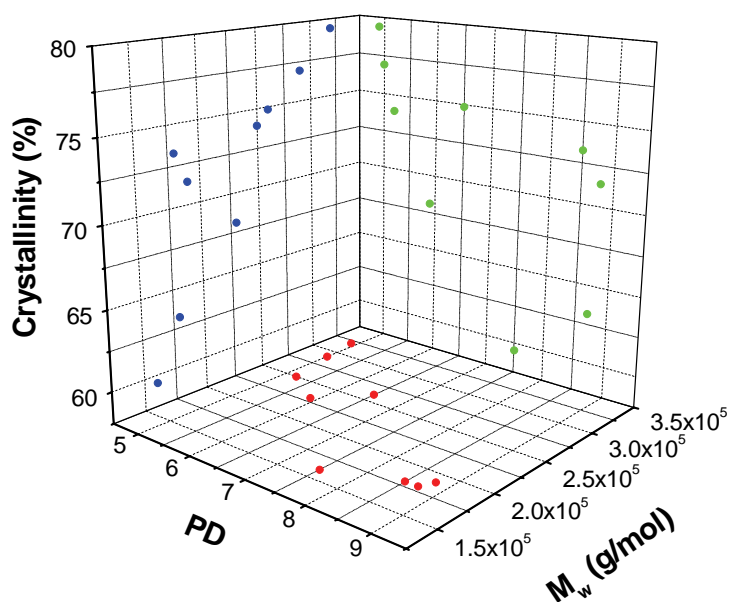


Figure 6.44 The effect of the molar mass and polydispersity on the crystallinity of all the samples.

Generally it can be said that the samples of low molar mass have a broader polydispersity and the higher molar mass samples have a narrower polydispersity indicating a narrower distribution of active sites producing higher molar mass chains.

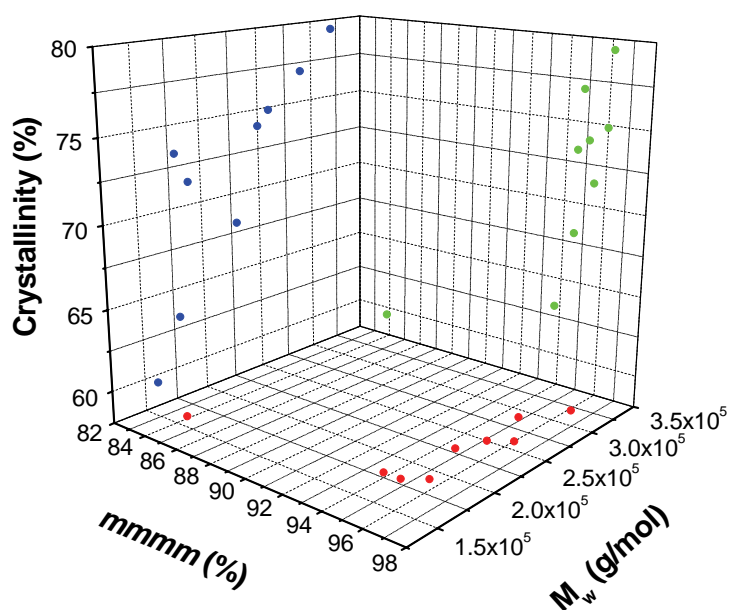


Figure 6.45 The effect of the molar mass and  $mmmm$  pentad content on the crystallinity of the samples.

It would also appear that the polydispersity has an influence on the crystallinity since the samples with a high degree of crystallinity also have low polydispersity values and vice versa, although the effect is not as strong as that of the molar mass. There is definitely a strong molar mass effect on the crystallinity with the samples of higher molar mass clearly enabling crystallisation to a higher degree.

Examination of the combined effect of the molar mass and  $mmmm$  pentad sequence content on the crystallinity of the samples is illustrated in Figure 6.45. There is clearly an increase in crystallinity as the  $mmmm$  pentad content is increased from approximately 84% to 94%. It is evident that there is a variation in the levels of crystallinity for the samples with relatively constant  $mmmm$  pentad content of approximately 94 – 96% which indicates that the effect of the molar mass on the crystallinity is significant. A closer look at the region of higher tacticity illustrated in Figure 6.46 reveals that there is definitely a correlation between the  $mmmm$  pentad content and the degree of crystallinity. The higher  $mmmm$  pentad contents correlate to higher degrees of crystallinity. It is also noteworthy that the higher molar mass chains also have a higher  $mmmm$  pentad content as expected since the more stereospecific sites have a higher  $k_p$ . Similar trends were observed by Sakurai *et al.* [30] with regards to the relationship of isotacticity to molar mass.

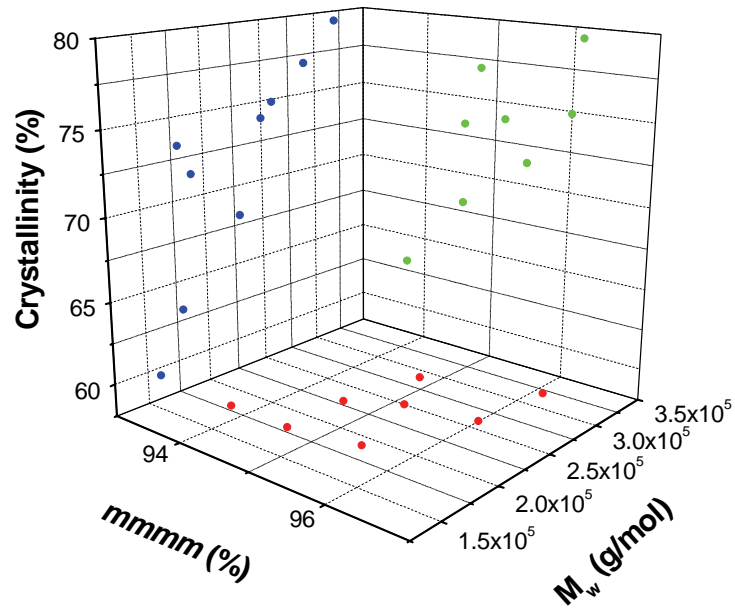


Figure 6.46 A closer examination of the effect of small changes in *mmmm* pentad content as well as changes in the molar mass on the crystallinity of the samples.

As to the dominant effect determining the crystallinity of the samples it is believed that large changes in *mmmm* pentad content clearly dominate over other effects such as the molar mass but that the molar mass and molar mass distribution definitely play a major role when the *mmmm* pentad values are similar.

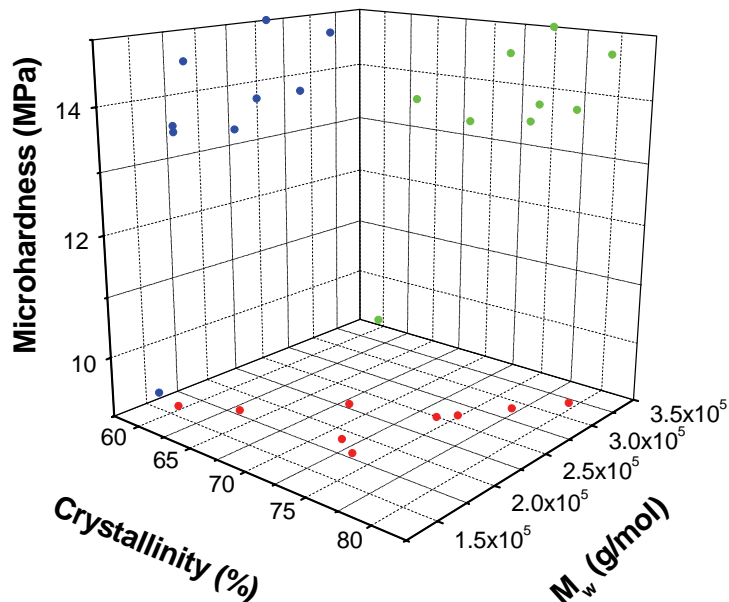
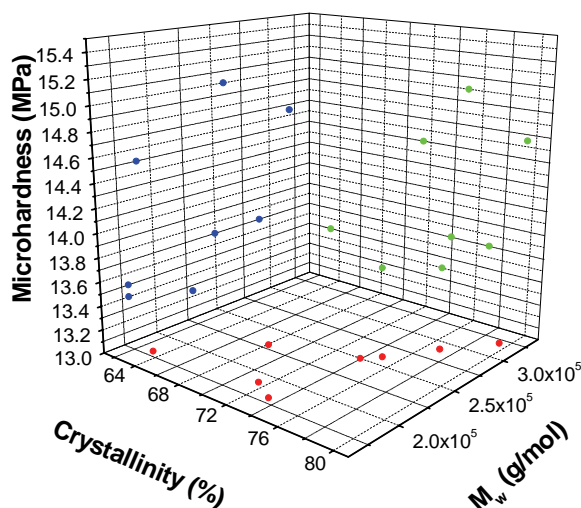


Figure 6.47 The effect of the crystallinity and the molar mass on the microhardness of the samples.

If one examines the combined effect of the molar mass and the crystallinity on the microhardness of the samples (Figure 6.47) it appears that the sharp increase in microhardness

observed from the single lowest point is not due to the molar mass of the sample. There is also no dramatic increase in the overall crystallinity of the sample. It would therefore seem as if neither factor was directly responsible for the sharp increase observed from the sample of lowest microhardness. A closer inspection of the region of small increase in microhardness is given in Figure 6.48.



**Figure 6.48** A closer inspection of the effect of crystallinity and molar mass on small changes in microhardness.

There would appear to be a slight correlation between both the crystallinity and molar mass on the microhardness with samples of high molar mass and high degrees of crystallinity generally having higher microhardness values.

Since the crystallinity is related in part to the tacticity of the samples, the combined effect of the molar mass and the *mmmm* pentad content on the microhardness was investigated. Figure 6.49 demonstrates that the sharp increase in microhardness is due mainly to an increase in the *mmmm* pentad content of the sample and not to the molar mass increase. It would therefore appear that changes in *mmmm* pentad content exert a strong influence on the microhardness of a sample.

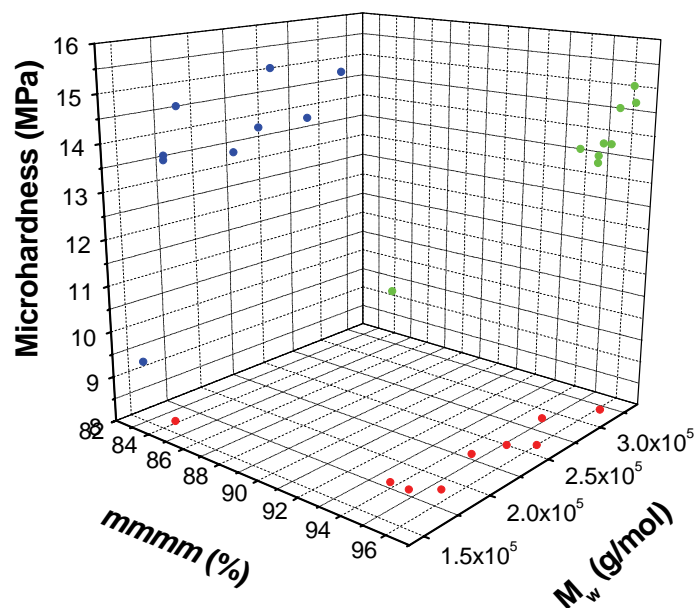


Figure 6.49 The effect of the molar mass and the *mmmm* pentad content on the microhardness of the samples.

If one removes the data point of lower tacticity and focuses on the data points of the samples of higher *mmmm* pentad content then some interesting relationships are revealed (Figure 6.50). There is a strong relationship between the *mmmm* pentad content and the microhardness of the samples, where the higher the *mmmm* pentad content the higher the microhardness value. This is very interesting since it means that the *mmmm* pentad content of a sample plays a more significant role in determining the properties of a material not simply through its influence on the crystallinity of a sample but possibly also on the way in which the sample absorbs energy. It is feasible that the higher *mmmm* pentad content enables easier recrystallisation upon the application of an external force to the sample, thereby improving the hardness of the sample upon indentation. The importance of the tacticity of the polypropylene chains on the properties of the polymer has also been noted by De Rosa *et al.* [31].

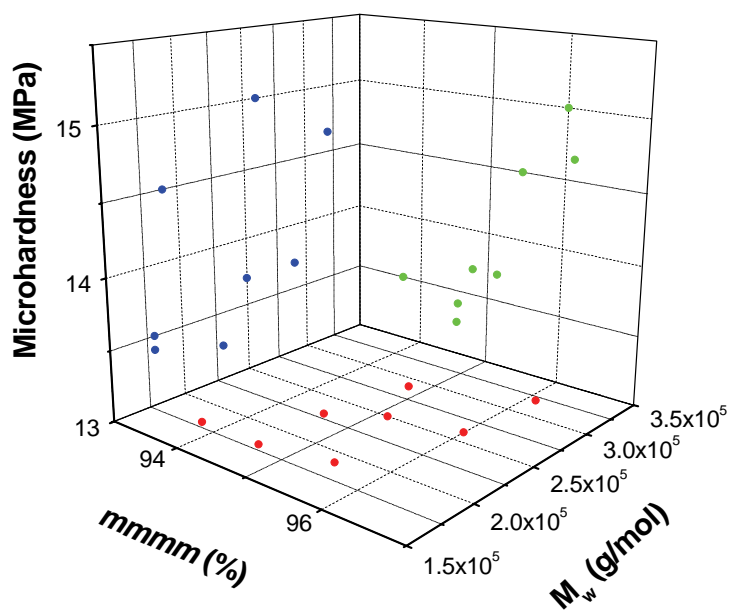


Figure 6.50 The combined effect of the molar mass and the *mmmm* pentad content on the microhardness of the samples.

Within a given series of polymers produced using the same type of external donor one can also see relationships between the molar mass and the microhardness of the samples (Figure 6.51).

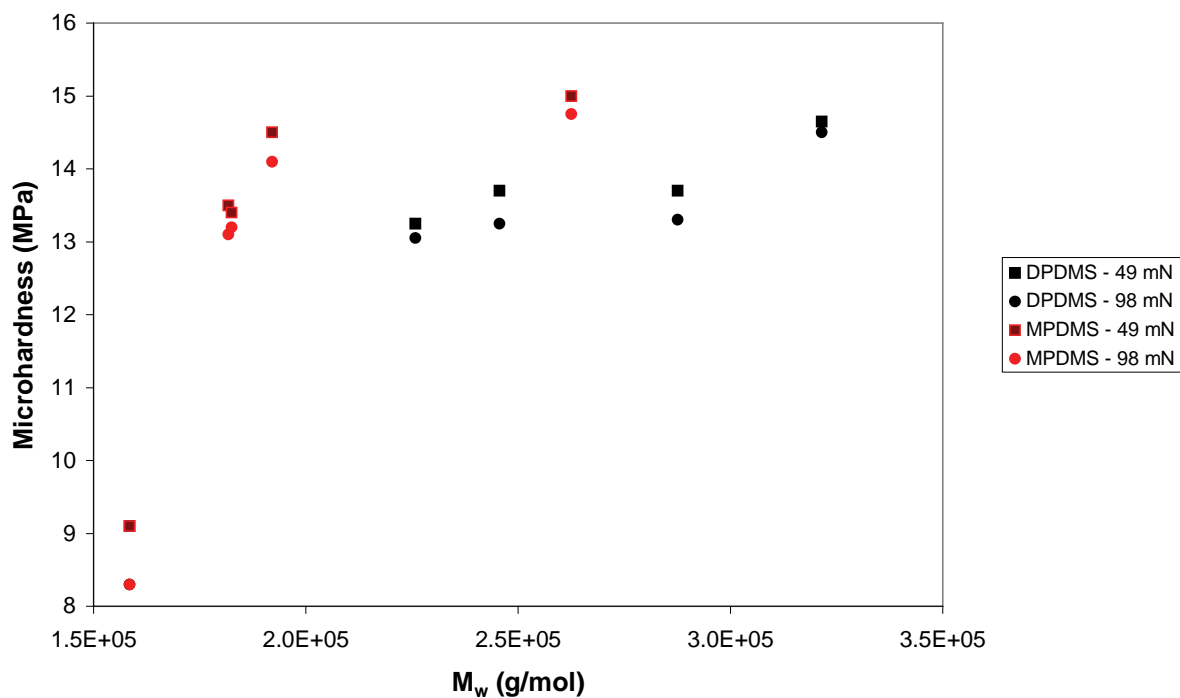
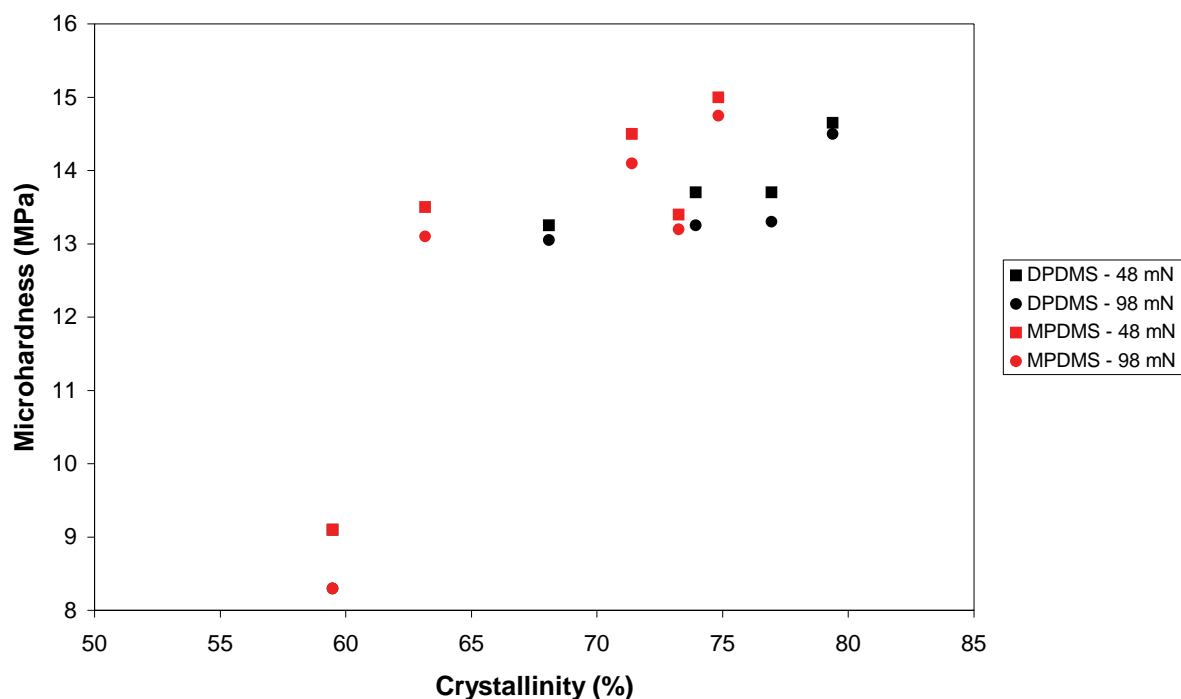


Figure 6.51 The effect of the molar mass on the microhardness of the samples produced using a certain donor type.



The molar mass effect, although not the dominant effect on the microhardness, is still important for a given series of polymers. It is possible that influence of the molar mass on the microhardness is due to its influence on the crystallinity of the samples but also the effect of molecular entanglements since the presence of more entanglements can also increase the hardness of a material.



**Figure 6.52** The effect of the crystallinity on the microhardness of the polymers produced using a certain donor type.

The effect of crystallinity on the microhardness for the different series of polymers is illustrated in Figure 6.52. Similarly to the case of the molar mass effect, the effect of increasing the crystallinity of a sample within a given series of polymers produced by the same type of catalyst system is evident.

However, the dominant effect as discussed earlier is the *mmmm* pentad content which increases with microhardness for both series' of polymers as illustrated in Figure 6.53. It is therefore evident that the external electron donor influences the properties of the polymer by improving the average *mmmm* pentad content of the samples. This is accomplished by the coordination of the external donor in the vicinity of the active sites, thereby converting some poorly isospecific sites (site type **B** in Busico's model) and aspecific sites (site type **C** in Busico's model) to isospecific sites.

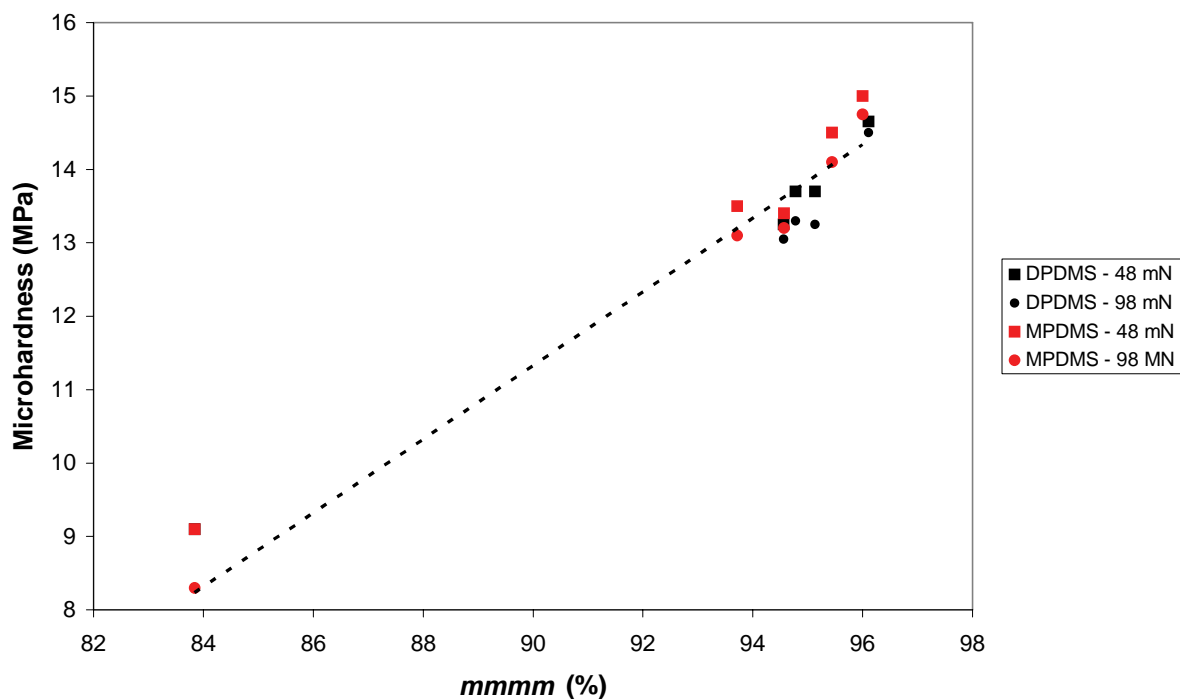


**Figure 6.53** The effect of the *mmm* pentad content on the microhardness of the samples for the different polymers produced using different external donor types.

The next question which arises is which sites are affected to what degree. It would appear as if the sites of type **B** in Busico's model are the prime candidates for conversion and the TREF data would seem to support this. The addition of an external donor to the system as well as subsequent increases in the external donor/catalyst ratio has the greatest influence on the 60, 80, 100, 105, and 110 °C TREF fractions since it is these fractions which are reduced in amount upon addition of an external donor. It is also these fractions which influence the properties of a material to the greatest extent as shown in Chapter 4. It is evident that the microhardness is increased by increasing the overall tacticity of the polymer chains and so the degree to which the active sites, producing material which elutes in these fractions, can be converted to site type **A**, producing highly isotactic material, is of paramount importance in determining the microhardness of the material.

### 6.3.6.2 DMA

The DMA technique is an extremely useful one and is often used to obtain an indication of the physical properties of samples. It is a very sensitive technique, able to detect a number of different transitions and relaxations which take place in a material at a certain temperature. The  $\tan \delta$  curves essentially represent the ratio of the ability of the material to

store energy and lose energy which is also sometimes referred to as the damping ability of a material. This can also be taken as a measure of the impact properties of a material.

It is evident from Figures 6.54 and 6.55 that the  $\beta$ -transition, corresponding to the glass transition temperature of iPP, which occurs over a temperature range in the region of 10 °C, is far greater for the sample produced without external donor present in the system. This is to be expected since the sample in question is less crystalline and therefore contains more amorphous material. The implications are that the chains have far greater mobility in the amorphous phase for the No ED sample compared to the samples produced with either DPDMS or MPDMS as external donor since the magnitude of the  $\beta$ -transition is related to the mobility of the chains.

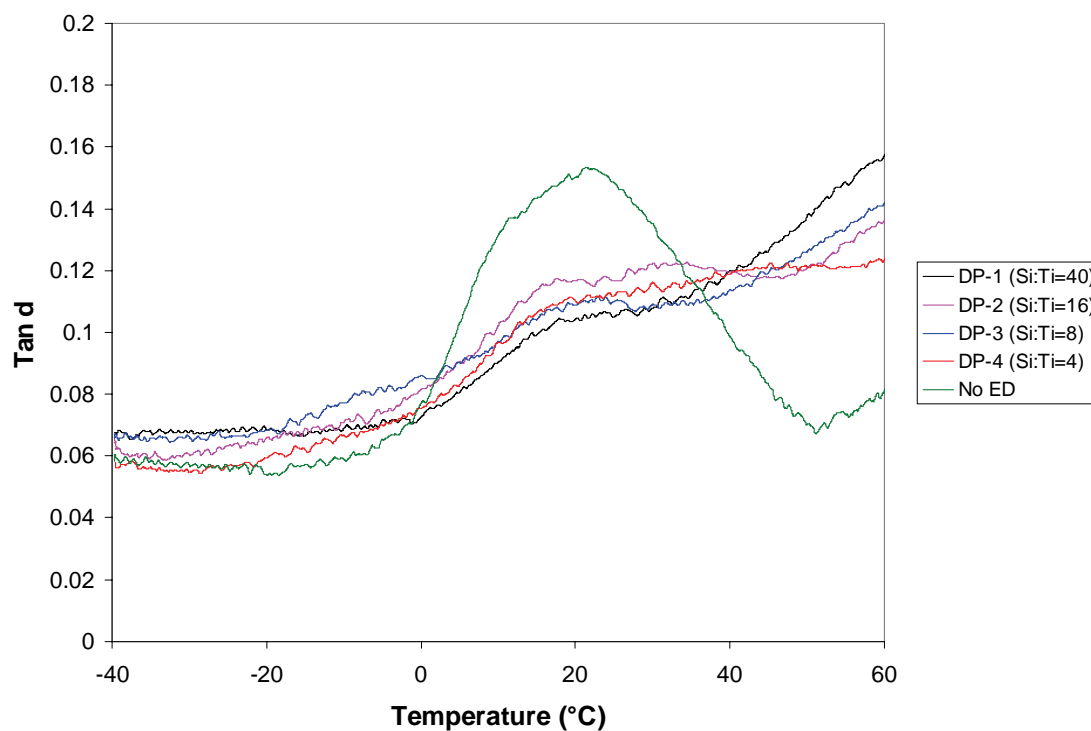


Figure 6.54 The  $\tan \delta$  curves for the samples produced using DPDMS and the No ED sample.

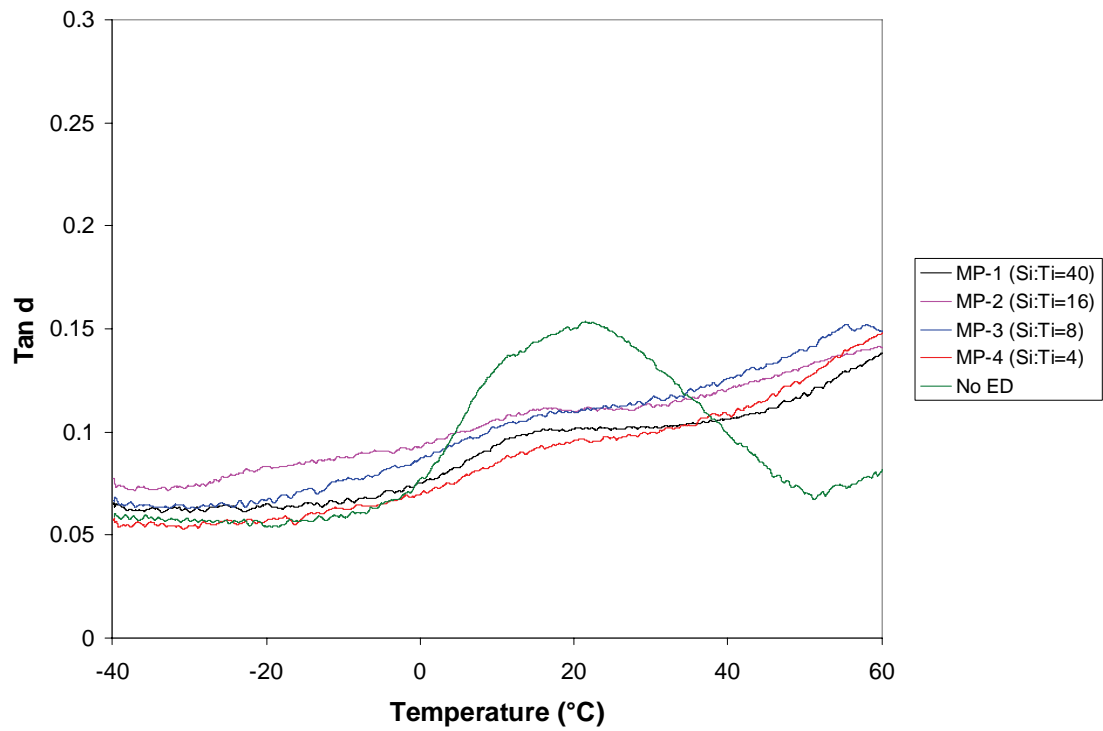


Figure 6.55 The  $\tan \delta$  curves for the samples produced using MPDMS and the No ED sample.

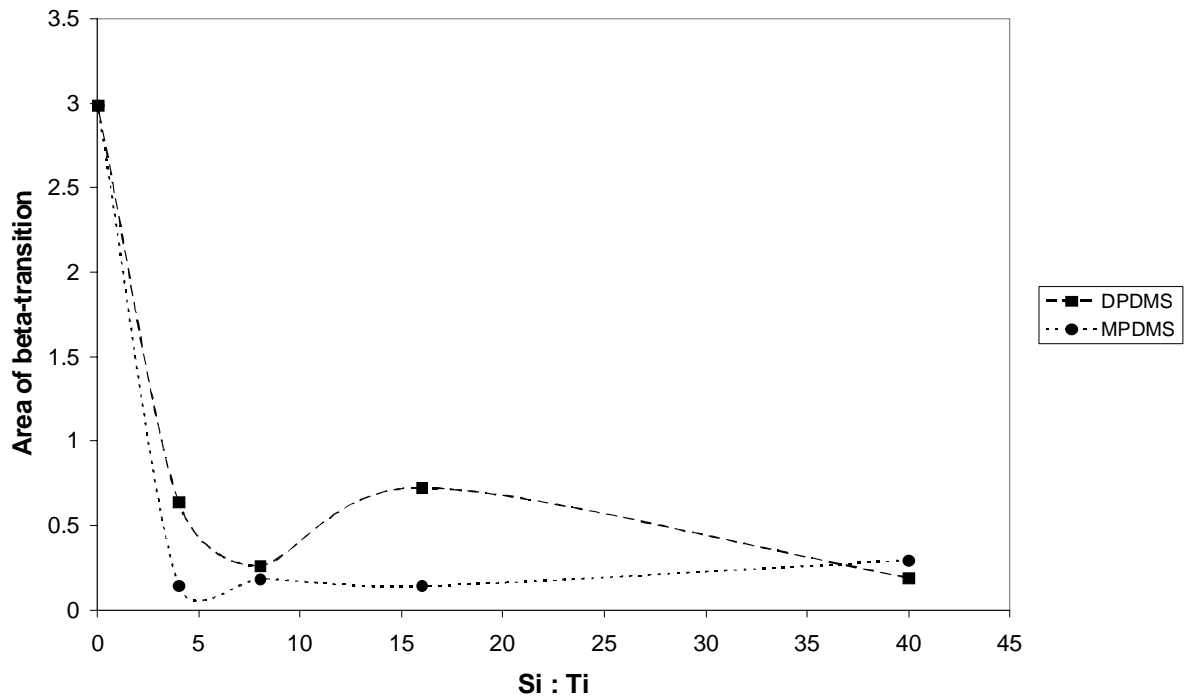


Figure 6.56 The magnitude of the area of the  $\beta$ -transition as a function of the external donor/catalyst ratio for the samples produced with both DPDMS and MPDMS.

The areas of the  $\beta$ -transitions of the samples, after subtraction of a linear baseline, are given in Figure 6.56. The decrease in mobility of the chains in the amorphous regions is evident

upon addition of an external donor, however, the effect of increasing the external donor/catalyst ratio is complex. There is a slight decrease in the magnitude of the transition for the DPDMS samples as the external donor/catalyst ratio is increased with the exception of sample DP-2 (with an external donor/catalyst ratio of 16). This is possibly related to the slightly lower crystallinity of this sample compared to sample DP-3, however, sample DP-4 has a similar level of crystallinity and a lower magnitude of the  $\beta$ -transition. There is also a possible molar mass effect, as discussed by Stern *et al.* [1] who found that the higher molar mass polymers were generally characterised by larger  $\beta$ -transitions. Sample DP-2 has a relatively high molar mass and a slightly lower *mmmm* pentad content than the samples at higher, and lower, external donor/catalyst ratios. It is also noted that the magnitude of the  $\beta$ -transition is greater for the samples produced with DPDMS than for the samples produced with MPDMS. This implies better mobility for the chains in the amorphous regions of these samples compared to the MPDMS samples and could be related to better-defined crystalline regions in the samples produced using DPDMS and also the higher average molar mass of the samples produced using DPDMS. This would result in the chains in the amorphous region being less restricted by the crystalline domains. The microhardness values of the samples produced using MPDMS are on average slightly higher than those produced using DPDMS, therefore the slightly lower mobility of the chains of the MPDMS samples would seem to correlate with a slightly higher microhardness value since there is more resistance to the motion of the chains. It would therefore seem as if upon modification of the catalyst one can convert a large portion of the active sites to those of type **A**, thereby increasing the microhardness of the samples but that this comes at a price in terms of the ability of the material to absorb energy and so the impact strength of the material decreases. It would appear as if the 60 °C to 110 °C fractions are key in determining this effect since it is a reduction in the amount of material eluted in these fractions which brings about an increase in the microhardness of the material and vice versa in terms of the energy absorbing abilities of the sample.

The storage modulus data for the samples produced using DPDMS are given in Figure 6.57. It is apparent that similarly to the magnitude of the  $\beta$ -transition the storage modulus of the No ED sample is the highest of all the samples. It is also interesting that the storage modulus of the samples increases as the external donor/catalyst ratio increases from 4 to 16 but that the modulus for the highest ratio of 40 is actually lower than one would expect. This is believed to be related to the molar mass of the important fractions eluting in the 80 – 115 °C temperature region. It would seem as if the higher the molar mass of these fractions, the higher the storage modulus, since it is evident that for the DPDMS samples the No ED sample

and DP-2 sample both have fractions of high molar mass eluting at these temperatures while the DP-1 sample's fractions consist of the lowest molar mass material of all the fractions eluting at these temperatures.

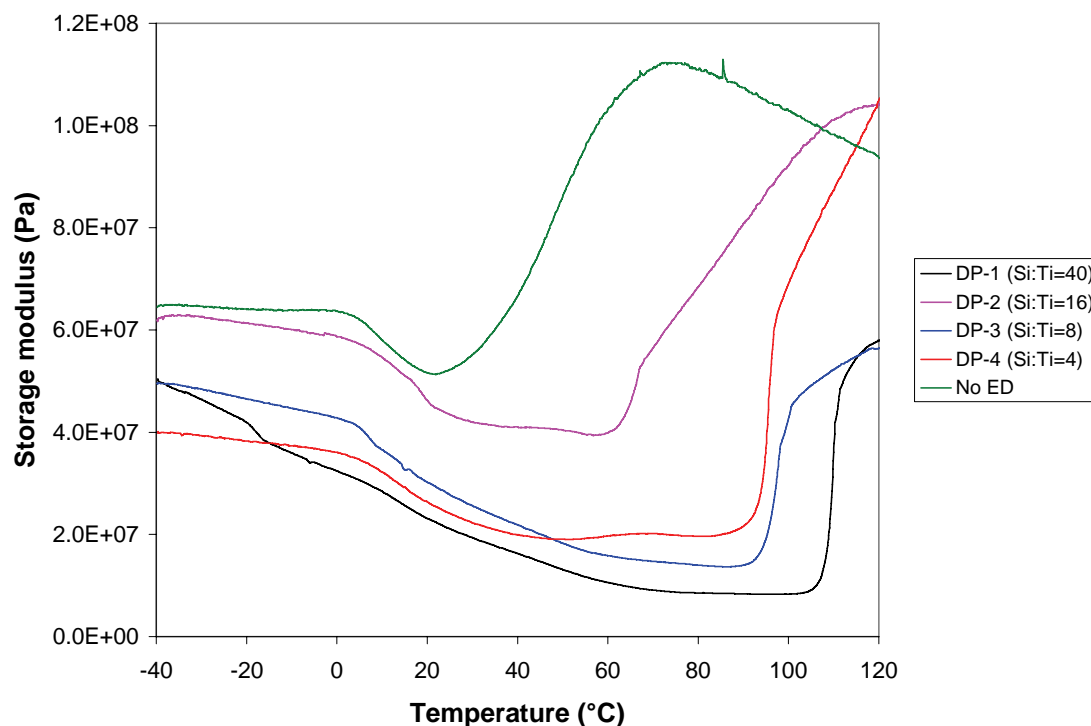


**Figure 6.57** The storage modulus curves for the samples produced using DPDMS and the No ED sample.

It is also interesting to note the dramatic increase in storage modulus observed at a certain temperature for a certain sample. This is related to the recrystallisation of the samples as the temperature is increased. The recrystallisation is known to occur [32] as a result of frozen-in-stress due to the sample preparation process. The recrystallisation process is strongly dependent on the external donor/catalyst ratio and it is clear that increasing this ratio produces material which generally only recrystallises at a higher temperature. This is due to the fact that the crystalline regions which are formed are more perfectly ordered due to the improvement in crystallisation of the types of chains present. Sample DP-2, however, recrystallises at a lower temperature than the trend suggests. The magnitude of the  $\beta$ -transition of this sample is also relatively high compared to the other samples in the series and so it is thought that the increased mobility of the chains in the amorphous region enables the recrystallisation of the crystalline regions at a lower temperature. The recrystallisation temperatures of the other DPDMS samples also correlate well with the magnitude of the  $\beta$ -transition.

The storage modulus data for the samples produced using MPDMS are given in Figure 6.58. Compared to the samples produced using DPDMS the modulus values are significantly lower for the samples produced using MPDMS. The most significant difference between the samples produced using DPDMS and those produced using MPDMS is the molar mass. Indeed the lower modulus values for the MPDMS samples correlates well with the slightly lower molar masses of the MPDMS samples' fractions in the 60 – 105 °C temperature regions. The molar mass of the No ED samples' aforementioned important fractions is also higher than that of the MPDMS samples. In this case the MP-1 sample's fractions are the second highest and the MP-2 sample's are the lowest in terms of molar mass which also correlates well with the modulus values providing further evidence that the storage modulus is indeed linked to the molar mass of these specific fractions of the material.

It seems therefore that the amount of material eluting in these fractions (representing the degree of active site conversion) affects the microhardness and damping ability of the materials while the molar mass of the fractions affects the modulus of the samples and also possibly the damping properties through the molar mass effect on the mobility of chains in the amorphous or ordered amorphous phase. It is therefore possible to tailor the properties of the polymer via chemical modification of the catalyst system used to make the polymers, as opposed to the physical alteration of the composition of the materials as performed in Chapter 4.

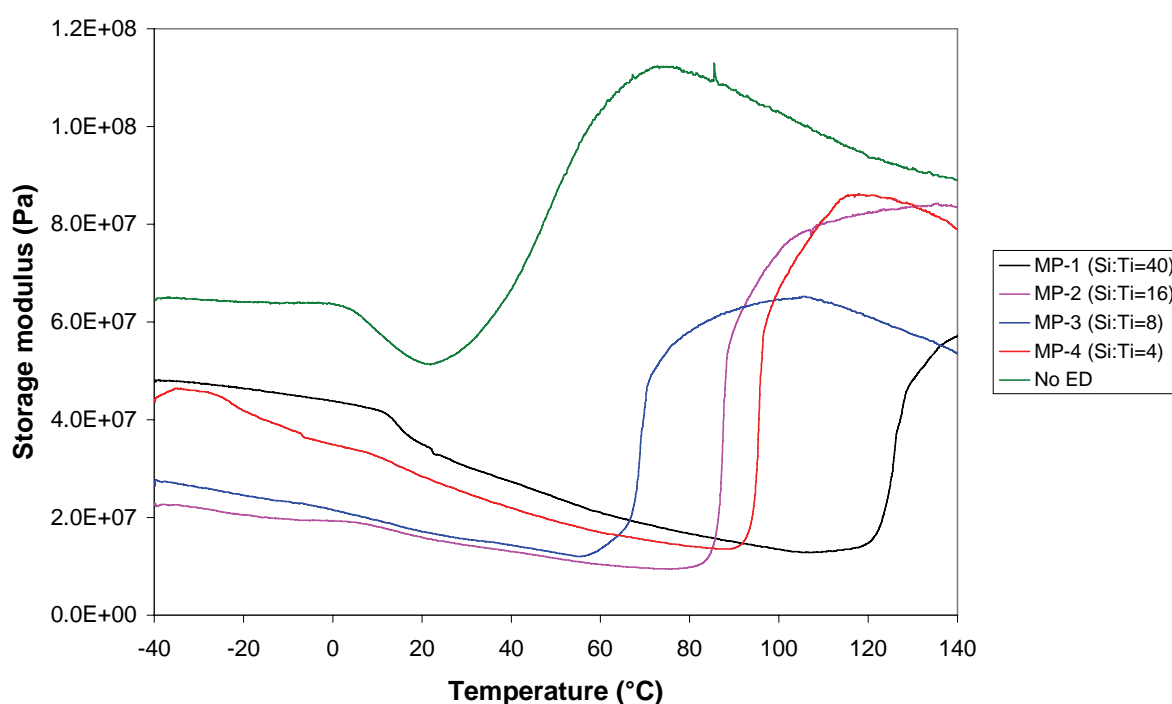


Figure 6.58 The storage modulus curves for the samples produced using MPDMS and the No ED sample.

The recrystallisation phenomenon is also observed for the samples produced using MPDMS as external donor. The sample produced at the highest external donor/catalyst ratio once again recrystallises at the highest temperature, however, the onset of recrystallisation for the other samples in the series is complex. The lower than expected recrystallisation temperature of sample MP-3 is possibly related to the lower crystallisation temperature of this sample (Figure 6.14).

## 6.4 Conclusions

With regards to the polymerisations themselves, a number of interesting conclusions can be drawn. Firstly, it seems as if the DPDMS external donor exerts a stronger influence on the nature of the active sites than the MPDMS external donor. The reason for this is that there is a more marked decrease in activity with increasing external donor/catalyst ratio for the samples produced with DPDMS. The effect on molar mass is also substantially different in that a definite increase in molar mass is observed upon increasing the external donor/catalyst ratio while using DPDMS, while when using MPDMS there is an increase in molar mass but the increase is slight until the high external donor/catalyst ratio of 40 is used. Then only does the molar mass increase significantly. The molar mass of the samples produced using DPDMS is significantly higher than that of the samples produced using MPDMS. The polydispersity of the samples produced using DPDMS is also narrower than that of the samples produced using MPDMS.

The addition of even a small amount of external donor brings about a sharp increase in the *mmmm* pentad content of the polymer produced. Further increase in the external donor/catalyst ratio does increase the *mmmm* pentad content but only slightly. Increasing the external donor/catalyst ratio for both types of donors does bring about a constant decrease in the amount of syndiotactic material present (*rrrm* and *rrrr* pentad content) in the polymers, indicating that although the average *mmmm* pentad content does not improve much, the donors are still coordinated in the vicinity of the active sites and prevent the chain end control mechanism from occurring to a certain extent.

In terms of the thermal properties of the samples, those produced using DPDMS melt at higher temperatures than those produced using MPDMS possibly related to the molar mass of the samples. The crystallinities of the samples increase upon addition of little external donor, however, the overall crystallinities slightly decrease again for higher external donor



ratios for both external donors investigated. The weight average lamellar thickness of the samples tends to increase with increasing external donor/catalyst ratio.

Crystallisation of the samples from solution is definitely different to the case of crystallisation in the solid state. CRYSTAF data indicate that the molar mass of the polymers is the most important factor regarding initiation of crystallisation, and that samples with higher molar mass crystallise out of solution at higher temperatures. The sample with an external donor/catalyst ratio of 4 had the highest onset of crystallisation temperature of all the samples for both external donor types investigated. Furthermore it was evident that the samples with the highest external donor/catalyst ratio were the highest melting irrespective of external donor type.

TREF fractionation of the samples revealed that the samples produced using DPDMS were eluted at mainly the 115 °C and 120 °C fractions while the samples produced using MPDMS had considerably less material in their 120 °C fractions and more material distributed over the 110, 115, and 120 °C fractions. Sample DP-2 appeared to elute more of its material in the 115 °C fraction than would have been expected compared to the trends observed for the other samples in the series. Sample MP-4 eluted more material in the 120 °C fraction than would be expected compared to the other MP-samples. Overall it would seem as if the DPDMS external donor exerted more influence on the active sites producing chains which elute in the lower temperature fractions than the MPDMS, i.e. is better at converting the active sites to those of increased stereospecificity than the MPDMS is. These fractions all showed the expected trend of decreased contribution to the composition of the polymer with increasing external donor/catalyst ratio, as the external donor coordinated to the aspecific and poorly isospecific sites, and either deactivated them or converted them to more stereospecific sites.

The molar mass of the fractions increased dramatically for all samples after the 105 °C fraction irrespective of external donor type, loading or even presence in the system. This is a clear indication that the molar mass plays a significant role in the fractionation mechanism of TREF. There are fractions present with negligible differences in *mmmm* pentad content which elute in successive fractions, with the higher molar mass sample eluting at the higher temperature. The fractionation mechanism of TREF is therefore a complex one with contributions from both the stereoregularity and molar mass of the chains. In terms of the polydispersity of the TREF fractions, it is evident that the lower temperature fractions have a broader distribution of molar mass chains than the higher temperature fractions. There is a minimum polydispersity value which was observed for the 100 °C fraction for all samples. The *mmmm* pentad content of the fractions generally increased with elution temperature for

all samples analysed as expected since a higher *mmmm* pentad content facilitates easier crystallisation of the chains.

The effect of the addition of external donor to the polymerisation system was also shown for those sites producing polymers eluting in the 60 °C fraction. The systematic deactivation of the sites producing material eluting in these fractions was demonstrated upon increasing the external donor/catalyst ratio. In general the thermal properties of the TREF fractions improved with fractionation temperature up to the 115 or 120 °C fractions after which there was a slight decrease in the properties due to the co-crystallisation of material trapped during the TREF crystallisation process.

Deconvolution of the molar mass data revealed that the molar mass distributions of all the samples could be described by 6 active sites. For the samples produced using DPDMS it would appear that the addition of a small amount of external donor converts many aspecific sites to isospecific sites but that further external donor addition deactivates sites but increases the stereoregularity and thus the  $k_p$  of the sites which remain. Using MPDMS as external donor does not appear to influence the stereospecificity of the sites at low external donor/catalyst loadings and that slight increases in molar mass are due to conversion of aspecific sites to stereospecific sites without increasing the stereoselectivity of the sites. Very high external donor/catalyst ratios would appear to be needed to significantly improve the stereospecificity of the sites and thus their  $k_p$ . This would seem to corroborate the hypothesis that the DPDMS as external donor exerts a greater influence on the active sites even at low external donor/catalyst ratios.

With regards to the microhardness of the samples, the addition of a small amount of external donor dramatically increases the microhardness of the polymer, while increasing the external donor/catalyst ratio increases the microhardness slightly for both external donor types. The crystallinity of the samples was shown to be clearly related to the molar mass and molar mass distribution as well as the *mmmm* pentad content of the samples. Higher molar masses, narrower molar mass distributions, and higher *mmmm* pentad contents improved the crystallinity of the samples over the range of microstructures studied here. The higher molar mass samples were also shown to have higher stereoregularity. The molar mass and crystallinity both show an effect on the microhardness, with the harder samples generally consisting of more crystalline material of a higher molar mass. However, the strongest property affecting the microhardness was the *mmmm* pentad content of the samples, where the samples with higher *mmmm* pentad content had higher microhardness values. It is evident that the external electron donor mainly exerts its influence on the poorly isospecific sites as evidenced by the significant decrease in the amount of material eluting in the 60 – 110 °C

fractions. It is also clear that the physical properties such as the microhardness are dependent on the amount of material in these medium – high temperature fractions since a reduction in the proportion of material eluting in these fractions means the conversion of more active sites and a higher overall *mmmm* pentad content.

DMA analysis showed that the ability of the materials to dissipate energy was related to the mobility of the amorphous regions in the polymers. The sample produced without external donor clearly had the best damping ability at low temperature and it is noted that this sample is the softest but that its damping ability was the best. A relationship seems to exist whereby increasing the amount of material eluting in the 80 – 110 °C fraction increases the damping properties of the material while at the same time decreasing the hardness of the material. The modulus of the samples appears to be related to the molar mass of these medium – high temperature fractions, where higher molar masses in these fractions result in a material with a higher modulus. Significant secondary crystallisation was observed for all samples due to the re-crystallisation of chains after the frozen-in-stress was removed upon heating. The temperature at which the recrystallisation takes place appears to be possibly related to the mobility of the amorphous domains. It is also noted that in general the samples produced using DPDMS have a higher modulus than the samples produced using MPDMS, and that this is also related to the higher molar mass of the 60 – 110 °C fractions.

## 6.5 References

1. Stern, C., Frick, A., & Weickert, G., *Relationship between the structure and mechanical properties of polypropylene: Effects of the molecular weight and shear-induced structure*. Journal of Applied Polymer Science, 2007. **103**: p. 519-533.
2. Samios, D., Tokumoto, S., & Denardin, E.L.G., *Investigation of the large plastic deformation of iPP induced by plane strain compression: Stress–strain behavior and thermo-mechanical properties*. International Journal of Plasticity, 2006. **22**: p. 1924–1942.
3. De Rosa, C., & Auriemma, F., *Structural-mechanical phase diagram of isotactic polypropylene*. Journal of the American Chemical Society, 2006. **128**: p. 11024-11025.
4. Bukatov, G.D., & Zakharov, V.A., *Propylene Ziegler-Natta polymerization: Numbers and propagation rate constants for stereospecific and non-stereospecific centers*. Macromolecular Chemistry and Physics, 2001. **202**: p. 2003-2009.

5. Garoff, T., Virkkunen, V., Jaaskelainen, P., Vestberg, T., *A qualitative model for polymerisation of propylene with a MgCl<sub>2</sub>-supported TiCl<sub>4</sub> Ziegler–Natta catalyst.* European Polymer Journal, 2003. **39**: p. 1679-1685.
6. Chadwick, J.C., *Advances in propene polymerization using MgCl<sub>2</sub>-supported catalysts. Fundamental aspects and the role of electron donor.* Macromolecular Symposium, 2001. **173**: p. 21-35.
7. Chadwick, J.C., van Kessel, G.M.M., & Sudmeijer, O., *Regio- and stereospecificity in propene polymerization with MgCl<sub>2</sub>-supported Ziegler-Natta catalysts: Effects of hydrogen and the external donor.* Macromolecular Chemistry and Physics, 1995. **196**: p. 1431-1437.
8. Chadwick, J.C., Van der Burgt, F.P.T.J., Rastogi, S., Busico, V., Cipullo, R., Talarico, G., Heere, J.J.R., *Influence of Ziegler-Natta catalyst regioselectivity on polypropylene molecular weight distribution and rheological and crystallization behaviour.* Macromolecules, 2004. **37**: p. 9722-9727.
9. Chadwick, J.C., Morini, G., Balbontin, G., Mingozi, I., & Albizzati, E., *Propene polymerization with MgCl<sub>2</sub>-supported catalysts: Effects of using a diether as external donor.* Macromolecular Chemistry and Physics, 1997. **198**: p. 1181-1188.
10. Matsuoka, H., Liu, B., Nakatani, H., & Terano, M., *Variation in the isospecific active sites of internal donor-free MgCl<sub>2</sub>-supported Ziegler catalysts: Effect of external electron donors.* Macromolecular Rapid Communications, 2001. **22**: p. 326-328.
11. Hasan, K.A.T.M., Liu, B., & Terano, M., *Effects of various preparation and polymerization procedures on the isospecific nature of TiCl<sub>3</sub>-based polypropylene catalysts.* Polymer Bulletin, 2005. **54**: p. 225-236.
12. Busico, V., Cipullo, R., Monaco, G., Talarico, G., Vacatello, M., Chadwick, J.C., Segre, A.L., & Sudmeijer, O., *High-resolution <sup>13</sup>C NMR configurational analysis of polypropylene made with MgCl<sub>2</sub>-supported Ziegler-Natta catalysts. 1. The “model” system MgCl<sub>2</sub>/TiCl<sub>4</sub>-2,6-dimethylpyridine/Al(C<sub>2</sub>H<sub>5</sub>)<sub>3</sub>.* Macromolecules, 1999. **32**: p. 4173-4182.
13. Busico, V., Corradini, P., De Biasio, R., Landriani, L., & Segre, A.L., *<sup>13</sup>C NMR evidence of the copresence of m-rich and r-rich sequences (stereoblocks) in polypropene molecules.* Macromolecules, 1994. **27**: p. 4521-4524.
14. Busico, V., Chadwick, J.C., Cipullo, R., Ronca, S., & Talarico, G., *Propene/ethene-[1-<sup>13</sup>C] copolymerization as a tool for investigating catalyst regioselectivity. MgCl<sub>2</sub>/internal donor/TiCl<sub>4</sub>-external donor/AlR<sub>3</sub> systems.* Macromolecules, 2004. **37**: p. 7437-7443.

15. Liu, B., Nitta, T., Nakatani, H., & Terano, M., *Precise arguments on the distribution of stereospecific active sites on MgCl<sub>2</sub>-supported Ziegler-Natta catalysts*. Macromolecular Symposium, 2004. **213**: p. 7-18.
16. Liu, B., Nitta, T., Nakatani, H., & Terano, M., *Stereospecific nature of active sites on TiCl<sub>4</sub>/MgCl<sub>2</sub> Ziegler-Natta catalyst in the presence of an internal electron donor*. Macromolecular Chemistry and Physics, 2003. **204**: p. 395-402.
17. Flory, P.J., *Principles of polymer chemistry*. 1953, New York: Cornell University Press.
18. Soares, J.B.P., & Hamielac, A.E., *Deconvolution of chain-length distributions of linear polymers made by multiple-site-type catalysts*. Polymer, 1995. **36**: p. 2257-2263.
19. Soares, J.B.P., *Mathematical modelling of the microstructure of polyolefins made by coordination polymerization: a review*. Chemical Engineering Science, 2001. **56**: p. 4131-4153.
20. Kissin, Y.V., *Molecular weight distributions of linear polymers: Detailed analysis from GPC data*. Journal of Polymer Science: Part A: Polymer Chemistry, 1995. **33**: p. 227-237.
21. Nele, M., & Pinto, J.C., *Molecular-weight multimodality of multiple Flory distributions*. Macromolecular Theory and Simulations, 2002. **11**: p. 293-307.
22. Fortuny, M., Nele, M., Melo, P.A., & Pinto, J.C., *Deconvolution of molecular weight distributions using dynamic Flory-Schultz distributions*. Macromolecular Theory and Simulations, 2004. **13**: p. 355-364.
23. Chadwick, J.C., Morini, G., Balbontin, G., Camurati, I., Heere, J.J.R., Mingozzi, I., Testoni, F., *Effects of internal and external donors on the regio and stereoselectivity of active species in MgCl<sub>2</sub>-supported catalysts for propene polymerization*. Macromolecular Chemistry and Physics, 2001. **202**: p. 1995-2002.
24. Kouzai, I., Wada, T., Taniike, T., & Terano, M., *Hydrogen effects for propylene polymerization with ultra low TiCl<sub>3</sub> loading MgCl<sub>2</sub>-supported catalyst*. Macromolecular Symposium, 2007. **260**: p. 179-183.
25. De Rosa, C., Auriemma, F., Paolillo, M., Resconi, L., & Camurati, I., *Crystallization behavior and mechanical properties of regiodefective, highly stereoregular isotactic polypropylene: Effect of regiodeflects versus stereodeflects and influence of the molecular mass*. Macromolecules, 2005. **38**: p. 9143-9154.
26. Ibhaddon, A.O., *Crystallization regimes and reptation in polypropylene molecular weight fractions*. Journal of Applied Polymer Science, 1999. **71**: p. 579-584.

27. Flores, A., Aurrekoetxea, J., Gensler, R., Kausch, H.H., & Balta' Calleja, F.J., *Microhardness-structure correlation of iPP/EPR blends: influence of molecular weight and EPR particle content*. Colloid Polymer Science, 1998. **276**: p. 786-793.
28. Wild, L., *Temperature rising elution fractionation*. Advances in Polymer Science, 1990. **98**(1): p. 1-47.
29. Koch, T., Seidler, S., Halwax, E., & Bernstorff, S., *Microhardness of quenched and annealed isotactic polypropylene*. Journal of Materials Science, 2007. **42**: p. 5318-5326.
30. Sakurai, T., Nozue, Y., Kasahara, T., Mizunuma, K., Yamaguchi, N., Tashiro, K., & Amemiya, Y., *Structural deformation behavior of isotactic polypropylene with different molecular characteristics during hot drawing process*. Polymer, 2005. **46**: p. 8846-8858.
31. De Rosa, C., Auriemma, F., Di Capua, A., Resconi, L., Guidotti, S., Camurati, I., Nifant'ev, I.E., & Laishev'tsev, I.P., *Structure-property correlations in polypropylene from metallocene catalysts: Stereodeficient, regioregular isotactic polypropylene*. Journal of the American Chemical Society, 2004. **126**: p. 17040-17049.
32. Menard, K.P., *Dynamic mechanical analysis: A practical introduction*. 1999, Boca Raton: CRC Press.

## Chapter 7. Synopsis and conclusions

### 7.1 Synopsis and conclusions

In order to correlate the data regarding the removal of certain fractions of the polypropylene homopolymer (sample PPH), as discussed in Chapter 4, with the chemical alteration of the active sites, as discussed in Chapter 6, it is necessary to compare the materials used in each section of the work. Although removing an entire fraction from a material is slightly different to the alteration of the proportion of material eluting in a given fraction, it is believed that the methodology is sound in that the importance of specific fractions is highlighted. Removing a fraction from the material also modifies the composition of the polymer which is exactly what is accomplished by changing the reaction conditions. On the one hand there is the effect of removing fractions, leaving behind a polymer which could have been produced by a hypothetical catalyst system consisting of active sites which are different to those which produced the original material. On the other hand there is the real chemical modification of the active sites and the production of polymers with different properties. Selected examples are discussed regarding the relationship between the methods.

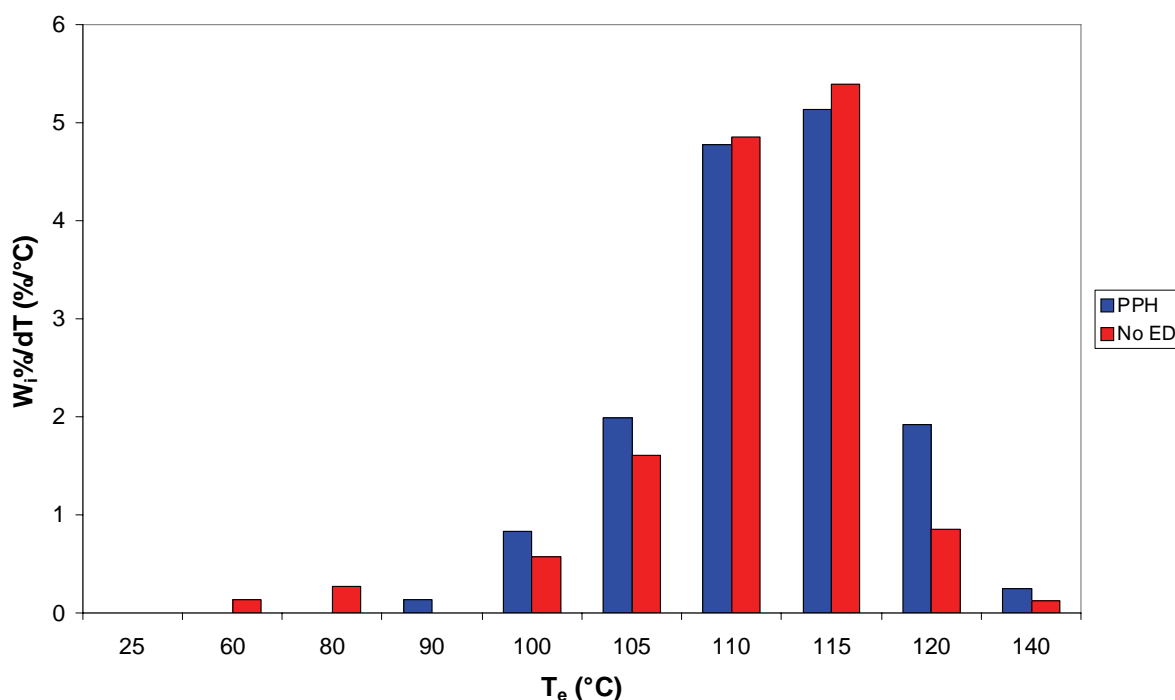
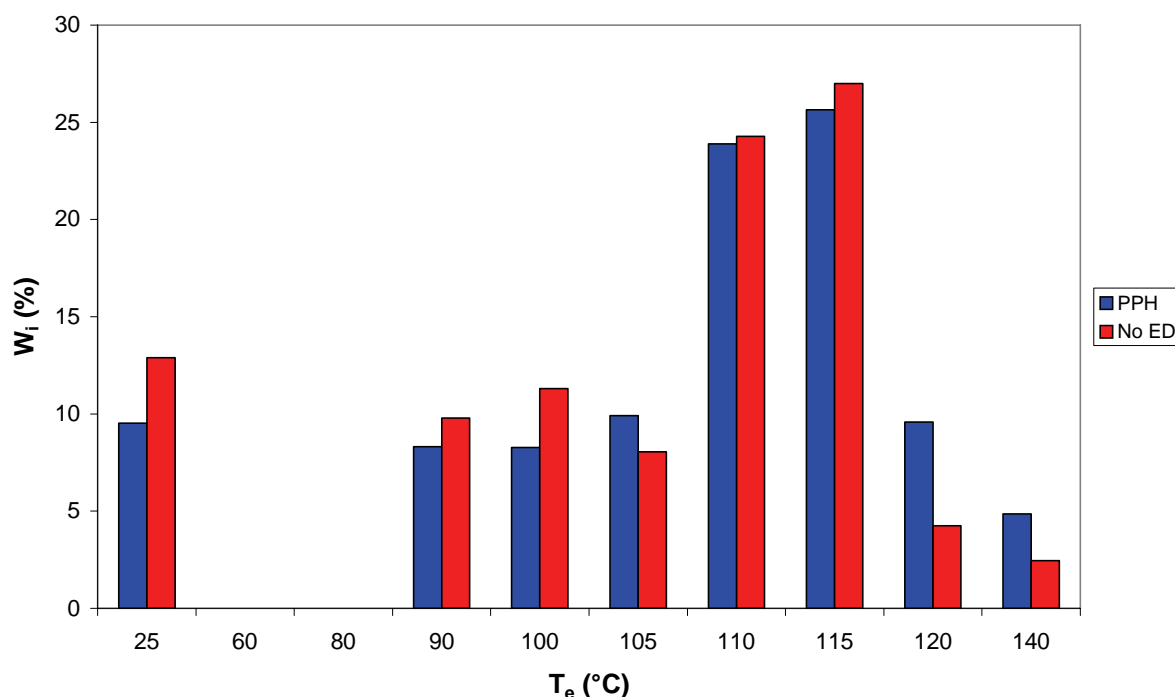


Figure 7.1 An illustration of the similarity in TREF profiles of the PPH sample and the No ED sample.

Figure 7.1 illustrates the comparison between the PPH sample discussed in Chapter 4 and the No ED sample discussed in Chapter 6. These samples are the most similar in terms of the amount of material eluting in each specific TREF fraction. The fractionation temperatures are slightly different for the lower temperature fractions therefore the 60 and 80 °C fractions of the No ED sample have been combined into a hypothetical 90 °C fraction so as to facilitate easier comparisons. This is illustrated in Figure 7.2.



**Figure 7.2 A more direct comparison between the amount of material eluting in each of the fractions of the PPH and No ED samples.**

It is clear that the No ED sample has more material eluting in the lower temperature fractions as evidenced by comparing the amount of material eluting in the 90 and 100 °C fractions. It is also evident that there is more material eluting in the highest temperature fractions for the PPH sample. This is consistent with the data discussed in Chapter 6 for the reduction in the amount of material eluting in the lower temperature fractions due to the conversion of some of the active sites into those producing more isotactic material.

The largest difference in the crystallinity of the PPH samples was brought about by the removal of the 91 – 100 °C to 106 – 110 °C fractions from the PPH sample, while the largest difference in physical properties was observed upon removal of the 26 – 90 °C fraction and the 106 – 110 °C fractions. It was also shown in Chapter 6 that reduction in the amount of material eluting in the 60 – 110 °C temperature range had a significant effect on the polymer



properties. The lower crystallinity values observed upon removing the 91 – 100 °C to 106 – 110 °C fractions from the PPH sample was due to significantly lower *mmmm* pentad contents for the residual material. As demonstrated in Chapter 6 the lower *mmmm* pentad contents have a direct bearing on the microhardness values of the sample hence the removal of these fractions would result in significant changes in the microhardness of the material.

It could, therefore, be said upon comparison of these two materials that the PPH sample would be expected to have a slightly higher *mmmm* pentad content based on the amount of material eluting in the fractions and this is indeed the case since the No ED sample has an *mmmm* pentad content of approximately 84% while that of the PPH sample is approximately 90%. This could be brought about via modification and tailoring of the type and amount of the electron donors present in the system as shown in Chapter 6. The slightly lower than expected microhardness values could very well be due to a molar mass effect on the microhardness, since Koch *et al.* [1] have demonstrated that higher molar mass polymers (with molar mass higher than 400 kg/mol) have lower microhardness values, and the PPH sample has a weight average molar mass in excess of 600 kg/mol. It is therefore believed that very large differences in molar mass could play a role but that the tacticity of the samples is still the dominant property governing the microhardness of the samples.

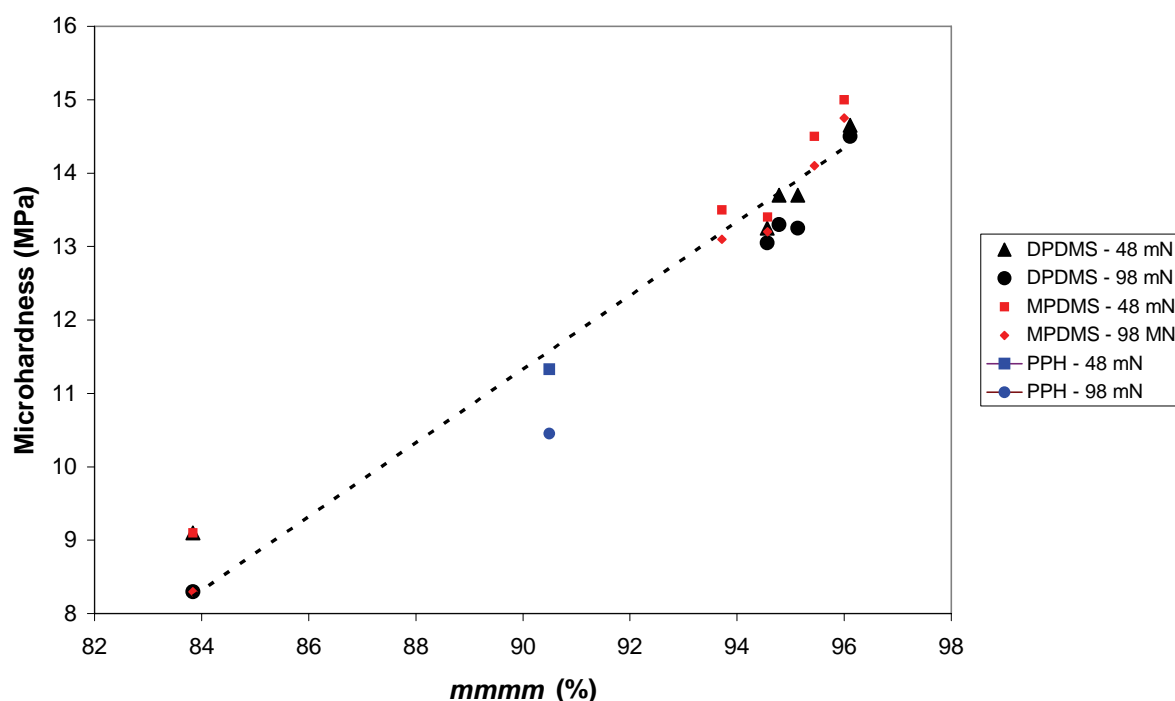
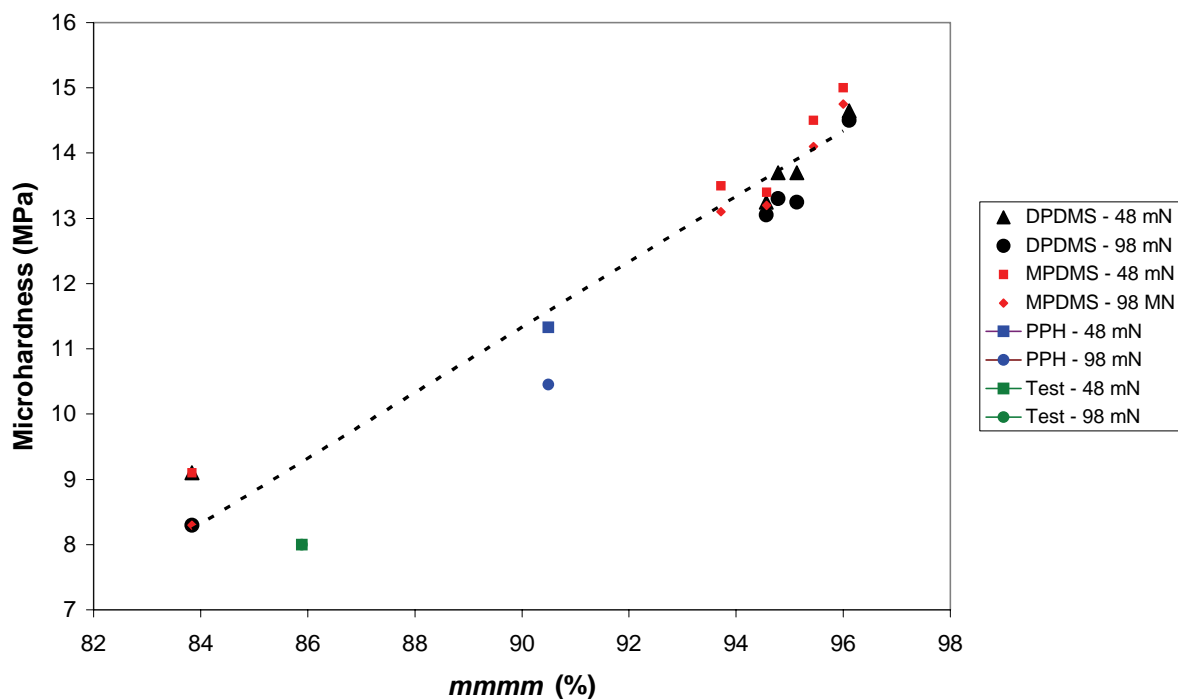


Figure 7.3 The relationship between the *mmmm* pentad content and the microhardness illustrating the position of the PPH sample relative to the other samples.

There would therefore definitely seem to be a correlation between the physical removal of material and the chemical alteration of the composition of a polymer via alteration of the active sites on the catalyst. This is evidenced by the changes in the properties upon addition of external donor to the catalyst system since the addition of the donor reduces the amount of material eluting in specific fractions by converting the active sites from poorly isospecific sites to highly isospecific sites. The fast switching of the active sites between the different types results in the production of chains containing blocks of highly isotactic chains and sequences which are less stereoregular. Long chains containing both types of sequences would be ideal to act as tie molecules, linking up the various crystalline regions with the less stereoregular blocks being excluded from the crystals and located in the inter-crystalline regions. These chains are believed to be found mainly in the medium to high temperature TREF fractions, hence these fractions' importance for polymer properties. Similar effects are obtained by removing certain fractions of a PP sample, thereby altering for example the average *mmmm* pentad content.

Higher average *mmmm* pentad contents lead to increases in the microhardness of the material as demonstrated in Chapter 6. This is illustrated in Figure 7.3 highlighting the microhardness of the PPH sample relative to the other samples, clearly showing the dependence of the microhardness on the average *mmmm* pentad content. The PPH sample has an average *mmmm* pentad content of approximately 90% and as expected the microhardness of this material lies between that of the No ED sample and the samples produced with external donors which all have higher *mmmm* pentad contents. Unfortunately the conditions under which the PPH sample was made are not known due to the commercial nature of the material, however, it is certainly possible, as evidenced by this material, to tailor the reaction conditions and donor loadings to such an extent that the properties of the polymers can be varied between the extremities of those used in this study.



**Figure 7.4** The relationship between the *mmmm* pentad content and the microhardness illustrating the position of the test sample (produced at an external donor/catalyst ratio of 2) relative to the other samples.

The two most important properties of polypropylene which exert the greatest influence on all other properties, namely the tacticity and molar mass, can therefore be tailored via choice of suitable reactions conditions and donor types and loadings. A reaction was also performed at an external donor/catalyst ratio of 2 in order to investigate the region between the ratios of 0 and 4. The microhardness and tacticity correlation of the sample is illustrated in Figure 7.4. With an *mmmm* pentad content of just under 86% the microhardness of the sample is in the region where it is expected. The molar mass of this sample is reasonably high compared to the other samples at approximately 600 kg/mol (due to the fact that the polymerisation was performed in the absence of hydrogen) and this is thought to be the reason for the slight depression in the values compared to the No ED sample since these relatively high molar masses exert an influence on the microhardness as discussed earlier [1]. This sample demonstrates in a single solution how one could alter the polymerisation conditions in order to tailor the properties of the polymer since the external donor added ensures a slightly higher *mmmm* pentad content compared to the No ED sample and the absence of hydrogen results in significantly higher molar mass of the polymer, the combined effect of which is evidenced by the microhardness data.

It is also noteworthy to mention the reciprocal relationship between the hardness of a material, as measured by the microhardness, and the impact properties, a measure of which is

the area of the  $\beta$ -transition of the  $\tan \delta$  DMA curve. This relationship is illustrated in Figure 7.5 for a number of the samples used in this study.

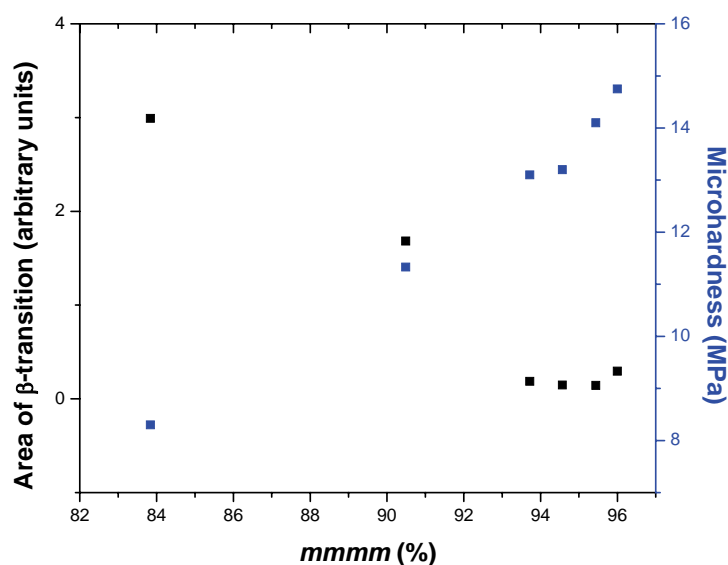


**Figure 7.5** An illustration of the reciprocal relationship between the microhardness and impact properties as measured by the damping ability of a material in DMA.

It is evident that in general the harder the sample, the less is its ability to dissipate energy at low temperature. Knowledge of these trends can prove extremely important, facilitating the tailoring of polymer properties for specific applications for a given polymer-catalyst system.

It was also observed and discussed in Chapter 6 that the molar mass of these important TREF fractions play a key role in determining the storage modulus of the samples. Deconvolution of the molar mass distribution of the PPH sample reveals that the optimum solution is one with only 5 active sites as opposed to the 6 sites found for the rest of the samples indicating a narrower distribution of molecular species. A comparison of the fraction percentage of each type of site for the sample with the 106 – 110 °C fraction removed and the PPH sample is given in Figure 7.6.

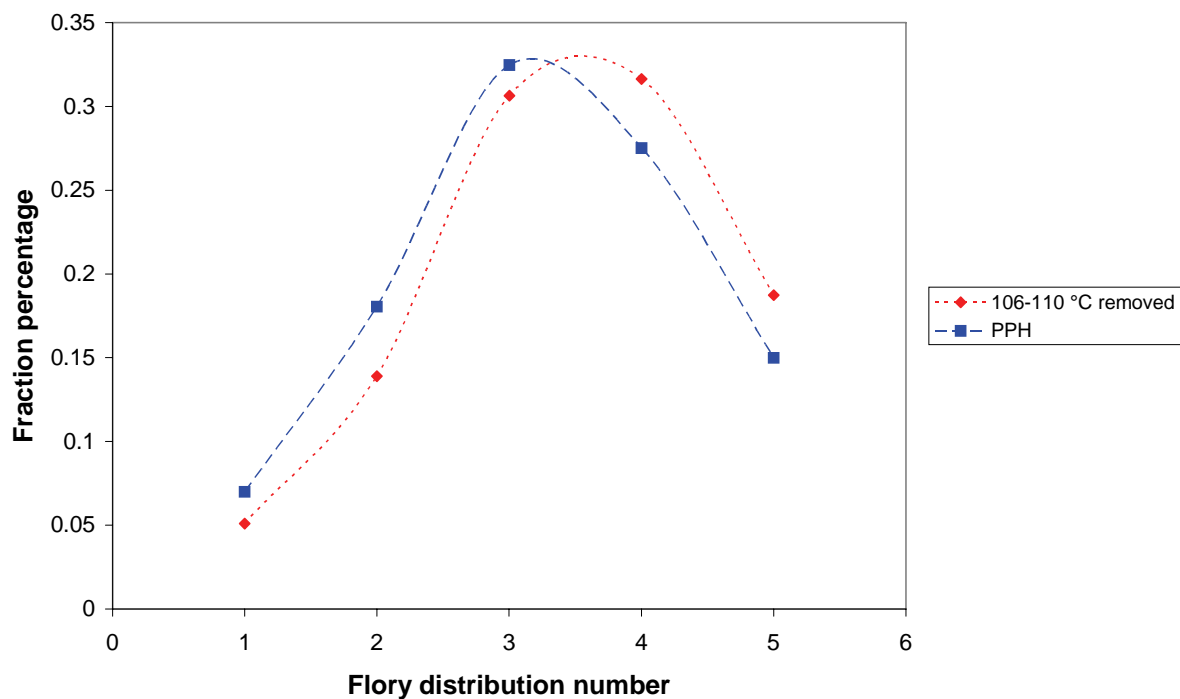


**Figure 7.6** A comparison of the fraction percentage of the different site types responsible for the molar mass distribution of the PPH sample with the 106 – 110 °C fraction removed and the original PPH sample.

The molar mass of the material produced at each site is compared in Figure 7.7.

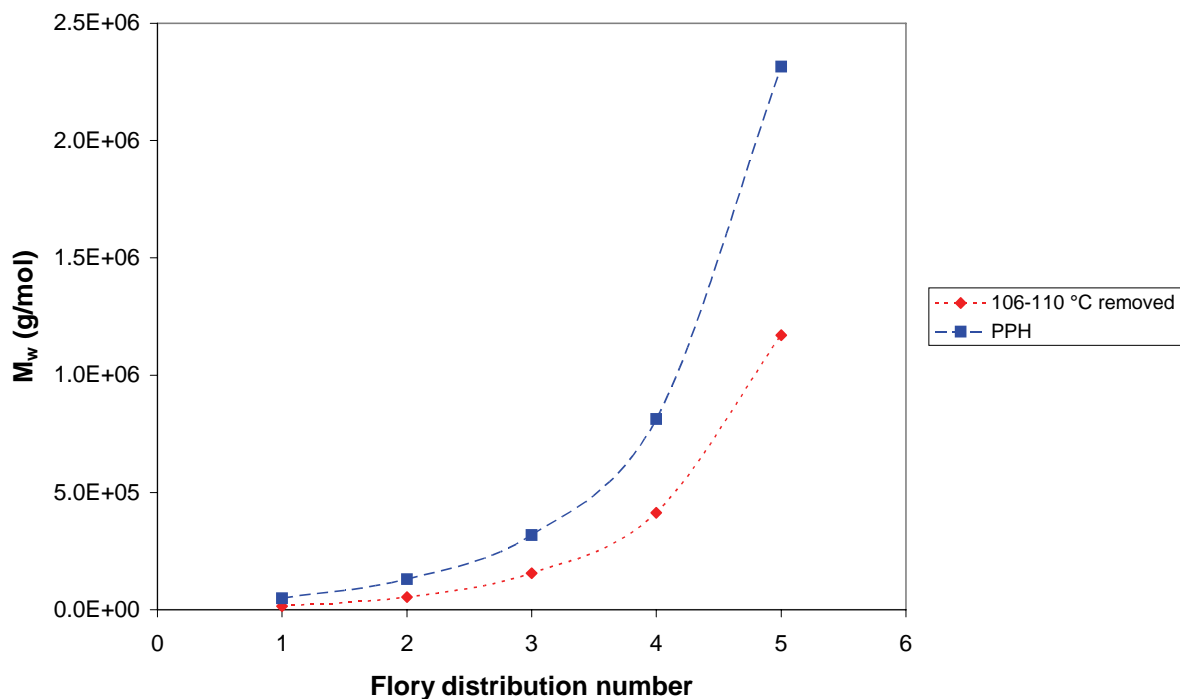


**Figure 7.7** A comparison of the molar mass of the chains produced at each active site type for the sample with the 106 – 110 °C fraction removed and the PPH sample.

It is evident that the proportion of sites producing high molar mass chains is higher for the sample with the 106 – 110 °C fraction removed but that the molar mass of the chains produced at all sites is much higher for the PPH sample. It would therefore seem as if a hypothetical catalyst system, producing the same distribution of molecular species as the PPH sample with the 106 – 110 °C fraction removed, would consist of active sites of lower stereoregularity and therefore lower  $k_p$  but that the proportion of sites producing high molar mass polymer would be slightly higher. This also correlates well with the actually average *mmmm* pentad content of the sample with the 106 – 110 °C fraction removed, since it is significantly lower than that of the PPH sample at approximately 84% compared to the 90% of the PPH sample.

Although the distribution of active sites for the PPH sample cannot be directly compared to that of the rest of the samples, since the number of sites describing the distribution of molecular species is different, one can still compare changes within a given polymer system as illustrated earlier for the PPH sample and the same sample with a fraction removed. Similar changes were also reflected in some of the distributions of the samples produced with and without external donors. This is illustrated in Figure 7.8 which compares the proportion of material produced at each active site for the No ED sample and the DP-3 sample.

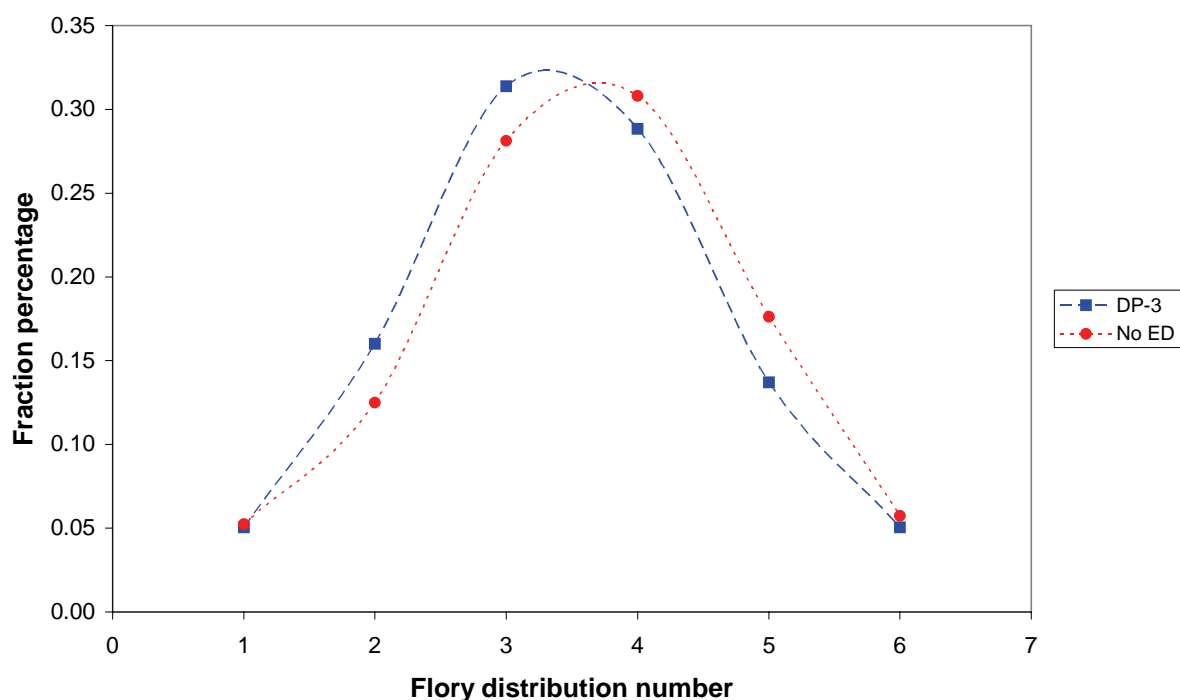


**Figure 7.8** A comparison of the fraction percentage of the different site types responsible for the molar mass distribution of the No ED and DP-3 samples.

The weight average molar mass of the chains produced at each site is illustrated in Figure 7.9.

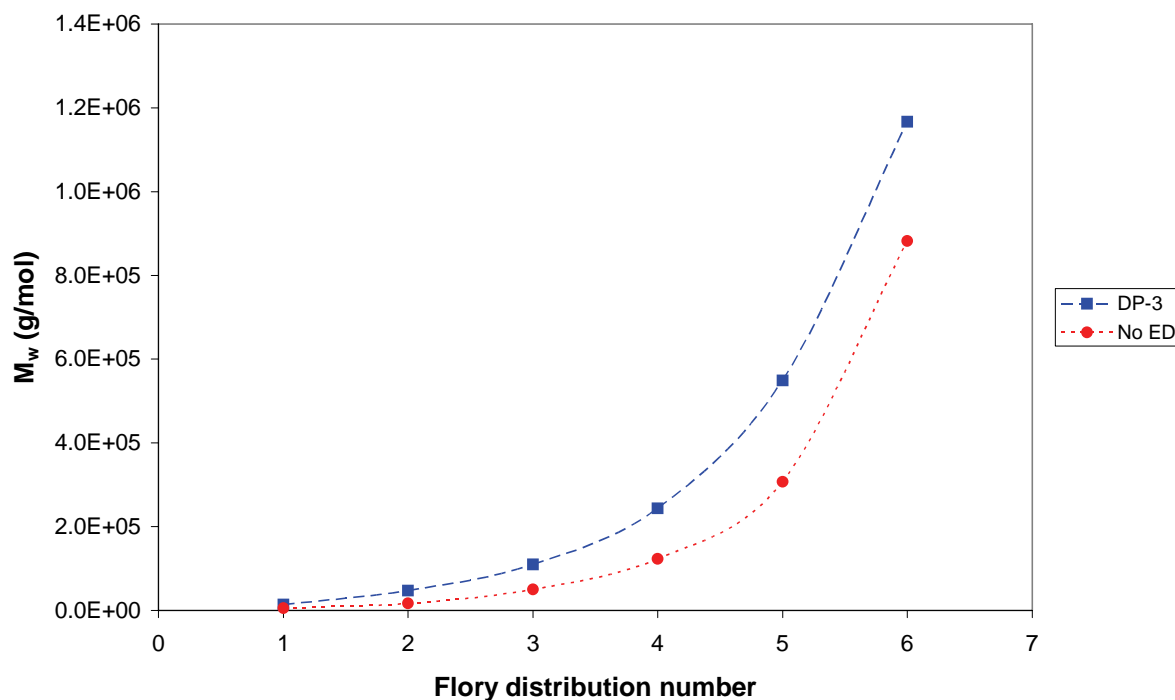


**Figure 7.9** A comparison of the molar mass of the chains produced at each active site type for the No ED and the DP-3 samples.

The DP-3 sample has a considerably higher molar mass and *mmmm* pentad content than the No ED sample and one can immediately see the similarity with the case presented earlier regarding the removal of a fraction from the PPH sample. In both cases the sample with the lower molar mass and lower *mmmm* pentad content was produced by a catalyst consisting of a higher proportion of sites producing higher molar mass chains but that the molar mass of the chains produced at all sites is significantly lower compared to that which was produced at the sites of the higher molar mass sample. Since, for the case of isotactic polypropylene, the higher molar mass is linked to higher stereospecificity at a given active site due to less 2,1 insertions resulting in chain termination, the distribution of chain lengths produced at each of the active sites also gives an indication of the stereospecificity of that particular site.

It is therefore clear that removing a fraction from a material can bring about similar changes in the composition of the material as if the material had been produced with a different catalyst system yielding different active sites. The importance of specific TREF fractions has been emphasised and correlated with the physical properties, both for the case of fraction removal and recombination of residual material and the case of chemical alteration of the active sites, and these methods can be related to one another with similar fractions having

been shown to be important in both cases. It has also been demonstrated that the DPDMS external donor exerts greater influence over the active sites due to its steric bulk and that therefore it is a more effective external donor than the MPDMS.

## **7.2 Recommendations for future work**

Many of the issues surrounding the analysis of the physical properties within this work centre around the amount of material available for analysis and thus it is believed that additional physical property measurement on a small scale could play a major role in assisting with this sort of study. Nanoindentation could prove to be extremely useful method to support the evidence presented here. Small scale impact tests would also provide more useful information on the behaviour of the polymers under this type of test.

For a number of the properties of polymers, such as the crystallinity and crystallisation of the sample, there are simultaneous affects taking place with regards to the effect of factors such as the molar mass and tacticity of the chains. It would be advantageous to further development work in the field, to investigate the magnitude of each effect on factors such as the crystallisation and degree of crystallinity so that one can better understand trends observed during polymer analysis. For example during TREF analysis small changes in the tacticity of the chains can dominate the effect of molar mass but at some point for very small increases in tacticity the molar mass effect becomes important and so this should be investigated further in order to determine the exact crossover points in terms of relative importance of molecular characteristics.

Further work can also be carried out regarding the rate of crystallisation of various samples, both in bulk and in solution, as some interesting trends were observed here and it is believed that more knowledge is required in this area also with regards to simultaneous effects. It would also be interesting to examine the recrystallisation of samples under applied loads in order to observe the effect of different energy absorption mechanisms at work and also to correlate the mechanisms with the nature of the polymer itself and thus with the polymerisation conditions also.

It would also be very interesting to investigate the effect of the addition of certain types of chains to a bulk material. This could also provide valuable insight into the types of chains required to improve polymer properties. Chains with different block lengths of highly isotactic sequences and less stereoregular sequences could be made and added to a standard test material.



The work carried out so far only involved the polypropylene homopolymer, however, there are a number of possibilities in terms of the analysis of copolymers and the effect of different proportions and types of active sites on the incorporation of comonomers into the chains and their subsequent effect on the properties of the material. If this could also be related to specific active sites then this would provide valuable information for tailoring polymers for certain applications requiring for example, lower levels of crystallinity.

On that note a study of this nature would also provide useful information for different catalyst systems with different donor types. Only one type of internal donor was used during this work and two types of external donor, however, the effects of different donor types such as the hindered diethers could also be extremely interesting. It would also be interesting to investigate different donor free catalysts and compare the results obtained with the current data and that obtained using other donor combinations and types. The use of different donors as well as different donor/catalyst ratios would also expand the region of properties being investigated, allowing even more in-depth analysis of the effect of different microstructures on the physical properties.

### 7.3 References

1. Koch, T., Seidler, S., Halwax, E., & Bernstorff, S., *Microhardness of quenched and annealed isotactic polypropylene*. Journal of Materials Science, 2007. **42**: p. 5318-5326.

## Appendix A. HT-GPC data

### A.1 HT-GPC data from Chapter 4

Table A.1 The HT-GPC data for the fractions of the TREF characterisation of the PP1P sample

$T_e$ (°C)	$M_n$ (g/mol)	$M_w$ (g/mol)	PD
25	3.1E+04	2.4E+05	7.7
70	8.5E+04	3.0E+05	3.5
80	1.1E+05	4.3E+05	4.0
90	1.7E+05	5.8E+05	3.3
95	2.7E+05	7.2E+05	2.7
100	2.5E+05	7.6E+05	3.1
105	1.3E+05	6.9E+05	5.1
140	2.1E+05	6.1E+05	2.9

Table A.2 The HT-GPC data for the PP1P samples with selected fractions removed

Temperature range of fraction removed (°C)	$M_n$ (g/mol)	$M_w$ (g/mol)	PD
<25	1.6E+05	5.6E+05	3.6
26-70	1.5E+05	5.5E+05	3.8
71-80	1.5E+05	6.1E+05	4.0
81-90	1.4E+05	5.1E+05	3.8
91-95	1.1E+05	5.0E+05	4.4
96-100	1.4E+05	5.1E+05	3.7
101-105	1.5E+05	5.7E+05	3.7
106-140	1.6E+05	6.0E+05	3.7

Table A.3 The HT-GPC data for the fractions of the TREF characterisation of the PPH sample

$T_e$ (°C)	$M_n$ (g/mol)	$M_w$ (g/mol)	PD
25	2.0E+04	1.1E+05	5.4
90	2.5E+04	1.7E+05	7.1
100	4.7E+04	1.7E+05	3.6
105	7.1E+04	2.3E+05	3.3
110	1.6E+05	4.9E+05	3.1
115	2.1E+05	7.0E+05	3.3
120	1.8E+05	5.2E+05	3.0
140	1.5E+05	4.5E+05	2.9

**Table A.4 The HT-GPC data for the PPH samples with selected fractions removed**

Temperature range of fraction removed (°C)	M <sub>n</sub> (g/mol)	M <sub>w</sub> (g/mol)	PD
<25	8.6E+04	6.0E+05	7.0
26-90	9.9E+04	6.5E+05	6.6
91-100	8.0E+04	6.7E+05	8.3
101-105	7.1E+04	5.5E+05	7.7
106-110	5.9E+04	4.0E+05	6.9
111-115	6.8E+04	3.6E+05	5.3
116-140	8.5E+04	5.4E+05	6.4

## A.2 HT-GPC data from Chapter 5

**Table A.5 The HT-GPC data for the various polymerisations performed**

Polymerisation variable under investigation	Variable	M <sub>n</sub> (g/mol)	M <sub>w</sub> (g/mol)	PD
Catalyst/cocatalyst pretreatment time	0.25 minutes	1.9E+04	4.1E+05	22.0
	2 minutes	1.8E+04	4.1E+05	22.2
	10 minutes	1.4E+04	2.9E+05	20.9
Polymerisation temperature at Al:Ti=20	20 °C	1.3E+05	7.6E+05	5.8
	40 °C	1.1E+05	4.4E+05	1.1
	70 °C	6.2E+04	3.8E+05	6.2
	80 °C	7.3E+04	3.1E+05	4.3
Cocatalyst/catalyst ratio	10	1.5E+05	6.1E+05	4.0
	20	6.2E+04	3.8E+05	6.2
	40	1.3E+05	7.1E+05	5.4
	60	1.0E+05	5.7E+05	5.5
	80	5.0E+04	3.4E+05	6.9
	100	1.6E+04	3.4E+05	20.9
PP Pressure (Mpa)	0.97	3.7E+04	4.0E+05	10.7
	1.46	3.1E+04	3.1E+05	9.9
	1.70	1.9E+04	2.5E+05	13.4
H <sub>2</sub> Pressure (kPa)	0	3.5E+04	4.0E+05	11.6
	10	2.4E+04	2.2E+05	9.2
	20	2.8E+04	2.0E+05	7.0
	60	2.7E+04	1.6E+05	6.2
	100	2.3E+04	1.5E+05	6.6
	400	9.8E+03	1.1E+05	11.0
DPDMS: The Si:Ti ratio at an Al:Ti=20	1.00	1.4E+05	8.6E+05	6.1
	2.94	1.3E+05	4.7E+05	3.6
	4.41	1.4E+05	4.8E+05	3.5
	8.82	2.2E+05	8.3E+05	3.7
	17.65	2.5E+05	1.1E+06	4.4
	40.00	4.0E+05	1.5E+06	3.7
DPDMS: The Si:Ti ratio at an Al:Ti=40	2.00	1.2E+05	6.0E+05	4.8
	5.88	8.8E+04	3.9E+05	4.4
	8.82	2.3E+05	6.9E+05	3.1
	17.65	2.4E+05	7.9E+05	3.4
	35.29	2.3E+05	1.0E+06	4.3

Polymerisation variable under investigation	Variable	M <sub>n</sub> (g/mol)	M <sub>w</sub> (g/mol)	PD
	80.00	3.8E+05	1.3E+06	3.3
DPDMS: The Si:Ti ratio at an Al:Ti=60	3.00	1.7E+05	9.5E+05	5.7
	8.82	2.5E+05	1.0E+06	4.0
	13.23	2.2E+05	8.4E+05	3.8
	26.47	8.7E+04	3.6E+05	4.2
	52.94	1.8E+05	9.0E+05	5.0
	120.00	3.9E+05	1.6E+06	4.3
DPDMS: The Si:Ti ratio at an Al:Ti=80	4.00	2.1E+05	1.0E+06	4.7
	11.76	3.7E+04	3.1E+05	8.2
	17.65	4.0E+04	3.3E+05	8.3
	35.29	7.4E+04	5.1E+05	6.9
	70.58	1.3E+05	5.4E+05	4.1
	176.45	2.5E+05	1.4E+06	5.6
MPDMS: The Si:Ti ratio at Al:Ti=80	88.21	3.9E+05	1.1E+06	2.7
	44.40	3.0E+05	8.0E+05	2.7
	22.05	1.4E+05	7.7E+05	5.5
	14.70	1.4E+05	8.3E+05	5.8
Repeating final reactions to check consistency using DPDMS at Si:Ti = 4	Reaction 1	3.6E+04	2.0E+05	5.4
	Reaction 2	4.6E+04	2.3E+05	5.1
	Reaction 3	4.5E+04	2.2E+05	5.0
	Reaction 4	5.6E+04	2.6E+05	4.7
Repeating final reactions to check consistency using DPDMS at Si:Ti = 8	Reaction 1	6.6E+04	2.9E+05	4.4
	Reaction 2	4.9E+04	2.4E+05	4.9
	Reaction 3	5.6E+04	3.0E+05	5.4
	Reaction 4	4.9E+04	2.6E+05	5.3
Repeating final reactions to check consistency using DPDMS at Si:Ti = 16	Reaction 1	6.3E+04	3.1E+05	5.0
	Reaction 2	5.5E+04	3.0E+05	5.4
	Reaction 3	6.1E+04	2.8E+05	4.7
	Reaction 4	5.8E+04	2.8E+05	4.9
Repeating final reactions to check consistency using DPDMS at Si:Ti = 40	Reaction 1	7.0E+04	3.7E+05	5.3
	Reaction 2	6.4E+04	3.6E+05	5.6
	Reaction 3	6.0E+04	3.2E+05	5.3
	Reaction 4	7.2E+04	3.9E+05	5.4
Repeating final reactions to check consistency using no external donor	Reaction 1	2.1E+04	1.5E+05	7.1
	Reaction 2	2.3E+04	1.6E+05	7.0
	Reaction 3	2.3E+04	1.6E+05	6.9
Repeating final reactions to check consistency using MPDMS at Si:Ti = 4	Reaction 1	2.0E+04	1.6E+05	8.2
	Reaction 2	2.4E+04	1.7E+05	7.1
	Reaction 3	2.1E+04	1.8E+05	8.4
Repeating final reactions to check consistency using MPDMS at Si:Ti = 8	Reaction 1	2.2E+04	1.8E+05	8.4
	Reaction 2	1.9E+04	1.7E+05	8.5
	Reaction 3	2.1E+04	1.8E+05	8.5
Repeating final reactions to check consistency using MPDMS at Si:Ti = 16	Reaction 1	2.5E+04	1.9E+05	7.8
	Reaction 2	2.5E+04	1.9E+05	7.5
	Reaction 3	2.2E+04	1.8E+05	8.5
	Reaction 4	2.3E+04	1.9E+05	8.4
Repeating final reactions to check consistency using MPDMS at Si:Ti = 40	Reaction 1	2.4E+04	2.1E+05	8.8
	Reaction 2	4.0E+04	2.6E+05	6.4

Polymerisation variable under investigation	Variable	M <sub>n</sub> (g/mol)	M <sub>w</sub> (g/mol)	PD
	Reaction 3	4.8E+04	3.0E+05	6.2
	Reaction 4	3.3E+04	2.4E+05	7.4

### A.3 HT-GPC data from Chapter 6

Table A.6 The HT-GPC data of the TREF fractions of sample DP-1

T <sub>e</sub> (°C)	M <sub>n</sub> (g/mol)	M <sub>w</sub> (g/mol)	PD
25	2.8E+03	1.9E+04	6.8
60	7.3E+03	5.0E+04	6.8
80	4.1E+03	4.1E+04	10.0
100	1.1E+04	3.7E+04	3.2
105	1.7E+04	4.6E+04	2.7
110	2.3E+04	7.5E+04	3.2
115	4.6E+04	1.9E+05	4.2
120	8.0E+04	3.2E+05	3.9
140	7.7E+04	2.9E+05	3.8

Table A.7 The HT-GPC data of the TREF fractions of sample DP-2

T <sub>e</sub> (°C)	M <sub>n</sub> (g/mol)	M <sub>w</sub> (g/mol)	PD
25	3.7E+03	3.4E+04	9.2
60	3.9E+03	4.1E+04	10.4
80	4.5E+03	4.5E+04	9.8
100	1.3E+04	5.1E+04	3.8
105	2.2E+04	6.4E+04	2.9
110	3.4E+04	1.1E+05	3.2
115	6.7E+04	2.8E+05	4.1
120	8.1E+04	3.1E+05	3.8
140	6.7E+04	2.6E+05	3.8

Table A.8 The HT-GPC data of the TREF fractions of sample DP-3

T <sub>e</sub> (°C)	M <sub>n</sub> (g/mol)	M <sub>w</sub> (g/mol)	PD
25	3.8E+03	3.4E+04	8.9
60	2.4E+03	3.3E+04	13.8
80	3.6E+03	3.9E+04	10.6
100	1.4E+04	4.3E+04	3.0
105	2.1E+04	5.4E+04	2.5
110	3.0E+04	9.3E+04	3.1
115	5.7E+04	2.1E+05	3.7
120	6.8E+04	2.5E+05	3.7
140	6.1E+04	2.4E+05	4.0

**Table A.9 The HT-GPC data of the TREF fractions of sample DP-4**

$T_e$ (°C)	$M_n$ (g/mol)	$M_w$ (g/mol)	PD
25	1.5E+03	7.1E+03	4.7
60	4.0E+03	3.0E+04	7.5
80	3.9E+03	3.5E+04	8.8
100	1.2E+04	3.8E+04	3.2
105	1.8E+04	4.7E+04	2.5
110	2.9E+04	8.6E+04	3.0
115	5.6E+04	2.3E+05	4.1
120	6.2E+04	2.7E+05	4.3
140	5.7E+04	2.3E+05	4.0

**Table A.10 The HT-GPC data of the TREF fractions of sample No ED**

$T_e$ (°C)	$M_n$ (g/mol)	$M_w$ (g/mol)	PD
25	4.4E+03	3.2E+04	7.2
60	6.2E+03	4.9E+04	7.9
80	1.3E+04	5.4E+04	4.2
100	1.6E+04	5.0E+04	3.0
105	2.7E+04	7.7E+04	2.9
110	4.7E+04	1.7E+05	3.7
115	6.3E+04	2.6E+05	5.1
120	6.1E+04	2.1E+05	3.4
140	5.6E+04	1.9E+05	3.3

**Table A.11 The HT-GPC data of the TREF fractions of sample MP-1**

$T_e$ (°C)	$M_n$ (g/mol)	$M_w$ (g/mol)	PD
25	4.2E+03	4.5E+04	10.8
60	6.1E+03	4.7E+04	7.7
80	7.3E+03	4.0E+04	5.5
100	1.3E+04	3.9E+04	3.0
105	2.4E+04	6.4E+04	2.7
110	4.0E+04	1.4E+05	3.5
115	8.1E+04	3.3E+05	4.1
120	7.7E+04	3.2E+05	4.1
140	5.0E+04	2.5E+05	5.0

**Table A.12 The HT-GPC data of the TREF fractions of sample MP-2**

$T_e$ (°C)	$M_n$ (g/mol)	$M_w$ (g/mol)	PD
25	1.6E+03	1.4E+04	8.9
60	2.3E+03	2.0E+04	8.6
80	3.5E+03	1.9E+04	5.5
100	8.4E+03	2.1E+04	2.5
105	1.4E+04	3.7E+04	2.7
110	2.4E+04	1.1E+05	4.4
115	4.5E+04	2.3E+05	5.1
120	5.1E+04	2.5E+05	4.9
140	5.0E+04	2.3E+05	5.6

**Table A.13 The HT-GPC data of the TREF fractions of sample MP-3**

$T_e$ (°C)	$M_n$ (g/mol)	$M_w$ (g/mol)	PD
25	2.3E+03	1.1E+04	4.8
60	3.1E+03	4.4E+04	14.0
80	3.9E+03	3.2E+04	8.2
100	9.3E+03	3.0E+04	3.3
105	1.7E+04	4.5E+04	2.7
110	2.4E+04	8.1E+04	3.3
115	5.1E+04	2.6E+05	5.0
120	4.6E+04	2.2E+05	4.8
140	5.2E+04	2.3E+05	4.4

**Table A.14 The HT-GPC data of the TREF fractions of sample MP-4**

$T_e$ (°C)	$M_n$ (g/mol)	$M_w$ (g/mol)	PD
25	1.7E+03	1.6E+04	9.3
60	2.7E+03	2.8E+04	10.4
80	3.3E+03	2.7E+04	8.1
100	9.4E+03	3.1E+04	3.3
105	1.5E+04	4.1E+04	2.7
110	2.3E+04	8.6E+04	3.8
115	4.2E+04	2.3E+05	5.5
120	4.9E+04	2.4E+05	4.9
140	5.3E+04	2.4E+05	4.6

## A.4 HT-GPC data from Chapter 7

**Table A.15 The HT-GPC data for the test sample**

Sample	$M_n$ (g/mol)	$M_w$ (g/mol)	PD
Test	1.2E+05	6.0E+05	4.83

## Appendix B. $^{13}\text{C}$ NMR data

### B.1 $^{13}\text{C}$ NMR data from Chapter 4

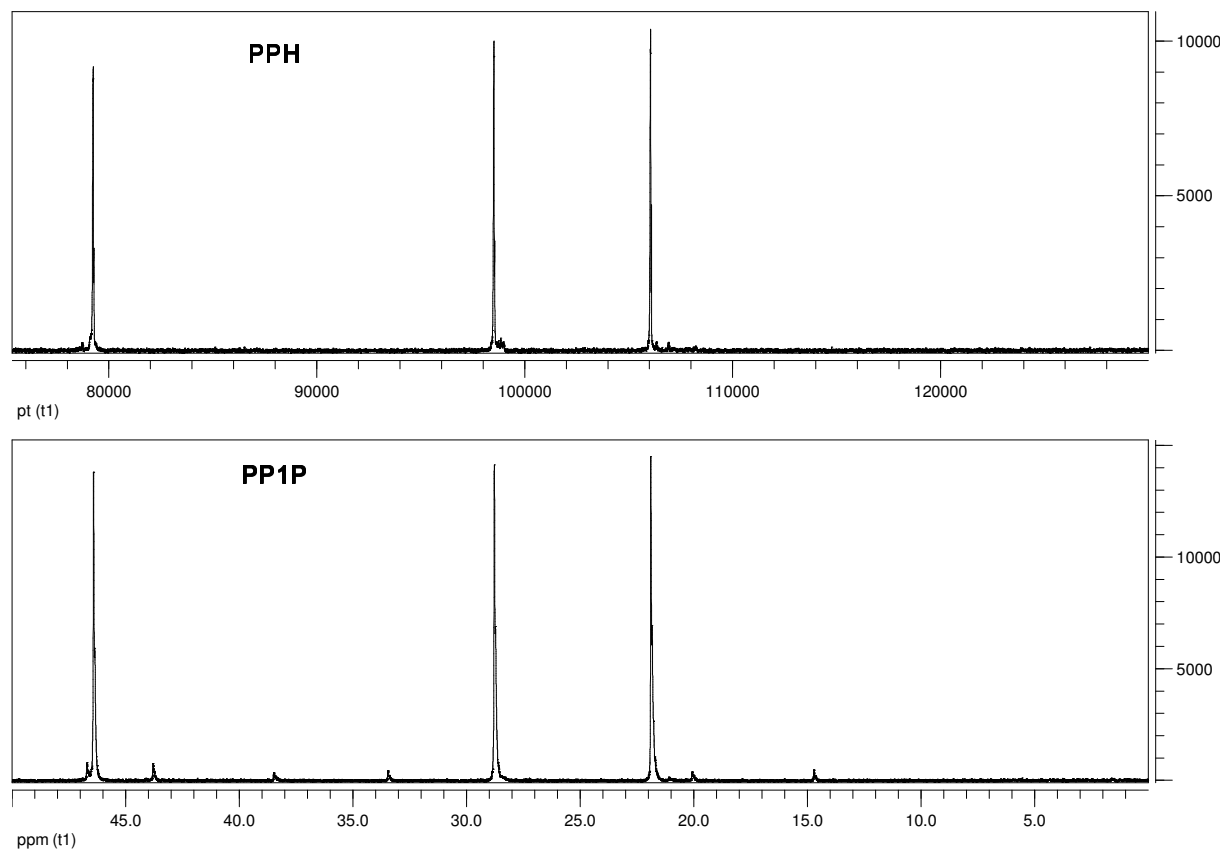


Figure B.1 The  $^{13}\text{C}$  NMR spectra of the PPH and PP1P samples.



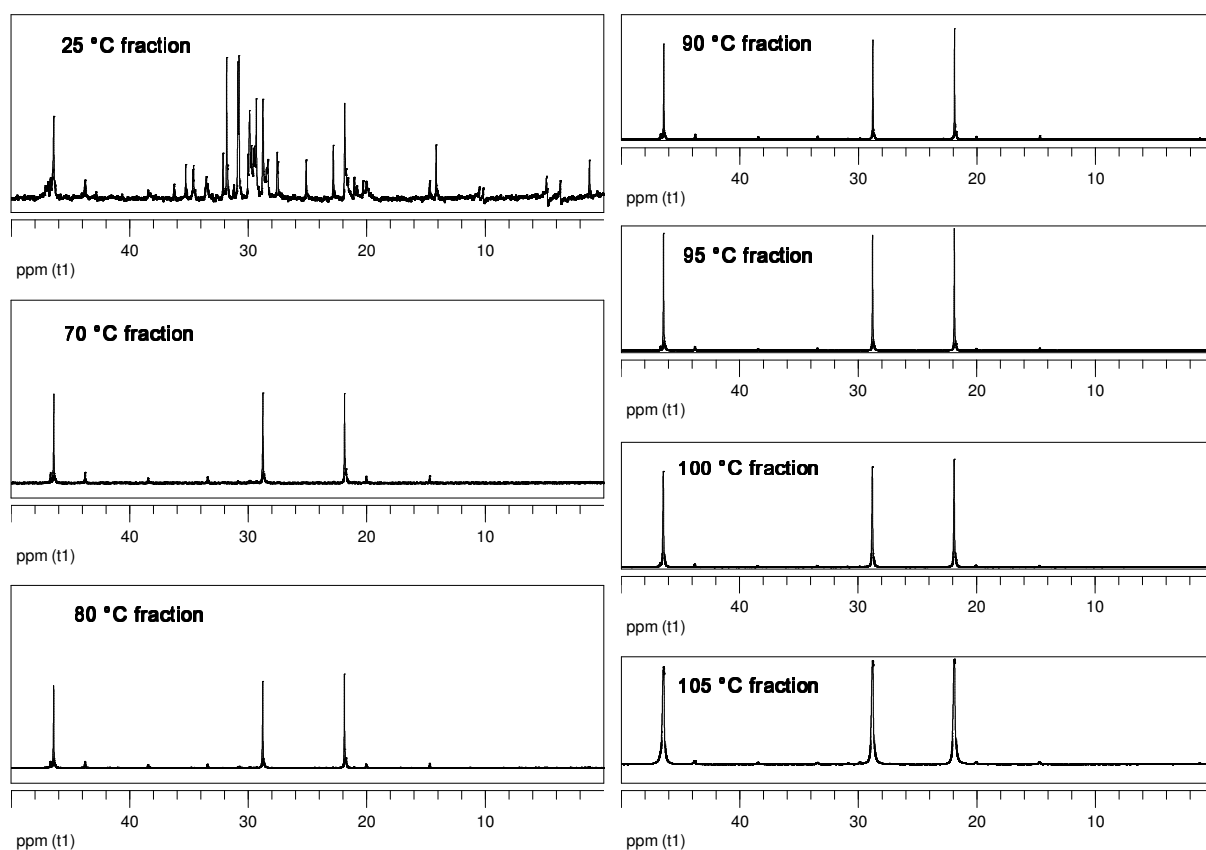


Figure B.2 The  $^{13}\text{C}$  NMR spectra for the TREF fractions of the PPIP sample.

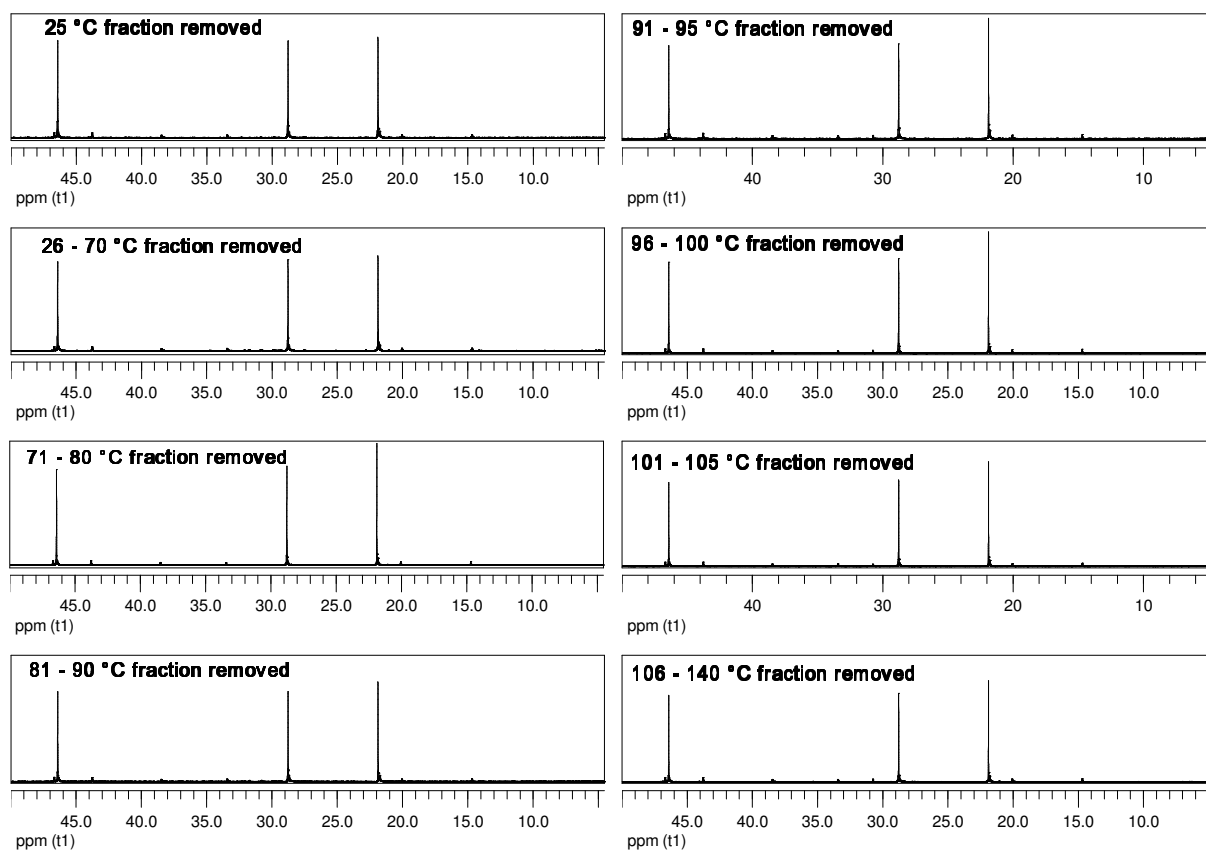


Figure B.3 The  $^{13}\text{C}$  NMR spectra for the PPIP samples with specific TREF fractions removed.

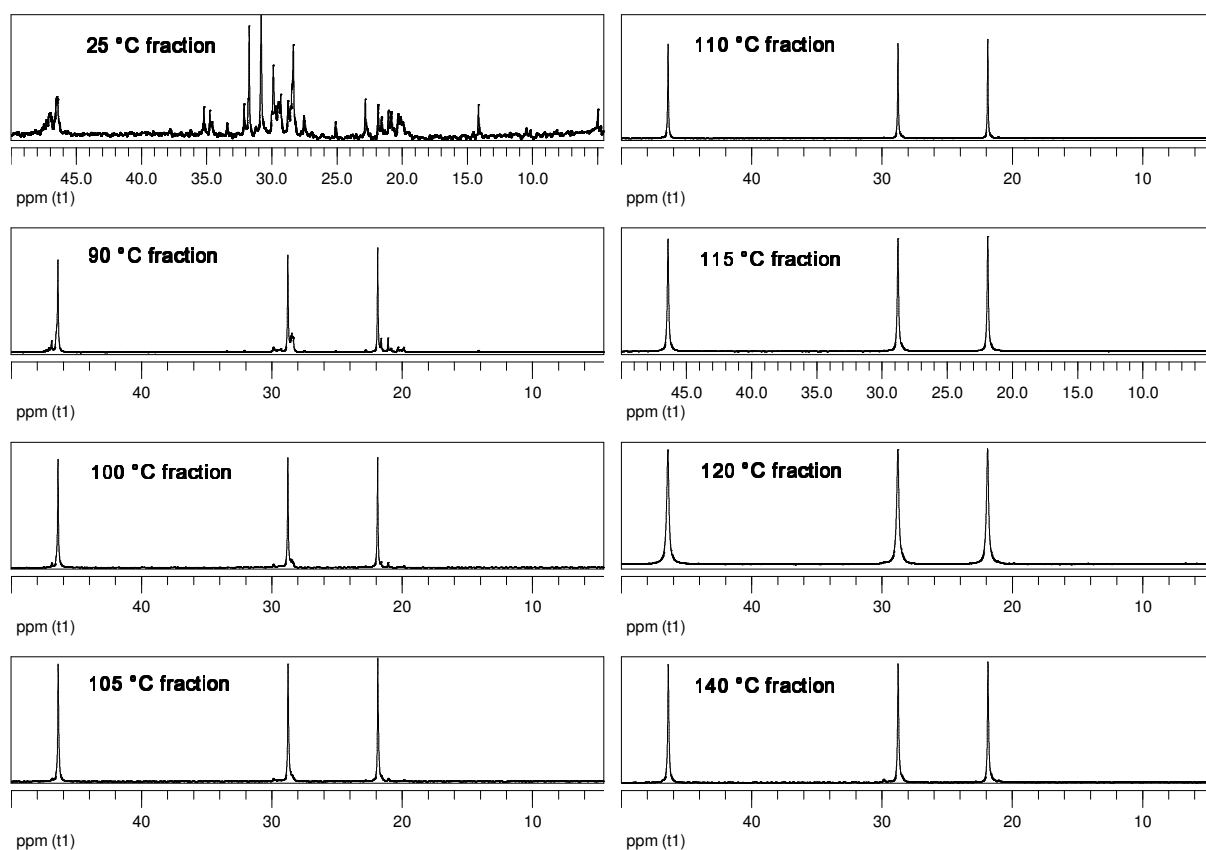


Figure B.4 The  $^{13}\text{C}$  NMR spectra for the TREF fractions of the PPH sample.

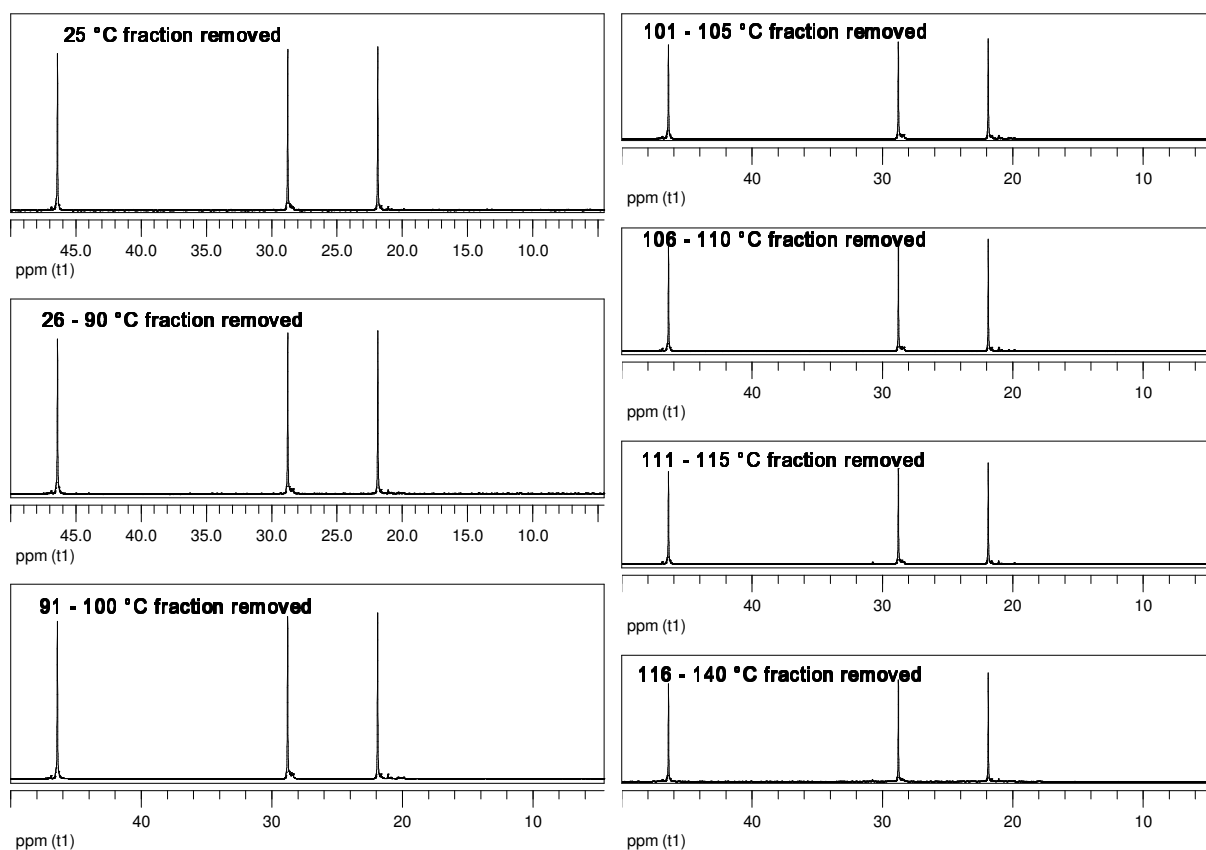


Figure B.5 The  $^{13}\text{C}$  NMR spectra for the PPH samples with specific TREF fractions removed.

## B.2 $^{13}\text{C}$ NMR data from Chapter 5

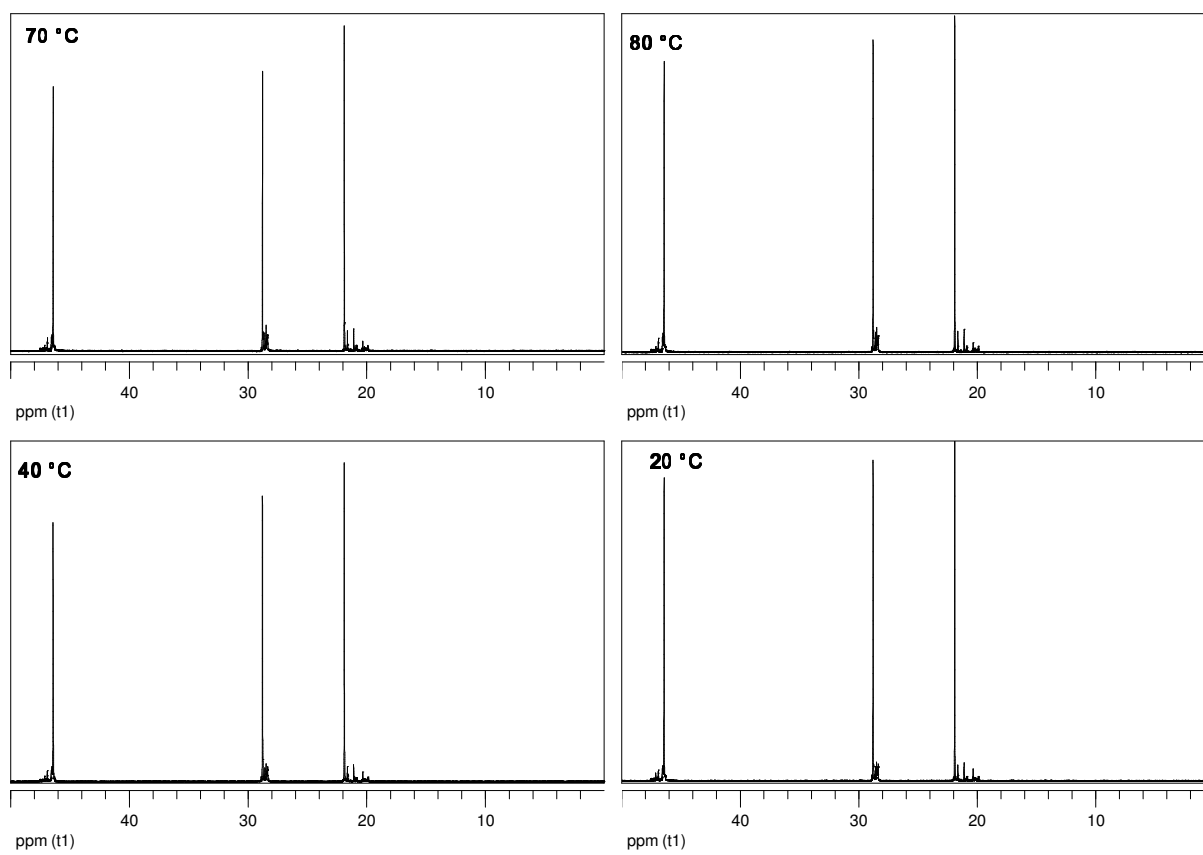


Figure B.6 The  $^{13}\text{C}$  NMR spectra for the polymerisations conducted at various temperatures at an Al:Ti = 20.

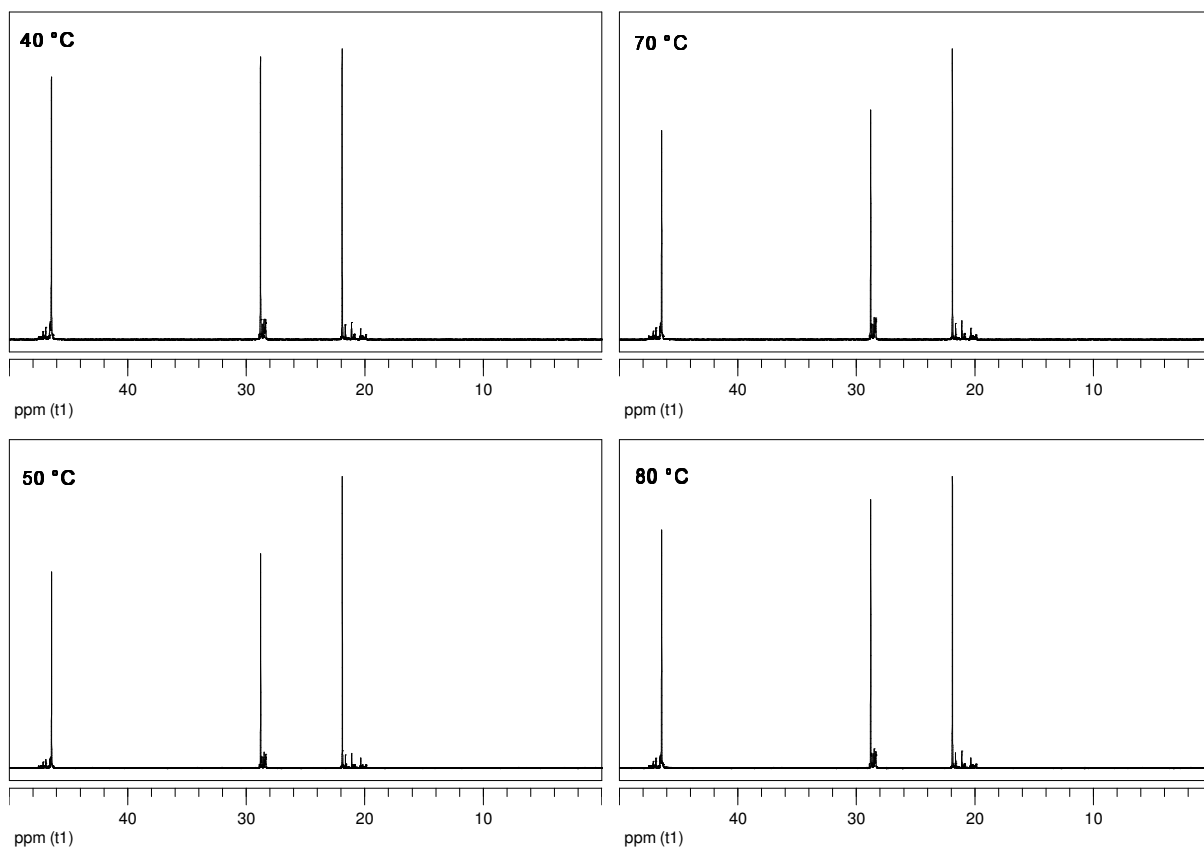


Figure B.7 The  $^{13}\text{C}$  NMR spectra for the polymerisations conducted at various temperatures at an Al:Ti = 80.

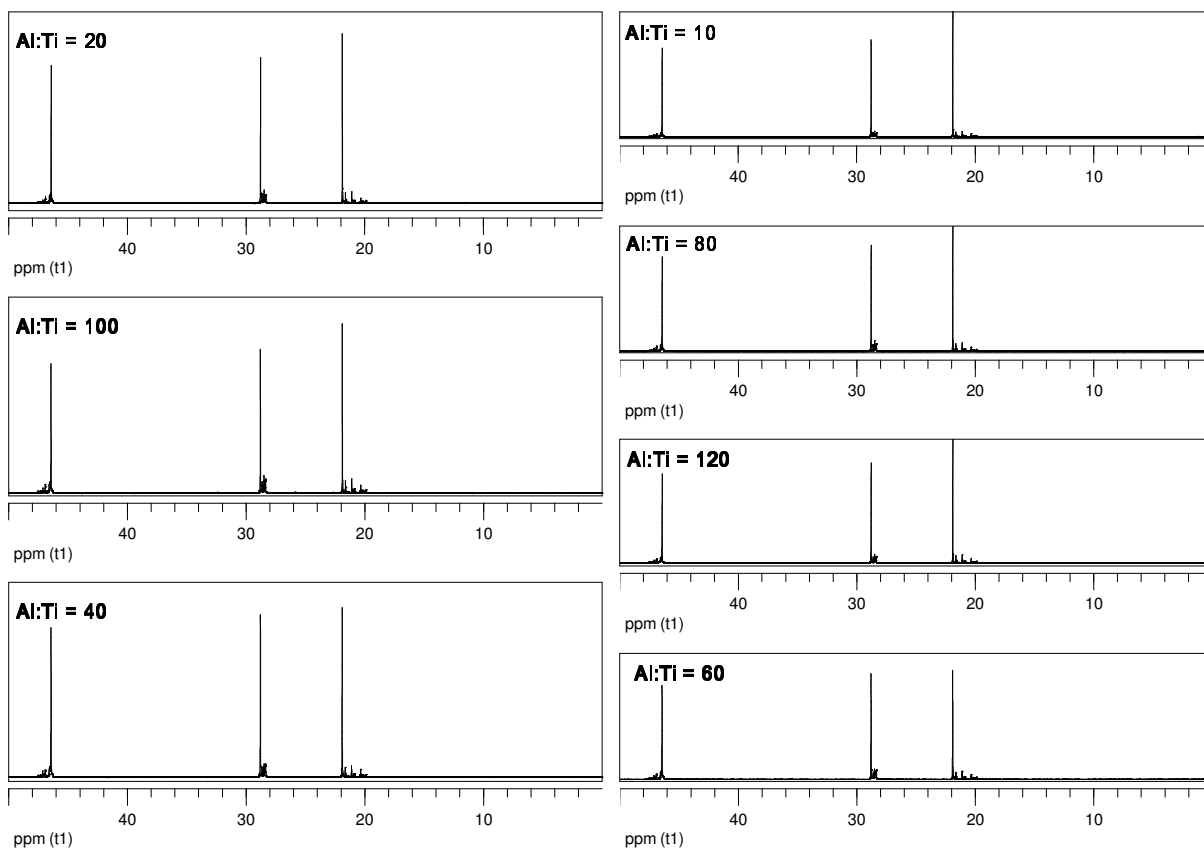
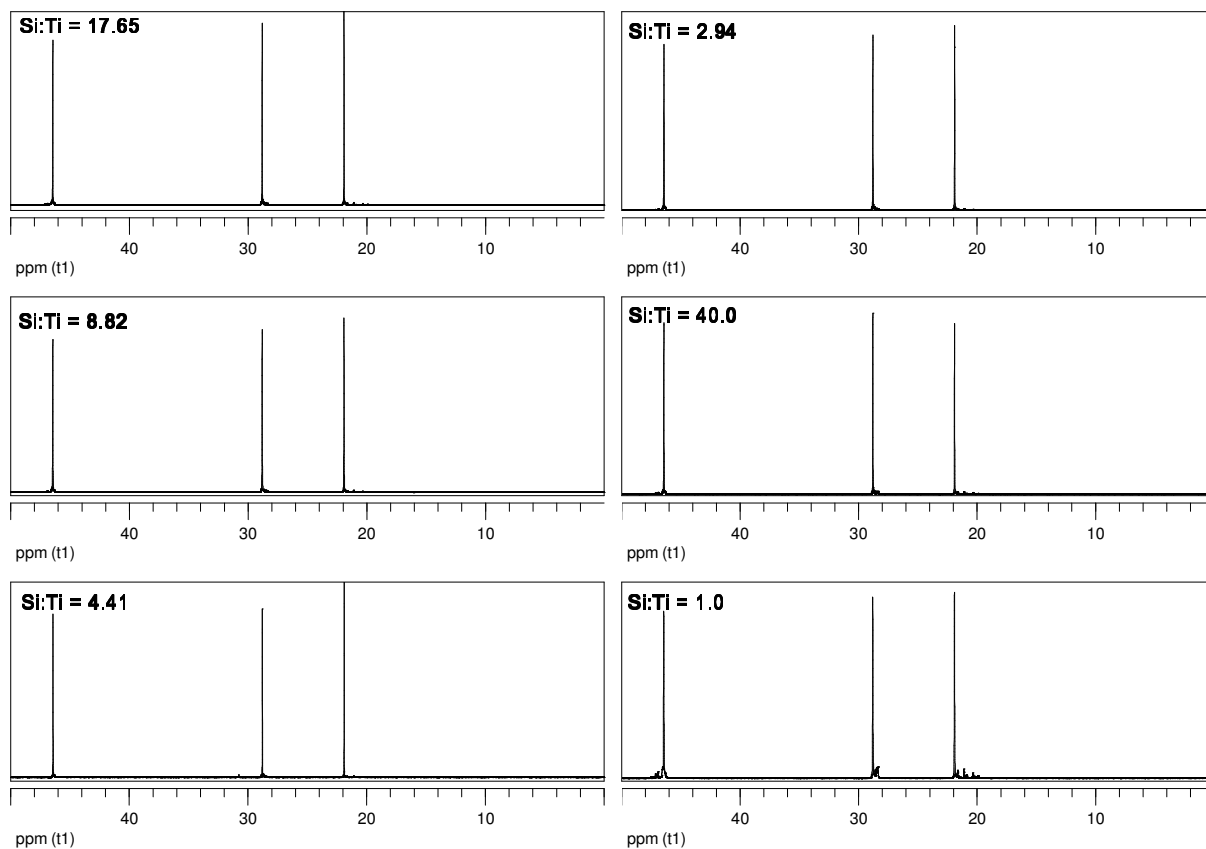
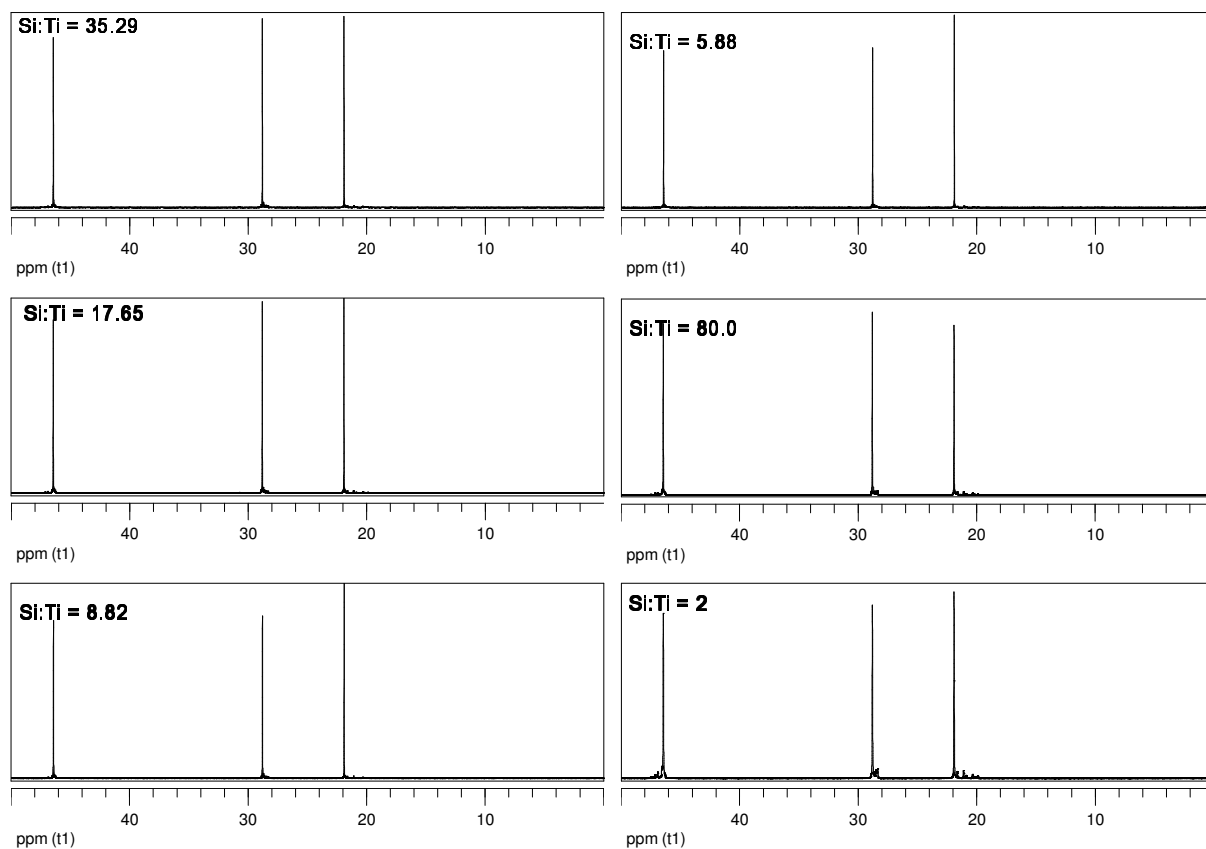


Figure B.8 The  $^{13}\text{C}$  NMR spectra for the polymerisations conducted at various cocatalyst/catalyst ratios.



**Figure B.9** The  $^{13}\text{C}$  NMR spectra for the polymerisations conducted using DPDMS at varying external donor/catalyst ratios at an Al:Ti = 20.



**Figure B.10** The  $^{13}\text{C}$  NMR spectra for the polymerisations conducted using DPDMS at varying external donor/catalyst ratios at an Al:Ti = 40.

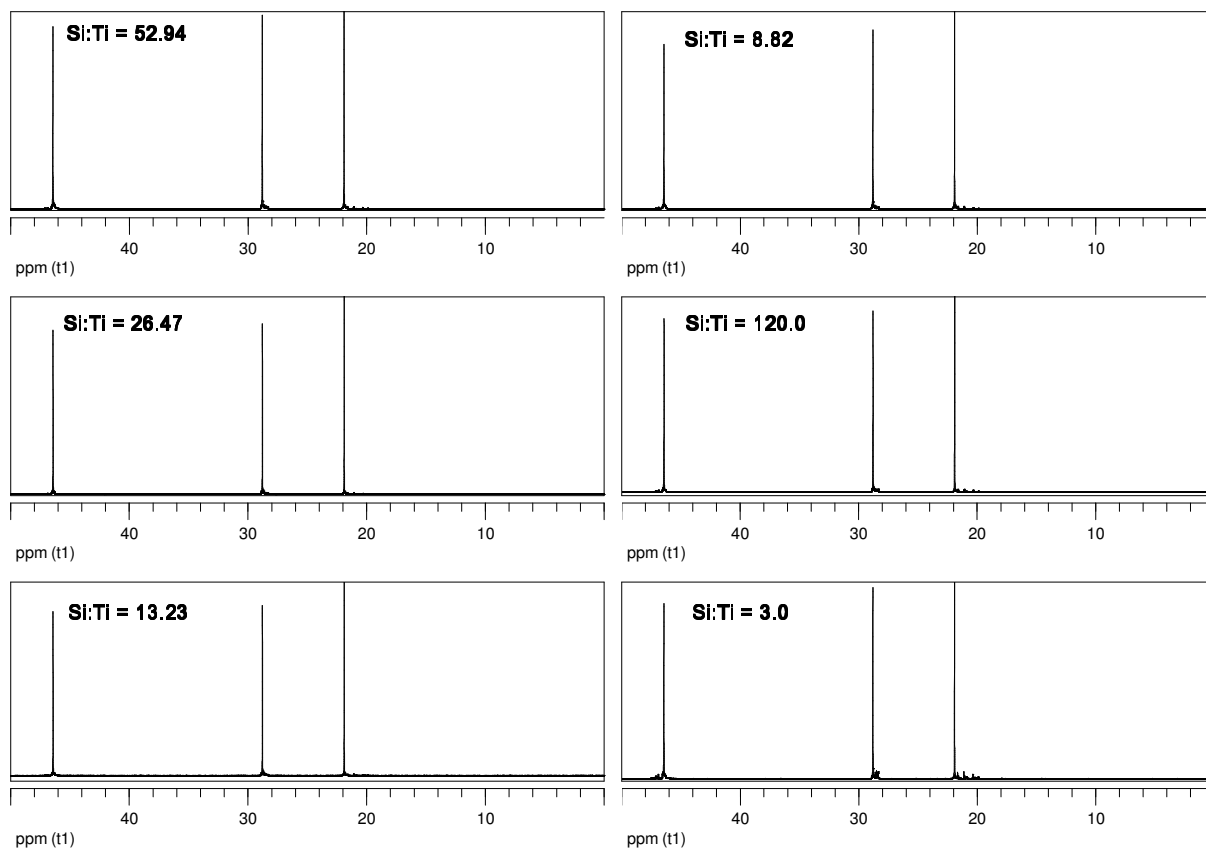


Figure B.11 The  $^{13}\text{C}$  NMR spectra for the polymerisations conducted using DPDMS at varying external donor/catalyst ratios at an Al:Ti = 60.

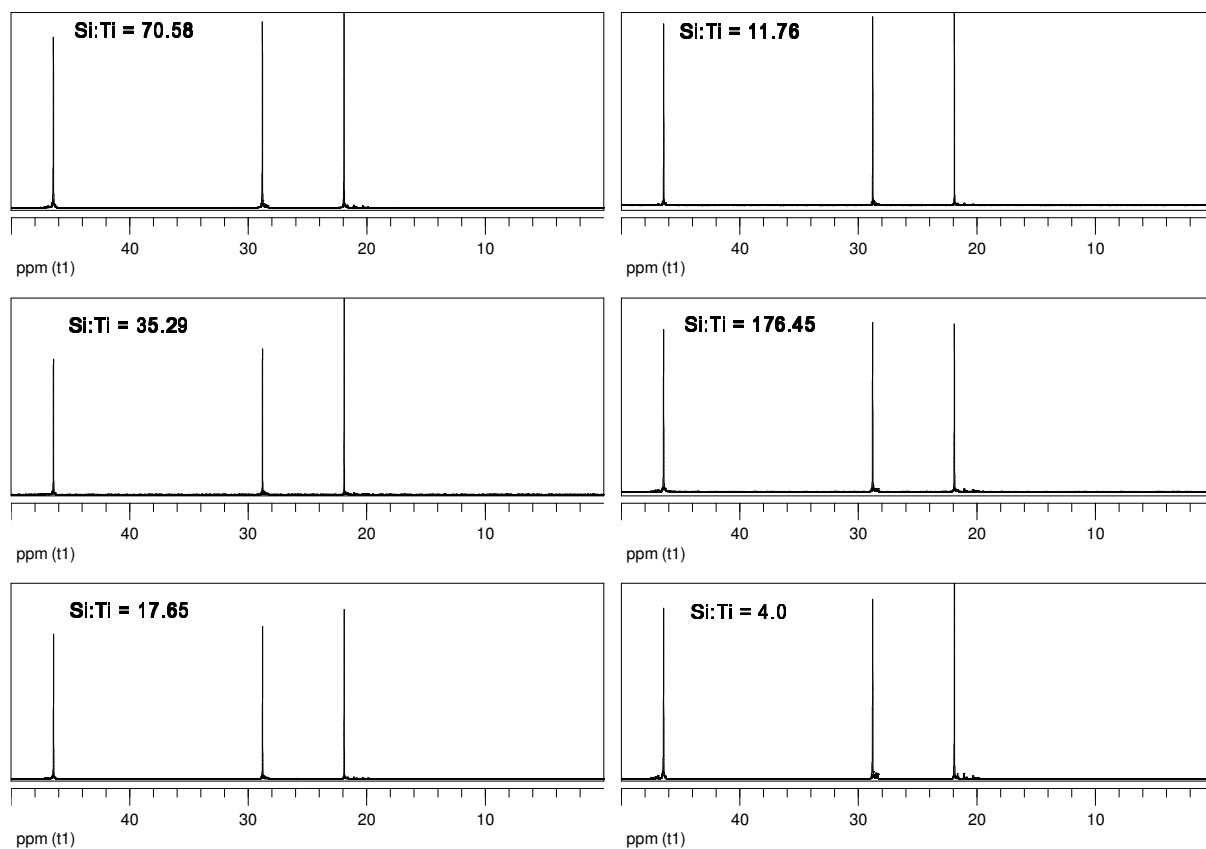
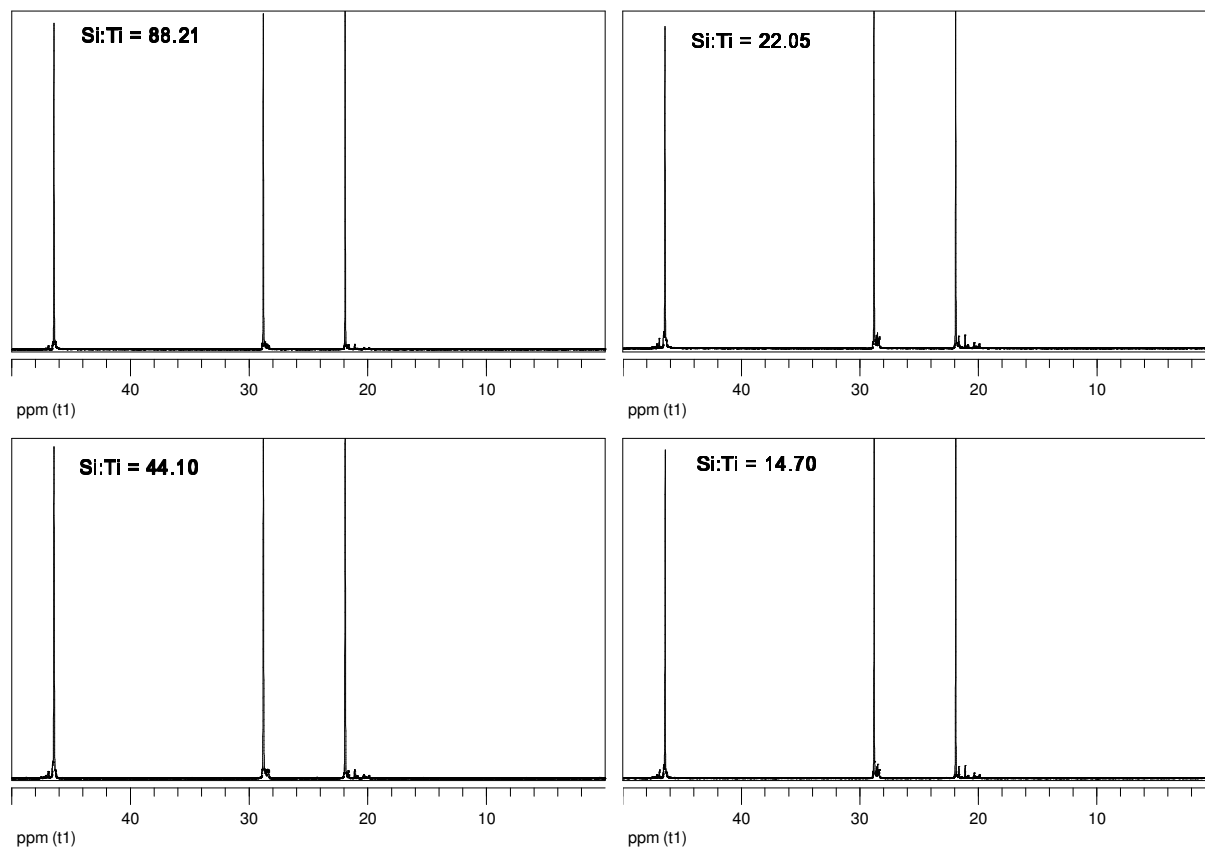


Figure B.12 The  $^{13}\text{C}$  NMR spectra for the polymerisations conducted using DPDMS at varying external donor/catalyst ratios at an Al:Ti = 80.



**Figure B.13** The  $^{13}\text{C}$  NMR spectra for the polymerisations conducted using MPDMS at varying external donor/catalyst ratios at an Al:Ti = 80.

## B.3 $^{13}\text{C}$ NMR data from Chapter 6

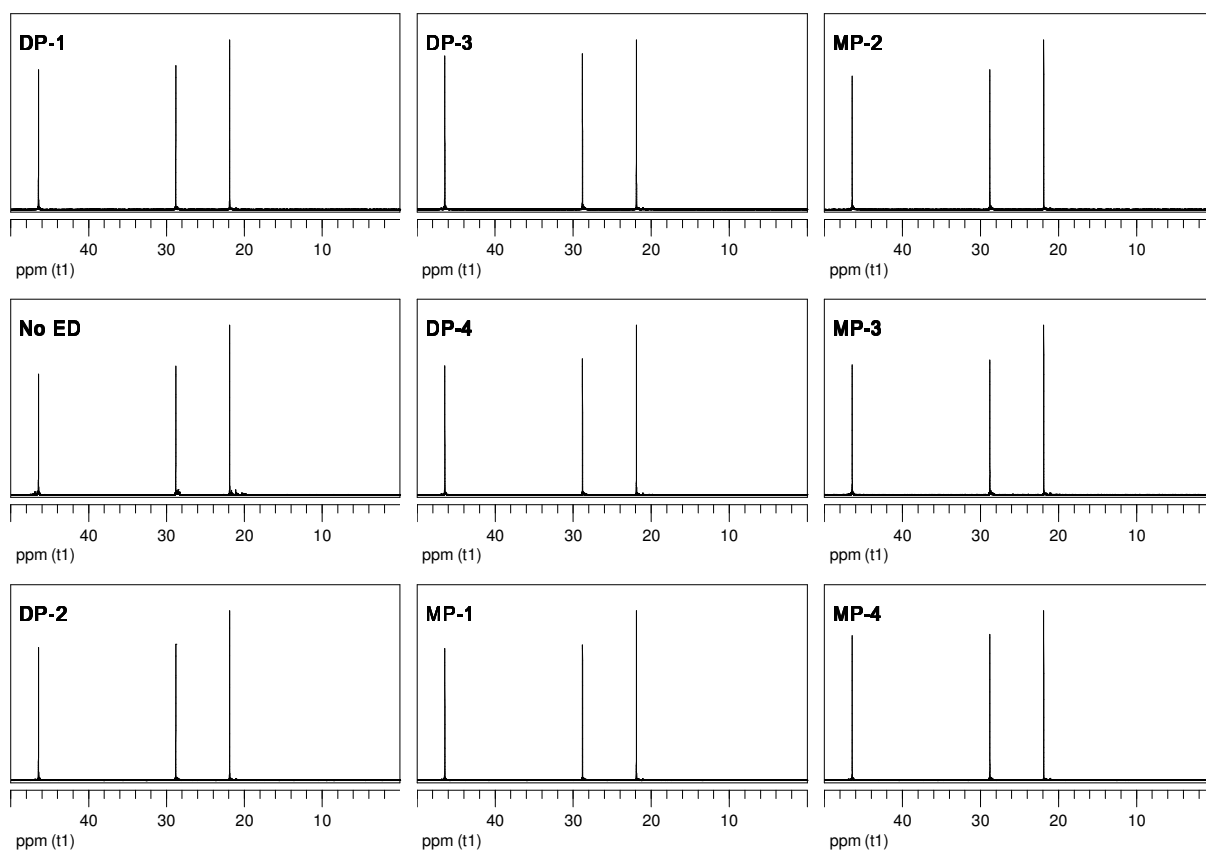


Figure B.14 The  $^{13}\text{C}$  NMR spectra for the polymerisations used for in-depth analysis.



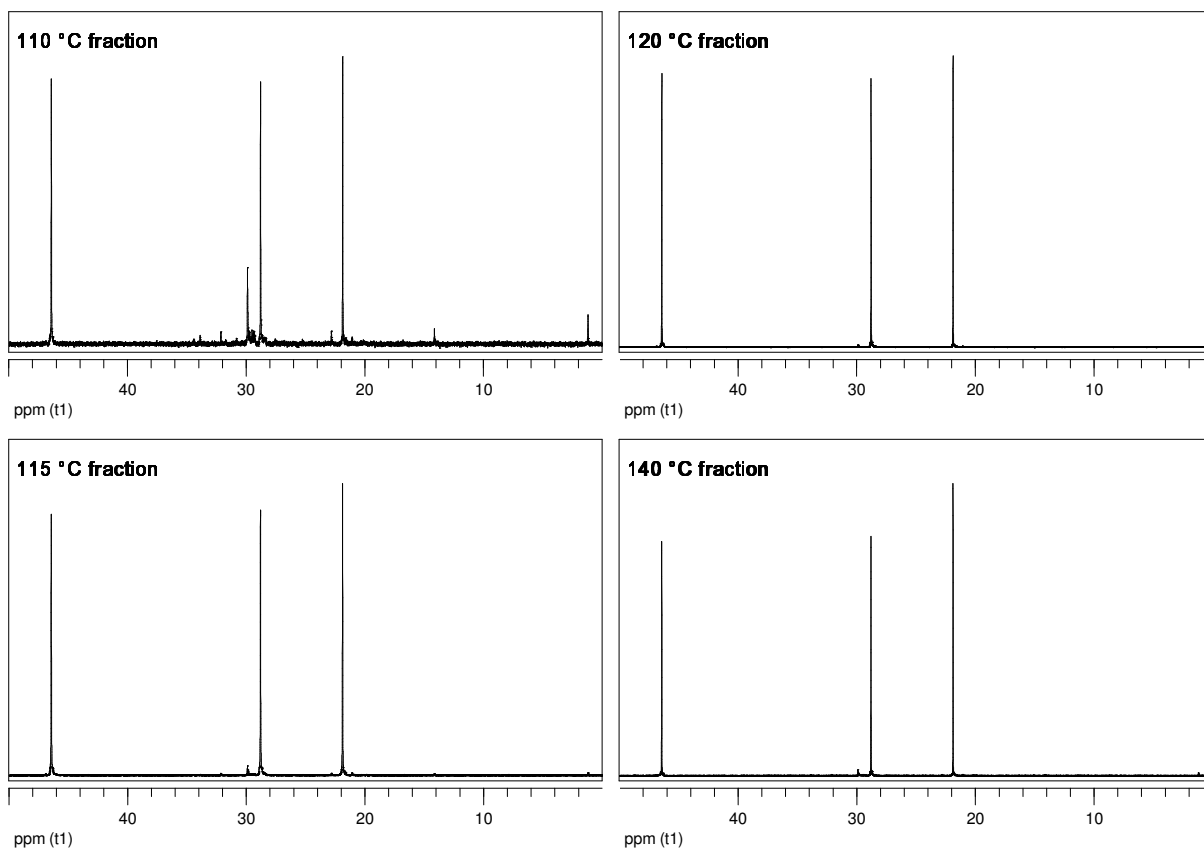


Figure B.15 The  $^{13}\text{C}$  NMR spectra for selected TREF fractions of sample DP-1.

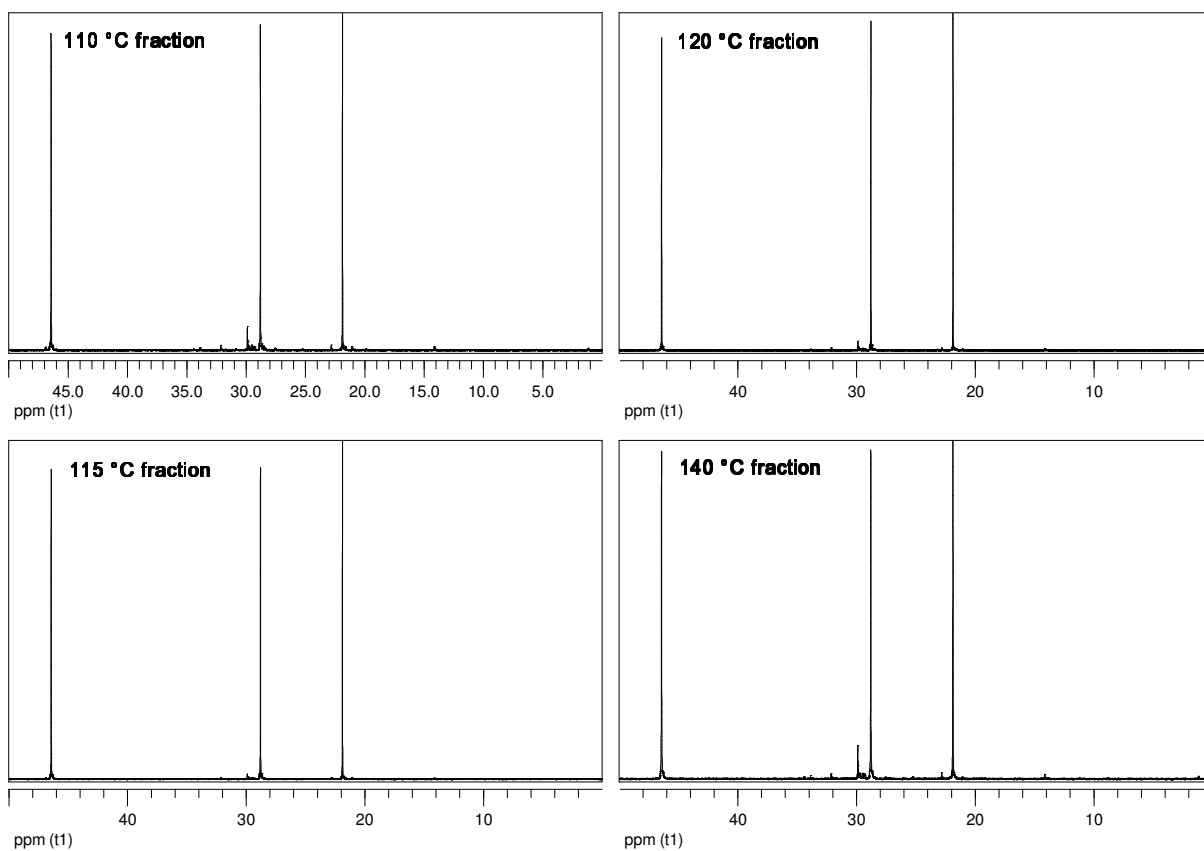


Figure B.16 The  $^{13}\text{C}$  NMR spectra for selected TREF fractions of sample DP-2.

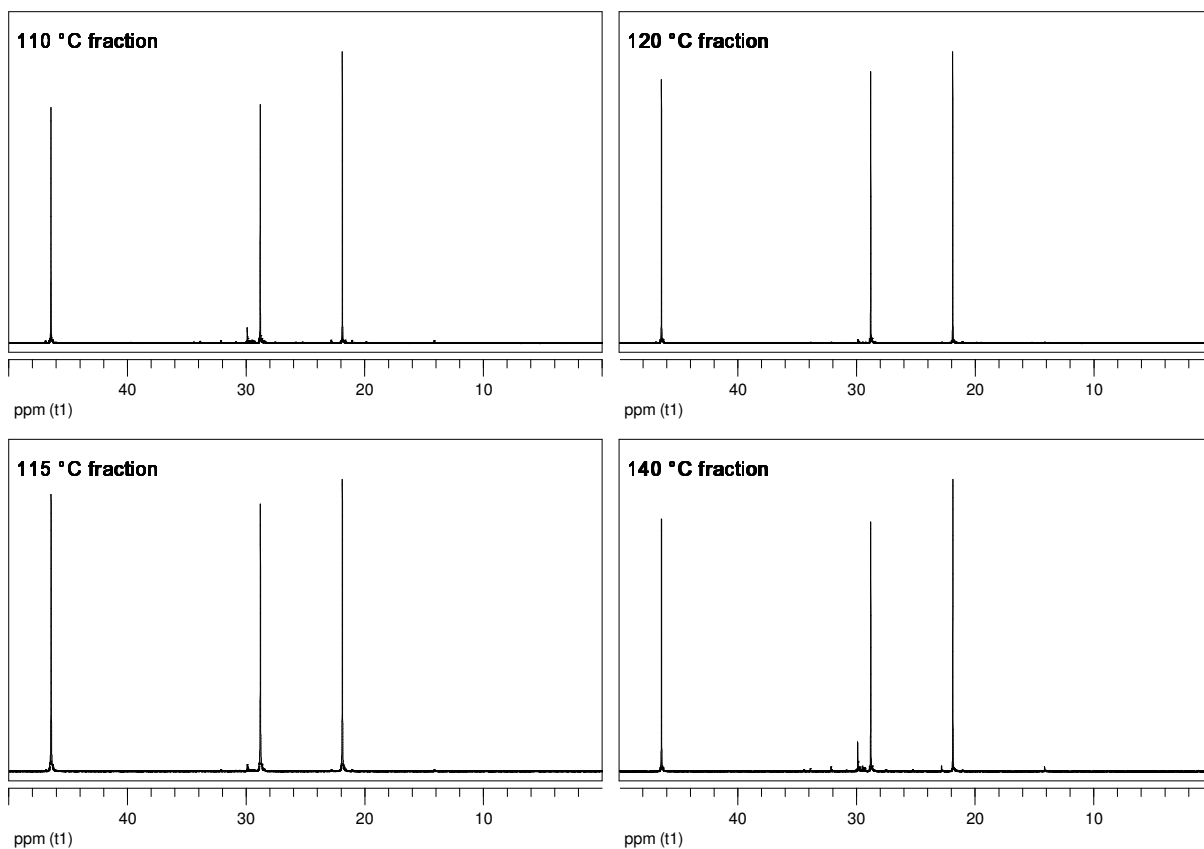


Figure B.17 The  $^{13}\text{C}$  NMR spectra for selected TREF fractions of sample DP-3.

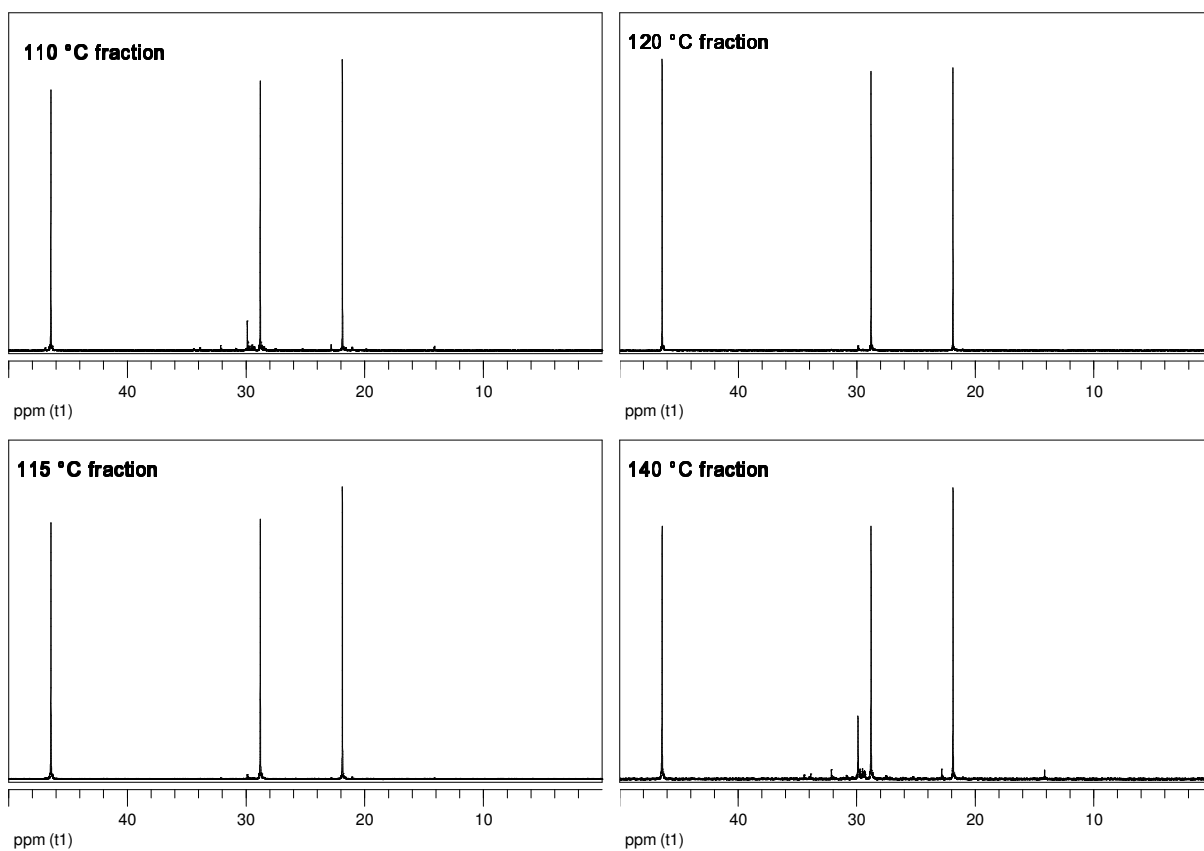


Figure B.18 The  $^{13}\text{C}$  NMR spectra for selected TREF fractions of sample DP-4.

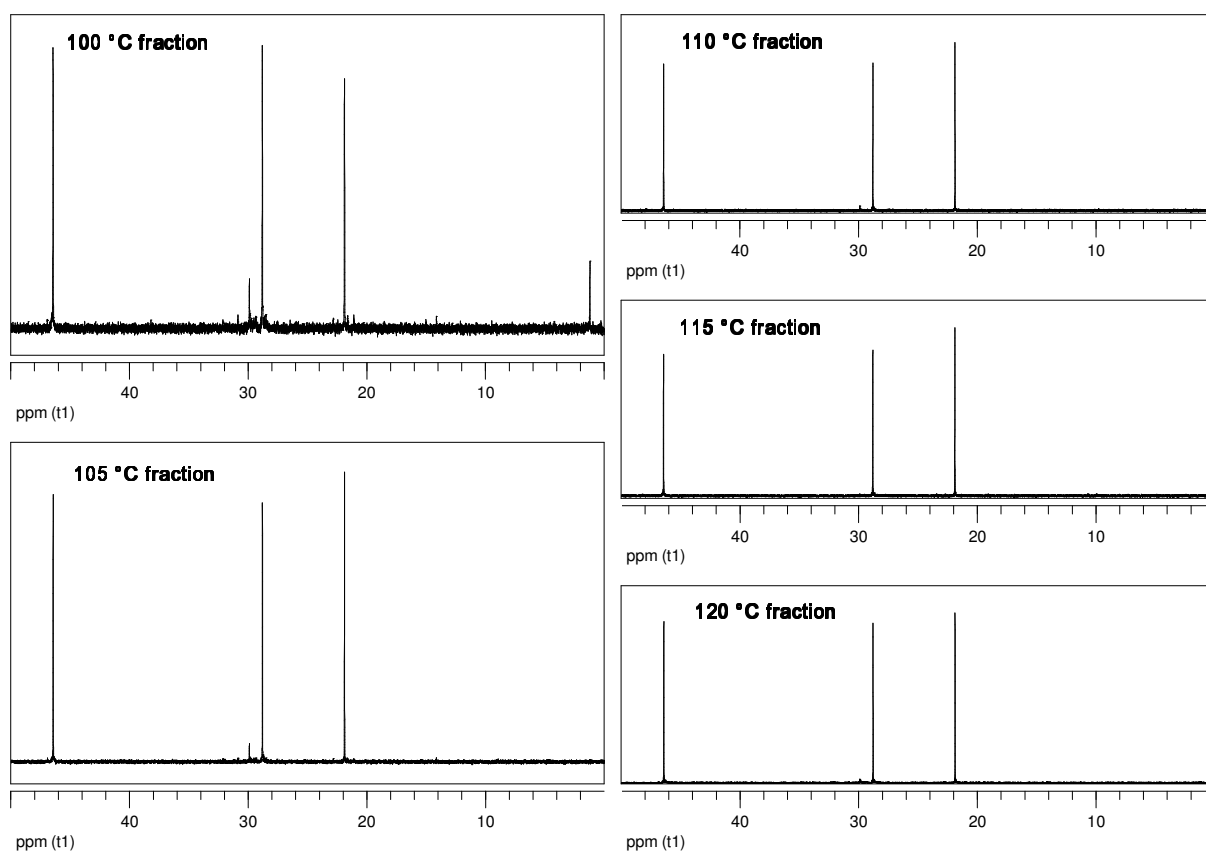


Figure B.19 The  $^{13}\text{C}$  NMR spectra for selected TREF fractions of sample MP-1.

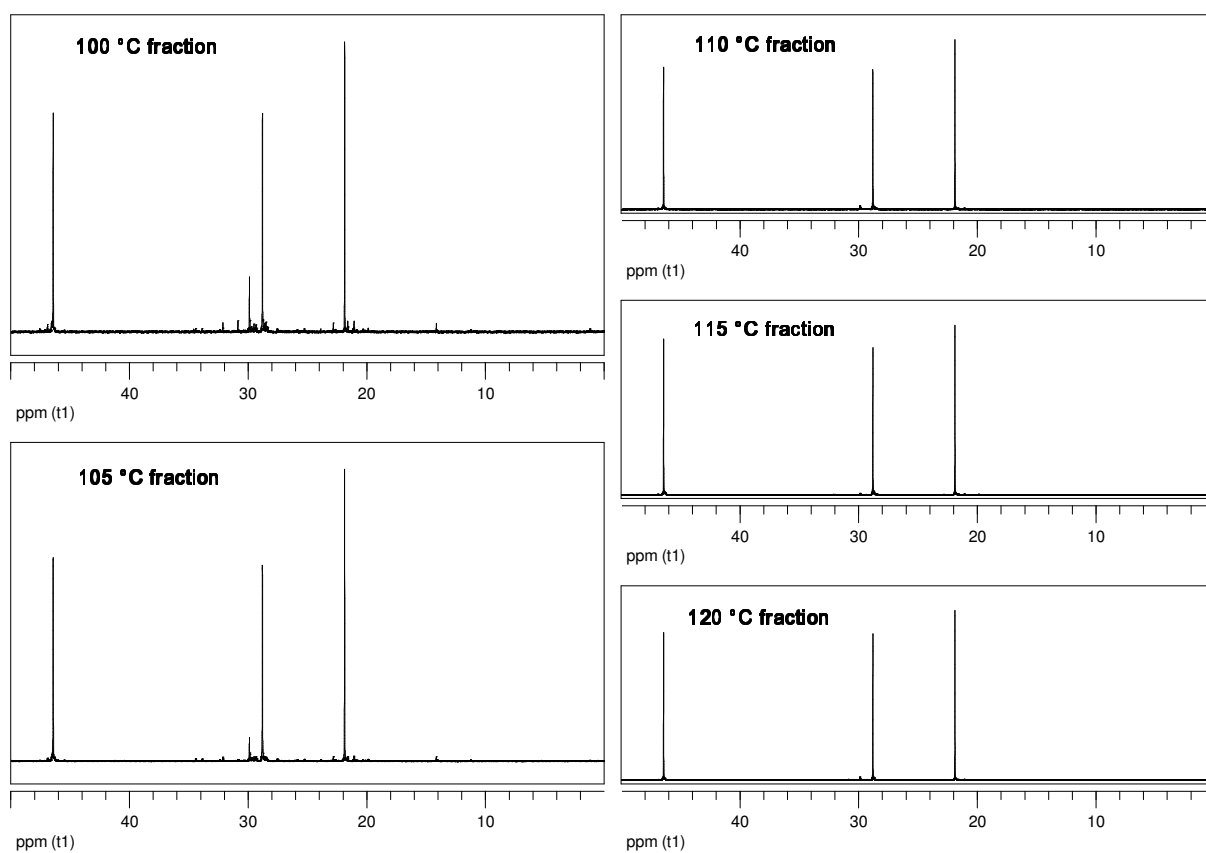


Figure B.20 The  $^{13}\text{C}$  NMR spectra for selected TREF fractions of sample MP-2.

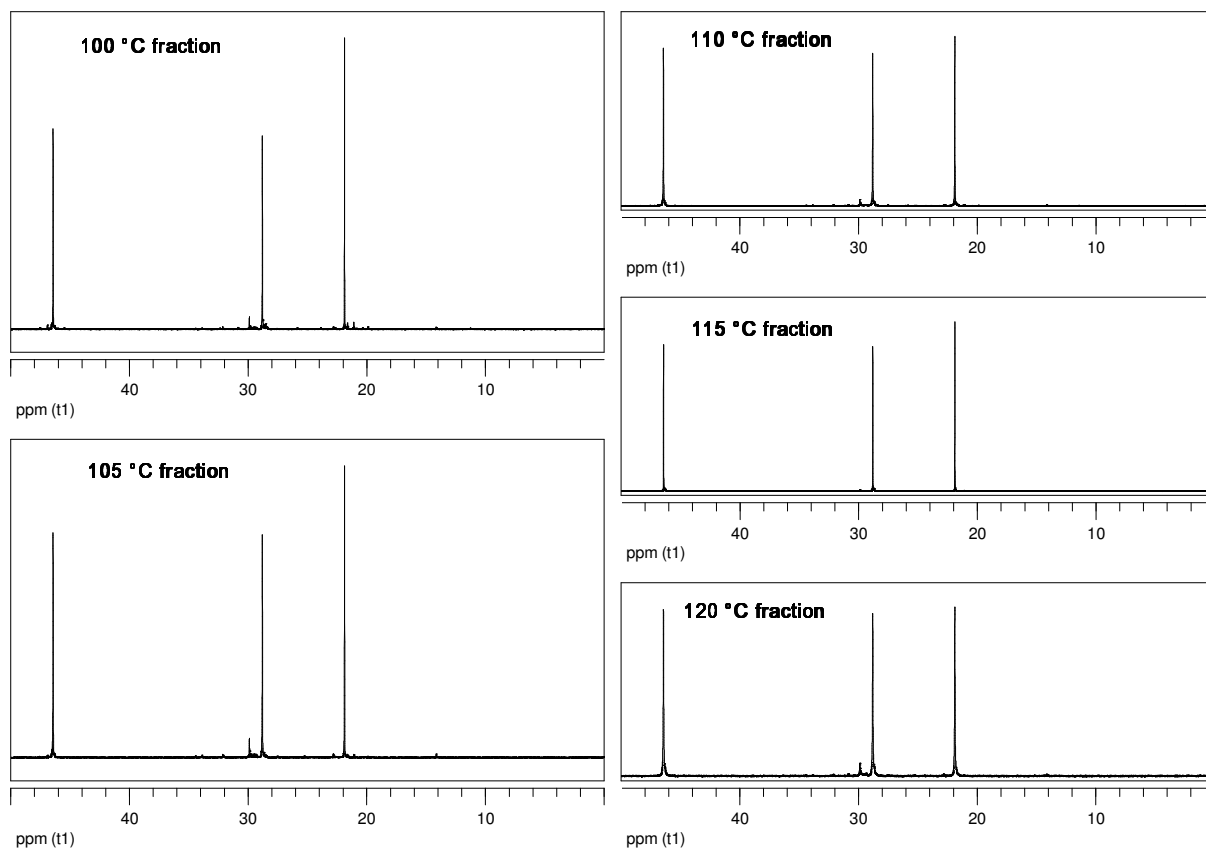


Figure B.21 The  $^{13}\text{C}$  NMR spectra for selected TREF fractions of sample MP-3.

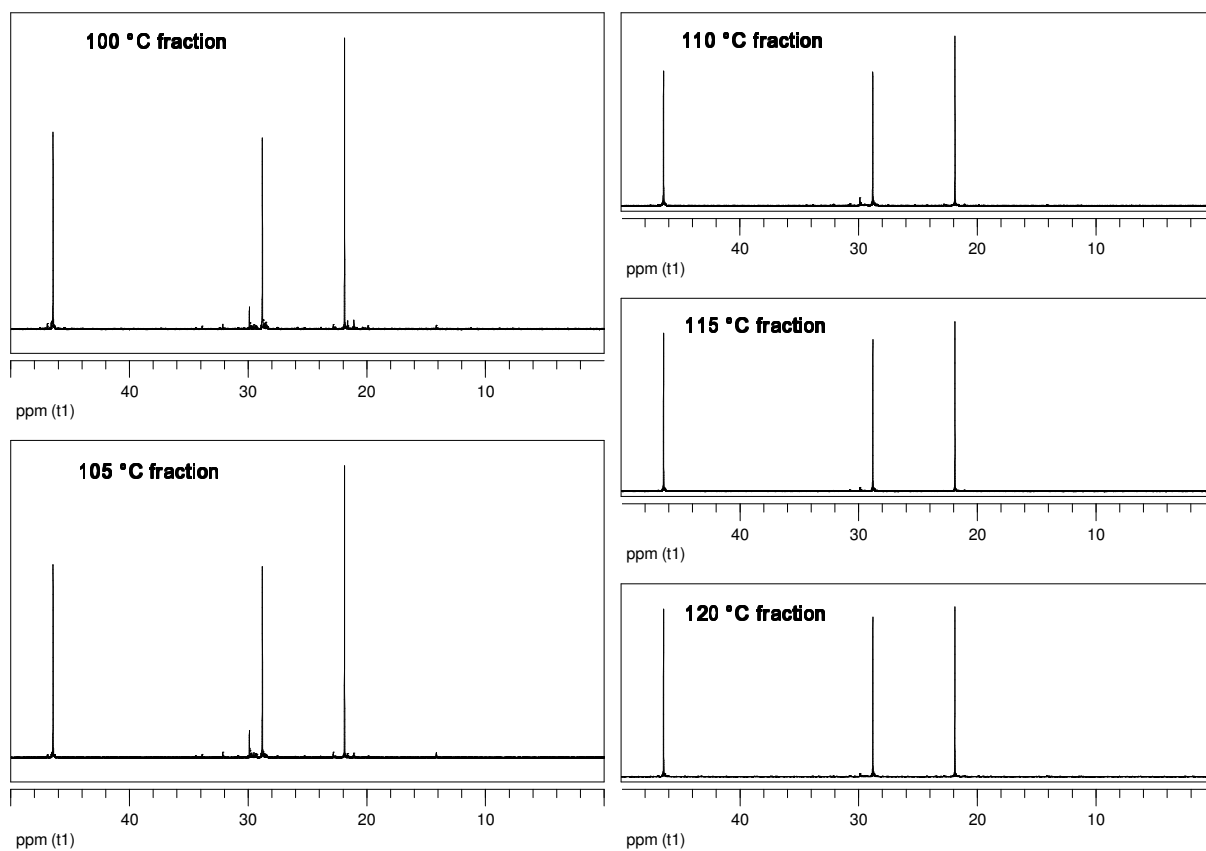


Figure B.22 The  $^{13}\text{C}$  NMR spectra for selected TREF fractions of sample MP-4.

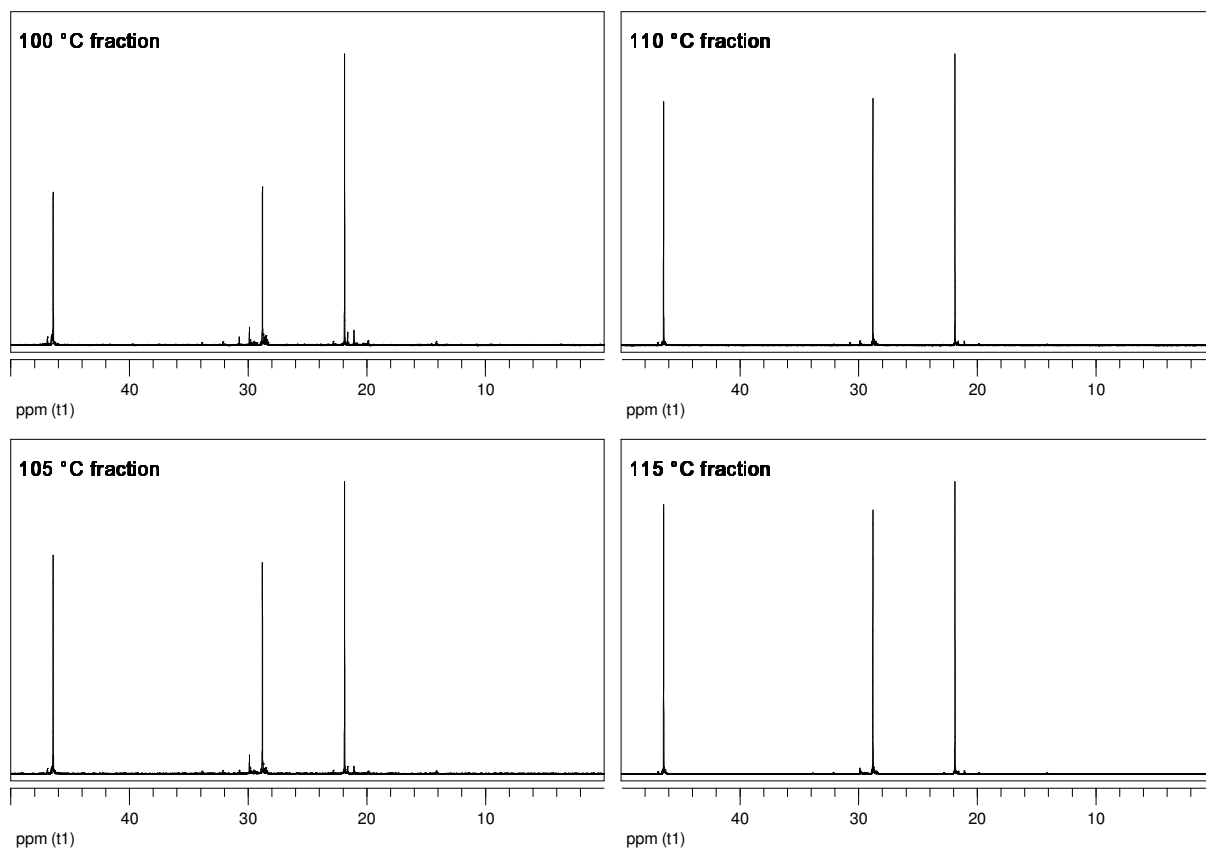


Figure B.23 The  $^{13}\text{C}$  NMR spectra for selected TREF fractions of sample No ED.

## B.4 $^{13}\text{C}$ NMR data from Chapter 7

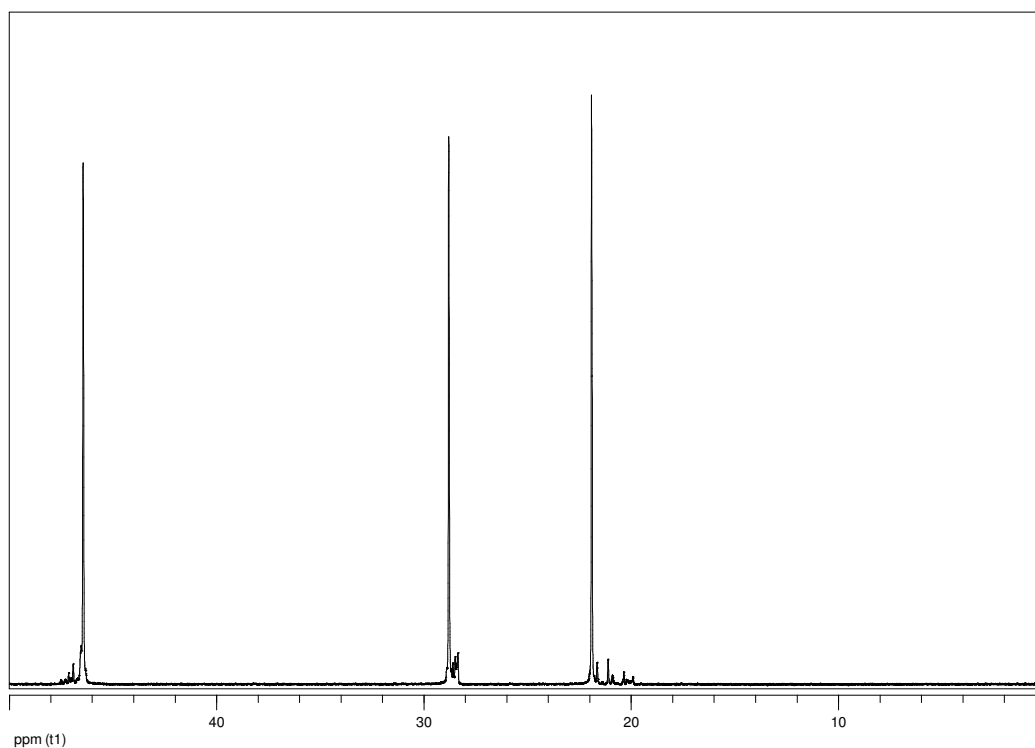


Figure B.24 The  $^{13}\text{C}$  NMR spectrum of the test sample.

# Appendix C. DSC data

## C.1 DSC data from Chapter 4

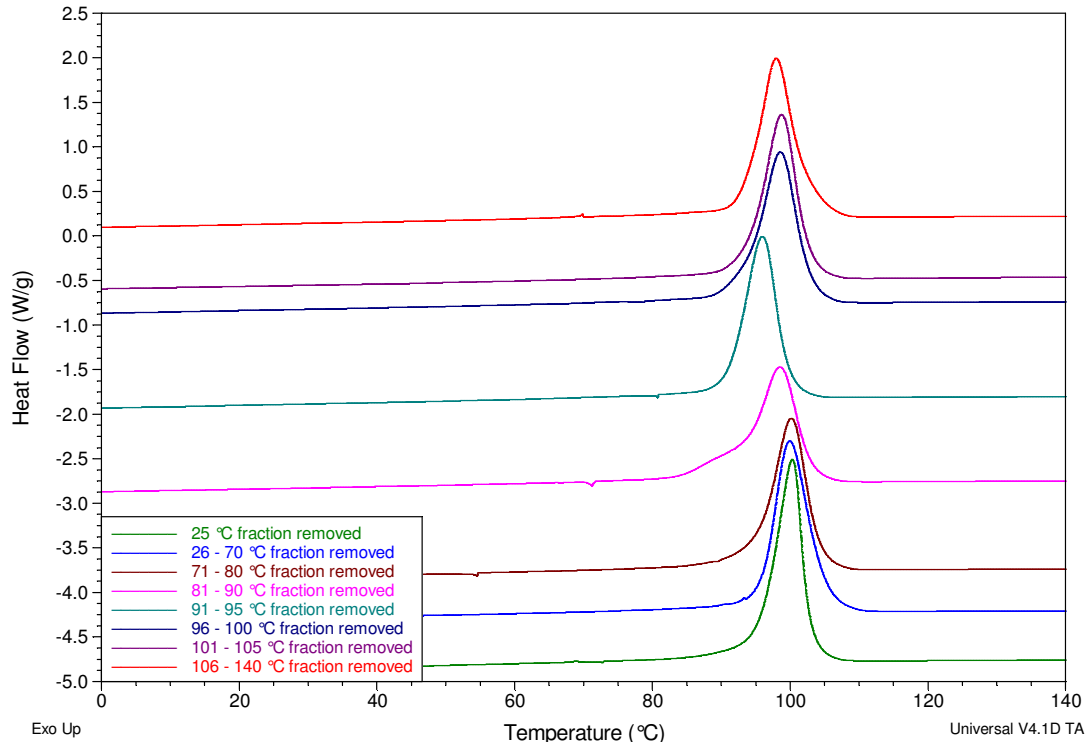


Figure C.1 The DSC crystallisation exotherms for the PP1P samples with selected fractions removed.

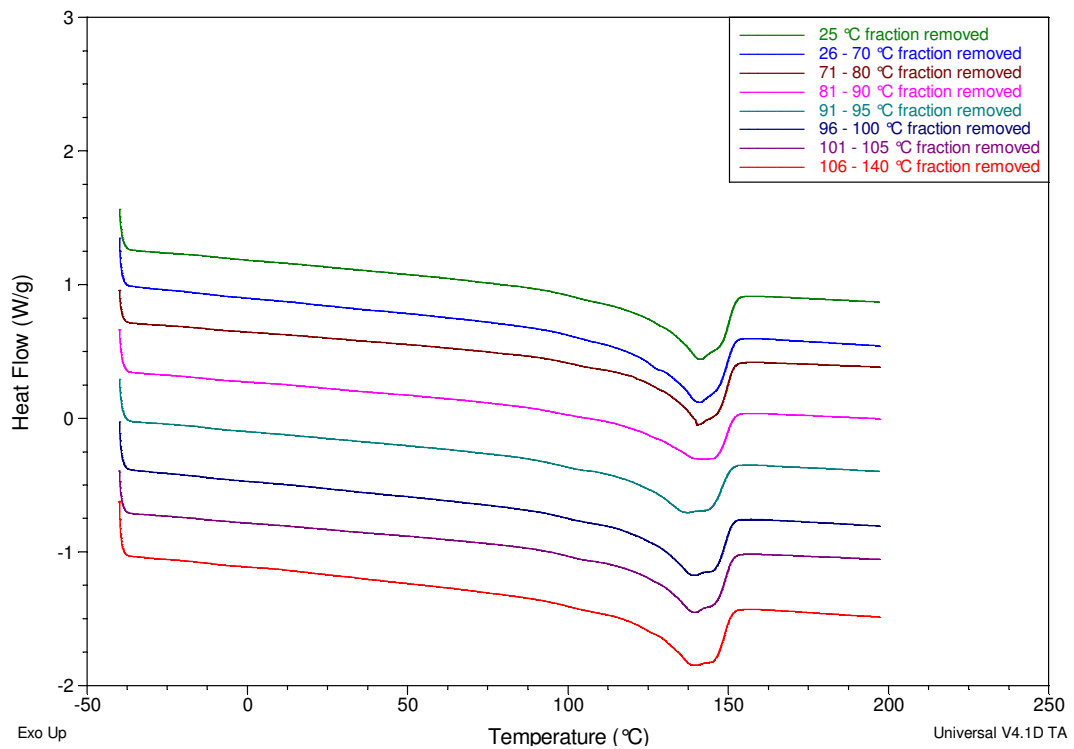
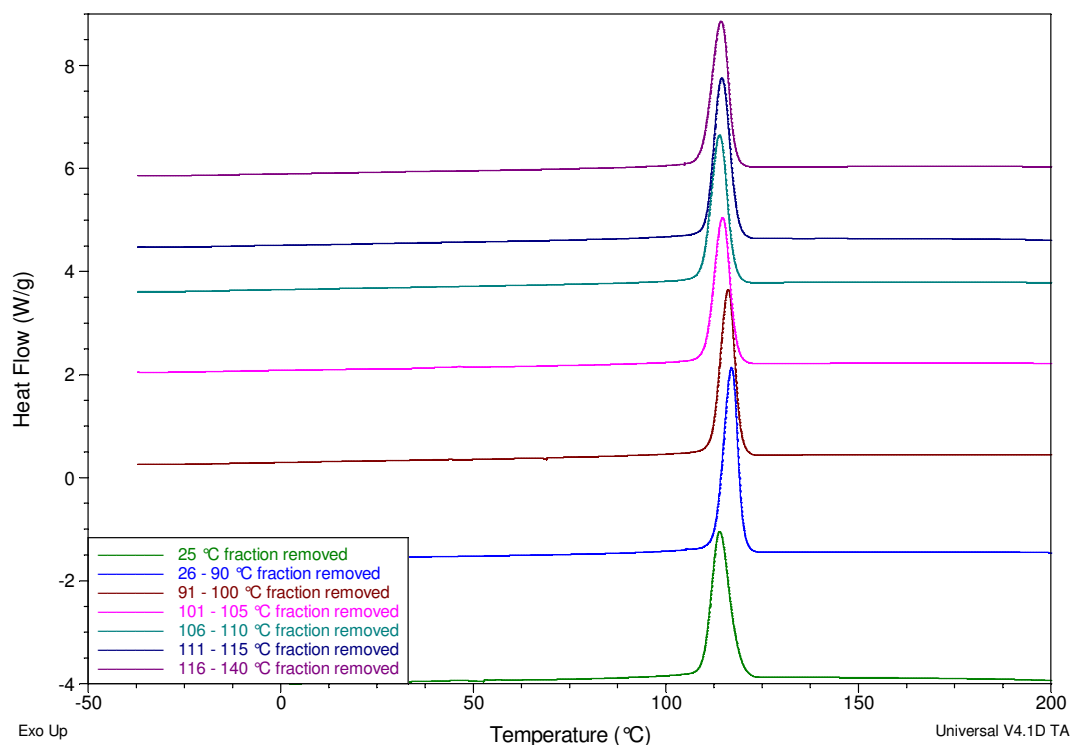
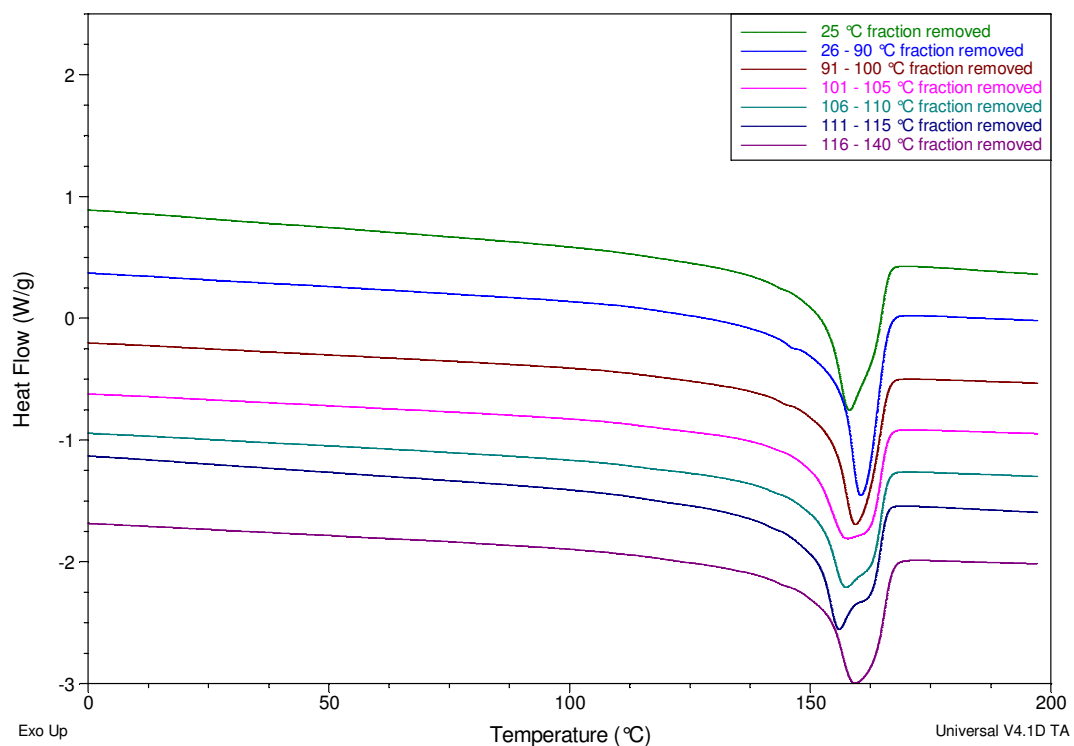


Figure C.2 The DSC melting endotherms for the PP1P samples with selected fractions removed.



**Figure C.3** The DSC crystallisation exotherms for the PPH samples with selected fractions removed.



**Figure C.4** The DSC melting endotherms for the PPH samples with selected fractions removed.

## C.2 DSC data from Chapter 5

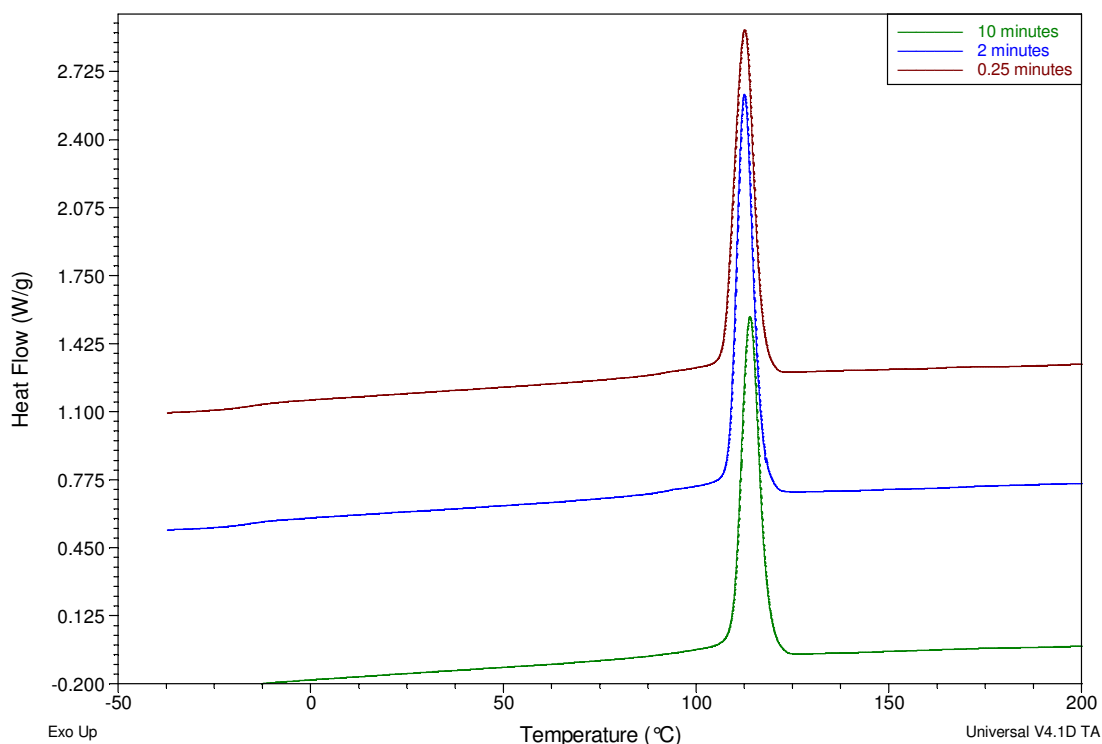


**Figure C.5** The DSC crystallisation exotherms for the samples produced while varying the pre-treatment time between the catalyst and cocatalyst. The pre-treatment time is indicated in minutes.

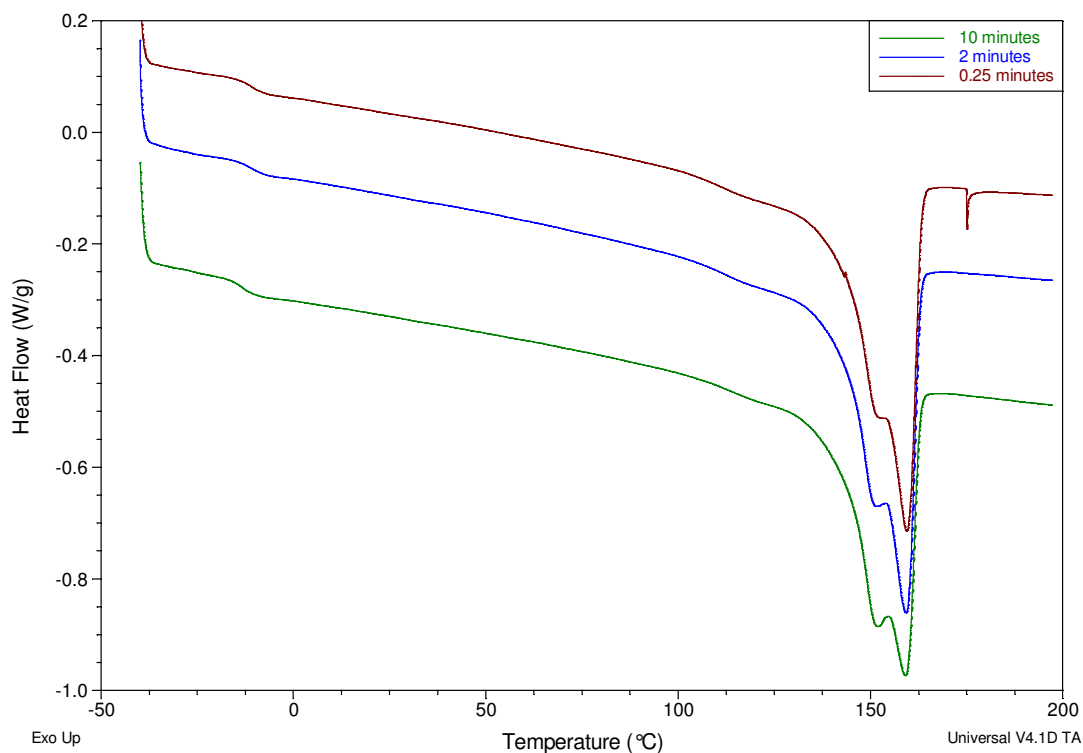


**Figure C.6** The DSC melting endotherms for the samples produced while varying the pre-treatment time between the catalyst and cocatalyst. The pre-treatment time is indicated in minutes.



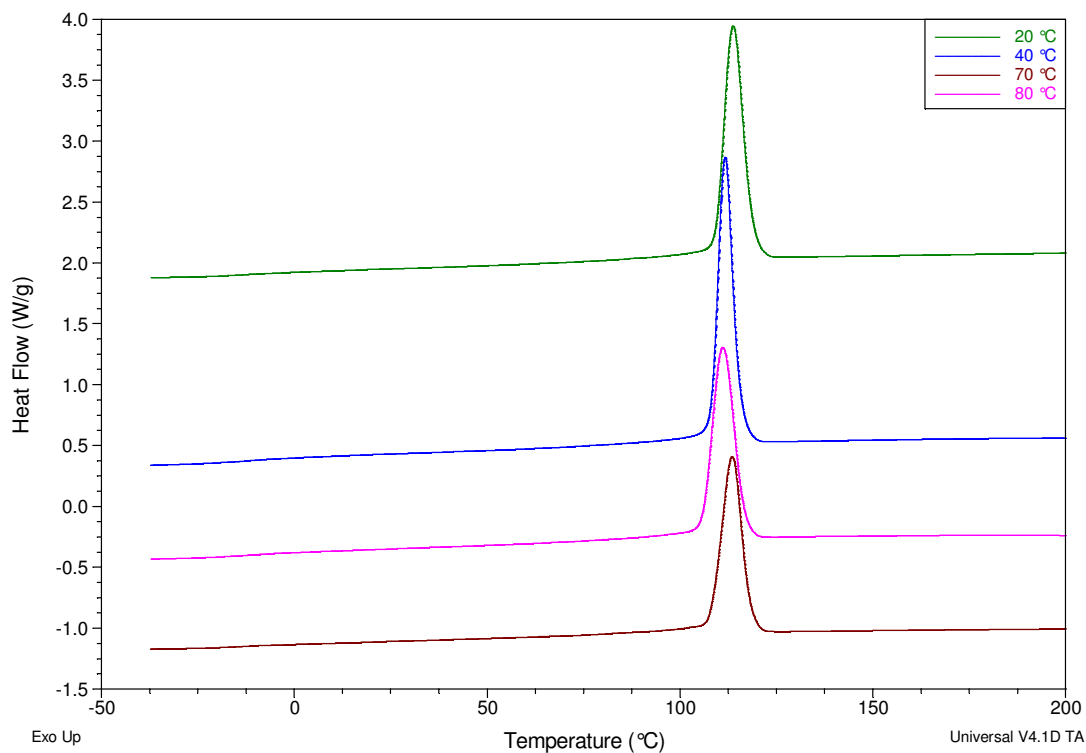


**Figure C.7** The DSC crystallisation exotherms of the polymers produced at different temperatures at an **Al:Ti = 20**.

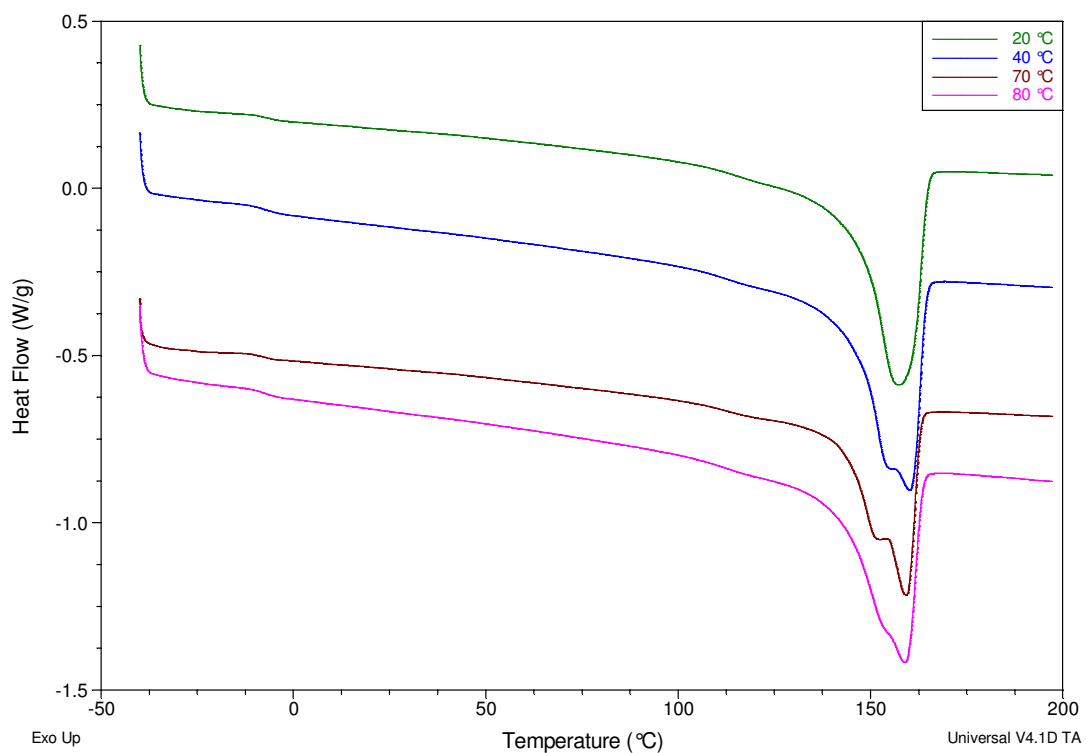


**Figure C.8** The DSC melting endotherms of the polymers produced at different temperatures at an **Al:Ti = 20**.

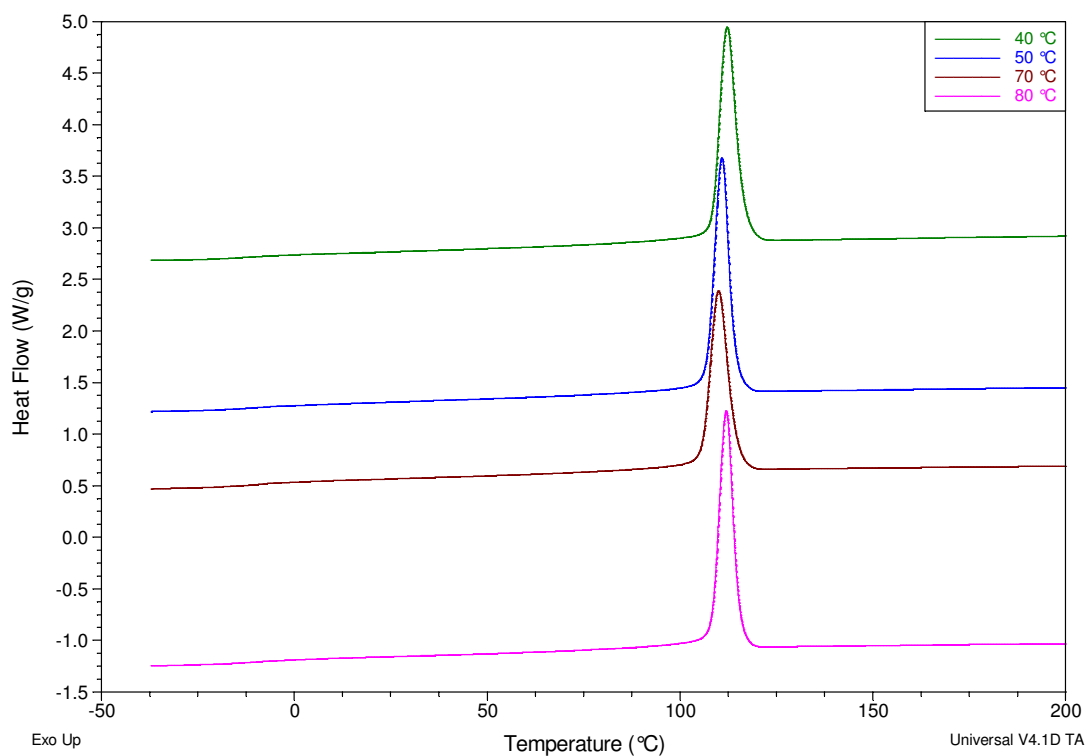


**Figure C.9** The DSC crystallisation exotherms of the polymers produced at different temperatures at an **Al:Ti = 80**.

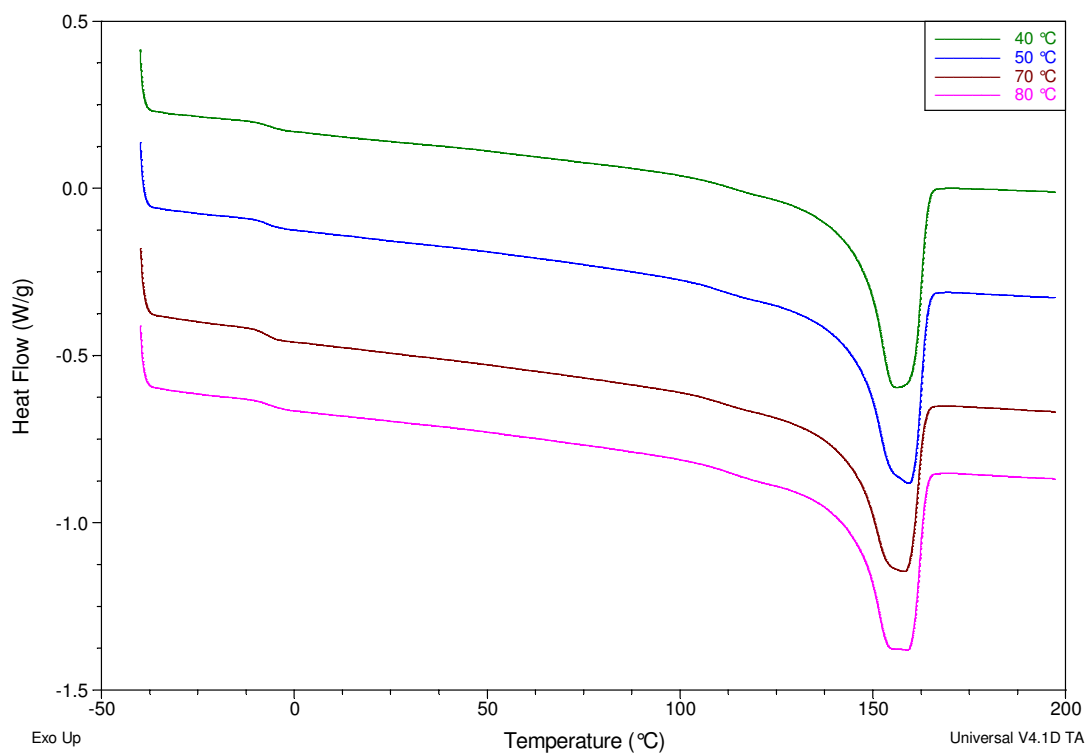


**Figure C.10** The DSC melting endotherms of the polymers produced at different temperatures at an **Al:Ti = 80**.

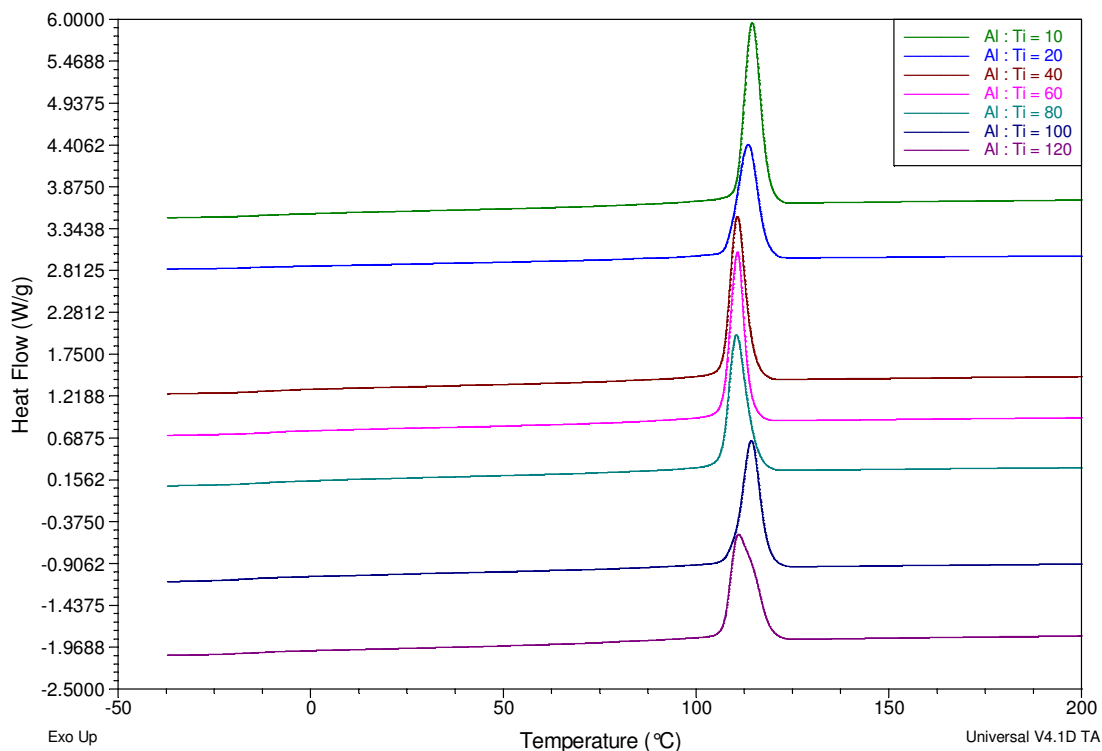


**Figure C.11** The DSC crystallisation exotherms for the samples produced at different catalyst/cocatalyst ratios.

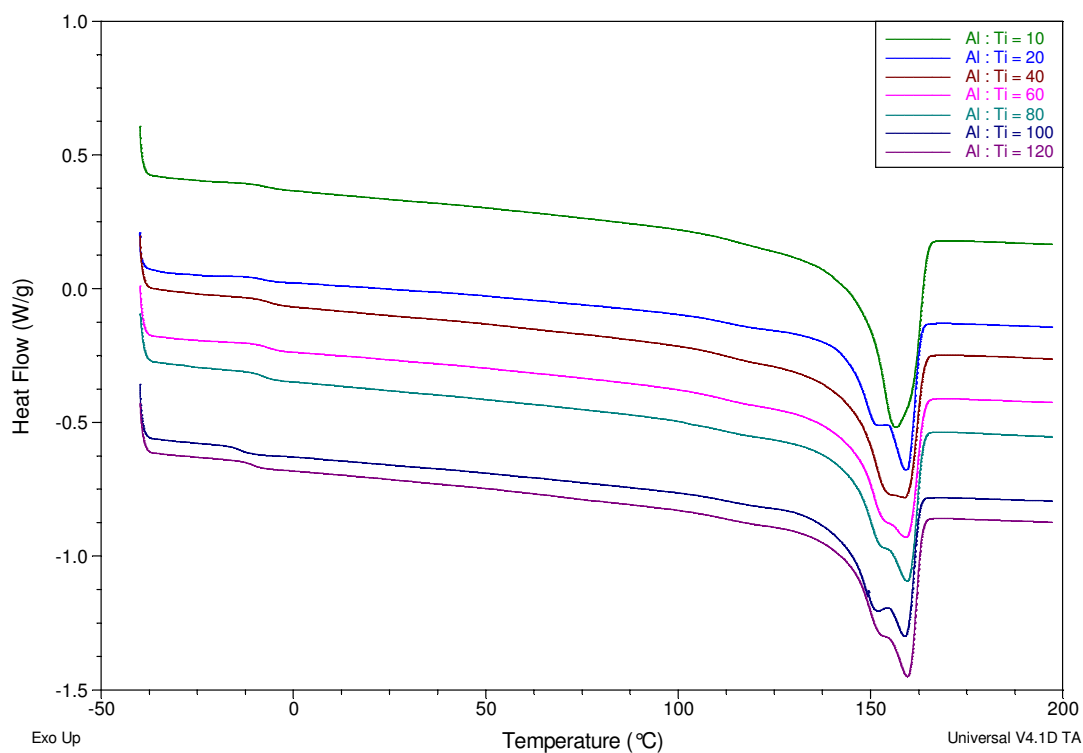


**Figure C.12** The DSC melting endotherms for the samples produced at different catalyst/cocatalyst ratios.

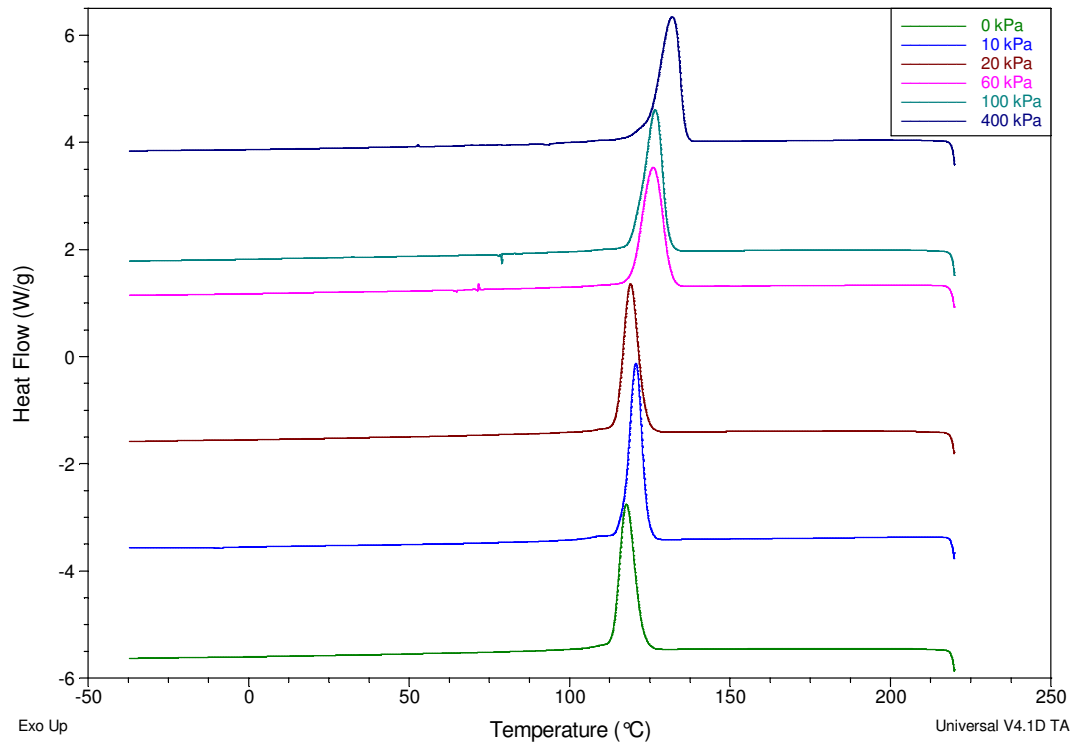


**Figure C.13** The DSC crystallisation exotherms for the samples produced at varying hydrogen pressures.

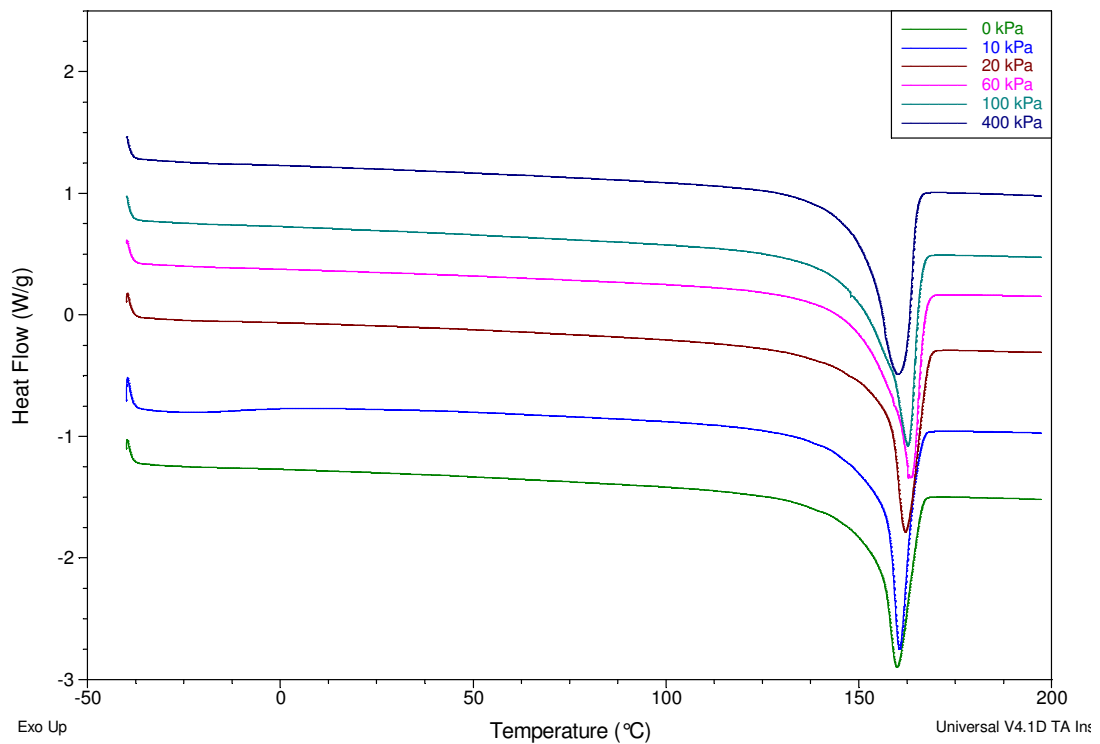


**Figure C.14** The DSC melting endotherms for the samples produced at varying hydrogen pressures.

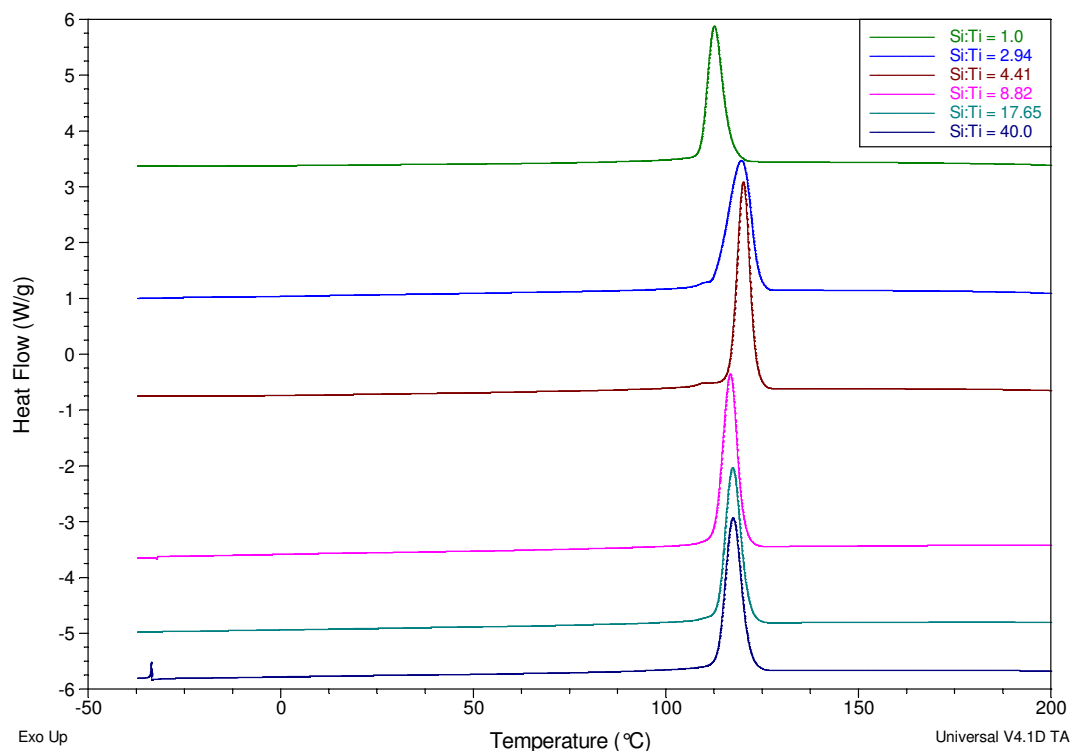


**Figure C.15** The DSC crystallisation exotherms for the polymers produced using DPDMS at an Al:Ti=20 while varying the Si:Ti.

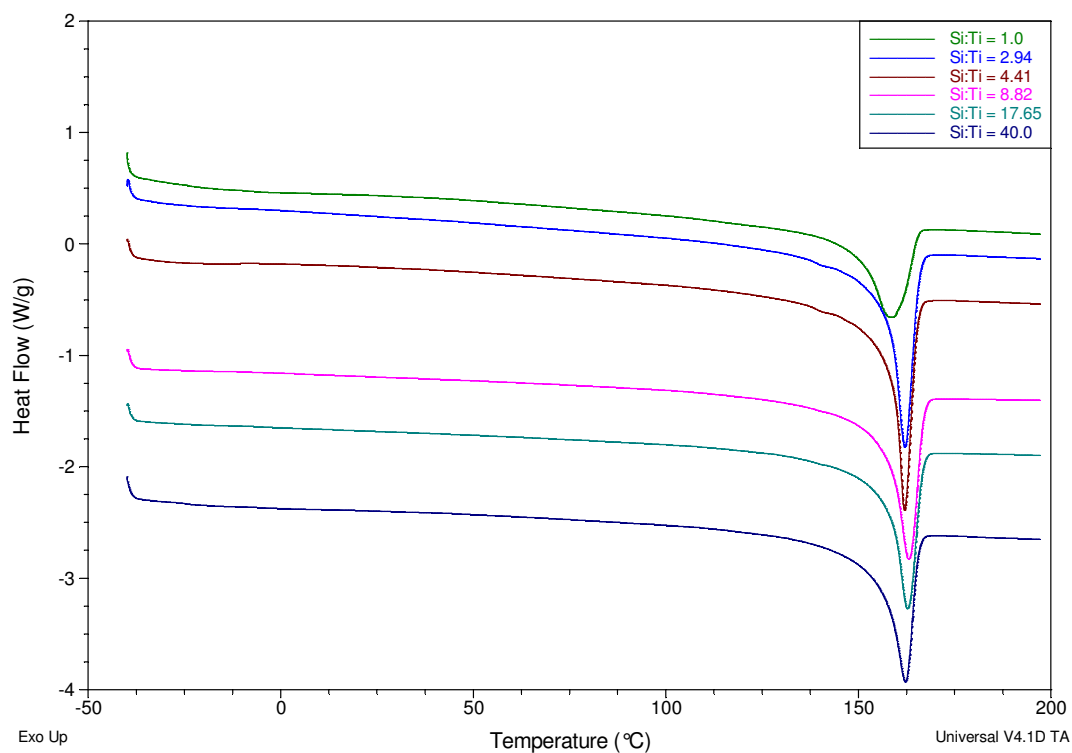


**Figure C.16** The DSC melting endotherms for the polymers produced using DPDMS at an Al:Ti=20 while varying the Si:Ti.

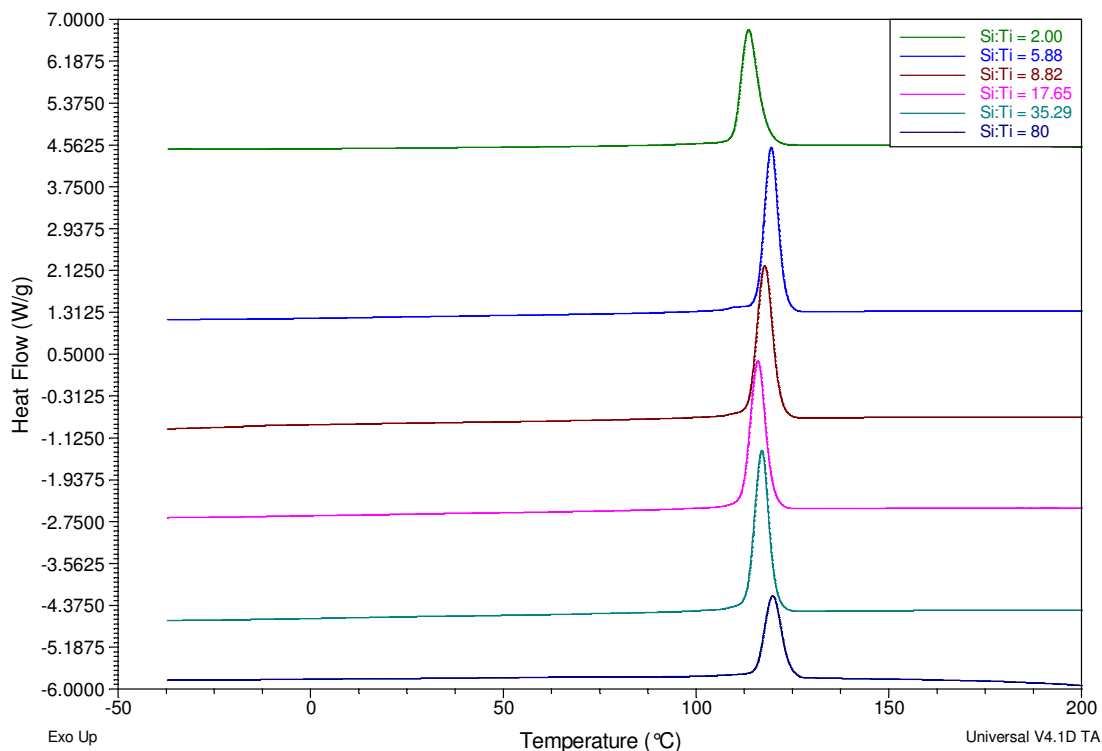


**Figure C.17** The DSC crystallisation exotherms for the polymers produced using DPDMS at an Al:Ti=40 while varying the Si:Ti.

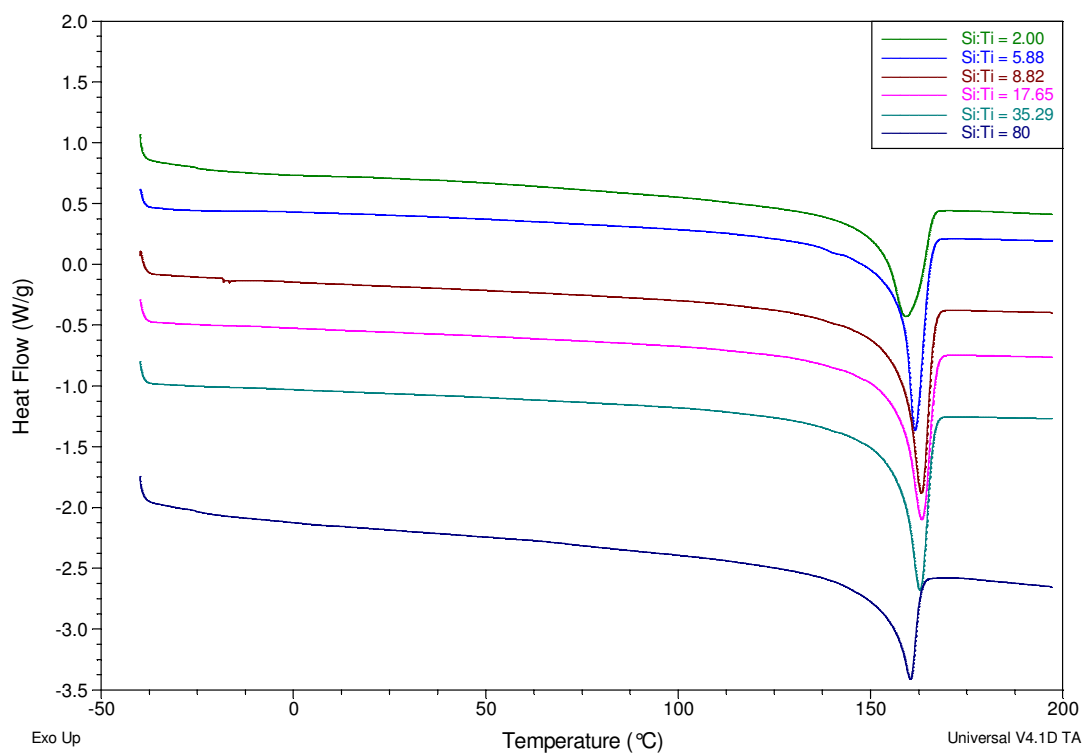


**Figure C.18** The DSC melting endotherms for the polymers produced using DPDMS at an Al:Ti=40 while varying the Si:Ti.

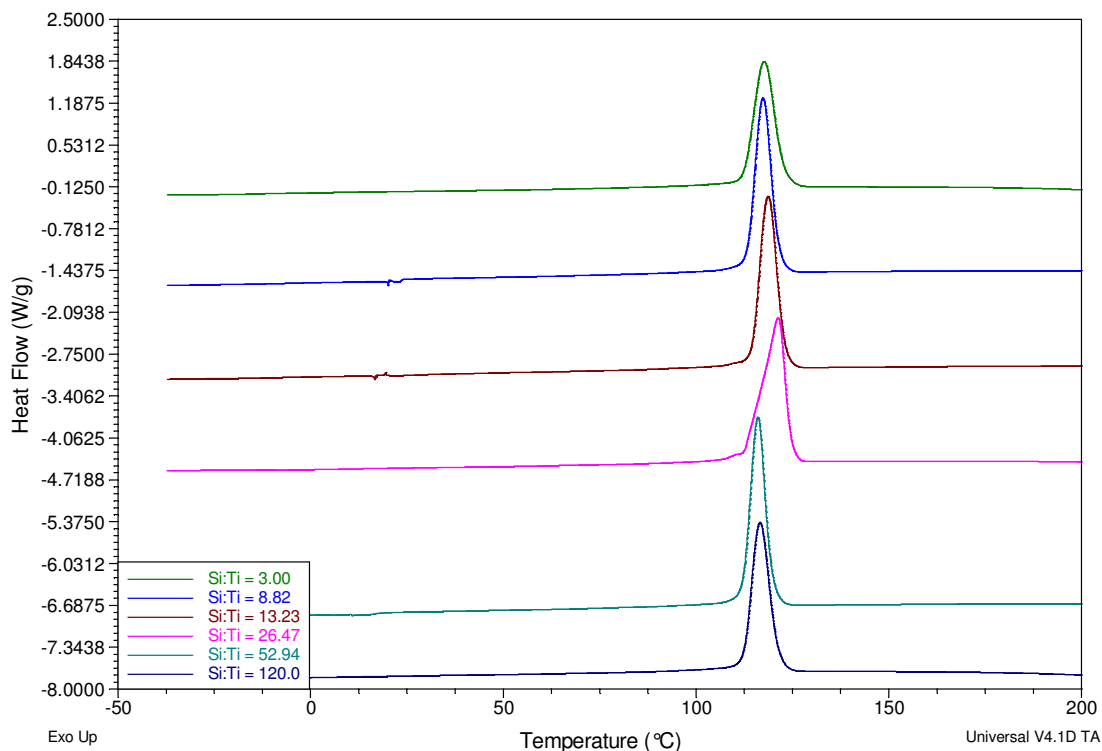


**Figure C.19** The DSC crystallisation exotherms for the polymers produced using DPDMS at an Al:Ti=60 while varying the Si:Ti.

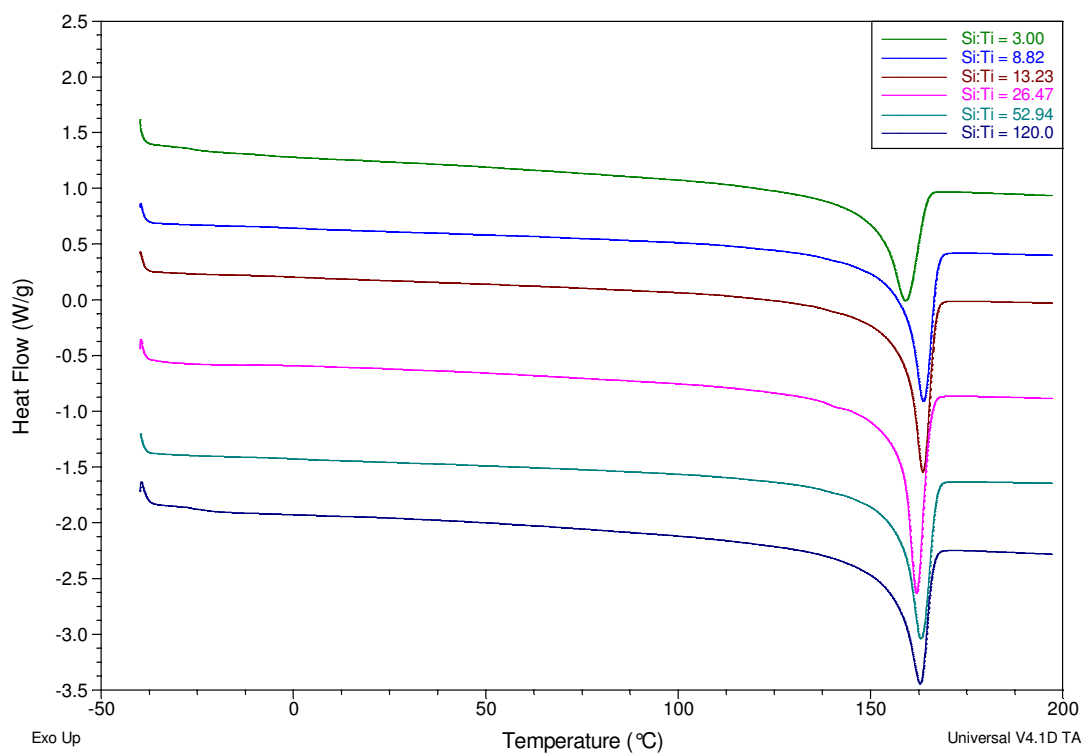


**Figure C.20** The DSC melting endotherms for the polymers produced using DPDMS at an Al:Ti=60 while varying the Si:Ti.

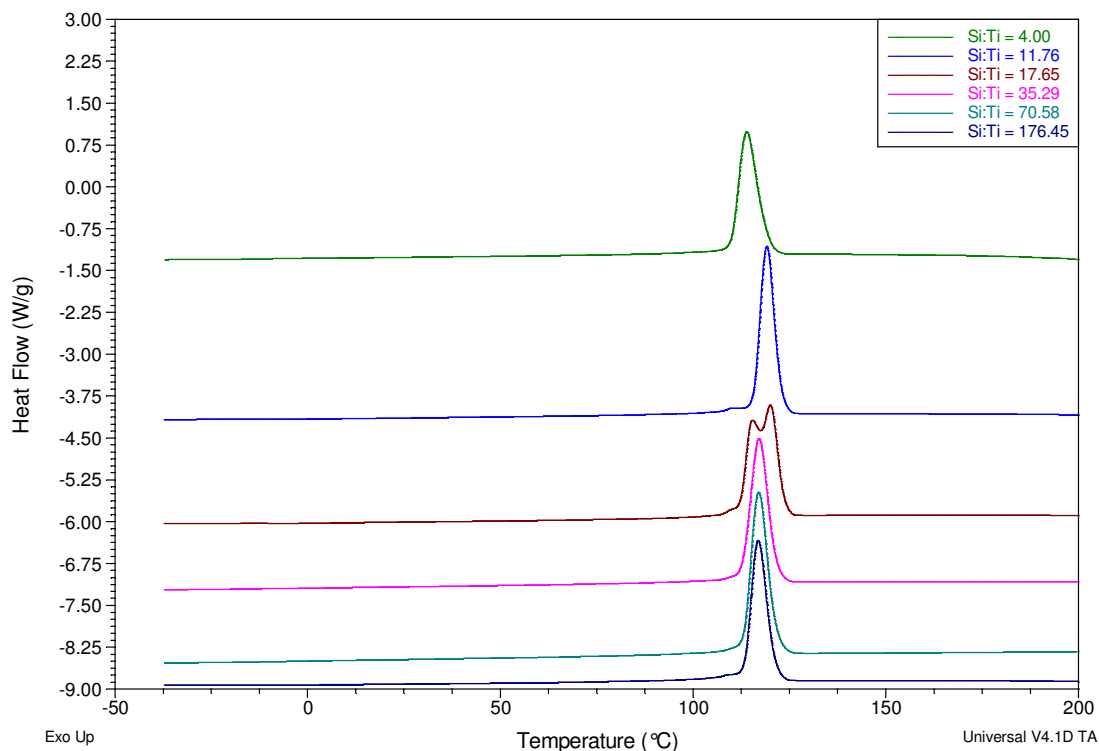


**Figure C.21** The DSC crystallisation exotherms for the polymers produced using DPDMS at an Al:Ti=80 while varying the Si:Ti.

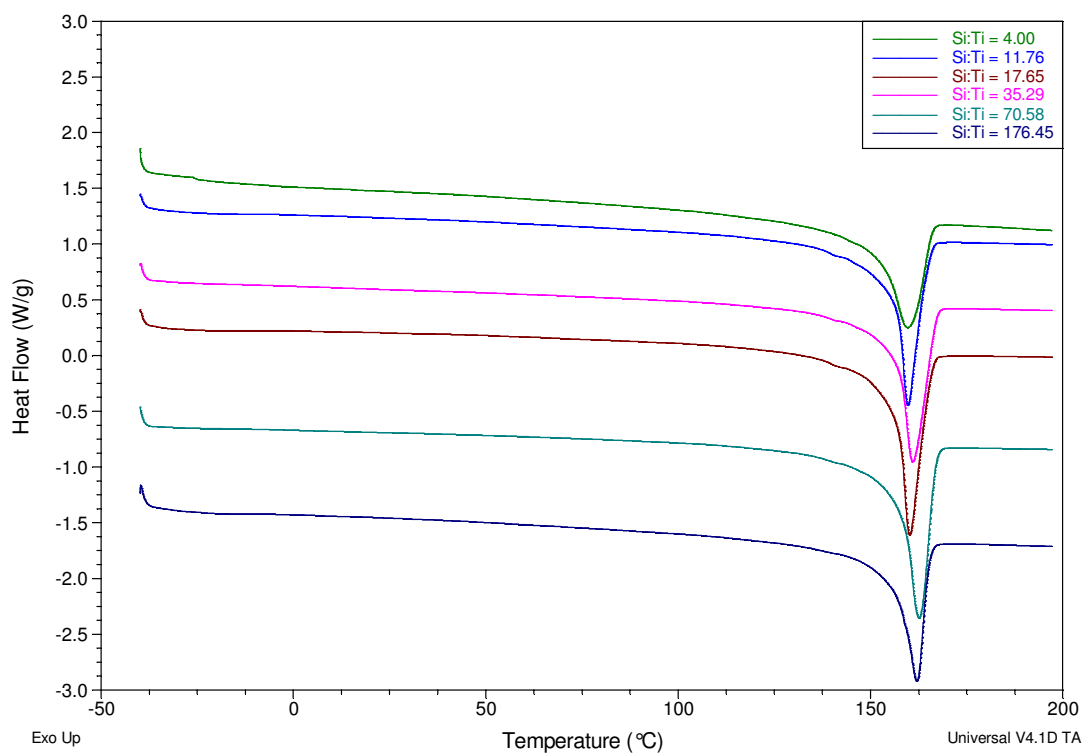


**Figure C.22** The DSC melting endotherms for the polymers produced using DPDMS at an Al:Ti=80 while varying the Si:Ti.



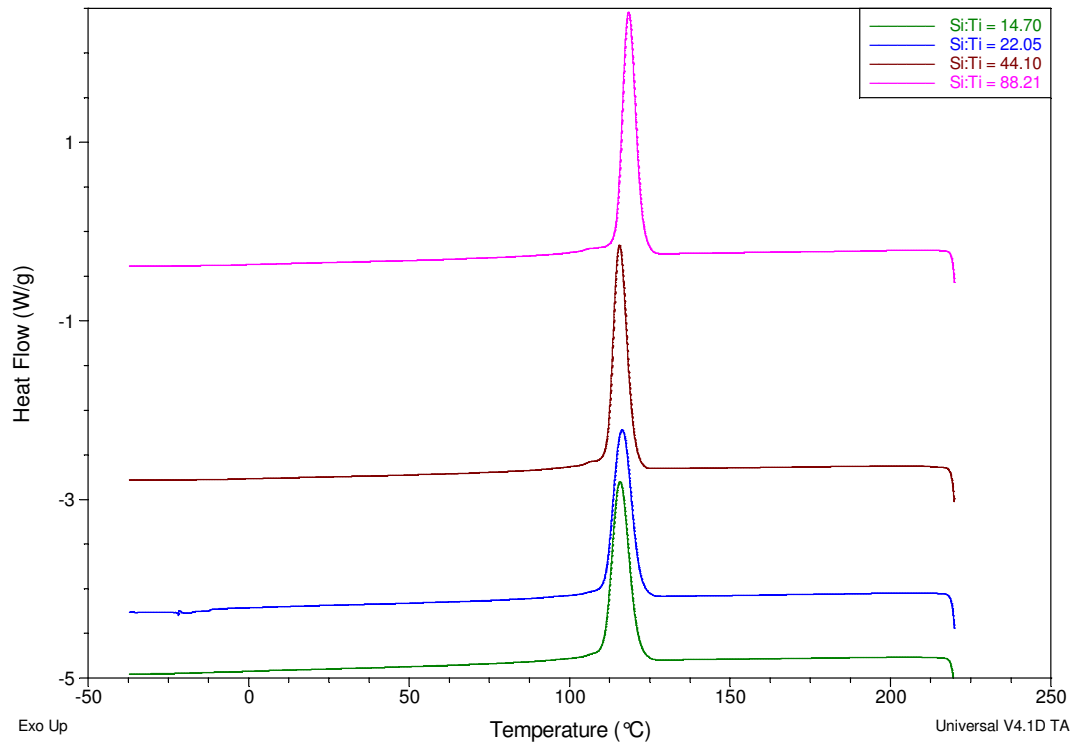


**Figure C.23** The DSC crystallisation exotherms for the polymers produced using MPDMS at an Al:Ti=80 while varying the Si:Ti.

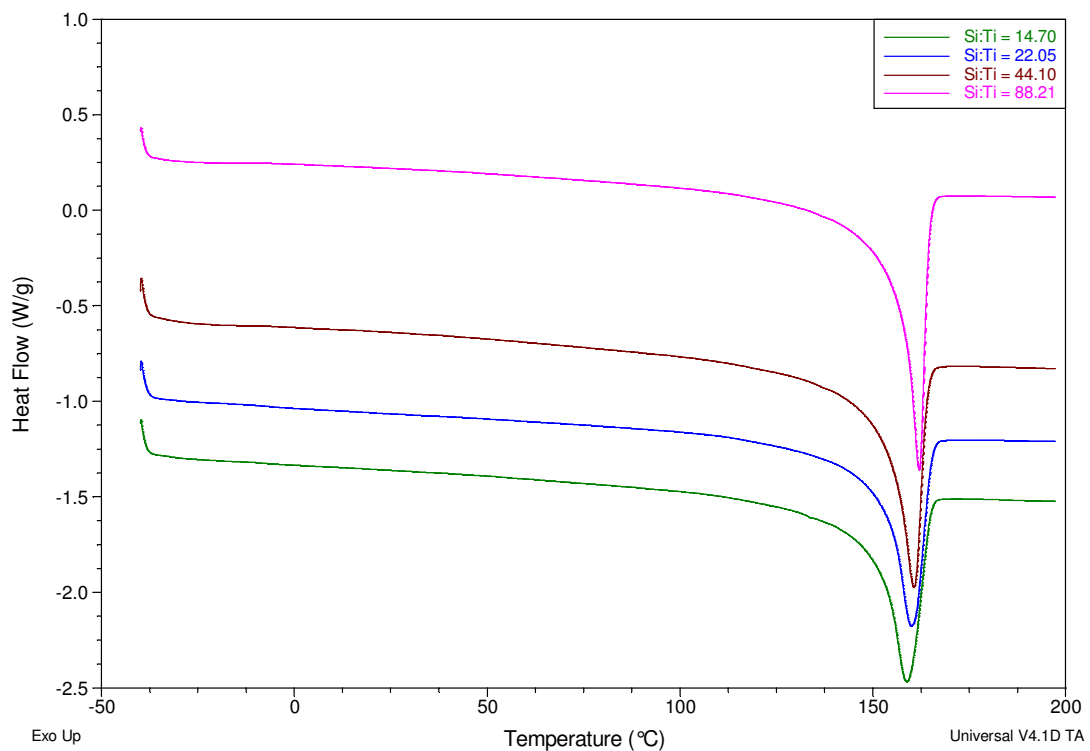


**Figure C.24** The DSC melting endotherms for the polymers produced using MPDMS at an Al:Ti=80 while varying the Si:Ti.

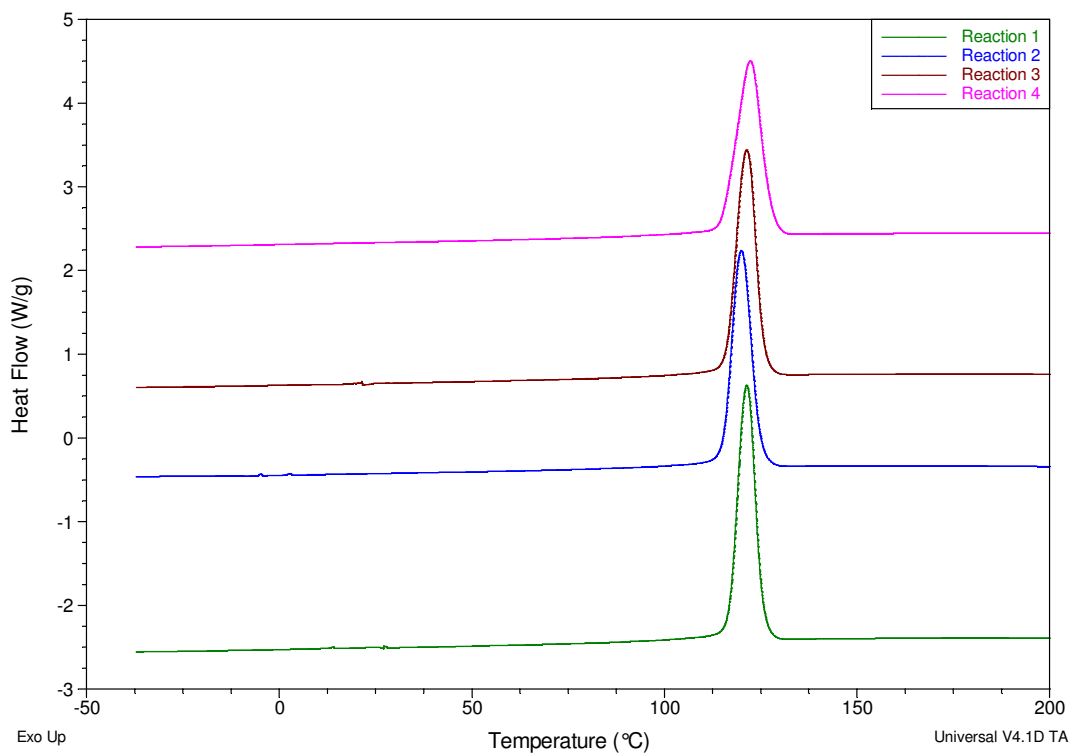


**Figure C.25** The DSC crystallisation exotherms for the polymers prepared to investigate repeatability using the DPDMS donor at an external donor/catalyst ratio of 4.

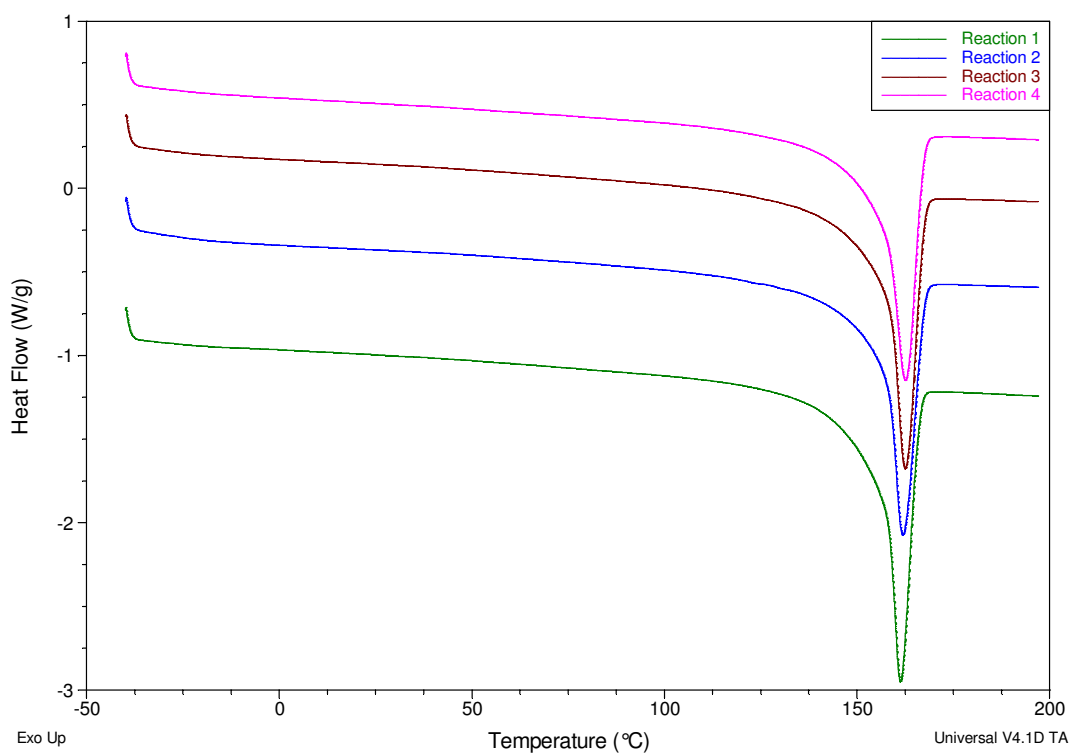


**Figure C.26** The DSC melting endotherms for the polymers prepared to investigate repeatability using the DPDMS donor at an external donor/catalyst ratio of 4.

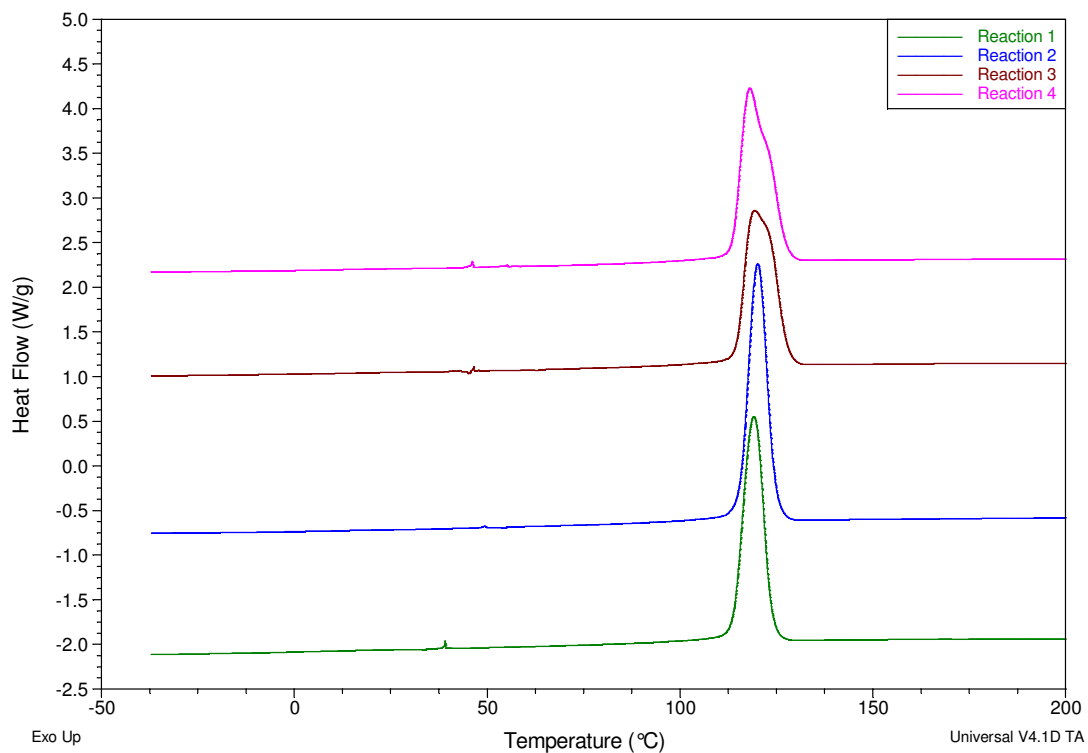


**Figure C.27** The DSC crystallisation exotherms for the polymers prepared to investigate repeatability using the DPDMS donor at an external donor/catalyst ratio of 8.

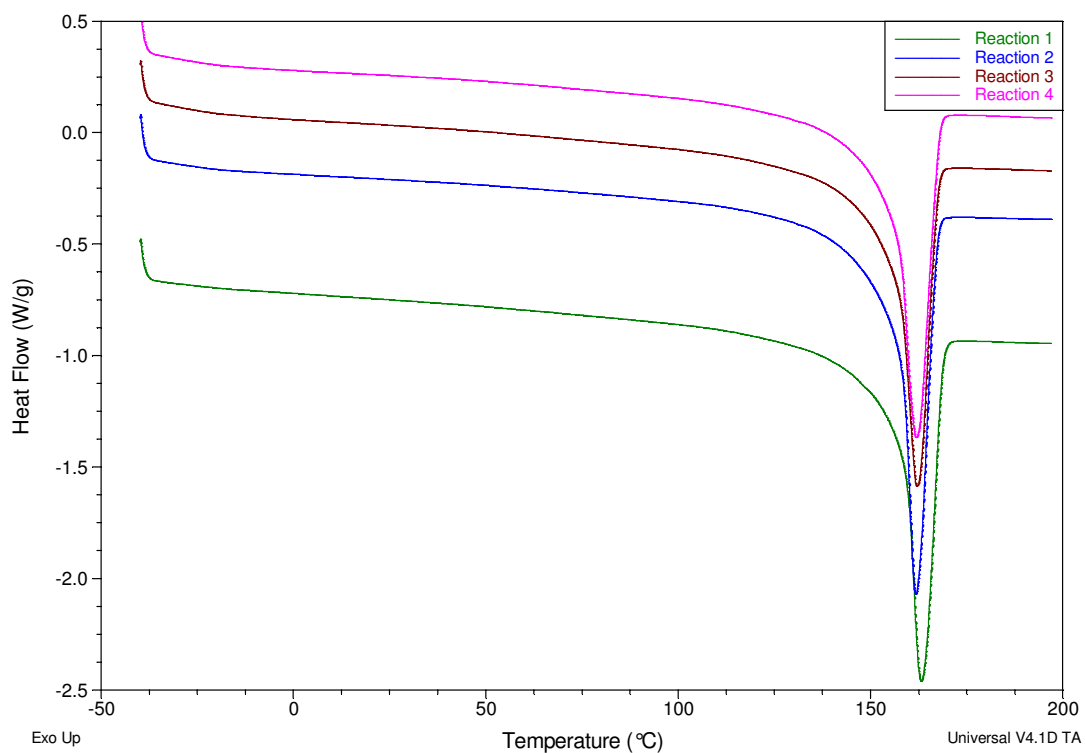


**Figure C.28** The DSC melting endotherms for the polymers prepared to investigate repeatability using the DPDMS donor at an external donor/catalyst ratio of 8.

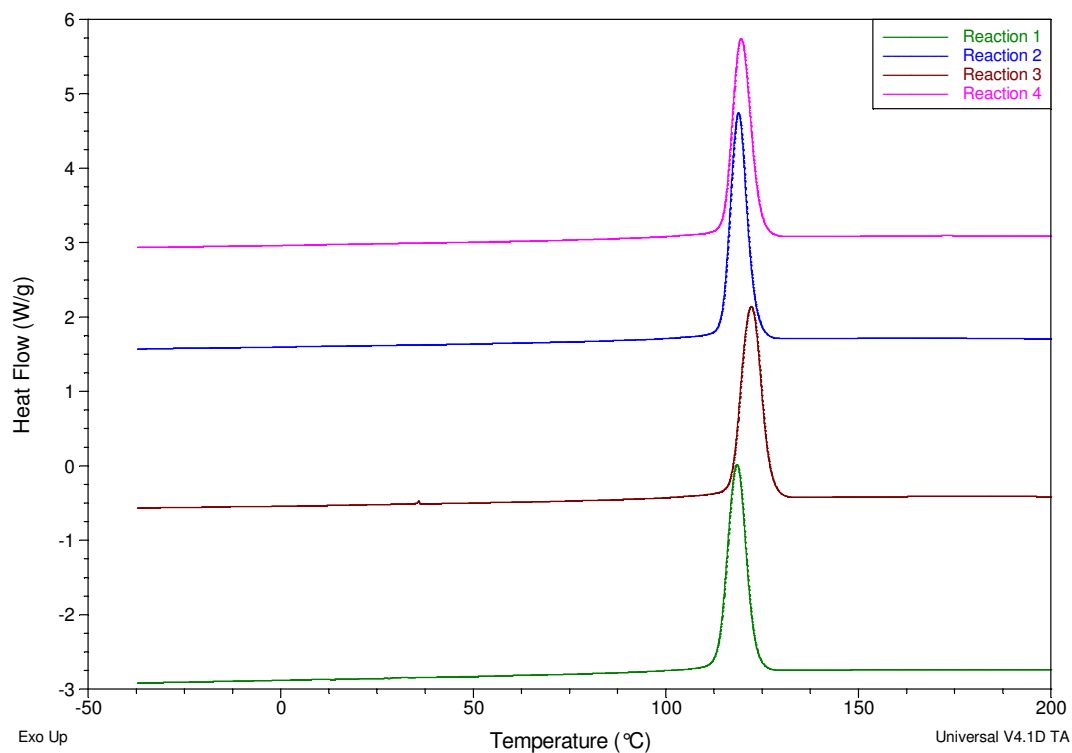


**Figure C.29** The DSC crystallisation exotherms for the polymers prepared to investigate repeatability using the DPDMS donor at an external donor/catalyst ratio of 16.

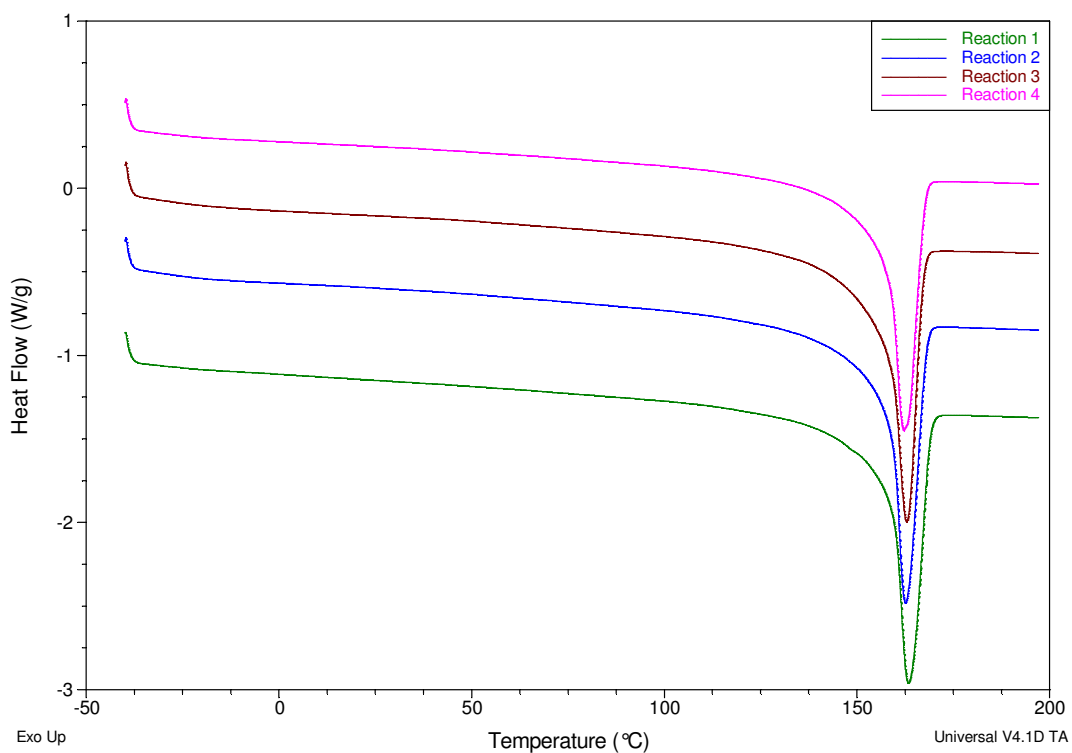


**Figure C.30** The DSC melting endotherms for the polymers prepared to investigate repeatability using the DPDMS donor at an external donor/catalyst ratio of 16.

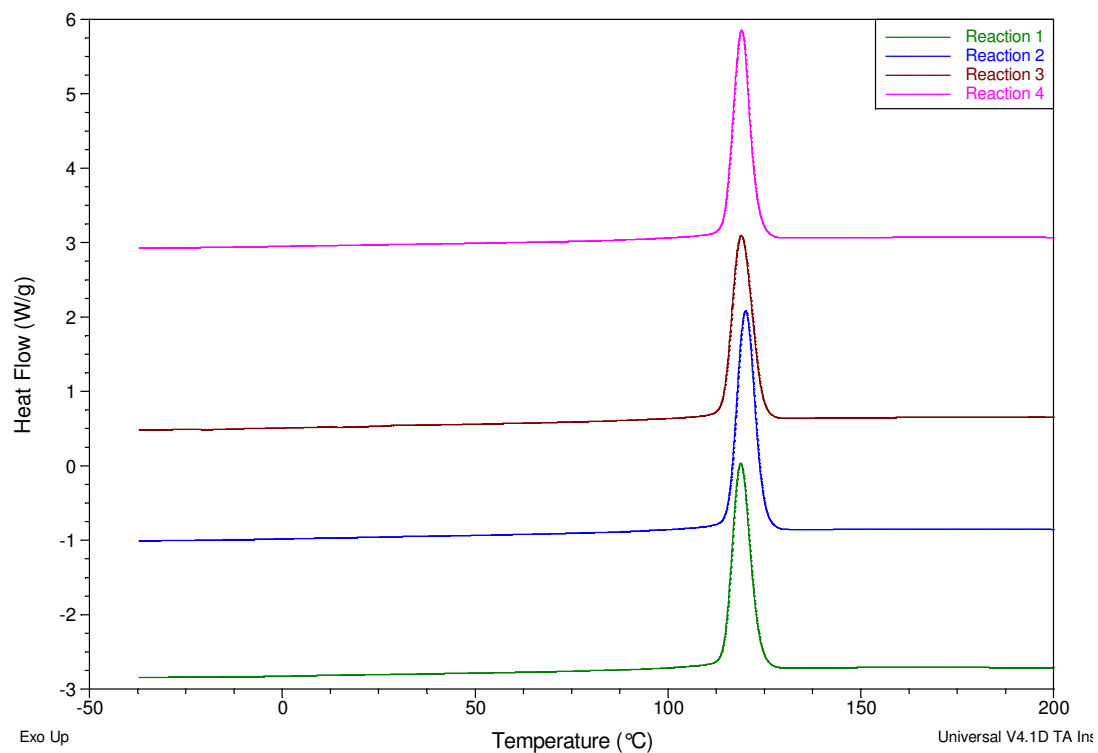


**Figure C.31** The DSC crystallisation exotherms for the polymers prepared to investigate repeatability using the DPDMS donor at an external donor/catalyst ratio of 40.

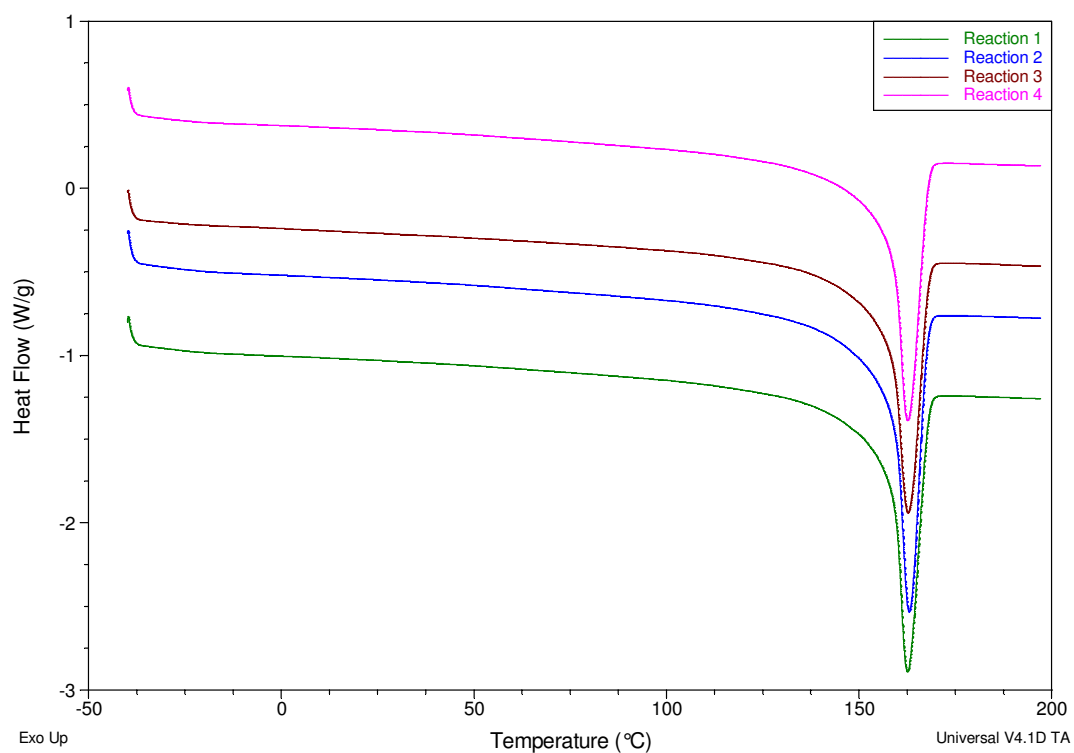


**Figure C.32** The DSC melting endotherms for the polymers prepared to investigate repeatability using the DPDMS donor at an external donor/catalyst ratio of 40.

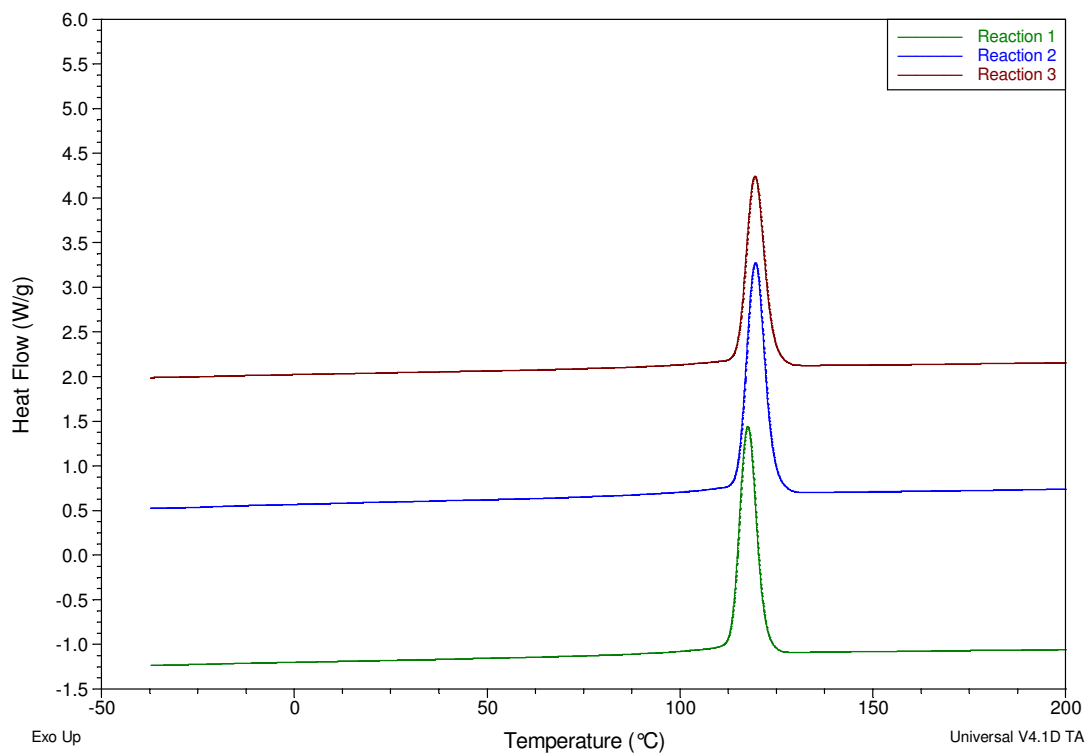


**Figure C.33 The DSC crystallisation exotherms for the polymers prepared to investigate repeatability using no external donor.**

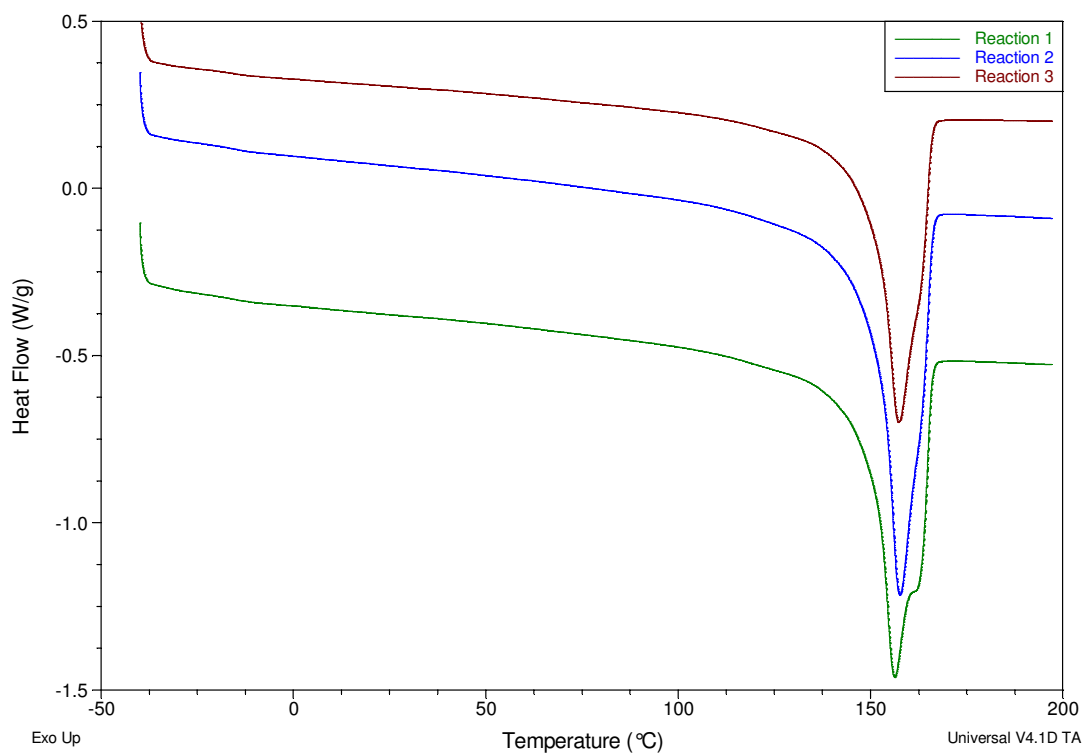


**Figure C.34 The DSC melting endotherms for the polymers prepared to investigate repeatability using no external donor.**

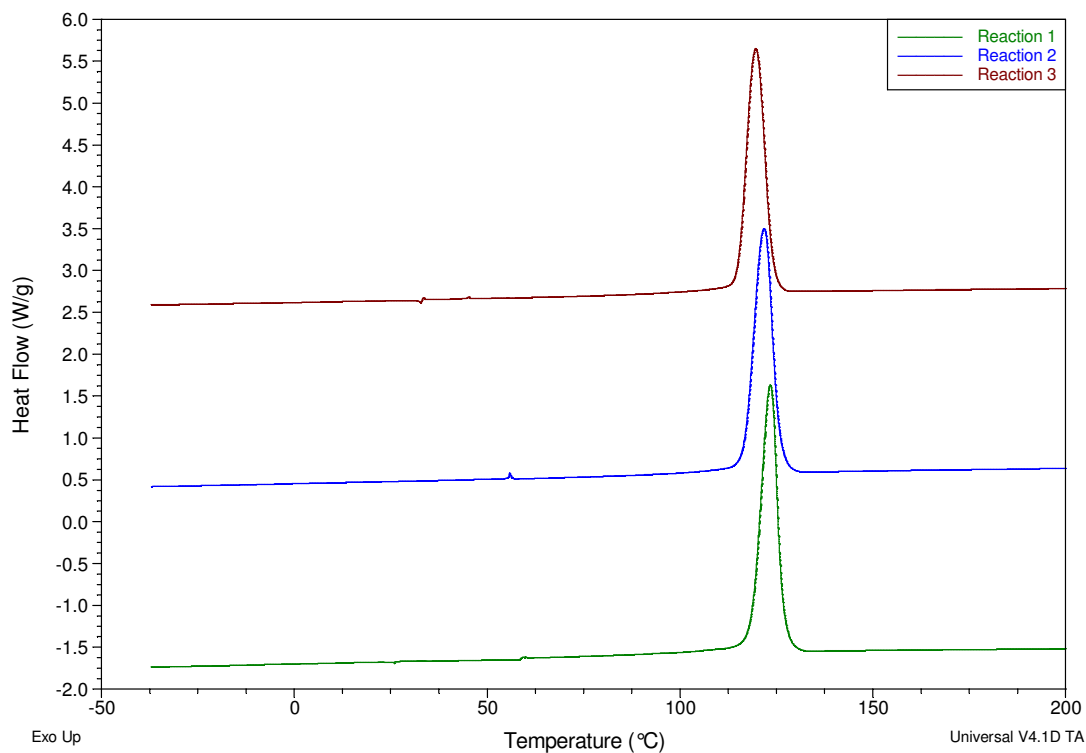


**Figure C.35** The DSC crystallisation exotherms for the polymers prepared to investigate repeatability using the MPDMS donor at an external donor/catalyst ratio of 4.

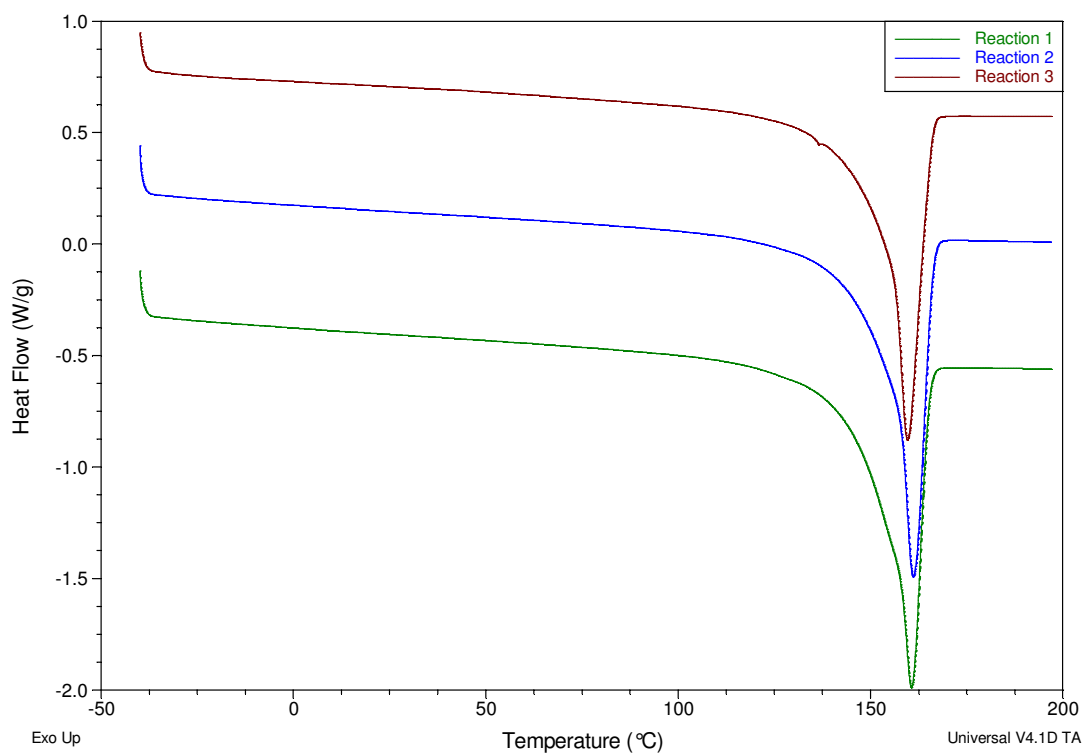


**Figure C.36** The DSC melting endotherms for the polymers prepared to investigate repeatability using the MPDMS donor at an external donor/catalyst ratio of 4.

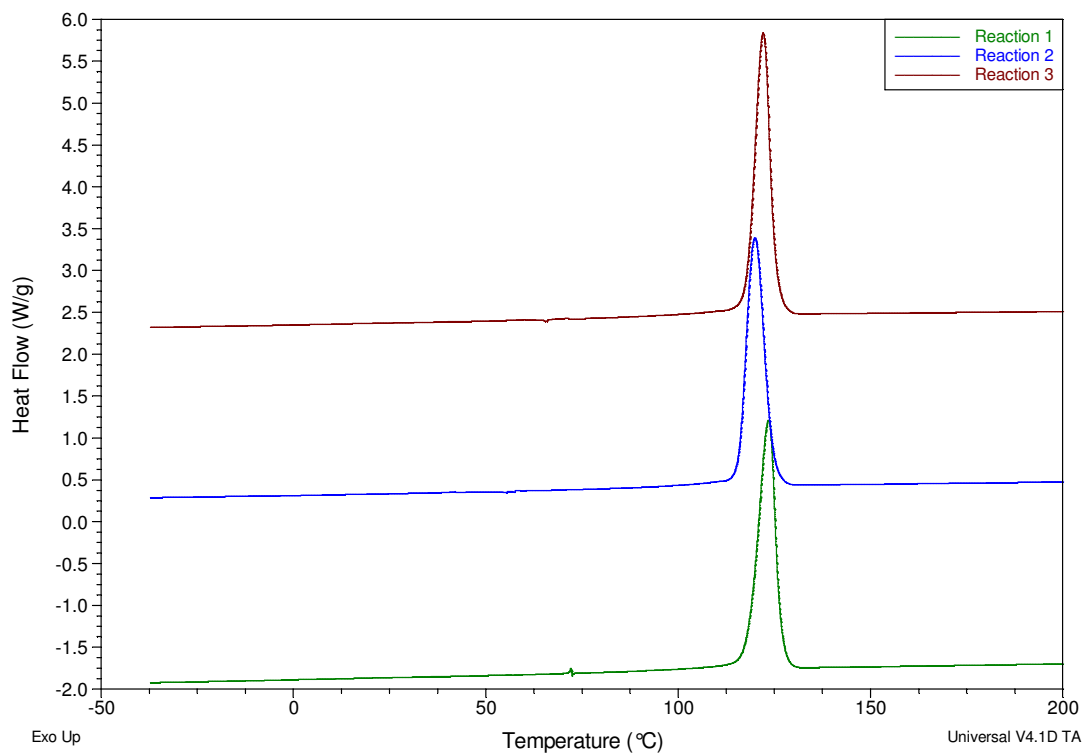


**Figure C.37** The DSC crystallisation exotherms for the polymers prepared to investigate repeatability using the MPDMS donor at an external donor/catalyst ratio of 8.

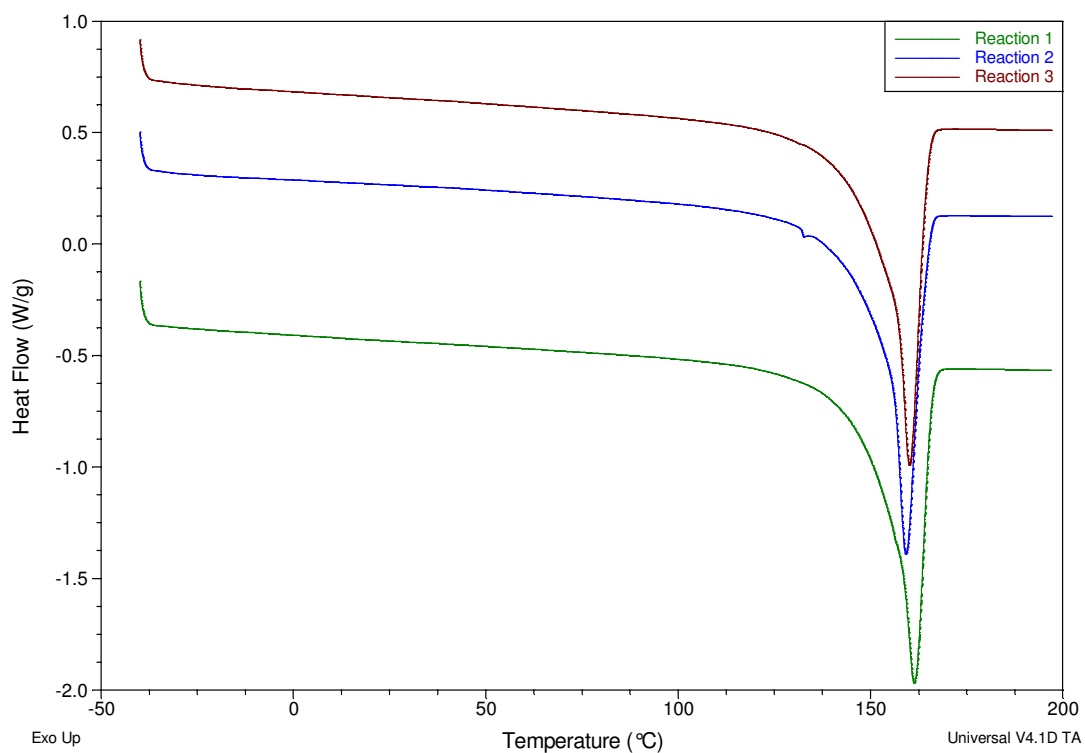


**Figure C.38** The DSC melting endotherms for the polymers prepared to investigate repeatability using the MPDMS donor at an external donor/catalyst ratio of 8.



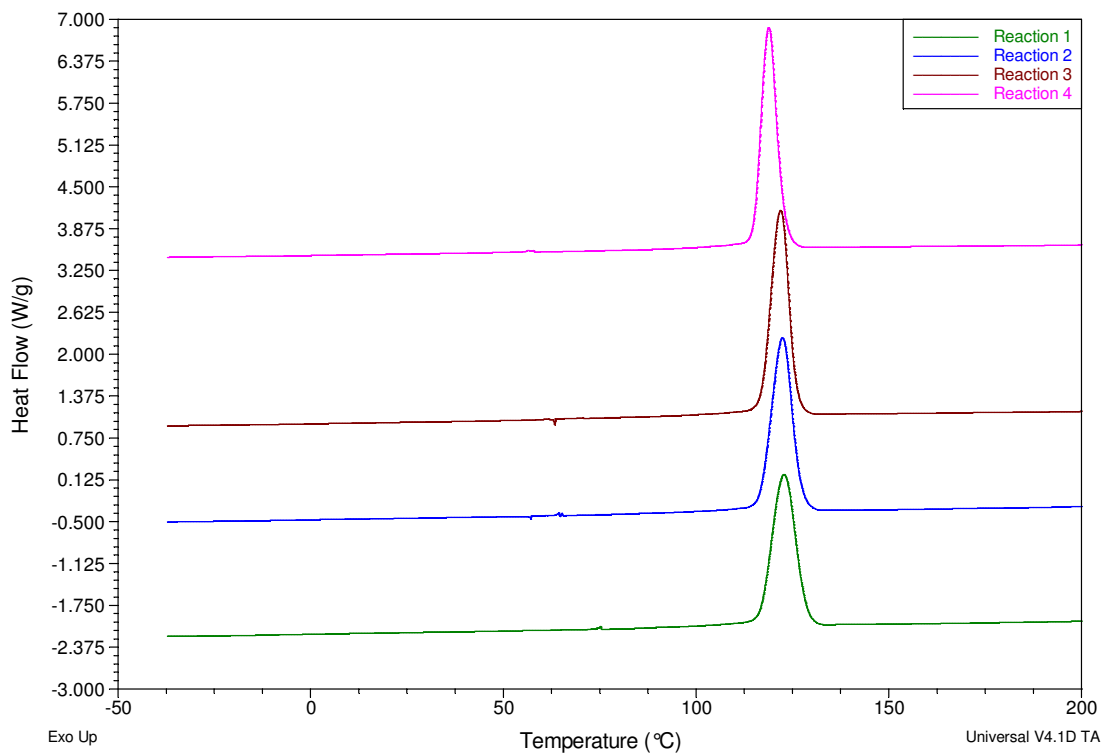


**Figure C.39** The DSC crystallisation exotherms for the polymers prepared to investigate repeatability using the MPDMS donor at an external donor/catalyst ratio of 16.

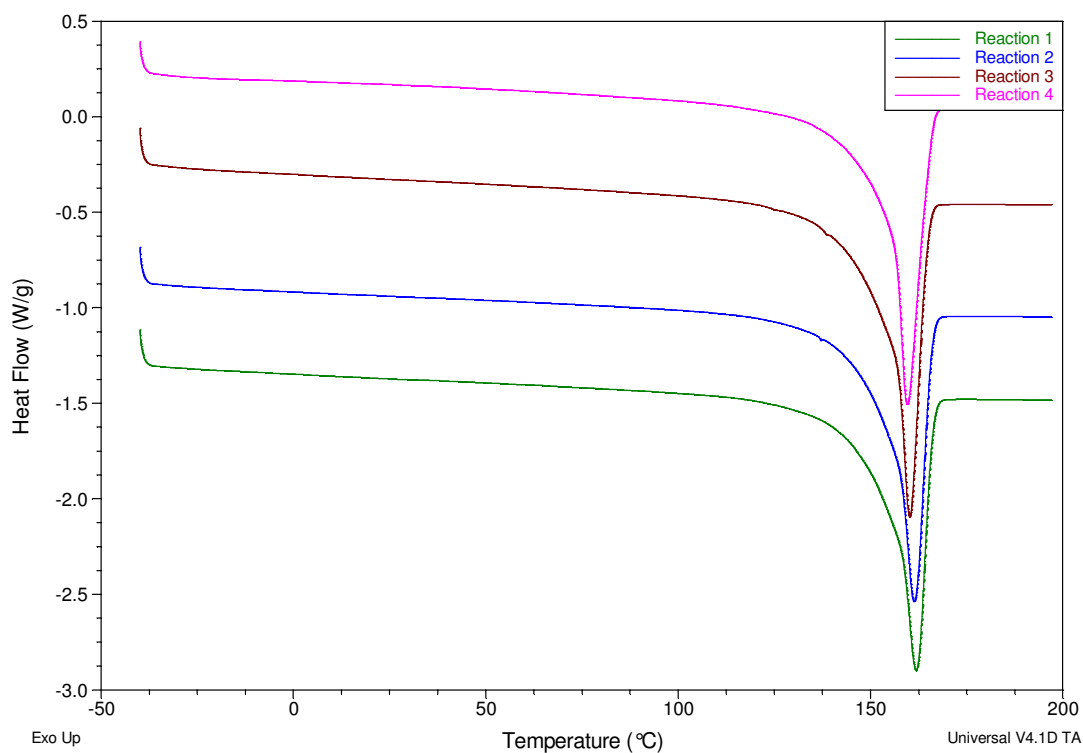


**Figure C.40** The DSC melting endotherms for the polymers prepared to investigate repeatability using the MPDMS donor at an external donor/catalyst ratio of 16.

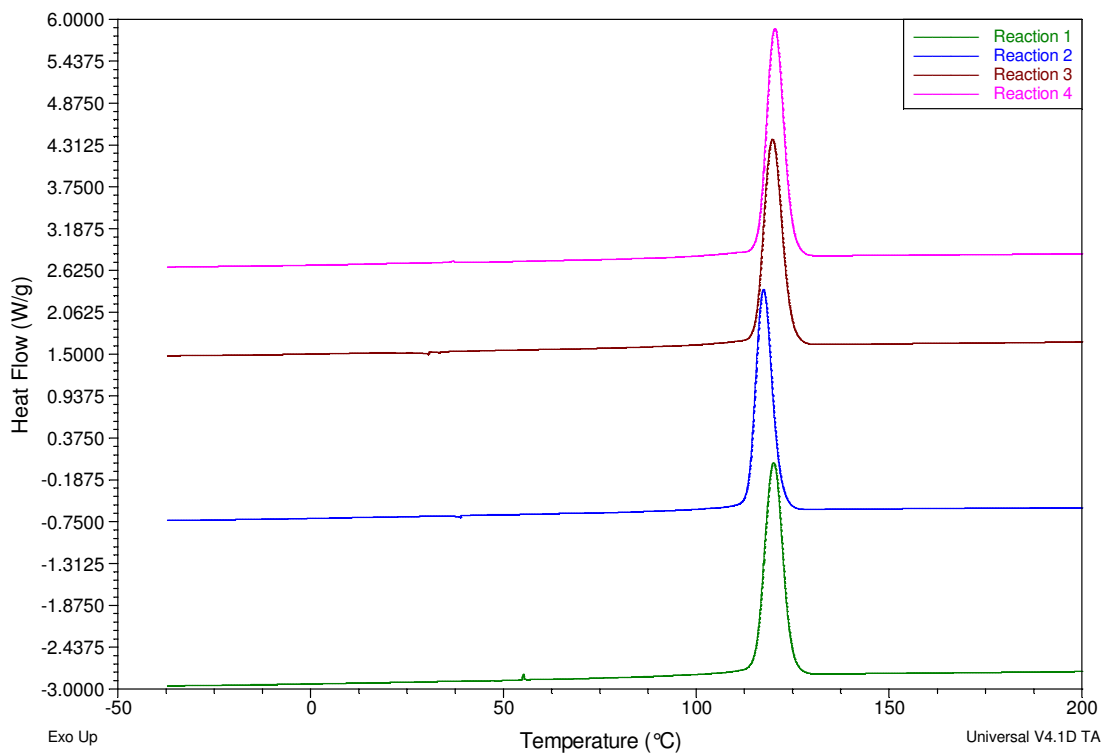


**Figure C.41 The DSC crystallisation exotherms for the polymers prepared to investigate repeatability using the MPDMS donor at an external donor/catalyst ratio of 40.**

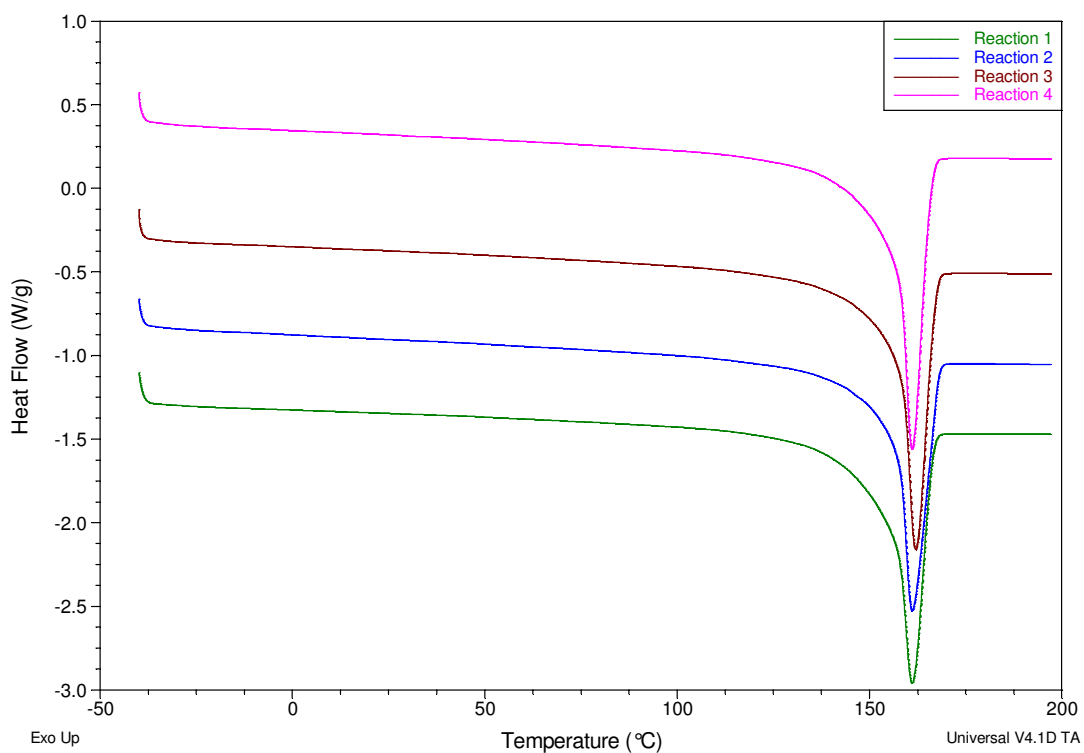


**Figure C.42 The DSC melting endotherms for the polymers prepared to investigate repeatability using the MPDMS donor at an external donor/catalyst ratio of 40.**

### C.3 DSC data from Chapter 6

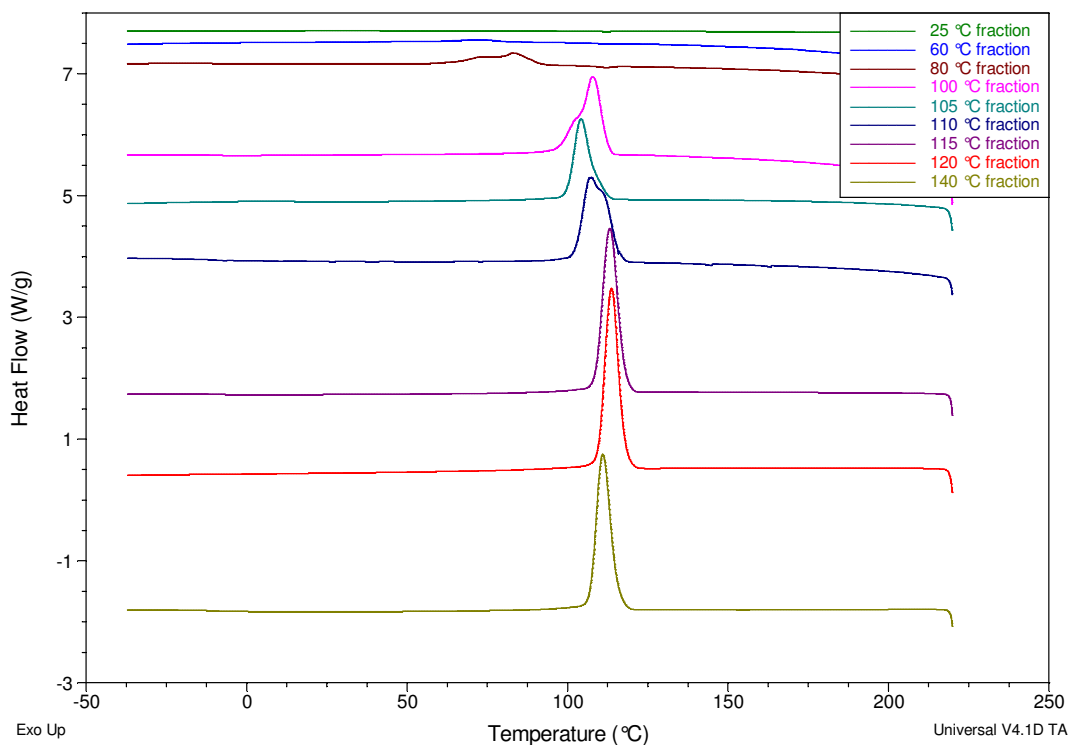


Figure C.43 The DSC crystallisation exotherms of the TREF fractions of sample DP-1.

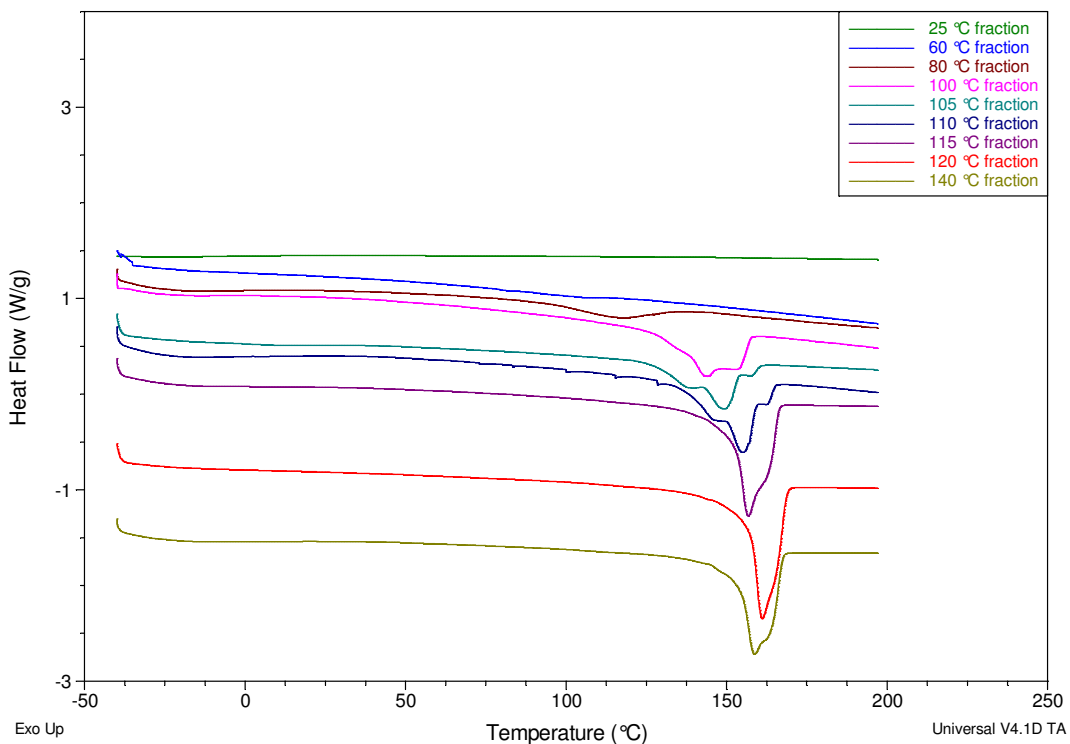


Figure C.44 The DSC melting endotherms of the TREF fractions of sample DP-1.

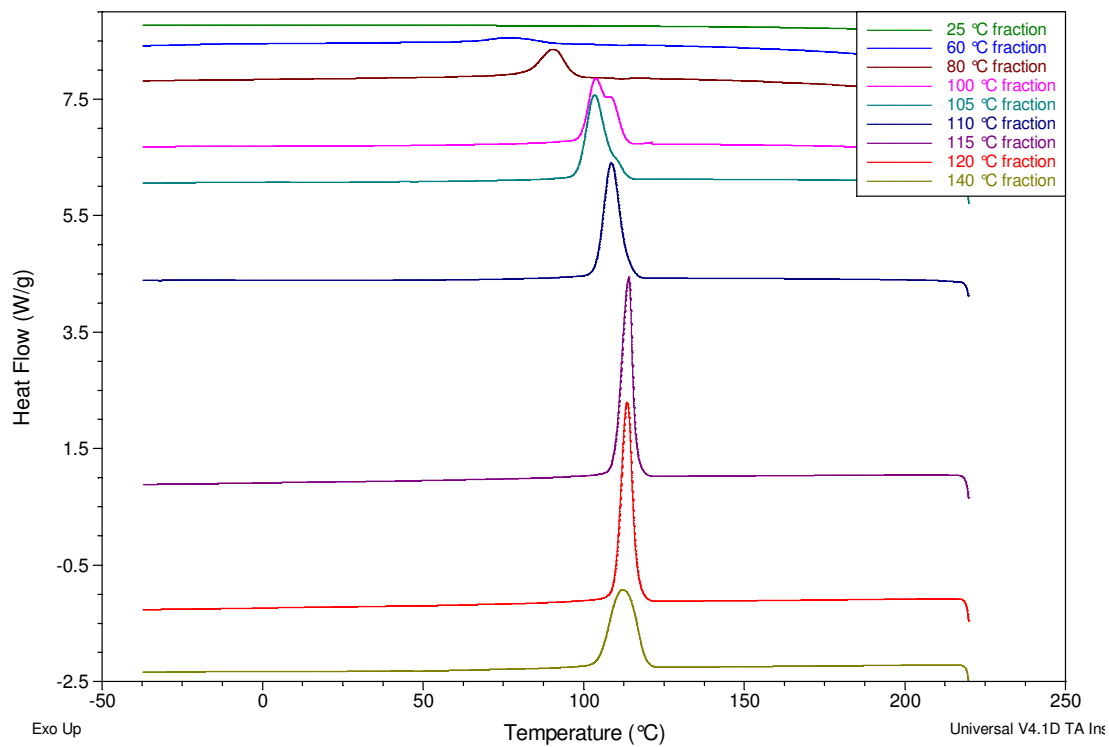


Figure C.45 The DSC crystallisation exotherms of the TREF fractions of sample DP-2.

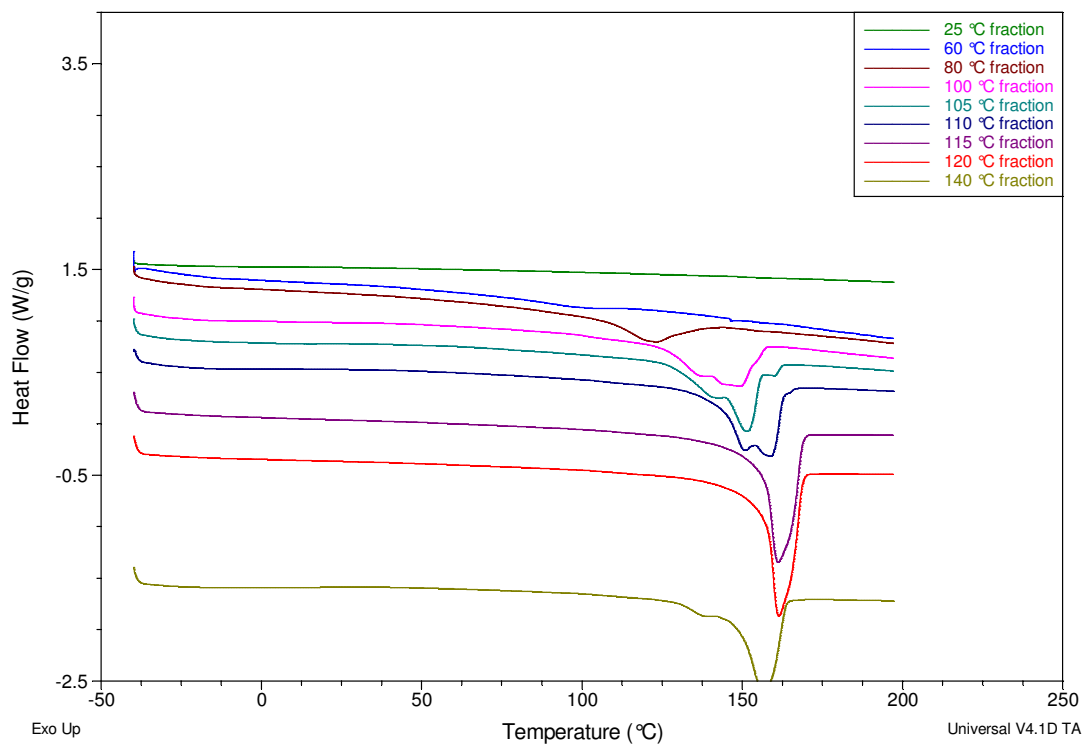
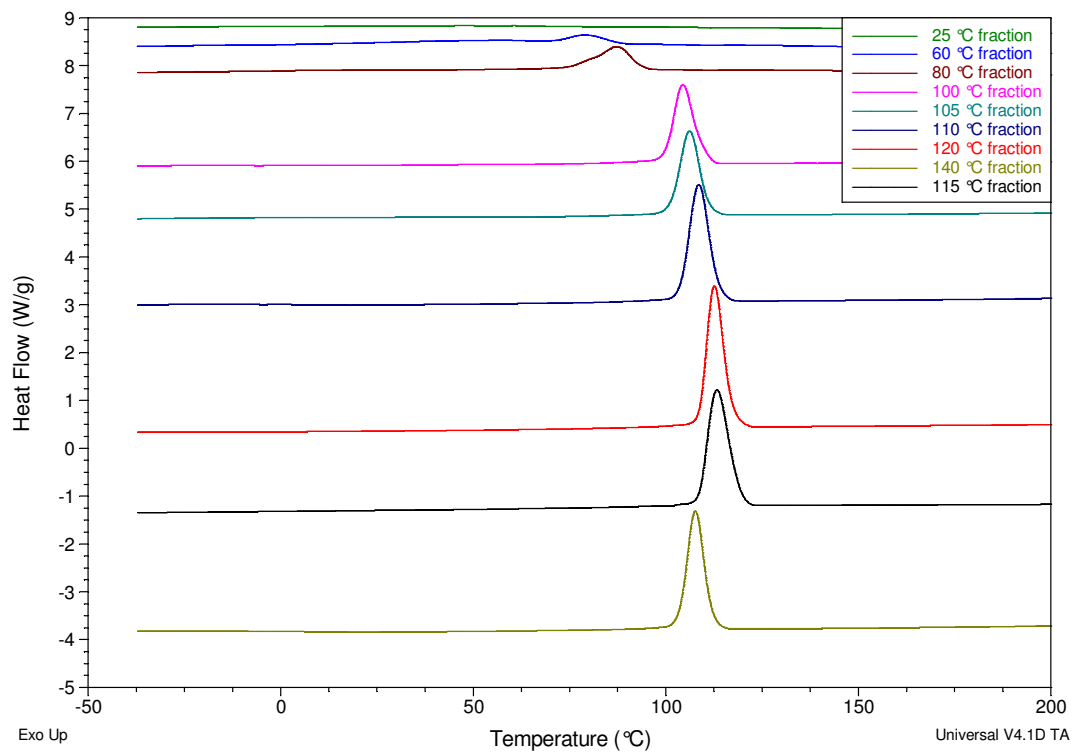
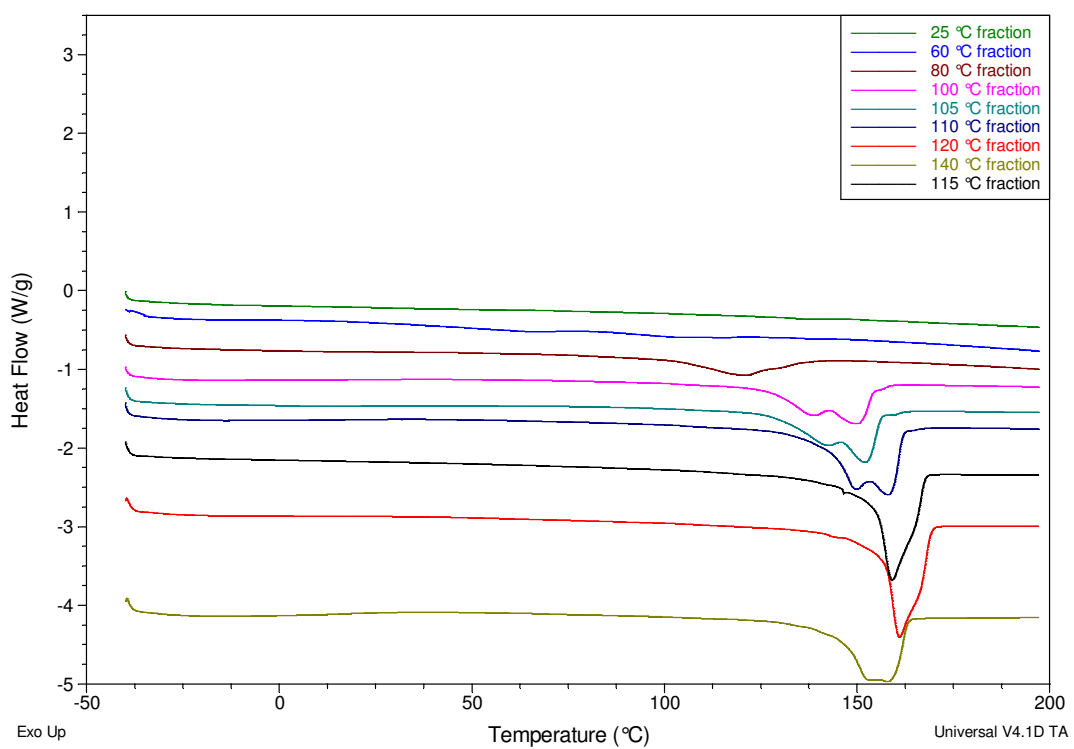


Figure C.46 The DSC melting endotherms of the TREF fractions of sample DP-2.



**Figure C.47** The DSC crystallisation exotherms of the TREF fractions of sample DP-3.



**Figure C.48** The DSC melting endotherms of the TREF fractions of sample DP-3.

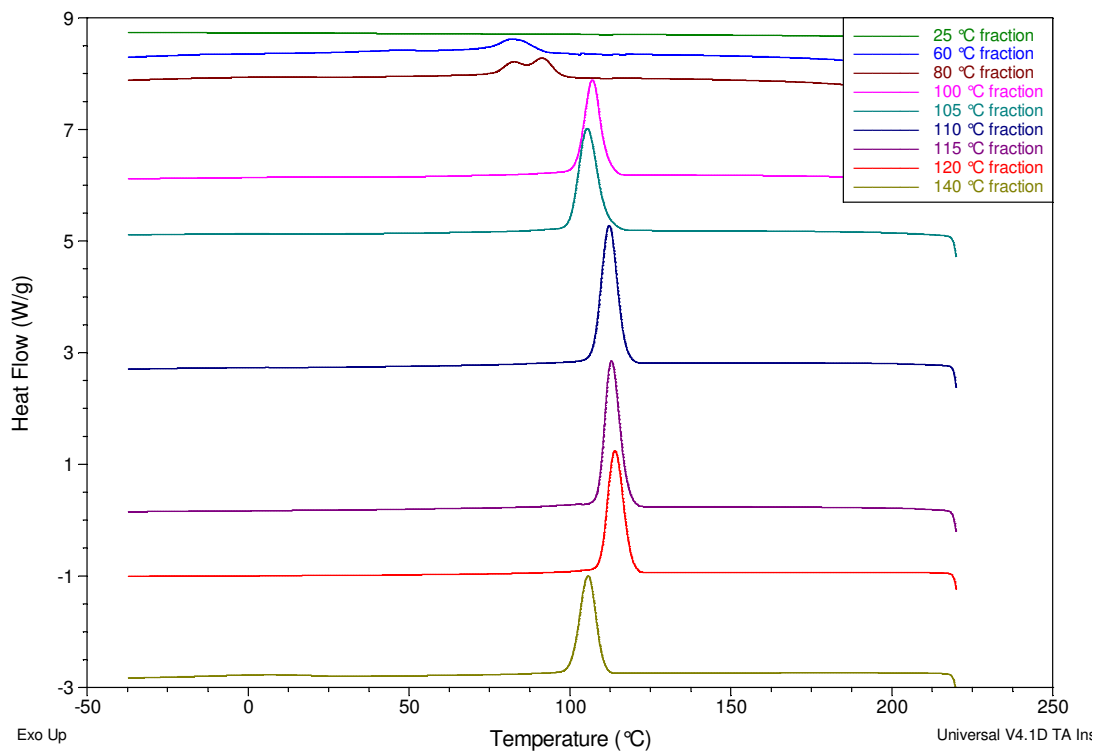


**Figure C.49** The DSC crystallisation exotherms of the TREF fractions of sample DP-4.

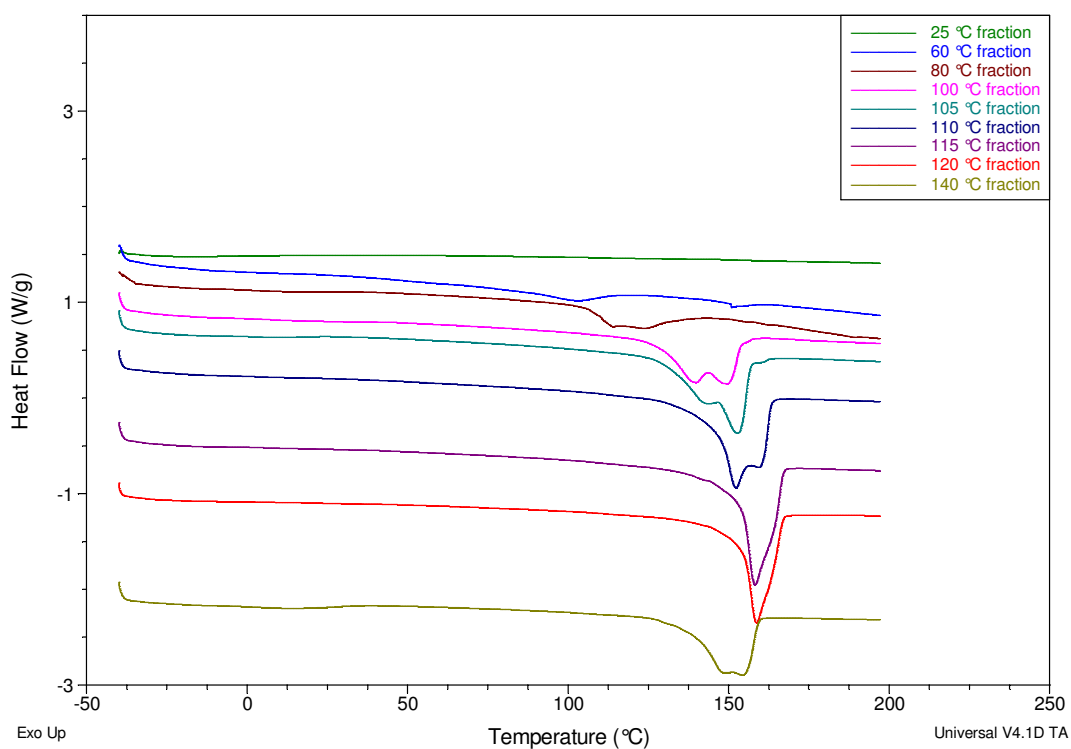


**Figure C.50** The DSC melting endotherms of the TREF fractions of sample DP-4.

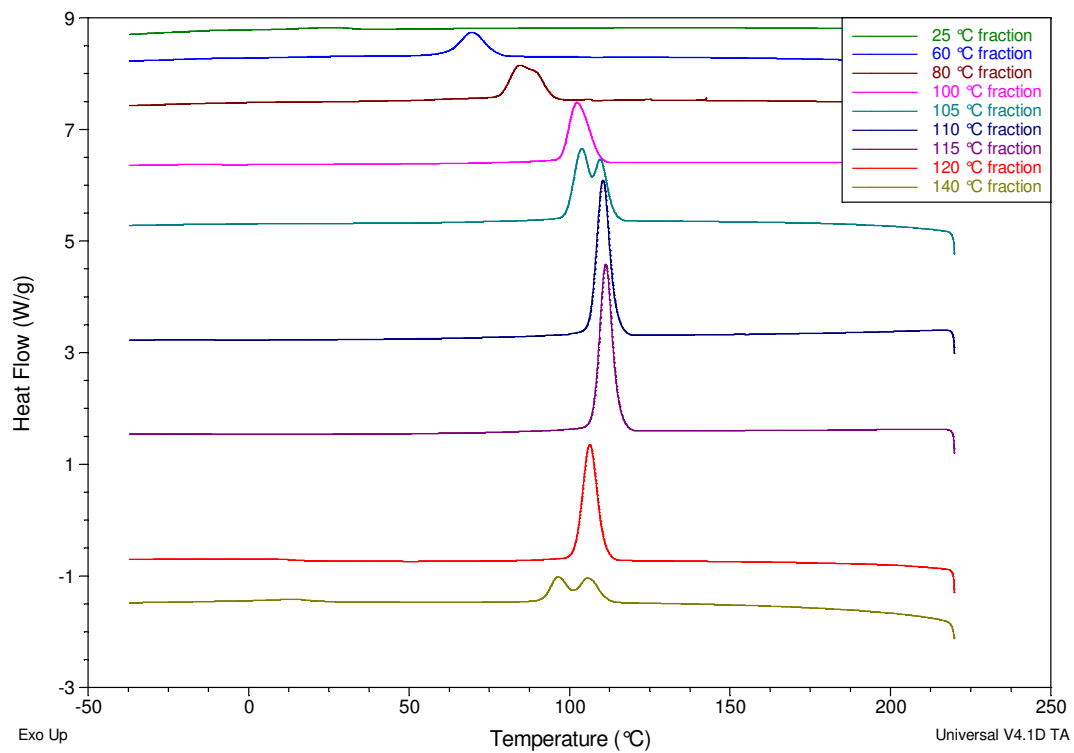


**Figure C.51** The DSC crystallisation exotherms of the TREF fractions of sample No ED.

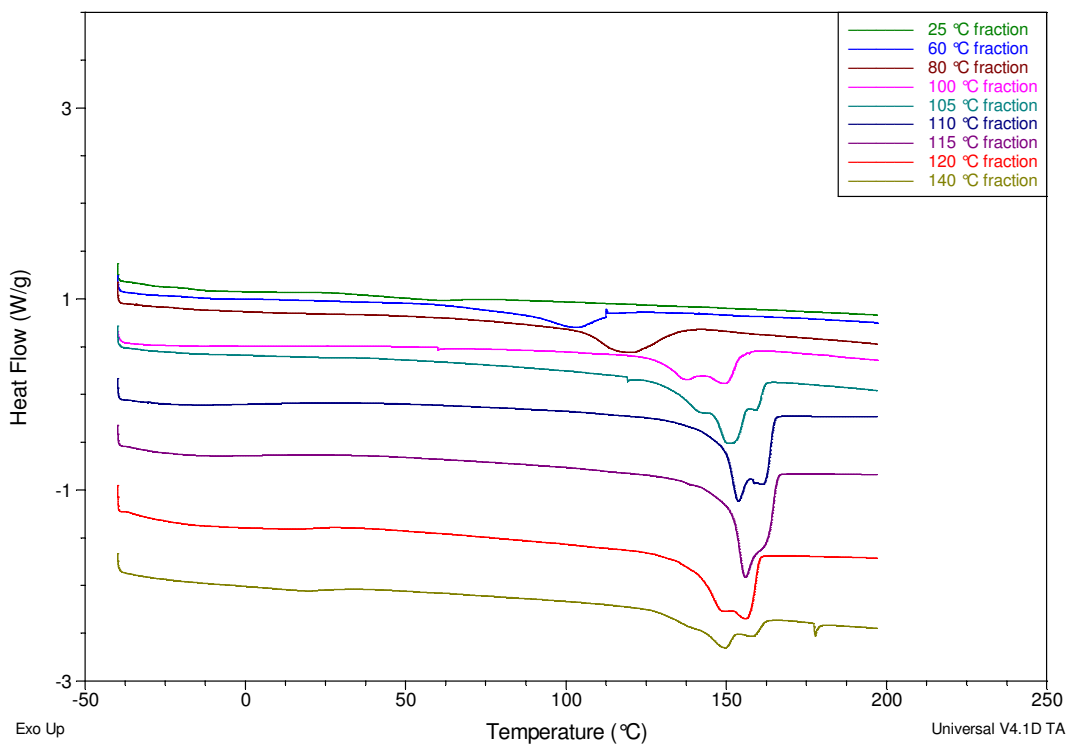


**Figure C.52** The DSC melting endotherms of the TREF fractions of sample No ED.

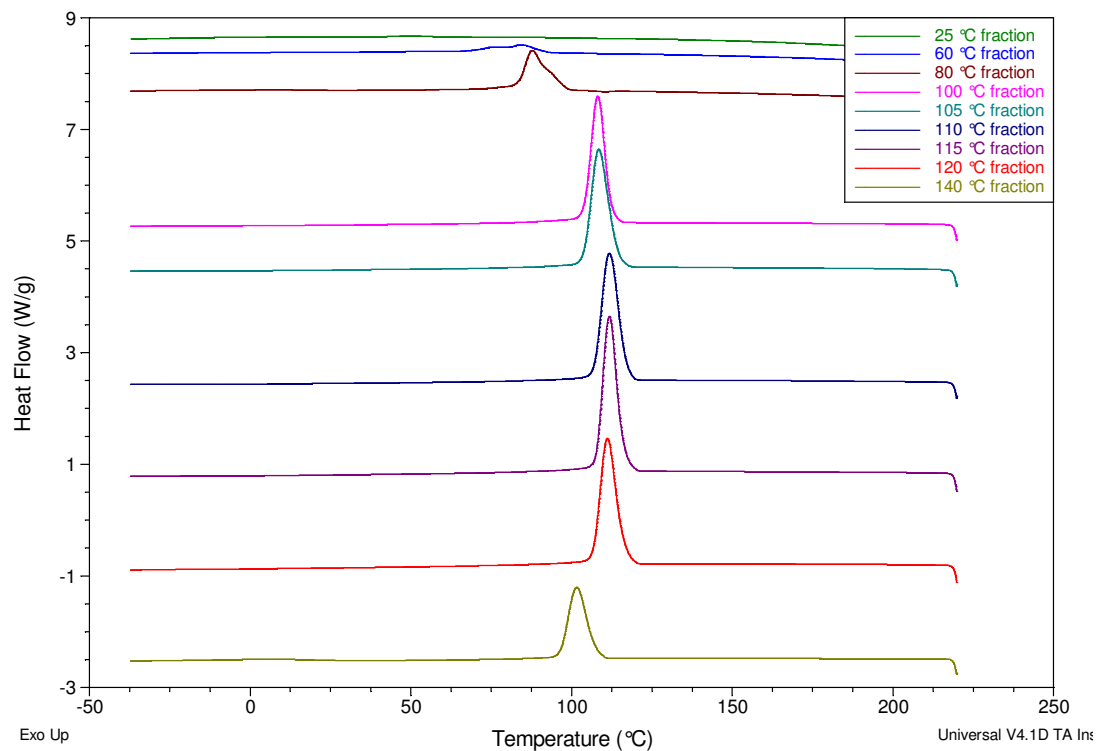


Figure C.53 The DSC crystallisation exotherms of the TREF fractions of sample MP-1.

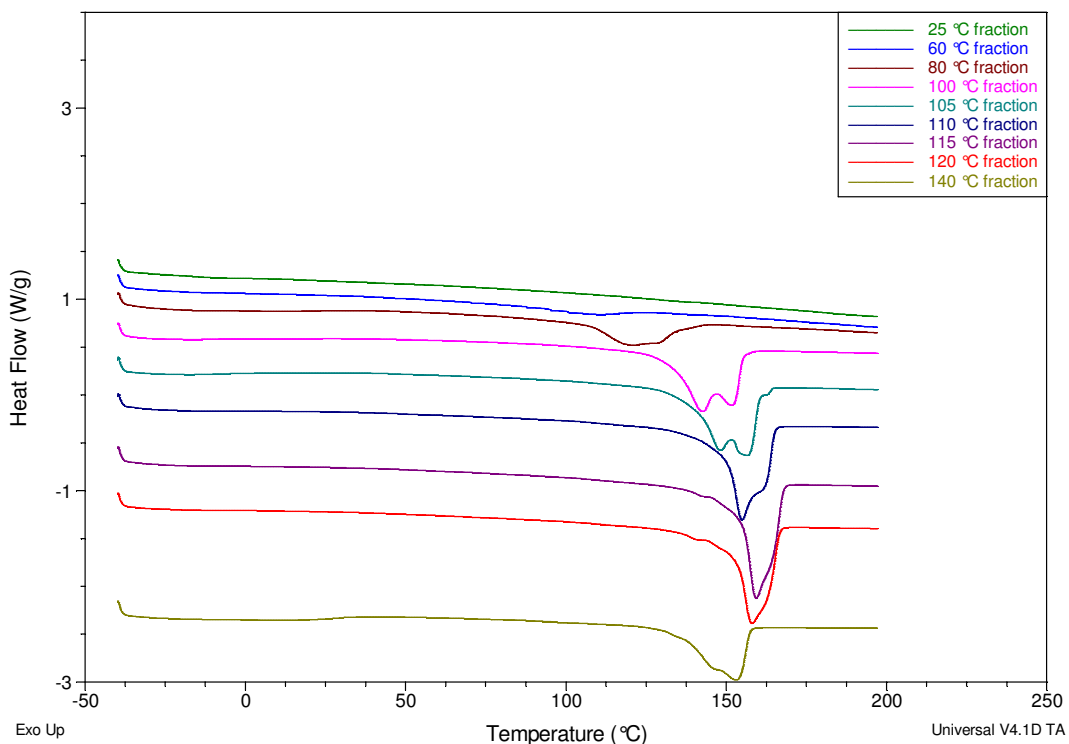


Figure C.54 The DSC melting endotherms of the TREF fractions of sample MP-1.



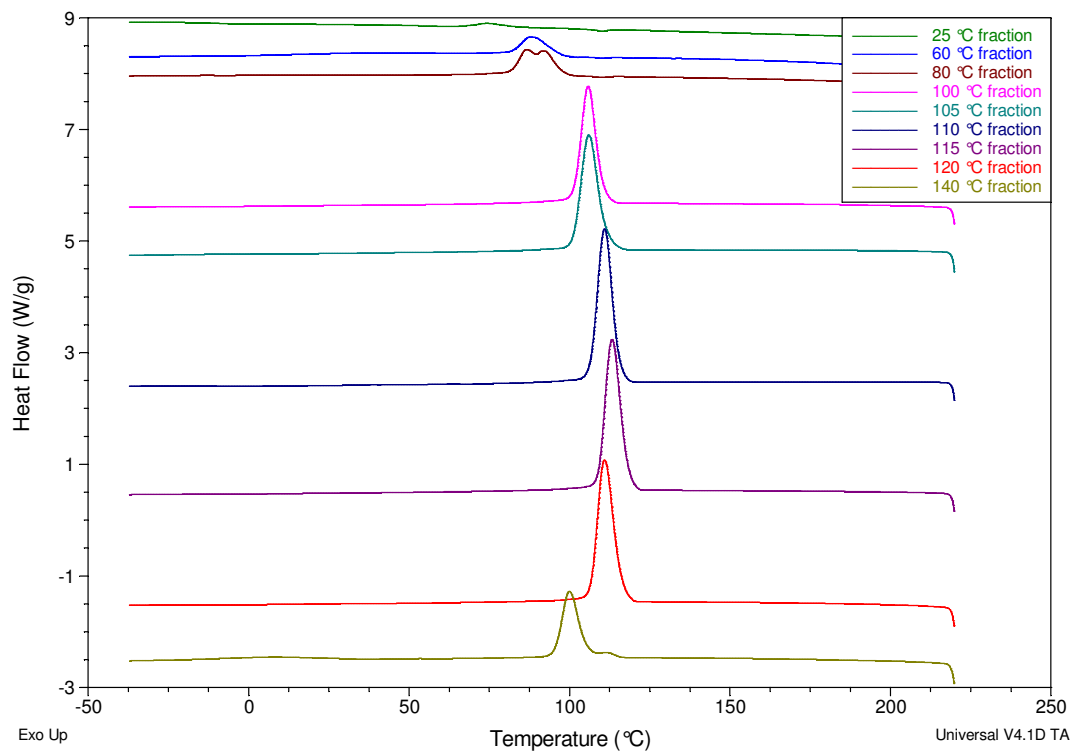


Figure C.55 The DSC crystallisation exotherms of the TREF fractions of sample MP-2.

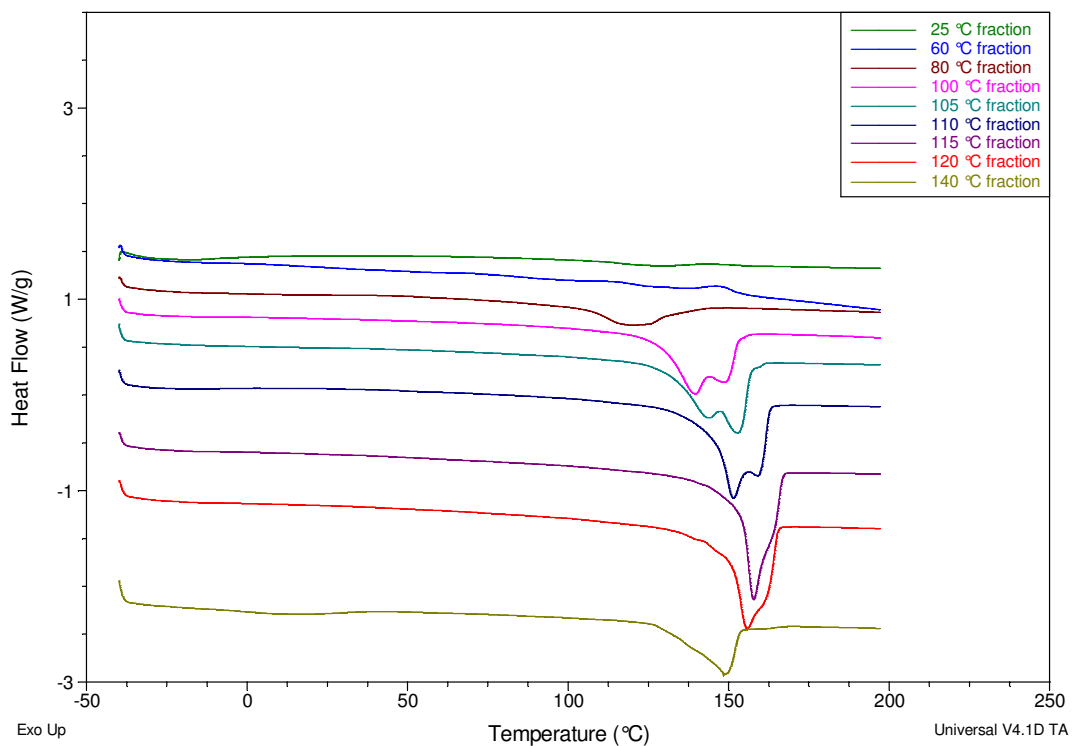
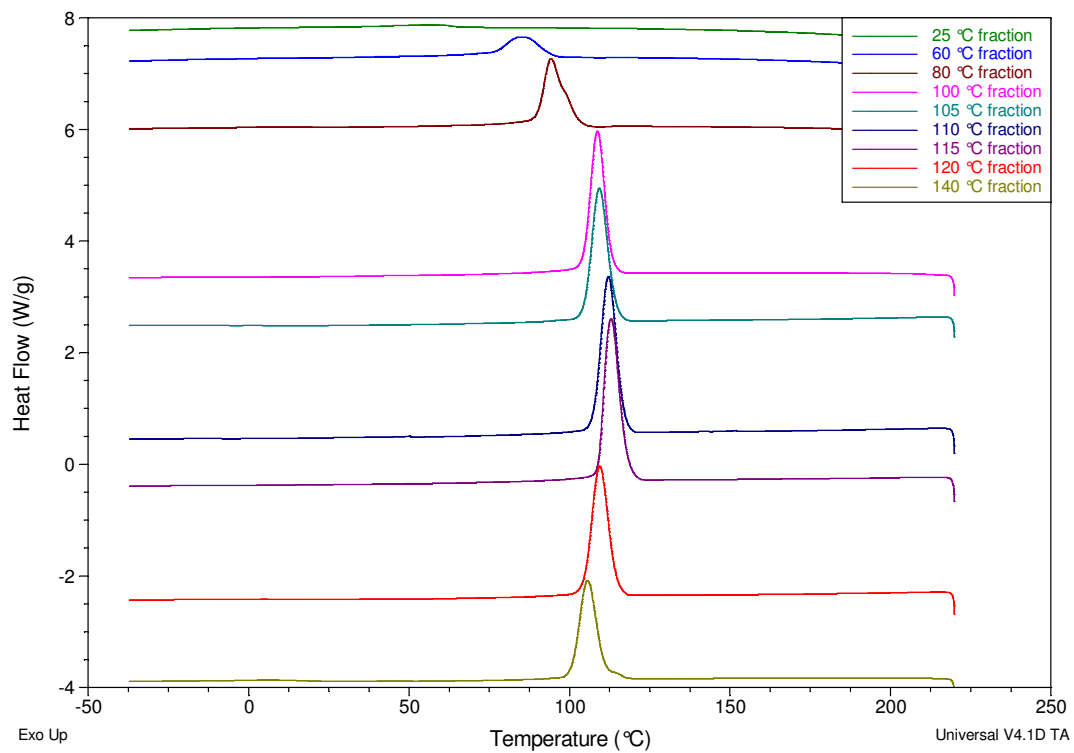
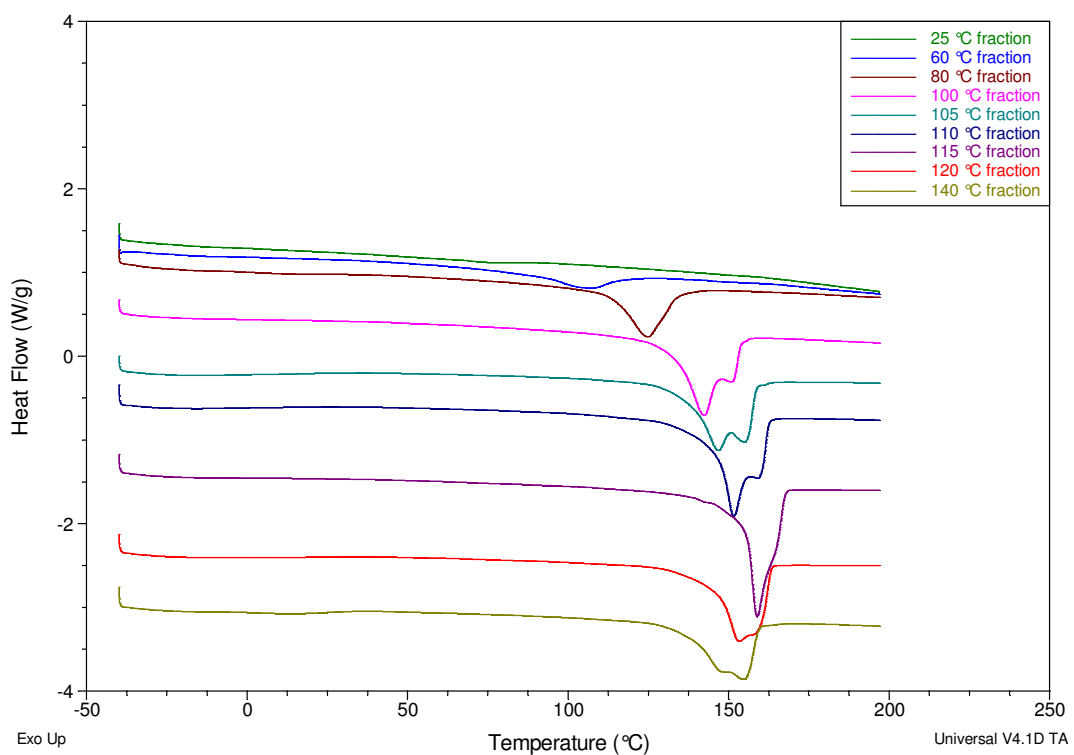


Figure C.56 The DSC melting endotherms of the TREF fractions of sample MP-2.



**Figure C.57** The DSC crystallisation exotherms of the TREF fractions of sample MP-3.



**Figure C.58** The DSC melting endotherms of the TREF fractions of sample MP-3.

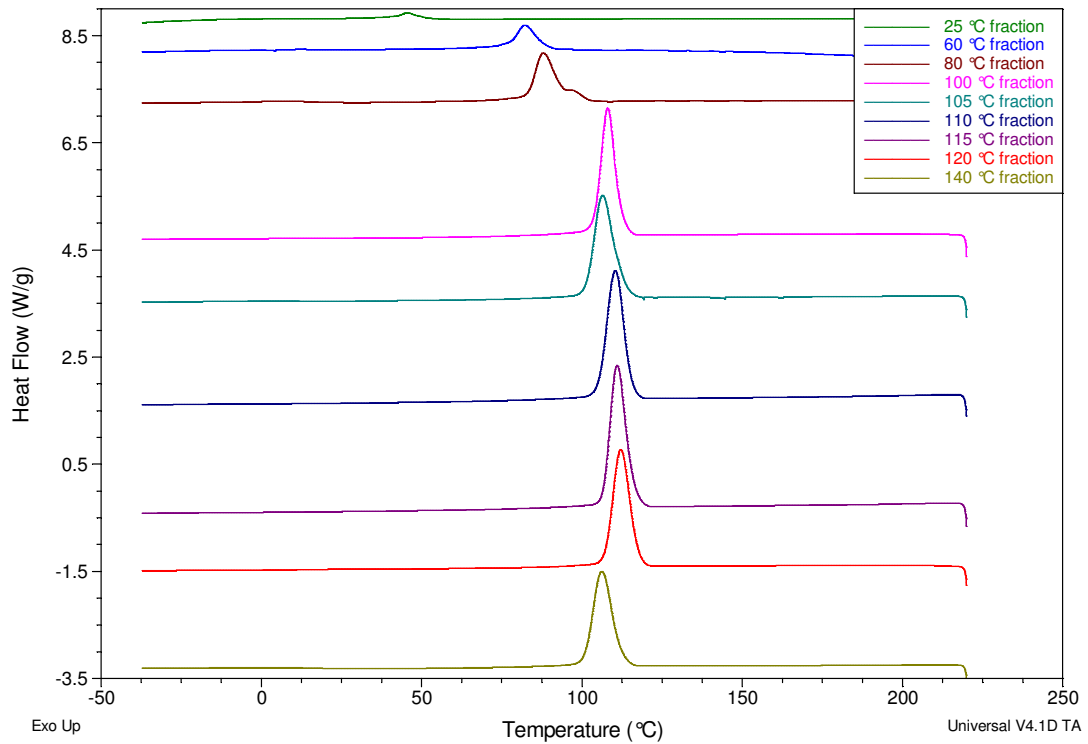


Figure C.59 The DSC crystallisation exotherms of the TREF fractions of sample MP-4.

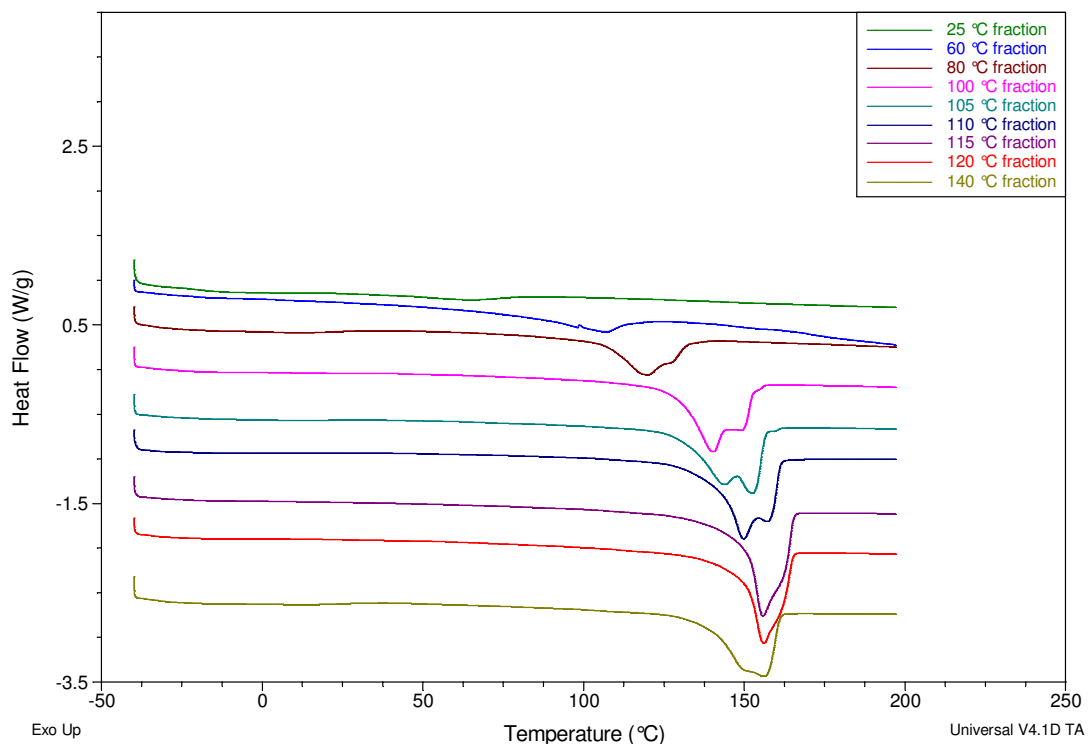
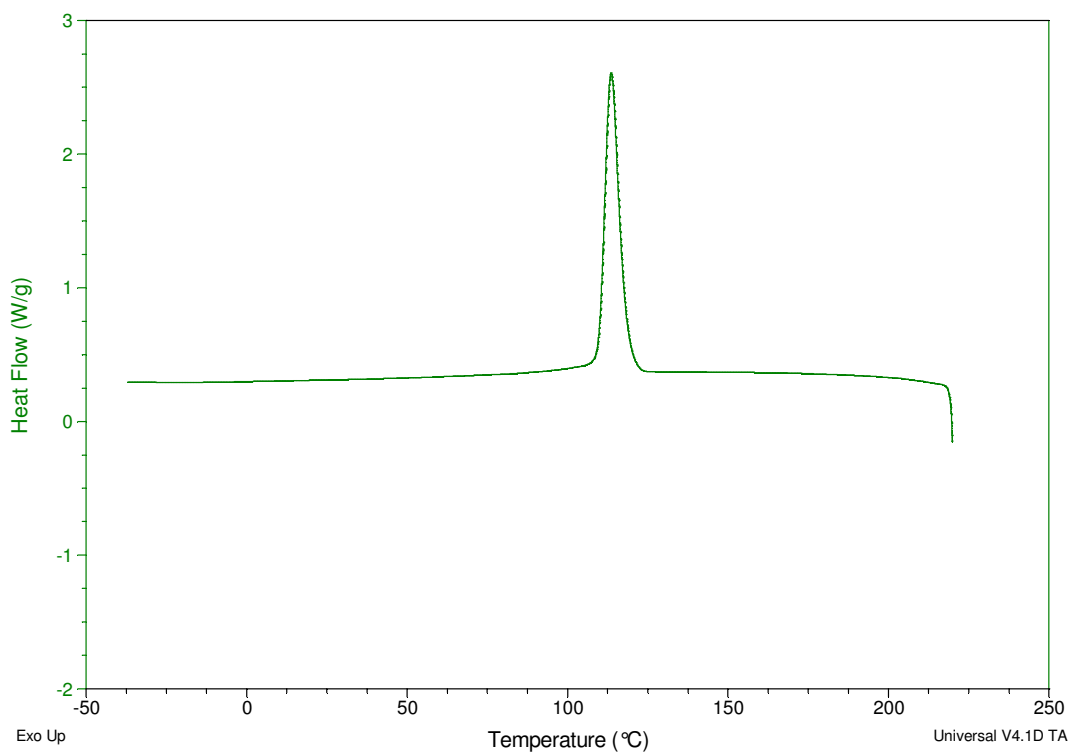
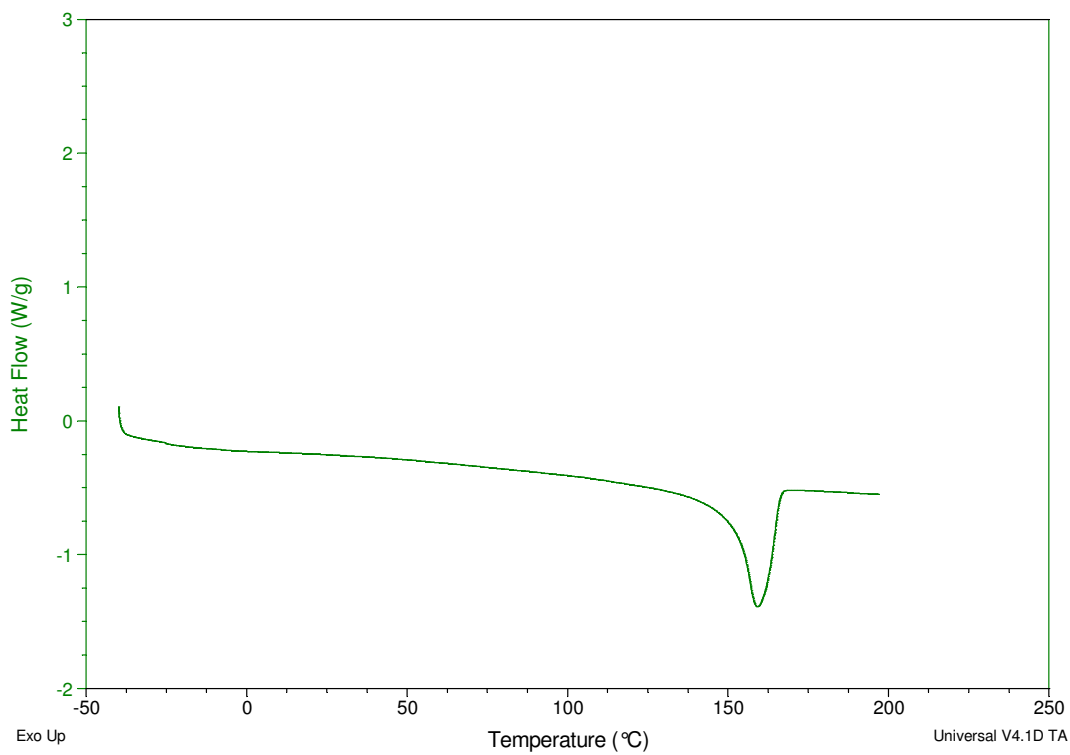


Figure C.60 The DSC melting endotherms of the TREF fractions of sample MP-4.

## C.4 DSC data from Chapter 7



**Figure C.61** The DSC crystallisation exotherm of the test sample.



**Figure C.62** The DSC melting endotherm of the test sample.